Modelling mitochondrial epilepsy *in vitro*: conceptualisation, mechanisms, and therapeutic implications

Felix Chan

Thesis submitted for the degree of Doctor of Philosophy at Newcastle University

April 2017

Advisor:

Prof. Mark Cunningham

Prof. Sir. Doug Turnbull

Abstract

Up to a third of patients with mitochondrial disease exhibit epilepsy which is difficult to control with existing pharmacotherapies. Anti-epileptic drug development in this field has stalled due to a paucity of pre-clinical models. To address this, I developed a novel *in vitro* model of mitochondrial epilepsy. The main features of the model are respiratory chain complex I and IV inhibition as well as astrocytic aconitase inhibition using pharmacological agents. In this way, I observed epileptiform discharges in rodent and murine hippocampal brain slices. Using immunohistochemical techniques, I confirmed findings from human neuropathological studies in that epileptic slices showed a selective loss of GABAergic interneurons, sparing of pyramidal neurons, and profound astrogliosis. To demonstrate the models clinical relevancy, I illustrated the model's predictive validity by observing that epileptic activity was unaffected by various antiepileptic drugs. These studies did reveal that there was an involvement of AMPA and $GABA_A$ receptors in the generation of the epileptiform discharges. Further experiments also implicated the astroglial glutamate-glutamine cycle in the process of epileptogenesis. Using metabolic tracing experiments, glutamine was observed to be depleted during the epileptic state. Glutamine supplementation sustained the synthesis of GABA in the epileptic tissue, presumably to restore metabolic homeostasis. Finally, aerobic respiration was inhibited alongside the upregulation of anaerobic glycolysis during the epileptic state. To dissect the role of glutamine in the modulation of mitochondrial respiration, I isolated neuronal and astrocytic populations and performed measurements of metabolic flux during the induction of seizure activity. Glutamine was able to rescue partial mitochondrial respiratory chain inhibition selectively in the astrocytes. Overall, I have developed an *in vitro* model of mitochondrial epilepsy and showed the interaction between astrocytes and neurons is prerequisite for seizure generation. Several pharmacological targets have emerged from these studies which may provide future novel therapeutic targets for this condition.

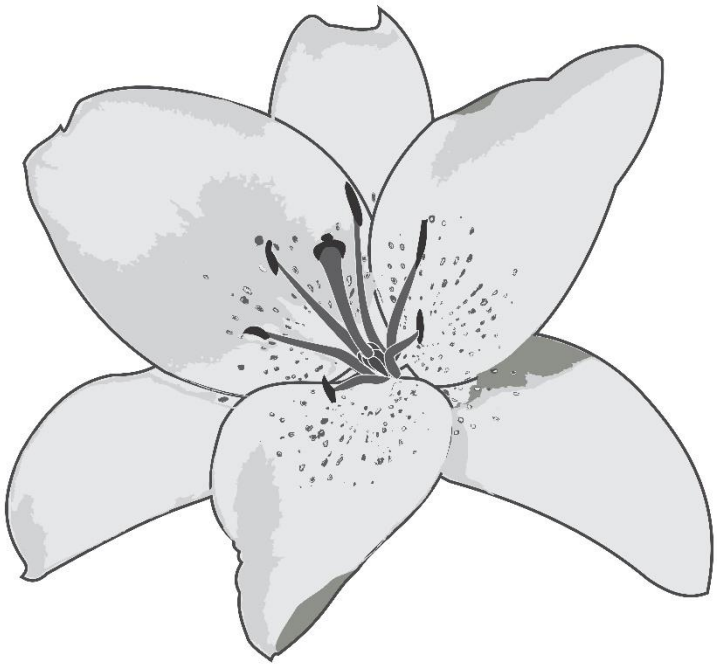

Dedicated to my mother, Lily Meliani Lauwensi, whose love and kindness have shaped me into the man and the scientist that I am.

Acknowledgments

First and foremost, I would like to thank my fantastic supervisory team that has given me excellent support throughout my Doctorate study. I am indebted to Professor Mark Cunningham, for whom I have developed a huge amount of respect for and for constantly pushing me to strive for the best scientific work possible. Equally, I would like to acknowledge Professor Sir Doug Turnbull, for being my role – model and mentor as a clinical academic who constantly challenge me with thought – provoking questions from the very first time I met him. Finally, I would like to thank Dr. Nichola Lax for being there for me every time I have a question and providing one of the best pastoral care that a graduate student can expect from their supervisory team.

All the work presented in this thesis is my own, except for Figure 3.1 which uses images and data obtained from work conducted by Dr. Nichola Lax (used and reproduced with permission). Some Matlab scripts have also been written by various third parties that are used to analyse the data presented in this thesis. A copy of the Matlab script has been reproduced with permission and attached in Appendix 1. I would like to thank and acknowledge both Dr. Katherine Newling and Stacey Aston for the writing of this script. I would also like to thank Dede for the consultation and help in the graphical preparation of some of the figures in this thesis. The study presented in this thesis is also not possible without financial contributions from various sources. I would like to acknowledge the EPSRC Industrial CASE Award (EP/K50499X/1) studentship in collaboration with GlaxoSmithKline that primarily funds this study. I would also like to acknowledge HelloBio for the travel grant for attending the Society for Neuroscience Meeting to present this work and the Network of European Neuroscience Schools (NENS) Exchange Grant for funding the collaborative work done with University of Copenhagen. I would also like to acknowledge Eisai and The Wellcome Trust Biomedical Vacation Scholarships grant for the contribution towards the perampanel study.

Throughout my PhD, all past and present members of the laboratory have assisted me in the completion of this study in various capacities. To that, I am forever grateful. I would like to acknowledge the past lab members; Dr Katherine Newling, Dr. Anais Thouin, Dr. Anna Simon, and Dr. Stephen Hall for largely training me in the wonderful world of neuroscience and tolerating the 18 – years old version of me starting out a doctorate study. I am equally indebted to all current members of the laboratory;

Dr. Georgia Rentesi, Dr. Tamara Modebadze, and (soon to be Dr) Anderson Brito da Silva for helping me grow and develop into the scientists that I am today. Thank you to Karen Parkin for checking up on me every morning. I also would like to acknowledge the Wellcome Trust Centre for Mitochondrial Research, members of which have largely also contributed towards the conception and development of this study. In particular, I would like to thank Dr. Nichola Lax and Dr. Monika Olahova for being my mentors and primary point of contact within the centre for any issues and questions that I have. I would also like to thank past and present members of the centre who have contributed to a dynamic discussion and study on mitochondrial research, particularly Alexia, Jono, and Craig (whom I started out with); Amy Reeve, Ollie, Pav, Lyndsey, Julie, Nishani, and Gavin F.

I have also obtained advice and support from various other affiliated academics throughout this study. I would like to acknowledge my progress review panels; Dr. Fiona LeBeau and Professor Robert (Bob) Lightowlers for providing sound advice throughout my PhD and for helping me learn how to ‘be realistic’, ‘edit’, and ‘prioritize’. I would like to thank Professor Zofia-Chrzanowska Lightowlers for believing in me from when she was my personal tutor during my Masters and to date, still asking how I am holding up. Equally, I would like to thank Dr. Gavin Clowry, who was my first ever scientific mentor and has really played a major role in the realization of my academic career. I would also like to thank Dr. Michele Sweeney (particularly), Dr. Lindsey Ferrie, Dr. Vanessa Armstrong, and Dr. Martin Edwards for providing me with invaluable teaching experience that would be useful for my professional career development. Various clinicians affiliated with the Newcastle upon Tyne Hospitals NHS Foundation Trust have also provided constructive criticism and inputs in the development of this study. In particular, I would like to thank Dr. Mark Baker for the support and advice that he is always willing to give in the clinical applications of the study. I would also like to thank Dr. Anita Devlin for reigniting my interests in ketogenic diet research and providing me with the opportunity to observe her very professionally run epilepsy clinic.

I have also worked closely with many talented undergraduate students who have helped with various aspects of this study. I would like to thank Heather Thompson for her hard work in helping optimize the Seahorse technique, Adam Skeen for his perseverance during the perampanel experiment, Angeline Kosim for her help with the oxidative stress assessment, Shuna Whyte for her assistance with

immunohistochemistry and microscopy, and Elizabeth J. Tilley for her hard work in helping with the pharmacology experiments.

As the study developed, I have also initiated active collaboration with various research institutions and groups in the use of novel approaches and techniques for in-depth research of mitochondrial epilepsy. I would like to acknowledge NeuroMet in University of Copenhagen whom I have spent a few months working in and have truly welcomed me as part of the member of the NeuroMet family (officiated by singing the NeuroMet song). I would like to thank Professor Helle Waagepetersen for replying to a string of random emails that eventually developed into one of the best collaboration and fruitful moments that has come out of my PhD. Professor Waagepetersen has given me a unique approach to science and the nurturing of a familial collaborative research environment; for which I truly respect her. I would also like to thank Caroline Marie Voss for training me in everything (literally, everything), Blanca Irene Aldana Garcia for active assistance in any issues I have with the machines and techniques there (and the discussions on Mexican food), and Jens Valde Andersen for being a good friend whilst I was there (thank you for lending me the eraser).

In Newcastle University, I would like to acknowledge Dr. Annette Meeson for kindly lending me the equipment and the bench space necessary to conduct the cell isolation described in this thesis. I would like to thank the members of her research group; Nani, Evie, and Kamilla; and Debra Jones, the technical manager, for welcoming me (a random stranger) into their workspace and helping me with any silly questions I might have. I would also like to thank Dr. Satomi Miwa for her expert advice on the Seahorse technique and Edward Fielder for being a good friend while I was working in the Centre for Aging and Vitality.

The research that I have conducted would not have run as smoothly as it had, had it not been for the hard work of all the support team in the Institute of Neuroscience. I would like to acknowledge all the postgraduate support officers that have helped me throughout my postgraduate study in the Institute: Helen Stewart, Suzi Engelbright, Caroline Risacher, and (the rockstar) Beckie Hedley. I would like to thank Dr. Ann Fitchett for giving me the opportunity to develop my public engagement skills; which I now have a true passion for. I would like to thank Carole Ainsley and Glynis Mitchinson for always being there for whatever issue I might have (in P2P ordering or in life). I would also like to thank Kay Garrick and Samantha Cook for their prompt professional help whilst they were working in the Institute, Karen Curry for help whilst I am employed

as research assistant in the Institute, and Brian Claydon for ‘showing me the black magic’ of IT (and the new computer during the crucial time of thesis writing).

I am also forever indebted to all my friends who are truly supportive in maintaining my sanity whilst I am doing my PhD. Truly, the experience of the weekly Forth Hotel pub quiz, courtesy of Helen Jones, is vital in this. As such, the quiz team members, past or present, have been such good friends to me for the past three years. To name a few; Clare, Grace, Gemma, Abi, Caroline, Chris T, Chris B, Conor G, Connor R, Joe C, Josh, and Carolyn are ‘core’ members of the team and my friendship group. I would also like to acknowledge all the postgraduate students of Institute of Neuroscience who have come to my quizzes and reignited my passion for extracurricular activities. I would also like to thank the other members of the office who have been such close friends to me; Sabine (and Tom), Yingdi, Jean, Myrto, Ruwaydah, and Nelson. My Indonesian friendship circle has also helped keep me grounded and rooted whilst I went through this emotional turmoil, for which I am thankful for. I would like to thank these lovely individuals: Vincent T, Sally, Angel K, Nora, Hans, Justine, Harata, Katherine S, Tiffany, Lusiana, Chris C, Victor T, Andre, Rio, Velasca, and Angel C for keeping up with all my antics. I would also like to thank ‘The Spice of Life’, particularly Liz and Michael; Trish from the Atrium, as well as ‘Happiness Inn’ for providing me with the necessary nourishment to keep me going through the long hours and late nights of writing a thesis.

Finally, I would like to thank my family members for being there throughout this whole journey. I would like to thank my mother for always believing in me and my abilities even when no one would. For that, I am eternally grateful. I would also like to thank my father who has been patient and supportive with me throughout. I would also like to thank my aunt, Rosalinda, and her family for helping me get through the rough patches of the final stages of writing. My cousins, particularly Wenni, Checil, Eldo, and Eldmond, have also helped in many ways towards the completion of this thesis. Lastly, but not least, I would also like to acknowledge Mega and Steve Young for being wonderful ‘surrogate parents’ while I am here in the UK.

Table of contents

List of figures

List of tables

List of abbreviations

2-DG	2-deoxyglucose
ACSF	Artificial cerebrospinal fluid
AMPA-R	α-amino-3-hydroxy-5-methyl-4-isoxazole propionic acid receptor
AMPK	5' adenosine monophosphate-activated protein kinase
ANLSH	Astrocyte-neuron lactate shuttle hypothesis
ANOVA	Analysis of variance
ATP	Adenosine triphosphate
BCA	Bicinchoninic acid assay
BSA	Bovine serum albumin
C57BL/6	C57 black 6
CA	Ammon's horn or *Cornu Ammonis*
CaMKII	calmodulin protein kinase type II
cAMP	Cyclic adenosine monophosphate
CB	Calbindin
CoQ10	Coenzyme Q10
CR	Calretinin
DAB	3,3'-diaminobenzidine
D-AP5	D-(-)-2-amino-5-phosphonopentanoic acid
dH_2O	Distilled water
DMF	N,N-dimethylformamide
DMSO	Dimethyl sulfoxide
DNA	Deoxyribonucleic acid
DNPH	2,4-dinitrophenylhydrazine
DPX	Distyrene, plasticiser, and xylene
EAAT	Excitatory amino acid transporter
ECAR	Extracellular acidification rate
EDTA	ethylenediaminetetraacetic acid
EEG	Electroencephalogram
FAD	Flavin adenine dinucleotide
FBS	Fetal bovine serum
FCCP	Carbonyl cyanide-p-trifluoromethoxyphenylhydrazone
GABA	Gamma-aminobutyric acid

GC-MS	Gas chromatography – mass spectrometry
GFAP	Glial fibrillary acidic protein
GHB	Gamma hydroxybutyrate
GLAST	Glutamate aspartate transporter
GSSG	Glutathione disulphide
HPLC	High performance liquid chromatography
HTn	4-hydroxy-trans-aconitate
I.D	Inner diameter
IC_{50}	Inhibitory concentration at 50%
KA	Kainate
KCN	Potassium cyanide
LCFA	Long chain fatty acids
LFP	Local field potential
LHON	Leber hereditary optic neuropathy
MACS	Magnetic activated cell sorting
MCT	Medium chain triglycerides
MELAS	Mitochondrial encephalopathy with lactic acidosis and stroke like episodes
MERRF	Myoclonic epilepsy with ragged red fibers
MES	2-(N-morpholino)ethanesulfonic acid
MIC	Minimal inhibitory concentration
MPP^+	1-methyl-4-phenylpyridinium
MTBSTFA	N-tert-butyldimethylsilyl-N-methyl-trifluoroacetamide
MTC	Maximal tolerable concentration
nACSF	Normal artificial cerebrospinal fluid
NAD	Nicotinamide adenine dinucleotide
NADPH	Nicotinamide adenine dinucleotide phosphate
NBQX	2,3-dioxo-6-nitro-1,2,3,4-tetrahydrobenzo[f]quinoxaline-7-sulfonamide
NeuN	Neuronal nuclei
NMDA-R	N-methyl-D-aspartate receptor
O.D	Outer diameter
OCR	Oxygen consumption rate
PBS	Phosphate buffered saline

PCP	Phencyclidine
PFA	Paraformaldehyde acid
Pfkfb3	6-phosphofructo-2-kinase/fructose-2, 6-bisphosphatase-3
PGC1-α	Peroxisome proliferator-activated receptor gamma coactivator-1 alpha
PKC	Protein kinase C
PLC	Phospholipase C
PMSF	phenylmethylsulfonyl fluoride
POLG	DNA polymerase gamma
PPAR	Peroxisome proliferator-activated receptor
PPP	Pentose phosphate pathway
PSA-NCAM	Polysialylated-neural cell adhesion molecule
PTZ	Pentylenetetrazol
PV	Parvalbumin
sACSF	Sucrose artificial cerebrospinal fluid
SV2A	Synaptic vesicle glycoprotein 2A
TBS	Tris-buffered saline
TCA	Tricarboxylic acid
U-^{13}C	Universally labelled ^{13}C
VIP	Vasoactive intestinal peptide

Chapter 1 General introduction

1.1 Mitochondria

Mitochondrion (plural-mitochondria) is one of the most primitive eukaryotic cell organelle, thought to originate from endosymbiotic relationship with the ancestral *archaebacteria* (Ettema, 2016). As one of the first cellular organelle to evolve, it clearly holds a vital role for eukaryotic cell evolution. Indeed, mitochondria are now understood to supply the majority of the eukaryotic cell's energy requirement by generating ATP via oxidative phosphorylation (Hatefi, 1985).

With advances in imaging technique, the structure of mitochondria is now very well described (Frey and Mannella, 2000). They are spherical in nature with two layers, the inner and outer mitochondrial membrane, separated by the intermembrane space. The inner membrane lines the matrix, which is highly folded with the cristae protruding in between (see Figure 1-1).

Along with its main function as a cellular powerhouse, mitochondria are also involved in many other important cellular processes, including maintenance of calcium homeostasis (Gunter and Pfeiffer, 1990), generation of endogenous reactive oxygen species (Zorov *et al.*, 2006), and regulation of apoptosis (Green and Reed, 1998).

Mitochondria are also highly dynamic, meaning that they continuously undergo morphological change and cellular transport (Detmer and Chan, 2007). The two main processes that regulate mitochondrial morphology are fusion and fission (van der Bliek *et al.*, 2013). If the balance between the two processes is even slightly perturbed, dramatic changes in the mitochondrial morphology can take place. In addition to the tight control of mitochondrial fusion and fission, mitochondria are transported along the cytoskeletal axis, either in an anterograde or retrograde direction, dependant on the cellular demands (Saxton and Hollenbeck, 2012).

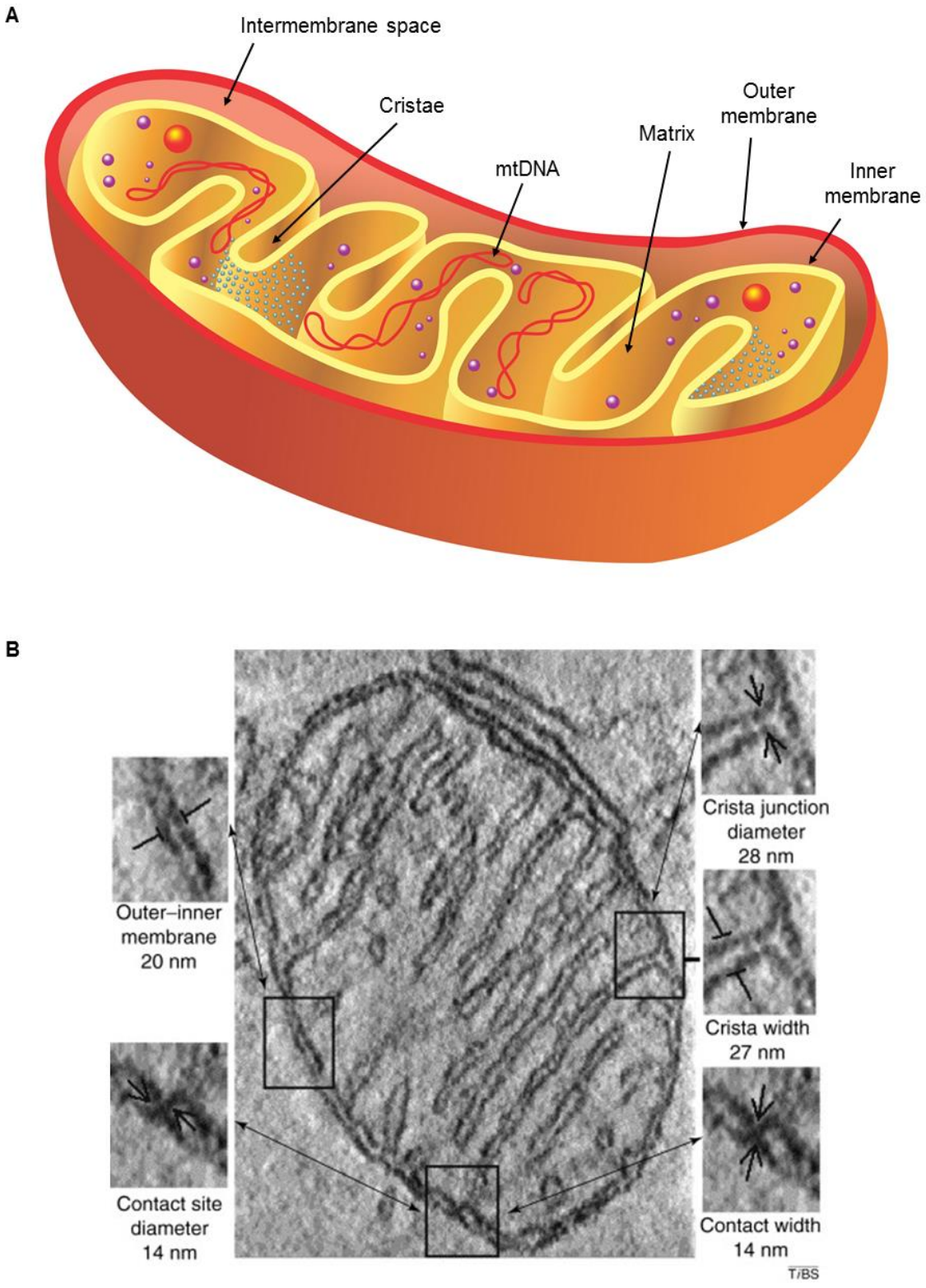

Figure 1-1 Mitochondria anatomy. Shown on (A) is a schematic representation of the mitochondrion with its corresponding structures and on (B) is an electron microscopy (EM) acquired image of a mitochondrion and its corresponding structures labelled. Image in (B) is reprinted from Trends in Biochemical Sciences, Volume 25, Issue 7, Frey TG and Mannella CA, The internal structure of mitochondria, Pages 319-324, Copyright (2000), with permission from Elsevier.

1.2 Mitochondrial ATP production

The mitochondria produces the majority of a cell's energy demand by generating ATP through a series of oxidation – reduction reactions, which are collectively called oxidative phosphorylation (Berg *et al.*, 2012g). The process of oxidative phosphorylation depends on a series of electron transfer through four mitochondrial respiratory complexes (see Figure 1-2), namely the NADH-Q oxidoreductase (complex I), succinate-Q reductase (complex II), Q-cytochrome c oxidoreductase (complex III), and cytochrome c oxidase (complex IV). The driving forces of the oxidative phosphorylation process are the substrates NADH and $FADH_2$, produced by the Krebs cycle (discussed further below in section 1.8.3). NADH enters the oxidative phosphorylation via complex I where it is oxidized and releases electrons, which are bound to the electron acceptors. This flow of electrons leads to the concomitant pumping of protons out of the mitochondrial matrix. $FADH_2$ enters the oxidative phosphorylation via complex II and similarly to NADH, it transfers its electron onto the acceptor molecules but without pumping protons (unlike complex I). This unique distinction between complex I and complex II in its capability to pump protons causes $FADH_2$ to generate less net total energy than NADH (Berg *et al.*, 2012g). Both of these acceptor molecules then move through complex III and complex IV, creating a chain of electron transfer while also pumping protons out of the mitochondrial matrix. At complex IV, the final acceptor molecule, which is oxygen, is reduced to form dihydrogen oxide (H_2O). This requirement of oxygen for the electron transfer chain reaction is what causes this process of mitochondrial ATP production to be described as an 'aerobic' process, specifically an aerobic respiration process (Berg *et al.*, 2012g).

A specific molecular assembly located in the inner mitochondrial membrane carries out the actual process of ATP synthesis, called the mitochondrial ATPase or ATP synthase or F_1F_0ATPase (complex V). Complex V utilizes the proton gradient created by the electron transfer chain and it is this proton-motive force that drives the catalytic unit to produce the energy providing molecule, adenosine triphosphate (ATP) (Elston *et al.*, 1998). Therefore, the process of electron transfer chain and ATP synthesis are two biochemically separate systems, which are coupled through the proton-motive force (Berg *et al.*, 2012g). This coupling is an important concept, as various molecules exist as a mitochondrial uncoupler, which could drive the electron transfer process without subsequently generating ATP (Terada, 1990).

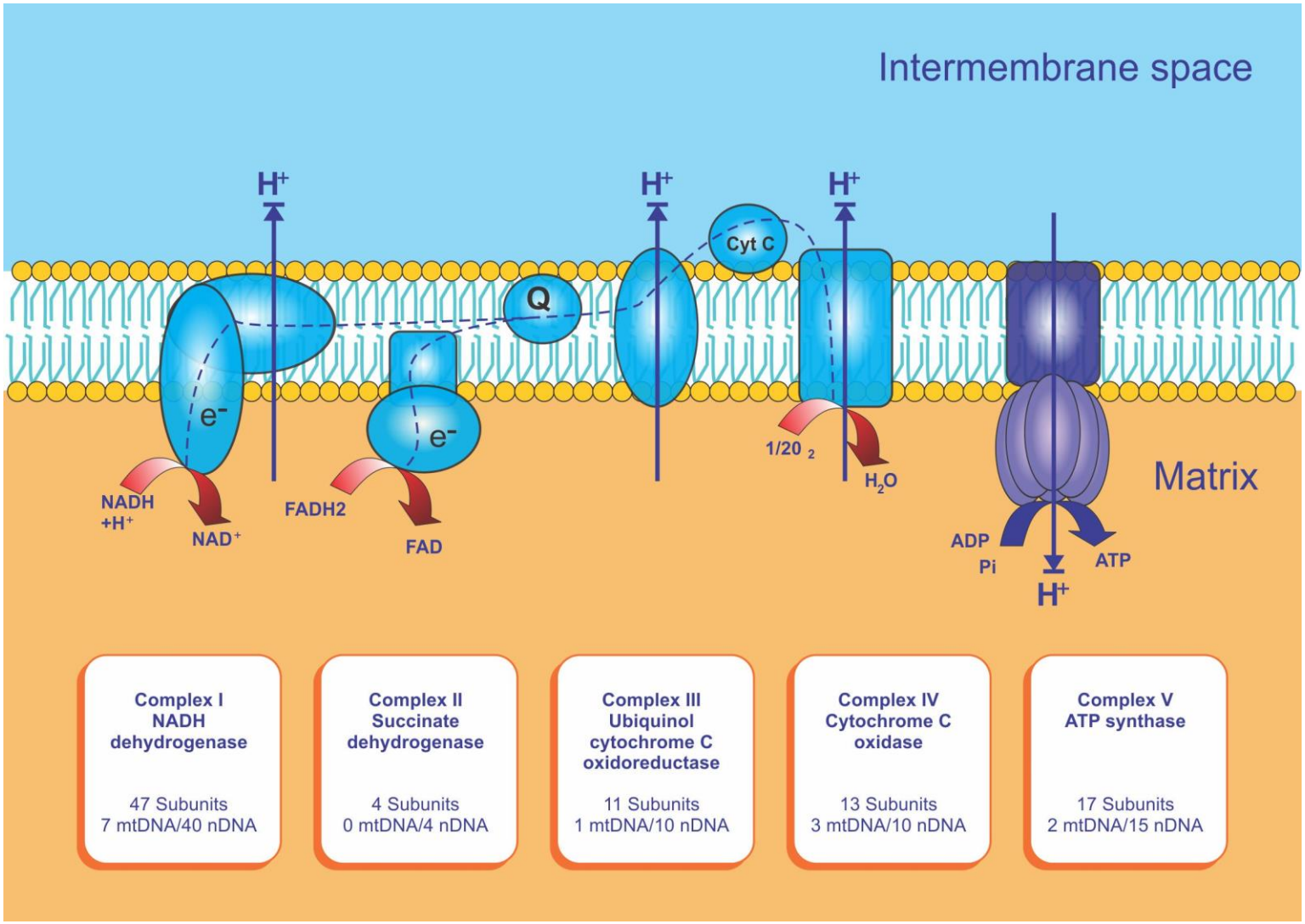

Figure 1-2 Mitochondrial ATP production through oxidative phosphorylation. Shown in the image are the electron transfer chain process through complex I to IV and the coupling to the ATP synthesis via complex V by the proton motive force. Shown in each complex as well is the subunit composition and the proportion of DNA encoding the subunits (mitochondrial or nuclear).

1.3 Mitochondrial supercomplexes

In recent studies, the mitochondrial respiratory complexes are found to interact and aggregate to form the supramolecular complexes, called the supercomplexes (see Figure 1-3). In mammalian mitochondria, for instance, a high proportion of the mitochondrial complex I is weaved with the mitochondrial complex III and together with a tetramer of complex IV constitute the 'respirasomes' (Schägger and Pfeiffer, 2000). These supercomplexes can form between any of the complexes (except for complex II), are known to be stable, and can be isolated from various organisms (Dudkina *et al.*, 2005). This assembly proves to be advantageous as it provides a dynamic and optimal electron flux, therefore increasing the efficiency of substrate utilization in aerobic respiration (Lapuente-Brun *et al.*, 2013). This may prove to be important in discussing mitochondrial energetics, as dysfunction of this assembly has been proven to cause the failure of respiratory chain and lead to the development of various syndromes in humans, such as in Barth syndrome (McKenzie *et al.*, 2006). Furthermore, each cell may have its own specific distribution of free-floating respiratory chain complex and supercomplexes. Neurons, for example, have been shown to have a higher proportion of complex I – III supercomplexes to the free-floating complex I, which is suggestive of a higher respiratory efficiency in neurons as compared to other cell types (Lopez-Fabuel *et al.*, 2016).

The use of molecular oxygen as the final electron acceptor in the electron transfer chain naturally leads to the possibility of a partial reduction, causing the generation of the superoxide ion (O_2^-) instead (Berg *et al.*, 2012g). These superoxide ions and their sister molecule, the peroxide ion (O_2^{2-}), are both reactive oxygen species and can damage the cells, causing oxidative stress (discussed further below in section 1.17). One potentially important role of the assembly of supercomplexes comes from the finding that the destabilization of supercomplexes lead to the increased generation of reactive oxygen species (Maranzana *et al.*, 2013). This suggests that the supercomplexes exist not only to increase the efficiency of mitochondrial respiration but also to limit the generation of reactive oxygen species. This limitation in the generation of reactive oxygen species may seem to appear beneficial, but in the case of neurons, they were found to be more vulnerable to the oxidative stress damage instead as their mitochondrial biology does not equip them with the necessary cellular machinery to combat reactive oxygen species production (Lopez-Fabuel *et al.*, 2016).

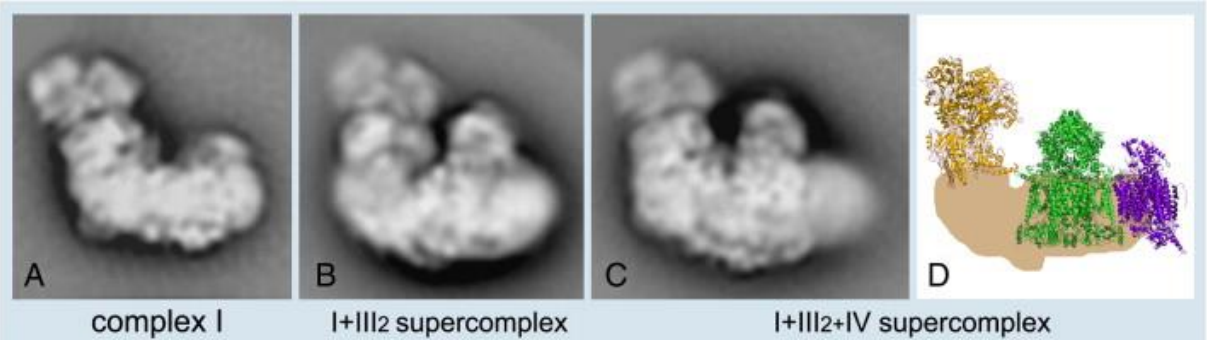

Figure 1-3 Electron microscopic view of mitochondrial supercomplexes. Electron microscopic images are obtained through negative staining and shows the averaged side views of bovine mitochondrial complex I (A) and its supercomplexes (B-C). Positions of individual mitochondrial complexes within the complex I+III$_2$+IV supercomplex or the more commonly referred to as 'respirasome' is illustrated in the schematic drawing in (D). Reprinted with modifications from Biochimica et Biophysica Acta, Volume 1797, Issues 6-7, Dudkina et al, Structure and function of mitochondrial supercomplexes, Pages 664-670, Copyright (2010), with permission from Elsevier. Also Springer special credit – 'Reprinted from Journal of Bioenergetics and Biomembranes, Volume 40, Issue 5, Dudkina et al, The higher level of organization of the oxidative phosphorylation system : mitochondrial supercomplexes, Pages 419 – 424, Copyright (2008), with permission from Springer'.

1.4 Mitochondrial DNA

Mitochondria is unique to the other cellular organelles, in that it has its own unique genome, in the form of the circular mitochondrial DNA (mtDNA). This DNA is conserved across species and is very important in facilitating the process of evolution due to its high rate of mutation (Brown *et al.*, 1979). Mitochondrial DNA is also different from nuclear DNA, in that it is exclusively maternally inherited (Giles *et al.*, 1980).

In humans, mitochondrial DNA is a compact double-stranded circular DNA, composed of 16,569 base pairs (Tuppen *et al.*, 2010). The two strands are composed of the cytosine-rich light (L) strand and the guanine-rich heavy (H) strand (see Figure 1-4). The complete sequence of the human mitochondrial DNA is well characterized and described (Andrews *et al.*, 1999). The human mtDNA contains a total of only 37 genes, all of which encode 13 polypeptides, all of which are core constituents of the mitochondrial respiratory chain complexes I, III, IV, and V, as well as the RNA necessary for the translation of the mitochondrial DNA (Tuppen *et al.*, 2010). The remaining components of the mitochondrial respiratory complexes are encoded by the nuclear DNA (Scarpulla, 1997). There are no introns or intergenic noncoding nucleotides in the mitochondrial DNA genome, except for the 1.1 kb displacement loop

(D-loop), which contains the transcriptional promoters and the proposed origins of replication (O_H) (Tuppen *et al.*, 2010).

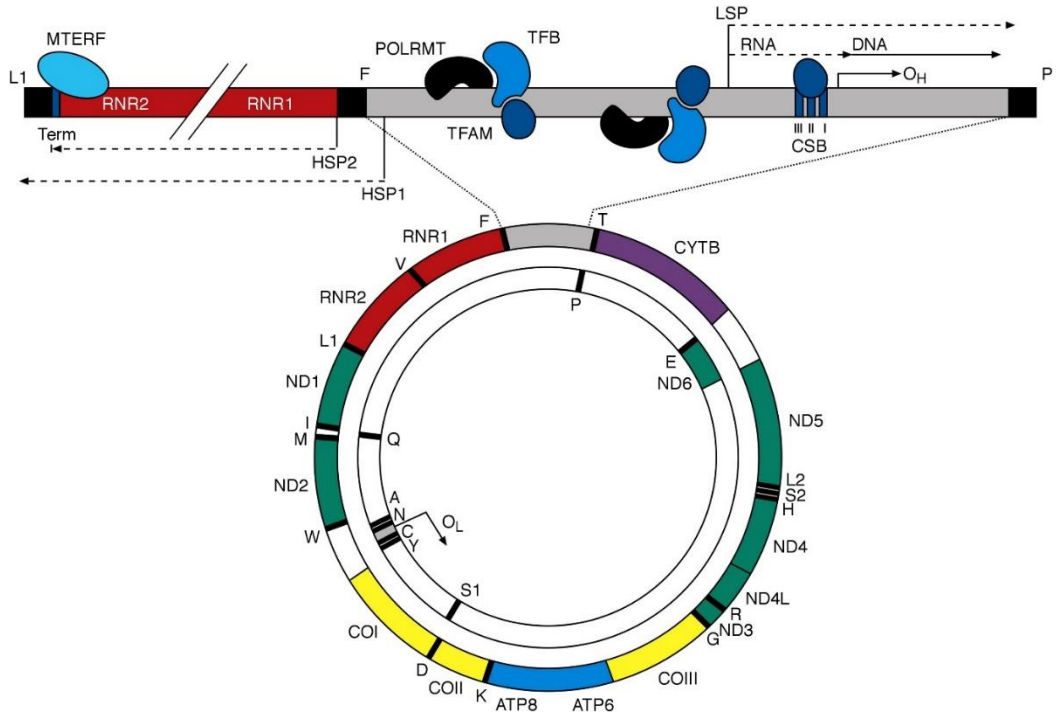

Figure 1-4 Human mitochondrial DNA. Shown is the schematic diagram of the human mitochondrial genome, with an enhanced view of the exceptional D-loop and transcription termination region. The two circles represents the double strand, with the outer circle being the heavy (H) strand and the inner circle being the light (L) strand. The human mitochondrial DNA encodes 2 mitochondrial-rRNAs (red), 22 mitochondrial-tRNAs (black bars), and 13 essential respiratory chain polypetides, including constituents of complex I (green), complex III (purple), complex IV (yellow), and complex V (blue). Reprinted from Biochimica et Biophysica Acta, Volume 1797, Issue 2, Tuppen et al, Mitochondrial DNA mutations and human disease, Pages 113 – 128, Copyright (2010), with permission from Elsevier.

In a normal cell, several hundreds or thousands of copies of the mitochondrial DNA are present at any one time. This unique property of mitochondrial DNA genetics allows for the presence of two or more variants of the mitochondrial genomes in a cell, a term also known as heteroplasmy, as opposed to homoplasmy when all the copies of a DNA within the cell are identical (Wallace and Chalkia, 2013). The finding that spontaneous *de novo* mutations in the mitochondrial DNA are suppressed in the female germ lines suggest the presence of a genetic bottleneck that is partly responsible for the presence of heteroplasmy (Stewart and Chinnery, 2015). Additionally, the phenotypic manifestation of these mutations depends on the presence of a specific proportion of the mutant mtDNA copies within a cell, a value that corresponds to the mitochondrial threshold effect (Rossignol *et al.*, 2003).

1.5 Mitochondria, metabolism, and the brain: the blood-brain barrier

The brain is a highly metabolically active organ. A human brain weighs only about 2 % of the total body weight and yet it consumes 20 % of the total oxygen consumption (Quastel and Wheatley, 1932). Therefore, it is clear that the brain is heavily reliant on aerobic metabolism through oxidative phosphorylation in the mitochondria. Unsurprisingly, any dysfunction of the mitochondria in the brain could affect its function at both a cellular and global network level (Picard and McEwen, 2014).

Any appreciation of metabolic rate *in vivo*, however, needs to consider various factors in addition to mitochondrial function and oxygen consumption. To sustain its function, the brain requires a continuous supply of oxygen and energy-yielding substrates. This high metabolic demand is tightly regulated by the functions of the blood-brain barrier (Paulson, 2002). The extremely high global cerebral oxygen consumption rate (~130μmol per 100 g per minute) is met by an equally very high rate of cerebral blood flow (~45 ml per 100 g per minute) (Jain *et al.*, 2010). The blood-brain barrier is composed of the highly impermeable tight junctions of the endothelial cells covered by the astrocytic end feet (see Figure 1-5) (Janzer and Raff, 1987). In addition to its tight regulation of cerebral blood flow, the blood-brain barrier has a unique distribution of transporters allowing for selective permeability to various substrates (McKenna *et al.*, 2006). Therefore, the discussion on pharmacological studies should pay attention to the complexity of the blood – brain barrier as not all compounds developed by the pharmaceutical industry will readily cross the blood – brain barrier (Witt *et al.*, 2001; Boonstra *et al.*, 2015).

Adding to the complexity of the brain's metabolism; it is established that the metabolism in the brain is compartmentalized. Metabolic compartmentalisation is defined as the presence of more than one distinct pool of a given metabolite in a tissue (McKenna *et al.*, 2006). The two major cells whereby the metabolism is highly compartmentalized are neurons, and glia (which includes astrocytes, oligodendrocytes, and microglia). Although all of these cell types have mitochondria, there exists a cell-specific mitochondrial expression and function that contributes to the metabolic compartmentation. Therefore, when considering brain metabolism, it is imperative that in addition to discussing them at an *in vivo* level, that it is also discussed at a cellular level to account for this metabolic compartmentalisation.

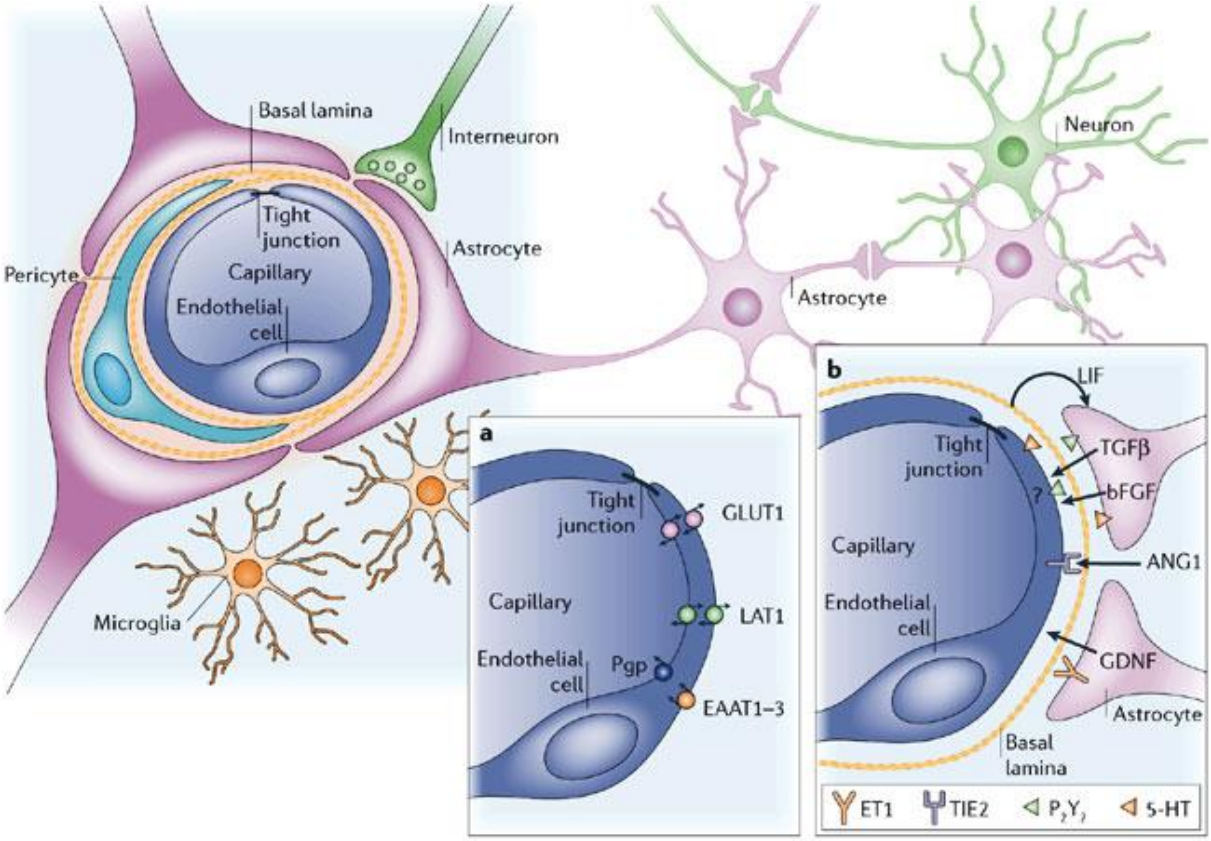

Figure 1-5 Cellular components of the blood-brain barrier. The blood-brain barrier is composed of capillary endothelial cells, wrapped by the astrocytic perivascular endfeet. The figure also shows other cellular components of the brain; neurons, pericytes, and microglia. Shown in (A) are the features of brain endothelial cells as observed in cell culture, complete with the transporters expression. Shown in (B) are the astroglial – endothelial interaction in the maintenance of the blood-brain barrier. Reprinted by permission from Macmillan Publishers Ltd: Nature Reviews Neuroscience (Abbott et al., 2006), copyright 2006.

1.6 Neurons

Neurons are the smallest functional unit of the nervous system. They are a specialised form of cells whose primary function is to communicate various bodily input and output via electrochemical network. Despite great variation in the size and morphological appearance, all neurons share the same basic structure (Young *et al.*, 2000) as shown below in Figure 1-6. All neurons have a large soma (or cell body) which contains the nucleus as well as the cells' organelles such as the ever-important mitochondria. Unique to the neurons are the two processes that extend from the cell body; namely a single axon and either one or multiple dendrites. These processes form the basis of the network communication between neurons via the formation of the

synapses. The pre-synaptic axon terminal and the post – synaptic dendrites; along with the astrocytic processes; make up what is called the 'tripartite synapse' (Perea *et al.*, 2009).

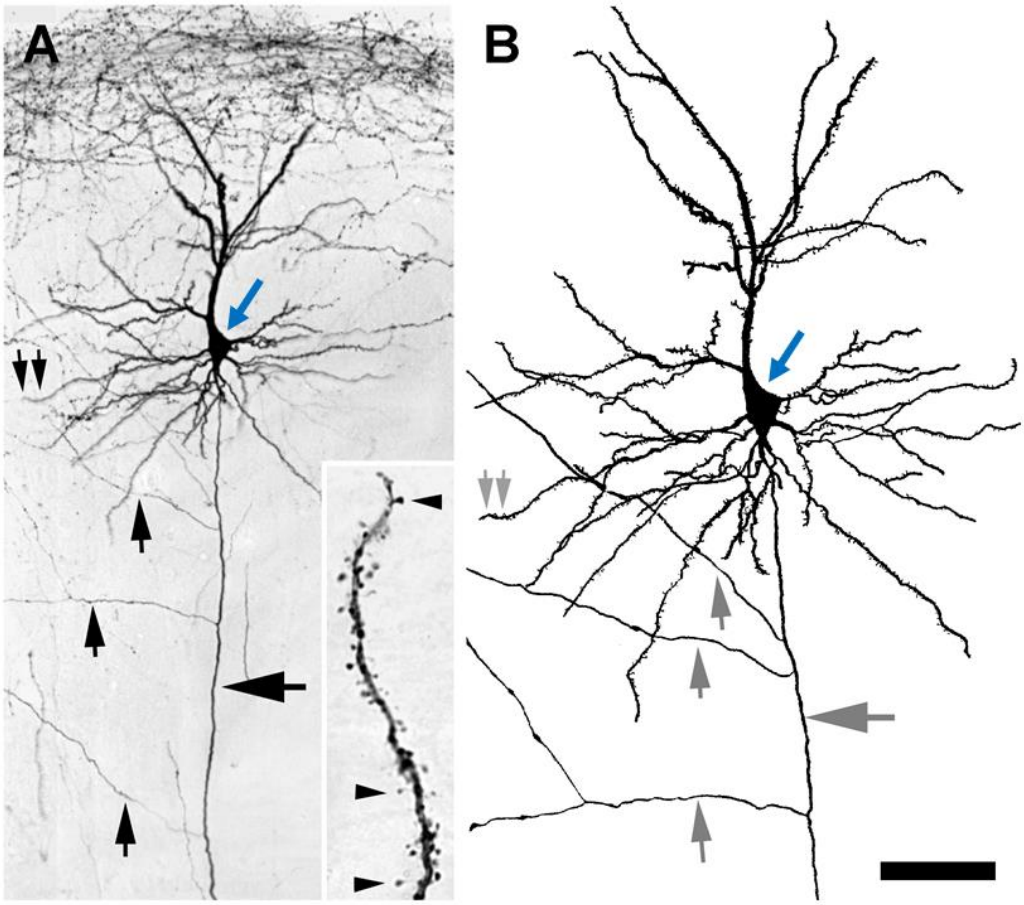

Figure 1-6 Basic structure of a neuron. Shown in (A) is an example of a pyramidal neuron in adult rat brains as labelled using the biotinylated dextran amine (BDA) labelling techniques and in (B) are the corresponding illustrative drawing of the same neuron. The horizontal arrow indicates the axon of the neurons that project deep into the white matter but also sends branches horizontally, as indicated by the vertical arrows. The double arrows indicate an example of a dendrite, with spiny appendages (arrowheads) distributed along the labelled dendrite; as shown in the inset. The blue arrow indicates the soma of the neuron; which in this case is pyramidal – shaped. The camera lucida drawing of the labelled neurons shown in A further clarified all these labelled structures. Scale bar in A indicates 75µm, in B indicates 50µM, and in the inset in A 10µm. Reprinted with modifications from PLOS One, Volume 7, Edition 11, Ling et al, Resolving the Detailed Structure of Cortical and Thalamic Neurons in the Adult Rat Brain with Refined Biotinylated Dextran Amine Labelling, Copyright (2012) as an open – access article distributed under the terms of the Creative Commons Attribution License.

Neurons are intrinsically electrically active cells. The communication of information between neurons is an electrochemical signal transmission; through the coupling of the neurotransmitter release and the electrical changes in the membrane potential. Signal communication is continued through the postsynaptic neurons by the generation of action potentials (for mechanisms of generation, see Figure 1-7). Based on their choice of neurotransmitters and the response they induce, the neurons are largely classified as either excitatory or inhibitory neurons (Hof *et al.*, 2014; Bear *et al.*, 2016b). The excitatory neurons release excitatory neurotransmitters (mostly glutamate, but also acetylcholine, norepinephrine, and other excitatory peptides) to induce depolarization in the synaptically connected post-synaptic neurons; therefore 'exciting' the neurons to increase action potential generation. Conversely, the inhibitory neurons release inhibitory neurotransmitters (mostly GABA, but also glycine) to induce hyperpolarization in synaptically connected post-synaptic neurons; therefore 'inhibiting' the neurons from generating action potential essentially silencing the postsynaptic communication.

1.6.1 Excitatory neurotransmission

As described above, excitatory neurons release excitatory neurotransmitters to induce depolarization in post – synaptic neurons. Of all the subtypes of the excitatory neurons, the most abundant are the pyramidal neurons (morphology as shown in Figure 1-6), which collectively make up approximately two-thirds of all the neurons in the mammalian cerebral cortex (Bekkers, 2011). The pyramidal neurons are named for their distinct morphological appearance: a pyramidal soma and a cluster of apical and basal dendrites (Spruston, 2008; Bekkers, 2011). These pyramidal neurons are primarily glutamatergic in nature; which means they release glutamate as their major excitatory neurotransmitter (Frotscher *et al.*, 1986; Bekkers, 2011; Ling *et al.*, 2012). Therefore, their neurotransmission is also dependent on the glutamate-gated channels (or glutamatergic receptors). The glutamate receptors are further subdivided into the fast excitatory ionotropic glutamate receptors and the slow excitatory metabotropic glutamate receptors (for further classification of the subtypes, see Table 1-1) (Bear *et al.*, 2016b; Forman *et al.*, 2017).

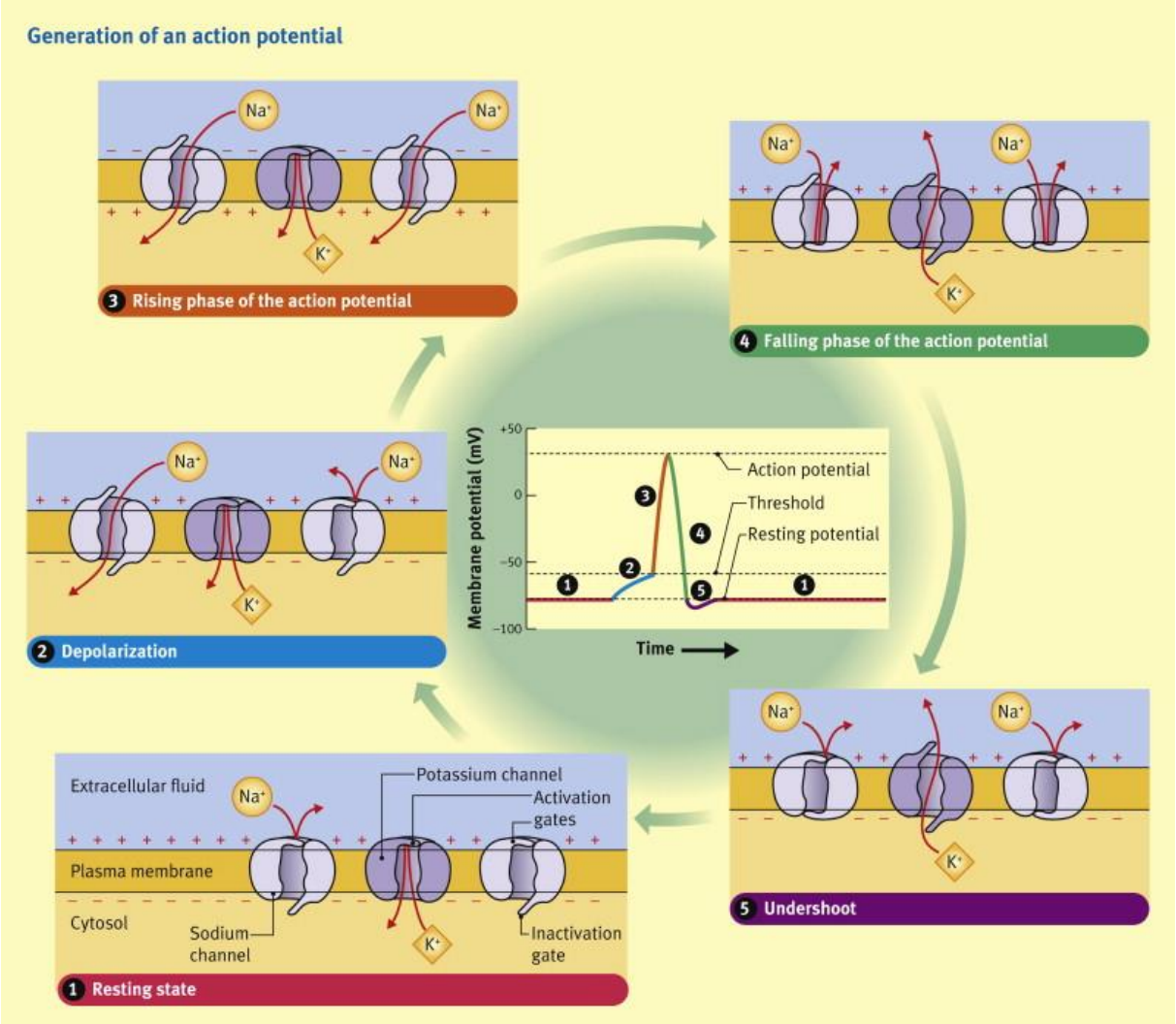

Figure 1-7 Generation of action potential. In short, neurons typically have a resting membrane potential of approximately - 60mV. At resting state (1), both the sodium and potassium channel are closed. Following excitatory signal through glutamate binding, the glutamate – gated channel opens and allows influx of the Na^+ ions into the cells, causing the membrane potential to be more positive or depolarized (2). Once it reaches the threshold value, the membrane potential reaches an all – or – none stage and recruits the voltage – gated sodium channel that rapidly depolarizes the potential until it reaches the peak value (3). The action potential is then fired and propagated. The inactivation gate of the voltage – gated sodium channel then closes to rapidly stops the sodium ion influx while the potassium channel activation gate opens to allow efflux of K^+ ions out of the cells, causing the membrane potential to be more negative or hyperpolarized (4). The membrane potential continues to be hyperpolarized to a value more negative than the resting membrane potential (the undershoot value). It takes a short delay to return the neurone's membrane potential to the resting state; which reflects the refractory period (5). This return to the resting state is facilitated through the closing of the activation gate of the voltage – gated sodium channel. Reprinted from Anaesthesia & Intensive Care Medicine, Volume 12, Issue 6, Fletcher A, Action potential : generation and propagation, Pages 258-262, Copyright (2011), with permission from Elsevier.

Table 1-1 Classification of glutamate receptor subtypes. Table adapted from (Forman et al., 2017)

Ionotropic glutamate receptor			
Subtype	**Subunits**	**Agonists**	**Actions**
AMPA	GluR1 GluR2 GluR3 GluR4	Glutamate or AMPA.	Increase Na^+ and Ca^{2+} influx (except for receptor with GluR2). Increase K^+ efflux.
Kainate	GluR5 GluR6 GluR7 KA1 KA2	Glutamate or kainate.	Increase Na^+ influx. Increase K^+ efflux.
NMDA	NR1 NR2A NR2B NR2C NR2D NR3A NR3B	Glutamate or NMDA and glycine Membrane depolarization	Increase Na^+ and Ca^{2+} influx. Increase K^+ efflux.
Metabotropic glutamate receptor			
I	mGluR1 mGluR5	Glutamate	Activates adenylyl cyclase to increase cAMP (mGluR1 only). Increases PLC activity to increase Ca^{2+} levels and stimulate PKC. Inhibits K^+ channels.
II	mGluR2 mGluR3	Glutamate	Inhibits adenylyl cyclase to decrease cAMP. Inhibits voltage – sensitive Ca^{2+} channels. Activate K^+ channels.
III	mGluR4 mGluR6 mGluR7 mGluR8	Glutamate	Inhibits adenylyl cyclase to decrease cAMP. Inhibits voltage – sensitive Ca^{2+} channels.

Of all the glutamate receptors, the ones that are relevant and discussed in this study are the AMPA (α-amino-3-hydroxy-5-methyl-4-isoxazole propionic acid) and the NMDA (N-methyl-D-aspartate) receptors (for schematic representation of these receptors, see Figure 1-8). Therefore, these receptors are discussed further below.

The ionotropic receptors are membrane – bound protein complexes, which form an ion – permeable pore in the cell membrane (Waxham, 2014). The ionotropic receptors mediate fast synaptic responses, while the metabotropic receptors mediate slow synaptic responses (Forman *et al.*, 2017). This is due to their difference in response to neurotransmitter binding. When a neurotransmitter binds to an ionotropic receptor, this binding directly results in the opening of the ion channels through an array of conformational changes. On the other hand, neurotransmitter binding to a metabotropic receptor mediates conformational changes as a G-protein coupled receptor via the cAMP-dependent protein kinase (Waxham, 2014).

The AMPA receptors mediate the majority of the fast excitatory neurotransmission and are expressed in an activity – dependent manner (Rogawski, 2013). Four subunits have been identified and it is believed that the AMPA receptor assembles as a tetrameric molecule (Kew and Kemp, 2005). Functional AMPA receptors have been identified not only in the hippocampal neurons, but also in the astrocytes (Martin *et al.*, 1993; Hall and Soderling, 1997; Fan *et al.*, 1999). Interestingly, the absence of the edited GluR2 subunit causes high calcium permeability (Vandenberghe *et al.*, 2000; Isaac *et al.*, 2007) and in the hippocampus, this is selectively expressed in the inhibitory interneurons (Kew and Kemp, 2005). This distinct AMPA-R expression has been shown to contribute towards the process of long – term potentiation (Wright and Vissel, 2012; Jia *et al.*); but may also be relevant in other neurological disorders such as the motor neuron disease (Wright and Vissel, 2012). The AMPA-R has a single binding site for its agonists (both glutamate and AMPA) but also has allosteric modulator site for barbiturate and alcohol (Forman *et al.*, 2017). The barbiturate allosteric binding is implicated in its antiepileptic and anaesthetic effect (Joo *et al.*, 1999; Nardou *et al.*, 2011); whereas the alcohol binding to AMPA-R is implicated in alcohol – craving behaviour and addiction (Cowen *et al.*, 2003; Möykkynen and Korpi, 2012; Cannady *et al.*, 2013).

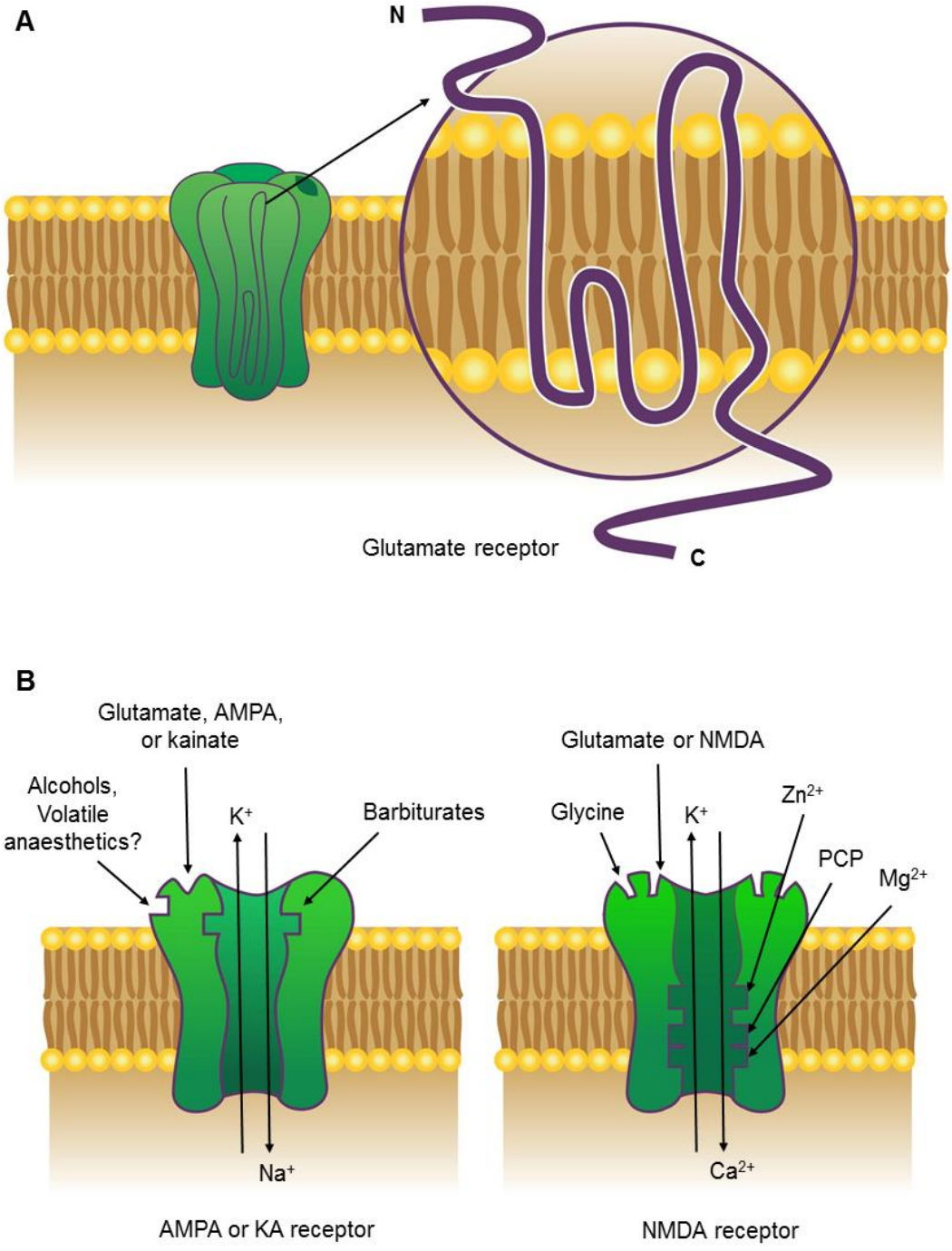

Figure 1-8 Schematic representation of the AMPA and NMDA receptors as well as the binding sites. The ionotropic glutamate receptors have a general structure shown in (A). They are tetrameric complexes composed of either homomeric subunits or different heteromeric subunits. The zoomed – in structure on the right shows one such subunit, which spans the membrane three times and has a partially spanning hairpin turn. The bolded dark green spot on the glutamate receptor marks the glutamate binding site to one of the subunit of the receptor. In (B) shown are major binding sites of the AMPA and NMDA receptors. The localization of these binding sites are schematically indicated in this diagram with precise location yet to be determined. Figure recreated and based from (Forman et al., 2017).

The NMDA receptors are constitutively expressed specifically in the neurons, unlike the AMPA receptors (Moriyoshi *et al.*, 1991). The NMDA receptors are oligomeric transmembrane complexes composed of the NR1 in combination with one or more of the NR2 subunits or both the NR2 and NR3 subunits (Kew and Kemp, 2005). There are several unique properties of the NMDA receptors that distinguishes it from the other glutamatergic receptors. The activation of the NMDA receptors require the binding of two distinct agonists; glutamate (or NMDA) and glycine (Cummings and Popescu, 2015). In a resting condition, the channel pore of the NMDA receptor is blocked by the magnesium ion (Mg^{2+}) (Nikolaev *et al.*, 2012). A sufficient trains of postsynaptic action potentials or subsequent activation of AMPA or kainate (KA) receptors in close proximity to the receptor is therefore additionally required to create membrane depolarization that would unblock the receptor gating system (Arvanian and Mendell, 2001; Fleming and England, 2010) Therefore, the gating of NMDA receptor depends on more intense levels of presynaptic activity than that of AMPA or KA receptors (Forman *et al.*, 2017). In addition to the agonist binding sites and the magnesium binding site, the NMDA receptor also has a binding site for the organic cation zinc (Zn^{2+}) as well as an allosteric binding site for its inhibitor, phencyclidine. Similar to magnesium, zinc is also a potent inhibitor of the gating of the NMDA receptor (Amico-Ruvio *et al.*, 2011; Sowa-Kućma *et al.*, 2013). Meanwhile, phencyclidine (PCP) is an established non – competitive antagonist of the NMDA receptor and is frequently used to recapitulate the psychotic features of schizophrenia as an animal model of this psychiatric condition (Balla *et al.*, 2001; Lee *et al.*, 2006; Domino and Luby, 2012).

1.6.2 Inhibitory neurotransmission

Inhibitory neurons (or more commonly known as the inhibitory interneurons) releases the inhibitory neurotransmitter, mostly GABA (but also glycine), to induce hyperpolarization of the postsynaptic neurons. The use of the term interneuron dates back to the studies of Santiago Ramon y Cajal who found the distinction between the cells with a long axon (the projection neurons) and the cells with a short axon (the intrinsic neurons, eventually known as the interneurons) (Hof *et al.*, 2014). These interneurons were found to be mostly GABA-ergic and constitute about 15 – 30 % of the total neuronal population (Jones, 2009).

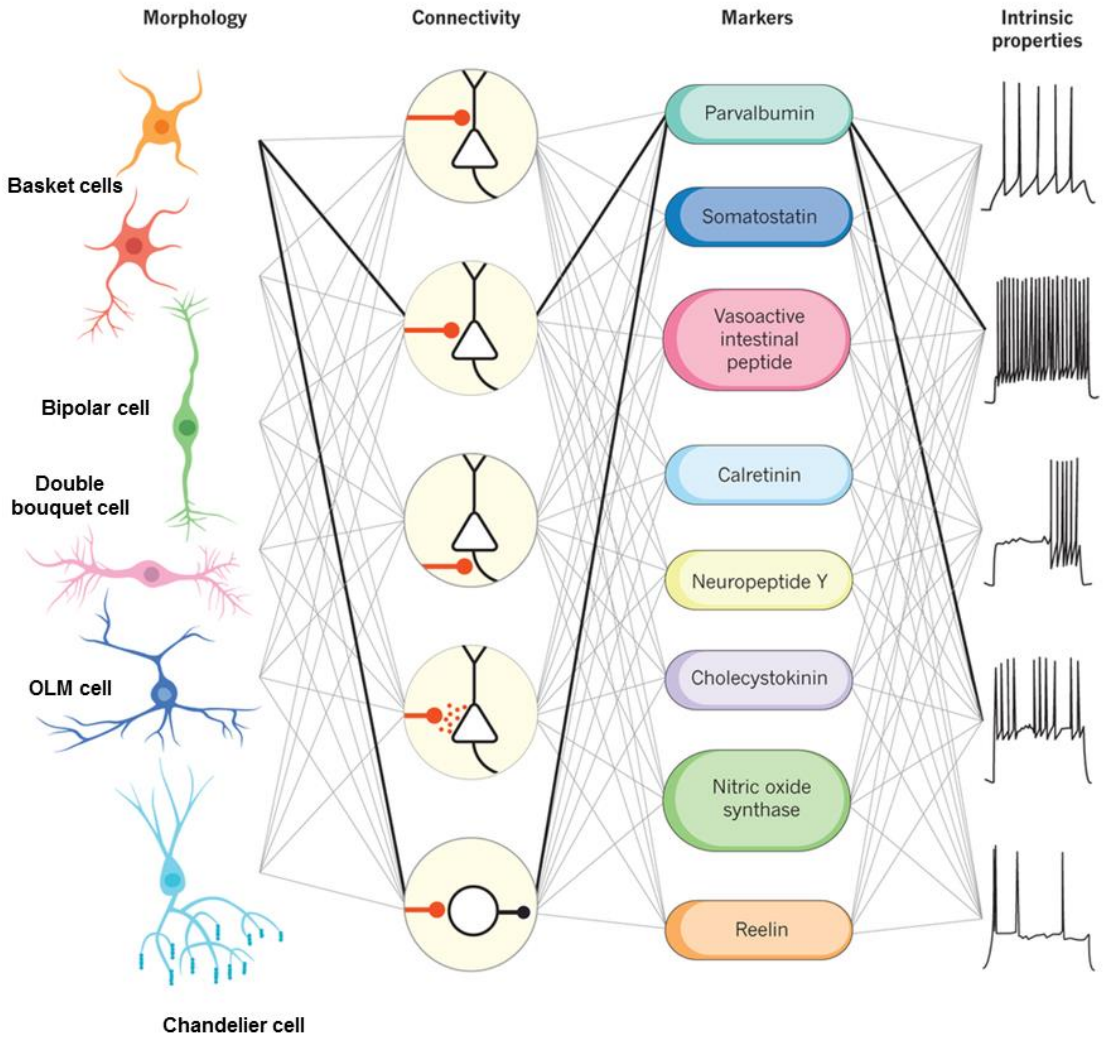

Figure 1-9 Interneuron morphology, connectivity, markers, and intrinsic properties. Shown are the variations in interneuron morphology, their respective connectivity, markers, and intrinsic properties. Highlighted are the properties of the fast – spiking cortical basket cells. Reprinted by permission and with slight modification from Macmillan Publishers Ltd: Nature (Kepecs and Fishell, 2014), copyright (2014).

Studies on inhibitory interneurons initially focused on the examination of the diverse morphological features that they have (Mendenhall and Murphey, 1974). Eventually, their connectivity and electrophysiological properties was studied (Bartos and Elgueta, 2012). However, the biggest stride in interneuron studies, perhaps, is the use of calcium binding proteins as interneuron markers (Van Brederode *et al.*, 1990; Demeulemeester *et al.*, 1991; Wild *et al.*, 2005; Zaitsev *et al.*, 2005). The finding of the selective expression of these calcium binding proteins allow for the use of immunohistochemistry to further classify these interneurons into specific subtypes. Nowadays, the classification of interneurons can be made based on any of these four

distinctive features (Maccaferri and Lacaille, 2003) (see Figure 1-9); despite the shared features that these cells may have following the distinctive classification (summarized and reviewed elegantly in (Kepecs and Fishell, 2014) and (Markram *et al.*, 2004)).

Inhibitory interneurons are of interest in the study of neuroenergetics as recent studies have demonstrated that inhibitory interneurons have much higher energetic demand than the excitatory neurons (Kann *et al.*, 2014). This has been shown *in vitro* in numerous studies in the context of gamma oscillations, a highly energetic physiological processes that depend on the temporal input of the fast – spiking inhibitory interneurons (Huchzermeyer *et al.*, 2008; Kann *et al.*, 2011; Whittaker *et al.*, 2011; Chan *et al.*, 2016; Jessen *et al.*, 2017). Furthermore, it was found that the inhibitory interneurons have higher expression of cytochrome c, a marker of mitochondrial respiration (Gulyás *et al.*, 2006) as well as a higher expression of cyclophillin-D, the modulator of the mitochondrial transition pore (Hazelton *et al.*, 2009). In post-mortem study of patients with mitochondrial disease, it was found that there was a dramatic loss of the inhibitory interneurons at the end-stage of the mitochondrial disease (Lax *et al.*, 2016). Collectively, all these studies led to the development of the 'interneuron energy hypothesis' (Kann, 2016), which postulates the importance of the inhibitory interneuron population at the core of various neurometabolic processes.

As with excitatory cells, the inhibitory interneurons utilize the major inhibitory neurotransmitters, GABA, for their neurotransmission. GABA, like glutamate, also has two major classes of receptors; the ionotropic GABA receptors ($GABA_A$ and $GABA_C$) and the metabotropic GABA receptors ($GABA_B$). The most abundant GABA receptors in the brain is the ionotropic $GABA_A$ receptor (Forman *et al.*, 2017); hence, this is further discussed below.

The $GABA_A$ receptor is generally a pentameric protein, composed of heteromeric subunits (Sigel and Steinmann, 2012). Sixteen different subunits have been cloned thus far from the $GABA_A$ receptor and most frequently, it is made up of two α subunits, two β subunits, and another subunit (usually the γ subunit) (Miller and Aricescu, 2014). The functional $GABA_A$ receptors have high heterogeneity (Nutt, 2006), meaning it is virtually impossible to determine the precise subunit composition of each $GABA_A$ receptor. In addition to its endogenous agonist (GABA), various synthetic molecules have been found and synthesized as $GABA_A$ agonists (such as muscimol). The $GABA_A$ receptor has various binding sites; most notably the distinct barbiturate and benzodiazepine binding sites; as well as the neurosteroid, picrotoxin, flumanezil,

penicillin, and furosemide binding site (Forman *et al.*, 2017). Both barbiturate and benzodiazepine are anticonvulsants that potentiate $GABA_A$ inhibitory neurotransmission but have been identified to have distinct binding sites (Eadie and Kwan, 2008; Schmidt and Wilensky, 2008; Greenfield Jr, 2013). Neurosteroids are endogenous steroids synthesized in the brain, adrenal glands, and the gonads; which exert a potent enhancement of the $GABA_A$ transmission (Lambert *et al.*, 2003; Wang, 2011). Finally, the remaining binding sites in the $GABA_A$ receptor pertains to antagonists of this receptor. Picrotoxin is perhaps the most classical of $GABA_A$ receptor antagonists. It is a potent non-competitive antagonist that works by disrupting the chloride (Cl^-) ion flow through the ion channel (Olsen, 2006). Flumanezil is a unique pharmacological tool, as on its own, it potentiates the $GABA_A$ neurotransmission; but when co-applied with benzodiazepines, it inhibits the potentiating effect of the benzodiazepines (Weiss *et al.*, 2002). Therefore, flumanezil is a potent inhibitor of the benzodiazepine binding site on the $GABA_A$ receptor. Penicillin, which is a member of the β-lactam antibiotic family, is known to be a weak $GABA_A$ receptor antagonist (Antoniadis *et al.*, 1980). It is thought to non-competitively interfere with the ion flow across the channel in a similar manner to picrotoxin; but at a different binding site (Tsuda *et al.*, 1994; Sugimoto *et al.*, 2002; Rossokhin *et al.*, 2014). Finally, furosemide is a well – characterized loop diuretic; which was found to have a unique inhibitory effect on the $GABA_A$ receptor. Its inhibitory effect seems to be region specific (restricted to the cerebellar cells), subtype specific, and acts as a sequential open channel blocker through inhibiting the dissociation of agonist while the channel is blocked (Korpi and Lüddens, 1997; Kolbaev *et al.*, 2002).

Hitherto, the basic principle underlying the excitatory and inhibitory neurotransmission has been discussed. The relevant receptors investigated within this study have also been described in detail. However, in reality, excitatory and inhibitory neurotransmission depends on various contributing factors and input. Therefore, the complexity of understanding these neurotransmissions should not be underestimated. Discussion on these contributing factors will be made as each experimental results described on these studies are examined and analysed in the context of the corresponding neurotransmission.

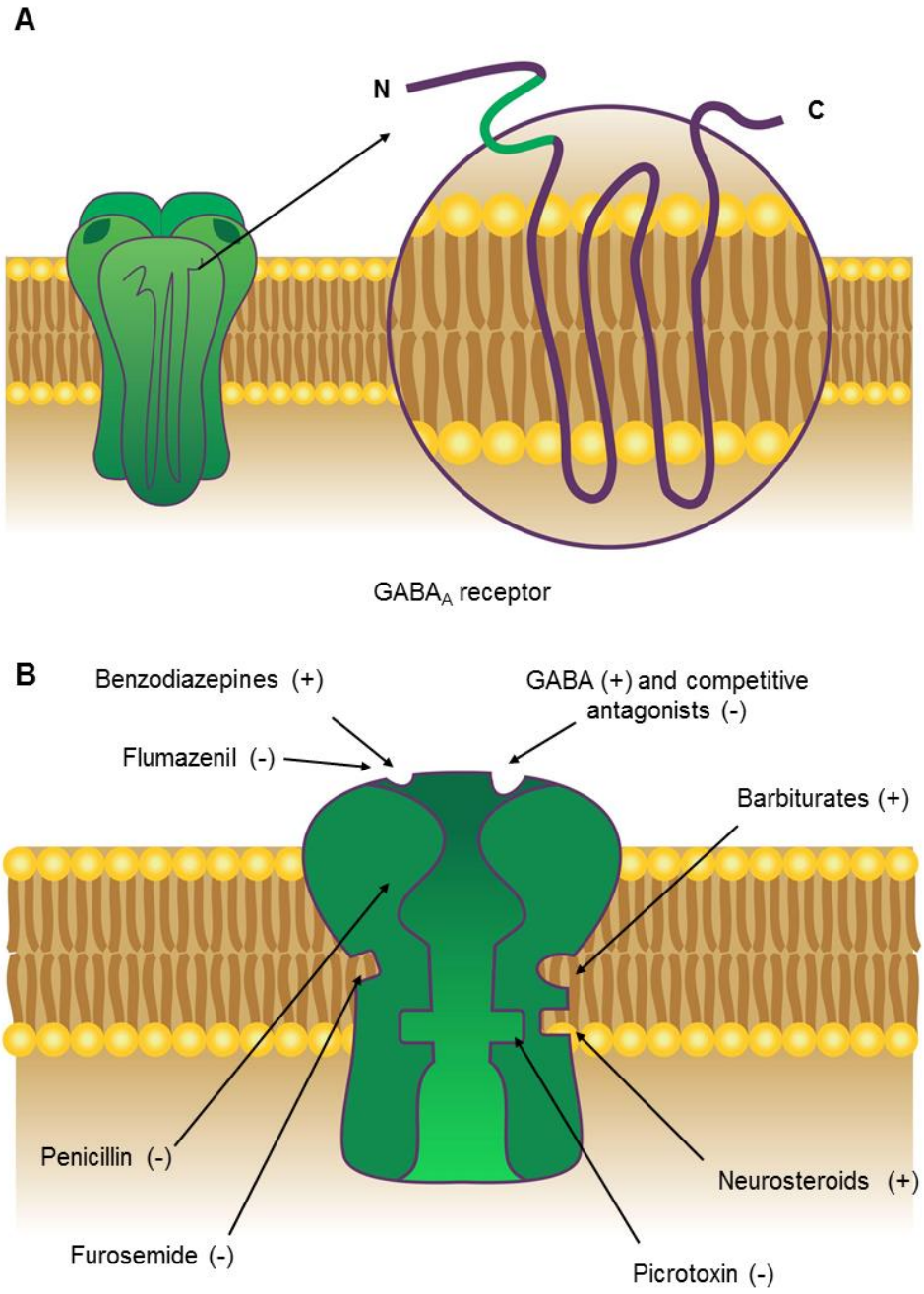

Figure 1-10 Schematic representation of the GABA$_A$ receptor and its binding sites. The ionotropic GABA$_A$ receptor is the most abundant GABA receptor in the brain and their general structure is a pentameric complexes (as shown in (A)). Activation of the receptor requires simultaneous binding of two GABA molecules to the receptors at the site indicated as the bolded dark green spot on the subunit. Each subunit of the receptor has four membrane – spanning regions with a cysteine loop in the extracellular N – terminus (shown by the light green region). In (B), the major binding sites of these receptors are schematically indicated. As with the glutamatergic receptors, the exact location of these binding sites are unknown. (+) indicates agonist or allosteric modulator of the receptor whilst (-) indicates competitive or non-competitive antagonist. Figure recreated and based from (Forman et al., 2017).

1.7 Astrocytes

The term neuroglia (or nerve glue) was first coined by Rudolph Virchow in 1859, who conceived these cells as the inactive 'connecting tissue' that holds neurons together in the central nervous system (Hof *et al.*, 2014). The work of Ramon y Cajal, with his various staining techniques, advanced this description of the neuroglia cells to three distinct supporting cell types; which are oligodendrocytes, astrocytes, and microglia (García-Marín *et al.*, 2007). Later, oligodendrocytes were found to be the myelinating cells of the central nervous system (Bradl and Lassmann, 2010); while the microglia was discovered to be the primary inflammatory cell of the central nervous system, acting as the resident macrophage of the brain (Prinz and Priller, 2014). Astrocytes, on the other hand, took centre stage as it was discovered that they closely associate with the neurons in the brain (see Figure 1-11) and are likely to participate in the process of neurotransmission (Olude *et al.*, 2015).

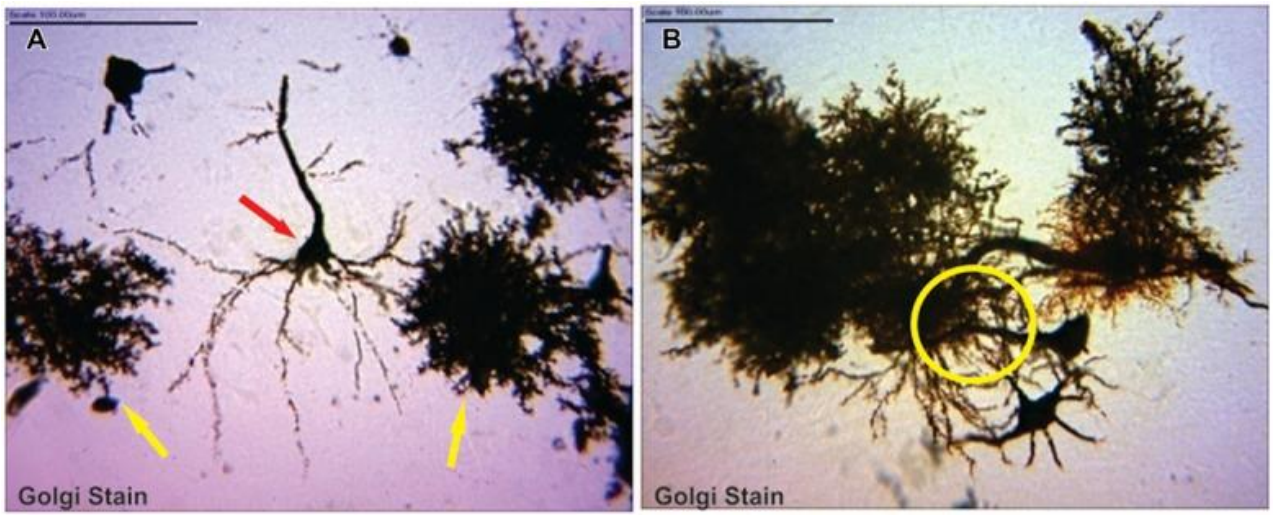

Figure 1-11 Astrocytes morphology in the context of neuronal population. Shown are images obtained from neocortical slices from African giant rat that were stained using the Golgi silver impregnation method. In (A), a typical pyramidal neuron (red arrow) is seen to make association with the astrocytes (yellow arrows). In (B), the astrocytes were found to be in synaptic association (yellow circumscribed area) with the neurons. Scale bar 100µm. Reprinted with modifications from Frontiers in Neuroanatomy, Volume 9, Edition 67, Olude et al, Astrocyte morphology, heterogeneity, and density in the developing African giant rat (Cricetomys gambianus), Copyright (2015) as an open – access article distributed under the terms of the Creative Commons Attribution License.

Astrocytes were named due to their star-shaped appearance under the microscope (García-Marín *et al.*, 2007; Hof *et al.*, 2014). They roughly constitute about

20 to 50 % of the volume of most brain areas occupied (Hof *et al.*, 2014); therefore their importance in brain pathology should not be understated. Astrocytes have various distinct morphological variation in the human brain (described and discussed extensively in Figure 1-12). Two of these astrocytic morphological types, the interlaminar and the polarized astrocytes, are specific to the human brain (Oberheim *et al.*, 2009). The other two subtypes, the fibrous and protoplasmic astrocytes, have been described in both humans and rodents; despite slight differences in the size of the soma between these two species (Matyash and Kettenmann, 2010). Furthermore, within species, there is also distinct functional and anatomical variation within the astrocytic population in different regions of the brain (Matyash and Kettenmann, 2010; Olude *et al.*, 2015). One such example is the lack of expression of functional NMDA receptor in the astrocytes of the hippocampus in mice (Seifert and Steinhäuser, 1995). These subtle differences could contribute to different functional properties of the astrocytes depending on the region of interest.

Subsequently, astrocytes were identified to serve many important functions in the maintenance of homeostasis in the central nervous system (reviewed elegantly in (Kimelberg and Nedergaard, 2010) and will be briefly discussed here). Due to the astrocytic expression of two potassium pumps (the ATP – dependent Na-K-ATPase and the Na-K-Cl cotransporter or NKCC pump) as well as the inward rectifying potassium channel (Kir), it is widely accepted that astrocytes play an important role in the buffering of extracellular K^+ (Kofuji and Newman, 2004; Witthoft *et al.*, 2013). The presence of various H^+ and HCO_3^- transporting enzymes in astrocytes also allows for these cells to actively participate in the regulation of brain pH (Chesler, 2003; Hansen *et al.*, 2015). Astrocytes also have various metabolic modulatory function such as the glutamate-glutamine cycle (Hertz, 2013) (discussed further below in section 1.8.6), the astrocyte-neuronal lactate shuttle (Chih and Roberts, 2003) (discussed further below in section 1.8.7), and the neurovascular coupling through the blood-brain barrier (Abbott *et al.*, 2006) (as discussed above in section 1.5). Astrocytes are also involved in water transport due to the specific expression of aquaporin channels (Satoh *et al.*, 2007; Hubbard *et al.*, 2015; Potokar *et al.*, 2016). Finally, astrocytes also demonstrate a high expression level of key antioxidant enzymes; therefore they are thought to be an important source of endogenous defence against oxidative stress (Fernandez-Fernandez *et al.*, 2012; Baxter and Hardingham, 2016).

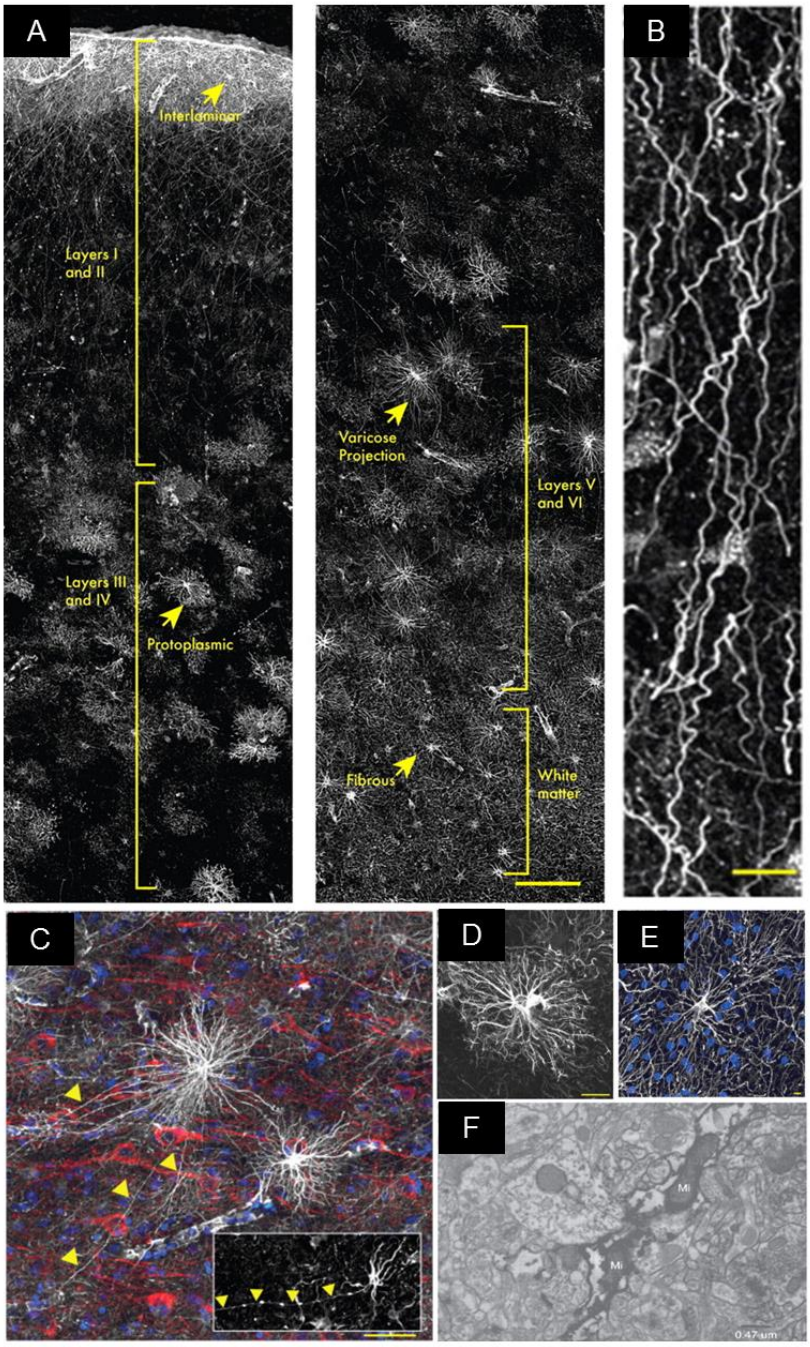

Figure 1-12 Astrocyte morphological variation in the human brain. Morphological studies are based on immunostaining of the GFAP protein in the human cortex. There is a regional specific distribution of astrocytes subtypes in the human brain as shown in (A). Layer I is composed of the cell bodies of the interlaminar astrocytes, with their respective processes extending through to layer II – IV with their characteristic tortuous processes (as shown in (B)). The polarized astrocytes with varicose projections (shown in (C) and projections shown with the yellow arrows) are found only in humans and seen sparsely across layers V – VI. The protoplasmic astrocytes (shown in (D)), the most common form of astrocytes, occupy most of the grey matter, especially in layers II – VI. Finally, the fibrous astrocytes (shown in (E)) are primarly found in the white matter and characteristically contain numerous overlapping processes. Scale bar in (A) 150µm, (B) 10µm, (C) 50µm, (D) 20µM, and (E) 10µm. Figure (A) and (F) is reprinted from Journal of Neuroscience, Volume 29, Edition 10, Oberheim et al, Uniquely Hominid Features of Adult Human Astrocytes, Page 3276 – 3287., Copyright (2009), with permission from the Society for Neuroscience. Figure (B), (C), (D), and (E) is reprinted from Brain Research Reviews, Volume 63, Issues 1 – 2, Matyash V and Kettenmann H, Heterogeneity in astrocyte morphology and physiology, Pages 2-10;, Copyright (2010), with permission from Elsevier. Permission also obtained from original images from (Oberheim, 2009) as with figure (A) and (F).

1.7.1 Astrogliosis

Another important role of astrocytes is their classical response to neuronal injury called reactive astrogliosis. Reactive astrogliosis is a pathological increase in the number and size of the astrocytes due to upregulation of various gene expression and molecular markers following neuronal injury (Zamanian *et al.*, 2012). One such marker of reactive astrogliosis is the glial fibrillary acidic protein (GFAP), which is known to be upregulated during astrogliosis but has eventually become used more extensively as an astrocytic marker due to its selective expression in the astrocytes (Hol and Pekny, 2015).

It is controversial whether reactive astrogliosis is largely beneficial or detrimental to the whole brain tissue in the context of neuronal injury (Sofroniew, 2009; Pekny and Pekna, 2014; Pekny *et al.*, 2014). In various studies using a wide array of model, reactive astrogliosis has been shown to be a protective mechanism in limiting the extent of the brain injury and inflammation to the area of gliosis (Bush *et al.*, 1999; Herx and Yong, 2001; Faulkner *et al.*, 2004; Myer *et al.*, 2006; Gadea *et al.*, 2008; Voskuhl *et al.*, 2009). On the other hand, in some models (particularly the spinal cord injury model), reactive astrogliosis has been demonstrated to be detrimental to neuroregeneration, especially in inhibiting new axonal growth following the neuronal injury (Liuzzi and Lasek, 1987; Snow *et al.*, 1990; Cirillo and Papa, 2016). This detrimental response from the reactive astrogliosis is usually characterized as a maladaptive response of gliosis (Pekny *et al.*, 2014). This distinction in the astrogliosis response to neuronal injury was also found to be model-specific and activates different gene expression pathways dependent on the injury types (Zamanian *et al.*, 2012). Therefore, it supports the view that reactive astrogliosis should be considered within the context of each injury and model (Sofroniew, 2009; Zamanian *et al.*, 2012; Pekny and Pekna, 2014).

Structurally, reactive astrogliosis is characterized by a hypertrophic response that varies with the severity of each insult (Sofroniew and Vinters, 2010). In a healthy astrocyte, each cell occupies a discrete domain and there is no overlap in the processes. Following a mild to moderate injury, the astrocytic processes are extended and no longer occupy discrete domains. When the injury reaches the severe stage, a glial scar is formed in addition to the reactive astrocytes. The glial scar is composed of newly proliferated astrocytes along with some other cell types such as fibromeningeal

cells and other neuroglial cells (Sofroniew, 2009; Wanner *et al.*, 2013; Silver, 2016). This glial scar forms a border around the extent of the injury and is usually very focal and well circumscribed. Therefore, the reactive astrogliosis can be graded in its response from a mild astrogliosis to a severe astrogliosis with glial scar formation (see Figure 1-13).

In the context of neurotransmission, reactive astrogliosis has been very closely associated with the loss of inhibition. The selective induction of reactive astrogliosis acutely cause an erosion of inhibition, which was speculated to be due to the failure of the astrocytic glutamate-glutamine cycle (Ortinski *et al.*, 2010). In a transgenic mice model of reactive astrogliosis, these animals were found to develop recurrent spontaneous seizure, which was thought to be due to alteration in the potassium channel expression (Yu *et al.*, 2014; Robel *et al.*, 2015). Indeed, reactive astrocytes and gliosis were found in various models of epilepsy and was associated with impairment in glutamatergic transmission (Represa *et al.*, 1995; Aronica *et al.*, 2000; Garzillo and Mello, 2002).

Indeed, reactive astrogliosis is a well-characterized response to neuronal injury which may have a beneficial or detrimental effects, depending on the injury type and model. Whatever the mechanisms or the modulators, it should be borne in mind that astrogliosis should be considered and examined in the context of various neurological disorders.

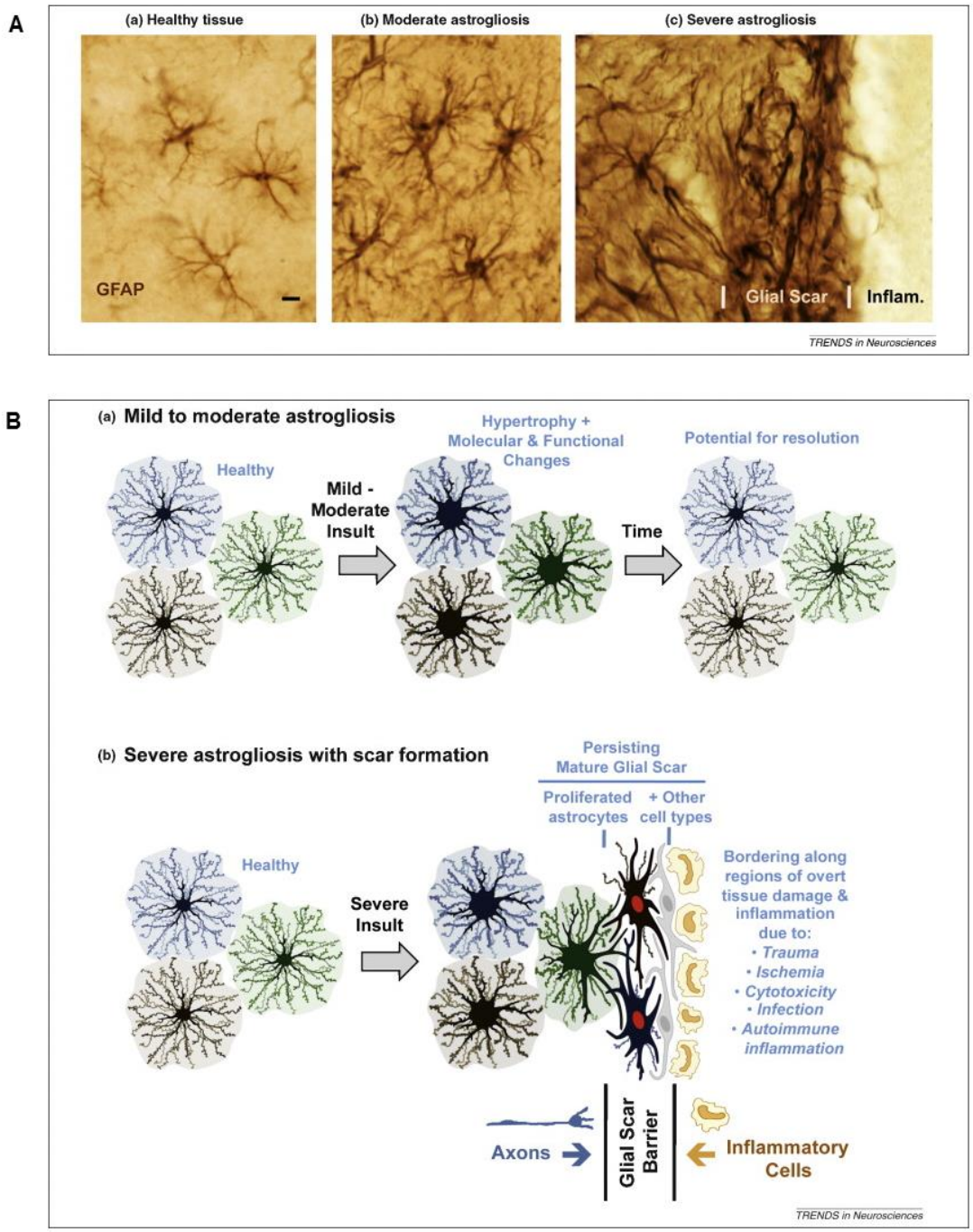

Figure 1-13 Progression of astrogliosis. Shown in (A) are photographs of astrocytes in healthy tissue (a) and the different stages of reactive astrogliosis (b-c) and glial scar formation (c) following various tissue insults of different severity. Astrocytes are labelled through immunostaining of the glial fibrillary protein (GFAP). Scale bar 8µm. Shown in (B) are schematic representations of the mechanisms involved in the different gradations of these reactive astrogliosis. In (a), mild to moderate reactive astrogliosis constitutes the changes in molecular expression and functional properties of the astrocytes associated with cellular hypertrophy. These changes are temporary and can still resolve itself should the insult be removed. Severe reactive astrogliosis (b), on the other hand, occurs with persisting scar formation along the border to areas of tissue damage and inflammatory reactions. This glial scar formation is comprised of newly proliferated astrocytes (with red nuclei in figure) and other glial cell types (with gray nuclei). Mature glial scars persist for long periods of time and act as both a barrier to axonal regeneration and to the spread of intense inflammatory reaction from the damaged tissue. Reprinted from Trends in Neuroscience, Volume 32, Issue 12, Sofroniew M.V., Molecular dissection of reactive astrogliosis and glial scar formation, Page 638-647., Copyright (2009), with permission from Elsevier.

1.7.2 Manipulation of astrocytic function

Currently, there are not many methods available to study astrocyte functions specifically, in isolation from the neuronal compartments. Most of our current knowledge on astrocytic function have been based on studies using astrocytic culture or co-culture with neurons (Jones *et al.*, 2012; Schildge *et al.*, 2013). However, it can be argued that the culture conditions are extremely artificial and do not represent *in vivo* conditions accurately. In the use of animal models, certain transgenic animal models have been developed with regards to the manipulation of specific astrocytic function (Yu *et al.*, 2014; Robel *et al.*, 2015; Srinivasan *et al.*, 2016). Whilst the use of genetically modified animals is certainly appealing due to its strength in the selective manipulation of astrocytic function, the generation of these animals tends to be expensive and time inefficient.

In an *in vitro* study, the most time efficient, cost effective, and reproducible method of manipulating cellular function is using pharmacological tools. There are very few pharmacological compounds available to modulate astrocytic function specifically. One such compound (used in this thesis) is fluorocitrate. Fluorocitrate is a specific astrocyte aconitase inhibitor (Hassel *et al.*, 1992). The specificity of this compound is reliant on the preferential uptake of citrate compounds into the astrocyte (Fonnum *et al.*, 1997). After being taken up by the astrocytes, fluorocitrate undergoes conversion to fluoro-cis-aconitate and eventually forms the by-product, 4-hydroxy-trans-aconitate (HTn), which is shown to form a tight bond with the aconitase molecule (Lauble *et al.*, 1996).

Metabolically, in addition to the inhibition of aconitase (a TCA cycle enzyme, TCA cycle to be discussed further below in section 1.8.3), fluorocitrate has been characterized to also cause many other metabolic changes. There is a significant decrease in glutamine production in the media of an astrocytic culture following fluorocitrate application (Hassel *et al.*, 1992; Fonnum *et al.*, 1997). Fluorocitrate has also been shown to significantly reduce cerebral oxidation of lactate and to a lesser extent, glucose (Ronald Zielke *et al.*, 2007). In rat kidney mitochondria, fluorocitrate was demonstrated to inhibit pyruvate carboxylation (Mehlman, 1968). All these studies indicated that the use of fluorocitrate can potentially cause a large metabolic change in the exposed tissue in addition to its effect as an aconitase inhibitor.

Intracerebral injection of fluorocitrate *in vivo* has been shown to lead to the development of convulsive seizures (Hornfeldt and Larson, 1990; Willoughby *et al.*, 2003; Mirsattari *et al.*, 2008). However, no single mechanisms has been ascribed to be responsible for this convulsive effect. In addition, another study using similar methods of delivery through intracerebral injection of fluorocitrate, albeit at a lower dose, did not find spontaneous seizure generation following the treatment (Lian and Stringer, 2004). Indeed, the selectivity of fluorocitrate inhibition towards the astrocytes has been shown to be dependent on concentration, time window, and method of delivery (Paulsen *et al.*, 1987). In the study using the lower concentration of fluorocitrate (which would be more specific in inhibition of astrocyte function), it was found that fluorocitrate increased the tissue susceptibility to various pro-convulsants, such as kainic acid and pilocarpine (Lian and Stringer, 2004). This was reproduced in the context of spreading depression and it was concluded that in the presence of fluorocitrate, neurons were more vulnerable to a convulsive state and the generation of cortical spreading depression (Largo *et al.*, 1997). Therefore, it seems more conclusive that fluorocitrate, as a modulator of astrocytic function, increased the neuronal vulnerability to a convulsive state; rather than acting as a direct pro-convulsant.

Interestingly, recent studies have shown that fluorocitrate may potentially modulate the function of other neuroglia cells, specifically the microglia in the context of understanding nociceptive pain transmission (Jiang *et al.*, 2009; Sung *et al.*, 2012; Xu *et al.*, 2016). It is important to note that these studies are still preliminary findings and further studies are required to truly establish the effect of fluorocitrate on microglia metabolism. However, the presence of such studies should revitalize the interest in the use of fluorocitrate as a modulator of glial function.

1.8 Energy metabolism in the brain

The main obligatory substrate for the brain is glucose (McKenna *et al.*, 2006). In addition to its role as an energy-providing substrate, glucose is also the carbon source for the biosynthesis of various essential compounds in the brain, including neurotransmitters (Dienel, 2014). Therefore, across all cell types in the brain (for instance neurons and astrocytes); there is a common metabolic pathway in energy metabolism that utilizes glucose as a substrate. However, it is accepted that under certain conditions, other substrates can be utilized by the brain. During starvation, for example, the brain preferentially uses ketone bodies rather than glucose as a metabolic substrate (Owen, 2005). Therefore, lipid metabolism may also play an important role in the provision of energy for the brain. Furthermore, there are also metabolic pathways that require the contribution of the two major cellular compartments of the brain, neurons and astrocytes. Such pathways include the astrocytic-neuron lactate shuttle hypothesis and the glutamate-glutamine cycle as well as the GABA shunt. All of these metabolic pathways are to be discussed in detail below.

1.8.1 Overview of glucose metabolism

Glucose enters the cell through a glucose transporter and undergoes glycolysis in the cytoplasm. Each glucose molecule would generate two molecules of pyruvate and the net result of glycolysis also includes 2 ATP molecules and 2 NADH molecules per molecule of glucose. Each of the pyruvate molecule can enter the mitochondria to undergo decarboxylation to generate acetyl-CoA. This acetyl-CoA enters the TCA cycle and generate 3 NADH and 1 $FADH_2$ as it undergoes the cycle. In addition, a molecule of GTP is generated and is readily converted to ATP per turn of the Krebs cycle. All these accumulated NADH and $FADH_2$ then enters the oxidative phosphorylation (discussed above in section 1.2) to generate the majority of the ATP via glucose metabolism. After accounting for all the steps that require ATP as an intermediary, the net result of ATP generated per molecule of glucose following all these steps is 30 ATP per molecule (Berg *et al.*, 2012g). It is important to note, however, that the metabolic processes in mitochondria are dependent on the presence of oxygen (see also above oxidative phosphorylation in section 1.2); hence making this complete glucose metabolism an ‘aerobic’ process (see Figure 1-14) (Berg *et al.*, 2012g).

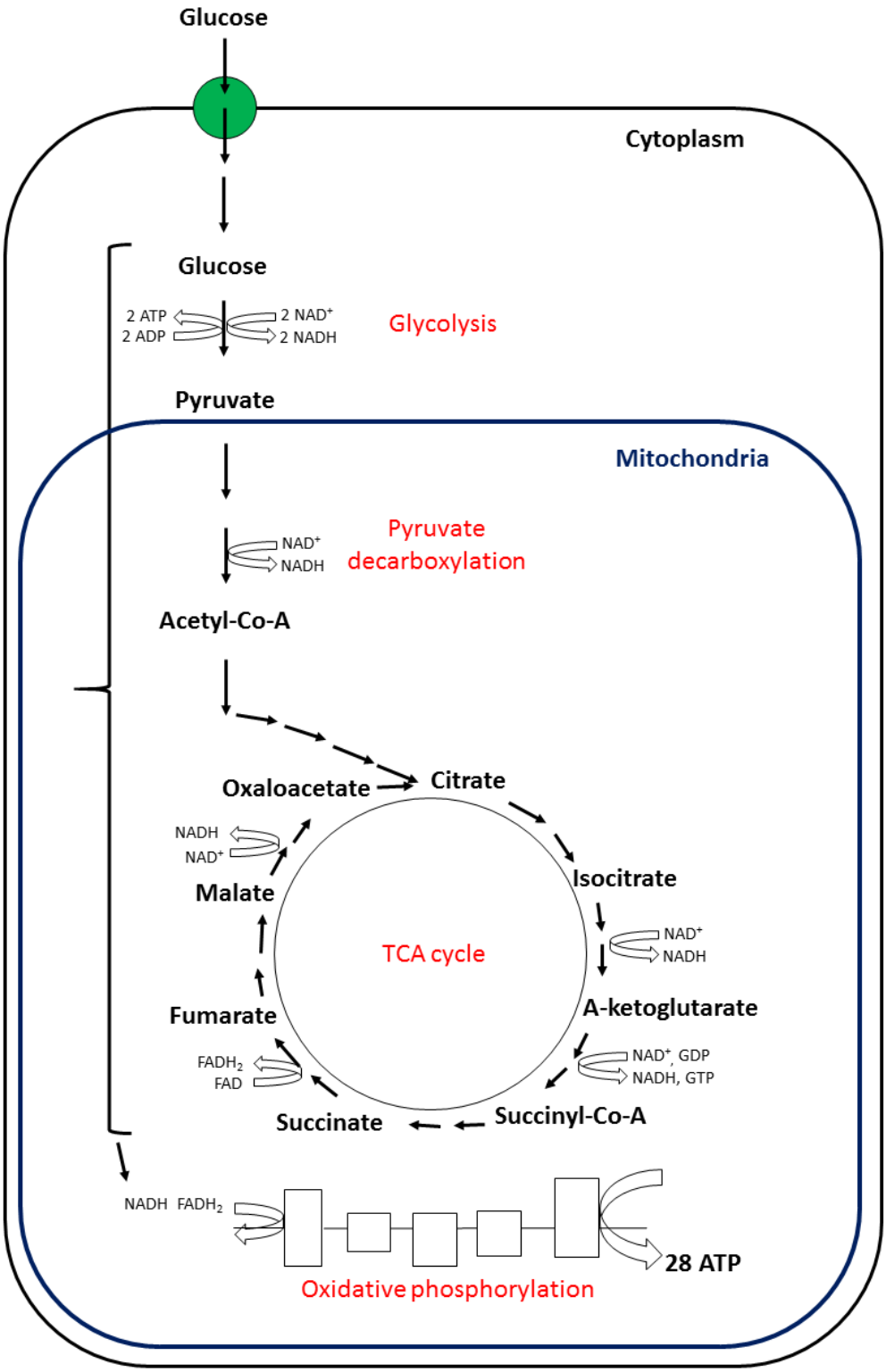

Figure 1-14 Overview of glucose metabolism. Shown above is an overview of glucose metabolism and the important byproducts of the metabolism. The processes involved are coloured red and is placed at its respective locations; whether in the cytoplasm or the mitochondria. In green is the glucose transporter that allows the glucose to enter the cell.

1.8.2 Glycolysis

Glycolysis is the first metabolic pathway, common to all tissues, in the metabolism of glucose (Berg *et al.*, 2012f). It is a sequence of chemical reactions that metabolizes a molecule of glucose to two molecules of pyruvate. The net results of this reaction are two molecules of pyruvate, two molecules of ATP, and two molecules of NADH (see Figure 1-15). In the brain, glycolysis is relatively rapid and has many major branching points, where the carbon atoms are redirected from the glycolytic pathways to other metabolic pathways. One such branching point is following the rate-limiting step of glucose conversion to glucose-6-phosphate by the enzyme hexokinase (Berg *et al.*, 2012f). Glucose-6-phosphate can enter the pentose phosphate shunt pathway for the generation of NADPH and various nucleotide precursors (Berg *et al.*, 2012b). NADPH is an important part of the endogenous oxidative defence system due to its strong reducing power (DeBerardinis *et al.*, 2007). Additionally, glucose-6-phosphate can also be converted to glucose-1-phosphate, an important precursor to glycogen (Dienel, 2014). In adult brain, glycogen is primarily stored in astrocytes and is usually the first fuel reserve utilized during an energy crisis (Brown and Ransom, 2007; Obel *et al.*, 2012). The next branching point in glycolysis is fructose-6-phosphate, which is a precursor to various glycoprotein components of the cell membrane (Dienel, 2014). Finally, 3-phosphoglycerate is also a branching point for the synthesis of various carbon compounds, such as the neurotransmitters, glycine and D-serine (Dienel, 2014).

As a product of glycolysis, pyruvate itself has multiple fates. Under normal aerobic conditions, most pyruvate will be decarboxylated by the pyruvate dehydrogenase complex to generate acetyl-CoA that would enter the TCA cycle (Berg *et al.*, 2012f). It can be transaminated to generate alanine by alanine transaminase (ALT) through a reaction coupled with the conversion of glutamate to alpha-ketoglutarate (Bak *et al.*, 2006). In the astrocytes, pyruvate is also an important source of anaplerosis and CO_2 fixation through the action of the enzyme pyruvate carboxylase, which converts it to oxaloacetate (Shank *et al.*, 1985). Finally, under anaerobic condition, pyruvate can also be reduced to form lactate by the enzyme lactate dehydrogenase, which is coupled to the oxidation of NADH to NAD^+ (Berg *et al.*, 2012f). This reaction is favourable under anaerobic condition as glycolysis requires NAD^+ to continue and the regeneration through oxidative respiration is unavailable under such condition.

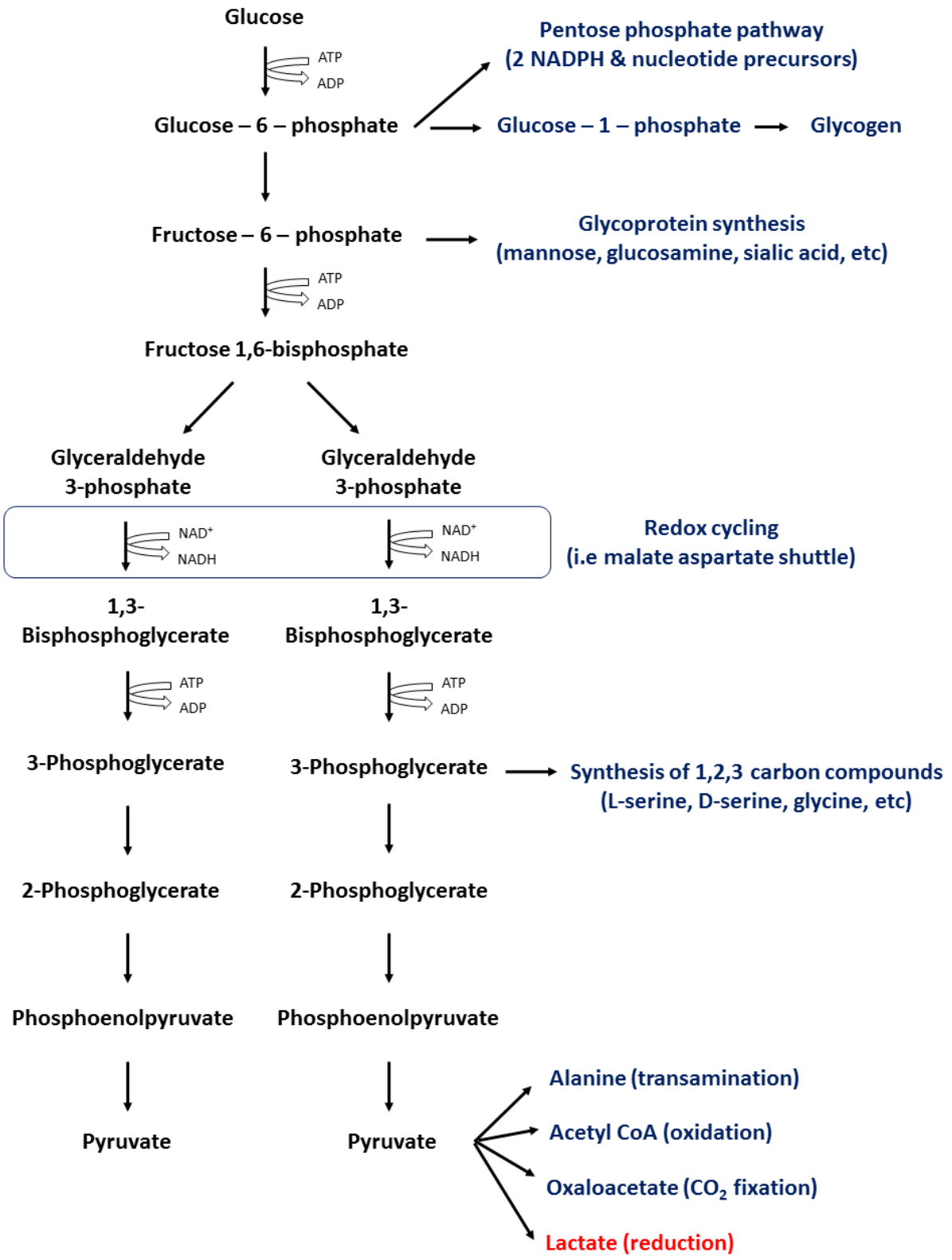

Figure 1-15 Glycolysis and its branching points. Shown are the steps involved in glycolysis as well as the important byproducts of the reaction. In blue are all the branching points that could occur in normal aerobic condition, whereas in red is the branching point that could occur under anaerobic condition.

Another important concept to discuss at this point is the NAD^+/NADH ratio, which acts as a good indicator of the redox status in the tissue (Dienel, 2014). NADH generated by glycolysis cannot directly cross the mitochondrial membrane to be oxidized via the electron transport chain. Therefore, to continue carrying on glycolysis, the tissue needs a pathway to replenish the NAD^+ pool. Under aerobic conditions, this is mediated by the redox shuttle system and the major system in brain is the malate-aspartate shuttle (see Figure 1-16) (Kane, 2014). Alternatively, pyruvate can also be reduced to lactate as mentioned above to regenerate the NAD^+ pool under anaerobic conditions (Berg *et al.*, 2012f). Under anaerobic conditions, NADH cannot be oxidized to NAD^+, therefore the NAD^+/NADH ratio would be less than 1 and indicates the failure of redox maintenance in the tissue. Therefore, the NAD^+/NADH ratio is an important concept in understanding the redox status of the tissue following metabolic dysfunction.

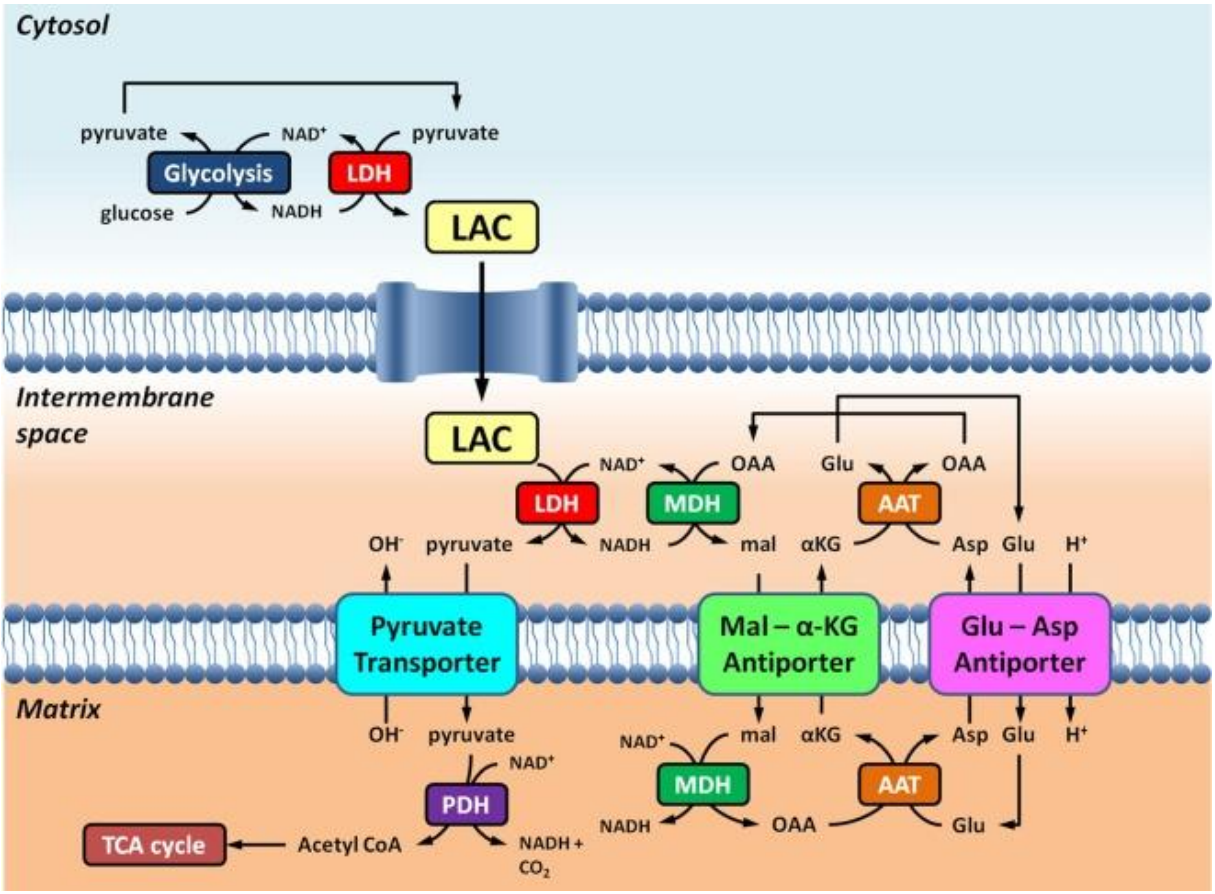

Figure 1-16 The redox shuttle system in the brain. There are two major ways for the brain to replenish NAD^+ content. Pyruvate can be reduced to lactate by the enzyme lactate dehydrogenase. Alternatively, a major redox shuttle system in the brain is the malate – aspartate shuttle, which involves various enzymes (such as malate dehydrogenase) and transporters (such as the malate – alpha ketoglutarate antiporter). Reprinted from Frontiers in Neuroscience, Volume 8, Edition 366, Kane D.A, Lactate oxidation at the mitochondria: a lactate – malate – aspartate shuttle, Copyright (2014) as an open – access article distributed under the terms of the Creative Commons Attribution License.

1.8.3 TCA cycle (Krebs cycle)

Following glycolysis, the majority of the pyruvate generated is decarboxylated by the pyruvate dehydrogenase complex to generate acetyl-CoA (Berg *et al.*, 2012f). Acetyl-CoA enters oxidative metabolism through the Krebs cycle (or the tricarboxylic acid cycle) (Berg *et al.*, 2012d). The TCA cycle is unique as it represents the metabolic pathway where glucose, amino acids, and lipid metabolism converges (see Figure 1-17) (Dienel, 2014).

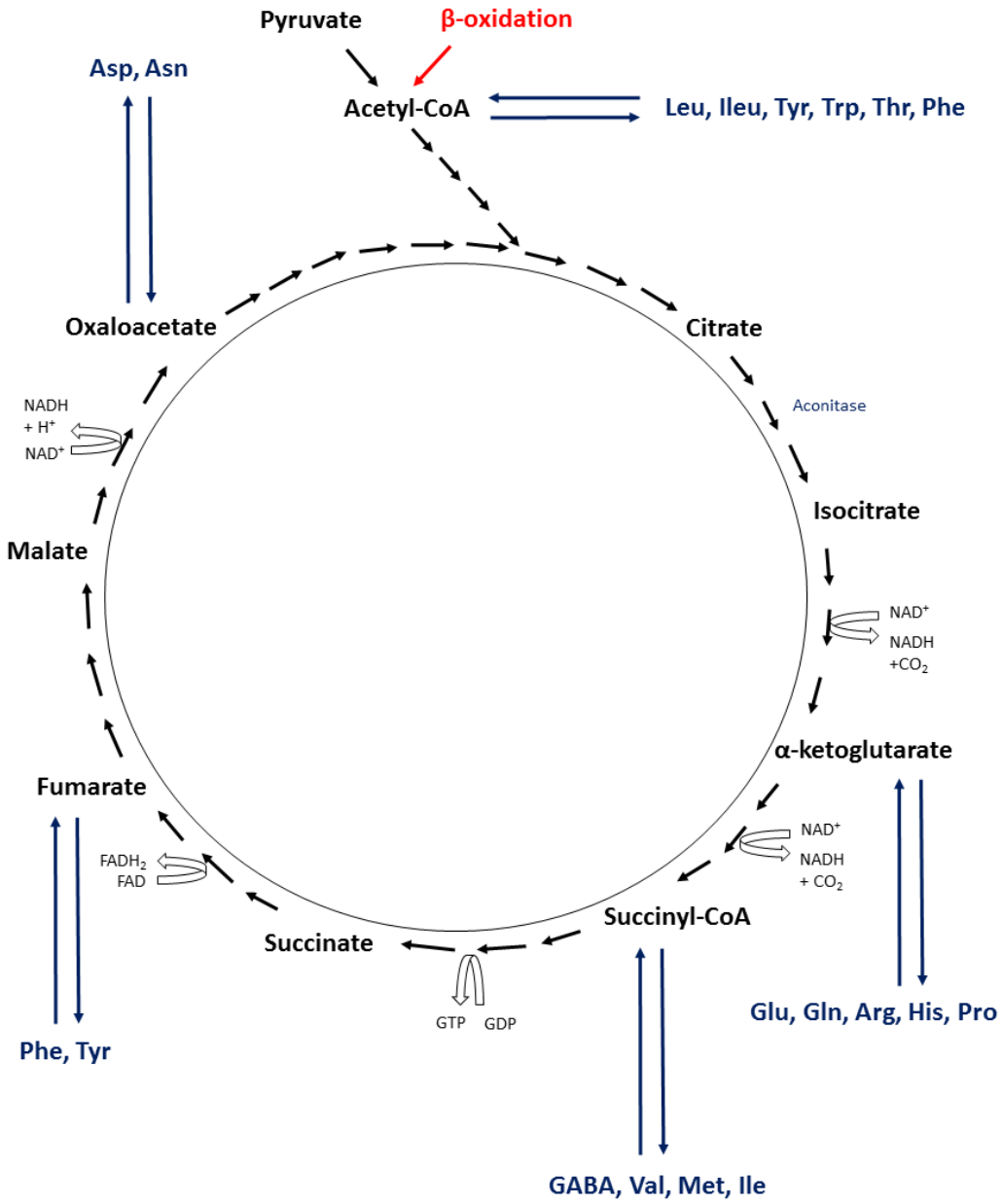

Figure 1-17 The TCA cycle and its branching point. Shown above is the TCA cycle or the Krebs cycle, its product, and its branching point. The step catalysed by the enzyme aconitase is highlighted as this is relevant to the study in this thesis. Blue represents the entry of amino acid metabolism and red represents the entry of lipid metabolism. Leu – leucine, Ileu – isoleucine, Tyr – tyrosine, Trp – tryptophan, Thr – threonine, Phe – phenylalanine, Glu – glutamate, Gln – glutamine, Arg – arginine, His – histidine, Pro – proline, Val – valine, Met – methionine, Asp – aspartate, Asn – asparagine.

The major products of the TCA cycle are the NADH and $FADH_2$. As mentioned previously in section 1.2, NADH enters the mitochondrial respiratory chain at complex I. $FADH_2$, in contrast, enters the mitochondrial respiratory chain directly from the TCA cycle without dissociating from the enzyme succinate dehydrogenase and forms complex II of the respiratory chain (Berg *et al.*, 2012d). Together, the oxidation of NADH and $FADH_2$ generated from the TCA cycle accounts for almost 90% of the energy requirement in human (Berg *et al.*, 2012d), highlighting the importance of this cycle in the generation of high energy ATP molecules. Another important by-product of the TCA cycle is the production of carbon dioxide (CO_2) and proton ions (H^+). This carbon dioxide has been shown to be a major source of acidification in cellular respiration as it is readily converted to bicarbonate (HCO_3^-) and proton ion (H^+) (Mookerjee *et al.*, 2015).

As shown in Figure 1-17, both amino acids and lipids enters energy-generating metabolism via the TCA cycle. Amino acids enter the TCA cycle through its intermediates. Glutamate, for example, enters the TCA cycle through the intermediate α-ketoglutarate following interconversion by the enzyme glutamate dehydrogenase (Bak *et al.*, 2006). Lipid metabolism through mitochondrial β-oxidation enters the TCA cycle after its conversion to acetyl-CoA (Berg *et al.*, 2012e) (to be discussed further below). Regardless, the TCA cycle represents an important converging metabolic pathway for the entry of various substrates to energy metabolism.

1.8.4 Fatty acid metabolism

Theoretically, fatty acids are the molecules with the highest efficiency in energy storage (Berg *et al.*, 2012e). However, the brain is suboptimal in its use of the hydrogen – rich fatty acids as a form of metabolic fuel. This is a very puzzling observation but is explained by various experimental observations. Catabolism of the fatty acids is mediated by mitochondrial β-oxidation and demands more oxygen than glucose catabolism, therefore cells such as neurons could potentially be hypoxic should it be forced to rely on fatty acids as metabolic substrate (Schönfeld and Reiser, 2013). Furthermore, β-oxidation generates superoxide, a potent reactive oxygen species (ROS) (Rodrigues and Gomes, 2012; Schönfeld and Wojtczak, 2012), that when handled improperly can cause severe oxidative stress. The rate of β-oxidation is also thought to be slower than glucose oxidation, making it difficult to rely on β-oxidation to

sustain rapid neuronal activity (Schönfeld and Reiser, 2013). Collectively, this makes it unfavourable for neurons to use fatty acid as the preferred form of metabolic fuel.

Regardless of all the disadvantages mentioned above, fatty acid metabolism still exists in brain tissue and is estimated to potentially account for up to 20% of the whole tissue metabolism (Panov *et al.*, 2014). A recent school of thought has hypothesized that fatty acid metabolism is more suitable to astrocytes rather than neurons (Schönfeld and Reiser, 2013; Murphy, 2014; Panov *et al.*, 2014). This is supported by various experimental evidence. For instance, astrocytes are better equipped with endogenous antioxidant systems to combat their natural reactive oxygen species formation due to their lack of mitochondrial supercomplexes organization (Lopez-Fabuel *et al.*, 2016). Astrocytes are therefore proposed to be a 'metabolic cauldron', without which, neuronal function would largely suffer (Panov *et al.*, 2014).

Another important cautionary note is that whilst most of the dietary long-chain fatty acids are metabolized through mitochondrial β-oxidation, some branched and very-long chain fatty acids are instead metabolized through the peroxisomal α- and β-oxidation processes (Wanders *et al.*, 2003). Therefore, the metabolism of each fatty acid should be considered in the context of its respective metabolic pathway. Furthermore, studies on fatty acid metabolism in the brain are relatively scarce and this area is still a growing field of study. Regardless, it proves worthwhile to investigate more on the exact roles that fatty acid play in energy metabolism of the brain.

1.8.5 Ketogenesis

As mentioned above, under starvation, the brain preferentially utilizes ketone bodies instead of glucose as metabolic fuel (Owen, 2005). Ketone bodies are collective groups of water-soluble molecules, comprised of β-hydroxybutyrate, acetoacetate, and acetone, that are generated from acetyl-CoA during starvation (see Figure 1-18) (Laffel, 1999). This acetyl-coA can either be generated from pyruvate following glycolysis or from β-oxidation of fatty acids (Laffel, 1999). The ketone bodies are utilized in the brain through the TCA cycle following re-conversion to acetyl-coA through ketolysis (Laffel, 1999)

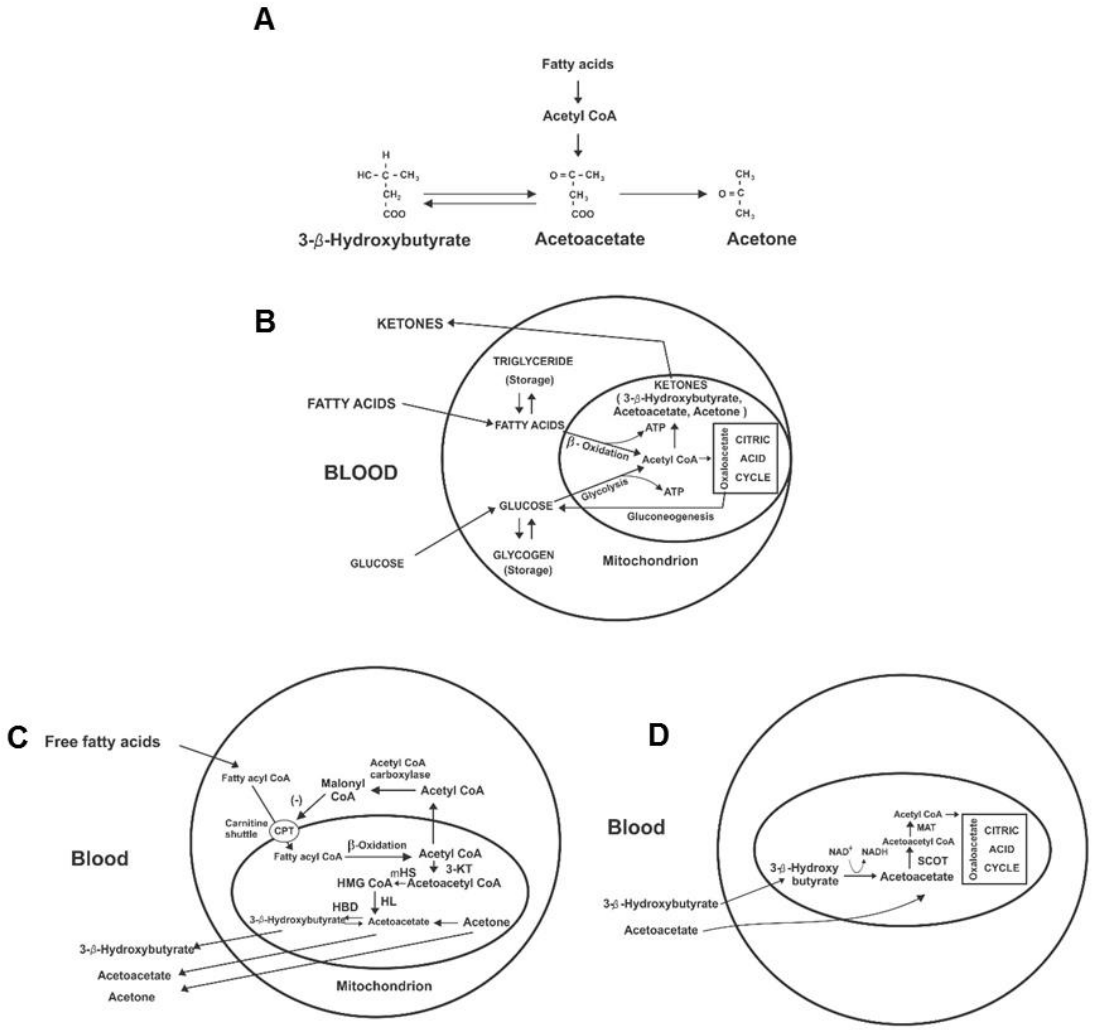

Figure 1-18 Ketone bodies and their respective metabolic pathways. Shown in (A) are the chemical structures of the three components of the ketone bodies, namely the β-hydroxybutyrate, acetoacetate, and acetone. The ketone bodies are generated through ketogenesis from acetyl-CoA, either obtained from glycolysis or β-oxidation, as shown in (B). Shown in (C) are the respective enzymes and transporters involved in ketogenesis. In (D), the use of ketone bodies or ketolysis is shown as it enters the TCA cycle to provide energy. HL – HMG CoA lyase, 3-KT – 3-ketothiolase, mHS – HMG CoA synthase, HBD – 3-HB dehydrogenase, SCOT – succinyl CoA-oxoacid transferase, and MAT – methylacetoacetyl CoA thiolase. Reprinted with slight modification from Diabetes Metabolism Research and Reviews, Volume 15, Issue 6, Laffel L, Ketone bodies: a review of physiology, pathophysiology and application of monitoring to diabetes, Page 412-426., Copyright (1999), with permission from John Wiley and Sons.

In vivo, the major site of production of the ketone bodies is the liver (Berg *et al.*, 2012e). Out of the three ketone bodies, acetoacetate and β-hydroxybutyrate are the most abundant, whereas acetone is the least abundant and rarely detectable in the blood (Laffel, 1999). Acetoacetate accumulates during fatty acid metabolism under hypoglycemic conditions, whereas β-hydroxybutyrate is formed through the reduction of acetoacetate in the mitochondria. Therefore, similarly, the utilization of β-hydroxybutyrate requires reconversion to acetoacetate, which is an energetically

favourable reaction as it yields NADH that is usable in oxidative phosphorylation (Berg *et al.*, 2012e). Acetone is only generated by the spontaneous decarboxylation of acetoacetate (Laffel, 1999), hence why it is the least abundant of the three molecules.

In the brain, it is thought that ketone body production is maintained through astrocytic fatty acid metabolism (Auestad *et al.*, 1991; Romano *et al.*, 2017). This astrocytic ketogenesis is tightly regulated by AMP-kinase (AMPK) and is upregulated in condition of energy crisis (Takahashi *et al.*, 2014). Thus, these astrocytic-generated ketone bodies may represent an important neuronal substrate in such conditions (see Figure 1-19).

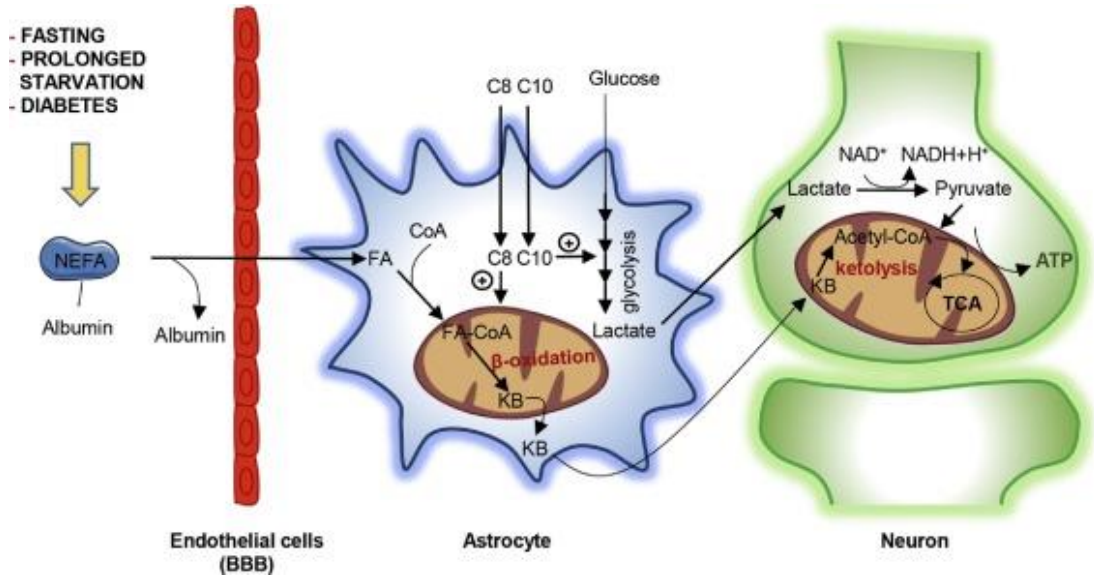

Figure 1-19 Utilization of fatty acids in the brain for ketone bodies metabolism. Recent evidence has shown that fatty acid metabolism in the brain may primarily be for ketone bodies production and utilization. The fatty acids mostly enter the brain as an albumin – bound form and is metabolized in the astrocytes through mitochondrial β-oxidation to generate ketone bodies. This ketone bodies are then taken up by the neurons and lysed in the mitochondria to generate acetyl-Co-A which would then supplement the TCA cycle in the neurons for ATP production. This ketone body production as well as glycolysis is shown to be modulated by the medium – chain fatty acids, octanoic acid (C8) and decanoic acid (C10). Reprinted from The International Journal of Biochemistry & Cell Biology, Volume 84, Romano et al, Fats for thoughts: An update on brain fatty acid metabolism, Page 40-45, Copyright (2017), with permission from Elsevier.

1.8.6 Glutamate-glutamine cycle

The glutamate-glutamine cycle is one of the many astrocytic mechanisms that directly modulate neurotransmission. The glutamate-glutamine cycle is an astrocytic metabolic pathway that is involved in the recycling of the neurotransmitters (Bak *et al.*, 2006). Together with the GABA shunt, these processes help maintain the excitatory and inhibitory neurotransmitter homeostasis by the degradation and production of glutamate and GABA (see Figure 1-20) (McKenna *et al.*, 2006).

Glutamine is the precursor to both glutamate and GABA (Dienel, 2014). However, the enzyme used to convert glutamate to glutamine, the ATP-dependent glutamine synthetase, is localized to astrocytes (Anlauf and Derouiche, 2013). Therefore, glutamine can only be synthesized by the astrocytes and in turn, astrocytes provide excitatory and inhibitory neurons with the precursors to glutamate and GABA respectively. The degradation of glutamate and GABA also occurs primarily in the astrocytic compartment. Glutamate readily enters the TCA cycle through interconversion to α-ketoglutarate, a reaction that is coupled with many other metabolic reactions (Berg *et al.*, 2012a). On the other hand, GABA is taken up by the astrocytes and undergoes transamination by GABA transaminase to generate succinate semialdehyde. Succinate semialdehyde is readily oxidized to form succinate that would enter the TCA cycle. Since the flux from α-ketoglutarate to glutamate, glutamine, and eventually to GABA bypasses some of the TCA cycle steps, this pathway is termed the GABA shunt and is often considered in close relation with the glutamate-glutamine cycle (Dienel, 2014).

This cycle is one example of how astrocytic metabolism complements and interacts with neuronal metabolism. The exact regulation and quantitative contributions of the different metabolic pathways towards this cycle are yet to be determined. However, the importance of this cycle in the brain homeostasis should not be undervalued.

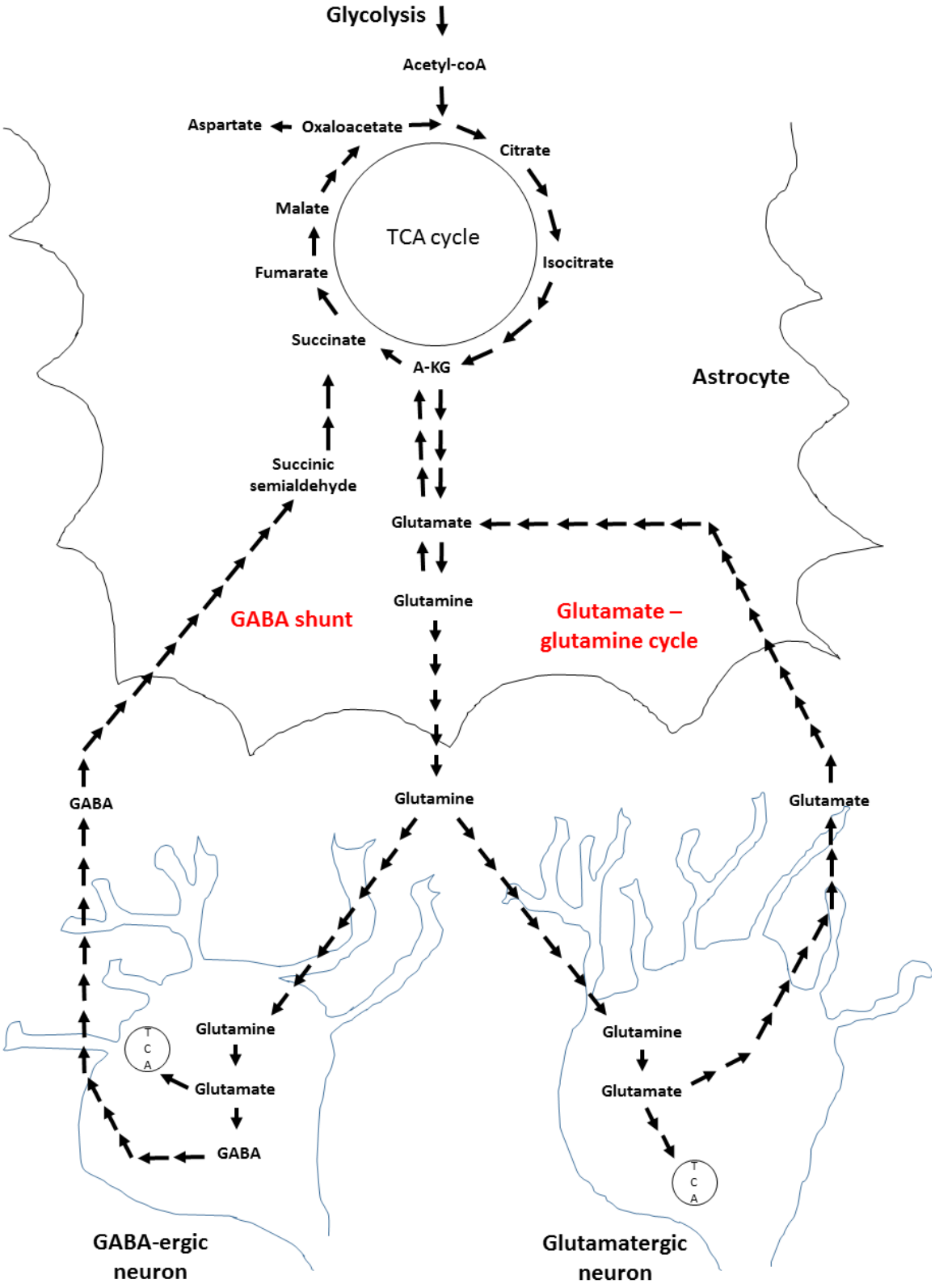

Figure 1-20 Glutamate - glutamine cycle and GABA shunt as an astrocytic - neuronal metabolic cooperation. Shown is a diagram representation of the glutamate – glutamine cycle and the GABA shunt that involves the neuronal and astrocytic compartment in the metabolic pathway.

1.8.7 Astrocyte-neuron lactate shuttle hypothesis

The astrocyte-neuron lactate shuttle hypothesis (ANLSH) was originally conceived from the observation that glutamate increased astrocytic glycolysis rate and was postulated to release lactate, which was used by neurons as preferential metabolic fuel during period of intense neuronal activity (Pellerin and Magistretti, 1994). Briefly, glutamate is taken up by astrocytes by excitatory amino acid transporters (EAAT) and stimulates ATP – dependent Na^+/K^+ ATPase, causing sodium influx into the astrocytes. This sodium influx then causes upregulation of aerobic glycolysis, specifically causing the astrocytes to generate lactate. This lactate is said to be released by the astrocytes and taken up by neurons, which would subsequently convert it to pyruvate and use it for energy metabolism. Since its existence, the theory has taken a life of its own and has incorrectly evolved into the statement that neurons depend on astrocytic supply of lactate for energy metabolism. There is a very large body of evidence that directly supports (Pellerin and Magistretti, 1994; Mangia *et al.*, 2009; Bélanger *et al.*, 2011; Genc *et al.*, 2011) or contradicts the ANLSH (Chih and Roberts, 2003; Ivanov *et al.*, 2013). Therefore, the true existence of this shuttle is yet to be determined. However, the original ANLSH has now been updated as to include only two components: the dependence of astrocytic glutamate uptake on glycolytic derived energy and the oxidation of lactate in neurons (Hertz, 2004). Even then, various evidence still arises to either support or question the existence of these two components (reviewed elegantly in (Hertz, 2004)). Regardless, the ANLSH represents an interesting mechanism whereby the astrocytic and neuronal metabolism might intersect. Therefore, its involvement in energy metabolism of the brain should be considered whenever the astrocytic and neuronal metabolism are perturbed.

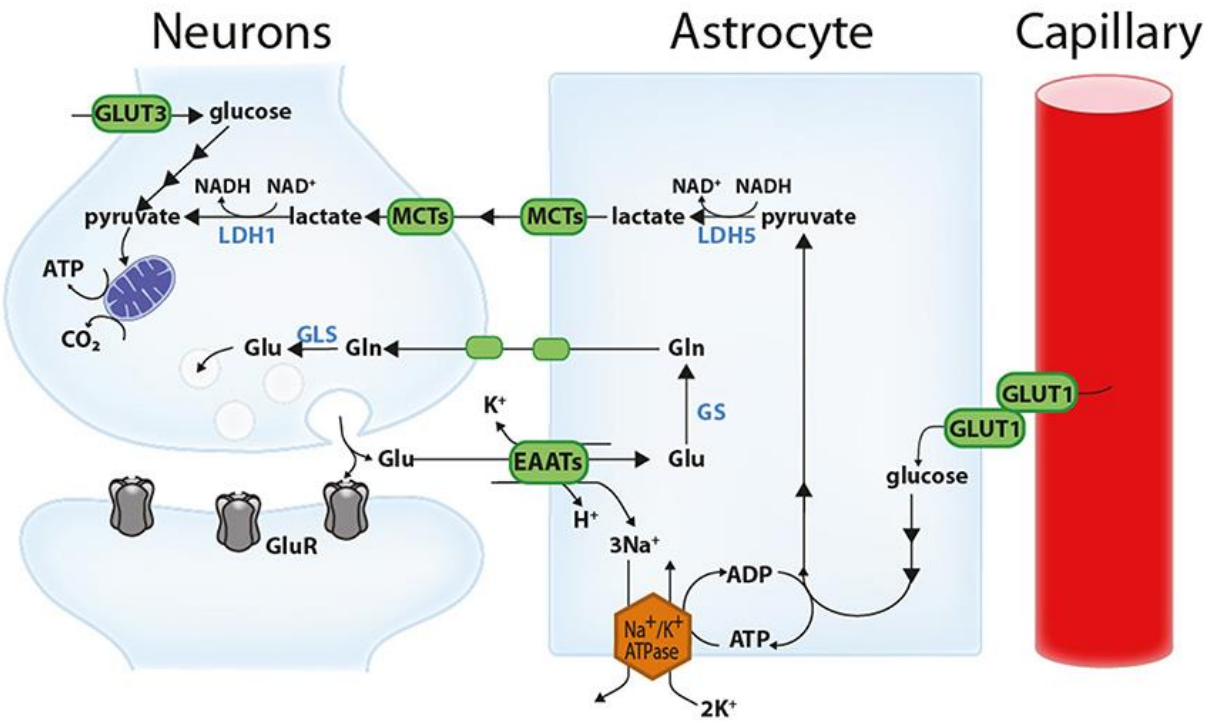

Figure 1-21 Astrocyte - neuron lactate shuttle hypothesis. There are now primarily two components to the shuttle, namely the upregulation of astrocyte aerobic glycolysis by glutamate uptake and the primary oxidation of lactate in neurons. GS – glutamine synthetase, GLS – glutaminase, LDH – lactate dehydrogenase, GLUT – glucose transporter, EAAT – excitatory amino acid transporters, and MCT – monocarboxylate transporters. Reprinted from Frontiers in Neuroscience, Allaman et al, Methylglyoxal, the dark side of glycolysis, Copyright (2015) as an open – access article distributed under the terms of the Creative Commons Attribution License. Also Elsevier special credit – 'Reprinted from Cell Metabolism, Volume 14, Issue 6, Belanger et al, Brain energy metabolism: focus on astrocyte – neuron metabolic cooperation, Pages 724-738, Copyright (2011), with permission from Elsevier'.

1.9 Mitochondrial disease

As mentioned above, mitochondrial DNA has a very high rate of mutation (Brown *et al.*, 1979). When mutation in the mitochondrial DNA is pathogenic, it causes impairment in the mitochondrial respiratory chain expression and typically leads to a severe multiorgan energy deficiency; collectively called mitochondrial disease (Tuppen *et al.*, 2010). Over the past few years, more and more genetic mutations are characterized as the cause of mitochondrial disease and this extends to nuclear DNA that was found to be involved in the maintenance and expression of the mitochondrial respiratory chain subunits (Scaglia, 2012). Regardless of the origin of the mutation, the genetic mutation has to lead to the deficiency of mitochondrial respiratory chain expression for the phenotype to manifest as mitochondrial disease (see Figure 1-22).

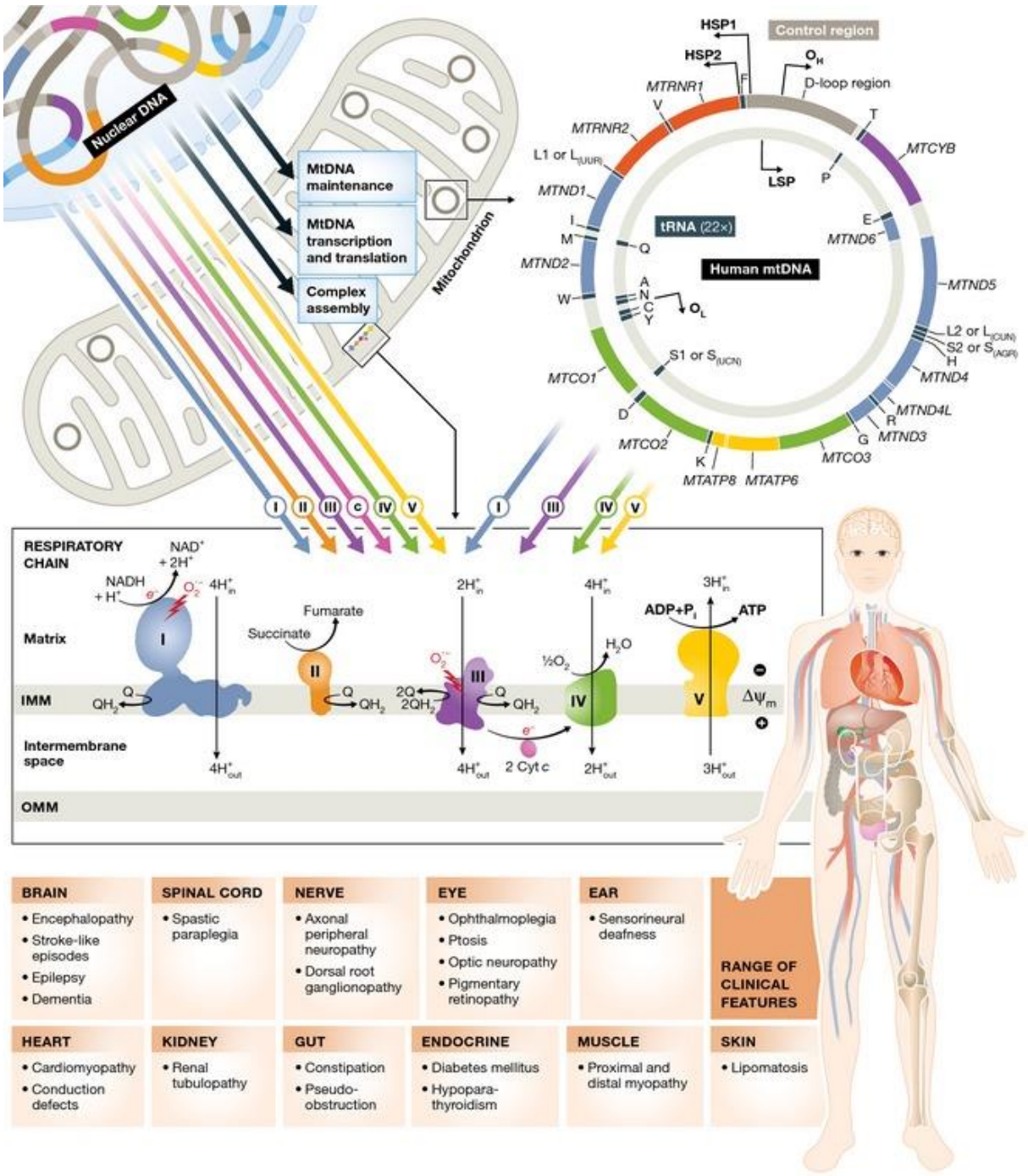

Figure 1-22 Overview of mitochondrial disease. Shown is the illustration of possible genetic mutations in the mitochondrial DNA or nuclear DNA which would subsequently affect the expression of the mitochondrial respiratory chain. This perturbed expression of the respiratory chain eventually leads to the manifestation of mitochondrial disease, which can have a range of clinical features across multiple organs. Reprinted from EMBO Molecular Medicine, Chinnery PF, Mitochondrial disease in adults: what's old and what's new?, Copyright (2015) as an open – access article distributed under the terms of the Creative Commons Attribution License.

Mitochondrial DNA mutation follows a unique pattern of inheritance, the maternal inheritance (Sato and Sato, 2013). However, the pathogenicity of these mutations also follows a unique principle due to heteroplasmy (Lightowlers *et al.*, 1997). Depending on the total amount of mutated mitochondrial DNA within a single cell, a pathogenic mutation may either manifest phenotypically or not. This is also known as the 'threshold effect' and also account for the variation in the severity of the clinical manifestations (Tuppen *et al.*, 2010). Furthermore, in mitochondrial disease, a phenotype is not associated strictly with a genotype. Instead, a majority of mutation at different sites within the mitochondrial or the nuclear DNA may lead to similar phenotypic manifestation (see Figure 1-23). In the North East of England, the most common pathogenic mutation is the m3243A>G mutation (Gorman *et al.*, 2015) and this mutation has a broad spectrum of phenotypes but is the most common cause of MELAS (Nesbitt and McFarland, 2011; Mancuso *et al.*, 2014).

In total, mitochondrial disease is estimated to have a prevalence of about 1 in 4,300 in the United Kingdom population and is therefore one of the most common adult forms of inherited neurological disorders (Gorman *et al.*, 2015). The collective term, mitochondrial disease, encompasses a multitude of syndromes and clinical manifestations. Some of these phenotypic manifestations is single organ (such as the eye in Leber Hereditary Optic Neuropathy), whilst most of the time, it typically is multiorgan (Mattman *et al.*, 2011). Typically, the brain, heart, and muscle are most severely affected, as these organs are classically the most metabolically active organs.

Out of the multisystem manifestations, neurological manifestations are by far the most common manifestations encountered in a clinical setting, putting the neurologists at the forefront of care of patients with mitochondrial disease (McFarland *et al.*, 2012). In a cohort study, the most common neurological manifestations are myopathy, chronic progressive external ophthalmoplegia, cerebellar ataxia, cognitive impairment, dysphagia, epilepsy, and stroke – like episode respectively (Ng *et al.*, 2015). It is important as well to note that these neurological manifestations can either manifests acutely or chronically; but, regardless of the timing of its manifestation, these neurological manifestations are known to be progressive and results in neurodegenerative features in these patients over time (Ng and Turnbull, 2016; Lax *et al.*, 2017).

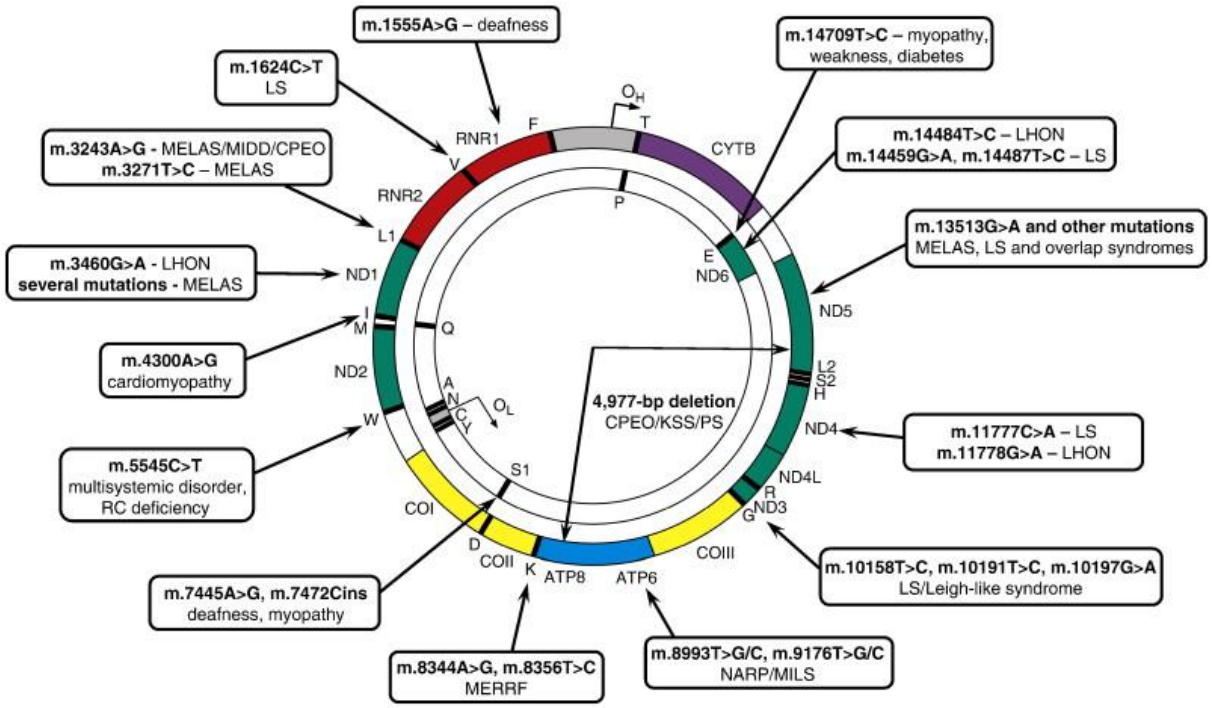

Figure 1-23 Some examples of the common genotype - phenotype correlation in mitochondrial disease. Shown is the mitochondrial DNA along with the common site of mutation and its associated clinical phenotypes. MELAS – Mitochondrial Encephalopathy with Lactic Acidosis and Stroke like episode, LS – Leigh Syndrome, LHON – Leber Hereditary Optic Neuropathy, CPEO – Chronic Progressive External Opthalmoplegia, MERRF – Myoclonic Epilepsy and Ragged Red Fibres, MILS – Maternally Inherited Leigh Syndrome, NARP – Neurogenic Weakness, Ataxia, and Retinitis Pigmentosa, and PS – Pearson Syndrome. Reprinted from Biochimica et Biophysica Acta, Volume 1797, Issue 2, Tuppen et al, Mitochondrial DNA mutations and human disease, Pages 113 – 128, Copyright (2010), with permission from Elsevier.

Although the phenotypic manifestation of mitochondrial disease largely varies, therapeutic strategy for mitochondrial disease, in general, is still lacking and very much in its infancy (Parikh *et al.*, 2009). Hitherto, treatment remains largely supportive and symptomatic and patients with mitochondrial disease tends to have poor prognosis (Avula *et al.*, 2014).

1.10 Mitochondrial epilepsy

The International League Against Epilepsy has proposed the diagnostic criteria of epilepsy as a neurological disease which has any of these conditions: (1) at least two unprovoked seizures occurring more than 24 hours apart; (2) one unprovoked seizure in addition to the risk of further seizures similar to the general recurrence risk after two unprovoked seizures (of at least 60 %), within the next 10 years; or (3) the diagnosis of an epilepsy syndrome (Fisher *et al.*, 2014). Practically, this definition is summarized as such that epilepsy is a disease of the brain where there is increased risk of developing unprovoked seizures.

Patients with mitochondrial disease are known to have a high risk of developing epilepsy. The most current epidemiological study places the overall prevalence of epilepsy in a cohort of patients with mitochondrial disease at 23.1% (Whittaker *et al.*, 2015). The development of epilepsy in patients with mitochondrial disease is fittingly termed ‘mitochondrial epilepsy’.

The manifestation of mitochondrial epilepsy is highly dependent on the clinical phenotype of the patients with mitochondrial disease (Finsterer and Mahjoub, 2013). In the epidemiological study mentioned above, mitochondrial epilepsy is most frequently associated with the m.3243A>G mutation (Whittaker *et al.*, 2015); which as mentioned above is most frequently associated with MELAS (Nesbitt and McFarland, 2011; Mancuso *et al.*, 2014). Epilepsy can also appear as the defining feature of the clinical phenotype of mitochondrial disease; such as in the case of MERRF (Myoclonus Epilepsy with Ragged Red Fiber), where myoclonus epilepsy is one of the characteristic symptoms of such patients (Bindoff and Engelsen, 2012).

Virtually any seizure semiology and combinations can occur in the population of patients with mitochondrial epilepsy (Bindoff and Engelsen, 2012). In the epidemiological study, aside from myoclonus in patients with MERRF, the most common seizure types seen in the cohort as a whole were focal seizures, with or without progression to bilateral convulsive seizures (Whittaker *et al.*, 2015). Indeed, a combination of different types of focal seizures, including motor seizures with or without loss of consciousness and awareness, is a typical observation in patients with mitochondrial epilepsy (Bindoff and Engelsen, 2012; Chevallier *et al.*, 2014). In patients with MELAS, the most common seizure types were generalized tonic clonic seizure,

with generalized or focal epileptiform discharges in the electroencephalogram (EEG) (Chevallier *et al.*, 2014).

The EEG manifestation of epileptiform discharges in patients with mitochondrial epilepsy can also largely vary. An epidemiological study has reported that the most common findings in the EEG of these patients is a generalized slowing (60%) and the most common epileptiform discharges seen in the trace is multifocal (41%), followed closely by focal (39%) and generalized seizures (39%) (Chevallier *et al.*, 2014). It therefore reaffirms that mitochondrial epilepsy is an umbrella term that encompasses a varying epileptic phenotype that can occur in patients with mitochondrial disease (Bindoff and Engelsen, 2012).

The epileptic manifestation in this cohort of patients does not seem to contribute towards overall risk of mortality (Whittaker *et al.*, 2015); however, when left uncontrolled, this severe epileptic phenotype can be extremely debilitating and lead to poor quality of life (Leppik, 2003; Lin and Thajeb, 2007). Mitochondrial epilepsy was reported with a varying degree of pharmacological response to conventional antiepileptics. In the adult population, antiepileptic use is generally well-tolerated and tends to provide early relief and seizure control (Bindoff and Engelsen, 2012; Finsterer and Mahjoub, 2013; Whittaker *et al.*, 2015). In a study in the paediatric population, a larger proportion of the cohort (60%) was found to be pharmacoresistant to initial therapeutic regimen of antiepileptic agents (Khurana *et al.*, 2008). All of these studies, however, agreed that response to antiepileptic drugs tend to deteriorate causing epileptic phenotypes to resurface and are frequently progressive (Leppik, 2003; Khurana *et al.*, 2008; Bindoff and Engelsen, 2012; Finsterer and Mahjoub, 2013; Whittaker *et al.*, 2015).

Mitochondrial epilepsy is clearly a distinct epileptic syndrome that is unique to the other types of epilepsy. It is typically associated with a more severe manifestation of an epileptic phenotype with a degree of pharmacoresistance that is rarely seen in the other epileptic patients. Very few therapeutic recommendations were made for patients with mitochondrial epilepsy. The only clinical guideline that existed was produced in 2010 by the Newcastle Mitochondrial Disease Guidelines and was largely based on clinical and anecdotal experiences (Schaefer *et al.*, 2010). This clearly indicates a gap of knowledge in the understanding of mitochondrial epilepsy. This thesis aims to address this gap and provides a novel approach to understanding this distinctive epileptic syndrome.

1.11 Animal models of mitochondrial epilepsy

Despite the bleak clinical picture of the patient population with mitochondrial epilepsy as described above in section 1.10, there has been very little progress in preclinical studies of mitochondrial epilepsy. One of the biggest aids in preclinical studies aimed at understanding any neurological disorder is the development of an animal model of such disease. To present, there have been a paucity of animal models truly developed for mitochondrial epilepsy and this has been a significant bottleneck in the study of mitochondrial epilepsy.

The only animal model developed that claims to model mitochondrial epilepsy is the *Sod2*$^{-/+}$ mice (Liang and Patel, 2004). This animal model was initially developed on the basis of the understanding of oxidative stress contribution towards epileptic seizure and was not based on any real clinical phenotype of patients with mitochondrial epilepsy. These mice had a partial deficiency of the mitochondrial superoxide dismutase that led them to develop increased incidence of spontaneous and handling-induced seizures (Liang and Patel, 2004). This epileptic phenotype was found to be progressive and associated with mitochondrial aconitase inactivation (Liang and Patel, 2004). Other studies using the same mice model had only mostly characterized the oxidative stress phenotype and had not reported any epileptic or neurological phenotypes (Williams *et al.*, 1998; Van Remmen *et al.*, 1999; Gyung and Pak, 2002; Gupta *et al.*, 2015). Since there is only one study to date that demonstrated an epileptic phenotype in such mice and the modelling of the mice was not based on any clinical phenotype, it is hard to endorse this animal model as capturing mitochondrial epilepsy.

In addition to the *Sod2*$^{-/+}$ mice, various other small studies have reported epileptic phenotype in various animal models exposed to mitochondrial respiratory chain inhibitors. The mitochondrial complex II inhibitor, 3-nitropropionic acid, has been shown to evoke convulsions in a dose-dependent manner in mice (Haberek *et al.*, 2000; Zuchora *et al.*, 2001). However, the 3-nitropropionic acid model was much more relevant and accepted as a model of Huntington Disease, rather than that of mitochondrial epilepsy (Chan *et al.*, 2016). One study has also reported that subcutaneous injection of potassium cyanide caused a dose-dependent tonic seizures in mice (Yamamoto and Tang, 1996). However, again, this model was only used in this single study and has not been replicated. Furthermore, similar to the *Sod2*$^{-/+}$ mice, the

model was not based on the clinical phenotype of patients with mitochondrial epilepsy; thus, the model can largely be said to not reflect mitochondrial epilepsy.

Conversely, a number of studies have focused on the involvement of mitochondria in other models of epilepsy, such as the kainic acid model (Liang *et al.*, 2000; Mohanan and Yamamoto, 2002; Yamamoto and Mohanan, 2003; Chuang *et al.*, 2004), the pilocarpine model (Kudin *et al.*, 2002; Kudin *et al.*, 2004; Gao *et al.*, 2007; Olav *et al.*, 2013), or the status epilepticus model (Cock *et al.*, 2002; Sleven *et al.*, 2006). The major issue with such studies is that the currently available model of epilepsy tends to manipulate specific mechanisms that are virtually impossible to achieve in a clinical setting. Furthermore, each model was found to be specific to the mechanisms manipulated and would fail to identify potential novel antiepileptic agents that do not mediate anticonvulsant effects through the manipulated mechanisms (Löscher, 2011). Thus, whilst it is encouraging to know that mitochondrial dysfunction is intimately involved in these models of epilepsy, it does not progress our specific understanding of mitochondrial epilepsy.

In order to combat this unfocused strategy in the modelling of neurological diseases particularly associated with mitochondrial dysfunction, a framework has been developed and proposed to prevent such shortcomings (Chan *et al.*, 2016). Four main stages are identified, namely: (1) the extrapolation of findings from human neuropathological and/or electrophysiological studies, (2) a pilot study using *in vitro* brain slice electrophysiological study to recapitulate the findings extrapolated, (3) validation of the model using various techniques, and (4) further extrapolation (see Figure 1-24). The effort in modelling mitochondrial epilepsy described in this thesis will largely follow such proposed framework to avoid any pitfalls in the process of *in vitro* modelling.

1.12 In vitro brain slice electrophysiology

The framework, as proposed above, has recommended the use of *in vitro* brain slice electrophysiology as a pilot study for the understanding of the electrophysiological correlate of mitochondrial dysfunction. The use of a brain slice as an *in vitro* model was pioneered by Henry McIllwain, who was first and foremost a neurochemist (Collingridge, 1995). Therefore, there is already such a rich historical precedence in

the use of a brain slice model in neurometabolic study. In addition, current neuroscientists have adapted the brain slice model as the gold standard for *in vitro* electrophysiological study aimed at the understanding of cellular and molecular processes underlying such electrophysiological process (Ting *et al.*, 2014). Originally conceived to be a model strictly for use in animals, the brain slice model has evolved even further and it is now possible to ethically obtain electrically active human brain slices from patients undergoing elective neurosurgical procedures (Jones *et al.*, 2016). Furthermore, it is now possible to maintain the brain slices in a culture setting in a technique called the 'organotypic brain slice culture' (Humpel, 2015).

From an electrophysiological standpoint, the basic approach used in a brain slice is extracellular local field potential recording, which shows the electrical network potential generated by the summation of the electrical currents flowing from a population of cells around the recording electrode (Sharott, 2013). A further step is the recording of individual cellular electrophysiological activity through the use of either patch clamp or sharp electrodes (Li *et al.*, 2004). Such an approach is useful in dissecting the functional property of specific cellular population during an electrophysiological phenomenon, but should always be paired with local field potential recordings so that such correlation can be made. Technological advances have also led to the development of the multielectrode array, that allows simultaneous electrophysiological recordings from multiple channels and allow temporal and spatial analysis of such electrophysiological phenomenon (Ferrea *et al.*, 2012). Finally, recent techniques have started to incorporate optogenetics, a genetic manipulation that would allow modulation and control of specific cellular population using light, in electrophysiological recordings from brain slices and opened up a whole new avenue in the understanding of cellular mechanisms underlying an electrophysiological system (Ting *et al.*, 2014).

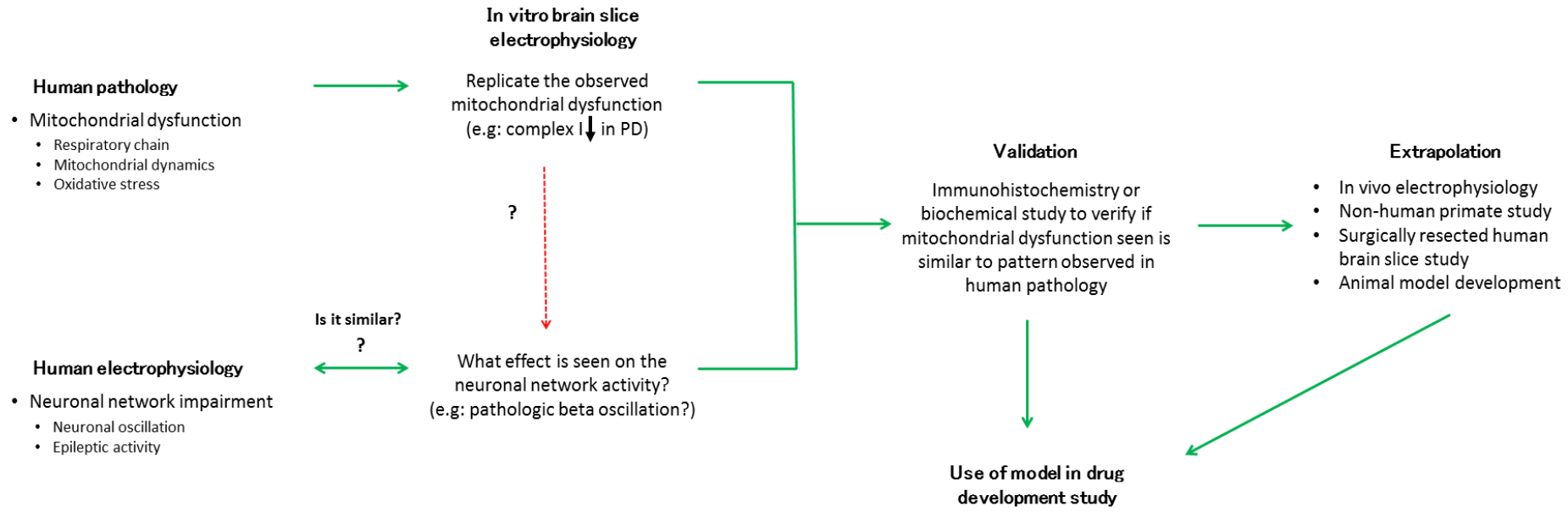

Figure 1-24 A neuropharmacological framework to understanding electrophysiological correlate of mitochondrial dysfunction. This framework was originally developed within the context of neuronal oscillation as a physiological correlate for mitochondrial dysfunction, but is readily applicable to the modelling of mitochondrial epilepsy. Reprinted with slight modification from Neuropharmacology, Volume 102, Chan et al, Neuronal oscillations: A physiological correlate for targeting mitochondrial dysfunction in neurodegenerative diseases?, Pages 48-58, Copyright (2016), with permission from Elsevier.

In addition to the wide variety of electrophysiological techniques that are employable in a brain slice setting, many other techniques are also useful and feasible to conduct in acute brain slice preparations. Live cell imaging allows the examination of various dynamic cell processes (such as the Ca^{2+} imaging) on a real-time setting (Dailey *et al.*, 2011). The use of various biosensors (such as the oxygen-sensitive microelectrodes) also allows for real-time imaging of biochemical processes in the slice as it incubates in various experimental conditions (Huchzermeyer *et al.*, 2008). The preservation of the brain slices in fixative following various experiments also allows for *post-hoc* examination of the cellular population using specific antibody-mediated immunohistochemistry or immunofluorescence (Park and Cunningham, 2007). The possibility of techniques that are usable in a brain slice setting, therefore, is endless and with continuous advancement of technology and knowledge, more advanced and delicate probing would even be possible in such a crude preparation.

Although the brain slice is a powerful platform for the understanding of cellular and molecular mechanisms underlying a neurological process, it is far from perfect and does have its own drawbacks and pitfalls as well. The largest criticism in the use of brain slice is its isolation of the studied structure from the overall neuronal network and connections that would have been present *in vivo*. The absence of wider networks and large scale connections could alter the functional profile of the structure studied and thus may undermine the relevance of the results found when translating the findings to an *in vivo* setting. Furthermore, the viability of the cells and tissue are highly susceptible to the brain slice preparation process and although this has been combatted in recent studies with the introduction of various ‘neuroprotective’ artificial cerebrospinal fluid media, one cannot ignore that the use of such ‘neuroprotective’ media may also alter the profile of such tissue from the actual *in vivo* setting (Buskila *et al.*, 2014; Ting *et al.*, 2014). Hence, whilst the use of acute *in vitro* slice preparation is favourable in its wide array of feasible techniques, the results from such a study should be critically analysed and be extrapolated to *in vivo* studies whenever possible (refer back to the framework described in Figure 1-24).

1.13 Temporal lobe and hippocampus in epilepsy

In epilepsy study, it is well known that the origin of a large proportion of the epileptiform discharges (estimated at about 60%) is from the temporal lobe (Téllez-Zenteno and Hernández-Ronquillo, 2012). It is such a large proportion that such cluster of epileptic manifestation is aptly referred to as 'temporal lobe epilepsy' (Engel Jr, 1996). Therefore, epilepsy study and modelling has largely focused on the development of a model using the temporal lobe as a focused area of interest.

Out of all the structures in the temporal lobe, the hippocampus has received significant coverage. This has originated from the finding that a large proportion of patients with temporal lobe epilepsy have a sclerotic hippocampus (Thom, 2014) and the removal of such sclerotic hippocampi led to the development of the epileptic surgical treatment for patients with temporal lobe epilepsy (Feindel *et al.*, 2009). These findings have solidified the place of hippocampus as a generator of epileptiform discharges in such patients (Avoli, 2007).

In addition to the reasons mentioned above, the structure of hippocampus, both in humans and rodents, have been extensively studied and characterized (Seress, 2007). Therefore, from a modelling standpoint, it provides advantages in that the cellular populations and functional profile of the underlying connections have been largely identified in previous studies.

The hippocampal anatomy will now be briefly reviewed below (Bear *et al.*, 2016a). The hippocampus is a subcortical structure located deep in the temporal lobe and is surrounded by the parahippocampal cortices (see Figure 1-25). The hippocampus comprises of two thin sheets of neurons that are folded onto each other; namely the dentate gyrus and the Ammon's horn. The Ammon's horn is further subdivided into four divisions: the CA1, CA2, CA3, and CA4 (CA stands for *Cornu Ammonis*, the Latin for Ammon's horn). This CA subfield is further subdivided into multiple layers (or strata); namely the stratum oriens, stratum pyramidale, stratum lucidum, stratum radiatum, stratum lacunosum, and stratum moleculare (see Figure 1-26). This stratum suborganization is important in the anatomical distribution of the cells of the hippocampus but the most important and by far, the most visible to the naked eye, is the stratum pyramidale. Stratum pyramidale is a distinct layer that is visible due to its dense organization of the cell bodies of the pyramidal cells and to a lesser degree, the interneurons of the hippocampus (Freund and Buzsaki, 1996).

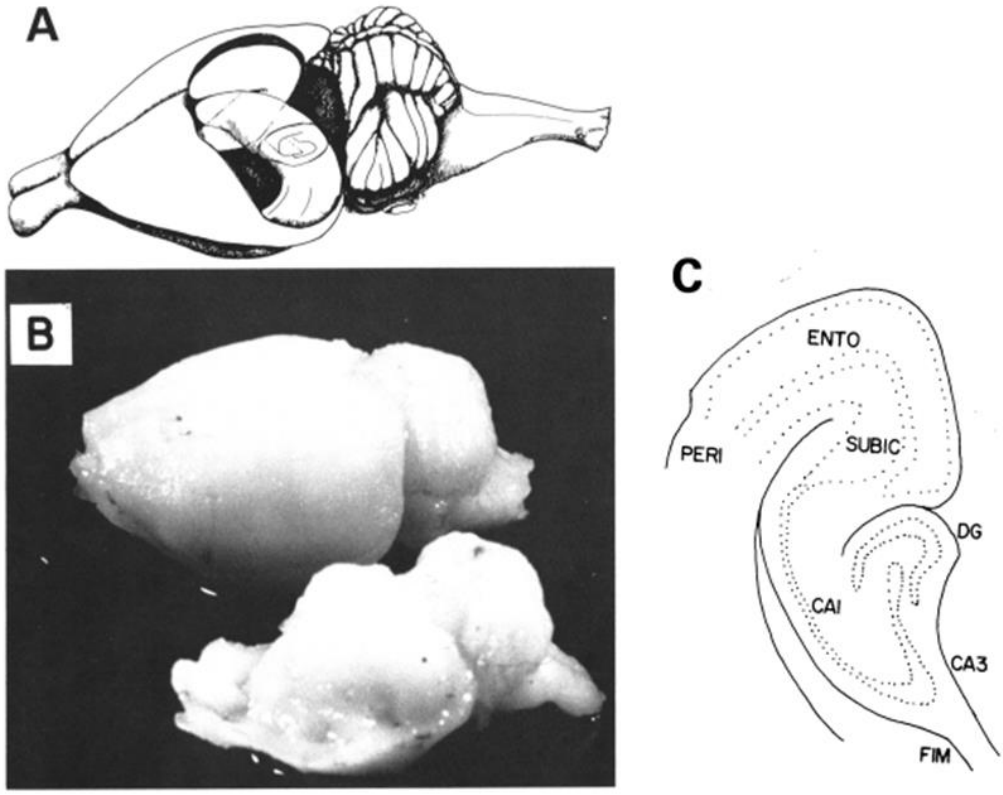

Figure 1-25 Macroanatomy of hippocampus. Shown in (A) is an illustration of the exposed hippocampus of the rat in situ. In (B) is a photograph of a rat brain with one side intact and the other side with the hippocampus exposed. In (C) is the illustration with anatomical labels corresponding to the structures of the hippocampus and the surrounding parahippocampal structures. DG – dentate gyrus, ENTO – entorhinal cortex, FIM – fibrria, PERI – perirhinal cortex, SUBIC – subiculum. Reprinted from Brain Research Bulletin, Volume 12, Issue 6, Teyler TJ and Discenna P, The topological anatomy of the hippocampus: A clue to its function, Pages 711-719, Copyright (1984), with permission from Elsevier.

From a neuroenergetic standpoint, the hippocampus has been shown to have a strong association between the neuroenergetic profile and the cognitive state that it is largely responsible for in physiological conditions (Rowe *et al.*, 2007; Kann *et al.*, 2011). Specifically, the CA3 seems to be the most energy-demanding region of the hippocampus and is tightly correlated with the higher power of neuronal gamma oscillation as compared to the CA1 (Kann *et al.*, 2011). This was further supported by the finding that some of the interneurons in the hippocampus CA3 have a higher expression of mitochondrial cytochrome c, as compared to the same population of interneurons in the dentate gyrus (Gulyás *et al.*, 2006).

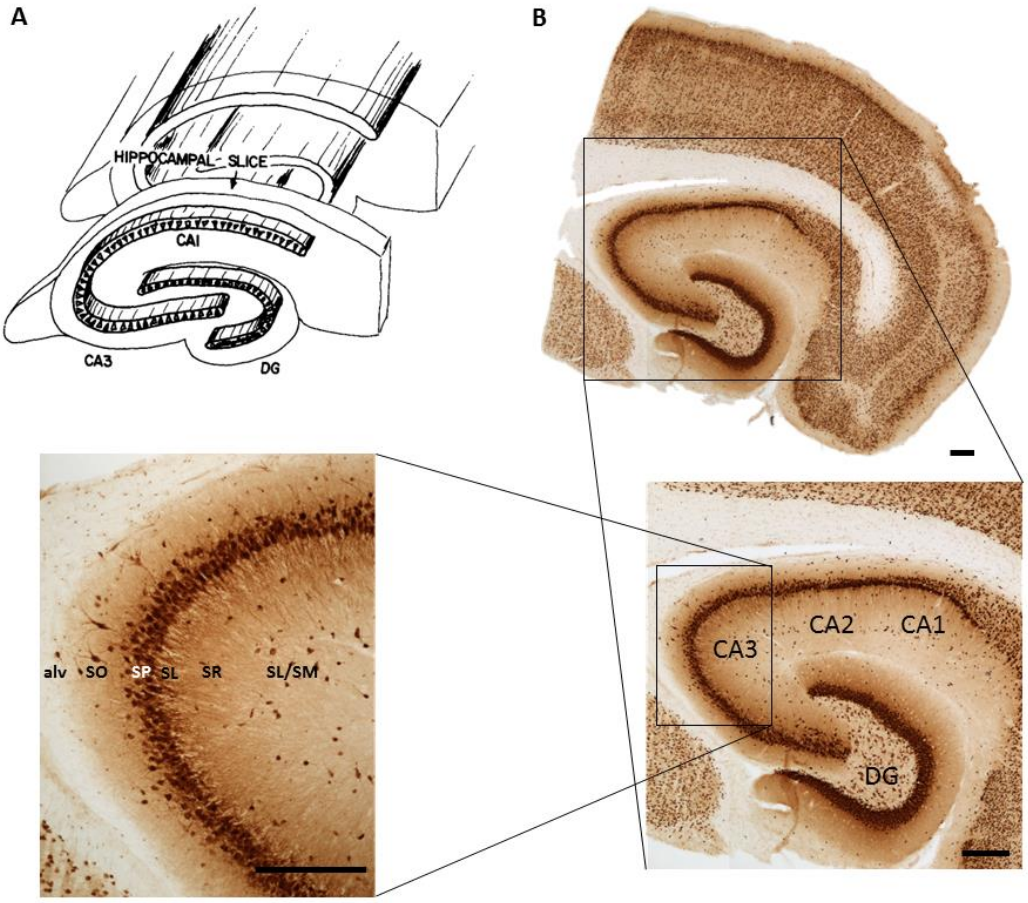

Figure 1-26 Hippocampus proper and the subdivisions. Shown in (A) is the illustrated diagram of the hippocampus proper after isolated and sliced. The CA1, CA3, and DG subfields are illustrated in the diagram. Shown in (B) is a photograph of a typical hippocampal brain slices that have been immunostained for NeuN to label the whole neuronal population in the slice. Zoomed in is the hippocampus proper and the respective subdivisions labelled. The CA3 is magnified further to showcase the layers (or strata) of the hippocampal CA subfield. In white is the stratum pyramidale, that is clearly different from the other layers of the hippocampal CA and is dense with neuronal cell bodies. DG – dentate gyrus, alv – alveus, SO – stratum oriens, SP – stratum pyramidale, SL – stratum lacunosum, SR – stratum radiatum, SL/SM – stratum lacunosum and stratum moleculare. Figure (A) is reprinted from Brain Research Bulletin, Volume 12, Issue 6, Teyler TJ and Discenna P, The topological anatomy of the hippocampus: A clue to its function, Pages 711-719, Copyright (1984), with permission from Elsevier. Scale bar 100µm.

1.14 Pharmacological treatment of epilepsy

The first-line treatment for epilepsy is the use of a pharmacological group of drugs, the antiepileptics, to try and achieve seizure control (or more significantly, seizure freedom). It is important to acknowledge that the conventionally available antiepileptic regimen is largely symptomatic, in that it controls seizure effectively. Neither effective prophylaxis nor disease-modifying treatment is currently available for epilepsy (McNamara, 2011).

The mechanism of action of an antiepileptic largely falls into three major categories: (1) the limitation of sustained, repetitive firing of neurons; (2) the potentiation of GABA-mediated synaptic inhibition; and (3) inhibition of voltage-activated Ca^{2+} channels, a mechanism specific to that of absence seizure (McNamara, 2011) (see Figure 1-27). Within this diverse category of antiepileptic mechanism of actions, there is further subdivision of mechanisms that further classify these drugs into their respective families (such as sodium channel blockers or benzodiazepines).

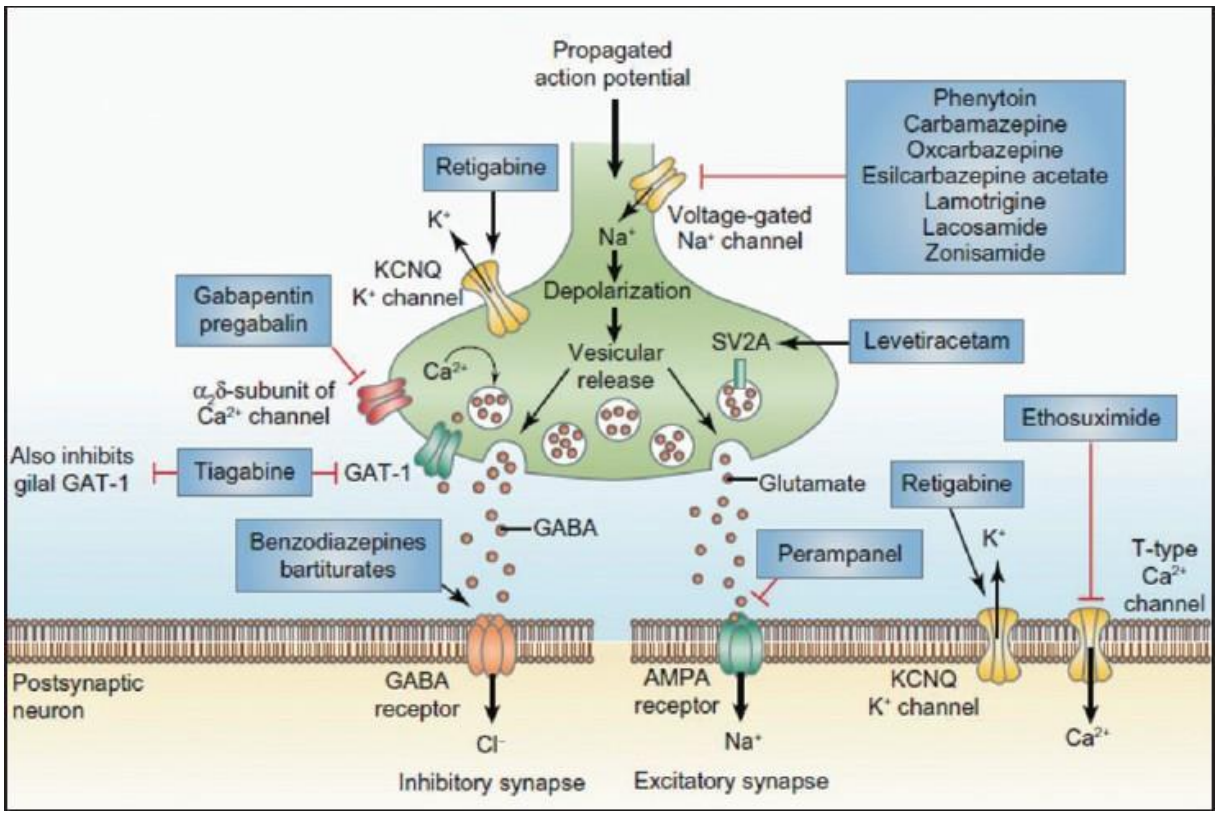

Figure 1-27 Mechanism of action of conventional antiepileptic drugs. Shown are the conventional antiepileptic drugs and the proposed main mechanism of actions. Largely, the antiepileptic drugs either exert its anticonvulsant activity through the taming of excitatory input or the potentiation of inhibitory input. Reprinted from Muller Journal of Medical Sciences and Research, Volume5, Issue 2, Singh SK and Brashier DBS, Perampanel: New drug for treatment of refractory partial onset seizures, Copyright (2014) as an open – access article distributed under the terms of the Creative Commons Attribution License.

There are currently about 28 antiepileptic drugs licensed for use in the United Kingdom (Sills, 2014). Even with this large choice of antiepileptic drugs, a significant proportion of the epileptic patients remains pharmacoresistant and could not achieve seizure freedom with conventional antiepileptics. In a population study in France, this number was placed at 15 % (Picot *et al.*, 2008); however, in the United Kingdom, this number was slightly higher and ranges from between 30 to 60 % (Kwan and Brodie, 2000; Tidman *et al.*, 2003). A proportion of these pharmacoresistant epilepsy patients can be attributed to mitochondrial epilepsy (Bindoff and Engelsen, 2012).

It is unclear what leads to this dichotomy in pharmacological response to antiepileptics. Clinically, there are predictors for negative response towards antiepileptic regimen, such as a higher pre-treatment seizure frequency (Hitiris *et al.*, 2007). The advent in pharmacogenomics has also suggested some potential genetic properties, such as the polymorphism in cytochrome P450, that can lead to this difference in pharmacological response (Glauser, 2011). Finally, interestingly, it was suggested that mitochondrial dysfunction in epilepsy may contribute towards pharmacoresistance (Yuen and Sander, 2011).

Despite the varying response of epileptic patients towards the antiepileptics, it should be acknowledged that there is still a large proportion of patients that do respond to these pharmacological treatments. Therefore, following the development of a new model of any form of epilepsy, pharmacological screening should be employed for these conventional antiepileptics. This will help provide an evidence-based therapeutic recommendation for the epileptic syndromes studied. Clinically, however, it should always be remembered that therapeutic regimen should be specifically tailored towards each patient's responses and form the basis of personalized medicine (Walker *et al.*, 2015).

1.15 Non-pharmacological treatment of epilepsy

1.15.1 Ketogenic diet

The ketogenic diet is by far, the most well-known and well-studied non-pharmacological intervention in epilepsy. It is a dietary intervention with the aim of increasing ketone bodies production; that surprisingly was found to have a capacity to control intractable seizure (Branco *et al.*, 2016). The diet has been in use since 1921 and is still in use in present days due to its time-tested efficacy, safety, and tolerability profile (Nordli and De Vivo, 1997). The classical ketogenic diet regime is highly restrictive, with ratios of fat to protein and carbohydrate combined of 3-4:1 with moderate energy restriction (Miranda *et al.*, 2012). Since then, the regime has evolved to a more lax regimen such as the medium chain triglycerides (MCT) diet with 30 to 60% of the energy obtained from MCT (Huttenlocher *et al.*, 1971), the modified Atkins diet (Kossoff *et al.*, 2006), and the low glycaemic index diet (Muzykewicz *et al.*, 2009). Across the classical and the alternative diets, the efficacy is largely promising and supports the use of any of these diets in treatment of intractable epilepsy (Miranda *et al.*, 2012).

The ketogenic diet is traditionally used in childhood (Neal *et al.*, 2008), although evidence has existed of efficacy in adults (Sirven *et al.*, 1999). In patients with mitochondrial epilepsy, ketogenic diet was also reported to have efficacy. In a small study of paediatric population with mitochondrial epilepsy, 50 % of the patients were able to achieve seizure freedom with the diet (Kang *et al.*, 2007). Furthermore, various case studies have reported on the success of seizure control in patients with mitochondrial epilepsy using the ketogenic diet (Martikainen *et al.*, 2012; Steriade *et al.*, 2014). These findings warrant further investigation into the efficacy of ketogenic diet as treatment of mitochondrial epilepsy.

Despite the large clinical evidence on the efficacy of the ketogenic diet, the mechanisms whereby the diet exerts its anticonvulsant effects is largely unknown and controversial (reviewed elegantly in (Nylen *et al.*, 2009) and (de Lima *et al.*, 2014)). The mechanisms that will be largely discussed in this study arises from the findings that the medium chain fatty acid, decanoic acid, was able to inhibit epileptiform discharges acutely due to inhibition of the AMPA-R (Chang *et al.*, 2015). This fatty acid was also found to modulate mitochondrial function by increasing mitochondrial complex I activity (Hughes *et al.*, 2014). Furthermore, decanoic acid and also octanoic

acid were found to modulate astrocyte ketogenesis (Thevenet *et al.*, 2016). Although all these findings are exciting, it should be recognized that many other hypothesis have been proposed for the mechanisms of ketogenic diet; such as the pH hypothesis, the metabolic hypothesis, the GABA shunt hypothesis, and the ketone hypothesis (Nylen *et al.*, 2009).

1.15.2 Surgical intervention

As briefly mentioned above, surgical treatments do exist for patients with intractable epilepsy and these typically represent last-line treatment options for such patients (Engel, 2003). Surgical treatments in epilepsy have a promising degree of success with a randomized clinical trial reporting 70% of patients with early surgical intervention able to achieve seizure freedom (Engel *et al.*, 2012). However, these surgical treatments largely depend on accurate localization of the seizure foci and may not be possible in patients where such foci are in the eloquent cortex. Furthermore, significant cognitive deterioration has been reported in some proportion of patients with epileptic surgery, even when such surgery afforded them seizure freedom (Baxendale, 2008). The increasing use of advanced imaging techniques (Raybaud *et al.*, 2006), brain stimulation (Jobst, 2010), and comprehensive pre-surgical electroencephalographic mapping (Zijlmans *et al.*, 2007) have somewhat circumvented these issues but the surgical regime currently available is far from perfect and is not suitable for just any patients with epilepsy.

No studies have been done on evaluating the use of surgical intervention for seizure control in patients with mitochondrial epilepsy. This is partly due to the difficulty in offering such option to these subset of patients as neurosurgical procedure requires general fitness and patients with mitochondrial disease tend to have multiorgan involvement. This would deem them an unsuitable patient group for surgical consideration.

The use of surgical intervention in patients with neurological disorders (such as epilepsy and tumour) has provided neuroscientists with the potential of obtaining acute human brain samples removed from these surgeries. This has led to the development of an array of human brain slice electrophysiology studies (Jones *et al.*, 2016), which provide strength in its direct examination of mechanisms specific to human.

1.15.3 Vitamin and supplements

In patients with mitochondrial epilepsy, physicians tended to treat the epileptic syndrome as a holistic approach towards therapy for mitochondrial disease and in their therapeutic regimens, they may have resorted to the use of various nutritional supplements and vitamins (elegantly reviewed in (Parikh *et al.*, 2009) and (Avula *et al.*, 2014)). These treatments are often referred to as 'mitochondrial treatment cocktail' and the most common starting composition are a combination of CoQ10 and a B vitamin (see Table 1-2) (Parikh *et al.*, 2009). These vitamins and supplements have not been assessed for efficacy and safety in a rigorous controlled clinical trial. The success in the use of these supplements, therefore, has largely been based on anecdotal evidence (Chinnery and Turnbull, 2001). Some have claimed that these supplements do not make a significant difference in patients with mitochondrial disease (Matthews *et al.*, 1993); whereas others have praised its benefits and efficacy (Hargreaves, 2014). Regardless, until proper clinical guidance based on pre-clinical and clinical evidence is produced, physicians are going to continue treatment for their patients with the only treatment option that they can offer, which is a personalized mitochondrial treatment cocktail.

Table 1-2 Typical composition of mitochondrial treatment cocktail. Table adapted from (Parikh et al., 2009).

Medication	**Dosage (adult)**	**Monitoring**	**Adverse effects**	**Comments**
CoQ10 as ubiquinol (preferred)	50-600 mg po daily	Pretherapy level and monitor CoQ1 level in leukocytes or plasma	Wakefulness, disruption of sleep, may interfere with warfarin concentration	Solubilized bioavailable formulation preferred. Absorption may improve when taken with meals
CoQ10 as ubiquinone	300-2400 mg po daily, 2-3x a day	Pretherapy level and monitor CoQ1 level in	Wakefulness, disruption of sleep, may interfere with warfarin concentration	Solubilized bioavailable formulation preferred. Absorption may

		leukocytes or plasma		improve when taken with meals
Riboflavin (B_2)	50-400 mg po daily	Not usually done	High doses may lead to anorexia and nausea	Change urine color and smell; less effects by bedtime administration
L-creatine	5 g po daily 1-2x a day	Renal function	Gastrointestinal upset	Primarily for myopathy patients
L-arginine	Acute stroke: 500mg/kg IV per day for 1- 3 days Maintenance: 150-300mg/kg PO or IV daily 2-3x a day	Plasma arginine	Hypotension (due to IV loading), hyponatremia, headache, nausea, diarrhea, myelinolysis (high dose)	Used with metabolic strokes, particularly in MELAS or those with low-normal plasma arginine; citrulline is used as alternative in urea cycle defects
L-carnitine	100-1000mg per dose, IV or po 2-3x a day	Pretherapy free and total plasma carnitine	GI upset, fishy odor, cardiac rhythm disturbances (in LCFA defects)	Only 10-20% absorbed. Acetyl-carnitine is an alternative
B50 or B100	1 tab po 1-2x a day	Not done	Toxic neuropathy (chronic large dose)	Poor palatability
Vitamin E	100-200 IU po daily	Not done	Possible cardiac risks at >400 IU/day	Absorption may improve when taken with meals
Vitamin C	50-200mg po daily	Not done	Increases iron absorption; high doses may	Easily absorbed water-soluble vitamin

			cause renal insufficiency	
Alpha-lipoic acid	50-200mg/d	Not done	Not known	None
Folinic acid as leucovorin	2.5-25mg po daily 1-2x a day	Spinal fluid folate and plasma / urine pipecolic acid	Rash and pruritus	Cerebral folate can be replenished with L-leucovorin or 5-methyl tetrahydrofolate.

1.16 Working hypothesis to understand mitochondrial epilepsy

Section 1.10 has outlined in detail the clinical features of mitochondrial epilepsy and subsequently, section 1.11 has reviewed currently available animal models for mitochondrial epilepsy. Whilst the clinical characteristics of mitochondrial epilepsy are relatively well studied, there is clearly a lack of animal models for mitochondrial epilepsy. This, in turn, leads to a lack of studies exploring the mechanisms behind the generation of mitochondrial epilepsy. Several reviews have attempted to address this by proposing various working hypothesis for the mechanisms underlying seizure generation in mitochondrial epilepsy (see one of the working hypothesis in Figure 1-28 and for the reviews, refer to (Zsurka and Kunz, 2015) and (Rahman, 2015))). However, all the mechanisms proposed in these reviews are based on inferences and theoretical postulation of possible underlying defects in neurotransmission caused by the primary mitochondrial deficiency. Very few experimental evidences have been provided to clearly support the mechanisms proposed. Therefore, more work needs to be done before such hypothesis on the pathophysiological mechanisms of mitochondrial epilepsy can be confidently used.

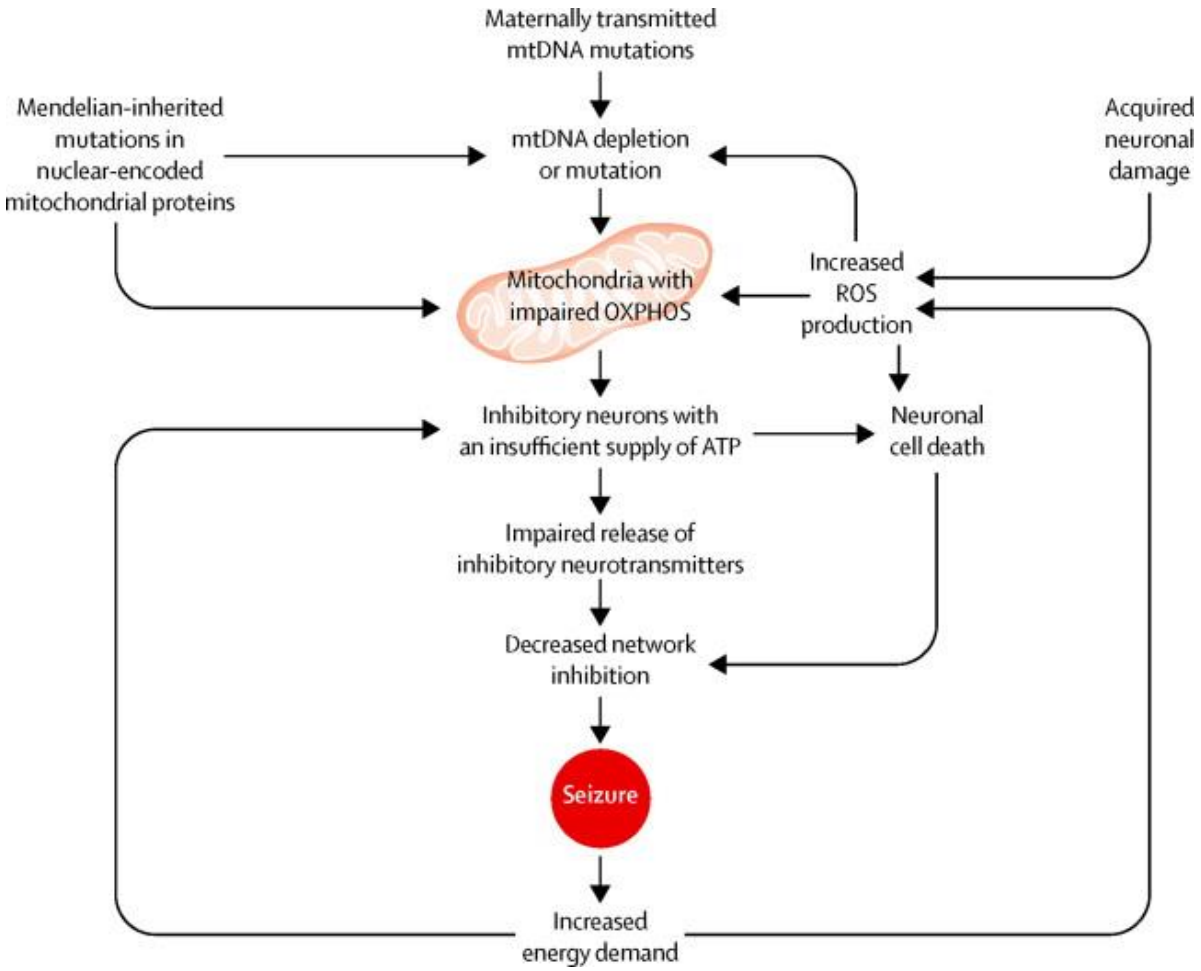

Figure 1-28 Current proposed working hypothesis for mechanisms underlying seizure generation in mitochondrial epilepsy. Reprinted from The Lancet Neurology, Volume 14, No 9, Zsurka G and Kunz WS, Mitochondrial dysfunction and seizures: the neuronal energy crisis, Pages 956-966, Copyright (2015), with permission from Elsevier.

There are, however, several mechanisms that are agreed upon by both reviews on seizure generation in mitochondrial epilepsy. Both reviews agreed that there must be some form of energy deficiency in the brain following the primary mitochondrial defects (Rahman, 2015; Zsurka and Kunz, 2015). Furthermore, both reviews also alluded to oxidative stress as the primary source of disruption in neurotransmission that would lead to seizure generation (Rahman, 2015; Zsurka and Kunz, 2015). It is proposed that due to the sensitivity of inhibitory interneurons and the astroglial and neuronal glutamate transporters to oxidative stress; that this is a very likely scenario in patients with primary mitochondrial defects (Zsurka and Kunz, 2015). Again, however, experimental evidence has not arisen to support this mechanism and as such, to this present time, this working hypothesis is still a putative pathophysiological mechanism.

1.17 Oxidative stress in epilepsy

As mentioned above, one of the mechanisms that is largely promising and agreed upon to be an important mechanism in seizure generation in mitochondrial epilepsy is oxidative stress (Rahman, 2012; Zsurka and Kunz, 2015). Oxidative stress is defined as the homeostatic imbalance where the production of reactive oxygen species (free radicals) could not be balanced with the antioxidant defence system (Betteridge, 2000). The major endogenous source of the reactive oxygen species is mitochondria, especially in those lacking the supercomplex organization (Ott *et al.*, 2007; Maranzana *et al.*, 2013).

In the brain, under oxygen saturation, about 1% of the respiratory chain electron flow is redirected towards production of reactive oxygen species in the form of superoxide and this can largely be attributed to complex I – mediated respiration (Kudin *et al.*, 2008). This is confirmed in a study using in situ mitochondria and further extended the finding to the TCA cycle α-ketoglutarate dehydrogenase as a potential source of reactive oxygen species that furthers the vicious cycle of oxidative stress (Adam-Vizi, 2005). Within the cellular population of the brain, mitochondrial supercomplexes of complex I is more frequently associated with neurons and so very few reactive oxygen species is produced by neuronal mitochondrial respiration (Lopez-Fabuel *et al.*, 2016). This is in direct contrast with astrocytes, where the predominating form of complex I is the free form, therefore, their mitochondrial respiration significantly generates reactive oxygen species (Lopez-Fabuel *et al.*, 2016). However, this is balanced by the strong antioxidant defence mechanism in astrocytes, mediated by the Nrf2-regulated pathway (Baxter and Hardingham, 2016).

Oxidative stress has been implicated in various neurological disorders, including epilepsy (Popa-Wagner *et al.*, 2013). In epilepsy, oxidative stress has been implicated in various models of epilepsy and the quenching of oxidative stress was repeatedly reported in various antiepileptic mechanisms of action (Devi *et al.*, 2008; Waldbaum and Patel, 2010; Shin *et al.*, 2011). However, there remains no clear consensus on how oxidative stress can contribute towards seizure generation. Seizure-induced oxidative stress has been reported to damage almost every macromolecule in the brain, from proteins, lipids, mitochondria (and mitochondrial DNA), and antioxidant mechanisms (Waldbaum and Patel, 2010). Therefore, the effect of oxidative stress

should probably be considered in the context of the individual model or characteristics of epilepsy in question.

With regards to mitochondrial epilepsy, the only experimental evidence available to support the involvement of oxidative stress is the *Sod2*$^{-/+}$ mice (Liang and Patel, 2004). Their spontaneous epileptic phenotype was associated by the authors with mitochondrial aconitase inactivation due to superoxide damage (Liang and Patel, 2004). Whilst this seems promising, this is a single study and a single evidence in an animal model that is not based on any clinical conditions. Therefore, very little can be said to confidently support that oxidative stress is indeed involved in mitochondrial epilepsy. However, this finding certainly provides promising evidence that oxidative stress may be associated with mitochondrial epilepsy.

1.18 Aims

The aims of this study are briefly summarized as follow:

1. To develop a novel *in vitro* brain slice model of mitochondrial epilepsy based on the neuropharmacological framework as proposed in Figure 1-24.
2. To examine the mechanisms underlying seizure generation in the model of mitochondrial epilepsy; utilizing various approaches such as electrophysiological, histopathological, and biochemical approach.
3. To conduct extensive pharmacological study and screening using the developed novel *in vitro* brain slice model of mitochondrial epilepsy.

These aims largely conform to the three overarching theme of this thesis on the understanding of the mitochondrial epilepsy: (1) the **conceptualization** of a new *in vitro* model of mitochondrial epilepsy, (2) the understanding of the **mechanisms** involved in seizure generation in mitochondrial epilepsy, and (3) the conduct of pharmacological study and screening to provide direct evidence-based recommendations and **therapeutic implications.**

Chapter 2 General methods

2.1 Animal provision

Adult male Wistar rats aged 10-12 weeks were obtained from Charles River Laboratories Inc. and housed in the Centre for Comparative Biology at Newcastle University under standard housing conditions. For some experiments in this thesis, I have used adult male C57 Black 6 mice (C57BL/6) aged 8-10 weeks, obtained from the same supplier.

Works presented in Chapter 5 were conducted at the University of Copenhagen. Adult male Wistar rats aged 10 weeks old were obtained from Charles River Laboratories Inc. and housed in the animal housing facility under standard housing conditions.

2.2 Brain slice preparation

All experimental and surgical procedures were carried out in accordance to the UK Animals (Scientific Procedures) Act 1986 with the approval of the Newcastle University Ethical Review Committee. All procedures were conducted under the following personal and project licenses granted by the UK Government Home Office:

- Felix Chan : PIL no 1886FA8EB
- Mark Cunningham : PPL no 60/4455

For works conducted at the University of Copenhagen, all experimental procedures were in accordance with the Danish National Ethics Committee and the European Convention ETS 123 of 1986.

2.2.1 Solutions for brain slice preparation

Normal-artificial cerebrospinal fluid (nACSF) contained 126mM NaCl, 3mM KCl, 1.25mM NaH_2PO_4, 1mM $MgSO_4$, 1.2mM $CaCl_2$, 24mM $NaHCO_3$, and 10mM glucose. Sucrose-artificial cerebrospinal fluid (sACSF) had the same composition, except for 2mM $MgSO_4$ and 2mM $CaCl_2$, and the substitution of equimolar 252mM sucrose for

the 126mM NaCl. All the salts used for the ACSF were obtained from VWR or Sigma Aldrich.

2.2.2 Slice Preparation (for *in vitro* electrophysiology)

Animals were given the inhaled anaethetic isoflurane (IsoFlo® - Abbott Laboratories Ltd UK). Following loss of consciousness, animals were injected intramuscularly with a mixture of ketamine (0.3 ml) (Narketan® 100mg/ml – Vetoquinol, UK) and xylazine (0.3 ml) (Xylacare® 20mg/ml – Animalcare, UK). Various reflexes were then assessed to measure depth of anaesthesia, including pedal withdrawal, tail pinch, and eye blink. Once reflexes disappeared, a midline incision was made across the abdomen. The diaphragm was sectioned to expose the heart. A catheter was inserted into the left ventricle and a small cut was made on the right atrium. Transcardial perfusion with ice-cold oxygenated (95% O_2/ 5% CO_2) sACSF was then conducted. The rat was then decapitated and the brain was extracted carefully and rapidly. The cerebellum was removed and the brain was sliced to 450µm thick slices along the horizontal axis using the 5100mz Vibratome (Campden Instruments, UK). Slices were then collected and trimmed down leaving behind the hippocampus and parahippocampal cortices. Slices were then transferred into a holding chamber and maintained at an interface between the nACSF and carbogen gas at room temperature for one hour to equilibrate.

2.2.3 Slice Preparation (for metabolic studies)

Animals were euthanized through decapitation using the guillotine. The head was immediately submerged in slushed sACSF saturated with carbogen gas (95% O_2/ 5% CO_2). The brain was then extracted carefully and rapidly. The hippocampi were separated from the cortices through gentle manual dissociation using the spatula. The hippocampi were then dissected and sliced along the coronal axis into 350µm thick slices using a McIlwain tissue chopper (The Vibratome Company, USA). Slices were then separated under a dissecting microscope and four hippocampal slices were placed in each chamber (for details on the incubation system, see section 2.11)**.** Slices were allowed to recover from slicing by incubation in nACSF for 30 minutes at 37^0C before any experimental manipulation.

2.3 Surgical human tissue collection and slice preparation

For some experiments, I have used human cortical slices obtained from routine neurosurgical procedures using protocols as described previously (Roopun *et al.*, 2010; Cunningham *et al.*, 2012; Simon *et al.*, 2014). Data from human slice studies presented in this thesis were obtained from 6 patients (two males; four females; mean age, 34.00 ± 4.50 years; range, 23-53 years; median 32.5 years); four of whom had medically intractable epilepsy and two of whom had peritumoural epilepsy; undergoing elective neurosurgical tissue resection. All patients had given their written informed consent, prior to the surgery, for use of the resected brain tissue. The study was approved by the County Durham and Tees Valley 1 Local Research Ethics Committee (06/Q1003/51; date of review 3 July 2006), and had clinical governance approved by the Newcastle upon Tyne Hospitals NHS Trust (CM/PB/3707). All aspects of the study conformed with The Code of Ethics of the World Medical Association (Declaration of Helsinki) as printed in the British Medical Journal (18 July 1964). Details on these 6 patients are summarised in Table 2-1.

Human slices were obtained from material removed as part of the elective neurosurgical treatment of the various conditions as described. Anaesthesia induction was conducted with intravenous remifentanil with or without alfentanil (0.2-0.4 and 1mg/kg respectively). Following the induction, a bolus dose of propofol (1-2 mg/kg) was administered intravenously. The patient also received the muscle relaxant, vecuronium (0.1mg/kg). After anaesthesia was established, it was maintained with remifentanil, oxygen, and desflurane at a minimum alveolar concentration volume of 0.5-1.0. Resected tissue was immediately transferred to oxygenated ice-cold sACSF and transported to the laboratory with transport time of under 5 minutes. Neocortical slices were cut into 450μm thick slices using the Microm HM 650V vibratome (Thermo Fisher Scientific, UK). They were then incubated in the holding chamber containing nACSF at room temperature for an hour prior to any experimentation.

Table 2-1 Summary of patient information.

No	Age at surgery (years)	Gender	Seizure semiology	Pathology	Type of surgery*	Brain region	Surgical outcome	Antiepileptic medication**
1	25	F	Complex partial seizures	Mesial temporal sclerosis	SAH	Right temporal lobe	Seizure-free with post-op nystagmus	CBZ
2	38	M	Complex partial seizures	Hippocampal sclerosis	SAH	Left temporal lobe	Seizure-free	VPA/ECBZ/LEV
3	23	F	Complex partial seizures	Mesial temporal sclerosis	SAH	Left temporal lobe	Seizure-free	LEV
4	29	F	Complex partial seizures	Mesial temporal sclerosis	SAH	Right temporal lobe	Seizure-free	LEV/LTG
5	36	M	Focal onset seizures	Grade III anaplastic astrocytoma	AL	Left temporal lobe	No reduction in seizure	CBZ
6	53	F	Generalised seizures	Glioblastoma multiforme	FC	Left frontal lobe	Seizure-free	PHT/CBZ

* SAH – selective amygdalohippocampectomy, AL – anterior lobectomy, FC – frontal craniotomy.

** CBZ – carbamazepine, VPA – valproate, ECBZ – eslicarbazepine, LEV – levetiracetam, LTG – lamotrigine, PHT – phenytoin

2.4 Electrophysiological experiment setup

Slices were placed in an interface recording chamber and maintained at 30-33^{0}C at the interface between nACSF and humidified carbogen gas. nACSF was circulated using a SciQ 400 series pump (Watson Marlow, UK) at a rate of 1-1.2 mls/min. Slices were allowed to adjust to the chamber condition for 30 minutes before any form of experiments were initiated.

Extracellular electrodes were prepared by pulling micropipettes from a thin walled borosilicate glass pipette (1.2mm O.D. x 0.94 mm I.D. – Harvard Apparatus Ltd, UK) with a PP-83 puller (Narishige, Japan). Electrodes were filled with nACSF and placed in the stratum pyramidale layer of the CA3 subregion of the hippocampus (see section 1.13) on the brain slice. Local field potentials (LFP) were recorded by the extracellular electrodes connected to a pre-amplifier EXT-10/2F headstage (npi electronic, Germany). The LFP was then band pass filtered between 10 Hz and 100 Hz by the AI-2130 differential amplifier (Axon Instrument, Molecular Devices, USA). The mains electrical noise was eliminated from the recorded LFP by the Hum-Bug noise eliminator (Quest Scientific Instruments, Canada). The obtained analog signal was digitized at 5 kHz by the ITC-16 multi-channel data acquisition interface (Digitimer, UK). The extracellular LFP was then recorded using the AxoGraph X software (Axograph Scientific, USA) recorded on a Macbook Pro computer (Apple, UK).

2.5 Mitochondrial epileptic induction

Following the 30 minute recovery period, 0.1mM fluorocitrate was applied to the circulating nACSF for one hour. Slices were then challenged via the circulating nACSF with 500nM rotenone (Sigma Aldrich, R8875) and 10μM potassium cyanide (Sigma Aldrich, 60178). Slices were monitored continuously for the presence of any epileptic activity using extracellular local field potential recordings.

Fluorocitrate was prepared as described in previous publication (Paulsen *et al.*, 1987). Briefly, 8mg of the fluorocitric acid barium salt (Sigma Aldrich, F9634) was weighed out and dissolved in 1ml of 0.1M hydrochloric acid (Sigma Aldrich, UK). A few drops of 0.1M sodium sulphate (Sigma Aldrich, UK) were added to precipitate the barium. 2ml of 0.1M Na_2HPO_4 (VWR UK) was added and they were then centrifuged

at 1000 x g for 5 minutes. The supernatant was then taken and the pH was adjusted to 7.4 before the volume was made up in 0.9% NaCl to 10ml. This created a 2mM stock solution of fluorocitrate. The stock solution was stored at 4^0C and used within a week of stock preparation.

2.6 Data analysis

Data were analysed off-line with Microsoft Excel (Microsoft Inc., USA), Matlab 2010a (MathWorks, USA), and Prism 7.0 (GraphPad Software, USA). An automated script was written in Matlab (courtesy of Dr. Katherine Newling, see Appendix 1. Matlab Script) to automatically detect burst discharges by setting a threshold against which the software detects the discharges. A 10-minute portion of the recording was used in any one time and the value of burst frequency were expressed as the amount of discharges per minute. These values were then arranged in a tabular format and appropriate statistical analysis were conducted using Prism 7.0. Normality of the data was tested with the Shapiro-Wilk normality test. For experimental treatment with just two conditions, a paired t-test was performed for parametric data or Wilcoxon matched-pairs signed rank test for non-parametric equivalent. When there are more than two conditions, a repeated-measure one-way analysis of variance (ANOVA) was performed for parametric data or Friedman test for non-parametric equivalent. If there is statistical significance, a post-hoc Sidak's multiple comparison test was then performed. A p-value of <0.05 was taken as significant.

2.7 Drugs

The following table lists the drugs used in this thesis for the *in vitro* electrophysiology experiments (see Table 2-2). Whenever possible, stock solutions of all drugs were prepared by dissolving in distilled H_2O. Otherwise, drugs were dissolved in DMSO (Sigma Aldrich UK) with a final concentration of <1% v/v. Stock solutions were either kept at 4^0C or frozen at -20^0C in aliquots as per instructions from the supplier.

Table 2-2 List of drugs used for in vitro electrophysiology experiments.

Drug Name	Supplier	Supplier Product Code
Fluorocitric acid barium salt	Sigma Aldrich	F9634
Rotenone	Sigma Aldrich	R8875
Potassium cyanide	Sigma Aldrich	60178
MPP^+-iodide	Sigma Aldrich	D048
Sodium azide	Sigma Aldrich	52002
NBQX	Abcam	AB120045
DAP-V	Abcam	AB120003
Gabazine	HelloBio	HB0901
Carbamazepine	Tocris	4098
Lamotrigine	Sigma Aldrich	L3791
Levetiracetam	Sigma Aldrich	L8668
Valproate acid	Sigma Aldrich	P4543
Diphenylhydantoin	Sigma Aldrich	D4505
Midazolam	Tocris	2832
Lorazepam	Sigma Aldrich	L1764
Sodium pentobarbital	Sigma Aldrich	P3761
Perampanel	Eisai	A gift from Eisai
Decanoic acid	Sigma Aldrich	C1875
Nonanoic acid	Sigma Aldrich	N29902
Octanoic acid	Sigma Aldrich	O3907
GABA	Tocris	0344
L-glutamine	Sigma Aldrich	G3126
L-glutamic acid	Sigma Aldrich	G1251
Alpha-ketoglutaric acid	Sigma Aldrich	K1128
DL-β-hydroxybutyrate	Sigma Aldrich	H6501
Glucose	VWR	10117HV
Sodium pyruvate	Acros Organics	A0327931
D-Lactate	Sigma Aldrich	71716
Coenzyme Q10	Abcam	AB143173
Bezafibrate	Sigma Aldrich	B7273

2.8 Immunohistochemistry

Slices that had been used for electrophysiological recordings were fixed in 4% paraformaldehyde (PFA) in 0.1M phosphate buffered saline (PBS) at the end of the recordings and stored at 4^0C. Control slices that had been incubating in the holding chamber for the same duration of time were also fixed. These slices were used for post-hoc immunohistochemistry (see Figure 2-1) to examine the cellular population in the tissue following electrophysiological experiments.

A day prior to use, slices were removed from the PFA and placed in a 30% sucrose in Tris-buffered saline (TBS) solution for cryoprotection overnight. Slices were then resectioned to 40µm thick sections using a freezing stage microtome (Shandon Life Sciences International, UK). Slices were placed in a 24 well-plate in TBS in a sequential order (5 wells for each slice). This allows an equal distribution of the dorsal and ventral portion of the slices in each well. Antigen retrieval was conducted by two 5-minute incubations in microwave-boiled 50mM sodium-citrate solution at pH 6.0. This was then followed by 3xTBS washes. Endogenous peroxidase activity was quenched by an hour incubation in 0.3% hydrogen peroxide (H_2O_2) in 70% methanol in TBS solution at room temperature. After another 3xTBS washes, sections were incubated in a 1% casein (FisherScientific, UK) in TBS solution for an hour for a non-specific binding block. This was then followed by 3xTBS washes and sections were then permeabilized by incubation in 0.05% Tween in TBS solution for 10 minutes. Following this, sections were then incubated in the primary antibody diluted in TBS with 5% normal serum (Vector Laboratories, UK) and 0.05% Tween. The choice of the serum depends on the secondary antibody used to detect the primary antibody binding and can either be normal goat, horse, or rabbit serum. The primary antibody was diluted according to the appropriate dilution factor as described in Table 2-3.

Table 2-3 List of primary antibodies used in this thesis.

Target protein	Supplier	Product code	Host species	Dilution
NeuN	Merck Millipore	ABN90P	Guinea pig	1:1000
GABA	Sigma Aldrich	A0310	Mouse	1:1000
CaMKII	Abcam	AB52476	Rabbit	1:1000
GFAP	Merck Millipore	AB5804	Rabbit	1:1000
PV	Sigma Aldrich	P3088	Mouse	1:1000
CB	Swant	CB38	Rabbit	1:10,000
CR	Swant	CG1	Goat	1:1000

Following the overnight incubation, sections were then incubated for 2 hours at room temperature on a rocking platform. Sections were then washed with 3x TBS washes and incubated in the appropriate secondary antibodies (see Table 2-4) diluted to 1:200 in 0.05% Tween in TBS solution for 2 hours at room temperature. Sections were then, again, washed with 3x TBS washes and incubated in horseradish peroxidase (Ready-To-Use Streptavidin Horseradish Peroxidase, VectorLabs, UK) for 2 hours at room temperature. Following yet another 3x TBS washes, the chromogenic reaction was then developed using DAB (SigmaFast® DAB tablets, Sigma Aldrich, UK) for 5 minutes before being washed with 3x TBS washes. Sections were then mounted onto gelatine-subbed glass slides (FisherScientific, UK). After air-drying overnight, slides were washed in distilled water and sections were then dehydrated by incubation in sequential ethanol concentration gradients; starting from 70%, 95%, and 100%; each for 5 minutes each, with a further 5 minutes in another 100% ethanol gradient. Sections were then bathed in Histoclear (National Diagnostics, USA) for 5 minutes twice before being coverslipped using DPX Mounting Media (FisherScientific, UK).

Table 2-4 List of secondary antibodies used in this thesis.

Antibody	**Supplier**	**Product code**
Biotinylated goat-anti rabbit IgG antibody	Vector Laboratories	BA-1000
Biotinylated horse-anti mouse IgG antibody	Vector Laboratories	BA-2000
Biotinylated goat-anti guinea pig IgG antibody	Vector Laboratories	BA-4000

Unless otherwise mentioned, all the reagents used here were obtained from Sigma Aldrich, UK. Tris-buffered saline (TBS) contains 0.06% Trizma® base and 0.85% NaCl and is pH adjusted to 7.4.

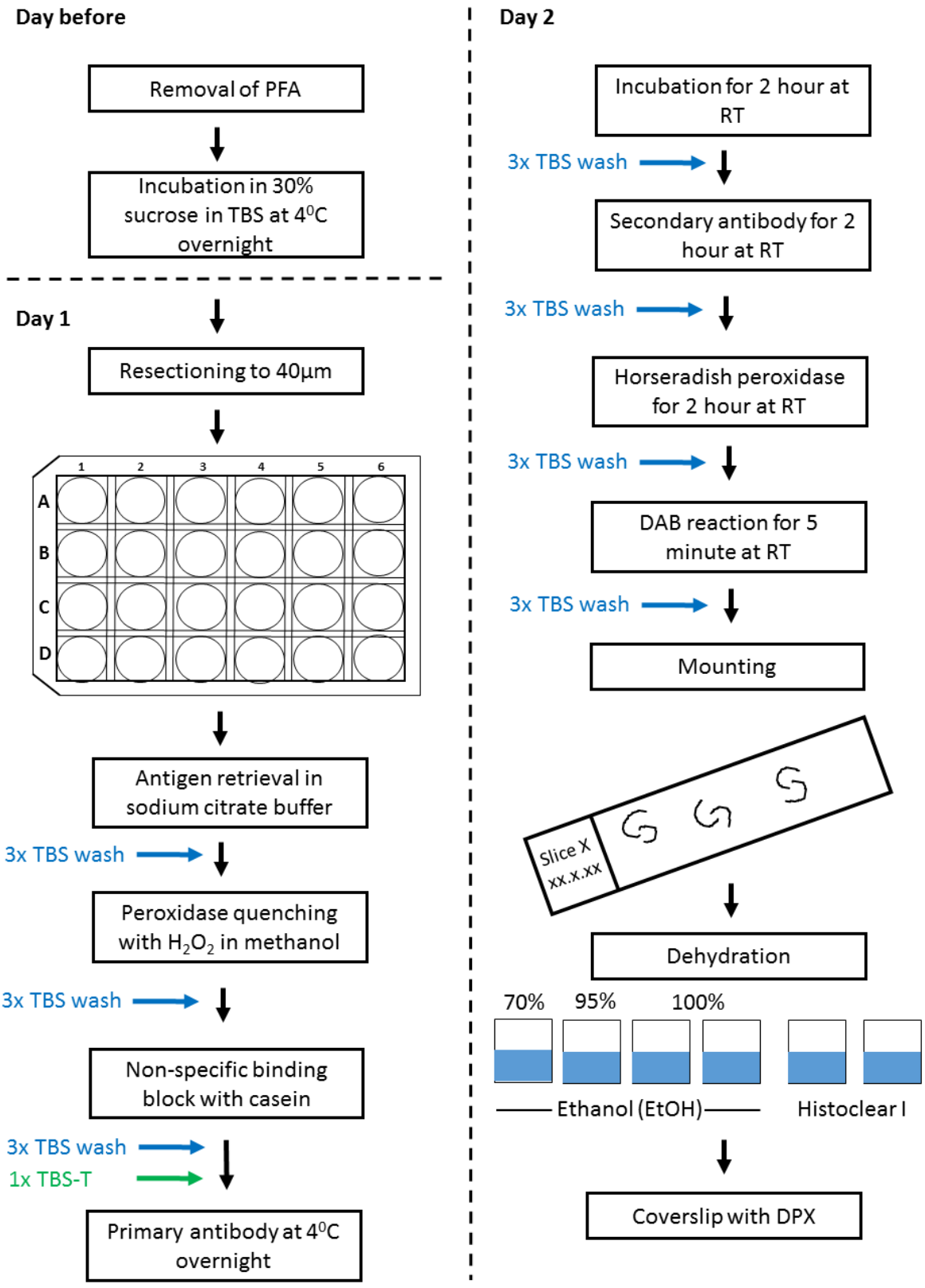

Figure 2-1 Flowchart of the standard immunohistochemistry protocol.

2.9 Microscopy, data acquisition, and data analysis

Microscope slides were visualized under stereology light microscope Olympus BX51 (Olympus Corporation, UK). The software Stereo Investigator (MBF Bioscience, USA) was used to analyse and perform the cell count. An outline was drawn at 2.5x magnification around the hippocampus CA3 and the area of the region was calculated. A meander scan was then performed at 20x magnification that allowed sequential scanning and counting of each portion of the region until the whole region was counted. The entire cell population was sampled according to the criteria of a clear and visible nuclear and cytoplasmic profile. This cell count was then divided by the area of count to generate the cell density (cells/mm^2). Statistical analysis was then conducted using Prism 7.0. Normality of the data was tested with the Shapiro-Wilk normality test. For experimental treatment with just two conditions, an unpaired t-test was performed for parametric data or Mann-Whitney test for non-parametric equivalent. When there are more than two conditions, a one-way analysis of variance (ANOVA) was performed for parametric data or Kruskal-Wallis test for non-parametric equivalent. A p-value of <0.05 was taken as significant.

All of the images presented in this thesis were taken using a camera attached to the microscope (Nikon Instruments, Japan) and using the software Picture Frame (Softonic, Spain). When necessary, for aesthetic purposes, images were processed using Adobe Photoshop CC 2014 (Adobe, USA).

2.10 Measurement of carbonylated protein

Protein carbonylation is a process of protein oxidation that is promoted by the process of oxidative stress, and hence, it can be indicative of oxidative damage in the tissue (Suzuki *et al.*, 2010). Carbonylated proteins can be derivatised by 2,4-dinitrophenylhydrazine (DNPH) to form hydrazones that are detected using a colorimetric assay (Levine *et al.*, 1994).

Following electrophysiological recording in which epileptic activity was induced, brain slices were homogenized using a T-18 digital Ultra-Turrax® blender (IKA Labortechnik, Germany) through a 3 x 15 seconds blending on ice, with 30 seconds break between each blend. To obtain an adequate protein yield, four brain slices were pooled together and homogenized in 1ml of ice-cold MES buffer, containing 50mM 2-

(N-morpholino)ethanesulfonic acid (MES), 1mM ethylenediaminetetraacetic acid (EDTA), 1% Tween-20, 1mM phenylmethylsulfonyl fluoride (PMSF), and 1x protease inhibitor cocktail. All reagents for the buffer were obtained from Sigma Aldrich, UK. Homogenate was then centrifuged at 10,000 x g for 10 minutes at 4^0C and the supernatant was taken. To remove the nucleic acids that may interfere with the assay, 1% streptomycin sulphate (Sigma Aldrich, UK) was added and the mixture was incubated at room temperature for 15 minutes. Samples were then centrifuged at 6,000 x g for 10 minutes at 4^0C. The supernatant was taken, snap-frozen in liquid nitrogen, and stored in -80^0C until processed.

On the day of processing, samples were thawed and 200µl of the samples were transferred to two tubes: the sample (S) and control (C) tubes. Into the sample tubes, 800µl of DNPH (Sigma Aldrich, UK) was added and into the control tubes, the same amount of 97% phosphoric acid (Sigma Aldrich, UK) was added. Both tubes were incubated in the dark for an hour and vortexed every 15 seconds to allow the derivatisation of the DNPH onto the carbonylated side chains. Into both tubes, 1 ml of 20% trichloroacetic acid (Sigma Aldrich, UK) was then added and incubated on ice for 5 minutes. Following centrifugation at 10,000 x g for 10 minutes at 4^0C; the supernatant was discarded and the pellet was resuspended in 1 ml of 10% trichloroacetic acid. Again, the tubes were incubated on ice for 5 minutes, centrifuged at 10,000 x g for 10 minutes at 4^0C, and the supernatant was discarded. Then, the pellets underwent 3 x wash using a 1:1 ethanol / ethyl acetate mixture. Each wash involved resuspending pellets in 1 ml of the mixture, a vortex, and centrifugation at 10,000 x g for 10 minutes at 4^0C. After the final wash, pellets were resuspended in 500µl of 6M guanidine hydrochloride (Sigma Aldrich UK). Tubes were then centrifuged at 10,000 x g for 10 minutes at 4^0C and 220µl of the supernatant was then put onto a 96-microwell plate to have their absorbance read at 360-385nm using the SpectraMax M3 plate reader (Molecular Devices, USA). The absorbance was then corrected by subtracting the control absorbance from the sample absorbance for each sample. Using the following equation, the value of the protein carbonyl was calculated.

$$Protein\ carbonyl\ \left(\frac{nmol}{ml}\right) = \left[\frac{(CA)}{0.011\ \mu M^{-1}}\right]\left(\frac{500\ \mu l}{200\ \mu l}\right)$$

The value for each sample was then normalized against the protein concentration. This was measured using a standard protein assay with the Bio-Rad Protein Assay Kit (Bio-Rad, USA). The values were tabulated and statistical analysis was performed as described in section 2.9.

2.11 Brain slice incubation for metabolic mapping

Following the brain slice preparation as described in section 2.2.3, slices were incubated in a specialized incubation system according to McNair *et al* (McNair *et al.*, 2016). The incubation system contains 9 incubation chambers, which holds a basket each whereon four hippocampal slices were placed. The baskets were placed at the interface of 10 ml nACSF which was pre-heated to 37^0C and equilibrated with humidified carbogen gas (5%CO_2/95%O_2). Following that, 0.1mM fluorocitrate was added to the nACSF and incubated for 30 minutes. Afterwards, 500nM rotenone and 10μM potassium cyanide was added to the nACSF and further incubated for another 30 minutes. This pre-incubation resembled the protocol described in section 2.5 and so, the slices were considered to be 'epileptic' at this stage of the incubation. 'Control' slices were exposed to vehicles instead of the epileptogenic compounds.

Slices were then gently rinsed with glucose-free nACSF before they were transferred to the incubation medium and left to incubate for one hour. Incubation medium consisted of nACSF containing the ^{13}C-labelled substrates (see Table 2-5) in addition to either the vehicles or the epileptogenic cocktail mixture, depending on the condition. In the case of conditions with the ^{13}C-glucose, the unlabelled glucose in the nACSF was replaced with the labelled glucose. Incubations were terminated after one hour by removing the basket, gently rinsing with ice-cold glucose-free nACSF, and submerging them in 5 ml of ice-cold 70% ethanol.

Table 2-5 List of isotopes used in this thesis.

^{13}C substrates	**Supplier**	**Product code**	**Concentration**
D-glucose (U-13C6, 99%)	Cambridge Isotope Laboratories	CLM-1396	10mM
L-glutamic acid (U-13C6, 99%)	Cambridge Isotope Laboratories	CLM-1800	0.5mM
L-glutamine (U-13C6, 99%)	Cambridge Isotope Laboratories	CLM-1822	2.5mM

The slices were removed from the basket and homogenized in the ethanol using the VibraCell^{TM} ultrasonicator (400W model, Sonic & Materials Inc, USA). Subsequently, the samples were centrifuged at 20,000 x g for 20 minutes at 4^{0}C to separate the denatured protein. The supernatant was taken as the extract sample and stored at -80^{0}C until freeze drying was performed. The pellets were dried at room temperature overnight, reconstituted in 500µl 1M KOH for at least 8 hours, and subjected to protein determination using the Pierce BCA Protein assay-kit (Thermo Fisher Scientific, USA) as per the supplier's instruction. Lactate release from the slices was measured in the incubation media using a lactate assay-kit (R-Biopharm AG, Germany) as per the supplier's instruction.

2.12 Gas chromatography – mass spectrometry analysis

Gas chromatography – mass spectrometry (GC-MS) is used to detect the incorporation of ^{13}C-labelling in various metabolites, including amino acids, lactate and alanine, and TCA cycle intermediates using an established protocol (Walls *et al.*, 2014; McNair *et al.*, 2016). Briefly, the extracts were freeze-dried and reconstituted in distilled water. An aliquot was taken and acidified using hydrochloric acid to pH 1-2 and dried under nitrogen gas flow. Metabolites then underwent extraction into 200µl of an organic phase consisting of 96% ethanol twice. 200µl of benzene was added to the combined organic phases before subsequent drying under nitrogen gas flow. Extracts were then reconstituted in N,N-dimethylformamide (DMF) (Sigma-Aldrich, USA) and N-tert-butyldimethylsilyl-N-methyl-trifluoroacetamide (MTBSTFA) (Sigma Aldrich, USA) was utilized to derivatise the metabolites. The analyses were conducted on an Agilent Technologies 7820A chromatograph, J&W GC column HP-5MS, parts no. 19091S-433 coupled to a mass spectrometer (Agilent Technologies 5977E, USA). Gas chromatography separates the metabolites by their boiling point and once each metabolite is isolated, they go through mass spectrometry to measure the mass of the metabolites as an indication of the ^{13}C-labelling incorporation (see Figure 2-2).

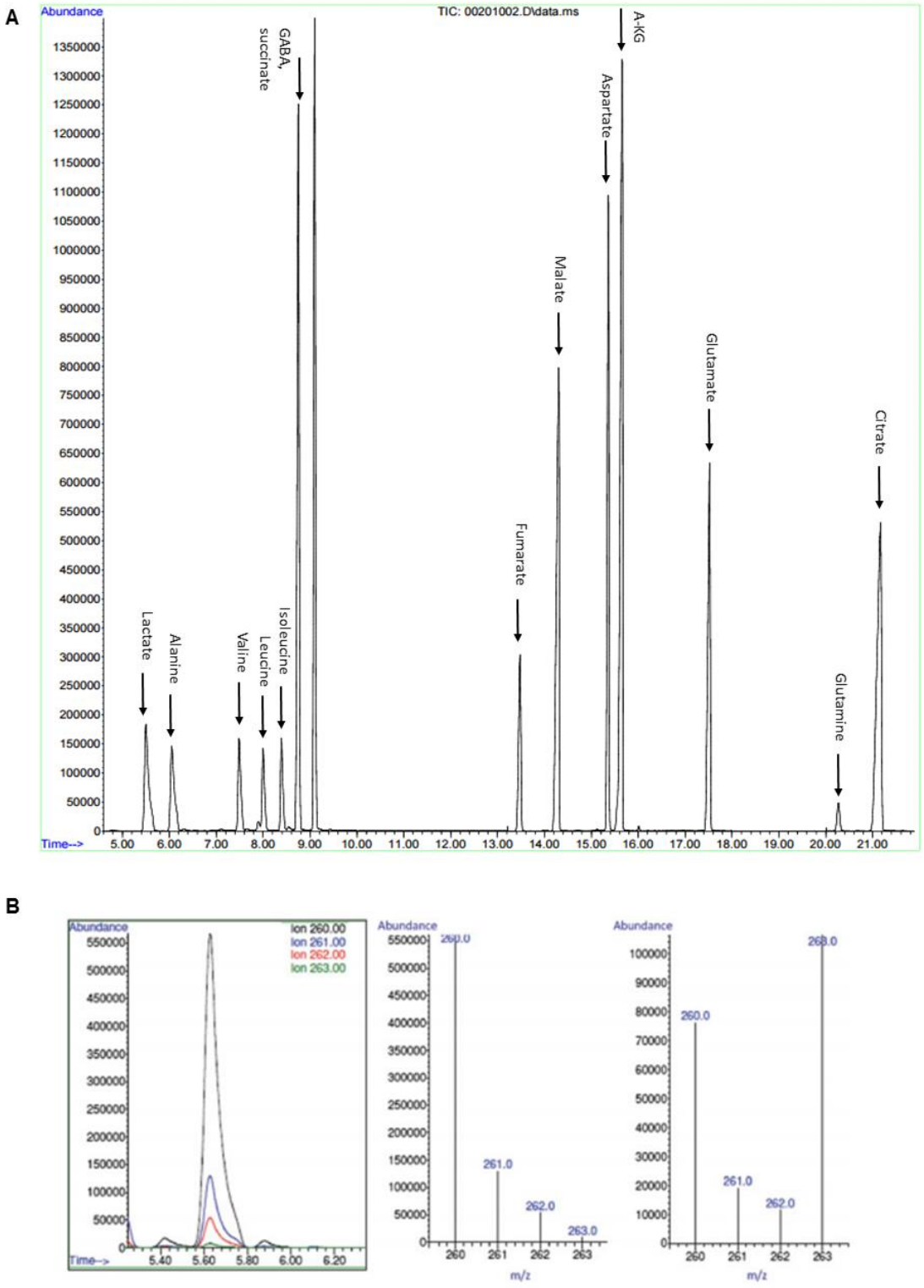

Figure 2-2 An example of a gas chromatograph and mass spectrometry analysis. Shown in (A) is an example of a gas chromatogram and the site within the trace that corresponds with the retention time of characterized metabolites. In (B), an example of a mass spectrum of an isolated metabolite is shown (left) and the m/z ratio was calculated to show the distribution of the relative abundance of the ^{13}C labelling (middle and right). In this example, 260.0 corresponds to the mass of the unlabelled molecule (M), 261.0 suggests incorporation of one carbon of the ^{13}C-labelled substrates in the metabolite (M+1), 262.0 has two (M+2), and 263.0 has three (M+3). Modified with permission from (Walls et al., 2014)

The most abundant isotope of carbon in nature has an atomic mass of 12. Carbon-13, on the other hand, only constitutes 1.1% of the naturally occurring carbon. ^{13}C-labelled substrates have had one or more of the carbon atom modified so that they have an extra mass of 13. In uniformly labelled ([U-^{13}C])-substrates, all the carbon atoms within that molecule are ^{13}C atoms. Therefore, for [U-^{13}C]-glucose, for instance, all six carbon atoms in the glucose are ^{13}C atoms. Following metabolism of the labelled substrates, these ^{13}C atoms can be incorporated into various metabolites (see Figure 2-3 and Figure 2-4) and hence, they can be tracked by measuring the mass of the metabolites in the sample. Each metabolite can theoretically be labelled by none or any number of the ^{13}C carbon atom. A non-labelled metabolite is the molecular ion (M) in the mass spectrum with its actual molecular mass. Each additional ^{13}C carbon-atom incorporation gives rise to an increase in mass by 1 as compared to the molecular ion (M+1, M+2, M+3, etc). These are collectively called the isotopologues of the given metabolite. ^{13}C-labelling data were corrected for natural abundance of ^{13}C (1.1%) by subtracting the mass distribution of a non-labelled standard containing the relevant metabolites. The percentage of the ^{13}C labelling was then calculated as described in a previous publication (Walls *et al.*, 2014).

These percentage values were then arranged in a tabular format and appropriate statistical analysis were conducted using GraphPad Prism 7.0. Normality of the data was tested with the Shapiro-Wilk normality test. For experimental treatment with two conditions, multiple unpaired t-test was performed with Holm-Sidak correction for parametric data or Mann-Whitney test for non-parametric equivalent. In the case of more than two conditions, a one-way analysis of variance (ANOVA) was performed for parametric data or Kruskal-Wallis test for non-parametric equivalent. If there is statistical significance, a post-hoc Sidak's multiple comparison test was then performed. A p-value of <0.05 was taken as significant.

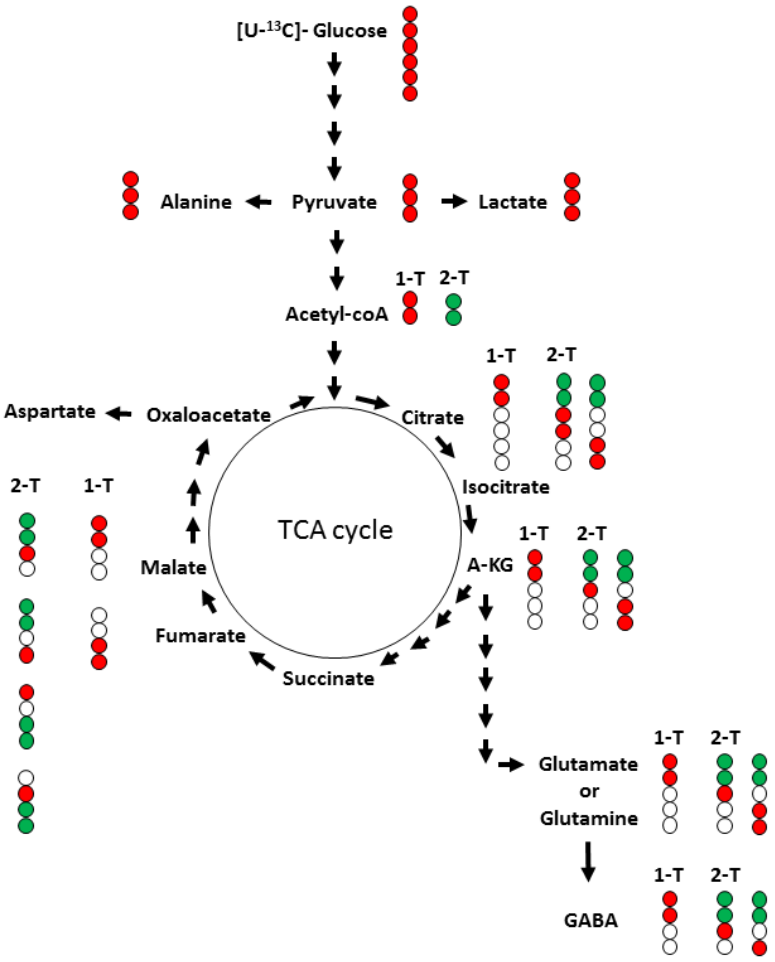

Figure 2-3 Incorporation of ^{13}C into various metabolites following [U-^{13}C]-glucose metabolism. Each circle represents a carbon atom. White circles represent ^{12}C and coloured circles represent ^{13}C. In particular, red circles represent the carbon atom from the metabolism of [U-^{13}C]-glucose and green circles represent carbon atoms from labelled acetyl-CoA introduced on the second turn of the TCA cycle. 1-T are molecules that could come about from the first turn of the TCA cycle and 2-T are molecules that could come about from the second turn of the TCA cycle. For example, on the first turn of the TCA cycle, one can only anticipate M+2 glutamate, whereas on the second turn, one can anticipate either M+3 or M+4 glutamate. This allows accurate dissection of the labelling from the first or second turn of the TCA cycle.

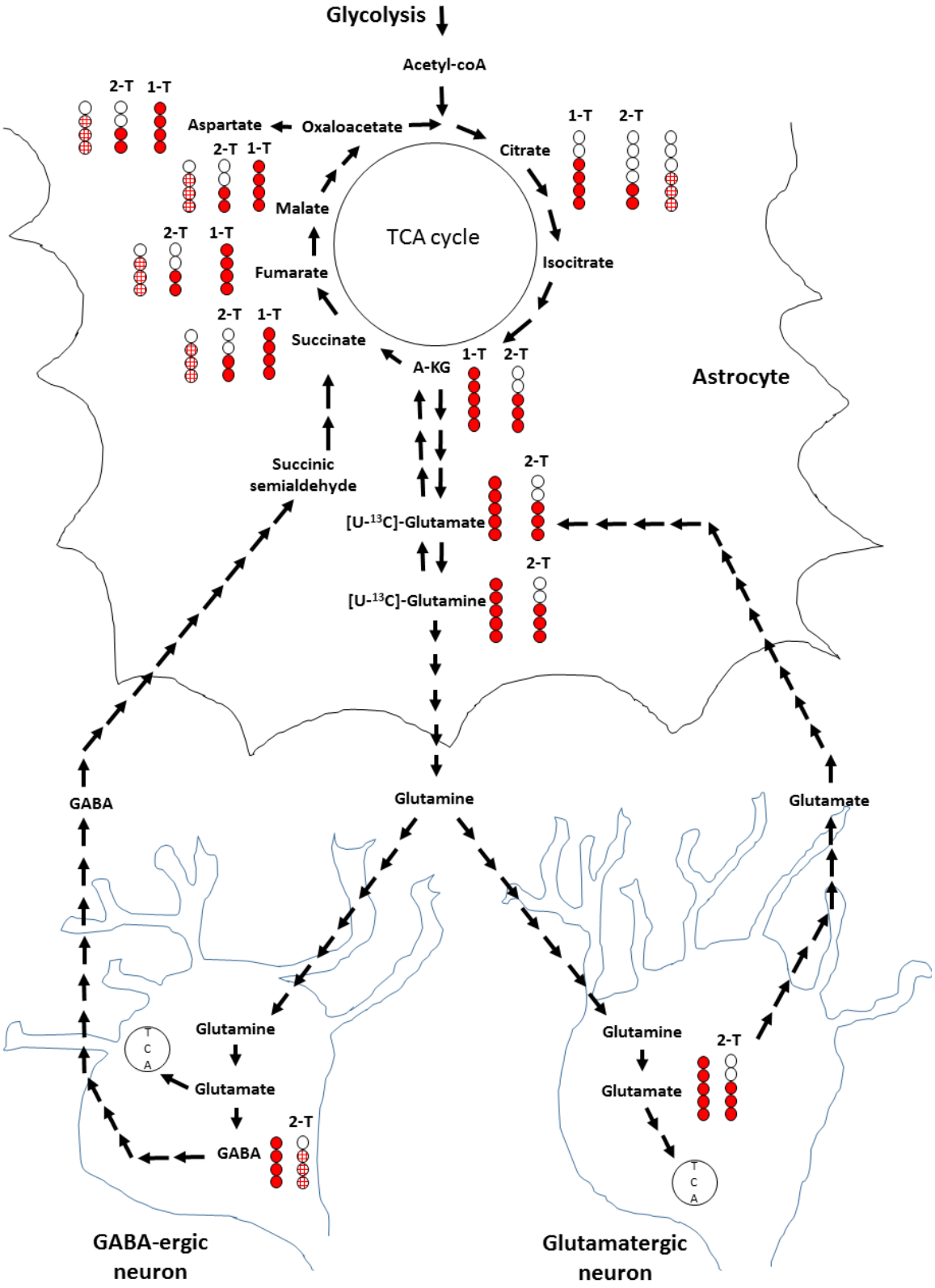

Figure 2-4 Incorporation of ^{13}C into various metabolites following [U-^{13}C]-glutamate or [U-^{13}C]-glutamine metabolism. Each circle represents a carbon atom. White circles represent ^{12}C and coloured circles represent ^{13}C. Patterned red circles represent molecules that enter the second turn of the TCA cycle via GABA. 1-T are molecules that could come about from the first turn of the TCA cycle and 2-T are molecules that could come about from the second turn of the TCA cycle. Circle with the TCA label represents entry into the TCA cycle in the neuronal compartment.

2.13 High performance liquid chromatography analysis

To quantify the pool of amino acids, reversed-phase high performance liquid chromatography (HPLC) was performed to separate the amino acids by polarity using an Agilent ZORBAX Eclipse plus C18 column (4.6 x 150mm, particle size 3.5µm; 959963-902, Agilent Technologies, USA). The HPLC included pre-column online *o*-phthaldialdehyde derivatization and fluorescence detection (338nm, 10nm bandwidth, and reference wave-length 390, 20nm bandwidth) using an Agilent 1260 Infinity system coupled to a 1260 Infinity fluorescence detector (McNair *et al.*, 2016).

A mobile phase gradient that consisted of a mixture of mobile phase A (10mM Na_2HPO_4; 10mM $Na_2B_4O_7$, pH 8.2; 5mM NaN_3) and mobile phase B [45% acetonitrile : 45% methanol : 10% water (v:v:v)] was utilized. The percentage of mobile phase B was increased linearly from 2 to 57% within 30 minutes, and from 57 to 100% in 6 seconds and returned again to 2% in 3.5 minutes; giving a total run time of 35 minutes. The flow of the mixed mobile phases was continuously maintained at 1.5 ml/minute. The separation of the amino acid was conducted according to the method supplied by the Agilent application note (Henderson and Brooks, 2010) and modified accordingly to separate the amino acids of interest (see example chromatogram in Figure 2-5). The amount of the amino acids was quantified by comparing the measured value against a standard curve generated by parallel injection of a mixture of amino acids of interest at increasing known concentrations.

Again, the data was tabulated and statistical analysis was conducted using GraphPad Prism 7.0 as described in section 2.9.

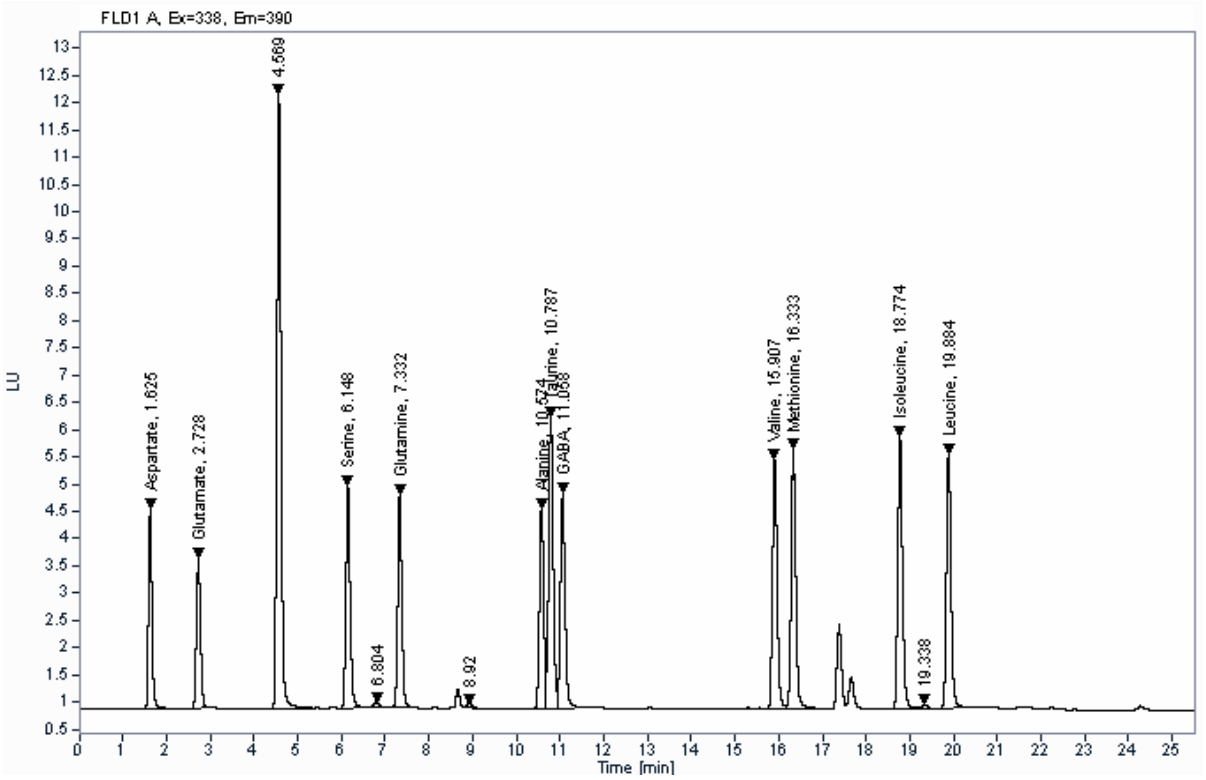

Figure 2-5 An example of a chromatogram with amino acids of interest. Amino acids are separated by polarity and by comparing the retention time in the trace against the standard, the locations of the amino acids are determined.

2.14 Magnetic-activated cell sorting

In order to probe the metabolism of specific cellular compartments, a novel method was devised utilizing magnetic-activated cell sorting (MACS) technology to acutely isolate specific cellular populations from the hippocampus. Since the mitochondrial epilepsy induction depends on the specific inhibition of astrocytic aconitase, it is imperative to assess the state of mitochondrial respiration in neurons and astrocytes separately. To isolate the neurons, the anti-PSA-NCAM microbeads (Miltenyi Biotec, Germany, 130-092-966) was used and for the astrocytes, the anti-GLAST (ACSA-1) microbeads (Miltenyi Biotec, Germany, 130-095-826) was used.

Animals were sacrificed through transcardial perfusion as described in section 2.2.2 and after the brain was removed from the skull, the two hippocampi were gently dissociated from the cortices using a spatula and the net weight of the tissue was determined. A net wet weight of circa 180-250mg of tissue was obtained per animal preparation from the two hippocampi. To dissociate the tissue, I used the Neural Tissue Dissociation Kit - Trypsin (Miltenyi Biotec, Germany, 130-093-231) and the

gentleMACS dissociator (Miltenyi Biotec, Germany, 130-093-235). Dissociation was performed as per the instruction on the kit.

After obtaining the cell lysate, the neuronal compartment was separated first. The process involved the use of the miniMACS separator (Miltenyi Biotec, Germany, 130-042-102) and the corresponding MS column (Miltenyi Biotec, Germany, 130-042-201) to separate the cells. Briefly, the cells were centrifuged at 300 x g for 10 minutes at 4^0C and resuspended in the MACS buffer (0.1M PBS (Sigma Aldrich, UK) with 0.5% bovine serum albumin (BSA) (Sigma Aldrich, UK), pH 7.2). After incubating for 10 minutes at 4^0C, the cells were labelled with the anti-PSA-NCAM Microbeads and incubated for 15 minutes at 4^0C. The cells were then washed with MACS buffer and centrifuged at 300 x g for 10 minutes. The supernatants were removed and the pellets were resuspended in MACS buffer before being passed through the column that has been placed in a magnetic field. The flow-through was collected as the negative fraction and then, the cells were then eluted from the column as the neuronal fraction. The negative fraction was then reprocessed to separate the astrocytes from the fraction. The cells were first labelled with the anti-GLAST (ACSA-1) -biotin microbeads as above and then, using the secondary anti-biotin microbeads. The incubation, wash, and separation process were similar to the neuronal process, as described above. The cells eluted from this column were then collected as the astrocytic fraction.

2.15 Measurement of metabolic fluxes using Seahorse XF24

The neurons and astrocytes isolated by the process outlined in section 2.14 were used for metabolic flux measurement using Seahorse XF24 Analyzer (Agilent Technologies, USA). Firstly, the Seahorse XF24 Cell Culture Microplates (Agilent Technologies, USA) were coated with 22.4µg/ml Cell-Tak (Corning, USA) made up in sterile 0.1M $NaHCO_3$ (Sigma Aldrich, UK) and alkalinized with 1M NaOH. The plates were incubated for 30 minute at room temperature and the plates were washed in distilled H_2O to remove the bicarbonate. The cell fraction was centrifuged at 10,000 x g for 30 seconds at 4^0C and resuspended in the 37^0C Seahorse media. Seahorse media consisted of Dulbecco's Modified Eagle's Medium (Sigma Aldrich, UK) resuspended according to the manufacturer's instructions and supplemented with 10mM D-glucose (Sigma Aldrich, UK) and 5mM pyruvate (Acros Organics, UK). Cell viability was determined using the tryptan blue cell viability assay and counted using

the automated cell counter Cellometer® Auto1000 (Nexcelom Biosciences, UK). The cells were then seeded at 300,000-400,000 cells/well. The plate was then centrifuged at 200 x g for 1 minute with zero deceleration. The plate was then incubated at 37^0C, 0% CO_2, for 30 minutes.

The Seahorse media was then supplemented with 3% fetal bovine serum (FBS) (Sigma Aldrich, UK) to create the experimental media. The elimination of FBS in the original seeding media was due to the interference from FBS in the cell adherence to the Cell-Tak coated surfaces. The experimental media was then supplemented with experimental treatments as necessary. With each experiment, around 10 wells of each cell population can be obtained. Two treatment conditions are then usually tested per each cell population. Each experiment also involve a cartridge which can hold four pharmacological treatments (Port A, B, C, and D) which would be injected into the media consecutively according to the protocol (see Chapter 6 for more details). Once the run has finished, the media was aspirated and the cells were fixed in 4% PFA for 30 minutes. Plates were washed with 0.1M PBS and stored at 4^0C until processing.

2.16 Post-hoc immunofluorescence

To visualize the cells that had undergone measurement of metabolic fluxes using Seahorse XF24, all of the wells on the plates were stained using a Hoechst stain bisbenzimide 2.5µg/ml in TBS (H33258, Sigma Aldrich, UK) for 30 minutes. The cells were then washed with TBS and visualized immediately under the inverted microscope Axiovert 200M (Zeiss, UK) with a fluorescent bulb HBO100 (Zeiss, UK) at excitation wavelength of 346nm and emission at 460nm. Images were taken at 4x magnification at four pre-determined sites in each well (see Figure 2-6).

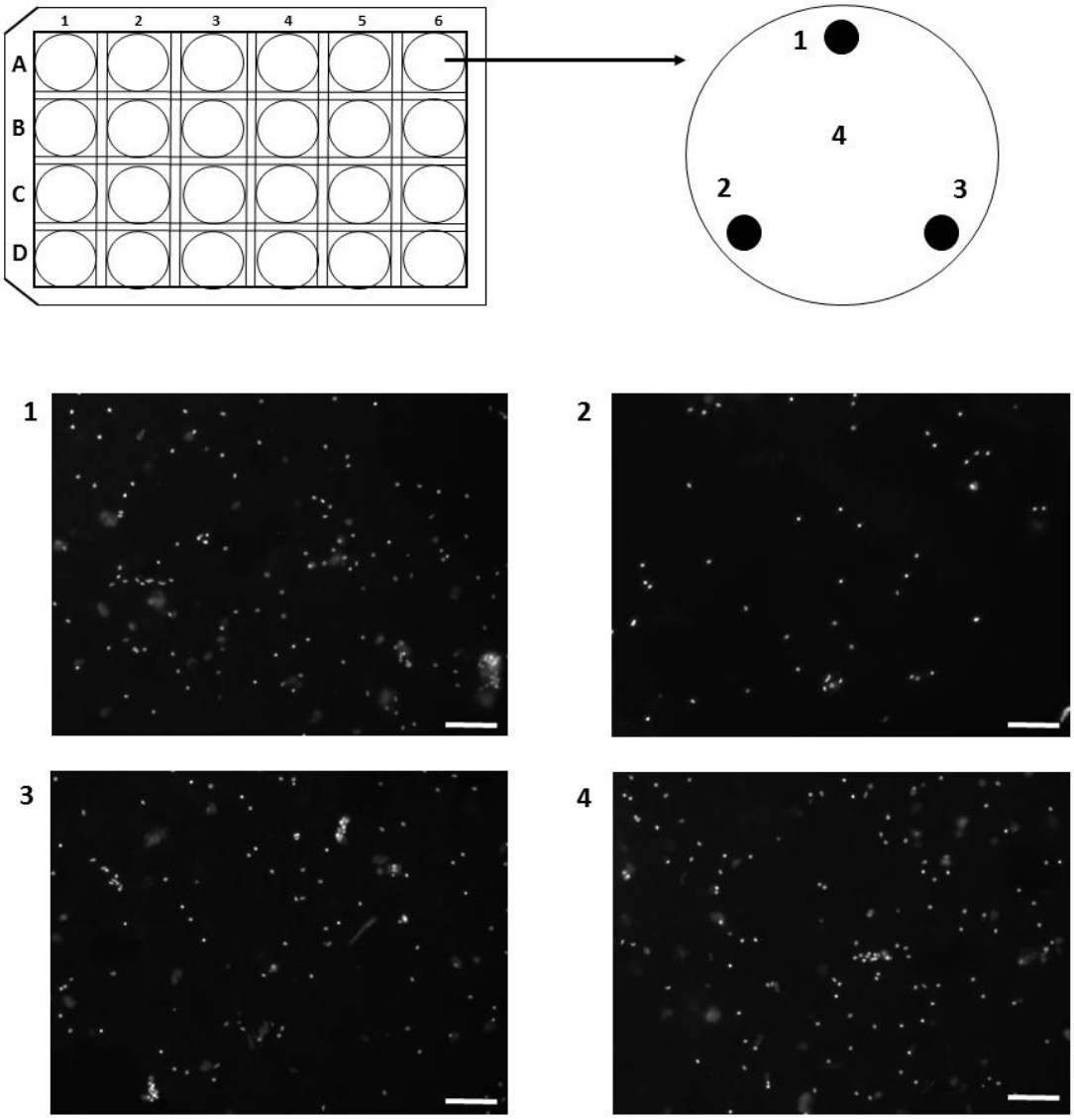

Figure 2-6 Seahorse plate layout and sites for image acquisition for cell counting. Shown on top left corner is a typical layout of a Seahorse XF24 well plate and four sites were chosen for image acquisition as shown on the zoomed-in diagram of the well on the top left corner. Images 1 to 4 corresponds to an example of images taken from the four sites of a well of the XF24 plate. Scale bar 10µm.

A Matlab script (courtesy of Stacey Aston, see Appendix 1. Matlab Script) was written to perform an automated cell count using threshold detection analysis on these images. An average was calculated for each well and using the ratio of the area of the visual field against the area of each well, the value was extrapolated to provide an estimate of the cell count in the whole well. Using the viability data from the tryptan blue assay, a viable cell count was obtained for each well (assuming that viability is equal across all wells with the same sample). The value for the Seahorse recording as conducted in section 2.15 was then normalized against the viable cell count.

Chapter 3 Developing an *in vitro* brain slice model of mitochondrial epilepsy

3.1 Introduction

About a quarter of the patient population with mitochondrial disease develop epilepsy (Whittaker *et al.*, 2015). Their epilepsy can virtually manifest in any seizure semiology and combinations; although classical absence seizures appear very rarely (Bindoff and Engelsen, 2012). Epilepsy can also be seen across multiple genotypes and phenotypes; with the most common syndromes associated with epilepsy reported to be the myoclonus epilepsy with ragged red fibres (MERRF) syndrome and the mitochondrial encephalopathy, lactic acidosis, and stroke-like episodes (MELAS) syndrome (Bindoff and Engelsen, 2012; Whittaker *et al.*, 2015). Furthermore, this epilepsy; the mitochondrial epilepsy; almost always never respond to traditional antiepileptic drugs and patients tend to deteriorate very rapidly with poor prognosis (Bindoff and Engelsen, 2012). Despite the severity of mitochondrial disease, very few animal models have been developed for the disease and the few models that were developed never phenotypically manifest as epilepsy (Tyynismaa and Suomalainen, 2009; Dunn *et al.*, 2012; Farrar *et al.*, 2013); reflecting the poor representation of mitochondrial disease phenotypes in these animal models.

Clearly, a fresh approach is required in developing a model of mitochondrial disease; particularly of mitochondrial epilepsy. A recent post-mortem neuropathological study on the investigation of neocortices of patients with mitochondrial epilepsy has shown profound interneuron loss as well as the extreme global loss of expression of mitochondrial complex I subunits and to a lesser degree, complex IV (Lax *et al.*, 2016). The author of this study further extended this finding to the demonstration of profound astrogliosis in the neocortex of these patients as well as a similar degree of complex I and complex IV loss in the astrocytes (Lax *et al.*, unpublished data; see Figure 3-1). Astrogliosis was indeed seen in some population of patients with mitochondrial disease (Sandbank and Lerman, 1972; Navarro-Sastre *et al.*, 2011); although it has not been previously investigated in the context of mitochondrial epilepsy.

This neuropathological finding, for the first time, implicated both the astrocytic and the neuronal compartment, in mitochondrial epilepsy. It is well demonstrated that the addition of high concentrations of complex I or complex IV inhibitors in acute brain slices alone did not cause epileptiform discharges in the hippocampal network recordings; despite a severe reduction in the interneuron firing rate and subsequent

disinhibition in the neuronal network (Kann *et al.*, 2011; Whittaker *et al.*, 2011). This indicates that the mere inhibition of mitochondrial complex I and IV using pharmacological tools is insufficient to modify the network into an epileptic state. Perhaps, an additional manipulation of astrocytic mitochondrial function is necessary for the generation of epileptiform discharges.

With that in mind, there are very few pharmacological tools that specifically modulate astrocytic function. One of the few pharmacological tools that existed is the Krebs cycle inhibitor, fluorocitrate. Fluorocitrate is a well-characterized selective inhibitor of the astrocytic aconitase, an enzyme involved in the Krebs cycle in the conversion of citrate to isocitrate (Hassel *et al.*, 1992; Swanson and Graham, 1994). It owes its selectivity to the preferential uptake of fluorocitrate by the glial cells (Fonnum *et al.*, 1997).

Taking all this into consideration, I combined the acute application of the astrocytic aconitase inhibitor, fluorocitrate, with the mitochondrial respiratory chain complex I and IV inhibitors, rotenone and potassium cyanide respectively, onto hippocampal brain slices to examine if this combination would generate epileptiform discharges. To validate the findings, all the exposed tissues were fixed in paraformaldehyde following the termination of the experiments and pathological studies are conducted to examine and compare the neuropathological results with the respective human neuropathological findings.

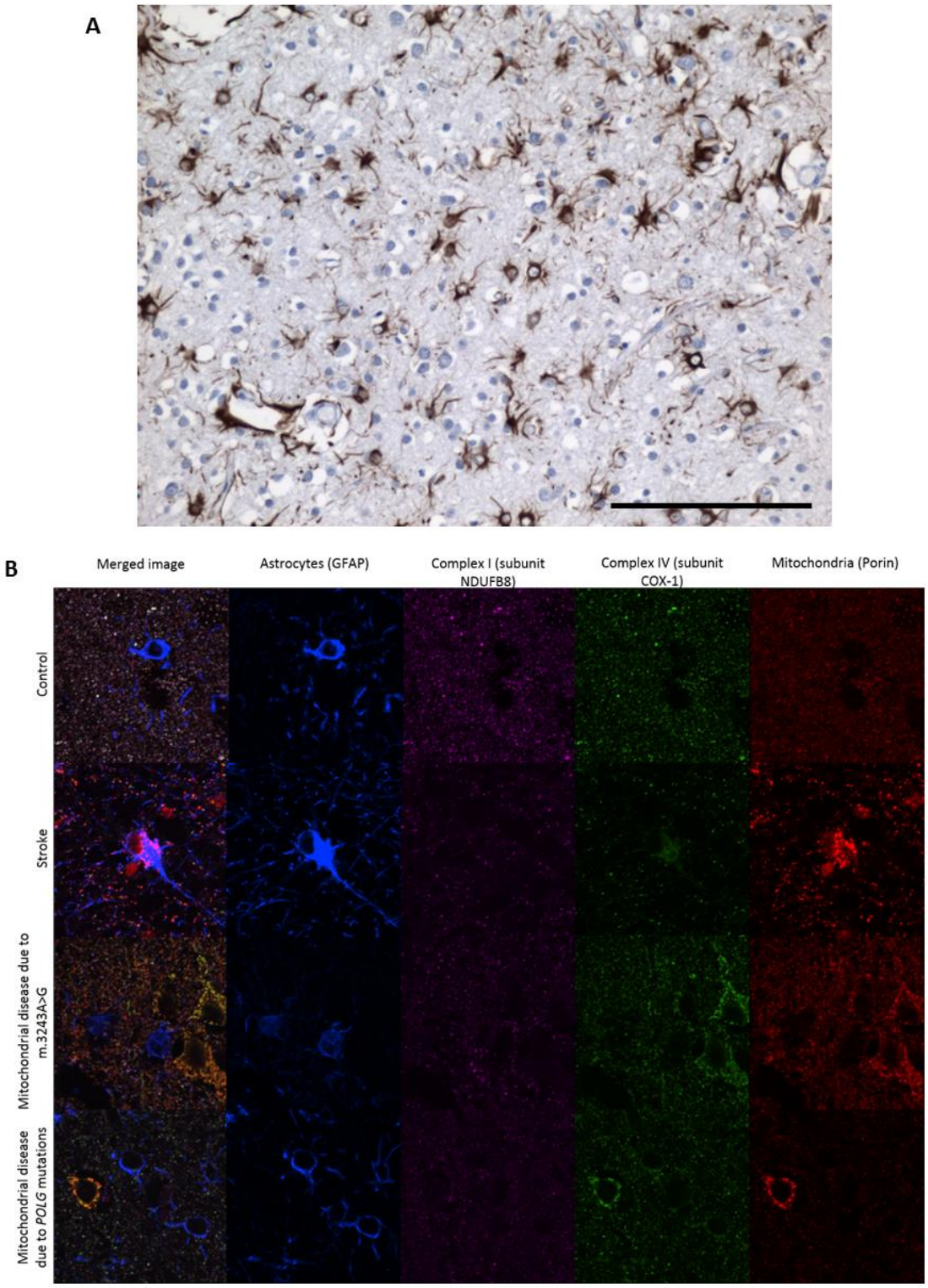

Figure 3-1 There is extensive astrogliosis and respiratory deficient astrocytes in the temporal cortex of patients with mitochondrial epilepsy. Shown in (A) is the immunostaining for glial fibrillary acidic protein (GFAP) in temporal cortex of a patient with mitochondrial epilepsy. The pattern of staining showed extensive reactive astrogliosis. In (B), a quadruple immunofluorescence assay was performed to evaluate the complex I and complex IV subunit expression within the mitochondria of the astrocytes. There was severe complex I deficiency and a subtler complex IV deficiency in the astrocytes of patients with mitochondrial epilepsy phenotype. Scale bar in (A) indicates 100µm. Image courtesy of Nichola Lax, unpublished data from an ongoing study.

3.2 Methods

Acute hippocampal slices were prepared from adult male Wistar rats and maintained as described extensively in Chapter 2. The combination of the three pharmacological agents (fluorocitrate, rotenone, and potassium cyanide) at the specific pro-convulsant concentration make up what was eventually known and described in the remainder of this thesis as the mitochondrial induction protocol (see section 2.5). For validation of the model, the concentration of these inhibitors was titrated higher to examine the impact of complete mitochondrial respiratory chain inhibition on the epileptic phenotype. Furthermore, to see if the protocol is specific to the respiratory chain inhibitors; an experiment substituting each of the respiratory chain inhibitors (rotenone and potassium cyanide) with their respective substitutes (MPP^+ and sodium azide respectively) was performed. The protocol was also applied to mice brain slices and human brain slices as will be discussed below. Quantification was conducted as detailed in section 2.6.

Subsequent to the termination of the electrophysiological experiments, these slices were fixed in 4% paraformaldehyde and post-hoc immunohistochemistry was performed as described in section 2.8. Slices were stained for various neuronal markers, including the excitatory and inhibitory neuronal markers, as well as the astroglial marker. For all the immunohistochemistry results presented here, the slices were recorded for up to 2 hours after application of rotenone and potassium cyanide before they were fixed in the 4% paraformaldehyde. Sections were imaged and analysis was conducted as described in section 2.9.

3.3 Results

3.3.1 Development of the brain slice model of mitochondrial epilepsy

As mentioned above, I attempted to model mitochondrial epilepsy based on recapitulating the findings from the post-mortem neuropathological studies showing a severe complex I and complex IV deficiency as well as an extensive astrogliosis. To replicate this dysfunction, I have chosen three pharmacological agents: rotenone (complex I inhibitor), potassium cyanide (complex IV inhibitor), and fluorocitrate (astrocytic aconitase inhibitor). The concentrations chosen for fluorocitrate was 0.1mM, which was the previously reported concentration whereby it is selectively inhibiting the astrocytic Krebs cycle (O'Dowd *et al.*, 1994). Initially, I used the concentrations used in previously published study for rotenone and potassium cyanide where at the concentrations used, the interneuron's firing rate was significantly reduced (Whittaker *et al.*, 2011); however, upon testing, it was apparent that these concentrations were too high and created generalized energy failure instead (to be discussed further below in section 3.3.2). Therefore, I titrated the concentrations of these respiratory chain inhibitors to the optimal concentrations as used below, 500nM for rotenone and 10µM for potassium cyanide.

Since the inhibitory effect of fluorocitrate relies on the uptake of the citric compound into the astrocytes, I chose to pre-incubate the tissue in 0.1mM fluorocitrate for an hour prior to the challenge with the mitochondrial respiratory chain inhibitors. During this pre-incubation, no epileptiform discharges were observed in the extracellular local field potential recordings (n=8). Subsequent to the pre-incubation with fluorocitrate, the slices were exposed to the concomitant application of the mitochondrial respiratory chain inhibitors; 500nM rotenone and 10µM potassium cyanide. Following this application, epileptiform discharges were robustly induced in the hippocampus CA3 (see Figure 3-2 for an example progression of activity following the mitochondrial epilepsy protocol). The mean onset of epileptic activity following this concomitant application is 26.32 minutes ± 3.98 minutes (data not shown on graph, n=8).

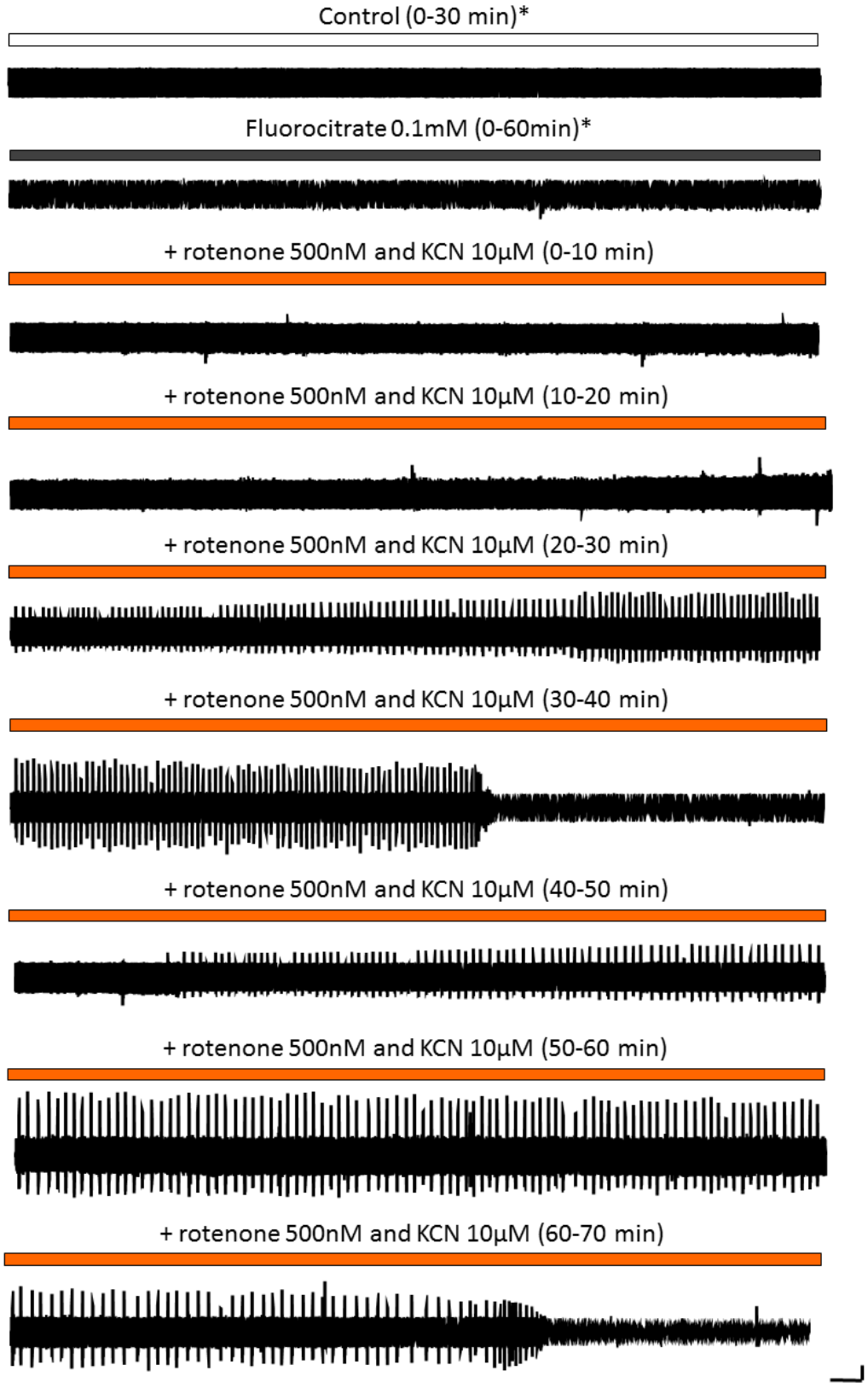

*Figure 3-2 The epileptic activity progression following the mitochondrial induction protocol. Shown are the electrophysiological recordings following each steps of the mitochondrial induction protocol. Each recording is a 10 minute recording shown for the respective time period as shown on the label. Scale bar indicates 0.05mV and 30 seconds. *Since the control and the fluorocitrate recording shows no epileptiform activity throughout the 30 minute control incubation and the 60 minute fluorocitrate incubation, only a representative 10 minute recording is shown for each of the incubation conditions; rather than the whole incubation conditions.*

The epileptiform discharges induced appear in two distinct form of activity: the interictal discharges and the ictal discharges (see Figure 3-3). Typically, following the onset of the seizure, the activity manifested as interictal discharges that gradually increase in amplitude and frequency (see Figure 3-2, time point 10-30 minutes after rotenone and KCN). These interictal discharges would eventually transform into a longer duration ictal discharges; which would then be followed by a period of silent network activity termed the post-ictal silencing (see Figure 3-2, time point 30-40 minutes after rotenone and KCN and also Figure 3-3 for the morphological feature of the interictal and ictal discharges). This silencing lasts for approximately 5 – 10 minutes before the interictal discharges re-manifested in a similar cycle as previously described. This interictal – ictal cycle lasted for the first 2 hours of the mitochondrial epilepsy induction. After 2 hours, the network shifted towards chronic continuous interictal discharges without any ictal discharges. This profile resembled the progression seen in the zero-magnesium model where the early tonic-clonic seizure-like activity progressed into the late recurrent discharges (Reddy and Kuruba, 2013). I have found that these late interictal discharges can last for a significant period of time after its establishment and have recorded the viability of these discharges up to five hours after the application of rotenone and KCN. Furthermore, there is no morphological distinction between the early interictal discharges and the late recurrent discharges, making it difficult to pinpoint exactly when the transition occurred. The only obvious change in the network activity after 2 hours of rotenone and cyanide application seems to be the absence of ictal discharges.

This induction of epileptiform discharges is dependent on the presence of all three components of the mitochondrial epilepsy induction protocol. The application of fluorocitrate on its own (n=6) or rotenone and cyanide on its own (n=6) did not induce epileptiform discharges in the hippocampus CA3; even up to three hours of incubation with these agents. Additionally, neither the combination of fluorocitrate and rotenone (n=6) nor the combination of fluorocitrate and potassium cyanide (n=6) was able to induce epileptiform discharges in the hippocampus CA3. Hence, there must be a synergistic effect between the three pharmacological components of the mitochondrial epilepsy induction protocol.

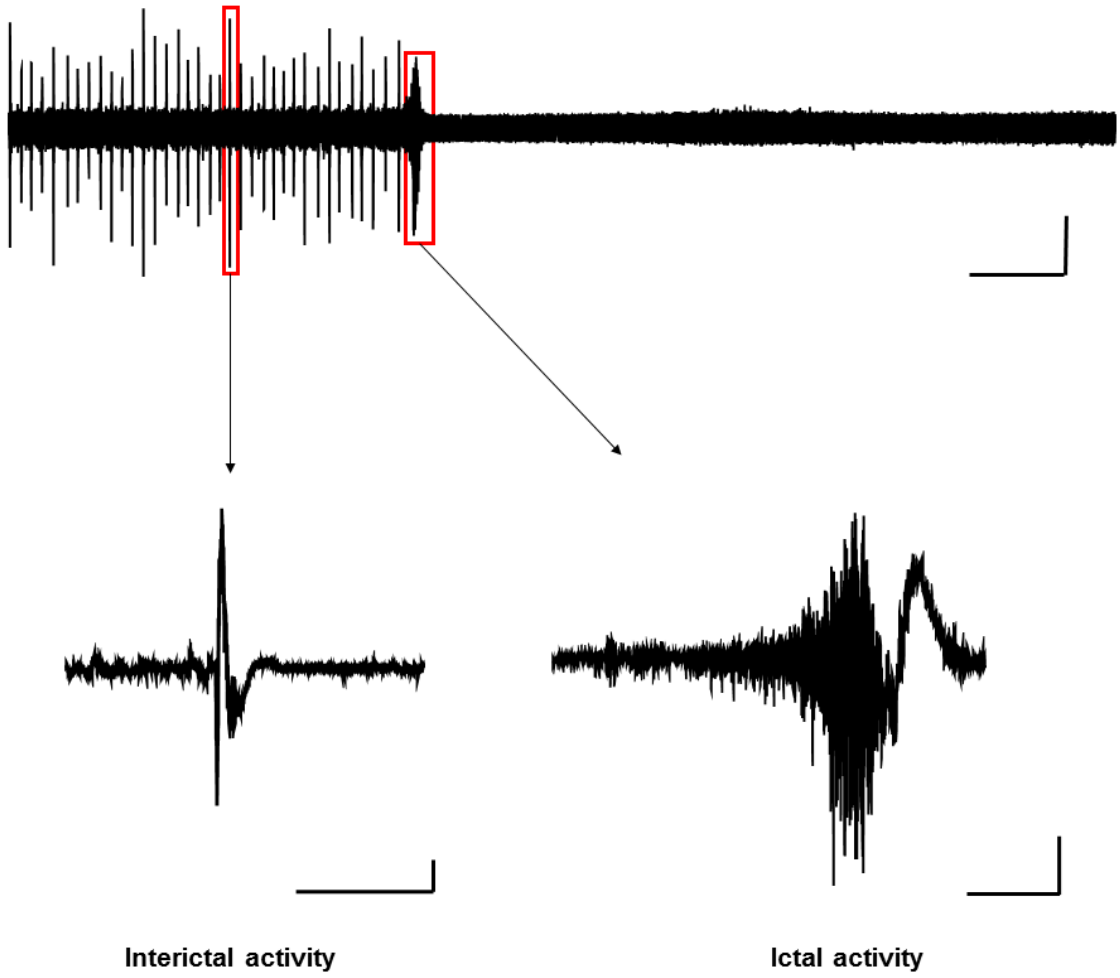

Figure 3-3 There are two distinct form of epileptiform discharges in this model of mitochondrial epilepsy. Shown is an example of an electrophysiological recording obtained from exposure to the mitochondrial induction protocol. On top is an example of a 10-minute recording with both the interictal and ictal activity. Boxed up in red and zoomed in are examples of an interictal activity (on the left) and an ictal activity (on the right). Scale bar on the top indicates 1mV and 1 minute. Scale bar on the interictal and ictal activity indicates 0.5mV and 5 seconds.

3.3.2 Generalized energy failure is induced at higher concentration of respiratory chain inhibitors

I initially started by using the concentrations utilized in previously published study from our group that showed that these concentrations of the mitochondrial respiratory chain inhibitors were able to reduce the firing rate of the inhibitory interneurons significantly (Whittaker *et al.*, 2011). These concentrations are 1µM for rotenone and 100µM for potassium cyanide. However, I found that when using these concentrations, instead of generating epileptiform discharges as shown in Figure 3-2, I was able to induce a generalized spreading depression in the hippocampus CA3 within 5-10 minutes of the joint application of these inhibitors (n=8, see Figure 3-4).

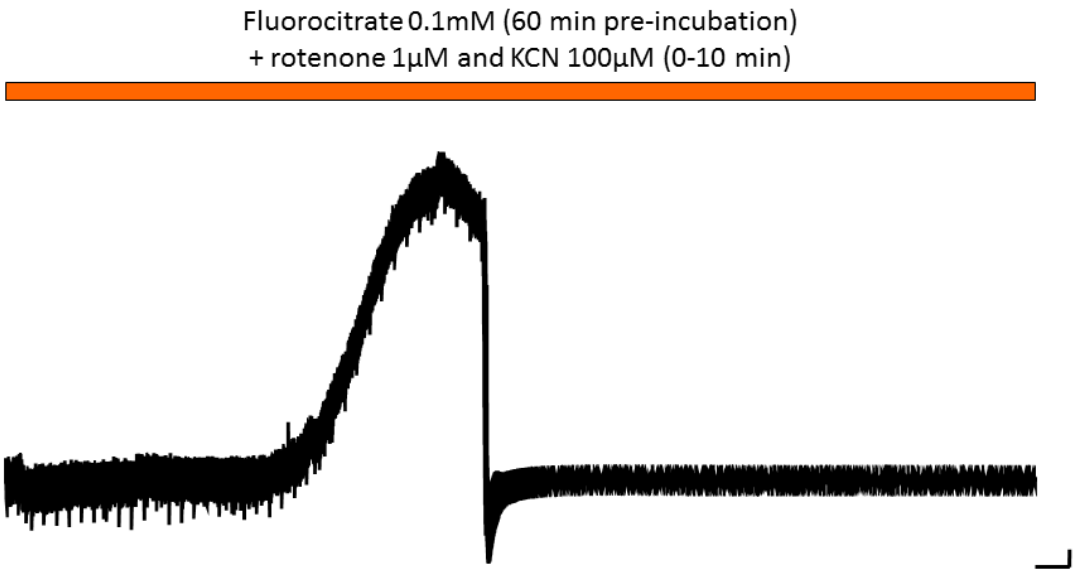

Figure 3-4 At higher concentration of rotenone and potassium cyanide, spreading depression is induced instead. Shown is an example of a 10 minutes electrophysiological recordings obtained from the hippocampus CA3 following exposure to 0.1mM for an hour followed by co-application of 1µM of rotenone and 100µM of potassium cyanide. Scale bar indicates 0.1mV and 30 seconds.

Following the spreading depression, there was no detectable network activity and this persisted even after washout of these inhibitors. This is very consistent with the cortical spreading depression pattern; an electroencephalogram feature where a giant wave of neuronal and glial depolarization occurs and is followed by a long lasting period of electrical silence across the entire cerebral cortex (Mayevsky *et al.*, 1996; Fabricius *et al.*, 2008). Classically, cortical spreading depression is associated with migraine and aura (Lauritzen; Noseda and Burstein, 2013). However, recent studies have implicated cortical spreading depression in conditions of high metabolic stress such as in hypoxic-ischemic injury (Fabricius *et al.*, 2006; Takano *et al.*, 2007). In studies of patients with mitochondrial disease, cortical spreading depression was found to be associated with stroke-like episodes in patients with the MELAS phenotype (Ohno *et al.*, 1997; Yonemura *et al.*, 2001). Therefore, I postulate that this activity is associated with a generalized energy failure in neuronal microcircuits and represents the progression from epileptiform discharges to a 'more severe electroencephalographic manifestation'. The concentration of these inhibitors were then titrated down to their optimal concentrations for epileptic activity induction as discussed extensively in section 3.3.1.

3.3.3 Respiratory chain inhibitors are substitutable

In order to ascertain if the mitochondrial epilepsy protocol is dependent on the specific use of rotenone and potassium cyanide as the mitochondrial complex I and IV inhibitor respectively, I devised a set of experiments whereby one component of the protocol is substituted with another characterized mitochondrial inhibitor. In one experiment, rotenone was substituted with MPP^+-iodide at the same concentration used for rotenone (500nM). In another series of experiments, potassium cyanide was substituted with sodium azide at the same concentration used for cyanide (10µM). Both MPP^+-iodide and sodium azide have been well described as a potent mitochondrial complex I and complex IV inhibitor respectively (Schapira, 2010; Lin *et al.*, 2012).

Both the substitution of 500nM rotenone with 500nM of MPP^+ iodide (n=8) and the substitution of 10µM potassium cyanide with 10µM sodium azide (n=6) were able to induce epileptiform discharges in the hippocampus CA3 respectively (see Figure 3-5). These epileptic activities are comparable to those induced by the components of the mitochondrial epilepsy protocol. Furthermore, both types of the discharges can be induced in the early stage of the epileptic induction using both these substitution protocols; the interictal and the ictal discharges. This indicates that the mitochondrial epilepsy protocol is not reliant on the specific use of rotenone and potassium cyanide. Rather, it requires a combination of a mitochondrial complex I and complex IV inhibitor with the astrocytic aconitase inhibitor to induce epileptiform discharges in the hippocampus CA3.

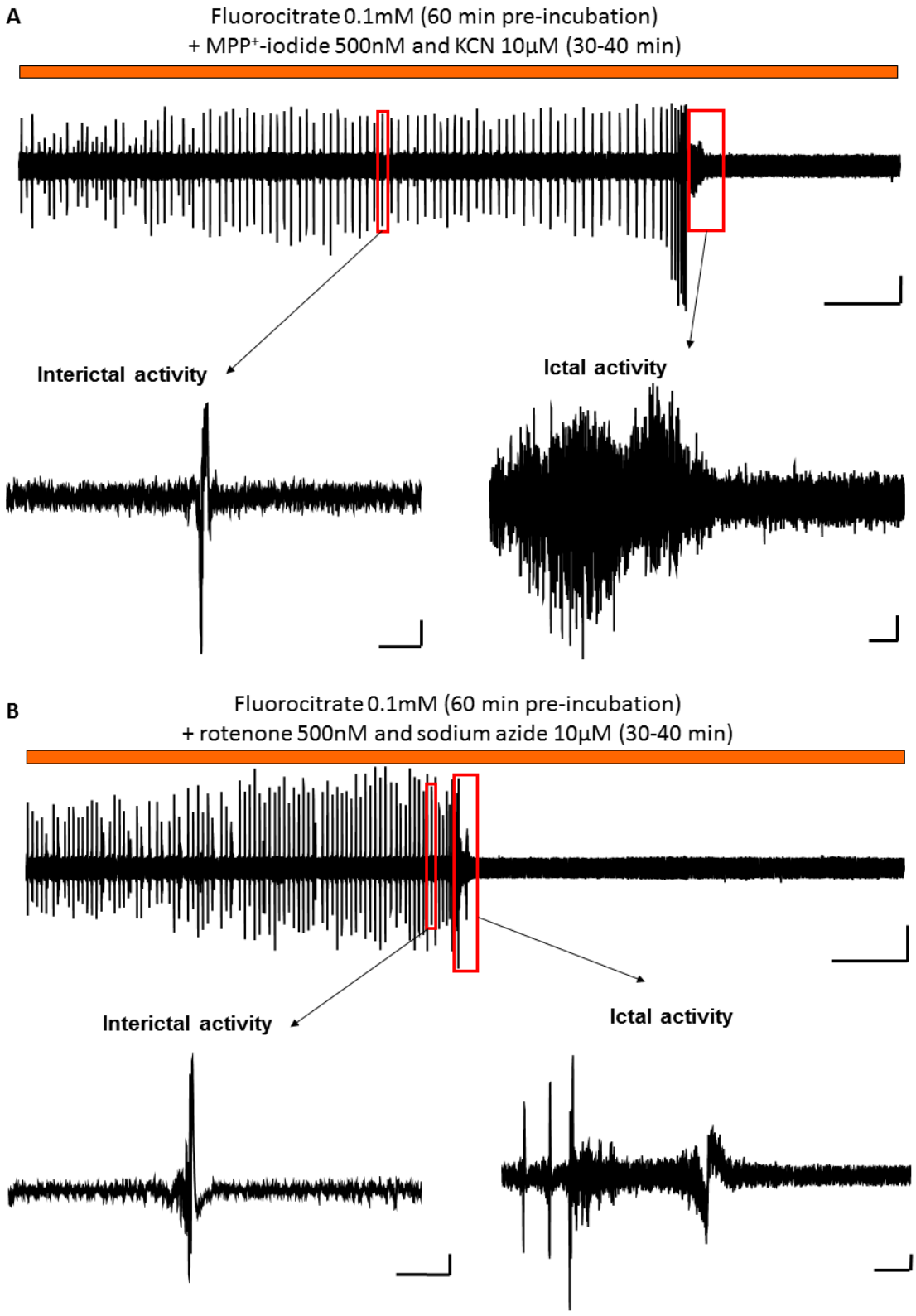

Figure 3-5 Similar pattern of epileptiform discharges can be induced by substitution of the mitochondrial inhibitors used. Shown in (A) is an example of electrophysiological recording obtained from the substitution of rotenone with MPP⁺-iodide in the mitochondrial epilepsy protocol and in (B) from the substitution of potassium cyanide with sodium azide. Shown as example are the zoomed-in examples of the interictal activity (on the left) and the ictal activity (on the right). Scale bar in (A) in the whole trace indicates 1mV and 1 minute, interictal activity 0.5mV and 1 second, and ictal activity 0.2mV and 3 second. Scale bar in (B) the whole trace indicates 2mV and 1 minute, interictal activity 1mV and 1 second, and ictal activity 2mV and 3 seconds.

3.3.4 The mitochondrial epilepsy induction is conserved across species

To validate this model further, I wanted to demonstrate that the mitochondrial epilepsy induction is not restricted to acutely prepared rat brain slices. Therefore, I chose to conduct this mitochondrial epilepsy induction using similar protocol in acute brain slices prepared from another commonly used laboratory murine, the C57BL/6 mice. I have used male mice (similar gender to the male rat) and 8-10 weeks old mice (age equivalent to the 10-12 weeks old rat used). Slice preparation was conducted in the same manner to rat brain slice preparation and experimental setup was consistent.

In addition to validation in mice, I also managed to use the mitochondrial epilepsy protocol in surgically resected human brain tissue obtained from patients undergoing neurosurgical procedures. Patients information from which brain slices were obtained are summarized in Table 2-1. Slice preparation was conducted as described in section 2.3 and experimental setup was kept consistent with the experiments using murine and rodent brain slices.

Epileptiform discharges were induced using the mitochondrial induction protocol in both C57BL/6 mice (n=10) and human (n=6) brain slices (see Figure 3-6). Both interictal and ictal discharges were observed following induction in both species. Overall, the pattern of induction in mice brain slices resembled the rat brain slices very closely. In human brain slices, however, onset of the epileptiform discharges vary quite considerably within the 2 hour of application of rotenone and cyanide. Furthermore, in some cases (as is shown in Figure 3-6), the intensity and the severity of the epileptiform discharges can vary quite significantly as well. In the particular case shown in Figure 3-6, two ictal discharges can be seen in a 10-minute recording, which is unseen of in rodent brain slices. Regardless, the pattern of activity is still the same in that interictal discharges are followed by ictal discharges, which then resulted in a post-ictal silencing before re-manifesting as interictal discharges. This subtle variety in the onset, intensity, and severity of the epileptiform discharges probably reflects the genetic and clinical variety of the human patients from which the brain slices were obtained from.

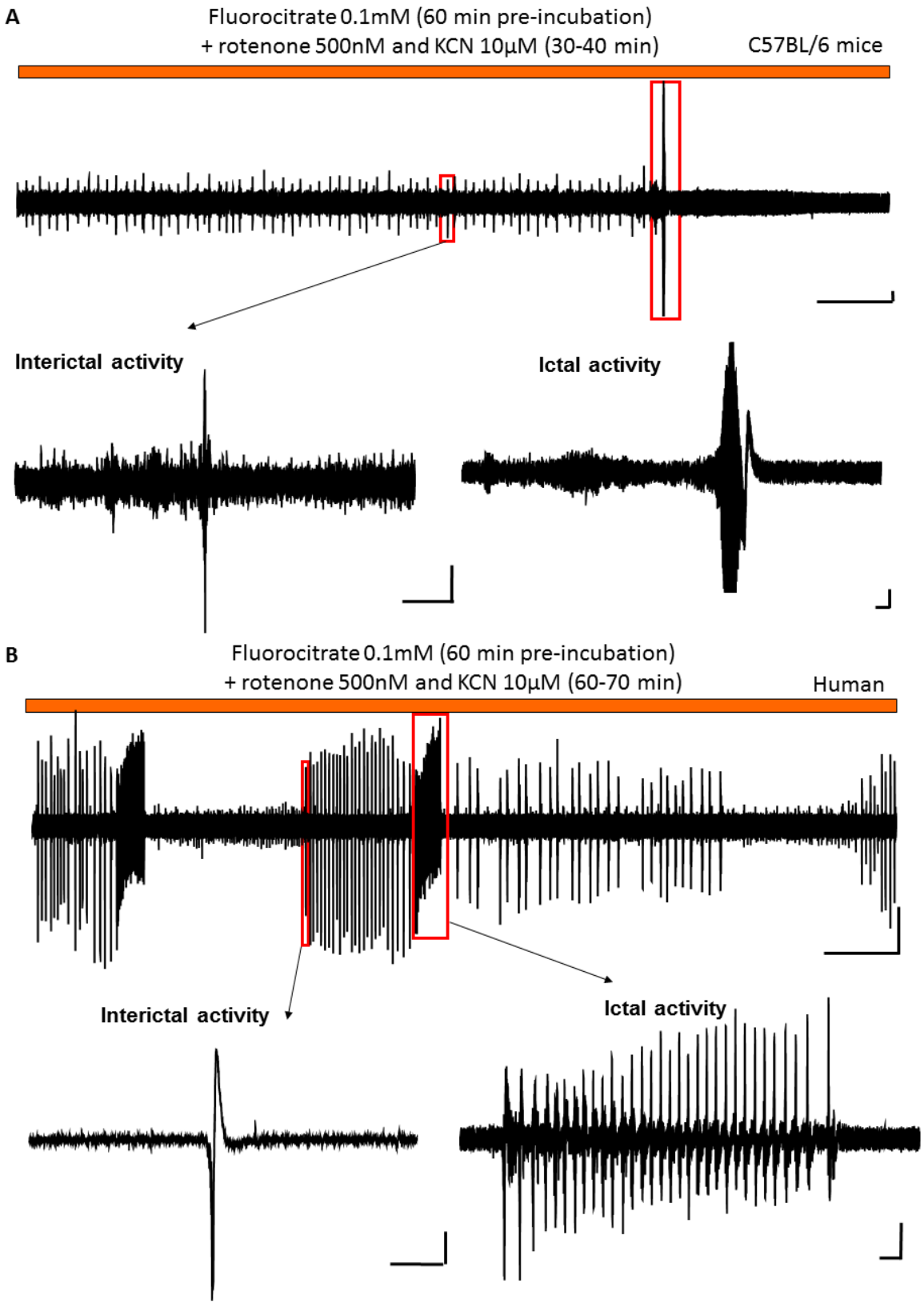

Figure 3-6 Mitochondrial epilepsy was able to be induced in both mice and human brain slices. Shown in (A) and (B) is an example of electrophysiological recordings obtained from C57BL/6 mice and human brain slices respectively. Shown as example are the zoomed-in examples of the interictal activity (on the left) and the ictal activity (on the right). Scale bar in (A) in the whole trace indicates 1mV and 1 minute, interictal activity 0.5mV and 2 seconds, and ictal activity 1mV and 10 seconds. Scale bar in (B) in the whole trace indicates 1mV and 1 minute, interictal activity 0.5mV and 0.5 second, and ictal activity 1mV and 1 second.

3.3.5 Quantification through automated burst detection demonstrates the stability of the epileptic activity

Hitherto, this model has shown that it can robustly produce epileptiform discharges in hippocampus CA3 *in vitro* and the epileptic activity induction is conserved across multiple species. In order to use this model for pharmacological studies (results discussed in Chapter 4), a method of quantification needs to be developed that can accurately and consistently detect the epileptiform discharges and quantify them. To address this, a Matlab script was written (courtesy of Dr. Katherine Newling, see Appendix 1) to automate the burst detection procedure. The script is based on automated burst detection by threshold analysis. Various parameters can be measured through the automated burst detection; including the frequency, amplitude, and duration of the epileptiform discharges. Since the planned pharmacological studies were to provide recommendations for therapeutic planning in patients with mitochondrial epilepsy, a clinically relevant parameter is required. The frequency of the epileptiform discharges has been shown to be the most clinically relevant quantifiable parameter as it is a predictor of the pharmacological response of the epileptiform activity (Hitiris *et al.*, 2007). Clinically, the response of an antiepileptic therapeutic intervention is usually measured by a 50% reduction in seizure frequency or the attainment of seizure freedom (Birbeck *et al.*, 2002). Whilst, scientifically, a reduction in amplitude and duration of an epileptiform discharges might represent an interesting phenomenon by a therapeutic intervention; it may not provide a meaningful insight into the potential clinical efficacy of the intervention. Therefore, I decided to quantify only the frequency of the epileptiform discharges and assessed whether there is a period of stability of the burst frequency to provide a platform for pharmacological screening (n=5, see Table 3-1 and Figure 3-7).

For 120 minutes following the application of rotenone and cyanide, the epileptiform activity gradually increased in terms of frequency with the onset of the first epileptiform discharges occurring after 30 minutes (although one slice did have a rapid onset at 10 minute after rotenone and cyanide application). There was an observable period of stability (± 10%) in frequency of epileptiform discharges at 120 to 180 minutes following rotenone and cyanide application. This corresponds very well to the previously discussed transition to the late recurrent interictal discharges. After 180 minutes, there was a slight reduction in the frequency of the epileptiform discharges. However, for the next 60 minutes, this epileptic activity was again relatively stable (±

10%). Therefore, despite the slight reduction in the frequency of the epileptic activity, it can be argued that the epileptiform discharges are relatively stable from 120 to 240 minutes after rotenone and cyanide application. This represents a window of stability for pharmacological studies to be conducted.

Table 3-1 Quantification of epileptic activity showed a period of stability (± 10%) at 120 minute up to 180 minutes, as well as from 190 to 240 minutes after rotenone and cyanide application.

Time (min)	Burst count (mean ± SEM) in burst/min	Time (min)	Burst count (mean ± SEM) in burst/min
10	1.80 ± 1.80	**130**	10.30 ± 1.97
20	3.10 ± 3.10	**140**	10.30 ± 1.95
30	6.22 ± 3.92	**150**	10.18 ± 1.96
40	5.83 ± 4.32	**160**	10.12 ± 1.86
50	9.29 ± 3.99	**170**	10.32 ± 2.16
60	10.81 ± 1.77	**180**	9.22 ± 1.60
70	11.04 ± 2.70	**190**	8.46 ± 1.33
80	11.16 ± 2.59	**200**	8.18 ± 1.12
90	12.36 ± 2.53	**210**	8.10 ± 1.02
100	10.86 ± 3.19	**220**	7.70 ± 1.07
110	11.18 ± 2.63	**230**	7.42 ± 0.40
120	9.82 ± 1.86	**240**	7.54 ± 0.84

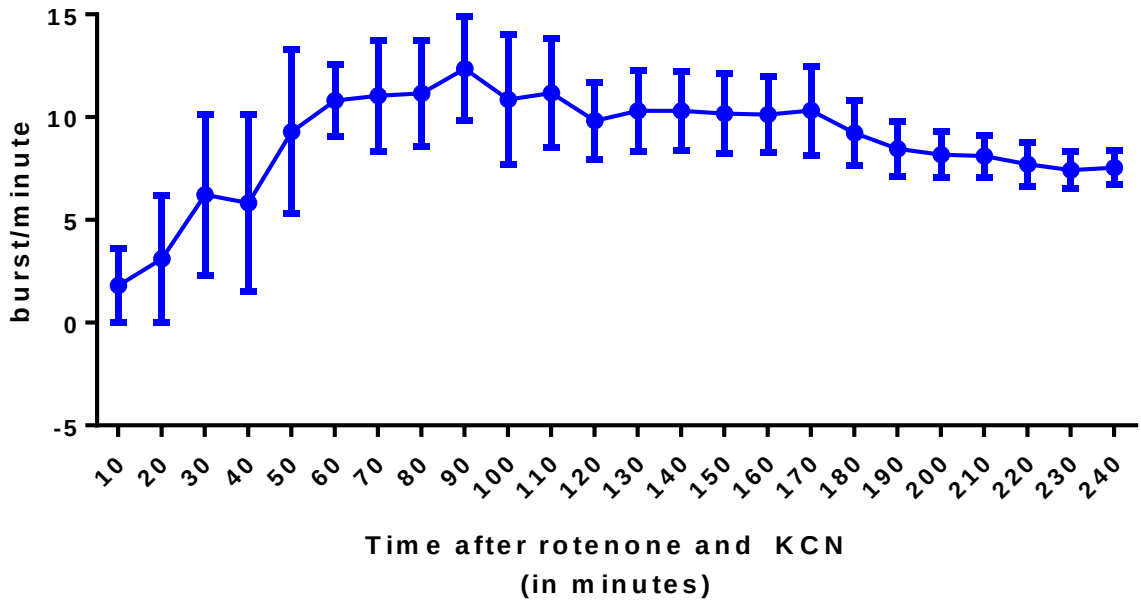

Figure 3-7 There is a period of stable frequency of epileptiform discharges after 2 hour of application of rotenone and potassium cyanide. This time period corresponds to the observation of when the activity transitions to the late recurrent interictal discharges.

3.3.6 Neuronal population loss in the epileptic tissue

It has long been recognized that severe and chronic epilepsy models (usually associated with status epilepticus) is associated with neuronal cell death (Dam, 1980; Meldrum, 1993; Dingledine *et al.*, 2014). Neuropathological findings in patients with mitochondrial epilepsy also showed a severe loss of neuronal population in the neocortex, particularly those of the GABAergic interneurons (Lax *et al.*, 2016). Since this model is based on the recapitulation of these neuropathological findings, it is unsurprising to expect a degree of neuronal loss in the hippocampus following the induction of the epileptiform activity. To examine this, post-hoc immunohistochemistry has been conducted on the pan-neuronal marker NeuN, a nuclear protein expressed exclusively in mature post-mitotic neuronal cells (Gusel'nikova and Korzhevskiy, 2015).

There is a global loss of neurons in both the neocortex and the hippocampus of the epileptic brain slices (see Figure 3-8). Prominent thinning of the pyramidal layer of the hippocampus was observed in the epileptic tissue. Quantification in the CA3 subfield of the hippocampus confirmed that there is a significant reduction ($p<0.05$) of the NeuN-positive cells in the epileptic tissue (344.10 ± 18.56 cells/mm^2, $n=9$) as compared against control tissue (487.60 ± 33.39 cells/mm^2, $n=17$). This indicates that there is a loss of neuronal population following the mitochondrial epilepsy induction protocol. To further characterize if there is a specific neuronal population that is more vulnerable to the epileptic induction, I have chosen to test against a panel of commonly used neuronal markers to confirm this finding.

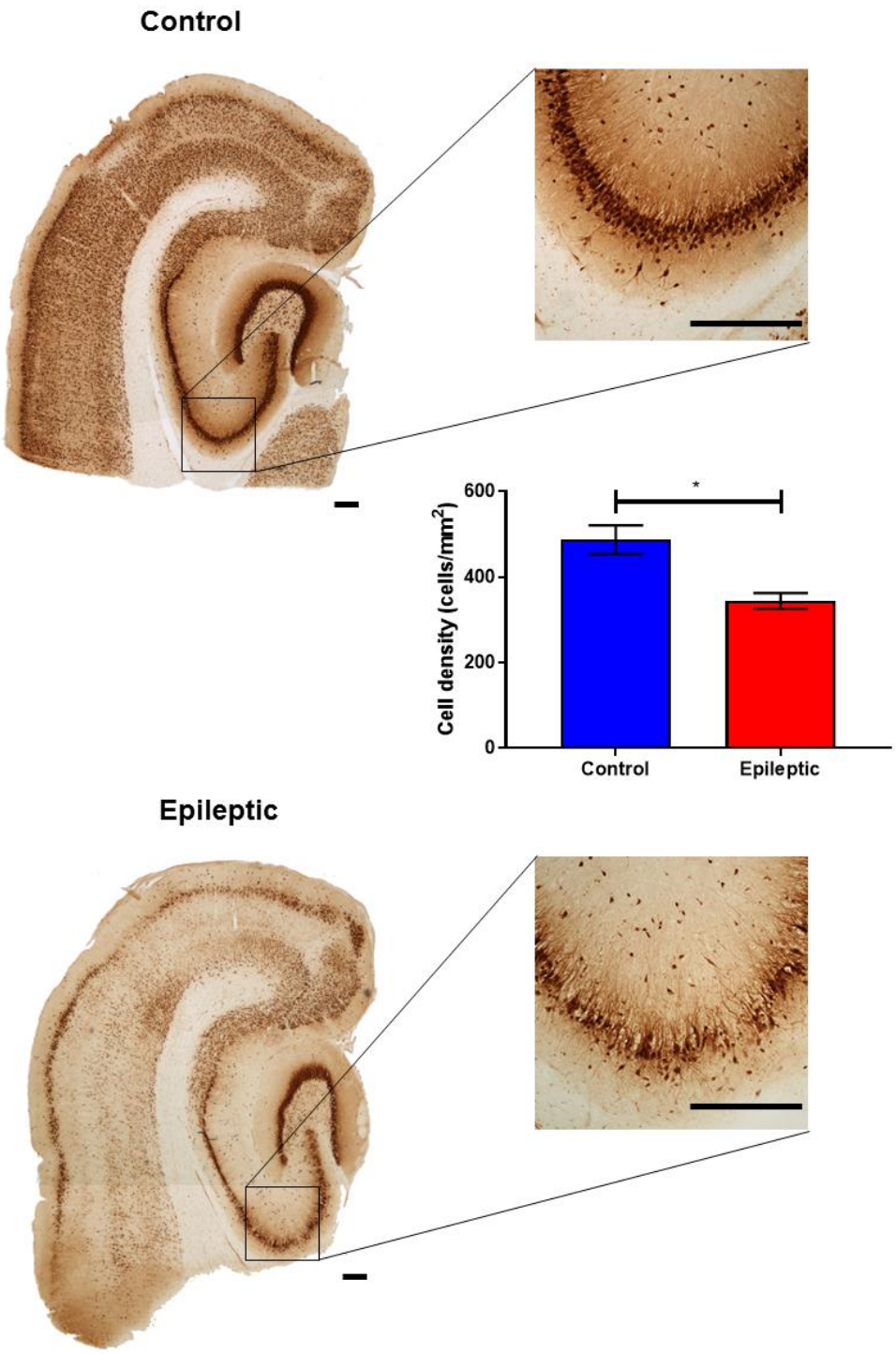

Figure 3-8 There is a significant neuronal loss in the epileptic hippocampus CA3 relative to control tissues. Shown is an example of control and epileptic slices stained for the NeuN protein. Insert showcases the higher magnification of the hippocampus CA3, where quantification was done. The bar chart shows the cell density measurements from the hippocampus CA3 in the control and epileptic slices respectively. Asterisk indicates significance at p< 0.05. Scale bar in both the whole brain image and the insert indicates 100µm.

3.3.6.1 Excitatory neurons

Pyramidal neurons are the most prominent member of the excitatory neuron grouping and make up about two-thirds of all the neurons in the mammalian cerebral cortex (Bekkers, 2011), placing them centre-stage for many important brain processes. One marker that is commonly used to detect excitatory pyramidal cells is the calmodulin protein kinase type II (CaMKII). It has comprehensively been demonstrated that GABA-ergic inhibitory cells lack the expression of CaMKII and thus, the protein is an excellent surrogate marker of the excitatory neuronal population (Benson *et al.*, 1992; Liu and Murray, 2012; Wang *et al.*, 2013).

There was no observable difference in the expression of CaMKII between control and epileptic brain slices (see Figure 3-9). Quantification confirmed this and showed that there is no significant difference ($p>0.05$) between the control tissue (97.48 ± 12.35 cells/mm^2, n=11) and the epileptic tissue (81.05 ± 8.25 cells/mm^2, n=7). This suggests that the excitatory pyramidal neurons are relatively spared by the mitochondrial epilepsy induction protocol.

3.3.6.2 Inhibitory neurons

Inhibitory interneurons contribute to only 20-30% of the neuronal population and yet are responsible for the inhibitory tone of the whole brain (Markram *et al.*, 2004). There is growing evidence that inhibitory interneurons, unlike the excitatory pyramidal neurons, have a heavy metabolic demand and hence, relatively higher mitochondrial function (Gulyás *et al.*, 2006; Hazelton *et al.*, 2009; Lin-Hendel *et al.*, 2016). This is confirmed in the neuropathological study of the patients with mitochondrial disease demonstrating significant loss of interneurons in those patients with epileptic phenotype (Lax *et al.*, 2016). Unsurprisingly, I chose to stain for GABA as a marker for inhibitory interneuron population in the hippocampus.

There is a considerable loss of expression of GABA in the epileptic tissue, as compared against control (see Figure 3-10). Quantification in the CA3 of hippocampus showed that there is indeed a significant reduction ($p<0.05$) of GABA-ergic cells in the epileptic tissue (89.80 ± 8.80 cells/mm^2, n=6) when compared against the control tissue (168.20 ± 23.39 cells/mm^2, n=6). This reduction in inhibitory interneuron population is reflective of alterations observed in human neuropathological studies.

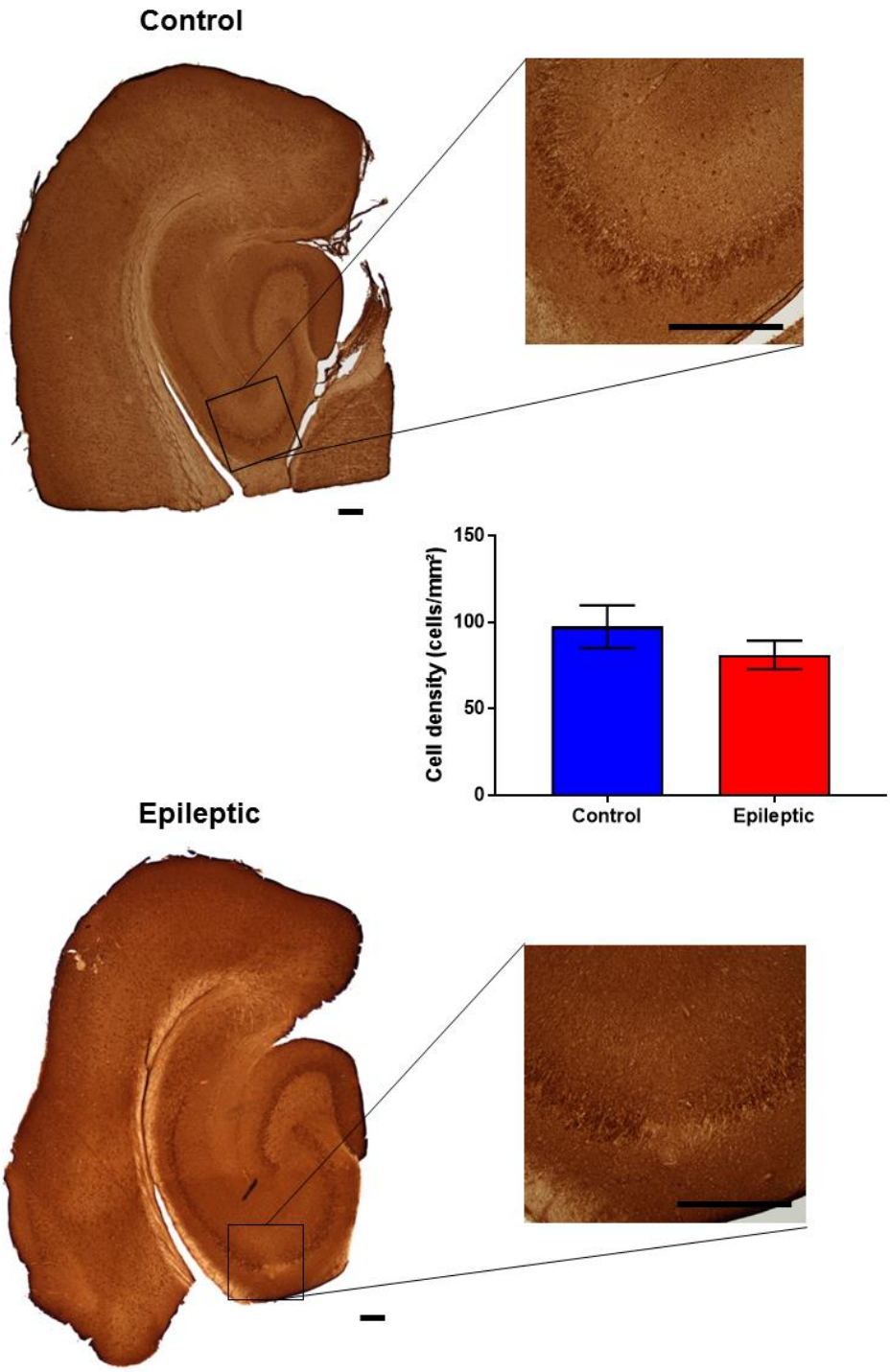

Figure 3-9 Excitatory cell population of the hippocampus CA3 is relatively spared in the epileptic tissue. Shown is an example of control and epileptic slices stained for the CaMKII protein. Insert showcases the higher magnification of the hippocampus CA3, where quantification was done. The bar chart shows the cell density measurements from the hippocampus CA3 in the control and epileptic slices respectively. Scale bar in both the whole brain image and the insert indicates 100µm.

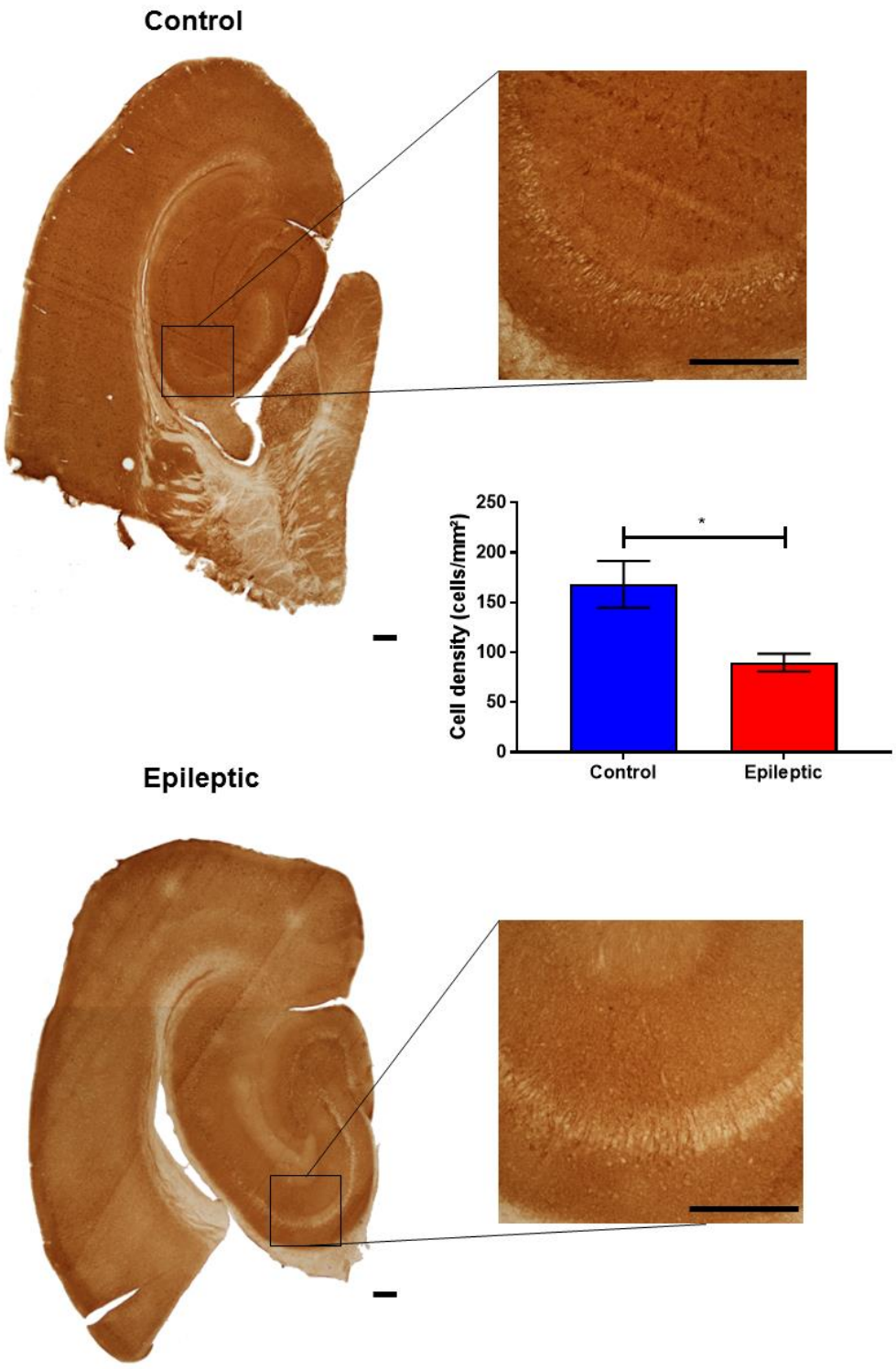

Figure 3-10 There is a significant reduction in the inhibitory neuron population in the epileptic tissue. Shown is an example of control and epileptic slices stained for the GABA protein. Insert showcases the higher magnification of the hippocampus CA3, where quantification was done. The bar chart shows the cell density measurements from the hippocampus CA3 in the control and epileptic slices respectively. Asterisk indicates significance at p< 0.05. Scale bar in both the whole brain image and the insert indicates 100µm.

3.3.7 There is no specific vulnerability of interneuron subtypes towards the mitochondrial epilepsy insult

Using GABA as a marker, I have observed a reduction in the number of inhibitory interneurons in epileptic tissue. However, there are many different types of interneurons with various distinct morphological and functional properties, such as the somadendritic – targeting basket cells or the dendritic – targeting Martinotti cells; which together make up more than 50% of the interneuron population in the cortex (Markram *et al.*, 2004). These interneurons can be defined through the differential labelling of the various calcium binding proteins that they express (Van Brederode *et al.*, 1990; Demeulemeester *et al.*, 1991; Wild *et al.*, 2005; Zaitsev *et al.*, 2005). Functionally, it has been demonstrated that these interneurons are also distinct in their mitochondrial and metabolic capacity. For instance, parvalbumin-expressing interneurons in the hippocampus have a strong co-localization with the mitochondrial enzyme, cytochrome c, but not the calretinin-expressing interneurons (Gulyás *et al.*, 2006). Therefore, I hypothesized that there could be selective vulnerability of specific interneuron subtypes towards the mitochondrial epilepsy induction protocol. As an initial screen, I have chosen three of the most commonly used calcium-binding proteins (parvalbumin, calbindin, and calretinin) to examine these specific interneuron populations.

3.3.7.1 Parvalbumin-expressing interneurons

Parvalbumin-expressing interneurons make up about 40% of the total interneuron populations, making them the most prominent subtypes of the inhibitory interneuron (Kelsom and Lu, 2013). There are two morphological types of interneurons that make up the parvalbumin-expressing interneuron population: the basket cell and the chandelier cell (Markram *et al.*, 2004; Kelsom and Lu, 2013). These parvalbumin-expressing interneurons are distinct in that they are rapidly recruited by excitatory synaptic input to generate high-frequency trains of action potentials that provide a rapid, stable, phase-locked, and timed inhibitory output (Bartos and Elgueta, 2012). It is due to this highly sophisticated and complex inhibitory output that the parvalbumin-expressing interneurons are thought to require the highly co-localized mitochondrial enzyme, cytochrome c (Gulyás *et al.*, 2006). Therefore, I examined the population of parvalbumin – expressing interneurons in the epileptic tissue, expecting a significant loss of this particular subtype of interneuron.

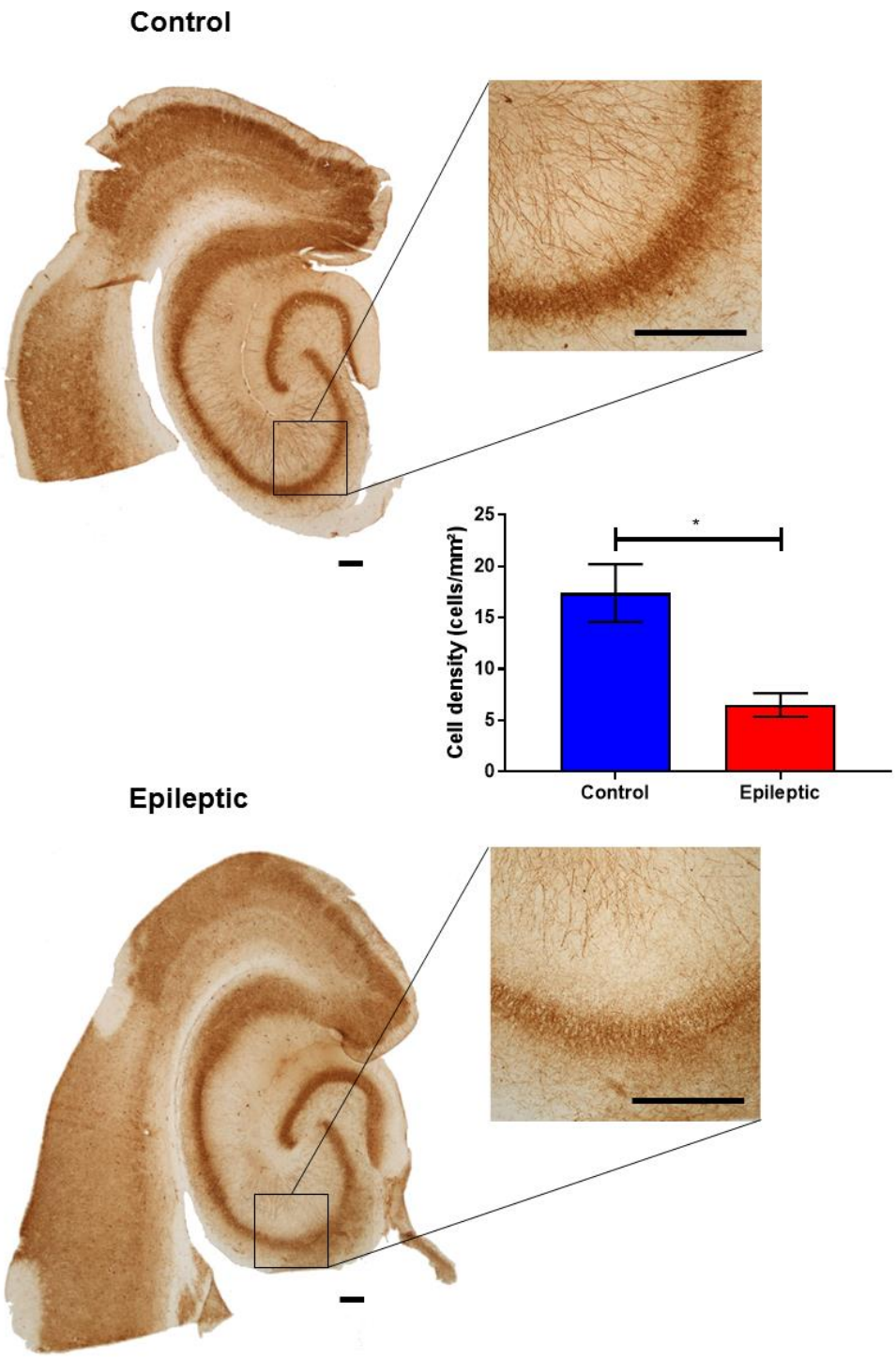

Figure 3-11 There is a significant reduction in the parvalbumin - expressing interneurons in the epileptic hippocampus CA3. Shown is an example of control and epileptic slices stained for the parvalbumin protein. Insert showcases the higher magnification of the hippocampus CA3, where quantification was done. The bar chart shows the cell density measurements from the hippocampus CA3 in the control and epileptic slices respectively. Asterisk indicates significance at p< 0.05. Scale bar in both the whole brain image and the insert indicates 100µm.

There was a significant reduction in the number of parvalbumin – expressing interneuron population in the epileptic tissue (see Figure 3-11). Furthermore, there is also a significant loss of the extensive dendritic arborisation in the stratum radiatum and lacunosum that is typically labelled by the parvalbumin antibody in the control hippocampus. When quantified, it was confirmed that there was a significant reduction ($p<0.05$) in the parvalbumin-expressing cell density in the epileptic tissue (6.51 ± 1.15 cells/mm^2, n=6) when compared against the control tissue (17.40 ± 2.81 cells/mm^2, n=6).

3.3.7.2 Calbindin-expressing interneurons

Another subtype of the interneuron family is the calbindin-expressing interneurons. These interneurons were found to have region-specific mitochondrial expression with those in the hippocampus CA3 strongly co-localizing with mitochondrial cytochrome c; whereas in the dentate gyrus this co-localization was not present (Gulyás *et al.*, 2006). Although calbindin is also expressed in the pyramidal cells in the hippocampus CA1, its expression in the CA3 is restricted to interneurons and they exhibit stellate-like appearance in all layers of this region (Freund and Buzsaki, 1996). I, therefore, examined the population of calbindin-expressing interneurons in the CA3 region of the hippocampus.

There was a generalized change in the calbindin expression in the epileptic slice (see Figure 3-12). The neocortex was very significantly affected in the epileptic slices, particularly in the deeper layers (cortical layer III-VI). The calbindin-expressing pyramidal cells of stratum pyramidale in CA1 were to a large degree well – preserved in the epileptic slice. In CA3, however, there was a significant loss of the calbindin – expressing interneurons typically found in stratum radiatum and lacunosum. Quantification of these cells confirmed that there was a significant loss ($p<0.05$) of the calbindin-expressing interneurons in the hippocampus CA3 of the epileptic tissue (15.70 ± 1.48 cells/mm^2, n=7) as compared against control (22.40 ± 1.82 cells/mm^2, n=5).

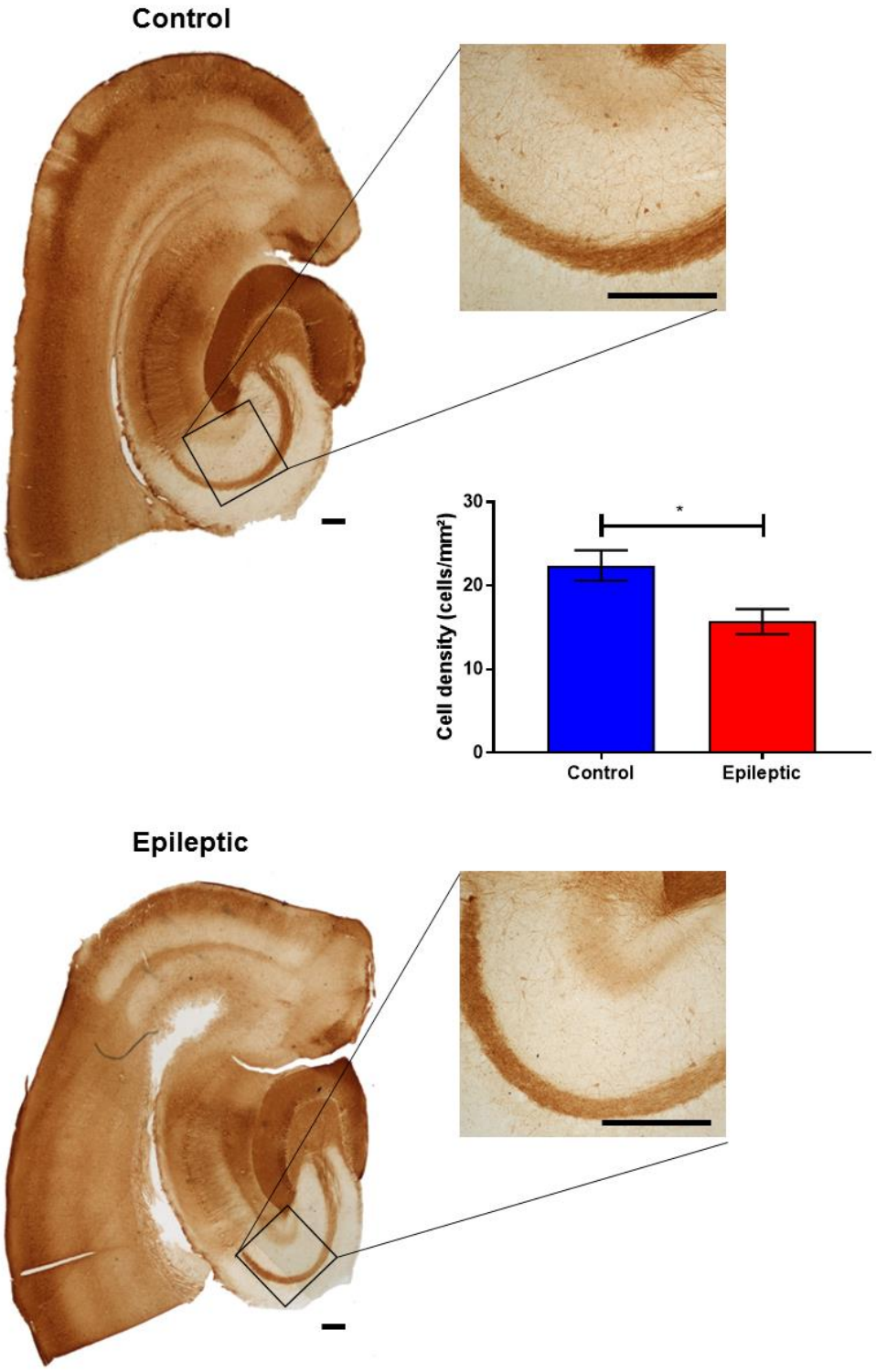

Figure 3-12 There is a significant reduction in the calbindin – expressing interneurons in the epileptic hippocampus CA3. Shown is an example of control and epileptic slices stained for the calbindin protein. Insert showcases the higher magnification of the hippocampus CA3, where quantification was done. The bar chart shows the cell density measurements from the hippocampus CA3 in the control and epileptic slices respectively. Asterisk indicates significance at p< 0.05. Scale bar in both the whole brain image and the insert indicates 100µm.

3.3.7.3 Calretinin-expressing interneurons

Calretinin-expressing interneurons are distributed across all layers and subfields of the hippocampus and the dentate gyrus (Freund and Buzsaki, 1996). The expression of mitochondrial cytochrome c is unique in that it weakly co-localizes with calretinin, unlike the parvalbumin and calbindin expressing interneurons (Gulyás *et al.*, 2006). With that in mind, it is possible that calretinin-expressing interneurons might not be as susceptible to the mitochondrial epilepsy induction protocol as the parvalbumin and calbindin-expressing interneurons appear to be.

Upon microscopic examination of the epileptic tissue, I found that there also appears to be a generalized change in the calretinin expression following the mitochondrial epilepsy induction (see Figure 3-13). There was a loss of calretinin-expressing cells across all layers of the neocortex. There also appeared to be a thinning of the calretinin-expressing cells in the stratum pyramidale of the hippocampus, across the CA1 and the CA3 subfields. This was also seen in the dentate gyrus, albeit less pronounced as the CA subfields. Quantification in CA3 revealed that there was indeed a significant reduction in the density of calretinin – expressing cells in the epileptic tissue (105.90 ± 10.21 cells/mm^2, n=9) as compared against the control tissue (145.20 ± 11.26 cells/mm^2, n=11).

Having now conducted the initial screen for the interneuron subtypes using three cellular markers; parvalbumin, calbindin, and calretinin; I have found that there was no specific vulnerability of a subtype of inhibitory interneurons in this model of mitochondrial epilepsy. However, there are other major subtypes of interneurons that were yet to be investigated, such as the somatostatin-expressing interneurons, the vasoactive intestinal peptide (VIP)-expressing interneurons, and the cholecystokinin-expressing interneurons. The vulnerability of a specific subtype of interneuron cannot therefore be confidently excluded without the complete assessment of all the subtypes of inhibitory interneurons observable in the hippocampus.

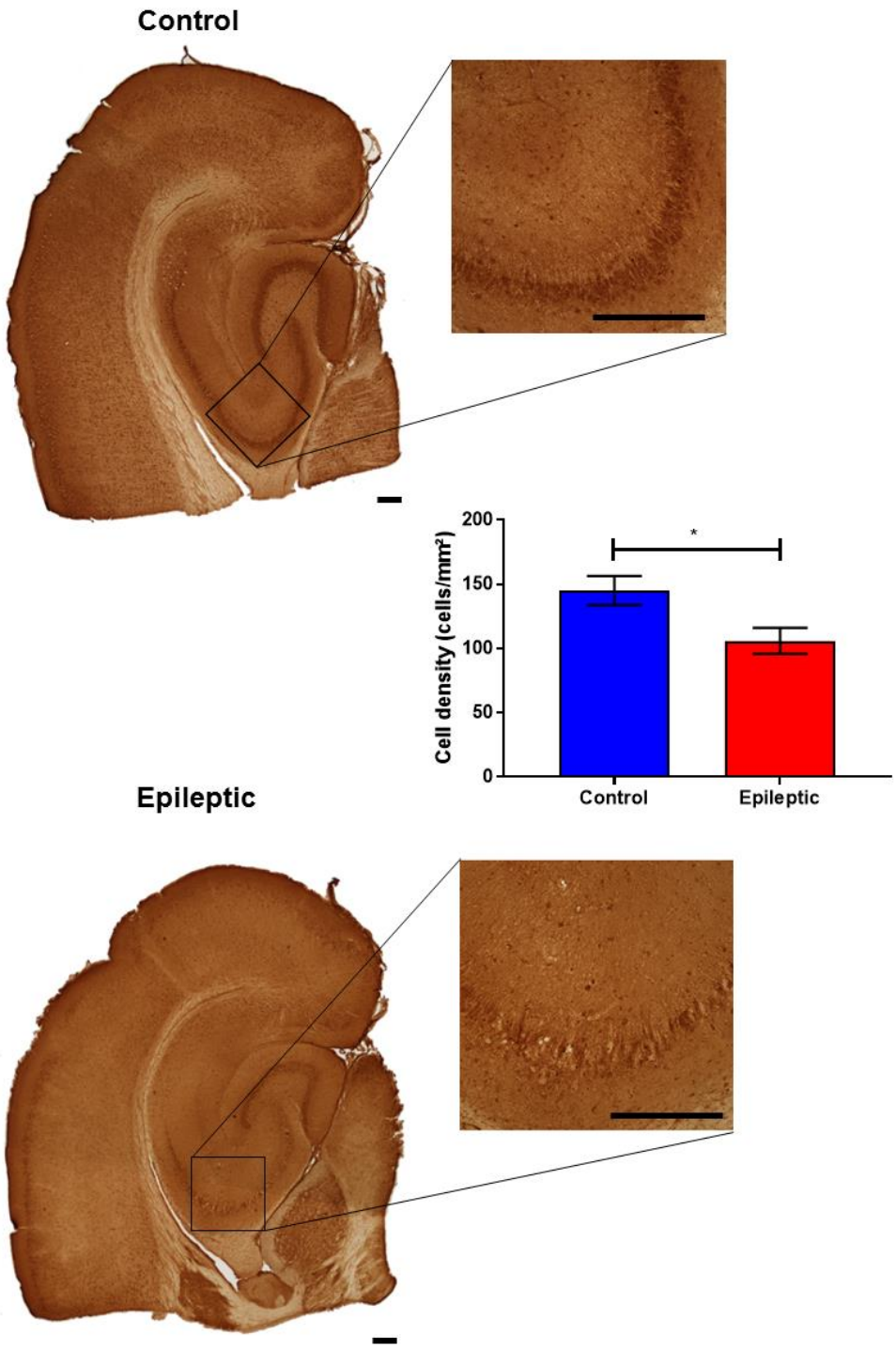

Figure 3-13 There is a significant reduction in the calretinin - expressing interneurons in the epileptic hippocampus CA3. Shown is an example of control and epileptic slices stained for the calretinin protein. Insert showcases the higher magnification of the hippocampus CA3, where quantification was done. The bar chart shows the cell density measurements from the hippocampus CA3 in the control and epileptic slices respectively. Asterisk indicates significance at p< 0.05. Scale bar in both the whole brain image and the insert indicates 100µm.

3.3.8 Extensive astrogliosis is present in epileptic tissue

Hitherto, the discussion of the neuropathological changes in this brain slice model of mitochondrial epilepsy has been limited to the neuronal compartment. However, the neuropathological study mentioned previously has clearly outlined that there is also an extensive involvement of the astrocytic compartment in the post-mortem brain tissue of patients with mitochondrial epilepsy. Profound astrogliosis was observed in the neocortex and the remaining astrocytes were found to have mitochondrial respiratory complex I and IV deficiency (see Figure 3-1). Therefore, it is important to consider the astrocytic compartment as well in the observation of the neuropathological changes in this model of mitochondrial epilepsy. To do this, I have stained for the glial fibrillary acidic protein (GFAP), a protein expressed exclusively in the astrocytes and found to be upregulated following astrogliosis (Hol and Pekny, 2015).

Following immunostaining, I found that expression of GFAP was significantly altered in the epileptic tissue (see Figure 3-14). In the control tissue, astrocytes were found across all layers in an organized and laminar labelling pattern. In the epileptic tissue, however, prominent glial scar was found in both the neocortex and the hippocampus. The glial scar is well-defined and encapsulated. At the core of each glial scar, no viable astrocytes were observed. The remaining astrocytes, either at the periphery of the glial scar or at the unscarred area, exhibited atypical dysmorphic morphology; indicative of reactive astrogliosis. Astrogliosis tends to follow a pattern of progression (Sofroniew; Sofroniew and Vinters, 2010) and in this model, it seems to have reached the end-stage of severe reactive astrogliosis followed by glial scar formation. Quantification was performed by delineating the area of reactive astrogliosis across the whole brain slice and calculating the proportion of the astrogliotic area against the area of the whole slice. Using this calculation, I found that there was significantly higher astrogliotic area in the epileptic tissue (32.77 ± 6.00 %, n=8) as compared against control (4.32 ± 1.95 %, n=11). This confirms that astrocytes are severely affected in this model of mitochondrial epilepsy to the end-stage of astrogliosis: severe reactive astrogliosis with glial scar formation.

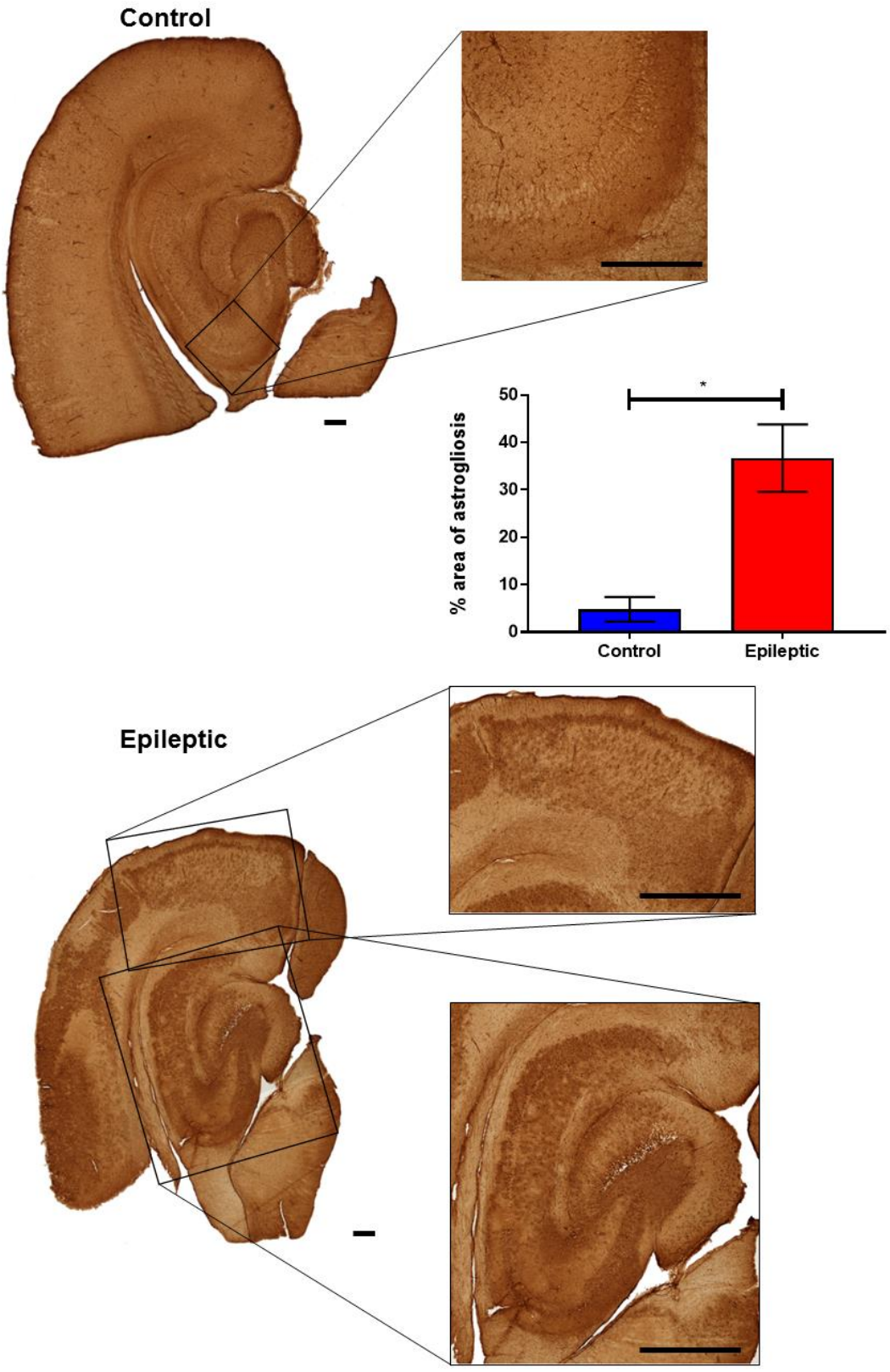

Figure 3-14 There is extensive astrogliosis and glial scar formation in the epileptic tissue. Shown is an example of control and epileptic slices stained for the glial fibrillary acidic protein. There appears to be extensive astrogliosis and glial scar formation in the epileptic tissue. Insert in the control tissue showcases normal astroglial labelling pattern in the hippocampus CA3 whereas insert in the epileptic tissue showcases higher magnification of the glial scar found in both the neocortex and the hippocampus. The bar chart shows quantification of the percentage of gliotic area in the control and epileptic slices respectively. Asterisk indicates significance at $p<0.05$. Scale bar in both the whole brain image and the insert indicates 100µm.

3.4 Discussion

3.4.1 Development of the *in vitro* model of mitochondrial epilepsy

This *in vitro* brain slice model of mitochondrial epilepsy is based on the principle of recapitulating the neuropathological findings from post-mortem studies on the neocortex of patients with mitochondrial epilepsy (Lax *et al.*, 2016). It has been argued that this approach of back translation from human studies to animal models may be the most effective approach in *in vitro* modelling of human diseases (Chan *et al.*, 2016). In previously published study, it was established that there is a severe interneuron loss in the cerebral cortex of patients with mitochondrial epilepsy and the deficiency of mitochondrial complex I and IV subunit expression in the remaining surviving interneurons (Lax *et al.*, 2016). The author further extended this neuropathological finding and described similar deficiency of mitochondrial complex I and IV subunit expression in astrocytes as well as a prominent pattern of reactive astrogliosis (Lax *et al*., unpublished data; see Figure 3-1).

This neuropathological study implicated that in addition to the neuronal compartment, the astrocytic compartment seems to be affected equally in patients with mitochondrial epilepsy. As a proof of concept, I conducted an experiment using acutely prepared rodent brain slices where I washed in mitochondrial complex I inhibitor (rotenone), complex IV inhibitor (potassium cyanide), and an astrocytic mitochondrial inhibitor (fluorocitrate). This combination of pharmacological agents at a specific concentration (discussed extensively in section 3.3.1) was able to induce epileptiform discharges robustly in the hippocampus CA3. This was the first study to describe an acute induction of epileptic activity through the manipulation of mitochondrial function. Interestingly, all three components of the induction protocol are required for induction of epileptiform discharges. The application of either one or two of the components alone cannot induce epileptiform discharges. This suggests a synergistic mechanism between the three pharmacological tools in modifying the metabolic state so that the network becomes hyperexcitable and produces epileptiform discharges.

Two forms of the epileptiform discharges have been extensively described and discussed above in section 3.3.1. Initially, the model manifested as interictal discharges which gradually build up in frequency and amplitude as time progressed. Eventually, this would manifest in the ictal discharges, which would be followed by a period of no observable activity in the network, which I have called the ‘post-ictal

silencing' period. Following the post-ictal silencing, the activity would re-manifest as interictal discharges which would then restart the cycle of interictal – ictal activity as above. At some point, the network activity transitioned to the late interictal recurrent discharges. The activity would continuously manifest as interictal discharges for a prolonged period of time without any ictal burst. This transition to the late recurrent discharges somewhat resembles the progression seen in the zero – magnesium model (Reddy and Kuruba, 2013). In the zero-magnesium model, this transition is associated with the erosion of inhibition in the tissue over time (Whittington *et al.*, 1995). Perhaps, this is the same in our model as the inhibition of mitochondrial respiration has been associated with the selective reduction in inhibitory tone (Whittaker *et al.*, 2011). In patients with mitochondrial disease, a variety of seizure semiologies can be found (Torbergsen *et al.*, 1991; Bindoff and Engelsen, 2012) but the most common seizure types in the most common phenotype associated with epilepsy (MELAS) is generalized tonic-clonic seizure with focal intermittent interictal discharges (Chevallier *et al.*, 2014). It can be argued that the generalized tonic-clonic seizure resembles the ictal discharges seen in this *in vitro* model and the focal interictal discharges resembles the interictal discharges. This further supports the face validity of this *in vitro* brain slice model of mitochondrial epilepsy.

In section 3.3.2, it was further described that at higher concentration of the respiratory chain inhibitors, generalized spreading depression was induced instead of the epileptiform discharges. In the context of mitochondrial disease, cortical spreading depression was found to be associated with stroke – like episodes in patients presenting with MELAS (Ohno *et al.*, 1997; Yonemura *et al.*, 2001). This further supports the suggestions that this *in vitro* brain slice model of mitochondrial epilepsy does replicate the features of mitochondrial disease, particularly MELAS. Furthermore, cortical spreading depression is an electroencephalographic feature where there is a wave of neuronal and glial depolarization followed by a persistent inhibition across the whole cortical area (Mayevsky *et al.*, 1996; Fabricius *et al.*, 2008). In this model, when spreading depression was induced; indeed, no further local field potential was observed. It can be argued that this post – spreading depression silencing very closely resembles the phenomenon of post – ictal silencing that was observed in the model. Perhaps, the ictal activity seen in this model is a subtler form of cortical spreading depression that is induced in lower degree of respiratory chain inhibition. If so, it can be argued then that the cortical spreading depression represents a progression of electroencephalographic manifestation of metabolic failure in the tissue.

To further validate the model, I have examined if substitution of the respiratory chain inhibitors, rotenone and potassium cyanide, with other established inhibitors would still induce epileptiform discharges. Section 3.3.3 has outlined that the substitution of rotenone with MPP^+-iodide or potassium cyanide with sodium azide still was able to induce similar epileptiform discharges in the hippocampus CA3 (see Figure 3-5). This suggests that the mitochondrial epilepsy induction is dependent on the presence of mitochondrial respiratory chain complex I and IV inhibition rather than the specific presence of rotenone and cyanide.

In section 3.3.4, an investigation was performed to see if the mitochondrial epilepsy induction protocol would similarly induce robust epileptiform discharges in acute brain slices from the commonly used laboratory mice, C57BL/6 mice; and from human patients who underwent elective neurosurgical procedures. The use of the mitochondrial epilepsy protocol was able to robustly produce the same interictal and ictal pattern of epileptiform discharges in the hippocampal brain slices from both species (see Figure 3-6). This further adds to the face validity of this brain slice model in that it is conserved across species. Furthermore, it has been discussed that the epileptic phenotype in mice very closely resembles that of rats, presumably due to its genetic similarity as members of the murine family (Consortium, 2004). The epileptic phenotype in human is slightly more variable and this is probably reflective of the genetic and clinical variety of the patients whose brain slices were obtained from (see Table 2-1 for patient information).

Finally, a quantification method was described in section 3.3.5. I have argued for the use of seizure frequency as the initial parameter to quantify in this model of mitochondrial epilepsy due to its high clinical relevance (Birbeck *et al.*, 2002). The use of the automated detection of epileptiform discharges represents a feasible, objective, and accurate measurement of the epileptic activity. The time-course experiment has shown a period of stable frequency of epileptiform discharges after 2 hours of application of rotenone and cyanide. This also coincides with the transition of the epileptic burst into the late recurrent interictal discharges. The presence of this time window is a golden opportunity to conduct pharmacological study which would require a stable functional system (to be discussed further below in section 4.4.1)

3.4.2 Neuropathological findings

Since the development of this model is based on the recapitulation of neuropathological findings from post-mortem study on patients with mitochondrial epilepsy, it is imperative to show that the model does indeed recapitulate the mitochondrial dysfunction observed in the human neuropathology. However, it is important to note that the post-mortem neuropathological study represents an investigation into the end-stage of a disease and may not provide insights into the acute stage of the disease. Furthermore, the patients studied in the neuropathological study have genetic abnormalities that lead to their disease development. These genetic abnormalities manifested as the loss of expression of a subunit of the mitochondrial respiratory chain. Acute pharmacological manipulation would not affect the expression of these subunits; rather, it just reduces the activity of the relevant mitochondrial respiratory complexes. Therefore, it would not be accurate to conduct post-mortem immunohistochemistry to detect against these mitochondrial complex subunits as was done in the human neuropathology. Rather, I have chosen to conduct an initial neuropathological examination on the neuronal and astroglial population in the epileptic tissue; both of which have been implicated in the human neuropathological studies.

3.4.2.1 Neuronal loss

As an initial screen for the whole neuronal population, I conducted immunolabeling of the NeuN protein (see section 3.3.6). The NeuN protein is a nuclear protein that is exclusively expressed in mature post-mitotic neuronal cells (Gusel'nikova and Korzhevskiy, 2015). The loss of expression of NeuN is closely associated with neuronal damage or death (Gusel'nikova and Korzhevskiy, 2015); therefore its use as a marker of neuronal loss is well-justified. In rare instances, the loss of expression of NeuN has been associated with the loss of antigenicity (Ünal-Çevik *et al.*, 2004). In this study, however, antigen retrieval was also shown to reverse this loss of antigenicity (Ünal-Çevik *et al.*, 2004) and since the technique I have used in the immunohistochemistry involved extensive antigen retrieval with heat-mediated sodium citrate buffer wash, I did not expect a loss of antigenicity in the assessment of NeuN expression in this model of mitochondrial epilepsy. Our results have

demonstrated a severe loss of NeuN expression across the whole brain slice and quantification in the CA3 region illustrated a significant reduction (see Figure 3-8). This strongly suggests that there is indeed neuronal loss following the mitochondrial epilepsy induction.

There are many mechanisms associated with neuronal loss in the epileptic tissue. One mechanism that may be relevant in this model is oxidative stress and the subsequent activation of apoptosis (Mendez-Armenta *et al.*, 2014). It has been shown in other model of epilepsy that seizure generation results in the mitochondria – independent reactive oxygen species production, eventually causing apoptosis in the tissue (Kovac *et al.*, 2014). Since mitochondria is a major source of the endogenous reactive oxygen species (Zorov *et al.*, 2014), it would not be surprising to expect oxidative stress following the mitochondrial epilepsy induction. This release of the reactive oxygen species can create a vicious cycle that further recruits more reactive oxygen species release from both the mitochondrial and extramitochondrial source (Kovac *et al.*, 2014; Zorov *et al.*, 2014). All this oxidative damage would inevitably upregulate the apoptotic signalling and system such as the caspase system (Kannan and Jain, 2000; Sinha *et al.*, 2013); leading to neuronal death and loss.

Interestingly, in a cell culture model, it has been found that spontaneous recurrent interictal discharges do not result in cell death but chronic status epilepticus does (Deshpande *et al.*, 2007). Indeed, acute epileptic models are rarely associated with neuronal loss due to the acute time course of the epileptic induction (Deshpande *et al.*, 2007; Deshpande *et al.*, 2008). However, it is clear in this model that there is extensive neuronal loss in the epileptic tissue. This may indicate the severity of the damage caused by the epileptiform discharges in this model, perhaps up to the level of that of status epilepticus.

To see if there is a specific subset of the neuronal population that is more susceptible to the mitochondrial epilepsy damage, I have conducted immunolabelling of the excitatory and inhibitory neuronal population through the labelling of the CaMKII and GABA protein respectively. Both CaMKII and GABA are well-characterized as specific markers of the excitatory and inhibitory neuron respectively (Benson *et al.*, 1992; Markram *et al.*, 2004). There was no significant difference in the CaMKII expressing cell population in the epileptic hippocampus CA3 (see Figure 3-9) whereas there was a significant reduction of GABA expressing cell population in the epileptic hippocampus CA3 (see Figure 3-10). This indicates that there is a selective

vulnerability of the inhibitory interneuron population towards the mitochondrial epilepsy insult. This fits with the current theories that the inhibitory interneurons have much higher metabolic demand than the excitatory neurons, leading to higher mitochondrial capacity and subsequently higher susceptibility to mitochondrial dysfunction (Gulyás *et al.*, 2006; Hazelton *et al.*, 2009; Kann *et al.*, 2014; Kann, 2016; Lin-Hendel *et al.*, 2016). Furthermore, it replicates the severe loss of inhibitory interneuron populations seen in the post-mortem neuropathological studies of patients with mitochondrial epilepsy (Lax *et al.*, 2016). However, a note of caution is that the loss of expression of GABA in the epileptic tissue might not necessarily mean the loss of the GABA-ergic cells. Indeed, it may simply indicate that the inhibitory cells have reduced GABA concentration and expression and are thus undetectable through the immunolabelling of GABA. This is certainly a possible scenario, but, taken together with the loss of NeuN expression, it strongly favours the hypothesis of the selective loss of inhibitory interneurons in the epileptic tissue.

To further dissect the susceptibility of the inhibitory interneuron population towards the mitochondrial epilepsy damage, I have screened for an initial panel of inhibitory interneuron markers (parvalbumin, calbindin, and calretinin) to see if there is a selective susceptibility of a subtype of interneurons towards the insult. Out of the three markers (see Figure 3-11, Figure 3-12, and Figure 3-13), all examined subtypes of inhibitory interneurons demonstrated a significant reduction in the epileptic hippocampus. This finding is surprising as immunolabeling with cytochrome c has revealed a strong co-localization with the parvalbumin and calbindin-expressing interneurons but not the calretinin-expressing interneurons of the hippocampus CA3 (Gulyás *et al.*, 2006). One would therefore expect that there would be a selective loss of the parvalbumin and calbindin-expressing interneurons due to their higher dependence and expression of mitochondrial cytochrome c. However, cytochrome c is merely a protein associated with complex IV of the respiratory chain and in this model, there is a concomitant inhibition of complex I and complex IV. Therefore, it would not be wrong to speculate that the calretinin-expressing interneuron loss may be due to the additional inhibition of complex I. Certainly, this finding potentially indicate that there is no selective susceptibility of a particular subtype of the inhibitory interneuron population towards the mitochondrial epilepsy insult. However, knowing that there are other major subtypes of interneurons that are yet to be investigated (such as the somatostatin, VIP, and cholecystokinin-expressing interneurons), no real conclusion

on the specific susceptibility of a particular subtype of interneuron can be made until the whole interneuron population is assessed and examined.

Regardless, collectively, all these findings confirmed that the neuronal compartment is severely affected in this model of mitochondrial epilepsy. There is a selective vulnerability of the inhibitory interneuron population towards the mitochondrial epileptic damage and this closely resembles the loss of interneuron seen in the human neuropathological study.

3.4.2.2 Astrogliosis

One vital component of the mitochondrial epilepsy induction protocol is fluorocitrate. Fluorocitrate has been shown to be a selective astrocytic aconitase inhibitor (Hassel *et al.*, 1992; Swanson and Graham, 1994; Fonnum *et al.*, 1997). Therefore, it is unsurprising to expect that the astrocytic component would be severely affected in this model of mitochondrial epilepsy. To investigate this, I performed immunolabeling against the glial fibrillary acidic protein (GFAP), a protein exclusively expressed in the astrocytes and is also a marker of astrogliosis (Hol and Pekny, 2015). The expression of GFAP was found to be significantly upregulated in the epileptic tissue (see Figure 3-14). Severe reactive astrogliosis was apparent across the whole brain slice in the epileptic tissue. Furthermore, glial scar formation is seen in the epileptic tissue in both the neocortex and the hippocampus. This glial scar is well-circumscribed and encapsulated an area of injury with no viable astrocytes at the core of the scar. According to a proposed grading system, the epileptic tissue in this model has exhibited feature of severe reactive astrogliosis followed by glial scar formation (Sofroniew and Vinters, 2010). Quantification of the proportion of gliotic area in the epileptic tissue has also shown a significant increase in percentage area of astrogliosis as compared against control. It is therefore very clear that there is extensive astrogliosis in this model of mitochondrial epilepsy and this closely resembles the astrogliosis seen in the neuropathological study of the patients with mitochondrial epilepsy (Lax *et al.*, unpublished data; see Figure 3-1).

In various other studies, reactive astrogliosis, especially the border – forming glial scar, is a protective mechanism to limit the extent of the brain injury to the area of gliosis and is closely regulated by inflammatory signals (Bush *et al.*, 1999; Herx and Yong, 2001; Faulkner *et al.*, 2004; Myer *et al.*, 2006; Gadea *et al.*, 2008; Voskuhl *et al.*,

2009). Indeed, in studies of temporal lobe epilepsy, chronic inflammation has been closely implicated in the epileptic tissue (Vezzani *et al.*, 2011; Volmering *et al.*, 2016). In mitochondrial epilepsy, preliminary observations have shown in post-mortem neuropathological studies that indeed, signs of inflammation are seen in the neocortex from patients with mitochondrial epilepsy (Lax *et al.*, personal communication and unpublished data). Therefore, it is not out of the realm of imagination to hypothesize that chronic inflammation may play a role in the seizure generation in patients with mitochondrial epilepsy. As a compensatory mechanism, therefore, astrocytes respond by activating reactive astrogliosis mechanism and forming glial scar, creating a border around the area of injury.

Another possible mechanism that has been shown to modulate reactive astrogliosis is oxidative stress. In various studies, oxidative stress has been linked to the proliferation of reactive astrocytes and therefore, the initiation of astrogliosis (Bates *et al.*, 2007; Borges *et al.*, 2015; Puttachary *et al.*, 2015). As discussed above, oxidative stress is closely associated with epilepsy and the major source of endogenous oxidative stress is mitochondria (Zorov *et al.*, 2006; Kovac *et al.*, 2014; Zorov *et al.*, 2014). Thus, oxidative stress can also be a potent modulator of reactive astrogliosis in this model of mitochondrial epilepsy.

Although not directly demonstrated in this model, reactive astrogliosis has been closely associated with neuronal death or apoptosis (Yu *et al.*, 2012; Livne-Bar *et al.*, 2016). It has been suggested that the astrocytic and the neuronal compartment is closely working together in the maintenance of the inhibitory – excitatory balance in the brain through various mechanisms. The selective induction of reactive astrogliosis through the use of genetically modified animals has been shown to lead to alteration in the potassium channel expression, causing tissue hyperexcitability and the subsequent development of seizure (Yu *et al.*, 2014; Robel *et al.*, 2015). Another interesting study has shown that induction of reactive astrogliosis caused an erosion of the inhibitory tone in the tissue through the failure of the astrocytic glutamate – glutamine cycle (Ortinski *et al.*, 2010). Whatever the mechanism, it seems quite clear that there is an accumulative dysfunction in the astrocytic and the neuronal compartment that leads to the generation of seizure in this model of mitochondrial epilepsy. The end-stage of this dysfunction and the epileptic damage is reactive astrogliosis (for the astrocytic compartment) and neuronal loss (for the neuronal compartment).

3.5 Summary, strength, and weakness

The findings in this chapter has presented the conceptualisation and the development of the novel *in vitro* brain slice model of mitochondrial epilepsy that will be investigated further throughout the remainder of this thesis. Various experiments have been conducted to add to the face validity of the model. Specifically, it has been shown that the mitochondrial epilepsy induction is dependent on the presence of all three components of the induction protocol; namely fluorocitrate, the astrocytic aconitase inhibitor, and a mitochondrial respiratory chain complex I inhibitor (either rotenone or MPP^+-iodide) as well as a mitochondrial respiratory chain complex IV inhibitor (either potassium cyanide or sodium azide). Furthermore, it has been shown that the mitochondrial epilepsy induction is conserved across species. At higher concentration of the respiratory chain inhibitors, cortical spreading depression is induced instead, which may represent an electroencephalographic manifestation of a generalized metabolic failure. I have also shown that quantification of the epileptic activity through automated burst detection is feasible and has shown a period of stable epileptic system after 2 hours of induction with rotenone and cyanide. This stable period of activity will be the stepping stone for the conduct of pharmacological study (described and discussed in detail below in Chapter 4). Post-hoc immunohistochemistry has shown a selective loss of inhibitory interneuron population in the epileptic hippocampus CA3. To present, there is no selective vulnerability of a specific subtype of interneuron population, but more subtype of interneuron needs to be investigated before this can be confidently concluded. Astrogliosis is also demonstrated prominently in the epileptic tissue with well-defined glial scar formation.

Overall, a novel *in vitro* brain slice model of mitochondrial epilepsy has been developed and validated through a series of control experiments presented in this chapter. It is quite clear that there is the implication of two cellular populations in this model of mitochondrial epilepsy; the neuronal and the astrocytic compartment. This led to the development of the ‘dual neuronal-astrocytic hit hypothesis’. This hypothesis postulates the requirement of both neuronal and astrocytic mechanisms to be recruited for the generation of seizure in mitochondrial epilepsy. These specific mechanisms are to be discussed and explored further in the studies presented in the remainder of this thesis.

The findings in this chapter have presented a sound approach to the development of an *in vitro* model of epilepsy. However, with any newly developed model of epilepsy, a certain degree of uncertainty needs to be placed in terms of what it actually is modelling. The development of this model is based on the recapitulation of neuropathological findings from human patients who have this condition. However, these patient populations come from a diverse genetic (m.3243A>G or m.8433A>G) and clinical phenotype (such as MELAS or MERRF). Therefore, whilst this model mimics the common pathological features in these syndromes; it does not specifically model any of these syndromes. It is therefore inaccurate to say that this is a model of MELAS or MERRF. Rather, this is a newly developed model of mitochondrial epilepsy, a common epileptic feature seen in all these patients; where the epilepsy is much more severe and pharmacoresistant than the normal epileptic phenotype. Regardless, this is still the first *in vitro* model of mitochondrial epilepsy and therefore, the merit and the importance of its development should not be undervalued.

Chapter 4 Pharmacological characterization of mitochondrial epilepsy

4.1 Introduction

Mitochondrial epilepsy is particularly challenging to manage in the clinic as the seizures tend to respond poorly to the currently available antiepileptic drugs (Whittaker *et al.*, 2015). Current practice in the management of mitochondrial disease, including epilepsy, remains largely supportive, symptomatic, and highly variable depending on the patient's presentation and the physician's judgment (Steele and Chinnery, 2015). It is this extreme pharmacoresistance that defines mitochondrial epilepsy as a unique subtype of epilepsy. In fact, some researchers have gone as far as postulating that underlying mitochondrial dysfunction may be the basis of pharmacoresistance in epilepsy (Yuen and Sander, 2011).

Given the promising development of this *in vitro* brain slice model of mitochondrial epilepsy (as detailed in Chapter 3), I seized on the opportunity to conduct pharmacological profiling on mitochondrial epilepsy. I started by assessing the contribution of various common glutamatergic and GABA-ergic receptors. Then, I tested the response of the epileptiform activity against various currently licensed-to-use antiepileptics from various subtypes, including sodium channel blockers, barbiturates, and benzodiazepines.

Ketogenic diet is a high-fat, moderate-protein, and low-carbohydrate dietary intervention that has shown promising clinical efficacy in controlling intractable seizure in children (Branco *et al.*, 2016). In a small study evaluating the efficacy of ketogenic diet in children with mitochondrial epilepsy, it was found that half of them could achieve seizure freedom with the undertaking of the diet (Kang *et al.*, 2007). Furthermore, various case reports had reported successful treatment of various phenotypes of mitochondrial epilepsy with variants of the ketogenic diet (Martikainen *et al.*, 2012; Steriade *et al.*, 2014). Although the mechanism by which ketogenic diet exerts its antiepileptic action is largely unknown, it has been proposed that ketogenic diet could have a multitude of protective effect towards the mitochondria (Branco *et al.*, 2016), hence its potential use in patients with mitochondrial epilepsy.

Despite the initial thought that the antiepileptic effect of ketogenic diet is mediated by the ketone bodies, it has been documented that the level of ketosis did not correlate with the degree of seizure control (Likhodii *et al.*, 2000). This suggests that another component of the diet is responsible for its antiepileptic properties and recent studies have entertained the idea of these components being the fatty acids. In particular, the

medium-chain fatty acids such as octanoic acid and decanoic acid have been demonstrated to be antiepileptic (Wlaź *et al.*, 2012; Chang *et al.*, 2013). Mechanistically, decanoic acid has been shown to modulate the AMPA-R (Chang *et al.*, 2015) and also upregulate mitochondrial respiratory chain complex I activity (Hughes *et al.*, 2014). Together, these data show that medium-chain fatty acids, particularly decanoic acid, has promising potential for use in mitochondrial epilepsy and therefore warrants further investigation in this model.

In spite of all the mechanisms listed above, there is no denying that the application of ketone bodies or fatty acids may alleviate the seizure in mitochondrial epilepsy simply through providing energy substrates for the system. All mechanisms considered, the basic scientific concept underlying mitochondrial epilepsy remains the 'neuronal energy crisis' (Zsurka and Kunz, 2015). Theoretically then, any substances applied to the epileptic brain that could be processed metabolically by the mitochondria would alleviate the 'neuronal energy crisis' and could then silence the pathological seizure discharges.

One of the most fundamental process in energy metabolism of the brain is glycolysis. Under physiological condition, glucose is the main obligatory substrate for energy metabolism in the brain (McKenna *et al.*, 2006). The only pathway by which glucose can enter metabolism is through glycolysis. Glucose is converted to pyruvate, which can then enter the Krebs cycle in aerobic metabolism. Glycolysis is unique to the other metabolic pathway in that it can occur anaerobically through the conversion of pyruvate to lactate, mediated by the enzyme lactate dehydrogenase. The astrocyte – neuron lactate shuttle hypothesis postulates that in conditions of increased network activity, glutamate can stimulate astrocyte to release lactate which is used by the neurons as a preferential energy substrate (Pellerin and Magistretti, 1994; Chih and Roberts, 2003; Bélanger *et al.*, 2011) . It would, therefore, prove interesting to examine the effect of lactate and pyruvate application in restoring the energy crisis of the epileptic tissue. Modulation of brain glycolysis may prove to be an interesting avenue for therapeutic development in mitochondrial epilepsy.

Another interesting substrate of the brain would have to be GABA. GABA is a metabolic substrate of the glutamate-glutamine cycle (Bak *et al.*, 2006; Hertz and Rothman, 2016) and is also the most abundant inhibitory neurotransmitter in the brain. The glutamate-glutamine cycle represents one of the most important processes in neurotransmitter recycling and is largely mediated by the communication between two

distinct cellular compartments: the neuronal and astrocytic compartment (Westergaard *et al.*, 1995). Of particular interest to me, with regards to this model, is that astrocytic impairment plays a crucial role in epileptogenesis and the glutamate-glutamine cycle may very well be the astrocytic process implicated in mitochondrial epilepsy.

Having considered all these, I applied various metabolic substrates of the ketogenic diet, glycolysis, and the glutamate-glutamine cycle in this *in vitro* brain slice model of mitochondrial epilepsy to tease out the specific metabolic processes that could possibly be implicated in this epileptic model.

4.2 Methods

Rat hippocampal slices were prepared as described in Chapter 2. Mitochondrial epilepsy were induced as described in section 2.5 and inhibitors were washed in until it reached the period of stability as described in section 3.3.5.

Once the epileptic activity was stable, the various pharmacological compounds or metabolic substrates were washed in the ACSF. For most experiments, two concentrations were generally used: the minimum inhibitory concentration (MIC) and the maximum tolerable concentration (MTC). Both concentration values were typically obtained through literature search. The MIC were first washed in for the first 30 minutes and then the MTC were washed in for the next 30 minutes. For characterization of receptor contribution, I used one concentration for each inhibitor, for which the concentration was known to adequately inhibit the target receptor selectively.

For some novel uncharacterized interventions, a dose-response curve has been generated. This is typically done by washing in four increasingly higher concentration of the compounds for 30 minutes each. In total, the pharmacological intervention typically took place within 1-2 hours of the stable period of epileptic activity. Dose-response curves were only generated when the suppressive effect appeared to be dose-dependent.

4.3 Results

4.3.1 Pharmacological response towards application of vehicle

In the development of any pharmacological agent, a serious consideration needs to be put in place for the vehicle formulations used in dissolving the compounds. Most pharmacological agents are water soluble, but an increasing number of new compounds are highly lipophilic and therefore poorly water soluble (Bittner and Mountfield, 2002). These compounds require an organic solvent for their dissolution and one of the most commonly used organic solvent is dimethyl sulfoxide (DMSO). Although these organic solvents are described as 'inert' compounds, several studies in various platforms have reported a 'vehicle effect', whereby the vehicle formulation used exhibited an effect on its own (Cavas *et al.*, 2005; Nasrallah *et al.*, 2008; Galvao *et al.*, 2014). This is particularly important when evaluating the pharmacological response of an anticonvulsant towards epileptiform discharges. The discovery of valproate as an anticonvulsant started through the finding that its use as a vehicle formulation for a lipophilic drug exhibited antiepileptic properties on its own (Beydoun *et al.*, 2008). In this study, I have used two vehicle formulations for the dissolution of all the pharmacological agents tested: water for the hydrophilic compounds and DMSO for the lipophilic compounds. Therefore, I have examined the effect of cumulative addition of these vehicles over four different concentrations towards the induced epileptiform discharges (see Figure 4-1).

There was no significant difference ($n=5$, $p>0.05$) in the frequency of epileptiform discharges following cumulative application of varying percentage of dH_2O (0.1 – 1 %). Specifically, there was no difference between baseline (14.20 ± 1.09 burst/min), following 0.1 % dH_2O addition (14.64 ± 1.00 burst/min), 0.25% dH_2O addition (13.92 ± 0.85 burst/min), 0.5% dH_2O addition (13.72 ± 0.93 burst/min), and 1% dH_2O addition (15.34 ± 2.34 burst/min).

Similarly, there was no statistically significant difference ($n=12$, $p>0.05$) in the frequency of epileptiform discharges following cumulative application of varying percentage of DMSO, ranging from 0.0001 – 0.1 %. Again, specifically, there was no difference between baseline (13.88 ± 1.85 burst/min), following 0.0001% DMSO addition (13.41 ± 2.28 burst/min), 0.001% DMSO addition (10.13 ± 2.70 burst/min), 0.01% DMSO addition (11.77 ± 2.97 burst/min), and 0.1% DMSO addition (10.34 ± 2.62 burst/min).

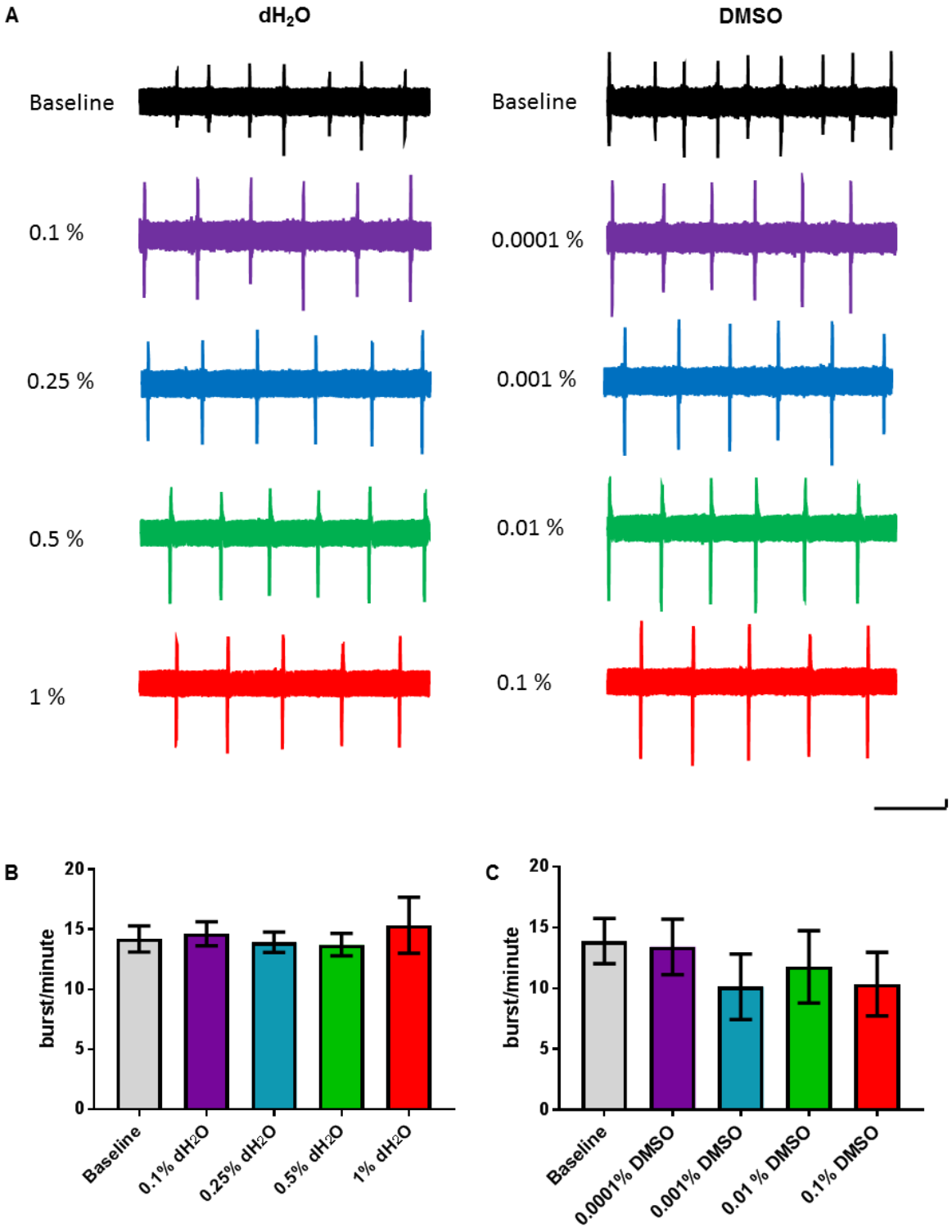

Figure 4-1 Epileptic activity does not respond towards vehicle application. (A) Shown on the left and right hand side is the response of the epileptic activity towards cumulative addition of water and DMSO respectively at varying % v/v. The corresponding bar chart summarizing the response towards water and DMSO is shown in (B) and (C) respectively. Scale bar 100µV and 10 seconds.

These results suggest that in this model of mitochondrial epilepsy, there was no demonstrable vehicle effect with addition of dH_2O up to 1% and DMSO up to 0.1%. Considering this, all of the drugs used in this chapter will be dissolved using either dH_2O or DMSO up to these concentrations. Any remaining pharmacological responses can then be confidently attributed to the mechanism of actions of the pharmacological agents tested.

4.3.2 Characterization of receptor contributions in mitochondrial epilepsy

Previous works on epilepsy models in acute brain slices have implicated various glutamatergic and GABA-ergic receptor contribution in seizure generation (Williamson and Wheal, 1992; Isaeva *et al.*, 2010). The three receptors that are most frequently implicated in epilepsy are the glutamatergic NMDA-R and AMPA-R as well as the GABA-ergic $GABA_A$ receptor. I hence decided to test the response of the epileptic activity to selective antagonism of NMDA-Rs by the bath application of D-AP5 (50μM), AMPA-Rs by NBQX (20μM), and $GABA_A$-Rs by gabazine (500nM) (see Figure 4-2.) These concentrations of D-AP5 and NBQX were chosen as they have been reported in the literature to generate a higher than 50% inhibitory effect in their respective inhibited receptors (Randle *et al.*, 1992; Wu *et al.*, 1999). On the other hand, I have chosen to use the IC_{50} of gabazine (~480nM) as a complete antagonism of inhibition could result in the slices progressing towards generalized spreading depression, as described in section 3.3.2 (Lindquist *et al.*, 2005).

Addition of 50μM D-AP5 for 60 minutes did not cause any significant change in the frequency of epileptiform discharges (9.42 ± 1.05 burst/min baseline vs 8.34 ± 2.18 burst/min drug, $p>0.05$, $n=5$).

In contrast, applying 20μM NBQX for 30 minutes caused a significant reduction in the frequency of epileptiform discharges (12.84 ± 3.37 burst/min baseline vs 0.02 ± 0.02 burst/min drug, $p<0.05$, $n=5$).

Applying the $GABA_A$ receptor antagonist, gabazine, at 500nM for 30 minutes caused an increase in the frequency of the epileptiform discharges, albeit this increase was not statistically significant (19.64 ± 6.00 burst/min baseline vs 25.98 ± 4.92 burst/min drug, $p>0.05$, $n=5$).

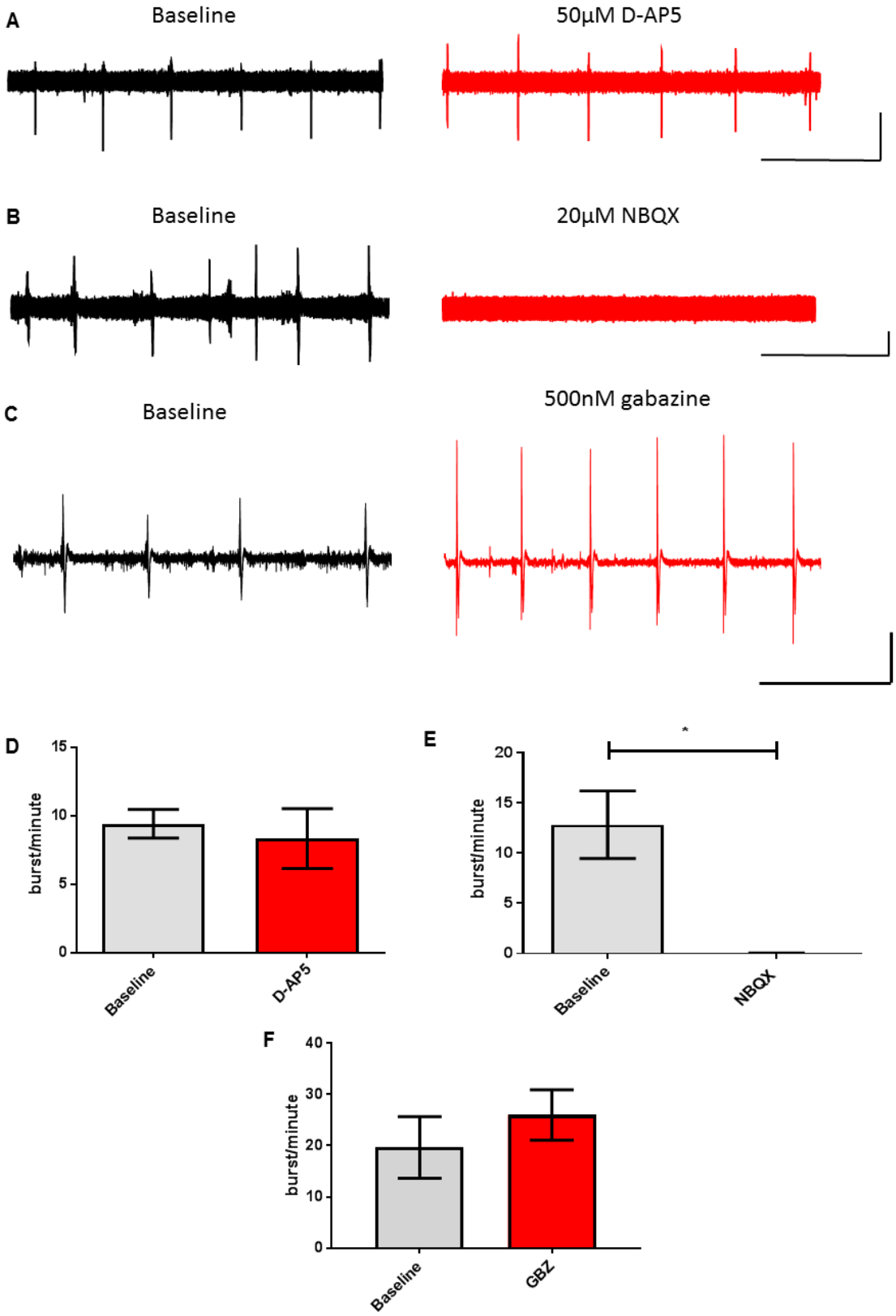

Figure 4-2 Epileptic activity is dependent on the contribution of AMPA-R, but not NMDA-R. A-C. Extracellular recordings of epileptic activity before (left) and after (right) addition of 50µM D-AP5 (A), 20µM NBQX (B), and 500nM gabazine (C). D-F. Corresponding bar charts of the burst count of each experimental condition. Asterisk indicates significance at p<0.05. Scale bars in (A) indicate 4 mV and 10 seconds, in (B) 0.2 mV and 10 seconds, and in (C) 0.05mV and 10 seconds.

4.3.3 Pharmacological responsiveness of mitochondrial epilepsy towards conventional antiepileptic drugs

Given the novelty of our model in replicating mitochondrial epilepsy, I decided to assess the pharmacological response of our model towards clinically used antiepileptic drugs. There are currently around 28 licensed-to-use antiepileptic drugs in the UK (Sills, 2014) for various indications. I have selected a range of antiepileptic drugs from various subtypes to test in this model as follow. Since the aim of this pharmacological testing was mainly for rapid antiepileptic drug screening, only two concentrations have been chosen per each antiepileptic drug; the literature – reported minimal inhibitory concentration (MIC) and maximal tolerable concentration (MTC).

4.3.3.1 Sodium channel blockers

Sodium channel blockers are one of the most commonly used and best-characterized antiepileptic drugs. By preventing the activation of sodium channels, these drugs block the voltage-dependent rapid repetitive firing of action potentials (Macdonald and Rogawski, 2008). I chose three drugs to test from this subgroup of antiepileptics, namely carbamazepine, phenytoin, and lamotrigine (see Figure 4-3).

Carbamazepine is one of the most widely prescribed 'first generation' antiepileptic drugs for partial and generalized tonic-clonic seizures (Fertig and Mattson, 2008). The bath application of carbamazepine (50μM) did not cause any significant change in the frequency of epileptiform discharges (13.90 ± 4.99 burst/min baseline vs 15.36 ± 4.83 burst/min 50μM) and increasing the drugs concentration to its MTC, 100 μM, still did not cause any significant change (13.48 ± 1.53 burst/min, $p>0.05$, $n=5$).

Lamotrigine, a phenyltriazine derivative, is utilized as monotherapy in paediatric patients and as adjunctive treatment for partial and primary and secondary generalized seizure in adults (Tomson *et al.*, 2008). Application of lamotrigine (10μM) did not cause any significant difference in the frequency of epileptiform discharges (10.86 ± 2.14 burst/min baseline vs 9.56 ± 1.55 burst/min 10μM) and despite the trend towards a decrease in frequency, increasing the concentration to 100μM still did not cause any significant change (7.68 ± 0.48 burst/min, $p>0.05$, $n=5$).

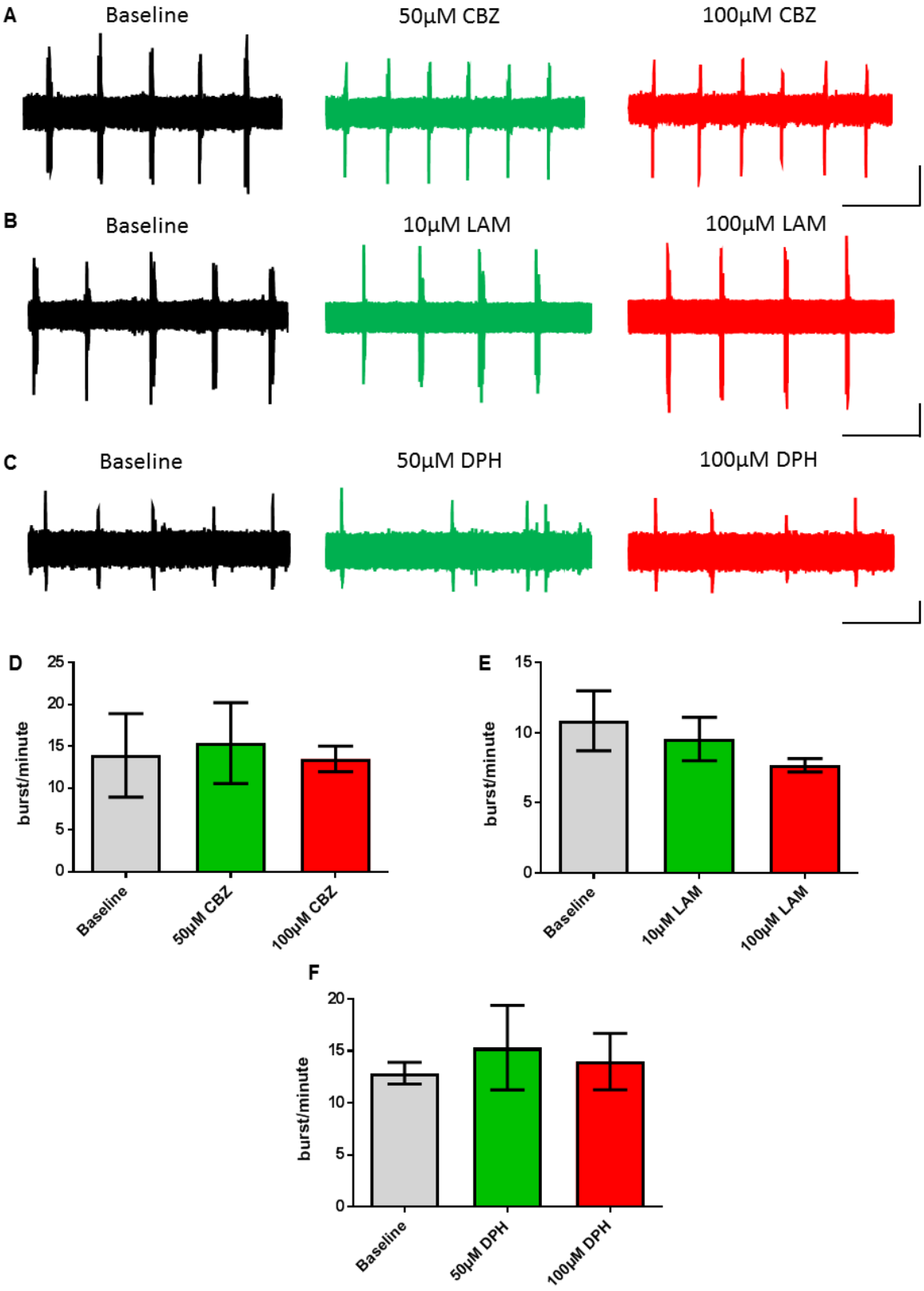

Figure 4-3 Epileptic activity exhibited pharmacoresistance against sodium channel blockers. A-C Extracellular recordings of epileptic activity before (left) and after addition of MIC (middle) and MTC (right) of carbamazepine (A), lamotrigine (B), and phenytoin (C). D-F. Corresponding bar charts of the burst count of each experimental condition. Scale bars in (a) indicate 0.5 mV and 10 seconds, in (b) 2 mV and 10 seconds, and in (c) 0.2mV and 10 seconds .

Phenytoin (diphenylhydantoin) is a member of the hydantoin family and is the most commonly prescribed agent from the family. It is indicated for partial seizures, with or without secondary generalization, and for primary generalized tonic-clonic seizures as well as being used as therapy for status epilepticus (Stern *et al.*, 2008). The application of diphenylhydantoin (50μM) did not cause any significant difference ($p>0.05$, $n=6$) in the frequency of epileptiform discharges (12.87 ± 1.05 burst/min baseline vs 15.31 ± 4.06 burst/min 50μM) nor did increasing the concentration to 100μM (13.98 ± 2.71 burst/min).

4.3.3.2 Levetiracetam

Levetiracetam has a unique mechanism of action among the other antiepileptic agents in that it binds to the synaptic vesicle SV2A receptor (Lynch *et al.*, 2004). In treating patients with mitochondrial epilepsy, levetiracetam is found to be particularly useful in controlling myoclonus (Schaefer *et al.*, 2010).

Applying levetiracetam at a bath concentration of 10μM did not cause any significant difference in the frequency of epileptiform discharges (11.52 ± 2.13 burst/min baseline vs 10.90 ± 1.93 burst/min 10μM). Increasing the concentration to 100μM still did not significantly modify the frequency of the discharges (9.08 ± 1.41 burst/min, $p>0.05$, $n=5$ – see Figure 4-4).

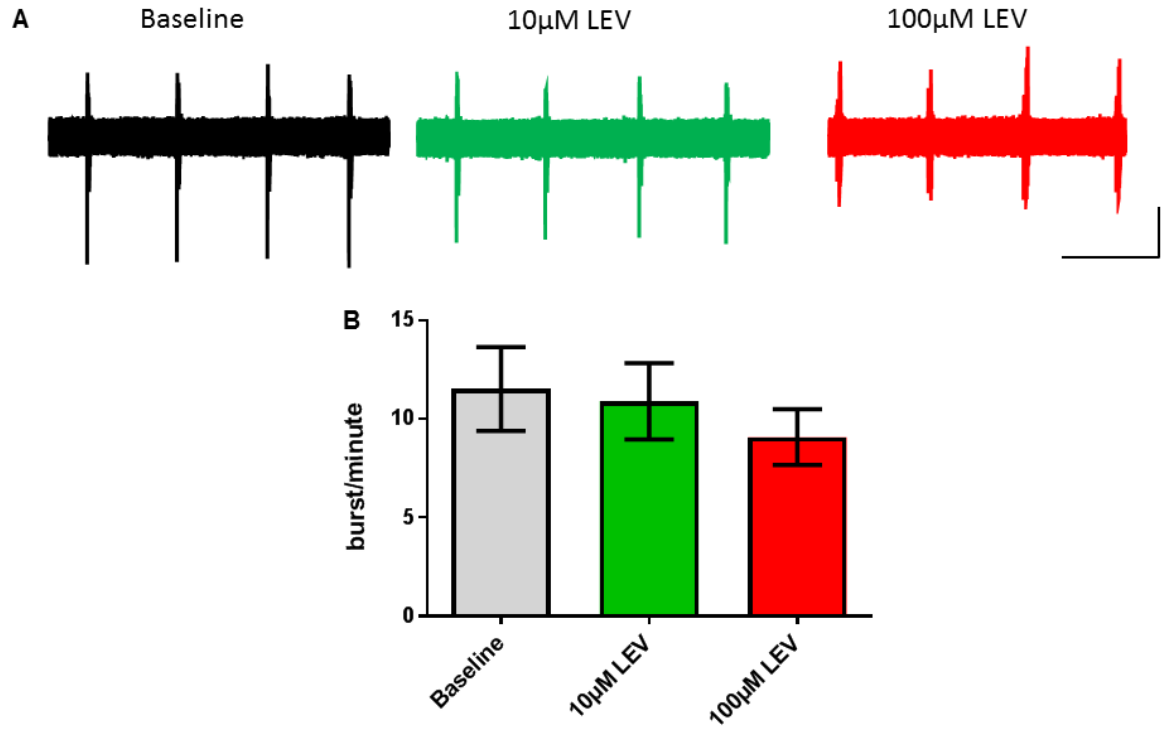

Figure 4-4 Epileptic activity is resistant against levetiracetam application. (A) shows the extracellular recordings of epileptic activity before (left) and after addition of 10µM levetiracetam (middle) up to 100 µM (right). (B) shows the corresponding bar chart of the burst count of the experimental condition. Scale bar indicate 1mV and 10 seconds.

4.3.3.3 Benzodiazepines

Benzodiazepines are currently used as first line treatment of status epilepticus due to their relatively rapid onset of action. It is well established that the primary target of benzodiazepines are the postsynaptic $GABA_A$ receptor and through allosteric binding, they increase the GABA receptor mediated current (Schmidt and Wilensky, 2008). I chose two different types of benzodiazepines to test; lorazepam, the first-line treatment for early stage of status epilepticus, and midazolam, the second-line (see Figure 4-5).

Lorazepam application at 50µM did not cause any significant difference in the frequency of epileptiform discharges (9.38 ± 1.80 burst/min baseline vs 8.70 ± 0.63 burst/min 50µM). Increasing the concentration to 100µM did not cause any significant difference in the frequency of the discharges (7.10 ± 0.56 burst/min, $p>0.05$, $n=4$).

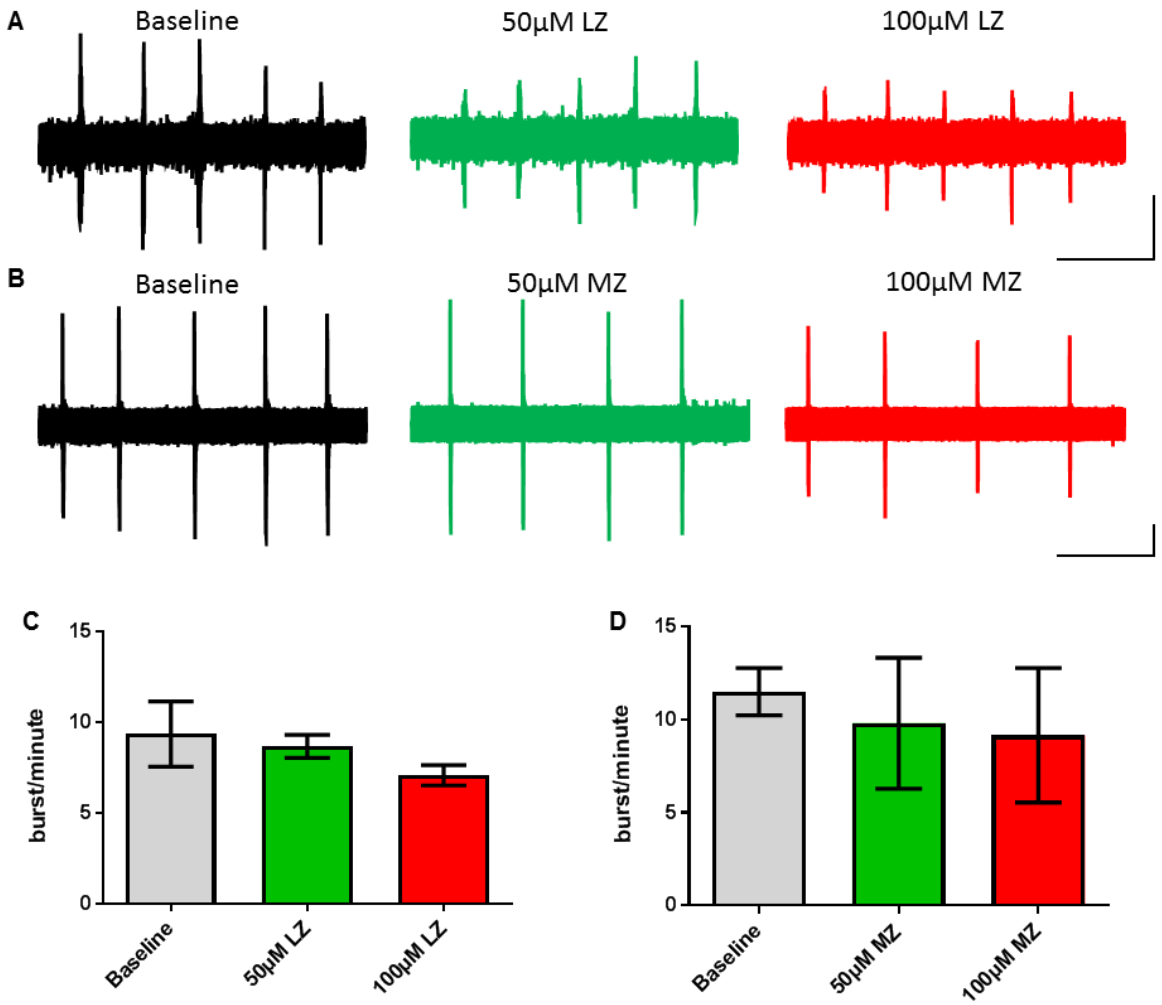

Figure 4-5 Epileptic activity is resistant against benzodiazepine application. A-B Extracellular recordings of epileptic activity before (left) and after addition of 50µM (middle) and 100µM (right) of lorazepam (A) and midazolam (B). C-D. Corresponding bar charts of the burst count of each experimental condition. Scale bars in (a) indicate 1 mV and 10 seconds and in (b) 2 mV and 10 seconds.

Similar to lorazepam, the bath application of midazolam (50µM) did not cause any significant difference in the frequency of epileptiform discharges (11.50 ± 1.27 burst/min baseline vs 9.80 ± 3.52 burst/min 50µM) and similarly, increasing the concentration to 100 µM still did not cause any significant difference (9.16 ± 3.61 burst/min, $p>0.05$, $n=5$).

4.3.3.4 Barbiturates

Barbiturates are central nervous system depressants that work by modulation of $GABA_A$-R, similar to benzodiazepines but at a different binding site and in a different manner. They are used as last-resort treatment for uncontrollable status epilepticus (Eadie and Kwan, 2008). Phenobarbitone is the classical anticonvulsant from the barbiturate subgroup; but pentobarbitone was chosen as it is much more potent than phenobarbitone in its modulation of GABA-R (Olsen, 2002).

The application of sodium pentobarbital at 100µM caused a reduction in the frequency of the epileptiform discharges (9.28 ± 2.67 burst/min baseline vs 2.80 ± 1.42 burst/min 100µM) but this was not statistically significant ($p>0.05$, $n=5$). Increasing the concentration to 200µM, however, caused a significant reduction ($p<0.05$, $n=5$) in the frequency of the epileptiform discharges (0.12 ± 0.12 burst/min).

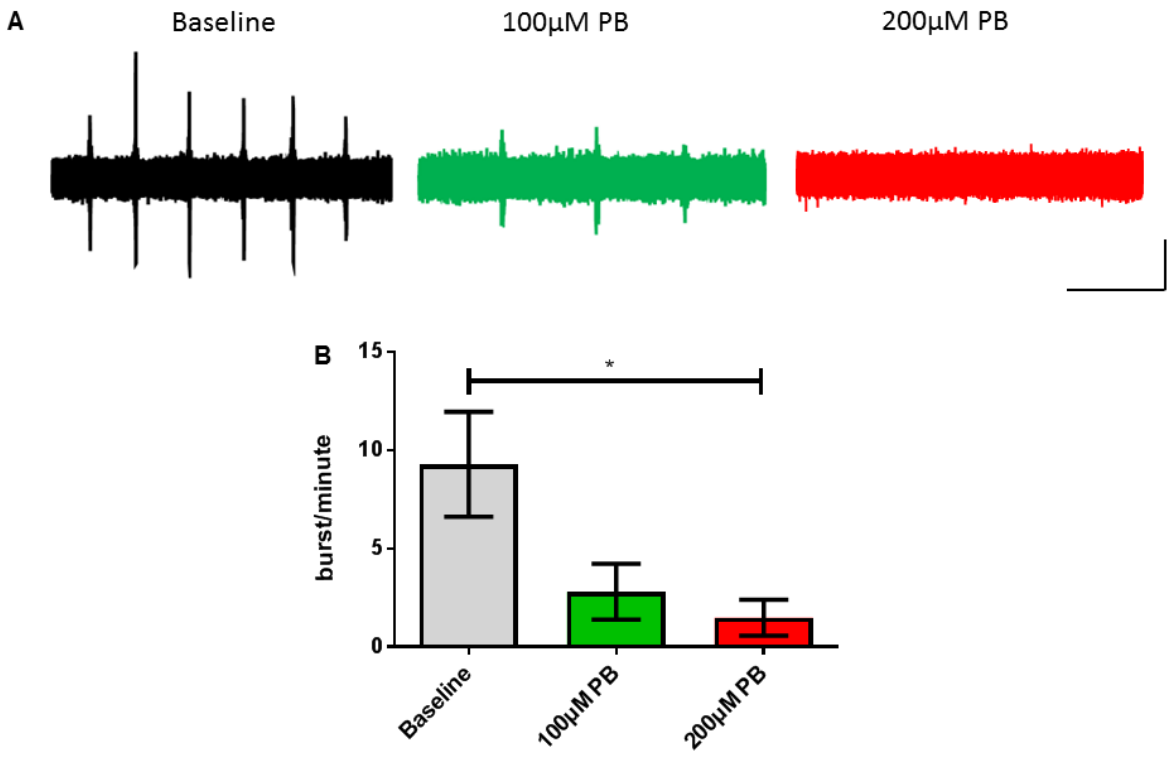

Figure 4-6 Epileptic activity is responsive to sodium pentobarbital application. (A) shows the extracellular recordings of epileptic activity before (left) and after addition of 100µM sodium pentobarbital (middle) up to 200 µM (right). (B) shows the corresponding bar chart of the burst count of the experimental condition. Scale bar indicates 0.5mV and 10 seconds. Asterisk indicates significance at p<0.05.

4.3.3.5 Valproate

Valproic acid is a branched-chain fatty acid, whose discovery as an antiepileptic drug was a serendipitous coincidence when it was used as a lipophilic vehicle and found to have a strong anticonvulsant property. Valproate has multiple anticonvulsant properties, including potentiation of GABA-ergic mechanisms, reduction of NMDA-R mediated excitation, and use-dependent reduction of the sodium current. Clinically, valproate is often used as monotherapy and add-on therapy for partial-onset seizures (Beydoun *et al.*, 2008). Available in many formulations, I chose to apply sodium valproate as it is water soluble and dissociates rapidly in the tissue to valproic acid.

The addition of sodium valproate (1mM) to the circulating nACSF did not cause any significant change ($p>0.05$, $n=5$) to the frequency of the epileptiform discharges nor did increasing it up to 2mM (12.26 ± 3.53 burst/min baseline vs 12.36 ± 3.16 burst/min 1mM vs 12.26 ± 3.90 burst/min 2mM).

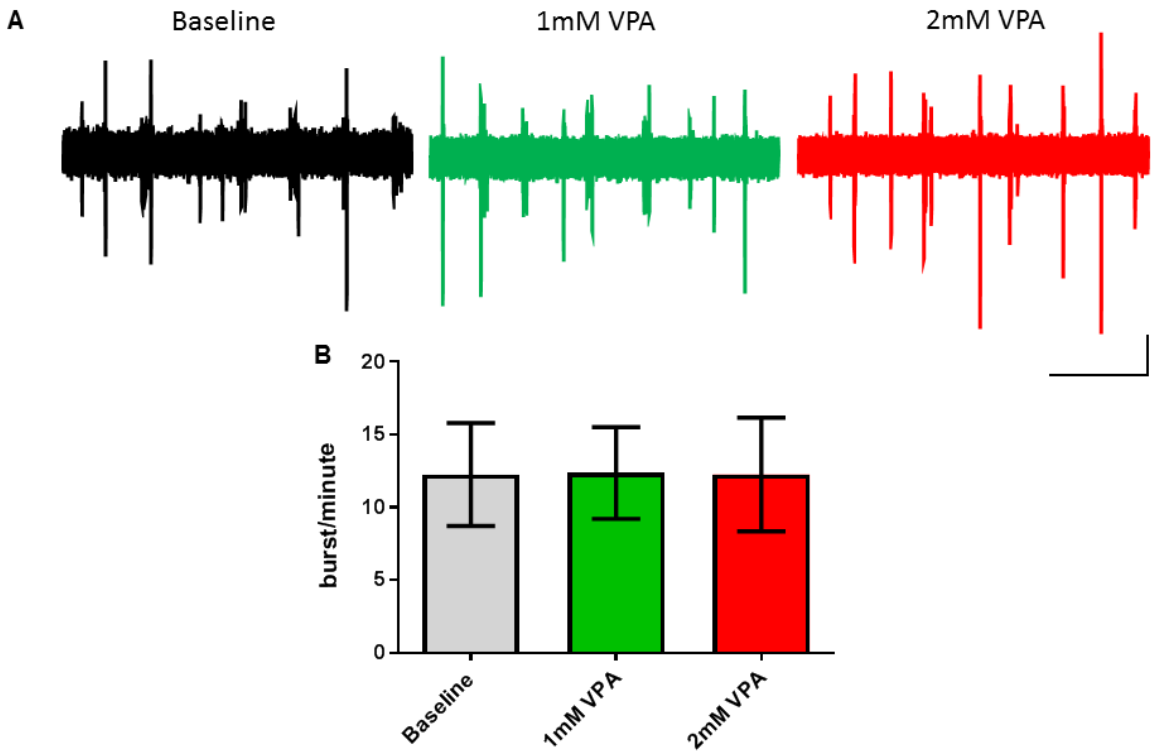

Figure 4-7 Epileptic activity is resistant against sodium valproate application. (A) shows the extracellular recordings of epileptic activity before (left) and after addition of 1mM sodium valproate (middle) up to 2mM (right). (B) shows the corresponding bar chart of the burst count of the experimental condition. Scale bar indicates 2mV and 10 seconds.

4.3.3.6 Perampanel

Perampanel is a relatively new antiepileptic drug with a novel mechanism of action in that it is a selective noncompetitive AMPA receptor antagonist (Hanada *et al.*, 2011). Clinically, perampanel is used as an adjunctive treatment for refractory partial-onset seizures (French *et al.*, 2013). Considering the response of the epileptiform discharges towards antagonism of the AMPA receptor with the competitive antagonist NBQX (as shown in section 4.3.2), I expected that the epileptiform discharge would also respond towards application of perampanel. Since perampanel is a novel antiepileptic drug and is not as well characterized as the other antiepileptic agents, I applied perampanel in an increasing cumulative concentration in its therapeutic range (0.1-10μM) (see Figure 4-13).

When perampanel was applied at 0.1μM, there was approximately a 20% reduction in the frequency of epileptiform discharges (13.86 ± 2.74 burst/min baseline vs 11.00 ± 2.58 burst/min 0.1μM) but this was not statistically significant ($p>0.05$, $n=5$). Increasing the concentration of perampanel to 0.3μM (8.76 ± 2.56 burst/min), 1μM (5.94 ± 2.37 burst/min), 3μM (2.58 ± 1.30 burst/min), and 10μM (0.92 ± 0.59 burst/min) caused a statistically significant reduction ($p<0.05$, $n=5$) in the frequency of the epileptiform discharges respectively. This reduction in epileptiform discharges seems to be dose-dependent with an IC_{50} value of 0.42μM.

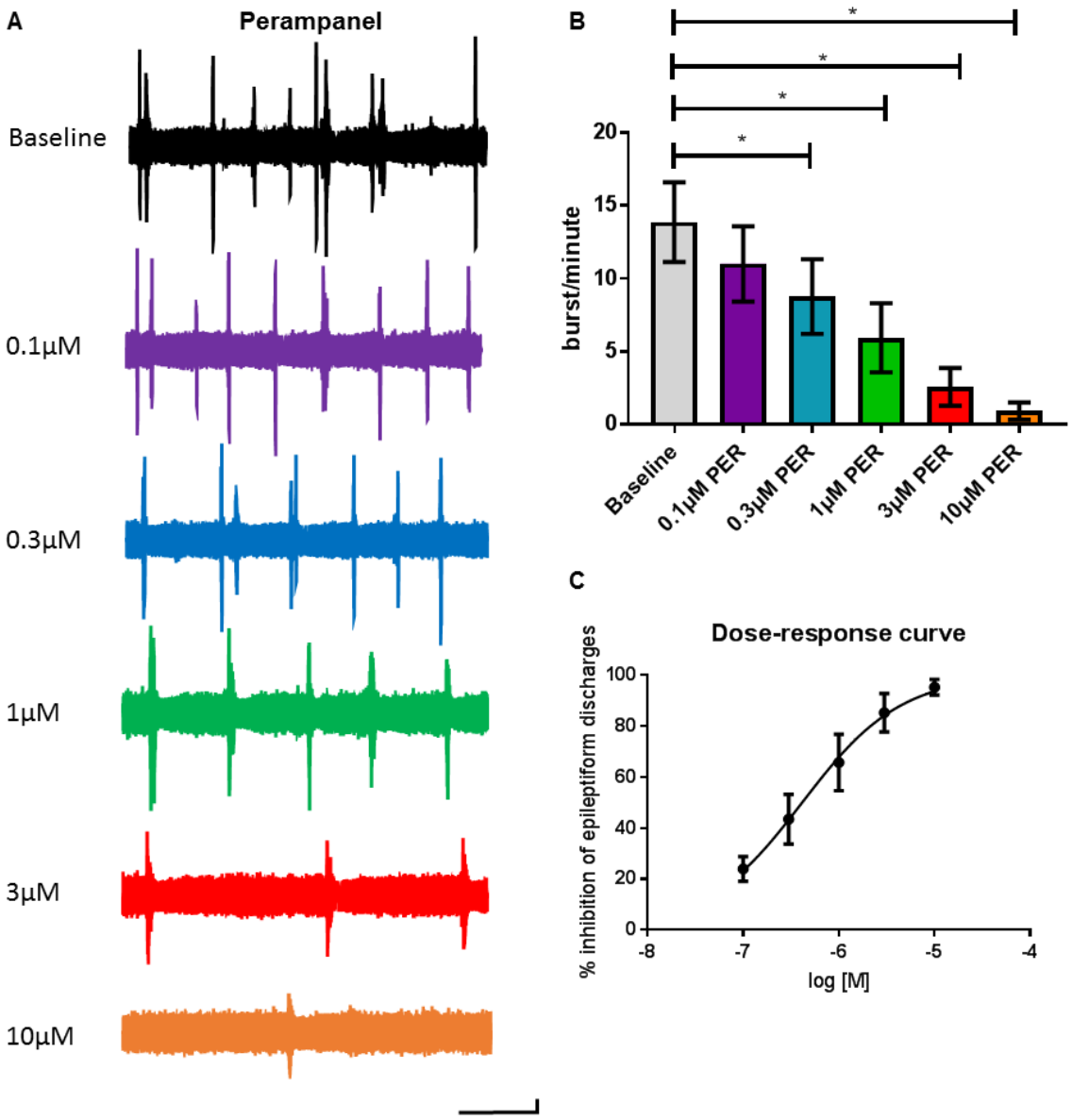

Figure 4-8 There is a dose-dependent reduction in the frequency of the epileptiform discharges following perampanel addition. (A) shows the extracellular recordings of epileptic activity following application of 0.1µM, 0.3µM, 1µM, 3µM, and 10µM perampanel respectively. (B) shows the corresponding bar chart of the burst count of the experimental condition and (C) shows a dose-response curve for perampanel. Scale bar indicates 1mV and 10 seconds. Asterisk indicates significance at p<0.05.

4.3.3.7 Summary of pharmacological responses towards antiepileptic drugs

The results presented in section 4.3.3.1 to 4.3.3.6 outlined the pharmacological response of the induced mitochondrial epileptic activity towards clinically used conventional antiepileptic drugs. In most scenarios, I tested two concentrations of these drugs; the minimal inhibitory concentration (MIC) and the maximal tolerable concentration (MTC). Figure 4-9 summarizes the pharmacological responses of the epileptic activity towards the MIC and MTC of these conventional antiepileptic agents.

When comparing the normalized percentage of the burst count against baseline following application of MIC of the drugs, there was no significant difference ($p>0.05$) between baseline and any of the pharmacological agents (100.00 ± 0.00 % baseline vs 116.90 ± 6.93 % carbamazepine, 90.49 ± 3.72 % lamotrigine, 116.70 ± 23.79 % phenytoin, 96.63 ± 10.95 % levetiracetam, 101.40 ± 12.20 % lorazepam, 78.13 ± 19.46 % midazolam, 53.99 ± 24.06 % pentobarbital, 105.40 ± 7.36 % valproate acid, and 76.05 ± 4.83 % perampanel).

In contrast, when comparing the normalized percentage following application of MTC of the drugs, there was a significant difference ($p< 0.05$) between baseline (100.00 ± 0.00 %) and pentobarbital (13.22 ± 13.22 %), as well as perampanel (4.79 ± 3.10 %). There was still no significant difference ($p>0.05$) between baseline and any of the remaining pharmacological agents (123.30 ± 18.67 % carbamazepine, 80.87 ± 13.63 % lamotrigine, 105.80 ± 13.29 % phenytoin, 81.11 ± 6.70 % levetiracetam, 85.74 ± 10.15 % lorazepam, 72.27 ± 20.32 % midazolam, and 91.30 ± 9.72 % valproate acid).

Therefore, out of all the tested conventional antiepileptic drugs, only sodium pentobarbital and perampanel demonstrated efficacy in this *in vitro* model of mitochondrial epilepsy. Furthermore, the higher concentration range (nearing MTC) is required with these two agents to demonstrate significant efficacy.

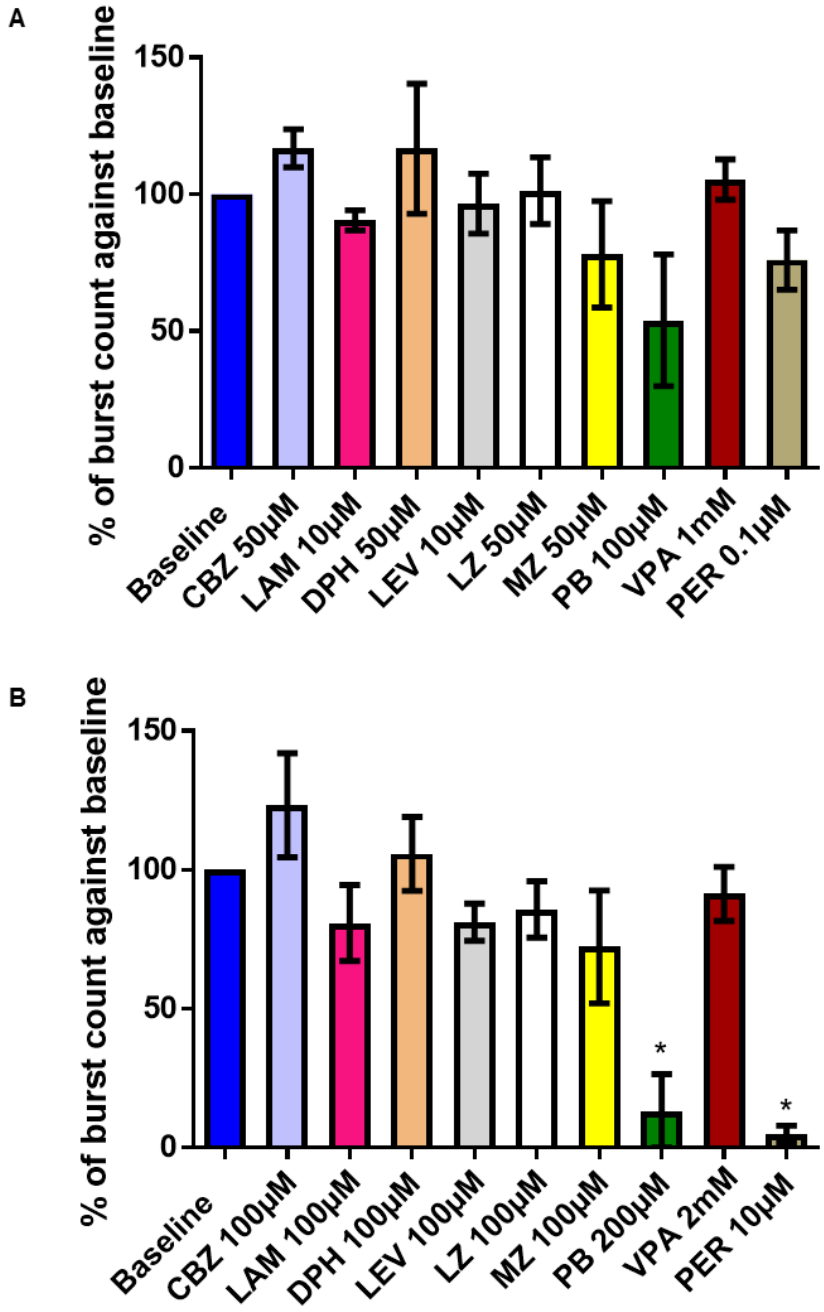

Figure 4-9 Summary of the response of the induced mitochondrial epileptiform discharges to the treatment with conventional antiepileptic agents. (A) shows the percentage of the burst count against baseline in the various experimental conditions using the minimal inhibitory concentration (MIC) of the conventional antiepileptic agents whereas (B) shows the percentage of the burst count against baseline when using the maximal tolerable concentration (MTC) of the same conventional antiepileptic agents. Asterisk indicates significance at $p<0.05$ when compared against the baseline. CBZ – carbamazepine, LAM – lamotrigine, DPH – diphenylhydantoin (phenytoin), LEV – levetiracetam, LZ – lorazepam, MZ – midazolam, PB – sodium pentobarbital, VPA – valproate acid, PER – perampanel.

4.3.4 Pharmacological responses towards substrates of the ketogenic diet

As mentioned above, ketogenic diet represents a form of dietary intervention that is commonly used in children with intractable seizures (Branco *et al.*, 2016) and has shown promises in controlling pharmacoresistant seizures in children with mitochondrial epilepsy (Kang *et al.*, 2007). Despite its well documented effectiveness in controlling intractable seizures, the mechanism whereby the ketogenic diet exerts its antiepileptic effect is largely unknown. Several components of the ketogenic diet have been identified to exhibit anticonvulsant or neuroprotective properties, including the ketone bodies themselves (β-hydroxybutyrate, acetone, and acetoacetate) (Rho *et al.*, 2002; Minlebaev and Khazipov, 2011) and the medium-chain fatty acids (such as decanoic acid and octanoic acid) (Hughes *et al.*, 2014; Chang *et al.*, 2015; Thevenet *et al.*, 2016). Considering this, I have chosen to examine the effect of acute application of three components of the ketogenic diet; β-hydroxybutyrate, decanoic acid, and octanoic acid; in this model of mitochondrial epilepsy.

4.3.4.1 Beta-hydroxybutyrate (β-HB)

Beta-hydroxybutyrate, along with acetone and acetoacetate, are collectively called the ketone bodies. They are formed from acetyl CoA when lipolysis is the predominant metabolic pathway *in vivo* (Berg *et al.*, 2012e). The brain preferentially uses the ketone bodies as metabolic fuel during chronic starvation (Berg *et al.*, 2012e) and the ketogenic diet aims to simulate this through a high-fat, low-carbohydrate dietary intervention. Unsurprisingly, then, the ketogenic diet leads to a high presence of the ketone bodies in the blood, ketosis (Neal *et al.*, 2008). To replicate this, I applied onto the circulating artificial cerebrospinal fluid increasing concentrations of the beta-hydoxybutyrate to examine its acute anticonvulsant properties (see Figure 4-10).

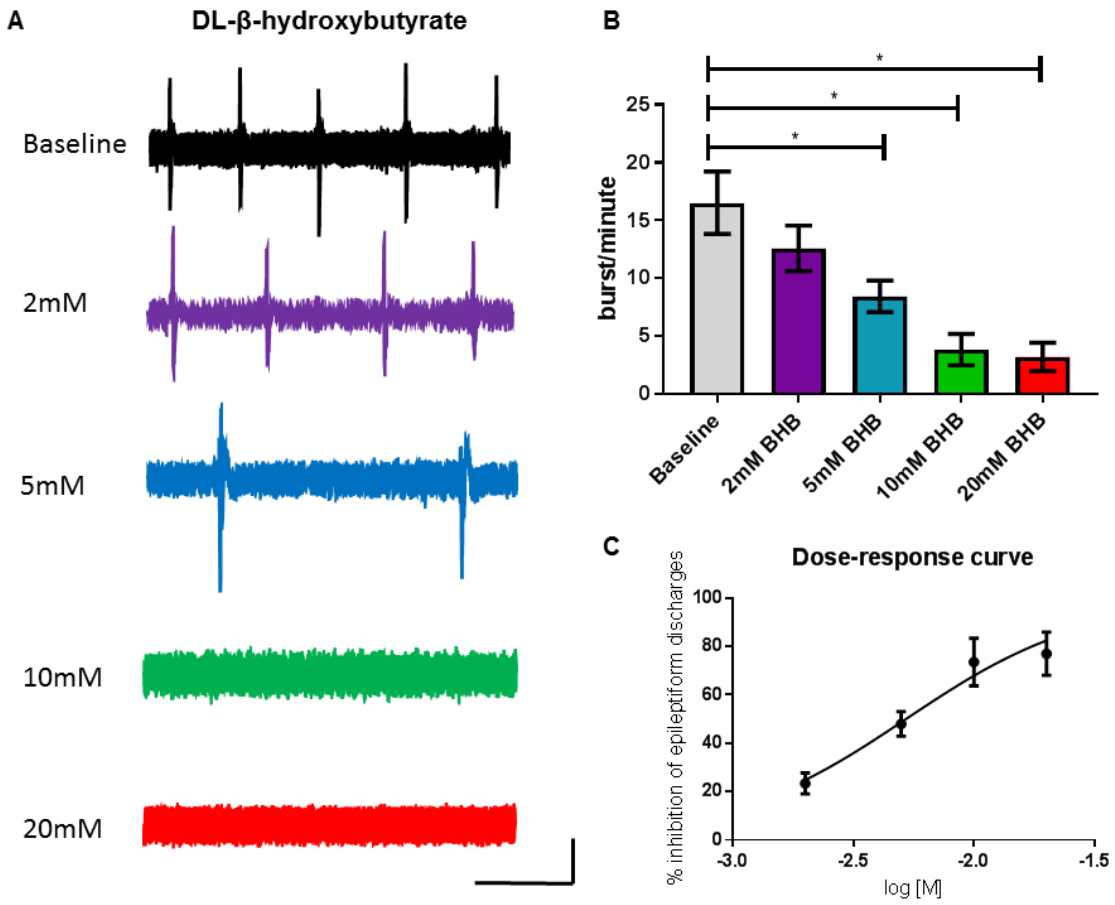

Figure 4-10 There is a dose-dependent reduction in epileptiform discharges following DL-β-hydroxybutyrate acute application. (A) shows the extracellular recordings of epileptic activity following application of 2mM, 5mM, 10mM, and 20mM DL-β-hydroxybutyrate respectively. (B) shows the corresponding bar chart of the burst count of the experimental condition and (C) shows a dose-response curve for β-hydroxybutyrate. Scale bar indicates 0.1mV and 10 seconds. Asterisk indicates significance at p<0.05.

Application of DL-β-hydroxybutyrate at 2mM caused approximately 20% reduction in epileptiform discharges (16.52 ± 2.69 burst/min baseline vs 12.58 ± 1.96 burst/min 2mM) and this was not statistically significant ($p>0.05$, $n=5$). However, increasing the concentration to 5mM (8.44 ± 1.36 burst/min), 10mM (3.84 ± 1.36 burst/min), and 20mM (3.22 ± 1.24 burst/min) caused a statistically significant ($p<0.05$, $n=5$) reduction in epileptiform discharges respectively. There appears to be a dose-dependent reduction in epileptiform discharges and hence, a dose-response curve was tabulated to obtain the IC_{50} value of 5.16mM.

4.3.4.2 Decanoic acid (C10)

Although the increased production of the ketone bodies is the main goal of the ketogenic diet, it is not a component of the diet itself. The components of the diet, the medium chain fatty acids, lead to the production of the ketone bodies after undergoing metabolism *in vivo*. The two main components of the ketogenic diet, octanoic acid (C8) and decanoic acid (C10), are also detectable in the plasma of the children on ketogenic diet, in addition to the ketone bodies (Haidukewych *et al.*, 1982). Although it has been shown that the level of these fatty acids in the plasma does not correlate with seizure control (Sills *et al.*, 1986), more recent studies on animal models have revived the interest in these fatty acids.

In particular, decanoic acid (C10) has been demonstrated to exhibit acute anticonvulsant properties in the pentylenetetrazol (PTZ) and low-Mg^{2+} model of epilepsy (Chang *et al.*, 2013; Chang *et al.*, 2015). Through works on the *Xenopus* oocytes, decanoic acid was suggested to directly inhibit the AMPA-R acutely (Chang *et al.*, 2015). Hitherto, I have applied two inhibitors of the AMPA-R (NBQX in section 4.3.2 and perampanel in section 4.3.3.6) and both of them were suppressive in this model of mitochondrial epilepsy. Therefore, to examine the inhibitory potential of decanoic acid (C10), I applied it onto the circulating NACSF in an increasing concentration, ranging from 100μM to 2mM (see Figure 4-11).

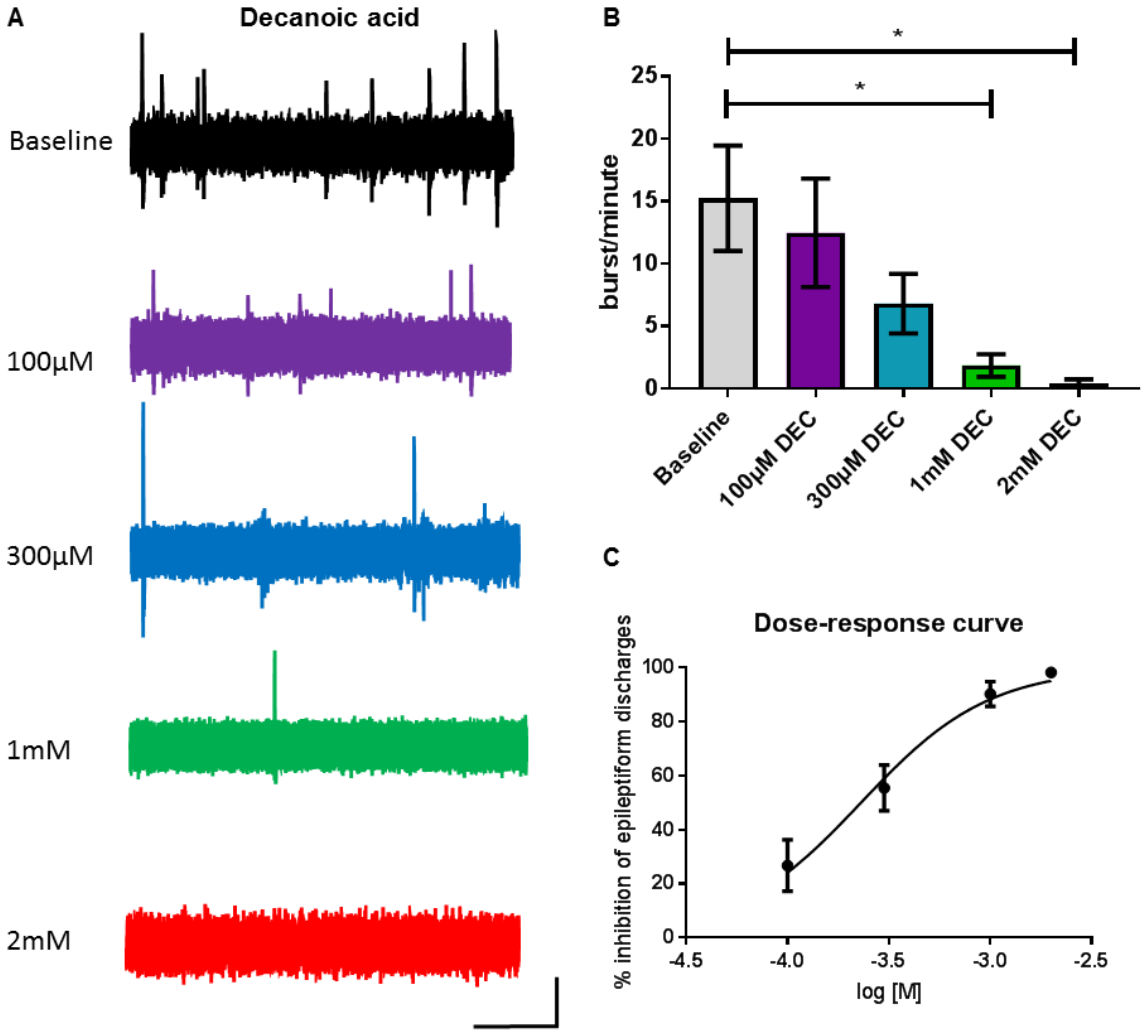

Figure 4-11 There is a dose-dependent reduction in the frequency of the epileptic activity following decanoic acid applications. (A) shows the extracellular recordings of epileptic activity following application of 100µM, 300µM, 1mM, and 2mM decanoic acid respectively. (B) shows the corresponding bar chart of the burst count of the experimental condition and (C) shows a dose-response curve for decanoic acid. Scale bar indicates 0.1mV and 10 seconds. Asterisk indicates significance at p<0.05.

Application of decanoic acid at 100µM and 300µM caused a reduction in the frequency of the epileptiform discharges (15.26 ± 4.22 burst/min baseline vs 12.48 ± 4.34 burst/min 100µM vs 6.82 ± 2.39 burst/min 300µM), however, this was not statistically significant ($p>0.05$, $n=5$). Increasing the concentration to 1mM (1.86 ± 0.91 burst/min) and 2mM (0.38 ± 0.38 burst/min), however, caused a statistically significant ($p<0.05$, $n=5$) decrease in the burst count. This reduction is dose-dependent with an IC_{50} value of 230.6µM.

4.3.4.3 Octanoic acid (C8)

As mentioned above, not only decanoic acid but also octanoic acid was found on the plasma of children on ketogenic diet (Haidukewych *et al.*, 1982). Interestingly, unlike decanoic acid, octanoic acid was found to have no inhibitory effect in the PTZ model of epilepsy (Chang *et al.*, 2013). Furthermore, octanoic acid was also shown to not modulate the AMPA-R activity, unlike decanoic acid (Chang *et al.*, 2015). Therefore, if the inhibitory effect of decanoic acid was truly due to its property in the AMPA-R modulation, then the application of octanoic acid would yield no inhibitory effect in this model of mitochondrial epilepsy. Hence, I added octanoic acid at a similar concentration range of decanoic acid to directly compare the effect of the two fatty acids (see Figure 4-12).

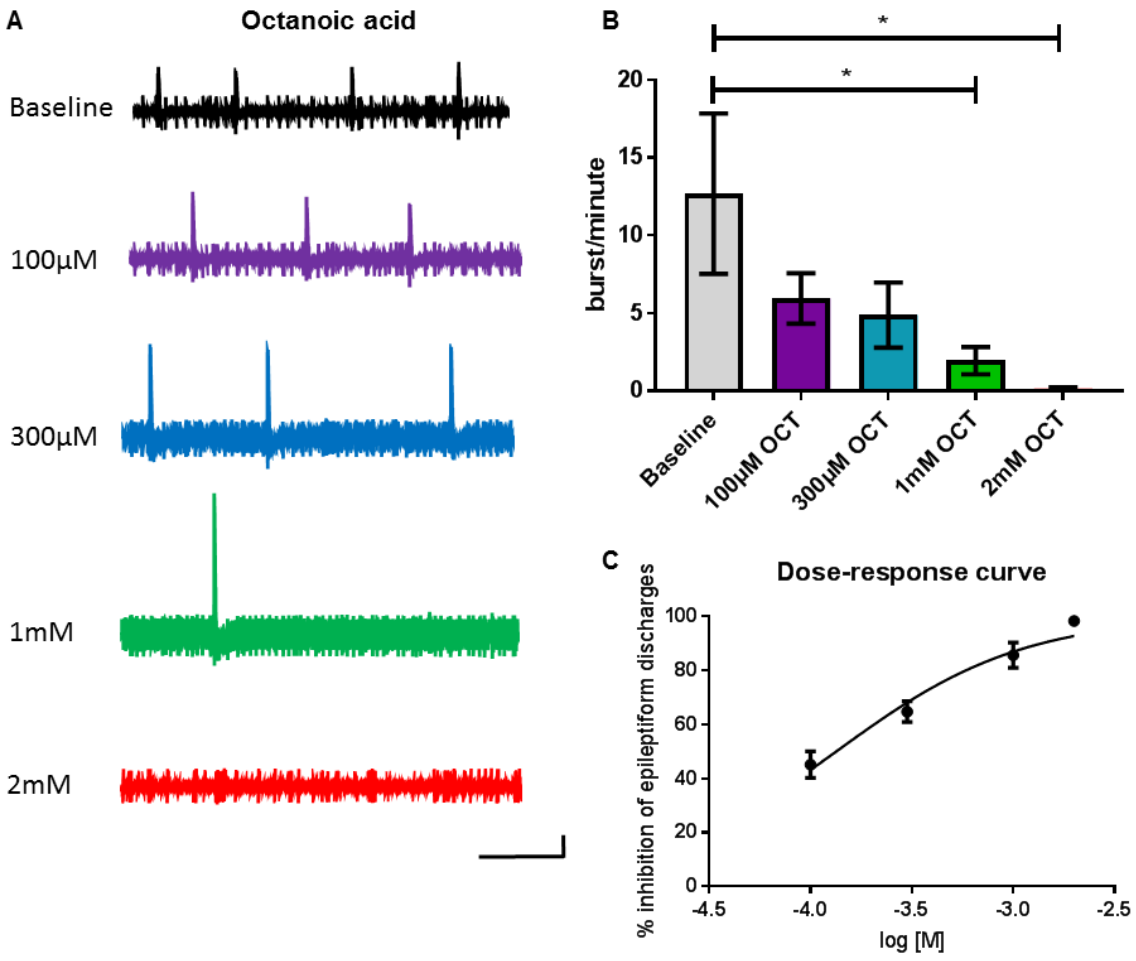

Figure 4-12 There is a dose-dependent reduction in the frequency of the epileptic activity following octanoic acid application. (A) shows the extracellular recordings of epileptic activity following application of 100µM, 300µM, 1mM and 2mM octanoic acid respectively. (B) shows the corresponding bar chart of the burst count of the experimental condition and (C) shows a dose-response curve for octanoic acid. Scale bar indicates 0.1mV and 10 seconds. Asterisk indicates significance at p<0.05.

Similar to decanoic acid, application of octanoic acid at 100μM and 300μM caused a reduction in the frequency of the epileptiform discharges (12.68 ± 5.16 burst/min baseline vs 5.95 ± 1.62 burst/min 100μM vs 4.88 ± 2.09 burst/min 300μM), however, this was not statistically significant ($p>0.05$, $n=6$). When I increased the concentration to 1mM (1.95 ± 0.87 burst/min) and 2mM (0.15 ± 0.09 burst/min), however, this caused a statistically significant ($p<0.05$, $n=6$) reduction in the burst count. This reduction is dose-dependent with an IC_{50} value of 134.2μM, which suggests that octanoic acid is more potent than decanoic acid in inhibiting the epileptiform discharges.

4.3.5 Pharmacological responses towards substrates of glycolysis

Under most physiological conditions, glucose is the obligatory main substrate for the brain (McKenna *et al.*, 2006). The only pathway by which glucose enters energy metabolism is through the cytoplasmic process of glycolysis. In my model, I have inhibited both the (astrocytic) Krebs cycle and the mitochondrial respiratory chain; the downstream process of glucose metabolism. Since glycolysis remains uninhibited, I postulated that the slices would upregulate glycolysis to meet the brain's energy requirement. Therefore, the addition of various substrates of glycolysis may rescue the epileptiform discharges induced through the restoration of the energy crisis induced by the mitochondrial epilepsy induction.

4.3.5.1 Glucose

As mentioned above, glucose is the main metabolic substrate of the brain. High glucose utilization has been reported during a state of seizure (Scorza *et al.*, 2002) and if glycolysis is upregulated, increasing extracellular availability of glucose might be crucial to maximize the reserve capacity of tissue's glycolysis. To examine this effect, I have applied increasing concentrations of glucose to the circulating aCSF bath, ranging from 2mM to 20mM (see Figure 4-13). It is important to note that the addition of the glucose is in addition to the pre-existing 10mM D-glucose in the aCSF composition.

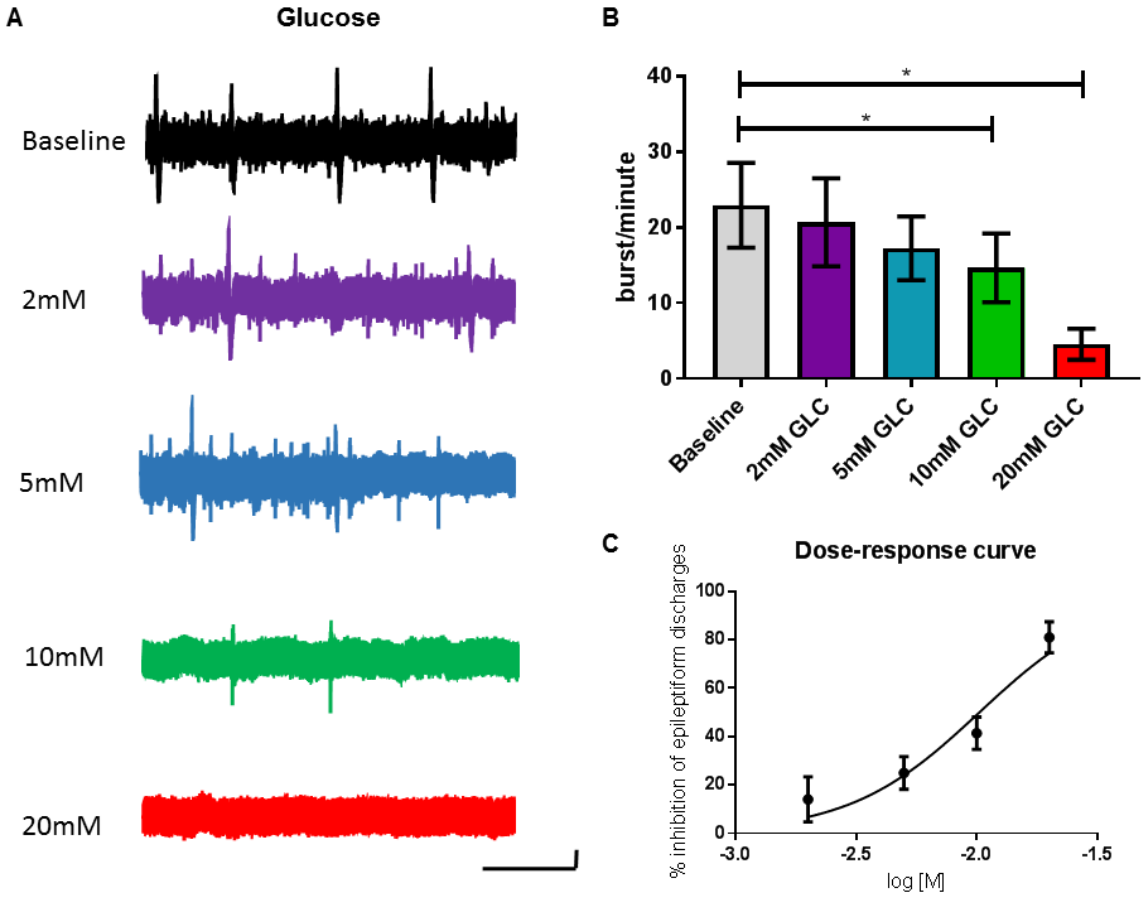

Figure 4-13 There is a dose-dependent reduction in the frequency of epileptiform discharges following extra addition of glucose. (A) shows the extracellular recordings of epileptic activity following application of 2mM, 5mM, 10mM, and 20mM D-glucose respectively. (B) shows the corresponding bar chart of the burst count of the experimental condition and (C) shows the dose-response curve for glucose. Scale bar indicates 0.05mV and 10 seconds. Asterisk indicates significance at p<0.05.

Applying D-glucose at 2mM and 5mM caused an insignificant ($p>0.05$, $n=6$) reduction in the epileptiform discharges as compared against baseline (22.97 ± 5.61 burst/min baseline vs 20.70 ± 5.61 burst/min 2mM vs 17.27 ± 4.20 burst/min 5mM). Application at 10mM and 20mM, however, caused a significant ($p<0.05$, $n=6$) reduction in the epileptiform discharges (14.67 ± 4.56 burst/min 10mM and 4.57 ± 2.05 burst/min 20mM respectively). There does appear to be a dose-dependent reduction in the frequency of the epileptiform discharges with the addition of glucose (IC_{50} = 10.27mM).

4.3.5.2 Pyruvate

Pyruvate is the end product of glycolysis. It has multiple fates following glycolysis; it can either enter oxidative metabolism through conversion to acetyl CoA or in anaerobic conditions, it can be reduced to lactate by the enzyme lactate dehydrogenase (Berg *et al.*, 2012f). Knowing that the addition of glucose can suppress the epileptiform discharges, I decided to apply pyruvate extracellularly at the same concentration range in order to compare the two substrates.

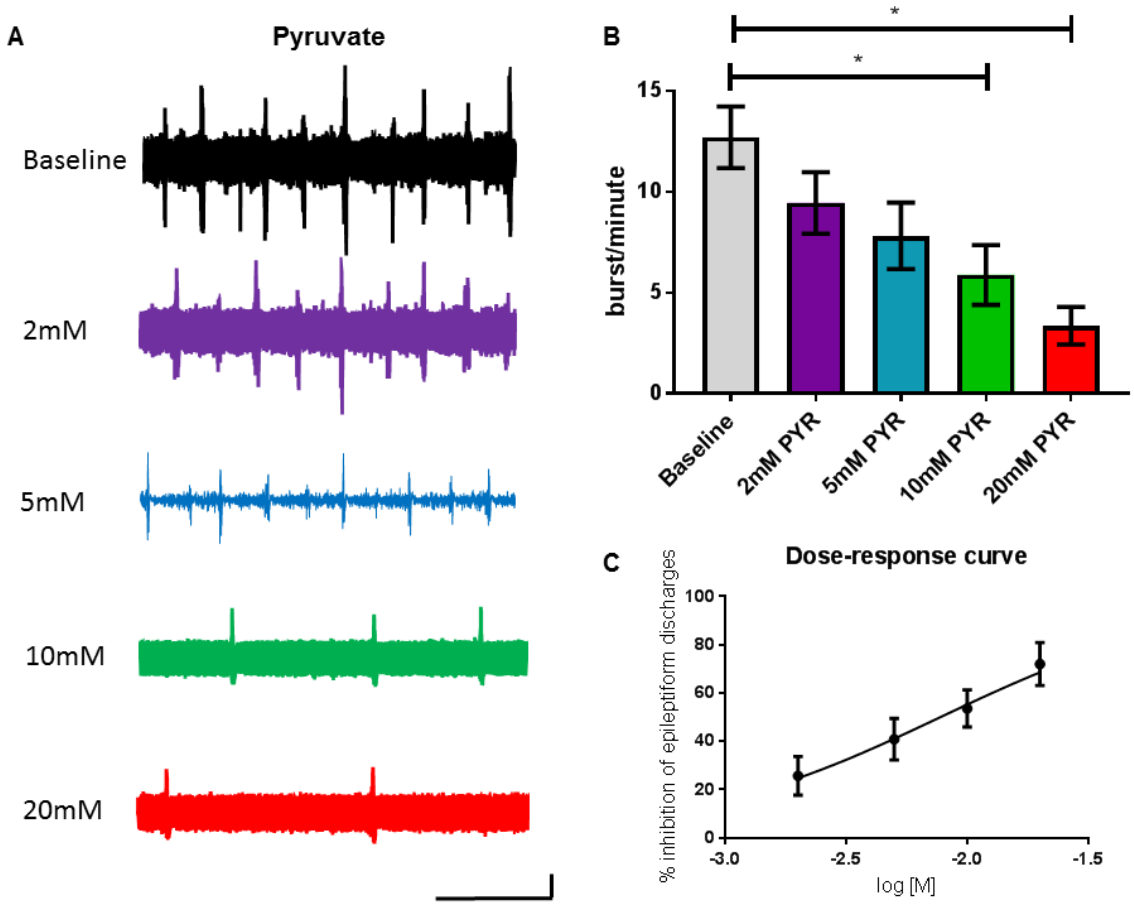

Figure 4-14 There is a dose-dependent reduction in the frequency of epileptiform discharges following addition of pyruvate. (A) shows the extracellular recordings of epileptic activity following application of 2mM, 5mM, 10mM , and 20mM sodium pyruvate. (B) shows the corresponding bar chart of the burst count of the experimental condition and (C) shows the dose-response curve for pyruvate. Scale bar indicates 0.05mV and 10 seconds. Asterisk indicates significance at p<0.05.

Pyruvate application at 2mM and 5mM did not cause a significant reduction ($p>0.05$, $n=14$) in the frequency of the epileptiform discharges as compared against baseline (12.69 ± 1.53 burst/min baseline vs 9.45 ± 1.53 burst/min 2mM vs 7.81 ± 1.64 burst/min 5mM). Increasing the concentration to 10mM and 20mM, however, caused a significant ($p<0.05$, $n=14$) reduction in the epileptiform discharges (5.88 ± 1.48

burst/min 10mM and 3.36 ± 0.93 burst/min 20mM). This reduction in the frequency of epileptiform discharges appears to be dose-dependent with an IC_{50} value of 7.74mM.

4.3.5.3 Lactate

Lactate is generated from pyruvate by the enzyme lactate dehydrogenase in an anaerobic manner (Berg *et al.*, 2012f). In the brain, it has been postulated that lactate, generated from astrocyte's glycolysis, is released by the astrocyte and preferentially used by neurons as metabolic substrate during increased neuronal activity (Pellerin and Magistretti, 1994). This is also known as the 'astrocyte-neuron lactate shuttle hypothesis' (Chih and Roberts, 2003). If the 'astrocyte-neuron lactate shuttle hypothesis' is applicable in this model, then the inhibitory effect of glucose and pyruvate as shown above in section 4.3.5.1 and 4.3.5.2 respectively could be through their respective conversion to lactate in the astrocyte's glycolytic process. To test this hypothesis, I applied equimolar concentration of lactate to the circulating aCSF bath as used with glucose and pyruvate (see Figure 4-15).

The addition of 2mM, 5mM, or 10mM L-lactate did not cause any significant reduction ($p>0.05$, $n=5$) in the frequency of the epileptiform discharges (21.70 ± 7.47 burst/min baseline vs 22.24 ± 6.71 burst/min 2mM vs 20.08 ± 5.73 burst/min 5mM vs 20.34 ± 7.93 burst/min 10mM). Surprisingly, however, adding 20mM L-lactate caused a sudden significant reduction ($p<0.05$, $n=5$) in the frequency of the epileptiform discharges (8.44 ± 3.29 burst/min 20mM).

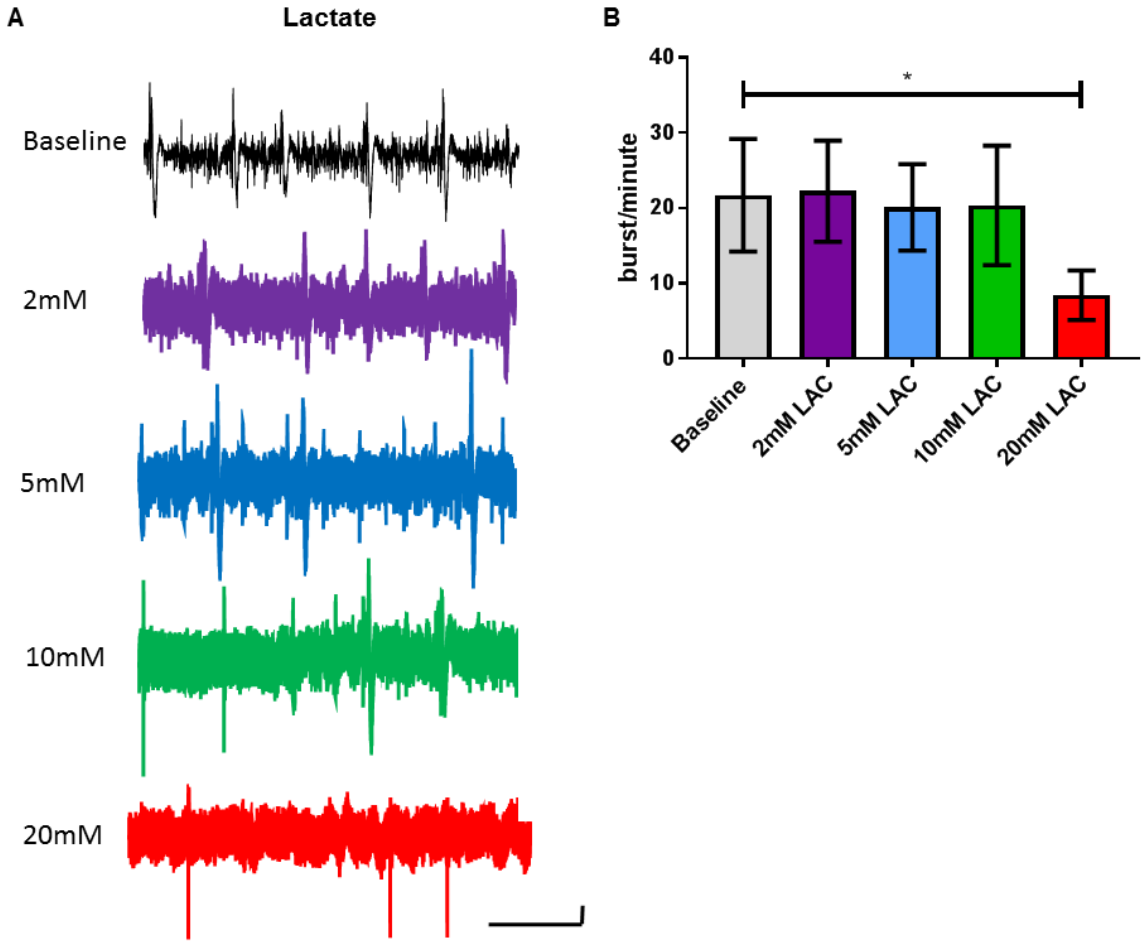

Figure 4-15 Epileptiform discharge is only suppressed by the addition of very high concentration of lactate. (A) shows the extracellular recordings of epileptic activity following application of 2mM, 5mM, 10mM, and 20mM L-lactate respectively. (B) shows the corresponding bar chart of the burst count of the experimental condition. Scale bar indicates 0.05mV and 10 seconds. Asterisk indicates significance at p<0.05.

4.3.5.4 Modulating glycolysis through stiripentol

Stiripentol is a clinically used antiepileptic agent for children with Dravet syndrome (Chiron *et al.*, 2000; Inoue *et al.*, 2009). The motivation to test stiripentol in this model developed from recent findings that stiripentol was able to inhibit the glycolytic enzyme, lactate dehydrogenase (Sada *et al.*, 2015). However, this effect was only seen at very high concentration of stiripentol (500μM) (Sada *et al.*, 2015) and at lower concentrations, stiripentol has been shown to modulate $GABA_A$-R mediated neurotransmission (Quilichini *et al.*, 2006; Fisher, 2011). Since the metabolic modulation was only seen at high concentrations, I decided to apply stiripentol through a gradually increasing concentration, ranging from the MIC (30μM) to the

supraphysiological concentration (500µM), unlike the experiments with the other antiepileptic drugs (as conducted in section 4.3.3).

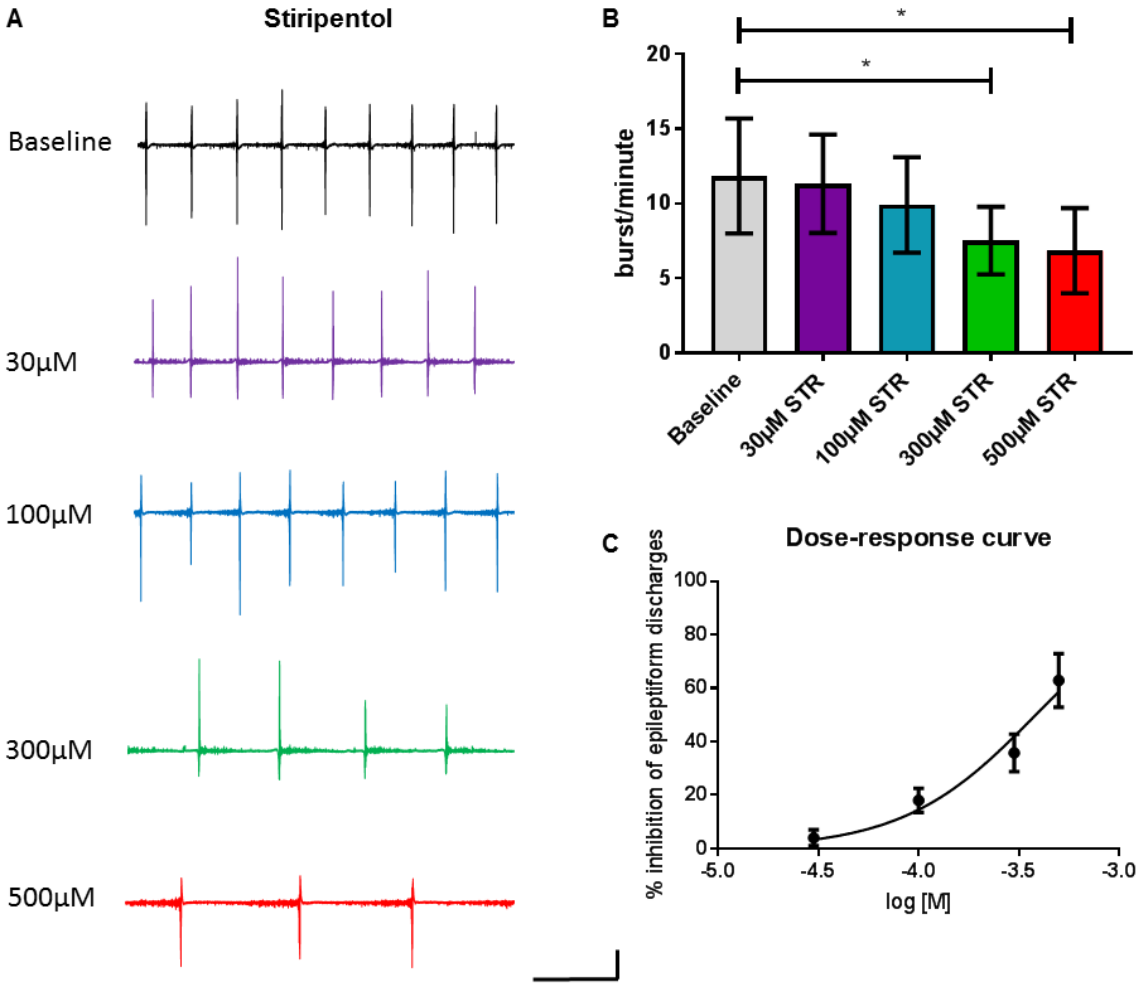

Figure 4-16 There is a dose-dependent reduction in the frequency of the epileptiform discharges following the addition of stiripentol. (A) shows the extracellular recordings of epileptic activity following application of 30µM, 100µM, 300µM, and 500µM of stiripentol respectively. (B) shows the corresponding bar chart of the burst count of the experimental condition and (C) shows the dose-response curve for stiripentol. Scale bar indicates 0.2mV and 10 seconds. Asterisk indicates significance at p<0.05.

At 30µM and 100µM, stiripentol did not cause any significant change ($p>0.05$, $n=5$) in the frequency of the epileptiform discharges (11.84 ± 3.85 burst/min baseline vs 11.32 ± 3.30 burst/min 30µM vs 9.90 ± 3.19 burst/min 100µM). Increasing the concentration to 300µM and 500µM caused a statistically significant reduction ($p<0.05$, $n=5$) in the burst count (7.52 ± 2.26 burst/min 300µM and 6.84 ± 2.85 burst/min 500µM respectively). This inhibition of epileptiform discharges is dose-dependent with an IC_{50} of 384.10µM.

4.3.6 Pharmacological responses towards substrates of the glutamate-glutamine cycle

The glutamate-glutamine cycle represents an important astrocytic process that is involved in the recycling of neurotransmitters, including glutamate and GABA (Bak *et al.*, 2006). Both neurotransmitters are recycled through the astrocytic TCA cycle and are regenerated through the formation of glutamine, the non-neuroactive precursor to both neurotransmitters. Since the astrocytic TCA cycle is directly inhibited in our model by the application of fluorocitrate, it can be hypothesized that downstream inhibition of the glutamate-glutamine cycle would occur. Therefore, the restoration of the cycle through external addition of the substrates of this cycle could potentially restore the metabolic dysfunction and suppress the epileptiform activity induced.

4.3.6.1 Glutamate

Glutamate is the major excitatory neurotransmitters in the brain, but in addition to this role in neurotransmission, glutamate is also involved in a lot of metabolic pathways in the nervous system, including the glutamate-glutamine cycle, the detoxification of ammonia, and the synthesis of peptides and glutathione (Cooper *et al.*, 2003). Therefore, the effect of glutamate should not be evaluated solely on its metabolic role as a substrate for the glutamate-glutamine cycle.

As described previously, the AMPA-R is implicated in the seizure generation (as discussed above in section 4.3.2, 4.3.3.6, and 4.3.4.2). In addition to AMPA, glutamate is a specific agonist for the AMPA-R (Gouaux, 2004). Therefore, since the inhibition of AMPA-R was able to suppress the epileptic activity significantly, the supplementation of agonist of this receptor is expected to increase the frequency of the epileptic activity instead. However, the metabolic role of glutamate, should it predominate over its role in neurotransmission, suggests that glutamate could suppress the epileptic activity, just like other metabolic substrates described above, like glucose, DL-β-hydroxybutyrate, and pyruvate.

Taking this into consideration, I applied glutamate at concentrations sufficient enough for it to be used as a metabolic substrate (see Figure 4-17).

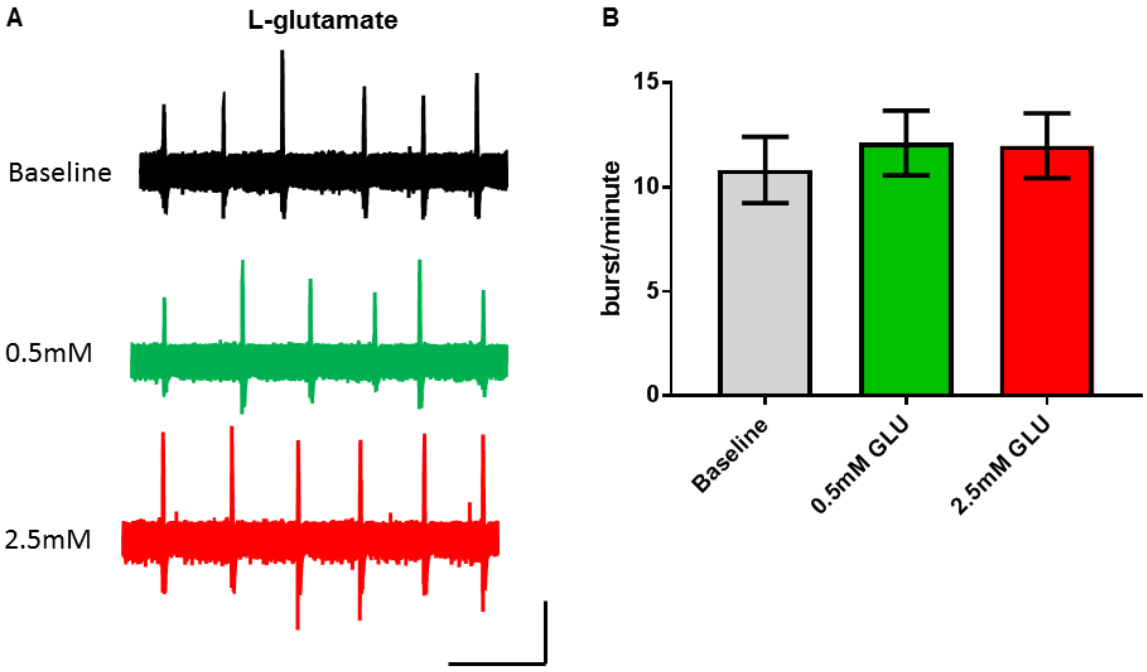

Figure 4-17 Epileptic activity is not responsive towards L-glutamate application. (A) shows the extracellular recordings of epileptic activity following application of 0.5mM and 2.5mM L-glutamate. (B) shows the corresponding bar chart of the burst count of the experimental condition. Scale bar indicates 0.2mV and 10 seconds.

The application of glutamate at either 0.5mM or 2.5mM did not cause any significant change ($p>0.05$, $n=6$) in the frequency of the epileptiform discharges (10.83 ± 1.59 burst/min baseline vs 12.12 ± 1.55 burst/min 0.5mM vs 11.98 ± 1.56 burst/min 2.5mM). There was, therefore, no effect whatsoever, neither metabolic nor neurotransmission associated, from the external supplementation of L-glutamate.

4.3.6.2 GABA

In contrast to glutamate, GABA is the major inhibitory neurotransmitters in the brain. However, similarly to glutamate, GABA is also involved as a metabolic substrate in the brain, including the glutamate – glutamine cycle and as precursor to many other substrates, including carnitine and γ-hydroxybutyrate (GHB) (Cooper *et al.*, 2003). Therefore, similar to glutamate, the pharmacological effect of GABA should be considered from both a metabolic and a neurotransmission standpoint.

Again, from results presented in the previous sections (specifically section 4.3.2, 4.3.3.3, and 4.3.3.4), the inhibition of $GABA_A$-R (with gabazine) caused an increase in the frequency of the epileptiform discharges and conversely, the potentiation of

$GABA_A$-R (with barbiturates) caused a significant suppression of the epileptiform discharges. Although $GABA_A$-R has many potential ligands, GABA is the only endogenous agonist for the $GABA_A$-R (Bergmann *et al.*, 2013). Therefore, the addition of GABA, as a $GABA_A$-R agonist, would be expected to suppress the epileptiform discharges. Similarly, as a metabolic substrate of the glutamate – glutamine cycle, GABA could also suppress the epileptiform discharges through metabolic modulation of the cycle. Therefore, if a suppressive effect is seen with the administration of GABA, it is still difficult to dissociate whether it is due to a receptor-mediated or a metabolic effect.

Putting this into consideration, I applied GABA at concentrations similar to glutamate where it should be at sufficient level to be used as a metabolic substrate (see Figure 4-18).

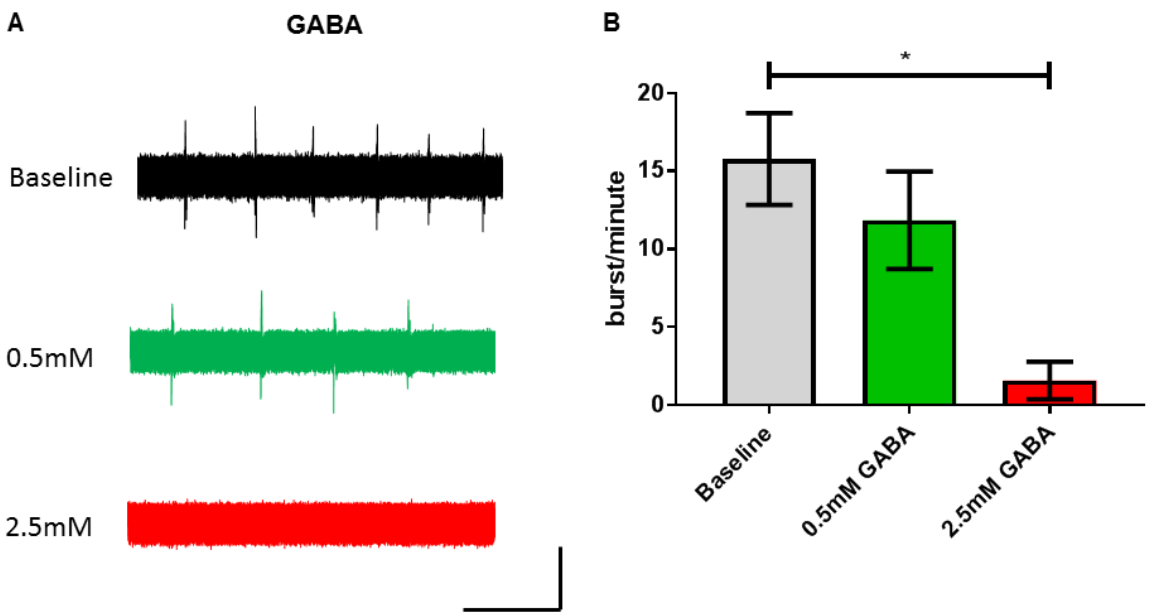

Figure 4-18 Epileptic activity is responsive to the application of GABA. (A) shows the extracellular recordings of epileptic activity following application of 0.5mM and 2.5mM GABA. (B) shows the corresponding bar chart of the burst count of the experimental condition. Scale bar indicates 0.05mV and 10 seconds. Asterisk indicates significance at p<0.05.

Application of GABA at 0.5mM did not cause any significant change ($p>0.05$, $n=8$) to the frequency of the epileptiform discharges (15.79 ± 2.94 burst/min baseline vs 11.85 ± 3.13 burst/min 0.5mM). Increasing the concentration to 2.5mM, however, caused a significant ($p<0.05$, $n=8$) suppression of the epileptiform discharges (1.58 ± 1.20 burst/min 2.5mM).

4.3.6.3 Glutamine

Glutamine is at the core of the astrocytic glutamate – glutamine cycle, as it is the precursor to both glutamate and GABA. The enzyme used to produce glutamine, glutamine synthetase, is primarily expressed in astrocytes (Anlauf and Derouiche, 2013). Therefore, glutamine represents an important mechanism in the interaction between astrocyte and neurons whereby recycling of both the excitatory and inhibitory neurotransmitters occur via astrocytic metabolism.

Considering the importance of glutamine for the glutamate – glutamine cycle, I applied equimolar concentration of glutamine as was used in the experiments with glutamate and GABA (see Figure 4-19).

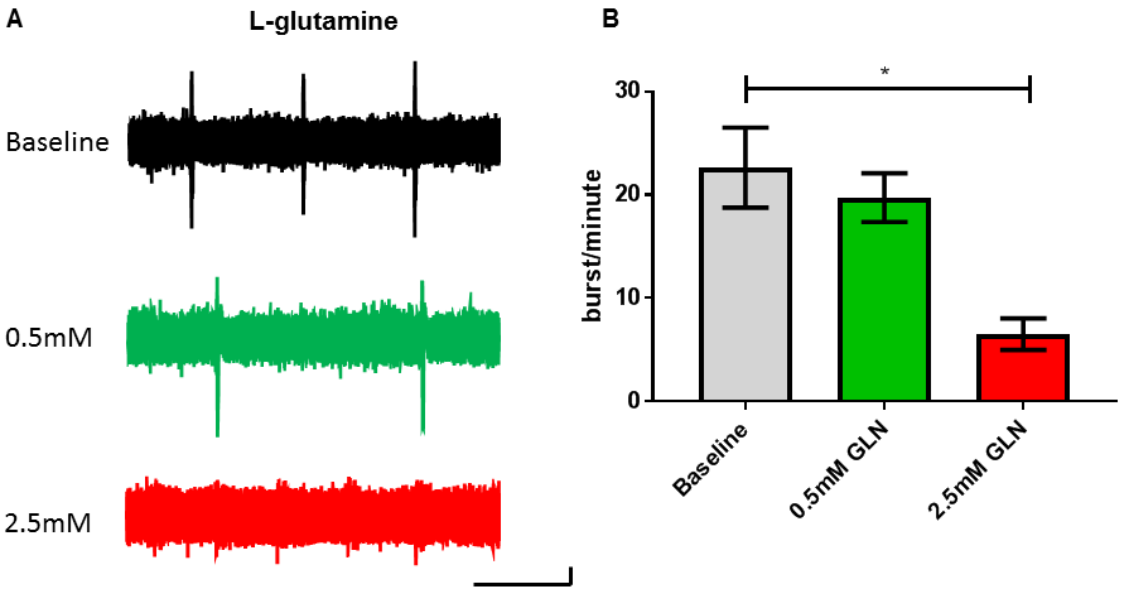

Figure 4-19 Epileptic activity is responsive to L-glutamine addition. (A) shows the extracellular recordings of epileptic activity following application of 0.5mM and 2.5mM L-glutamine. (B) shows the corresponding bar chart of the burst count of the experimental condition. Scale bar indicates 0.05mV and 10 seconds. Asterisk indicates significance at p<0.05.

There was a similar pattern of response by the epileptic tissue to L-glutamine as was demonstrated with GABA. Application at 0.5mM did not cause any significant change ($p>0.05$, $n=5$) in the frequency of the epileptiform discharges (22.60 ± 3.17 burst/min baseline vs 19.60 ± 1.93 burst/min 0.5mM). Increasing the concentration to 2.5mM caused a statistically significant reduction ($p<0.05$, $n=5$) in the frequency of the epileptiform discharges (8.55 ± 2.42 burst/min 2.5mM).

4.3.7 Synergism between benzodiazepine and GABA

Hitherto, our results have shown that the GABAergic system, involving the $GABA_A$-R, is heavily implicated in the process of seizure generation. Both benzodiazepine and barbiturates have a well characterized binding site as the allosteric modulator of the $GABA_A$-R s (Kucken *et al.*, 2000; Greenfield Jr, 2013). It is well characterized, however, that barbiturates can directly activate the $GABA_A$-R, even in the absence of GABA (Rho *et al.*, 1996). In contrast, benzodiazepines cannot activate the $GABA_A$-R when the tissue is devoid of GABA, even when it is administered at a very high concentration (Schmidt and Wilensky, 2008; Krisko *et al.*, 2017). The discrepancy in the response of the epileptiform discharges in this model to benzodiazepines and barbiturates suggested that the tissue might be devoid of GABA, hence the lack of response of the benzodiazepines.

To investigate this hypothesis, I devised an experiment to assess the synergistic effect in the co-application of the benzodiazepine, lorazepam, and GABA (see Figure 4-20). I have chosen the lower concentration range of GABA (0.5mM), where it has been shown that there was no significant suppressive effect from this concentration of GABA. Similarly, I have chosen the minimal inhibitory concentration of lorazepam, 50µM.

The application of lorazepam at 50µM on its own caused an increase in the frequency of the epileptiform discharges by 1.69 ± 15.77% (n=4) whereas the application of GABA at 0.5mM on its own suppressed the frequency of the discharges by 28.69 ± 7.29 % (n=6). These two effects are significantly different ($p<0.05$) when compared with the co-application of 50µM lorazepam and 0.5mM GABA, which caused a 77.75 ± 8.43 % suppression in the frequency of the epileptiform discharges (n=4).

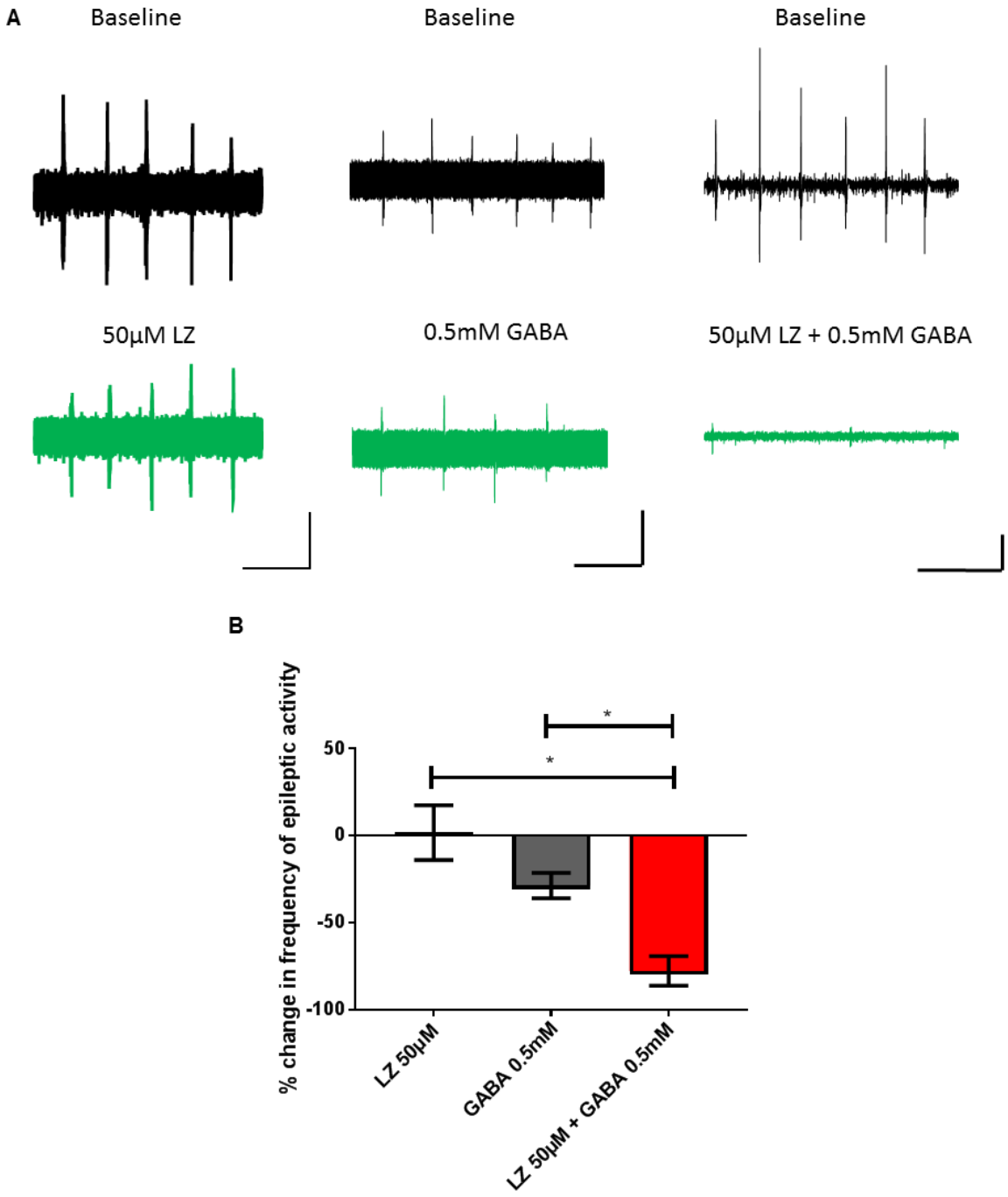

Figure 4-20 There is a synergistic effect with the co-application of the benzodiazepine lorazepam and GABA. (A) shows the electrophysiological recordings obtained following the application of 50µM lorazepam alone (left), 0.5mM GABA alone (middle), and 50µM lorazepam and 0.5mM GABA together (right). (B) shows the corresponding bar chart summarizing the percentage change in the frequency of epileptiform discharges induced by each of the experimental conditions. Scale bar in (A) left indicates 0.1mV and 10 seconds and in (A) middle and right indicates 0.05mV and 10 seconds.

This synergistic effect between benzodiazepine and GABA again suggested that the lack of response of the epileptiform discharges in this model to benzodiazepine administration is potentially due to the reduction in the epileptic tissue concentration of GABA.

4.3.8 The use of mitochondrial – targeting compounds

At present, there is no evidence-based therapeutic intervention for mitochondrial disease. Most physicians have reported the use of various vitamins, nutritional supplements, antioxidants, and mitochondrial – targeting compounds in their care for patients with mitochondrial disease (Parikh *et al.*, 2009). Various anecdotal evidences and small studies have reported promising effects of the use of these compounds (Parikh *et al.*, 2009; Frantz and Wipf, 2010; Pfeffer *et al.*, 2012; Avula *et al.*, 2014). Although none of these compounds were specifically examined for their anticonvulsant properties, their modulation of mitochondrial function may represent a novel approach to the treatment of mitochondrial epilepsy. Therefore, I decided to examine some of the more promising compounds for their potential anticonvulsant properties in this *in vitro* model of mitochondrial epilepsy.

4.3.8.1 Coenzyme Q10 (CoQ10)

Coenzyme Q10 (CoQ10) is a natural electron acceptor in the electron transport chain and has been demonstrated to exhibit strong antioxidant properties (Frantz and Wipf, 2010). Although primarily used for mitochondrial disease with a pathogenic mutation resulting in primary CoQ10 deficiency, it has shown promising effects in patients with secondary CoQ10 deficiency as well (Hargreaves, 2014). By far, the prevalent expert opinion in the use of CoQ10 in patients with mitochondrial disease is that it is beneficial (Parikh *et al.*, 2009). Therefore, I decided to apply CoQ10 acutely to the induced epileptic activity to examine its anticonvulsant activity (see Figure 4-21).

The application of coenzyme Q10 (CoQ10) at 100μM up to 200μM did not cause a significant change ($p>0.05$, $n=5$) in the frequency of the epileptiform discharges (9.56 ± 1.03 burst/min baseline vs 10.08 ± 2.39 burst/min 100μM vs 10.40 ± 3.04 burst/min 200μM). This suggests that coenzyme Q10 has exhibited no anticonvulsant properties and is probably not of benefit to patients with mitochondrial disease with epileptic component.

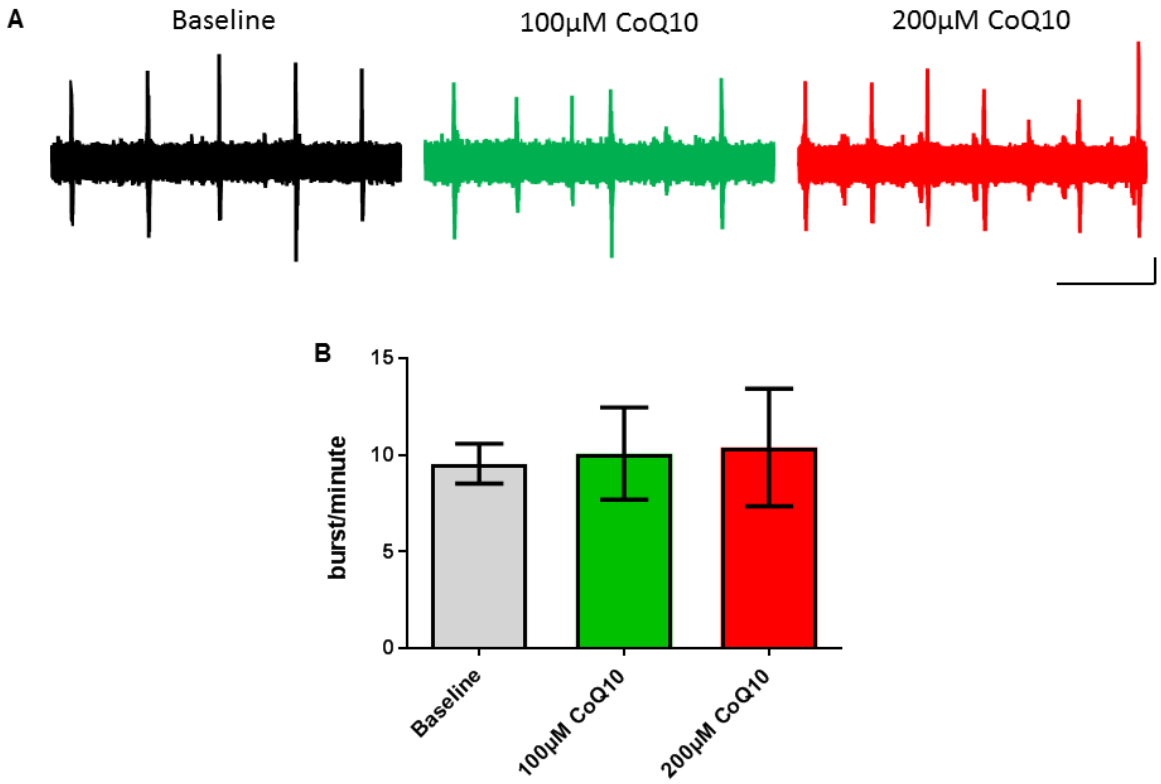

Figure 4-21 Coenzyme Q10 did not exhibit any anticonvulsant property. (A) shows the extracellular recordings of the epileptic activity before (left) and after addition of 100µM of coenzyme Q10 (CoQ10) (middle) up to 200µM (right). (B) shows the corresponding bar chart of the burst count of the experimental condition. Scale bar indicates 0.1mV and 10 seconds.

4.3.8.2 Bezafibrate

Bezafibrate is a hypolipidemic drug that is commonly used for patients with dyslipidemia (Krisko *et al.*, 2017). The mechanisms whereby bezafibrate exerts its pharmacological effect is through the activation of the peroxisome proliferator-activated receptor α (PPARα) (Krisko *et al.*, 2017). In the brain, PPARα is shown to be expressed strongly in the neurons and moderately in the astrocytes (Warden *et al.*, 2016) and in the hippocampus, PPARα has been shown to exhibit a role in the process of learning and memory, through the modulation of synaptic function (Roy *et al.*, 2013).

Bezafibrate, itself, has been shown to exhibit promising effects in patients with mitochondrial disease (Bonnefont *et al.*, 2009). This effect is replicated *in vitro* through the demonstration that it can correct mitochondrial respiratory chain deficiency through stimulating mitochondrial biogenesis (Bastin *et al.*, 2008; Johri *et al.*, 2012; Yatsuga and Suomalainen, 2012). Again, similar to coenzyme Q10, bezafibrate has not been evaluated for its anticonvulsant properties but due to its well established effect on the

modulation of mitochondrial function via the PPAR system, I believe it is worthwhile to investigate the effect of acute application of bezafibrate in this model of mitochondrial epilepsy.

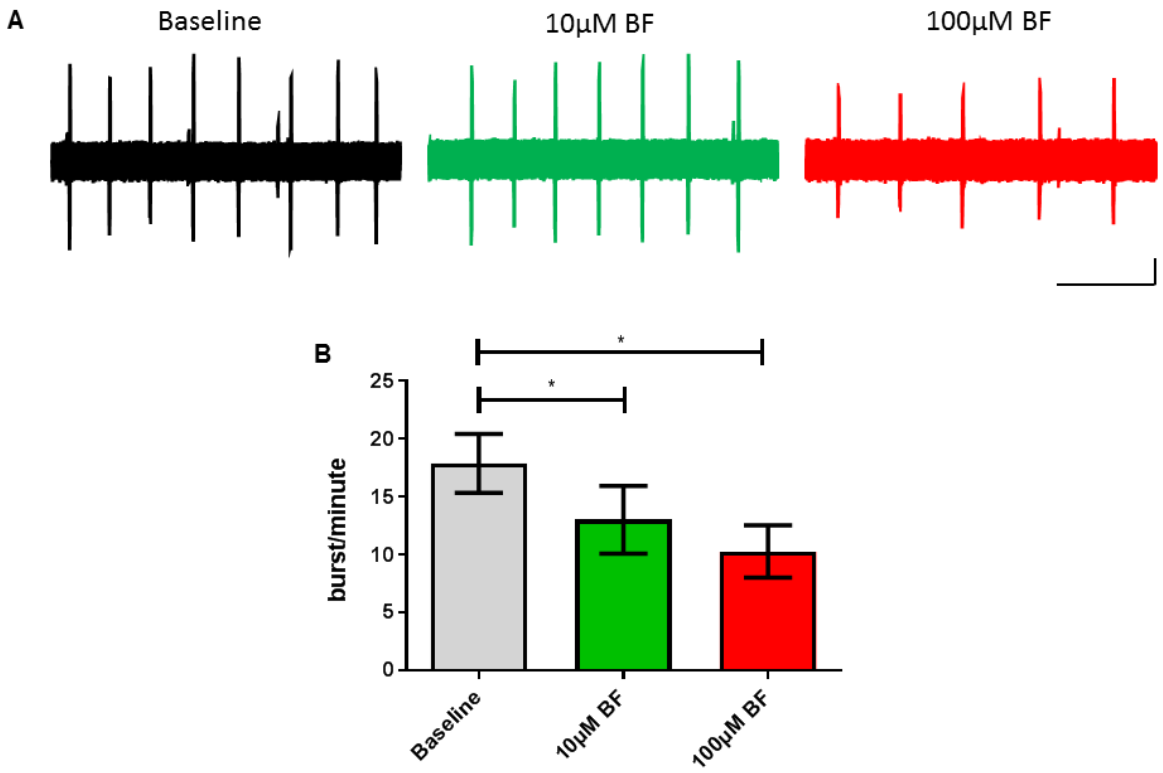

Figure 4-22 Bezafibrate exhibited an anticonvulsant property in the in vitro model of mitochondrial epilepsy. (A) shows the extracellular recordings of the epileptic activity before (left) and after addition of 10µM of bezafibrate (middle) up to 100µM (right). (B) shows the corresponding bar chart of the burst count of the experimental condition. Scale bar indicates 0.2mV and 10 seconds.

Applying bezafibrate at 10µM and up to 100µM caused a statistically significant reduction ($p<0.05$, $n=7$) in the frequency of the epileptiform discharges (17.90 ± 2.55 burst/min baseline vs 13.03 ± 2.92 burst/min 10µM vs 10.29 ± 2.26 burst/min 100µM). This suggests that unlike coenzyme Q10, bezafibrate exhibited potential use as anticonvulsant in mitochondrial epilepsy.

4.4 Discussion

4.4.1 Execution of an *in vitro* pharmacological study

The process of conducting any pharmacological study requires a number of critical experiments to be done to verify the validity of the study. First and foremost, a stable system is required for the pharmacological intervention to be conducted on. One must be certain that the system would not fluctuate or deteriorate over time regardless of the drug application. In this model of mitochondrial epilepsy, a period of stability of the epileptiform discharges has been described previously (see section 3.3.5). Specifically, the epileptic network manifested as a stable interictal activity over a period of 2 hours after 120 minutes of incubation with the rotenone and cyanide. The natural progression of the frequency of the interictal activity over this 2-hour time period is within a 10% variation, resulting in a relatively stable system. Therefore, all of the pharmacological experiments discussed in this chapter is conducted over this 2-hour stable time period.

Next, the 'vehicle effect' needs to be demonstrated and addressed before any conduct of a pharmacological study. A 'vehicle effect' is an effect whereby the vehicle formulation caused a change towards the system on its own, in the absence of the active compounds tested (Sanchez *et al.*, 2001). This is particularly important for evaluating newer compounds, which tend to be highly lipophilic and poorly water soluble (Bittner and Mountfield, 2002). In this study, the two vehicles that I have used for the dissolution of all of the pharmacological compounds are distilled water (dH_2O) for hydrophilic compounds and dimethyl sulfoxide (DMSO) for lipophilic compounds. I have assessed the effects of cumulative addition of increasing concentrations of dH_2O (up to 1%) and DMSO (up to 0.1%) on the frequency of the epileptiform discharges over the 2 hour stable time period (see section 4.3.1). There was no significant difference whatsoever following the application of either dH_2O or DMSO up to their respective highest concentration range. Therefore, the impact of 'vehicle effect' in this model of mitochondrial epilepsy can be excluded and any pharmacological responses described in this chapter can be confidently attributed to the pharmacological actions of the drugs.

4.4.2 Receptor contributions in mitochondrial epilepsy

As mentioned above in section 4.3.2, previous works on the characterization of epilepsy models in acute brain slices have implicated the contribution of various glutamatergic and GABA-ergic receptor in the process of epileptogenesis (Williamson and Wheal, 1992; Isaeva *et al.*, 2010). The receptors that are most commonly associated with seizure generation are the ionotropic glutamatergic receptors, N-methyl-D-aspartate (NMDA) receptor and the α-amino-3-hydroxy-5-methyl-4-isoxazole propionic acid (AMPA) receptor, as well as the ionotropic GABAergic receptor, the $GABA_A$ receptor.

The NMDA, AMPA, and $GABA_A$ receptors are all ionotropic receptors. This means that they mediate fast synaptic responses through the facilitation of the flow of ions across the plasma membranes. In the case of NMDA and AMPA, they respond to their endogenous ligand, glutamate, and allows the flow of cations (usually Na^+ or K^+) and in the case of $GABA_A$, it allows the flow of anions (Cl^-) in response to its endogenous ligand, GABA (Forman *et al.*, 2017).

The NMDA receptor is constitutively expressed mostly in neuronal cells throughout the whole brain, particularly in the hippocampus, cerebellum, and the cerebral cortex (Moriyoshi *et al.*, 1991). The NMDA receptor is unique to the other ionotropic glutamate receptors in that it requires the binding of both glutamate and glycine for the activation of the channel, as well as their dependence on an intense trains of presynaptic activity for the removal of the receptor block by the magnesium ion (Mg^{2+}) (Forman *et al.*, 2017). D-AP5 (D-(-)-2-amino-5-phosphonopentanoic acid) is a competitive NMDA receptor antagonist at the glutamate binding site. The application of D-AP5 caused no significant change in the frequency of the epileptiform discharges. This indicates that there is no contribution from the NMDA receptor towards the generation of epileptiform activity in this model of mitochondrial epilepsy. This is unsurprising as NMDA receptor activation in epileptic tissue is typically a secondary process, associated with the spread of the epileptic activity rather than seizure initiation (Rogawski, 2013; Forman *et al.*, 2017).

Unlike the NMDA receptor, the AMPA receptor mediate a larger proportion of excitatory neurotransmission and is expressed in an activity-dependent manner (Rogawski, 2013). Furthermore, functional AMPA receptor has been found to be expressed not only in hippocampal neurons, but also in the astrocytes (Martin *et al.*,

1993; Hall and Soderling, 1997; Fan *et al.*, 1999). NBQX (2,3-dihydroxy-6-nitro-7sulfamoyl-benzo[f]quinoxaline-2,3-dione) is a very potent competitive AMPA/KA receptor antagonist (Randle *et al.*, 1992). The complete suppression of the epileptic activity by application of NBQX implicated the contribution of the AMPA and potentially also KA receptor in this model of mitochondrial epilepsy. This corroborates previous reports that AMPA receptor is heavily implicated in the onset of an epileptiform activity (Rogawski, 2013; Forman *et al.*, 2017). Kainate receptor activation by kainate produces epileptic activity *in vitro* as a kainate model of epilepsy but its activation is not usually implicated in other more commonly used epileptic models, such as the kindling model (Fritsch *et al.*, 2014). It is generally less well understood than AMPA receptor and is more associated with the spread and severity of epileptiform discharges, like the NMDA receptor (Vincent and Mulle, 2009).

The most abundant GABA receptors in the central nervous system are the ionotropic $GABA_A$ receptor (Forman *et al.*, 2017). The $GABA_A$ receptor is widely expressed in the brain, in neurons and astrocytes alike (Fraser *et al.*, 1994; Galanopoulou, 2008). $GABA_A$ receptor is a pentameric receptor with two binding sites for its endogenous ligand, GABA, and multiple allosteric sites. Gabazine is a selective $GABA_A$ receptor antagonist, at the GABA binding site (Forman *et al.*, 2017). Antagonism of $GABA_A$ receptor by gabazine caused a slight increase in the frequency of the mitochondrial epileptiform discharges, although it is not statistically significant. This potentially implicates the $GABA_A$ receptor as an important modulator of the inhibitory neurotransmission in the mitochondrial epilepsy model. Antagonism of $GABA_A$-R by addition of exogenous GABA or potentiation of $GABA_A$-R by the allosteric modulators such as benzodiazepine or barbiturate may prove to be beneficial in controlling the epileptiform discharges in this model of mitochondrial epilepsy.

Overall, the NMDA receptor has not contributed towards seizure generation in this model of mitochondrial epilepsy. The glutamatergic AMPA-R and the GABAergic $GABA_A$-R, however, may play a role in the generation of epileptiform discharges in this model of mitochondrial epilepsy. These two receptor system may represent an important therapeutic target for drug development in mitochondrial epilepsy.

4.4.3 Use of antiepileptic drugs in mitochondrial epilepsy

Mitochondrial epilepsy is characteristically known as a very pharmacoresistant subtype of epilepsy, with very few seizure control afforded by currently available conventional antiepileptics (Bindoff and Engelsen, 2012; Whittaker *et al.*, 2015). Antiepileptic drug itself is a diverse family of pharmacological agents that exerts anticonvulsant activity through a myriad of mechanisms of actions. To screen the entire antiepileptic drug population is time consuming and inefficient so I have sampled some relevant antiepileptic drugs from the major subclasses of antiepileptic agents and applied the minimal inhibitory concentration (MIC) as well as the maximal tolerable concentration (MTC) of each drugs. The conventional drugs that I have chosen are sodium channel blockers (specifically carbamazepine, lamotrigine, and phenytoin), levetiracetam, benzodiazepines (specifically lorazepam and midazolam), barbiturates (specifically pentobarbitone), and valproate acid. I have also screened for two newer generation antiepileptic drugs that shows promising potential for use in mitochondrial epilepsy; the AMPA receptor antagonist, perampanel; and the metabolic modulator, stiripentol.

The sodium channel blockers act by stabilizing the inactivated state of the sodium channel, therefore producing a use-dependent inhibition of action potentials (Fertig and Mattson, 2008; Stern *et al.*, 2008; Tomson *et al.*, 2008). The three drugs that I have chosen; carbamazepine, lamotrigine, and phenytoin; are clinically indicated for slightly different seizure syndromes but they all generally act through the inactivation of the sodium channel. These three drugs showed no capacity whatsoever in controlling the epileptic activity induced (see Figure 4-3). This corroborates previous finding in the low magnesium – high potassium model of epilepsy where the high – frequency ictal discharges respond to sodium channel blockers, but not the late interictal discharges (Gáll *et al.*, 2017). Since the mechanism of action of these sodium channel blockers is through a use-dependent inhibition, it would not be surprising then to expect that only the high frequency ictal discharges would be responsive to these drugs and not the lower firing rate interictal discharges (Fertig and Mattson, 2008). In this model of mitochondrial epilepsy, the randomness of the appearance of the ictal discharges prevented me from being able to assess the anticonvulsant properties of these drugs towards the ictal discharges. As discussed in section 4.4.1, a stable system is required for accurate assessment of a pharmacological response and in this model, the stable electrophysiological system is the interictal discharges.

Levetiracetam is a unique antiepileptic drug that exerts its anticonvulsant activity through the inhibition of exocytosis of synaptic neurotransmitters via the SV2A receptor (Lynch *et al.*, 2004). Clinically, levetiracetam was suggested in existing guideline as one of the preferable antiepileptic drug to use for control of seizure in patients with mitochondrial epilepsy (Schaefer *et al.*, 2010). The application of levetiracetam in this model of mitochondrial epilepsy has shown no effect towards the frequency of the epileptiform discharges (see Figure 4-4). This suggests that the epileptic activity in the mitochondrial epilepsy model is independent of the contribution of the exocytosis of synaptic neurotransmitters. It is very much agreed that levetiracetam binds to SV2A, however, very little is known on the function of the SV2A signalling. A recent study has suggested that unlike what was previously hypothesized, the SV2A synaptic vesicle selectively regulates exocytosis of GABA, rather than glutamate (Tokudome *et al.*, 2016). This may cast doubt on whether or not the anticonvulsant property of levetiracetam is indeed associated with the SV2A system and may be more complicated than previously thought. Very little is indeed known about the SV2A system and without further elucidation on the function of the SV2A protein, little can be speculated from a pathophysiological perspective in explaining the resistance to levetiracetam in my model of mitochondrial epilepsy.

Benzodiazepine is one of the allosteric modulator of the $GABA_A$ receptor. It has its own binding site on the $GABA_A$ receptor and allosterically modulate the GABA receptor current to increase inhibitory tone (Schmidt and Wilensky, 2008). Clinically, benzodiazepine is the first line drug for status epilepticus due to its rapid onset of action (Schmidt and Wilensky, 2008). I have chosen to evaluate two drugs from the benzodiazepine family; the water-soluble formulation, midazolam, and the lipophilic formulation, lorazepam. Both benzodiazepines did not cause any significant change in the frequency of the epileptiform discharges (see Figure 4-5). This lack of response to benzodiazepine does not necessarily exclude the implication of $GABA_A$ receptor system in the model of mitochondrial epilepsy. As mentioned above, the $GABA_A$ receptor is composed of many different subunits, and benzodiazepine selectively binds to the α-subunit of the $GABA_A$ receptor (Smith, 2001). The lack of response to benzodiazepines then suggests that the inhibitory modulation via the α-subunit of the $GABA_A$ receptor is not a prime therapeutic target in mitochondrial epilepsy.

Barbiturate is another allosteric modulator of the $GABA_A$ receptor. Similar to benzodiazepine, it has its own binding site on the $GABA_A$ receptor in its allosteric

modulation of the inhibitory tone. No specific binding site can be identified due to the low affinity of barbiturate towards the receptor, however, it is known to be distinct from the benzodiazepine binding site (Bureau and Olsen, 1993). As mentioned above, phenobarbitone is the classically used antiepileptic from this subgroup, but pentobarbitone is known to be much more potent than phenobarbitone in the modulation of $GABA_A$-R (Olsen, 2002), therefore, its use is much more relevant in our context to evaluate the contribution of the $GABA_A$-R. The induced mitochondrial epileptic activity in this model shows profound responsiveness to the application of pentobarbitone. This suggests that the potentiation of $GABA_A$-R inhibitory current, as previously hypothesized in section 4.4.2, can indeed suppress the epileptiform discharges in this *in vitro* model of mitochondrial epilepsy. Furthermore, barbiturate is also well – characterized as having a dual mechanism as an AMPA-R inhibitor (Joo *et al.*, 1999; Forman *et al.*, 2017). Since inhibition of AMPA-R by NBQX was able to suppress the epileptiform discharges, the inhibitory effect of barbiturates could be mediated through its dual mechanism of actions.

This discrepancy between the response of the mitochondrial epileptiform discharges to benzodiazepine and barbiturate poses an important question in the modulation of the $GABA_A$-R neurotransmission in my model of mitochondrial epilepsy. It has been shown in previous study that barbiturates can directly activate the $GABA_A$-R at high concentrations, even in the absence of GABA (Rho *et al.*, 1996). Unlike barbiturates, benzodiazepines are unable to activate $GABA_A$-R when the tissue is devoid of GABA (Krisko *et al.*, 2017). This could potentially explain the discrepancy of the pharmacological response in this model. To address this, I co-applied the benzodiazepine, lorazepam and low concentration of GABA to evaluate any synergistic effect. This resulted in a synergistic summation of inhibitory effect, to almost a complete suppression (see Figure 4-20). This experiment suggested that the epileptic tissue in my model of mitochondrial epilepsy could have reduced tissue concentration of GABA, hence the lack of response of benzodiazepine on its own. It also corroborates the contribution of the $GABA_A$-R mediated inhibitory neurotransmission in the development of the epileptic activity in this model of mitochondrial epilepsy.

Valproic acid is a branched-chain fatty acid, which was surprisingly discovered to have a strong anticonvulsant property (Beydoun *et al.*, 2008). Up until the present time, there is no single mechanism of action that valproate can be attributed to. Instead, it is suggested to have a broad spectrum of activity, including the potentiation of GABA-

ergic signalling, reduction of NMDA-R mediated excitatory input, and use-dependent inhibition of the sodium channel (Löscher, 2002). In this model of mitochondrial epilepsy, valproate was found to have no inhibitory effect in the induced epileptiform discharges (see Figure 4-7). Mechanistically, there is perhaps no inference that can be made in explaining the resistance of the tissue to valproate as there is no single agreed mechanism that valproate was expected to act on. However, this resistance to valproic acid represents an interesting phenomenon when explaining the role of fatty acids in controlling seizure generation in this model of mitochondrial epilepsy (to be discussed further below in section 4.4.4). Regardless, valproic acid should be avoided as an antiepileptic agent for use in patients with mitochondrial epilepsy due to its well characterized hepatotoxicity in this subset of patient (Schaefer *et al.*, 2010; Li *et al.*, 2015).

Hitherto, most of the conventional antiepileptic drugs exhibited little, if any, effects on the epileptiform discharges in this model of mitochondrial epilepsy. The only pharmacological agents that seemed to exhibit therapeutic potential is barbiturates. Even with barbiturates, significant inhibitory effect was only apparent at its reported maximal tolerable concentration (200µM). It is important to note that the responses of these conventional antiepileptic drugs have only been tested at two concentration points that represent the safe and recommended therapeutic range for clinical use of these antiepileptic drugs in conventional epileptic patient. However, current clinical practice in the management of mitochondrial epilepsy often involves aggressive treatment with very high doses of antiepileptic drugs (Schaefer *et al.*, 2010; Whittaker *et al.*, 2015), which may not be represented by the concentrations tested in this study. Therefore, the lack of responses to these conventional antiepileptic drugs does not necessarily suggest the need for immediate exclusion of these drugs in the care of patients with mitochondrial epilepsy. This is particularly true for drugs that seemed to exhibit clinical efficacy but no responses in this model, such as levetiracetam or lamotrigine (Schaefer *et al.*, 2010). Perhaps, these drugs warrant further investigation in this model with regards to its effect on a higher than maximal tolerable concentration – the suprathreshold concentrations.

By the definition of ILAE, an epileptic syndrome is classified as pharmacoresistant when the epileptic activity fails to respond and achieve sustained seizure freedom with adequate trials of two tolerated and appropriately defined antiepileptic drug schedules (whether as monotherapies or in combination) (Kwan *et*

al., 2010). If this is to be applied to the context of an animal model, this *in vitro* brain slice model of mitochondrial epilepsy can be classified as a pharmacoresistant epilepsy model. Considering the extreme pharmacoresistance that has been displayed, it can even be claimed that the epileptic activity in this model presents as a 'super – refractory' epilepsy. The face validity of the model and the presence of extreme pharmacoresistance in this model raised the opportunity to evaluate the use of the newer generation of antiepileptic drugs in the context of mitochondrial epilepsy.

One such drug is perampanel, a first-in-class antiepileptic drug, with a novel mechanism of action on the modulation of AMPA receptor. Unlike NBQX, however, perampanel is a noncompetitive selective AMPA receptor antagonist, suggesting that it would not be displaced even in conditions where there is a high tissue concentration of glutamate (Chen *et al.*, 2014). Considering the responsiveness of the epileptic activity in this model to NBQX, perampanel is expected to also be able to suppress the induced mitochondrial epileptic activity. Indeed, the application of perampanel caused a dose-dependent reduction in the frequency of the epileptiform discharges with an almost complete suppression achievable with its MTC of 10μM (see Figure 4-8). The IC_{50} value in this model of 0.42μM is comparable with previously reported IC_{50} value of 0.56μM in the kainate model and 0.23μM in the electrical stimulation of the Schaffer collaterals (Ceolin *et al.*, 2012; Rogawski and Hanada, 2013; Chen *et al.*, 2014). This reaffirms the vital role that AMPA-R plays in the seizure generation in this model of mitochondrial epilepsy and supports the consideration of perampanel for use in patients with mitochondrial epilepsy.

Another drug that I tested in this model is stiripentol. Stiripentol is clinically only used in pediatric patients with Dravet syndrome (Chiron *et al.*, 2000; Inoue *et al.*, 2009). The relevance of stiripentol in this model of mitochondrial epilepsy is in the recent finding that stiripentol was able to inhibit the glycolytic enzyme, lactate dehydrogenase, and exhibited anticonvulsant activity through this mechanism (Sada *et al.*, 2015). The application of stiripentol in this model of mitochondrial epilepsy did result in a dose-dependent reduction in the frequency of epileptiform discharges, however complete suppression was not achievable even in the highest concentration tested of 500μM (see Figure 4-16). The maximum concentration of 500μM was the reported concentration where stiripentol inhibited the lactate dehydrogenase enzyme (Sada *et al.*, 2015) and at this concentration, only around 60% of inhibition was achieved in this model of mitochondrial epilepsy. In human, the therapeutic range of stiripentol has

been fitted to the concentration range of 30 - 100μM (Quilichini *et al.*, 2006). At this concentration range, stiripentol caused minimal inhibitory effect in this model of mitochondrial epilepsy. Furthermore, at this concentration range, stiripentol is well characterized to modulate $GABA_A$ receptor in a barbiturate-like manner (Quilichini *et al.*, 2006; Fisher, 2011; Grosenbaugh and Mott, 2013). Therefore, it does not exclude the possibility that the inhibitory effect that stiripentol was able to afford in this model of mitochondrial epilepsy is attributed to its modulation of $GABA_A$ receptor, as barbiturate does. Furthermore, to achieve a 50% suppression with stiripentol, a relatively high concentration of 384.10μM is required, which may not be achievable in the clinical setting.

To conclude, both of the newer generation antiepileptic drugs showed inhibitory effects in this model of mitochondrial epilepsy. However, perampanel is clearly more potent and was able to achieve complete suppression at its maximal concentration. Stiripentol, however, needs a significantly higher concentration before it produces sizable inhibitory effect, hence, the use of stiripentol in mitochondrial epilepsy needs to be evaluated and considered further.

4.4.4 Ketogenic diet in mitochondrial epilepsy

As mentioned above, ketogenic diet is a form of nutritional intervention by employing a high-fat, moderate-protein, and low-carbohydrate diet in order to favour the ketone bodies production (Branco *et al.*, 2016). Many studies have reported the success of ketogenic diet in controlling intractable seizures, especially in paediatric population (Branco *et al.*, 2016; Martin *et al.*, 2016; Lambrechts *et al.*, 2017). In patients with mitochondrial epilepsy, ketogenic diet has also been shown in various studies to be effective in controlling the various phenotypes of the epilepsy (Kang *et al.*, 2007; Martikainen *et al.*, 2012; Steriade *et al.*, 2014). As well characterized as the clinical efficacy of ketogenic diet is, little is known about the mechanisms whereby ketogenic diet is anticonvulsant. Some components of the diet have been identified to potentially exhibit anticonvulsant properties. I have chosen to examine the acute anticonvulsant activity of three components of the diet, namely the ketone body β-hydroxybutyrate and the medium-chain fatty acids; decanoic acid (C10) and octanoic acid (C8).

The ketone bodies are the primary product of the ketogenic diet. Composed of the β-hydroxybutyrate, acetone, and acetoacetate; collectively, these products are

formed through the generation of acetyl CoA via the breakdown of lipids (Berg *et al.*, 2012e). I have applied β-hydroxybutyrate acutely and found that there is a dose-dependent reduction in the frequency of the epileptiform discharges with about 80% reduction in epileptic activity at the highest concentration tested (20mM) (see Figure 4-10). This suggests that β-hydroxybutyrate, on its own, have an acute anticonvulsant property. This is consistent with previous studies reporting direct anticonvulsant property of β-hydroxybutyrate in the pilocarpine model of epilepsy (Yum *et al.*, 2012b; Yum *et al.*, 2012a). The mechanisms whereby β-hydroxybutyrate is directly anticonvulsant, however, remains largely unknown. Within the context of mitochondrial epilepsy, it is possible that β-hydroxybutyrate acts as a metabolic substrate to achieve burst suppression. It has been shown that replacement of glucose with β-hydroxybutyrate, can hyperpolarize the neurons; resulting in enhanced inhibition (Sada *et al.*, 2015). When comparing the IC_{50} of glucose (10.27mM), pyruvate (7.74mM), and β-hydroxybutyrate (5.16mM); it is clear that β-hydroxybutyrate exhibited the highest potency in achieving burst suppression and perhaps reflect the shift of preferred metabolic fuel usage towards ketone bodies. This shift may be able to enhance general inhibitory tone through the hyperpolarization of the neurons; as previously reported. Another potential mechanism reported in previous study is through the enhancement of the synthesis of kynurenic acid (Chmiel-Perzyńska *et al.*, 2011). Kynurenic acid is a metabolic product of L-tryptophan metabolism and has been shown to possess AMPA-R antagonism (Weber *et al.*, 2001). B-hydroxybutyrate at high concentrations (15mM) has been shown to increase synthesis of kynurenic acid as well as upregulate the kynurenine aminotransferase activity in the glia (Chmiel-Perzyńska *et al.*, 2011). Therefore, it is plausible that the β-hydroxybutyrate produces burst suppression through the antagonism of AMPA-R via upregulating the generation of kynurenic acid.

In human studies, the role that ketone bodies play in the control of seizure remains controversial. On one hand, past study has shown that level of ketosis does not necessarily correlate with the degree of seizure control (Likhodii *et al.*, 2000). A more recent study, however, has suggested relatively good correlation between blood ketosis level, but not urinary ketosis, and seizure reduction (van Delft *et al.*, 2010). Clearly, a more direct investigation is needed into the link between ketone bodies generation and seizure control. This uncertainty in the role of ketone bodies production in seizure suppression leads to studies on the other components of the ketogenic diet that may also exhibit anticonvulsant properties.

Another interesting component of the ketogenic diet is the medium-chain fatty acids. The two main fatty acid components of the diet are the octanoic acid (C8) and the decanoic acid (C10); both of which are detectable in the plasma following administration of the diet (Haidukewych *et al.*, 1982). I have demonstrated that the mitochondrial epilepsy in this brain slice model is responsive to both decanoic acid (see Figure 4-11) and octanoic acid (see Figure 4-12). This is consistent with recent studies that has found that decanoic acid (C10) has acute anticonvulsant properties in various *in vitro* epileptic models (Chang *et al.*, 2013; Chang *et al.*, 2015). This anticonvulsant property of C10 was suggested to be through the inhibition of AMPA-R currents and was, interestingly, shown to be specific to only C10 and not C8 (Chang *et al.*, 2015). This same author had also demonstrated in previous study that C8 has no acute anticonvulsant property, unlike C10 (Chang *et al.*, 2013). This is in direct contrast with our results and the results from a Polish group investigating the same medium chain fatty acids (Wlaź *et al.*, 2012; Wlaź *et al.*, 2015); both of which demonstrated that C8 is as effective as, if not more effective than, C10 in its acute anticonvulsant activity. In this model of mitochondrial epilepsy, C8 (IC_{50} = 134.2μM) is clearly more potent than C10 (IC_{50} = 230.6μM). This suggests that the inhibitory effect mediated by both C8 and C10 is unlikely through the modulation of AMPA-R. Specific to this model of mitochondrial epilepsy, C8 and C10 may be able to exert its inhibitory effect through metabolic modulation. Fatty acids and lipids are known to be the most efficient molecules in terms of ATP generated per molecule (Berg *et al.*, 2012e). Therefore, it would be unsurprising if the application of C8 and C10, especially at the high concentration range (1-2mM), can provide metabolic relief in the form of ATP production for the epileptic tissue. However, this still does not explain the potency of C8 as compared against C10. A recent study has addressed this issue through an elegant investigation into the distinction in the metabolic fate of C8 and C10. In the study, it was found that C10 upregulated astrocytic glycolysis and lactate production; whereas C8 upregulated astrocytic ketogenesis by almost two-fold, instead of upregulating glycolysis (Thevenet *et al.*, 2016). Considering that ketone bodies have been shown above to have an inhibitory effect on its own, it is not surprising then that C8 would have a more potent inhibitory effect in this scenario, as compared to C10.

To summarize, all the three components of the ketogenic diet investigated; β-hydroxybutyrate, octanoic acid, and decanoic acid; have been demonstrated to have acute anticonvulsant properties. This highly suggests that ketogenic diet may have efficacy in controlling mitochondrial epilepsy. However, preclinical studies on ketogenic

diet tend to be conducted *in vivo* either using animals fed on the ketogenic diet (Likhodii *et al.*, 2000) or using genetically modified animals (Giménez-Cassina *et al.*, 2012). This tends to be a more accurate representation of the ketogenic diet as the diet influences systemic metabolism *in vivo* and this modulation of metabolism may not be inducible through the acute application of a single component of the diet. However, the *in vitro* study conducted here is the only method to dissect the acute anticonvulsant property of each individual components of the diet. Therefore, future study should translate the findings from this *in vitro* study to *in vivo* animal model, as both findings should be complementary to each other.

4.4.5 Modulating glycolysis in mitochondrial epilepsy

In a physiological condition, glucose is the compulsory main substrate for brain energy provision and the only pathway from which glucose can enter metabolism is through glycolysis (McKenna *et al.*, 2006). Since components of the mitochondrial epilepsy model do not directly target glycolysis, it remains the only uninhibited metabolic pathway and if any upregulation was necessary to compensate for the metabolic inhibition, glycolysis would most probably be the first pathway to be upregulated. To investigate this, three substrates of glycolysis were added onto the brain slices; glucose, pyruvate, and lactate; at similar increasing concentration range (2-20mM) so as to provide direct comparison between the three substrates.

Addition of glucose was able to significantly suppress the induced epileptic activity with 50% suppression achieved by the addition of extra 10mM glucose into the nACSF bath (see Figure 4-13). This suggests that glycolysis is not saturated in the epileptic tissue and the upregulation of glycolysis can potentially provide metabolic relief for the epileptic tissue. However, the total maximal concentration of available glucose at 50% seizure reduction in this scenario would be 20mM (10mM already in the nACSF bath and extra 10mM glucose). This is potentially difficult to achieve in an *in vivo* setting as the maximal brain concentration at hyperglycemia is reported to be around 5mM (Silver and Erecinska, 1994). Therefore, the strategy of loading the brain with glucose to alleviate metabolic demand in the mitochondrial epileptic tissue may need to be re-evaluated.

Similar to glucose, the addition of pyruvate was able to significantly suppress the epileptiform discharges in the model of mitochondrial epilepsy (see Figure 4-14). This reaffirms that glucose is most likely suppressive through upregulation of glycolysis via the generation of pyruvate. Pyruvate, itself, has two metabolic fates; either to enter oxidative metabolism through conversion to acetyl CoA; or to be reduced to lactate by the enzyme lactate dehydrogenase (Berg *et al.*, 2012f). To distinguish which pathway provides the metabolic relief, I have added lactate at a similar concentration range and demonstrated that lactate was not suppressive in the mitochondrial epilepsy model, except when it is applied at very high concentration of 20mM (see Figure 4-15). This suggests that pyruvate is likely to exert its inhibitory effect through entering oxidative metabolism; rather than through anaerobic glycolysis. It also presents empirical evidence that oxidative metabolism has not been completely inhibited by the components of the mitochondrial epilepsy protocol. The lack of response of lactate also directly contradicts the astrocyte – neuron lactate shuttle hypothesis; which proposes that lactate is preferentially used by neurons as metabolic substrate during conditions of increased neuronal activity (Pellerin and Magistretti, 1994). The inhibitory effect that was afforded by lactate at 20mM was indeed surprising as no indication of any inhibitory effect was seen at any of the lower concentrations. Lactate, interestingly, is being investigated as a potential novel signalling molecules in the brain; found to interact with the HCA1 receptor, a putative G-protein coupled receptor, and the K_{ATP} channels (Bozzo *et al.*, 2013; Mosienko *et al.*, 2015). It is still unclear, however, how lactate acts as a signalling molecule and whether or not it affects inhibitory or excitatory neurotransmission.

Metabolic modulation seems to represent an interesting approach to provide seizure suppression in this model of mitochondrial epilepsy. It is clear that reserve capacity for oxidative metabolism still persists even following all the metabolic inhibitions during mitochondrial epilepsy induction. Any form of therapeutic intervention that can upregulate or make use of this reserve capacity may be able to modulate the epileptic network and alleviate the metabolic stress in such tissue.

4.4.6 Application of substrates of glutamate – glutamine cycle in mitochondrial epilepsy

As mentioned above, the glutamate – glutamine cycle is an important astrocytic process implicated in the recycling of both the excitatory neurotransmitter, glutamate and the inhibitory neurotransmitter, GABA; via the non-neuroactive precursor molecule, glutamine (Bak *et al.*, 2006). This cycle is heavily reliant on the astrocytic TCA cycle as its intermediary pathway. Since fluorocitrate, as part of the protocol for mitochondrial epilepsy induction, inhibits astrocytic TCA cycle specifically; it would be unsurprising to expect a downstream inhibition of the glutamate – glutamine cycle. To examine the role that this cycle plays in mitochondrial epilepsy, I have added the three main substrates of these cycles; glutamate, GABA, and glutamine; onto the epileptic tissue to assess its effect on the epileptiform discharges.

The addition of glutamate caused no effect whatsoever in the frequency of the epileptiform discharges (see Figure 4-17). This was starkly different to the addition of GABA, which caused a complete suppression at the high concentration of 2.5mM. This inhibitory effect of GABA is unsurprising in the context of inhibitory neurotransmission. Previous sections have outlined in detail the implication of $GABA_A$-R in seizure generation and therefore, this inhibitory effect can easily be attributed to the agonism of the $GABA_A$-R by its only known endogenous ligand, GABA (Bergmann *et al.*, 2013). However, both GABA and glutamate can also enter the astrocytic TCA cycle as a metabolic substrate through the glutamate – glutamine cycle. In this case, one would expect that both GABA and glutamate would be equally inhibitory towards the epileptiform discharges through the alleviation of metabolic demand by the same pathway. This has been shown to not be the case and therefore, it can be concluded that the inhibitory effect afforded by GABA is more likely to be through the enhancement of inhibitory tone by the agonistic action on $GABA_A$-R.

Interestingly, the addition of glutamine was able to cause significant suppression at the high concentration of 2.5mM. This could be mediated through the increased synthesis of GABA as glutamine is the precursor molecule to both glutamate and GABA (Bak *et al.*, 2006). Oral administration of glutamine has been shown to increase the level of GABA measured in the striatal tissue as well as in the extracellular fluid (Wang *et al.*, 2007). Another possibility, however, is that glutamine can also enter the astrocytic TCA cycle, similar to glutamate and GABA, and enter oxidative metabolism to alleviate the metabolic stress. Both possibilities certainly do seem

feasible and possible within the context of this model. Glutamine is an interesting molecule as it is non-neuroactive (McKenna *et al.*, 2006); therefore it would not affect neurotransmission on its own, unless it has been converted to either glutamate or GABA. However, recent studies have shown that glutamine is a key player in the neuronal – astrocytic interaction by mediating the regulation of the inhibitory postsynaptic current (IPSC) in a co-culture of neurons and astrocytes (Kaczor *et al.*, 2015). The mechanisms by which glutamine regulates this is unknown. Therefore, not much can be inferred still about how glutamine provides an anticonvulsant activity but any of the mechanisms discussed above may contribute to this effect within the context of this model of mitochondrial epilepsy.

Taken together, these results have reaffirmed the importance of GABA-ergic neurotransmission in the process of seizure control. Glutamine represents an interesting therapeutic candidate as it may either modulate the inhibitory neurotransmission via conversion to GABA or modulate metabolism by entering the TCA cycle. These results warrant further investigation into the glutamate – glutamine cycle, specifically the role that glutamine plays in mitochondrial epilepsy.

4.4.7 The use of mitochondrial – targeting compounds

As mentioned above, there is no clinical guideline in an evidence-based therapeutic intervention in patients with mitochondrial disease. Most physicians have resorted to the use of mitochondrial – targeting compounds in their attempt for the achievement of some form of modulation of mitochondrial function (Parikh *et al.*, 2009; Pfeffer *et al.*, 2012). Out of the many mitochondrial – targeting compounds described in various studies, I have decided to examine the effect of two of the most promising compounds, coenzyme Q10 (CoQ10) and bezafibrate.

Among all the mitochondrial – targeting compounds, CoQ10 is the most popular in the management of mitochondrial disease, due to its well-documented tolerability and safety even at high doses and its dual action as a respiratory chain component and antioxidant (Schon *et al.*, 2010). In a certain subgroup of patients with mutations resulting in a primary CoQ10 deficiency, the administration of CoQ10 can be lifesaving (Hargreaves, 2014). However, evidence of its use in the other group of patients without the primary CoQ10 deficiency remains largely anecdotal and lacks any assessment of

efficacy through a rigorously controlled clinical trial (Parikh *et al.*, 2009; Schon *et al.*, 2010).

In this model of mitochondrial epilepsy, the application of coenzyme Q10 (CoQ10) has been shown to have no anticonvulsant effect. The *in vitro* model of mitochondrial epilepsy that I have developed has a mitochondrial respiratory chain deficiency in complex I and IV through the administration of rotenone and potassium cyanide, respectively. CoQ10 is a component of the electron transport chain, as the mobile electron carrier from complex I and complex II to complex III (Voet and Voet, 2011a). It does not, however, on its own upregulate the mitochondrial respiratory chain activity. In fact, administration of CoQ10 in a neuronal cell-line deficient of CoQ10 only partially rescues the mitochondrial respiratory chain activity despite its strong antioxidant property (Duberley *et al.*, 2014). Indeed, CoQ10 has been shown to have a dual action as a potent cellular antioxidant (Leibovitz *et al.*, 1990). This suggests that the metabolic modulation mediated by coenzyme Q10 through upregulation of electron transport and as a potent antioxidant has no direct benefit in mitochondrial epilepsy. Although oxidative stress is likely to occur in the epileptic tissue due to the inhibition of mitochondrial respiratory chain, the mere scavenging of these free radicals without any real effect on the mitochondrial respiratory chain activity may prove to be of no real benefit to the epileptic tissue.

Bezafibrate is developing as a mitochondrial – modulating compound through its effect on mitochondrial biogenesis (Johri *et al.*, 2012; Yatsuga and Suomalainen, 2012). Unlike coenzyme Q10, bezafibrate has been shown to correct mitochondrial respiratory chain deficiency in a patient line deficient in complex I, III, and IV (Bastin *et al.*, 2008). This effect is proposed to be through the PPARgamma coactivator-1 alpha (PGC1-α) mediated by the activation of the peroxisome proliferator-activated receptor (PPAR) system (Liang and Ward, 2006; Bastin *et al.*, 2008; Schon *et al.*, 2010).

When I applied bezafibrate acutely in the model of mitochondrial epilepsy, there was a significant reduction in the frequency of the epileptiform discharges following the application of both 10μM and 100μM. This was unprecedented as bezafibrate has never been evaluated as a potential anticonvulsant agent. A mechanistic approach would suggest that the metabolic modulation afforded by bezafibrate can directly alleviate the metabolic stress imposed on the tissue that resulted in seizure generation. This could be through its correction of the mitochondrial respiratory chain deficiency, as described above in a previous study (Bastin *et al.*, 2008), but this correction is

proposed to be through the upregulation of mitochondrial biogenesis via PGC1-α activation (Bastin *et al.*, 2008; Schon *et al.*, 2010). PGC1-α is a transcription co-activator and its stimulation through the activation of the PPAR system upregulates mitochondrial biogenesis (Liang and Ward, 2006). This activation of the gene expression and subsequent stimulation of mitochondrial biogenesis tends to not be an acute effect and hence, most studies on the effect of bezafibrate has been through the introduction in a rodent's diet, rather than an acute application (Johri *et al.*, 2012; Chandra *et al.*, 2016). Therefore, it is unlikely that the acute anticonvulsant effect is mediated through an upregulation of mitochondrial biogenesis.

An interesting aspect of the pharmacological action of bezafibrate that tends to be overshadowed in recent studies is its effect on modulating lipid metabolism. As a hypolipidemic agent, bezafibrate is known to increase mitochondrial fatty acid oxidation (Krisko *et al.*, 2017). This has been confirmed *in vitro* in patients' cell line in that it shifts the metabolic profile of the cell towards increased beta oxidation and anaerobic glycolysis (Scatena *et al.*, 2003; Li *et al.*, 2010). Even more interesting is that in human studies, bezafibrate was found to be mildly ketogenic in that it increases β-hydroxybutyrate level in the postprandial plasma (Tremblay-Mercier *et al.*, 2010). When co-applied with the medium chain triglycerides, the combination of bezafibrate and the medium chain lipids increased initial ketone body production by twofold (Courchesne-Loyer *et al.*, 2015). It is therefore highly likely that bezafibrate increases fatty acid oxidation to favour ketogenesis. As discussed in section 4.4.4, ketone bodies and fatty acids have a suppressive effect towards the induced epileptic activity. Perhaps, in the epileptic tissue, the underlying metabolic profile has shifted towards a reliance on fatty acid metabolism and the administration of bezafibrate has upregulated this process, particularly towards ketogenesis, resulting in the alleviation of the metabolic stress and the suppression of the epileptiform activity.

Regardless of the results described above, the practice of using mitochondrial – targeting compounds in the care of patients with mitochondrial disease is likely to continue. However, it seems imperative that research is directed towards promising candidate compounds and evidence is collected through well designed studies and rigorously controlled clinical trials to support its use in patient care. According to our results alone, coenzyme Q10 is likely to be of no benefit for patients with mitochondrial epilepsy whereas bezafibrate could be of benefit. Specifically, bezafibrate might be useful not only for its effect towards upregulation of mitochondrial biogenesis but also

for its modulation of lipid metabolism. More mitochondrial – targeting compounds should be screened for using this model of mitochondrial epilepsy as emerging evidence suggests that metabolic modulation might be a novel approach in developing therapies for patients with mitochondrial epilepsy.

4.5 Summary, strength, and weakness

This chapter provides a comprehensive pharmacological study and investigation into possible therapeutic targets for mitochondrial epilepsy. Specifically, three distinct systems have been identified; namely the AMPA-R system, the $GABA_A$-R system, and metabolic modulation. The antagonism of the AMPA-R system by perampanel (and other potential modulators; like NBQX, decanoic acid (C10), and potentially β-hydroxybutyrate via kynurenic acid) represents an interesting approach in targeting excitatory input in mitochondrial epilepsy. Conversely, the potentiation of the inhibitory transmission via the $GABA_A$-R system is another distinct therapeutic approach presented in this Chapter. Barbiturate seems to be the most directly relevant antiepileptic drug with regards to this system; although benzodiazepine may be relevant if combined with a drug that can increase the tissue concentration of GABA. Direct agonism of $GABA_A$-R by increasing the tissue availability of GABA may be another approach in targeting the $GABA_A$-R system in terms of controlling the mitochondrial epileptic activity. Finally, metabolic modulation by the use of various substrates to alleviate metabolic demand in the epileptic tissue seems to have a positive effect on the epileptic network. In particular, the ketone bodies appear to be the most potent metabolic substrates; with various other compounds potentially working by modulating ketone bodies production (such as octanoic acid (C8) and bezafibrate). The modulation of glycolysis and the spare capacity of oxidative metabolism by supplementation of glucose and pyruvate may also be relevant; although feasibility needs to be investigated *in vivo* in allowing for the high concentrations required for a suppressive effect to be achieved in the brain.

These pharmacological studies provide the first evidence – based suggestions and recommendations in term of pharmacological therapy in mitochondrial epilepsy. Since it is conducted on a well-validated model and on a stable system, these further add to the predictive validity of the results presented here. However, the efficacy or the lack thereof from these pharmacological agents have only been investigated in the context of the interictal discharges. What this translates to in the clinical setting is yet to be known. Empirically, there are two types of epileptiform discharges that can be observed in this model; the interictal and the ictal discharges. Since the ictal discharges appear to follow no specific pattern, it is difficult to conduct pharmacological studies on these activities. However, the importance of this discharge should not be overlooked as theoretically, some of these pharmacological interventions (such as the sodium

channel blockers) may work on the ictal discharges but not the interictal discharges. Therefore, none of the drugs presented in this Chapter should be excluded from therapeutic regimen without further consideration or research. Additionally, all of the results presented in this Chapter come from investigation using an *in vitro* brain slice model. Some of the therapeutic interventions examined in this Chapter, particularly the metabolic modulators, are better suited to be investigated in an *in vivo* context. Modulation of metabolism by a substrate or compound (such as the components of the ketogenic diet) can easily occur systematically and produce different effects in the neurotransmission when the systemic metabolism is accounted for. Therefore, all the therapeutic leads that have been instigated from the results in this Chapter should be furthered into an *in vivo* setting using an animal model. However, such an *in vivo* animal model of mitochondrial epilepsy is yet to exist. This means, however, that when such an animal model is inevitably to be developed in the near future, these pharmacological studies should be revisited and re-evaluated. Until then, the results in this Chapter still provides the first real evidence – based pharmacological studies in mitochondrial epilepsy and thus, should not be taken lightly in the development of clinical guidelines and pharmacological regimens for the care of patients with mitochondrial epilepsy.

Chapter 5 Probing the state of metabolism during mitochondrial epilepsy

5.1 Introduction

Patients with mitochondrial disease normally present with varying degrees of oxidative phosphorylation defects, ranging from 0 to 100% of the normal activity, primarily due to heteroplasmy (Lightowlers *et al.*, 1997). However, mitochondrial disease with an epileptic phenotype typically presents with a more severe respiratory chain deficiencies, particularly in complex I and IV (Lax *et al.*, 2016). Epilepsy has been associated with cerebral hypometabolism (Abou-Khalil *et al.*, 1987; Henry *et al.*, 1993; Dubé *et al.*, 2001), therefore it is no surprise that a more severe metabolic deficiency would be associated with the development of epilepsy in mitochondrial disease.

In our model, I have replicated this severe metabolic deficiency through the co-application of two mitochondrial respiratory chain inhibitors; rotenone and potassium cyanide; in addition to the application of a Krebs cycle inhibitor, fluorocitrate. A severe inhibition of metabolism from the combination of these pharmacological agents would therefore be expected. To observe and quantify this state of metabolism, I performed incubation with ^{13}C-labelled substrates (such as ^{13}C-glucose) to probe various metabolic pathways during the state of seizure. Using state-of-the-art analytical chemistry techniques (as described in section 2.11 - 2.13), I was able to ascertain which metabolic pathways are implicated in the generation of mitochondrial epilepsy in this model.

A pathway of particular interest is the glutamate-glutamine cycle, which involves both the neuronal and astrocytic cellular compartments (Westergaard *et al.*, 1995; Hertz and Zielke, 2004; Bélanger *et al.*, 2011). The use of fluorocitrate in this model, which targets astrocytic aconitase specifically, would perturb astrocytic metabolism and the expectation would be that this results in the downstream inhibition of the glutamate-glutamine cycle. Through incubation with ^{13}C-glutamate and ^{13}C-glutamine, both of which were substrates of the cycle, I have probed and characterised the involvement of the glutamate-glutamine cycle in this model.

5.2 Methods

All the work presented in this chapter was conducted by myself in the laboratory of Professor Helle Waagepetersen at the University of Copenhagen. Animal preparation was as described in section 2.1 and 2.2.3. Once rodent brain slices were obtained, they were incubated as described in section 2.11. The conditions of the incubation is listed in Table 5-1. Condition 1 to 4 constitutes the probing of glucose metabolism with the various components of the mitochondrial epilepsy protocol present. Condition 5 to 6 assesses the glutamate-glutamine cycle during a state of seizure with a low concentration of ^{13}C-labelled glutamate. Condition 7 to 8 assesses the glutamate-glutamine cycle during the rescue of the seizure state with a suprathreshold concentration of glutamine as shown in section 4.3.6.3. Analysis was conducted as described in section 2.12 and 2.13.

Table 5-1 List of experimental conditions for metabolic mapping. PI 30 min refers to time point 30 minute of the pre-incubation and PI 60 min refers to time point 60 minute of the pre-incubation. Rot refers to rotenone and cyan refers to potassium cyanide.

Group	PI 30 min	PI 60 min	Experimental medium
1	0.9% NaCl	DMSO+ddH_2O	10mM [U-^{13}C]-glucose + 0.9% NaCl + DMSO + ddH_2O
2	0.1mM fluorocitrate	500nM rot + 10µM cyan	10mM [U-^{13}C]-glucose + 0.1mM fluorocitrate + 500nM rot + 10µM cyan
3	0.1mM fluorocitrate	DMSO+ddH_2O	10mM [U-^{13}C]-glucose + 0.1mM fluorocitrate + DMSO + ddH_2O
4	0.9% NaCl	500nM rot + 10µM cyan	10mM [U-^{13}C]-glucose + 0.9% NaCl + 500nM rot + 10µM cyan
5	0.9% NaCl	DMSO+ddH_2O	0.5mM [U-^{13}C]-glutamate + 0.9% NaCl + DMSO + ddH_2O
6	0.1mM fluorocitrate	500nM rot + 10µM cyan	0.5mM [U-^{13}C]-glutamate + 0.1mM fluorocitrate + 500nM rot + 10µM cyan
7	0.9% NaCl	DMSO+ddH_2O	2.5mM [U-^{13}C]-glutamine + 0.9% NaCl + DMSO + ddH_2O
8	0.1mM fluorocitrate	500nM rot + 10µM cyan	2.5mM [U-^{13}C]-glutamine + 0.1mM fluorocitrate + 500nM rot + 10µM cyan

5.3 Results

5.3.1 Glycolysis is significantly upregulated in epileptic tissue

To measure the glycolytic activity in the tissue, I have incubated the slices with 10mM [U-^{13}C]-glucose and traced the^{13}C-labelling in the two glycolytic substrates, lactate and alanine (see Figure 5-1).

There was no significant difference ($p>0.05$, $n=8$) between any of the group in the alanine M+1 labelling. However, there was a significant reduction ($p \leq 0.001$; $n=8$) in the alanine M+2 labelling in the group exposed to fluorocitrate only (7.12 ± 0.60 %), rotenone and cyanide only (8.04 ± 0.49 %), and to the combination of fluorocitrate, rotenone, and cyanide (8.19 ± 0.68 %) as compared against control (16.89 ± 1.26 %). There was also a significant difference ($p \leq 0.001$; $n=8$) in the alanine M+3 labelling in the group exposed to fluorocitrate only (66.21 ± 1.80 %), rotenone and cyanide only (68.06 ± 1.43 %), and to the combination (56.95 ± 3.47 %) as compared against control (44.61 ± 2.29 %). A significant difference ($p \leq 0.001$) was also observed between the fluorocitrate and the combination group as well as between the rotenone and cyanide only group and the combination group.

There was no significant difference ($p > 0.05$, $n=8$) between any of the group in the lactate M+1 and M+2 labelling. There was, however, a significant difference ($p \leq 0.001$; $n=8$) in the lactate M+3 labelling between the group exposed to fluorocitrate only (57.07 ± 2.61 %), rotenone and cyanide only (82.18 ± 2.62 %), and to the combination (74.23 ± 2.90 %) as compared against control (40.90 ± 4.22 %). Furthermore, there was also a significant difference ($p \leq 0.001$) between the fluorocitrate and the rotenone and cyanide group as well as the combination group; and also a significant difference ($p \leq 0.05$) between the rotenone and cyanide and the combination group.

This difference in glycolytic activity was also reflected in the amount of alanine. There was a significant increase ($p \leq 0.01$, $n=8$) in the amount of alanine in the fluorocitrate group (12.16 ± 7.11 nmol/mg protein) and in the rotenone and cyanide group ($p \leq 0.05$, 10.80 ± 2.84 nmol/mg protein) as compared against control (4.29 ± 1.16 nmol/mg protein).

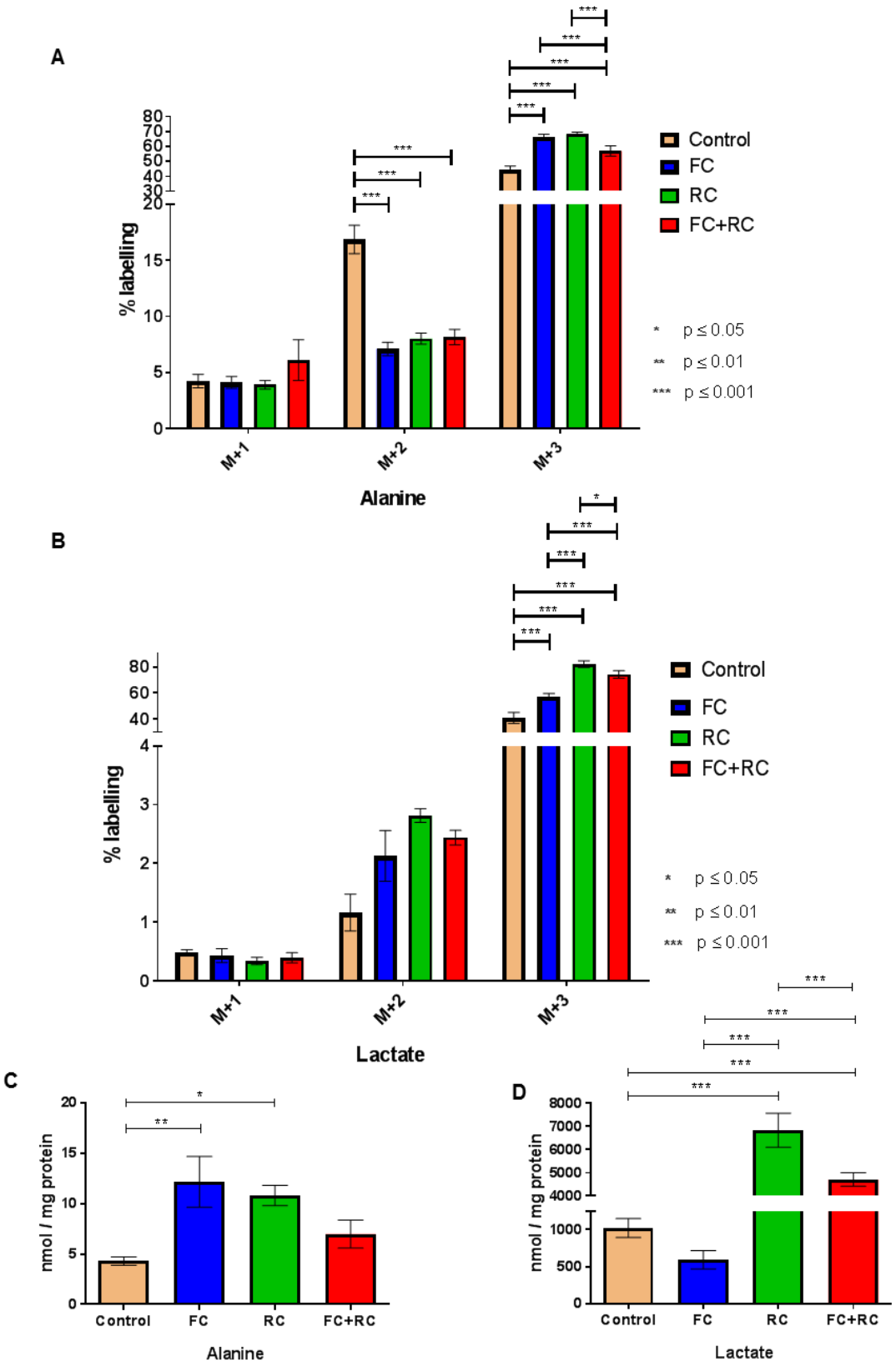

Figure 5-1 Glycolysis is significantly upregulated by the various components of the mitochondrial epilepsy protocol. A and B show the ^{13}C labelling for alanine and lactate respectively. C shows the amount of alanine and D shows the amount of lactate released to the media as measured by the colorimetric assay. Results are from condition 1, 2, 3, and 4. Condition 1 indicates control, 2 indicates FC+RC, 3 indicates FC, and 4 indicates RC.

As another indicator of glycolytic activity, the amount of lactate released from the tissue in the media was also quantified. There was a significant increase ($p \leq 0.001$) in the amount of lactate released in the group exposed to rotenone and cyanide only (6838.00 ± 734.50 nmol/mg protein, n=8) and to the combination (4710.00 ± 285.7 nmol/mg protein, n=24) as compared against control (1020.00 ± 127.90 nmol/mg protein, n=16) and the group exposed to fluorocitrate only (4710.00 ± 285.70 nmol/mg protein, n=8). Interestingly, the lactate release was also significantly lower ($p \leq 0.001$) in the group exposed to the combination as compared against to rotenone and cyanide only.

5.3.2 Krebs cycle activity is significantly downregulated in epileptic tissue

In order to gain additional insights of the metabolic state associated with this model, I measured the activity of the Krebs cycle in the tissue following the incubation with 10mM [U-^{13}C]-glucose (see Figure 5-2). Specifically, this can be measured by the incorporation of the ^{13}C labelling in the Krebs cycle intermediates: citrate, alpha-ketoglutarate, succinate, fumarate, and malate.

There was a significant reduction ($p \leq 0.001$; n=8) in the citrate M+1 labelling in the group exposed to fluorocitrate only (1.16 ± 0.07 %), rotenone and cyanide only (1.01 ± 0.33 %), and to the combination (0.52 ± 0.19 %) as compared against control (4.49 ± 0.37 %). The citrate M+2 labelling was significantly increased ($p \leq 0.01$; n=8) in the group exposed to fluorocitrate (24.08 ± 0.45) and to rotenone and cyanide only (24.26 ± 1.34) as compared against the control group (21.40 ± 0.48). This increase was also significant ($p \leq 0.001$) against the group exposed to the combination (19.59 ± 1.47). The labelling pattern for citrate M+3 and M+4 is similar in that there is a statistically significant difference ($p \leq 0.001$; n=8) between all the group, except for when comparing the group exposed to rotenone and cyanide only and the group exposed to the combination. In the case of citrate M+3 labelling, there was a significant reduction in the group exposed to fluorocitrate only (4.66 ± 0.44 %), rotenone and cyanide only (1.37 ± 0.52 %), and to the combination (1.05 ± 0.29 %) as compared against control (9.76 ± 0.45 %). Similarly, with the M+4 labelling, there was a significant reduction in the group exposed to fluorocitrate only (9.80 ± 0.55 %), rotenone and cyanide only (4.38 ± 0.30 %), and to the combination (2.74 ± 0.40 %) as compared against control (16.01 ± 0.54 %). There was a significant difference ($p \leq 0.001$; n=8)

between all the group in the citrate M+5 labelling. The labelling was reduced in the group exposed to fluorocitrate only (10.67 ± 0.63 %), rotenone and cyanide only (4.91 ± 0.60 %), and to the combination (2.16 ± 0.18 %) as compared against control (13.81 ± 0.43 %). For M+6 labelling, there was a significant reduction ($p \leq 0.001$; n=8) in labelling in the group exposed to rotenone and cyanide only (0.69 ± 0.21 %) and to the combination (0.36 ± 0.09 %) as compared against control (8.76 ± 0.47 %) and to the fluorocitrate (7.31 ± 0.35 %).

No significant difference ($p > 0.05$, n=8) was observed between any of the groups in the alpha-ketoglutarate M+1 and M+3 labelling. For M+2 labelling, there was a significant reduction ($p \leq 0.001$; n=8) in the group exposed to fluorocitrate only (6.90 ± 1.81 %), rotenone and cyanide only (2.09 ± 0.43 %), and to the combination (3.01 ± 1.05 %) as compared against control (22.85 ± 1.31 %). Additionally, there was also a statistically significant difference ($p < 0.05$) between the group exposed to fluorocitrate only and to rotenone and cyanide only. Considering the M+4 labelling, there was a statistically significant reduction ($p \leq 0.01$; n=8) in the group exposed to fluorocitrate (6.09 ± 0.88 %) and also ($p \leq 0.001$; n=8) in the group exposed to rotenone and cyanide only (2.63 ± 0.75 %) as well as the group exposed to the combination (3.50 ± 0.94 %) as compared against control (11.83 ± 0.86 %). Regarding the M+5 labelling, there was a statistically significant reduction ($p \leq 0.001$; n=8) in the group exposed to rotenone and cyanide only (2.02 ± 0.27 %) and to the combination (2.07 ± 0.60 %) as compared against the control group (8.60 ± 0.65 %).

There was a significant reduction ($p \leq 0.001$; n=8) in the succinate M+1 labelling in the group exposed to fluorocitrate only (0.32 ± 0.07 %), rotenone and cyanide only (0.16 ± 0.06 %), and to the combination (0.11 ± 0.06 %) as compared against control (2.28 ± 0.33 %). Similarly, there was a significant reduction ($p \leq 0.001$; n=8) in the succinate M+2 labelling in the group exposed to fluorocitrate only (1.89 ± 0.39 %), rotenone and cyanide only (0.33 ± 0.07 %), and to the combination (0.50 ± 0.13 %) as compared against control (7.90 ± 0.56 %). In addition, there was a significant difference between the group exposed to fluorocitrate only against the group exposed to rotenone and cyanide only and against the group exposed to the combination. The labelling pattern for succinate M+3 and M+4 is similar in that there is a statistically significant difference ($p \leq 0.001$; n=8) between all of the group, except for when comparing the group exposed to rotenone and cyanide only and the group exposed to the combination. Regarding the M+3 labelling, there was a significant reduction in the group exposed to

fluorocitrate only (1.81 ± 0.39 %), rotenone and cyanide only (0.14 ± 0.03 %), and to the combination (0.11 ± 0.02 %) as compared against control (5.14 ± 0.34 %). Similarly, with the M+4 labelling, there was a significant reduction in the group exposed to fluorocitrate only (1.98 ± 0.47 %), rotenone and cyanide only (0.24 ± 0.11 %), and to the combination (0.18 ± 0.07 %) as compared against control (6.46 ± 0.35 %).

When examining the fumarate M+1 labelling, there was no significant difference ($p > 0.05$, n=8) between any of the groups. With M+2, however, there was a significant reduction ($p \leq 0.001$; n=8) in the labelling in the group exposed to fluorocitrate only (3.59 ± 0.48 %), rotenone and cyanide only (2.46 ± 0.32 %), and to the combination (1.98 ± 0.32 %) as compared against control (7.23 ± 0.67 %). Additionally, there was a significant difference ($p \leq 0.01$) between the group exposed to fluorocitrate only and the group exposed to the combination. Considering the M+3 labelling, there was a significant reduction ($p \leq 0.001$; n=8) in the group exposed to fluorocitrate only (3.76 ± 0.60 %), rotenone and cyanide only (4.04 ± 0.62 %), and to the combination (3.11 ± 0.43 %) as compared against control (6.58 ± 0.58 %). With the M+4 labelling, there was a significant difference ($p \leq 0.05$; n=8) between the group exposed to fluorocitrate only (3.12 ± 0.57 %) and the control group (4.89 ± 0.59 %). There was also a significant reduction ($p \leq 0.001$) in the group exposed to rotenone and cyanide only (0.37 ± 0.06 %) and the group exposed to the combination (0.40 ± 0.11 %) as compared against the group exposed to fluorocitrate only and the control group.

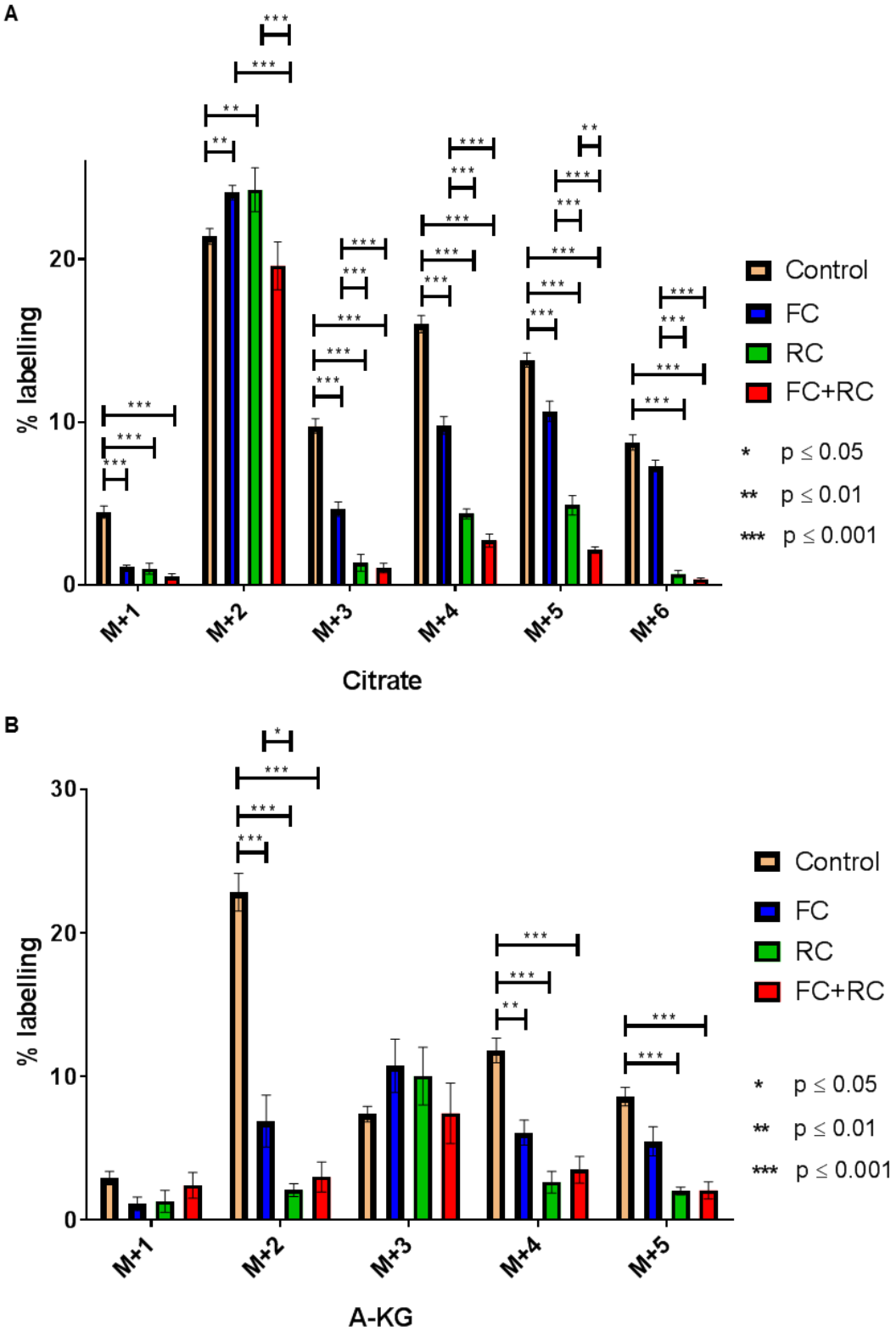
A
% labelling
0
10
20
M+1
M+2
M+3
M+4
M+5
M+6
Citrate
Control
FC
RC
FC+RC
* p ≤ 0.05
** p ≤ 0.01
*** p ≤ 0.001
B
% labelling
0
10
20
30
M+1
M+2
M+3
M+4
M+5
A-KG
Control
FC
RC
FC+RC
* p ≤ 0.05
** p ≤ 0.01
*** p ≤ 0.001

C

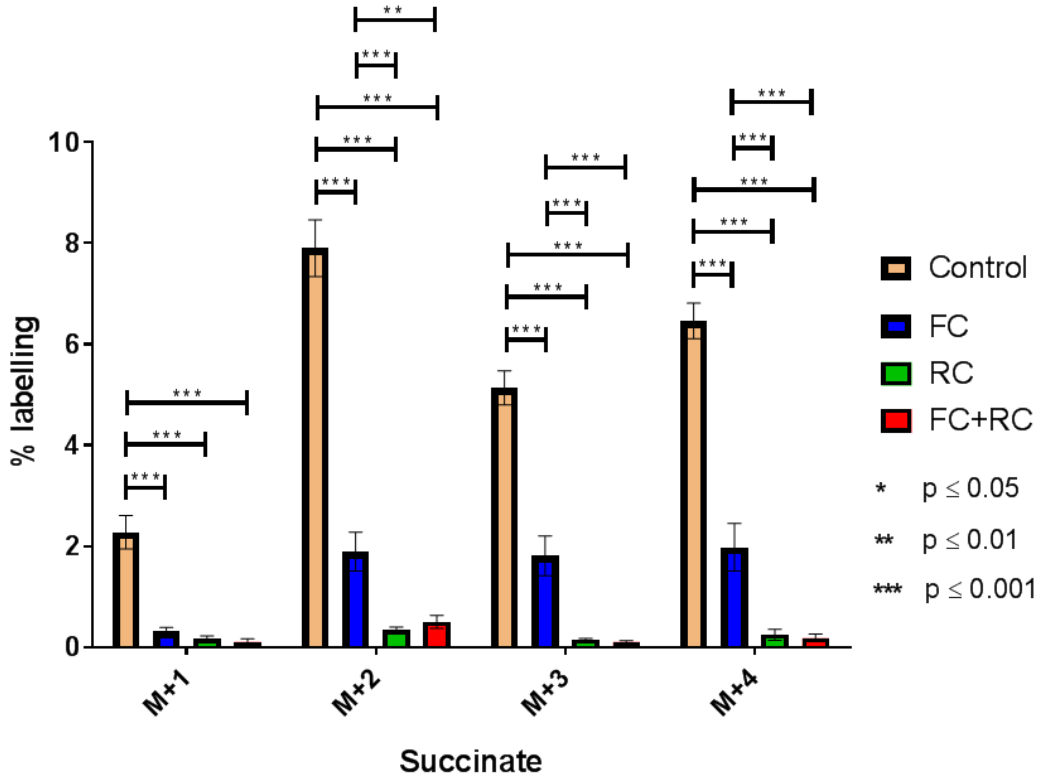
% labelling
10
8
6
4
2
0
M+1
M+2
M+3
M+4
Succinate
Control
FC
RC
FC+RC
* p ≤ 0.05
** p ≤ 0.01
*** p ≤ 0.001

D

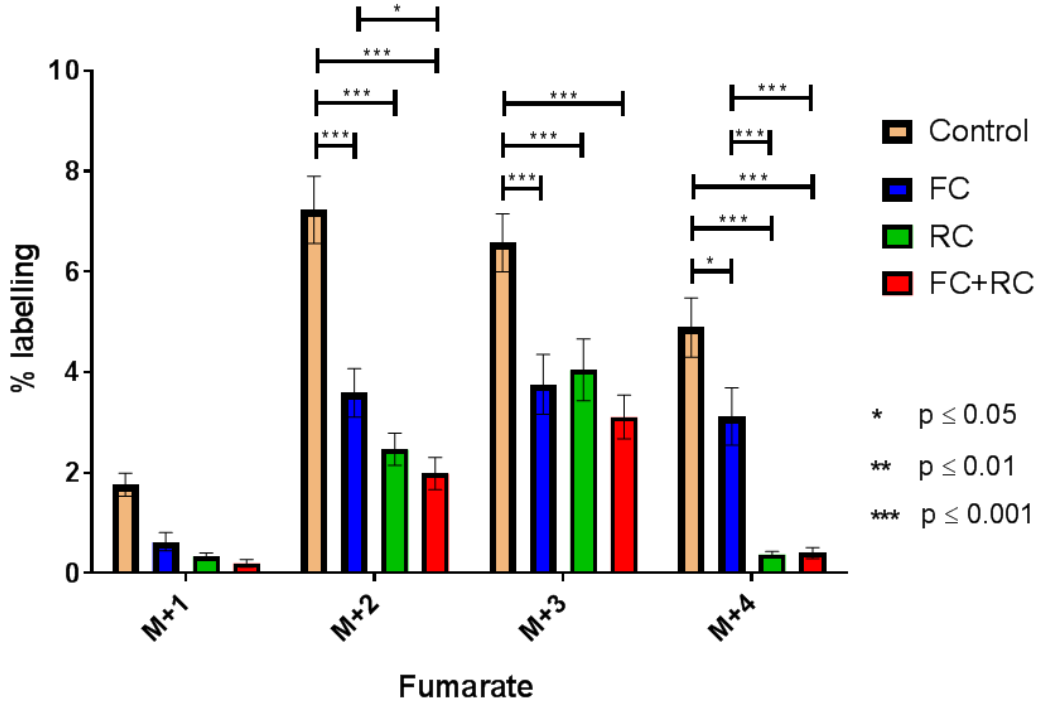
% labelling
10
8
6
4
2
0
M+1
M+2
M+3
M+4
Fumarate
Control
FC
RC
FC+RC
* p ≤ 0.05
** p ≤ 0.01
*** p ≤ 0.001

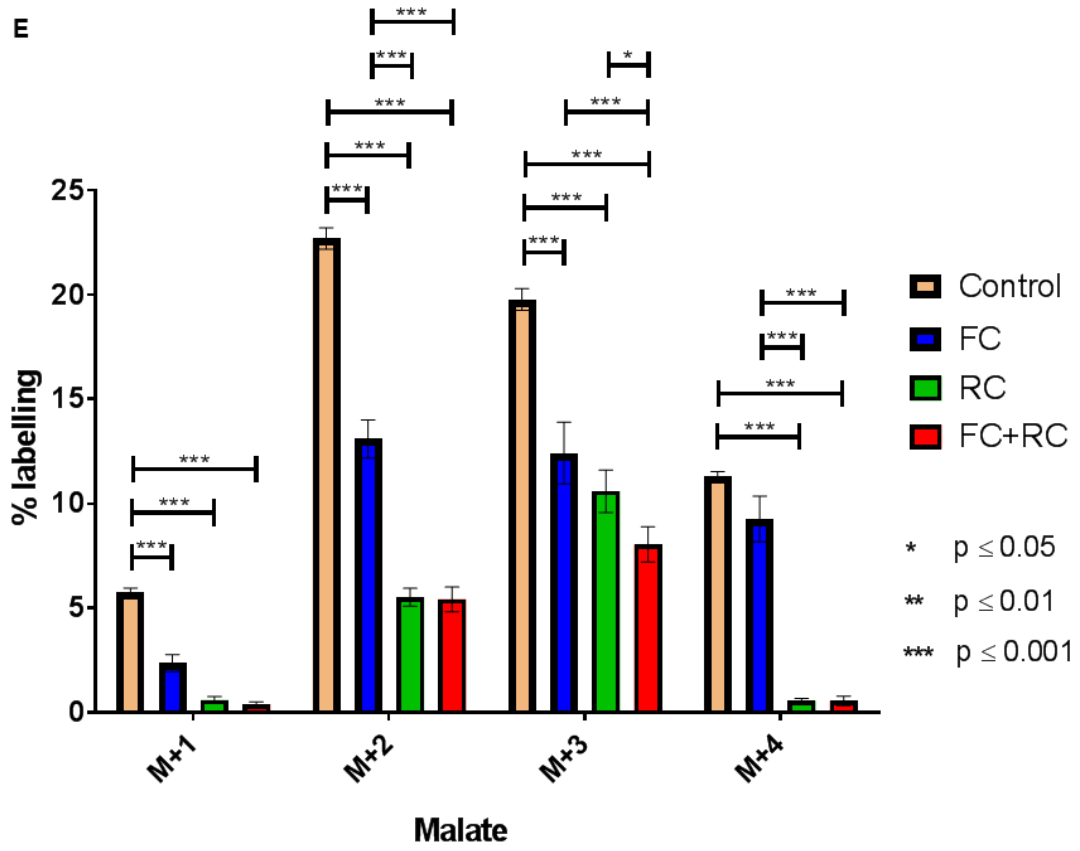

Figure 5-2 Krebs cycle activity is significantly decreased by the various components of the mitochondrial epilepsy protocol. A-E shows the ^{13}C labelling for citrate, alpha-ketoglutarate, succinate, fumarate, and malate respectively. Results are from condition 1, 2, 3, and 4. Condition 1 indicates control, 2 indicates FC+RC, 3 indicates FC, and 4 indicates RC.

There was a significant reduction ($p \leq 0.001$; n=8) in the malate M+1 labelling in the group exposed to fluorocitrate only (2.36 ± 0.41 %), rotenone and cyanide only (0.60 ± 0.16 %), and to the combination (0.39 ± 0.12 %) as compared against control (5.75 ± 0.20 %). The labelling pattern for malate M+2 showed a statistically significant difference ($p \leq 0.001$; n=8) between all the group, except for when comparing the group exposed to fluorocitrate only and the control group. There was a significant reduction in the M+2 labelling in the group exposed to fluorocitrate only (13.09 ± 0.92 %), rotenone and cyanide only (5.52 ± 0.43 %), and to the combination (5.42 ± 0.59 %) as compared against control (22.68 ± 0.51 %). In M+3, again, there was a significant reduction ($p \leq 0.001$; n=8) in labelling in the group exposed to fluorocitrate only (12.42 ± 1.48 %), rotenone and cyanide only (10.58 ± 1.01 %), and to the combination (8.04 ± 0.85 %) as compared against control (19.76 ± 0.52 %). Additionally, there was a significant difference ($p \leq 0.001$) between the group exposed to fluorocitrate alone and the group exposed to rotenone and cyanide alone ($p \leq 0.05$), as compared against the group exposed to the combination. With M+4, there was a significant reduction ($p \leq$

0.001; n=8) in labelling in the group exposed to rotenone and cyanide only (0.57 ± 0.11 %) and to the combination (0.56 ± 0.23 %) as compared against control (11.29 ± 0.24 %) and to the fluorocitrate (9.26 ± 1.09 %).

5.3.3 Aspartate labelling pattern indicates metabolic compartmentalization

Aspartate is primarily synthesized and stored in the neurons and regulated by cycling in its second compartment in the oligodendrocytes (Baslow, 2003). To evaluate metabolic compartmentalization, I evaluated the incorporation of 13-C into the amino acid aspartate following incubation with 10 mM [U-^{13}C]-glucose (see Figure 5-3).

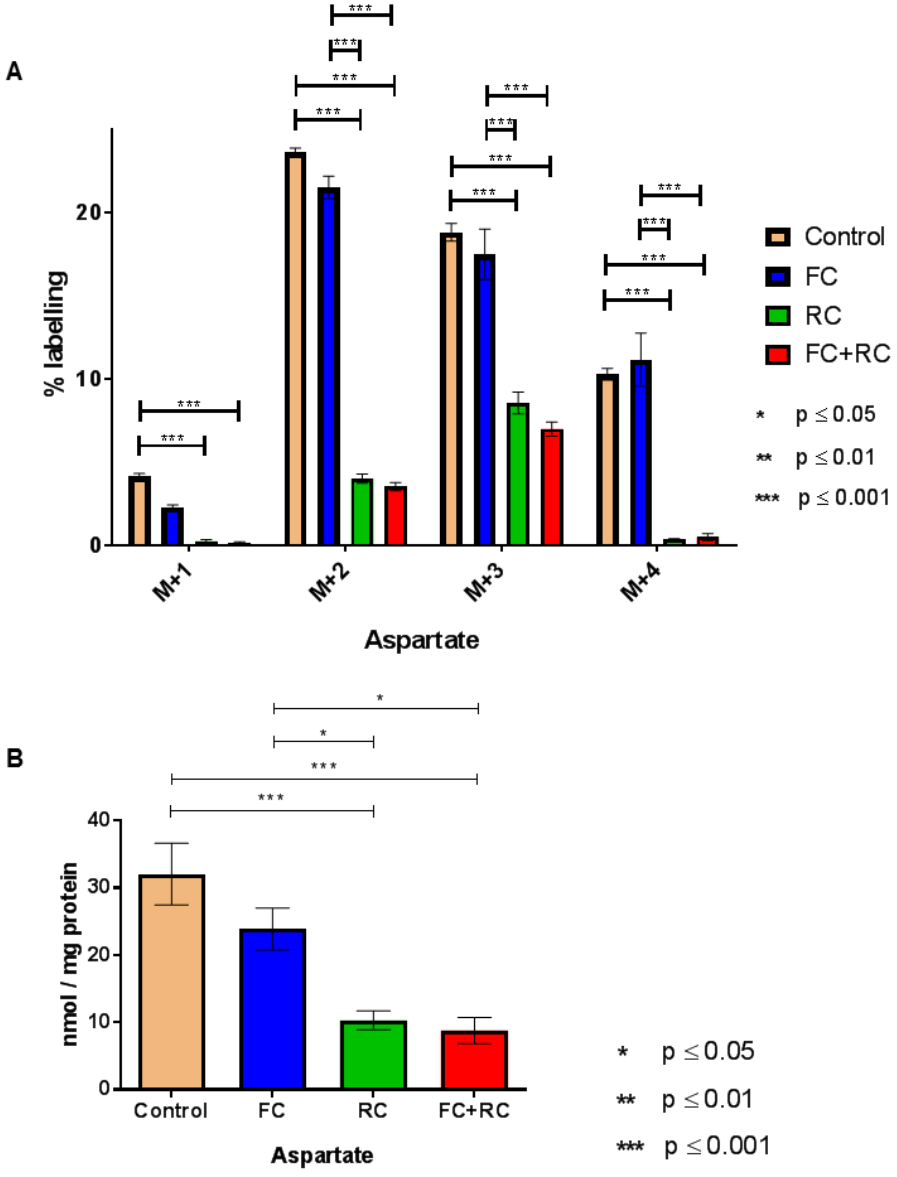

Figure 5-3 Aspartate labelling is significantly modified by the rotenone and cyanide component of the mitochondrial epilepsy protocol. A shows the ^{13}C labelling for aspartate and B shows the amount of tissue aspartate. Results are from condition 1, 2, 3, and 4. Condition 1 indicates control, 2 indicates FC+RC, 3 indicates FC, and 4 indicates RC.

There was a significant reduction ($p \leq 0.001$; n=8) in the aspartate M+1 labelling in the group exposed to rotenone and cyanide only (0.27 ± 0.11 %) and to the combination (0.17 ± 0.06 %) as compared against control (4.15 ± 0.19 %). The labelling pattern for aspartate M+2, M+3, and M+4 was similar in that there was a statistically significant difference ($p \leq 0.001$; n=8) in the group exposed to rotenone and cyanide only and to the combination as compared against the group exposed to fluorocitrate only and to the control group. There was a significant reduction in M+2 labelling in the group exposed to rotenone and cyanide only (4.04 ± 0.29 %) and to the combination (3.56 ± 0.25 %) as compared against control (23.65 ± 0.26 %) and to the fluorocitrate (21.56 ± 0.67 %). Similarly, with M+3, there was a significant reduction in labelling in the group exposed to rotenone and cyanide only (8.59 ± 0.65 %) and to the combination (7.01 ± 0.43 %) as compared against control (18.85 ± 0.53 %) and to the fluorocitrate (17.52 ± 1.52 %). Again, with M+4, there was a significant reduction in labelling in the group exposed to rotenone and cyanide only (0.37 ± 0.05 %) and to the combination (0.52 ± 0.22 %) as compared against control (10.31 ± 0.35 %) and to the fluorocitrate (11.19 ± 1.59 %).

There was also a statistically significant reduction ($p \leq 0.001$; n=8) in the tissue amount of asparate in the group exposed to rotenone and cyanide only (10.31 ± 1.40 nmol/mg protein) and the group exposed to the combination (8.79 ± 1.93 nmol/mg protein) as compared against the control group (32.07 ± 4.58 nmol/mg protein). To a lesser degree, there was also a statistically significant reduction ($p \leq 0.05$) in the group exposed to rotenone and cyanide only as well as the group exposed to the combination as compared against the group exposed to fluorocitrate only (23.89 ± 3.13 nmol/mg protein).

5.3.4 Glucose input into the glutamate – glutamine cycle is significantly altered in the mitochondrial epilepsy condition

Glucose is the primary source of the carbon atom for glutamate, whereas the nitrogen is primarily sourced from the branched chain amino acid (Daikhin and Yudkoff, 2000). Considering the significant alteration in glucose metabolism as described previously in section 5.3.1 to 5.3.3, I considered it worthwhile to assess the relative contribution of glucose into the glutamate – glutamine cycle following incubation with 10 mM [U-^{13}C]-glucose (see Figure 5-4).

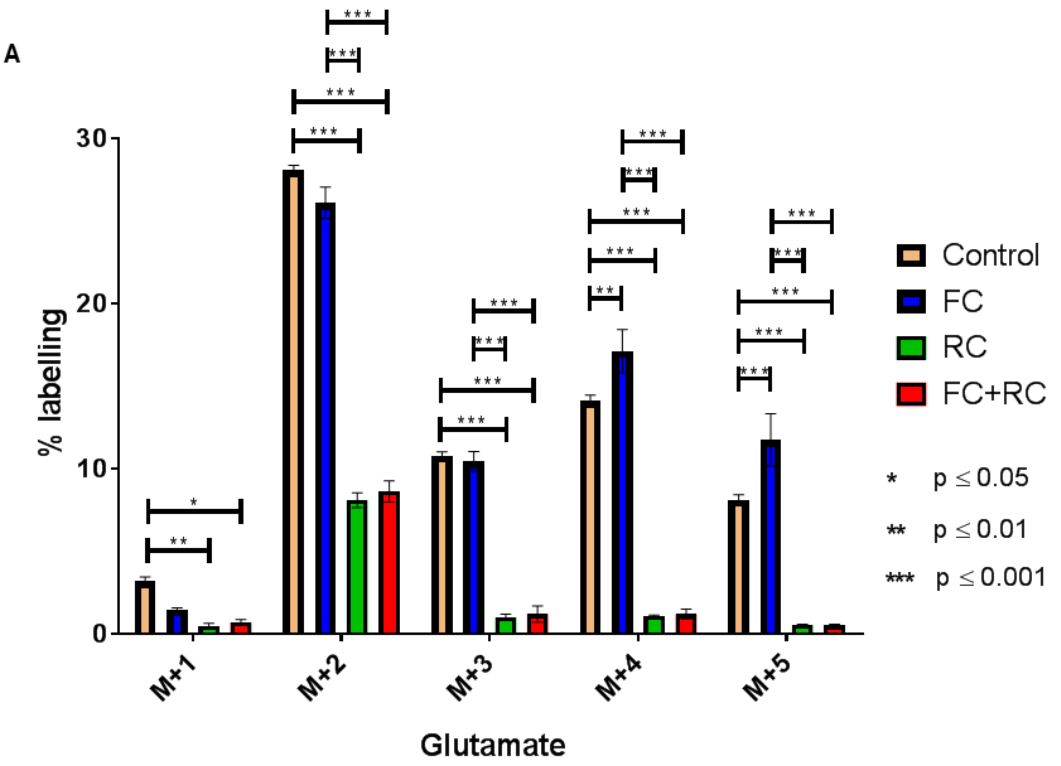
A
% labelling
30
20
10
0
M+1
M+2
M+3
M+4
M+5
Glutamate
Control
FC
RC
FC+RC
* p ≤ 0.05
** p ≤ 0.01
*** p ≤ 0.001

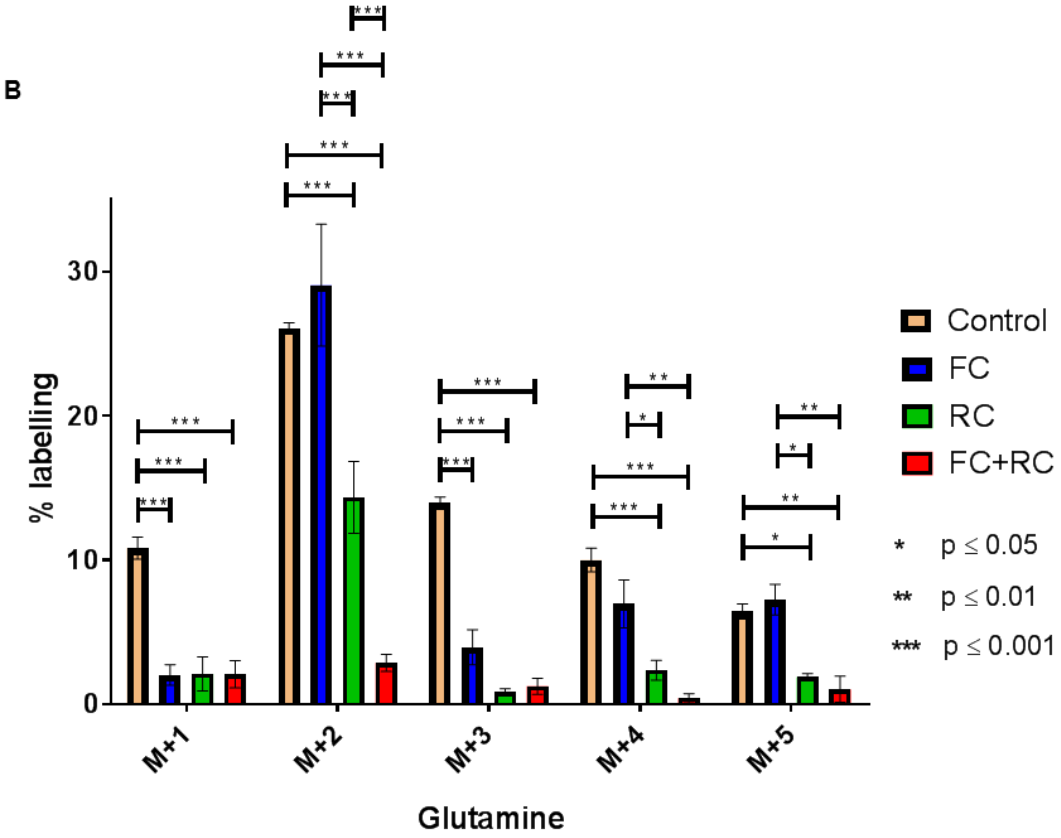
B
% labelling
30
20
10
0
M+1
M+2
M+3
M+4
M+5
Glutamine
Control
FC
RC
FC+RC
* p ≤ 0.05
** p ≤ 0.01
*** p ≤ 0.001

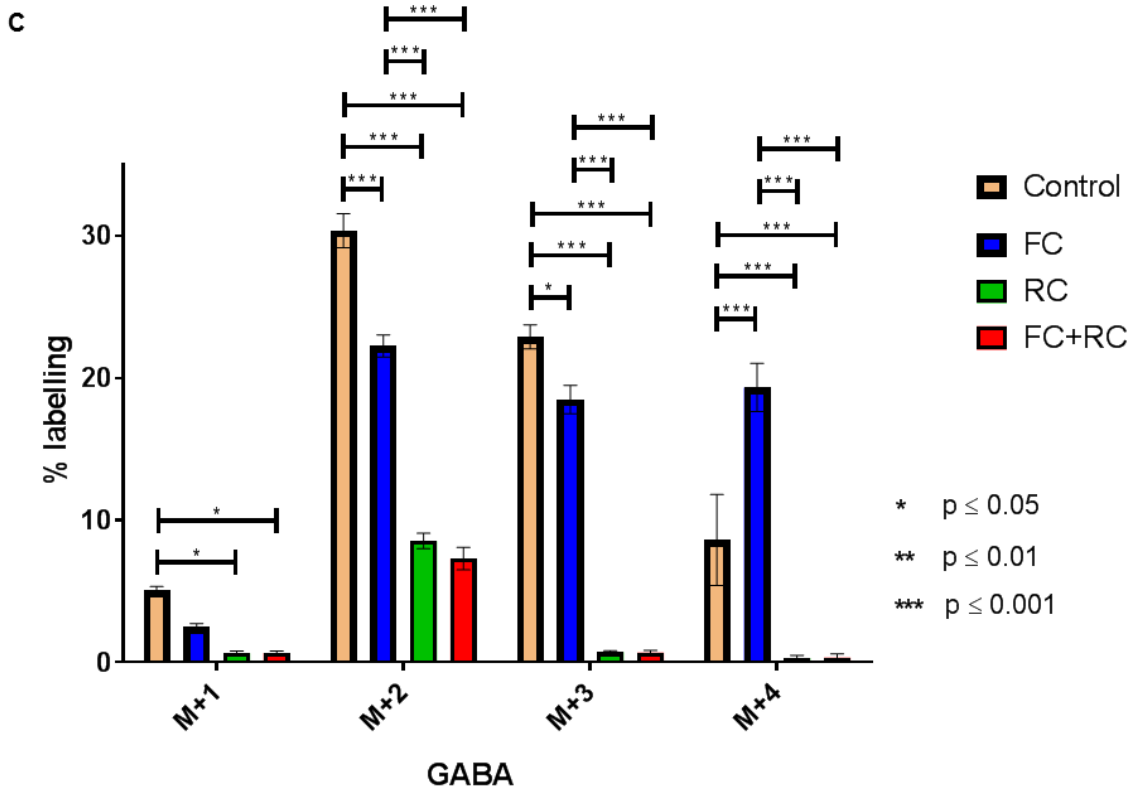

Figure 5-4 The glutamate-glutamine cycle is significantly affected by the mitochondrial epilepsy protocol. A-C shows the ^{13}C labelling for glutamate, glutamine, and GABA respectively. Results are from conditions 1, 2, 3, and 4. Condition 1 indicates control, 2 indicates FC+RC, 3 indicates FC, and 4 indicates RC.

There was a significant reduction ($p \leq 0.01$; n=8) in the glutamate M+1 labelling in the group exposed to rotenone and cyanide only (0.47 ± 0.17 %) and to a lesser degree ($p \leq 0.05$) the combination (0.70 ± 0.17 %) as compared against control (3.19 ± 0.27 %). The labelling pattern for glutamate M+2 and M+3 was similar in that there was a statistically significant difference ($p \leq 0.001$; n=8) in the group exposed to rotenone and cyanide only and to the combination as compared against the group exposed to fluorocitrate only and to the control group. With M+2, there was a significant reduction in labelling in the group exposed to rotenone and cyanide only (8.10 ± 0.45 %) and to the combination (8.63 ± 0.64 %) as compared against control (28.09 ± 0.29 %) and to the fluorocitrate (26.10 ± 0.96 %). Similarly, with M+3, there was a significant reduction in labelling in the group exposed to rotenone and cyanide only (1.01 ± 0.19 %) and to the combination (1.21 ± 0.49 %) as compared against control (10.80 ± 0.24 %) and to the fluorocitrate (10.45 ± 0.60 %). There was a slightly higher M+4 labelling ($p \leq 0.01$; n=8) in the group exposed to fluorocitrate only (17.12 ± 1.31 %) as compared against control (14.13 ± 0.34 %). Conversely, there was a reduction in labelling in the

group exposed to rotenone and cyanide only (1.07 ± 0.07 %) and the combination group (1.21 ± 0.30 %) as compared against the control and fluorocitrate group. Similarly, with M+5, there was a significantly higher labelling ($p \leq 0.001$; n=8) in the group exposed to fluorocitrate only (11.76 ± 1.59 %) as compared against control (8.13 ± 0.31 %). Additionally, there was a reduction in labelling in the group exposed to rotenone and cyanide only (0.55 ± 0.03 %) and the combination group (0.52 ± 0.06 %) as compared against the control and fluorocitrate group.

With regards to glutamine M+1 labelling, there was a significant reduction ($p \leq 0.001$; n=8) in the group exposed to fluorocitrate alone (2.03 ± 0.71 %), rotenone and cyanide only (2.10 ± 1.18 %) and the combination (2.08 ± 0.94 %) as compared against control (10.83 ± 0.76 %). There was a significant difference ($p \leq 0.001$; n=8) between all the group in the glutamine M+2 labelling, except for the difference between the group exposed to rotenone and cyanide only and to the combination which was not statistically significant. The M+2 labelling was reduced the most in the group exposed to the combination (2.86 ± 0.59 %) as compared against the group exposed to the rotenone and cyanide only (14.34 ± 2.50 %), to fluorocitrate only (29.07 ± 4.22 %), and the control group (26.08 ± 0.38 %). With M+3, there was a significant reduction ($p \leq 0.001$; n=8) in the labelling in the group exposed to fluorocitrate alone (3.95 ± 1.22 %), rotenone and cyanide only (0.84 ± 0.23 %) and the combination (1.24 ± 0.55 %) as compared against control (13.99 ± 0.39 %). Regarding the M+4 labelling, there was a significant reduction ($p \leq 0.001$; n=8) in the group exposed to rotenone and cyanide only (2.36 ± 0.69 %) and to the combination (0.41 ± 0.31 %) as compared against control (10.00 ± 0.82 %) and to the fluorocitrate (26.10 ± 0.96 %). There was also a significant difference ($p \leq 0.05$) between the rotenone and cyanide group as well as the combination group ($p \leq 0.01$) when compared against control. With M+5, there was a significant reduction ($p \leq 0.05$; n=8) in the group exposed to rotenone and cyanide only (1.88 ± 0.23 %) and also ($p \leq 0.01$) in the group exposed to the combination (1.04 ± 0.90 %) as compared against the control group (6.43 ± 0.52 %) and the group exposed to fluorocitrate (7.26 ± 1.06 %).

Taking into account the glutamate and the glutamine labelling, there was similarly a significant reduction ($p \leq 0.05$; n=8) in the GABA M+1 labelling in the group exposed to rotenone and cyanide alone (0.66 ± 0.15 %) and to the combination (0.67 ± 0.13 %) as compared against control (5.08 ± 0.27 %). Regarding M+2 and M+4 labelling, there is a similar pattern of labelling in that there is a significant difference ($p \leq 0.001$; n=8)

between all the groups, except between the group exposed to rotenone and cyanide alone and the group exposed to the combination. In GABA M+2, there was a significant reduction in the group exposed to fluorocitrate alone (22.24 ± 0.78 %) as compared against the control group (30.34 ± 1.21 %). Moreover, there was a significant reduction in the group exposed to rotenone and cyanide only (8.53 ± 0.54 %) and to the combination (7.30 ± 0.80 %) as compared against the control group and the group exposed to fluorocitrate alone. In contrast, with GABA M+4, there was a significant increase in the group exposed to fluorocitrate alone (19.32 ± 1.70 %) as compared against the control group (8.61 ± 3.19 %). However, similar to M+2, there was a significant reduction in the group exposed to rotenone and cyanide only (0.30 ± 0.19 %) and to the combination (0.33 ± 0.26 %) as compared against the control group and the group exposed to fluorocitrate alone. Finally, with GABA M+3, there was a significant reduction ($p \leq 0.05$; n=8) in the group exposed to fluorocitrate alone (18.47 ± 0.99 %) as compared against the control group (22.88 ± 0.85 %). In addition, there was a significant reduction ($p \leq 0.001$; n=8) in the group exposed to rotenone and cyanide alone (0.74 ± 0.08 %) and to the combination (0.68 ± 0.17 %) as compared against the control group and the group exposed to fluorocitrate alone.

5.3.5 The amount of glutamine is significantly reduced in the epileptic tissue, despite the sustained amounts of glutamate and increased amount of GABA

Despite the replacement of the unlabelled glucose with [U-^{13}C]-glucose, conditions 1 to 4 still represents the scenario observed in the mitochondrial epileptic protocol in which there is equimolar amounts of glucose without any additional external substrates. Therefore, conditions 1 to 4 can be used to assess the level of the substrates of the glutamate-glutamine cycle (see Figure 5-5) in the typical mitochondrial epilepsy model conditions.

There was no significant difference ($p \geq 0.05$; n= 8) across all the groups with regards to the amount of tissue glutamate.

Interestingly, there was a significant reduction ($p \leq 0.05$; n=13) in the group exposed to the combination (0.09 ± 0.06 nmol/mg protein) as compared against the group exposed to fluorocitrate alone (3.34 ± 1.64 nmol/mg protein) and the control group (2.64 ± 0.50 nmol/mg protein).

With regards to the amount of GABA, there was a significant increase ($p \leq 0.001$; n=8) in the group exposed to rotenone and cyanide alone (33.44 ± 2.83 nmol/mg protein) and also ($p \leq 0.05$) in the group exposed to the combination (28.03 ± 2.45 nmol/mg protein) as compared against the control group (16.4 ± 1.23 nmol/mg protein). Additionally, there was also a statistically significant increase ($p \leq 0.001$) in the group exposed to rotenone and cyanide alone as compared against the group exposed to fluorocitrate alone (19.03 ± 2.60 nmol/mg protein).

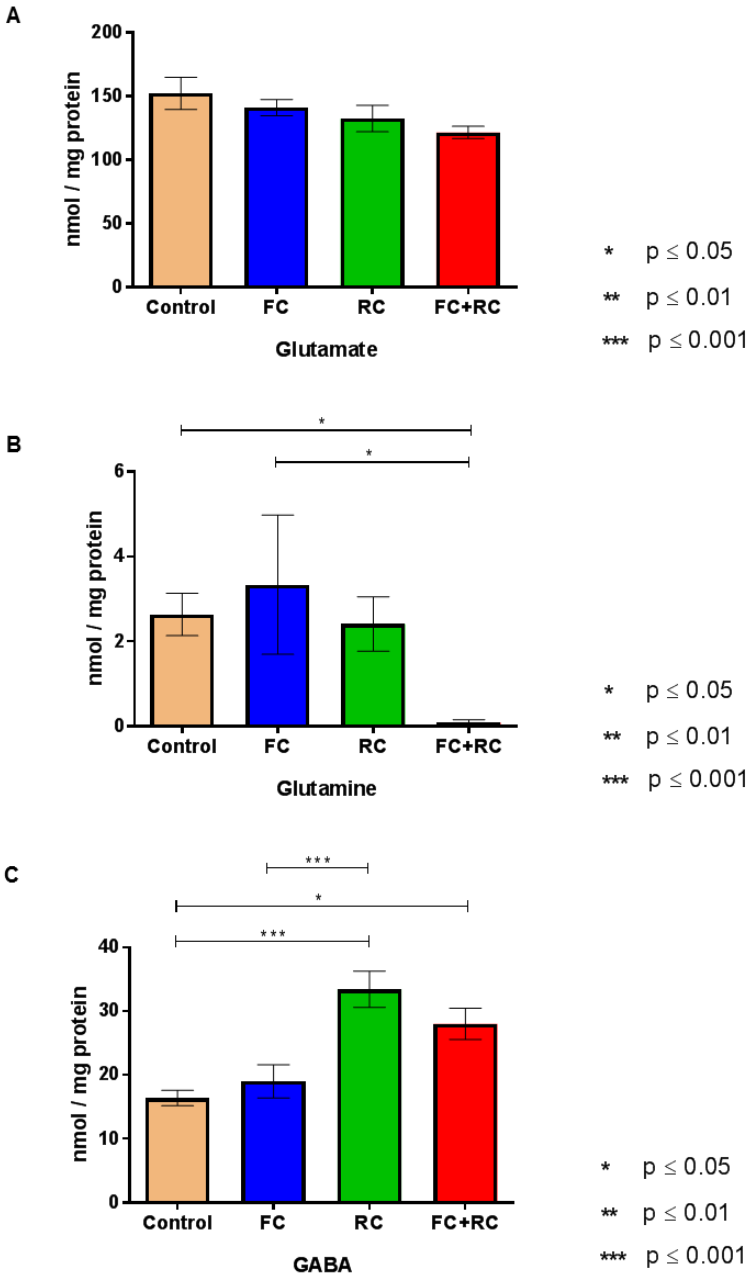

Figure 5-5 The amounts of the substrates of the glutamate-glutamine cycle are significantly altered in the mitochondrial epileptic condition. Shown in A to C are amounts of tissue glutamate, glutamine, and GABA respectively following the various conditions of the mitochondrial epilepsy protocol. Results are from conditions 1, 2, 3, and 4. Condition 1 indicates control, 2 indicates FC+RC, 3 indicates FC, and 4 indicates RC.

5.3.6 The activity of the glutamate-glutamine cycle via the Krebs cycle is significantly reduced

As described in section 4.3.6.3, the bath application of L-glutamate (0.5mM) did not cause any significant change in the electrophysiological recordings of the mitochondrial epileptic activity. Therefore, by adding 0.5mM [U-^{13}C]-glutamate, I can probe the activity of the glutamate-glutamine cycle without interfering with the seizure state. The assessment of the incorporation of the ^{13}C into the substrates of the cycle; glutamate, glutamine, and GABA; would give an indication of the activity of the glutamate – glutamine cycle (see Figure 5-6).

There was no significant difference ($p \geq 0.05$; n= 8) between the control and the epileptic group with regards to glutamate M+1 labelling. There was, however, a significant reduction ($p \leq 0.001$; n=8) in the epileptic group compared against the control group, with regards to the M+2 (0.01 ± 0.01 % epileptic vs 1.79 ± 0.06 % control), M+3 (0.98 ± 0.12 % epileptic vs 7.61 ± 0.27 % control), and M+4 (2.50 ± 0.06 % epileptic vs 1.33 ± 0.13 % control). In contrast, there was a significant increase ($p \leq 0.001$; n=8) in the M+5 labelling in the epileptic group (63.20 ± 1.07 %) as compared against the control group (39.14 ± 3.60 %).

Taking into account the glutamine M+1 labelling, there was a significant reduction ($p \leq 0.01$; n=8) in the epileptic group (2.43 ± 0.55 %) as compared against the control group (4.84 ± 0.26 %). There was a significant reduction ($p \leq 0.001$; n=8) in the epileptic group as compared against the control group, with regards to the M+2 (0.13 ± 0.06 % epileptic vs 3.19 ± 0.17 % control) and M+3 (0.93 ± 0.12 % epileptic vs 11.79 ± 0.81 % control) labelling. Conversely, there was a statistically significant increase ($p \leq 0.05$; n=8) in the glutamine M+4 labelling in the epileptic group (1.30 ± 0.20 %) when compared against the control group (0.69 ± 0.09 %). Moreover, there was a significant increase ($p \leq 0.01$; n=8) in the glutamine M+5 labelling in the epileptic group (41.89 ± 1.51 %) when compared against the control group (30.11 ± 3.30 %).

There was a significant reduction ($p \leq 0.001$; n=8) in the epileptic group as compared against the control group, with regards to the GABA M+1 (0.43 ± 0.09 % epileptic vs 5.01 ± 0.41 % control) and M+2 (0.94 ± 0.15 % epileptic vs 7.36 ± 0.63 % control) labelling. In contrast, there was no statistically significant difference ($p \geq 0.05$; n= 8) between the epileptic group and the control group, with regards to the GABA M+3 and M+4 labelling.

A

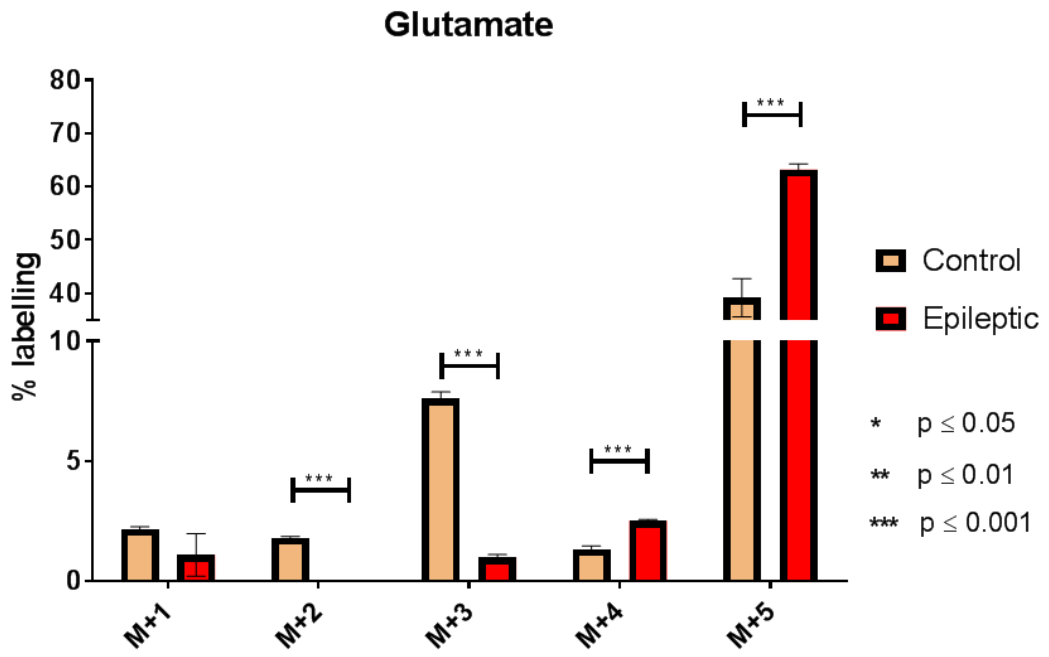
Glutamate
% labelling
80
70
60
50
40
10
5
0
M+1
M+2
M+3
M+4
M+5
***
Control
Epileptic
* p ≤ 0.05
** p ≤ 0.01
*** p ≤ 0.001

B

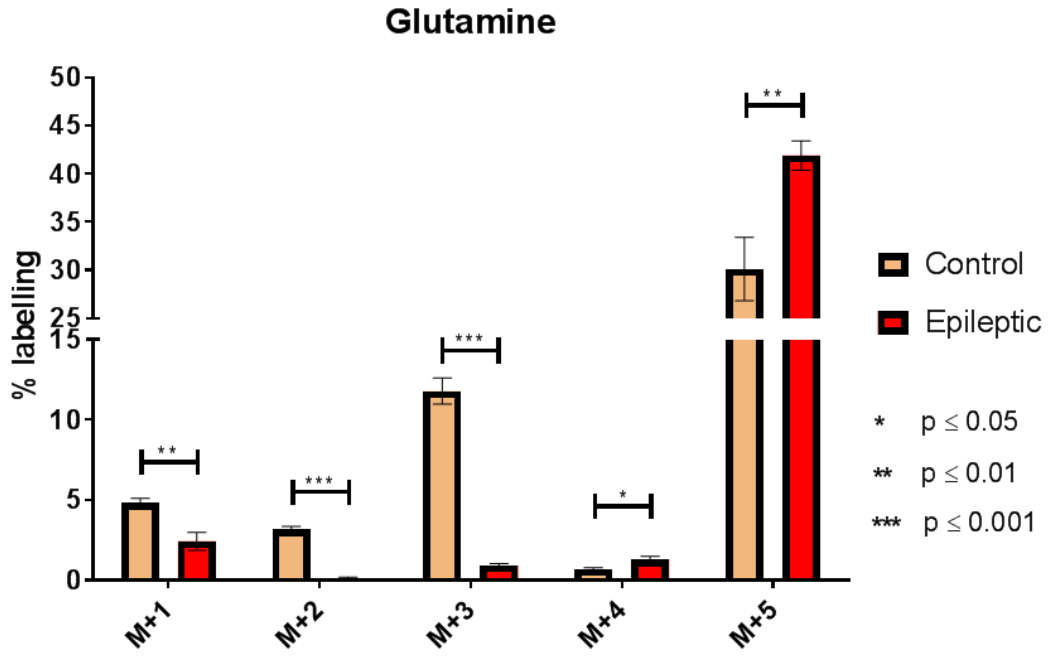
Glutamine
% labelling
50
45
40
35
30
25
15
10
5
0
M+1
M+2
M+3
M+4
M+5
**
***
*
Control
Epileptic
* p ≤ 0.05
** p ≤ 0.01
*** p ≤ 0.001

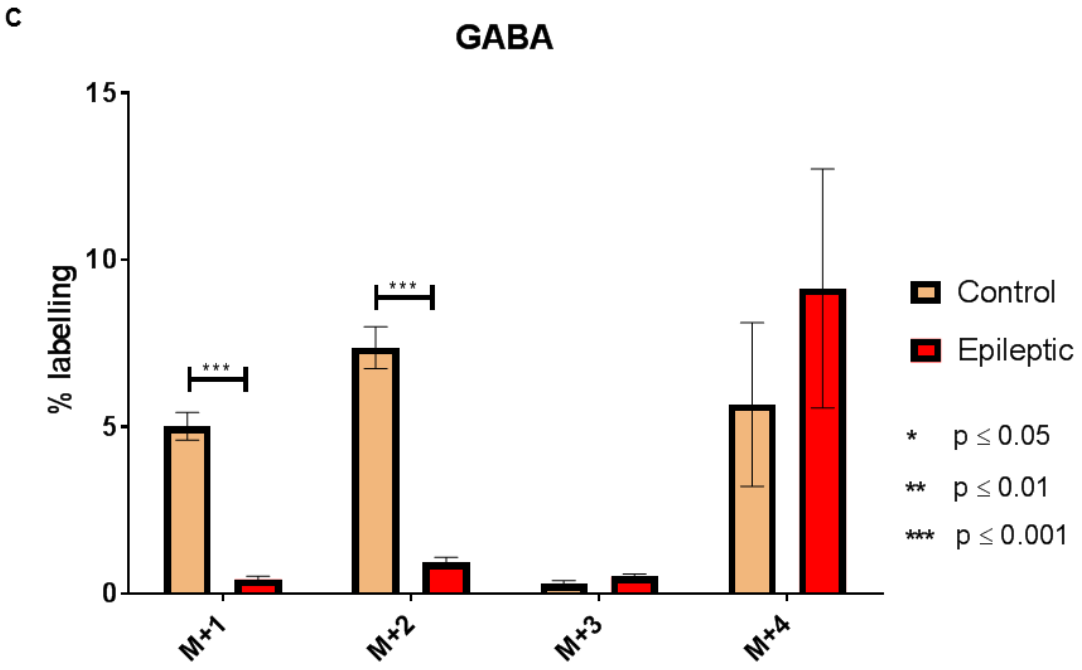

Figure 5-6 The immediate activity of the glutamate-glutamine cycle is sustained but recycling via the Krebs cycle is significantly reduced. Shown in A to C are the ^{13}C labelling for glutamate, glutamine, and GABA respectively. Results are from conditions 5 and 6. Condition 5 indicates control and 6 indicates epileptic.

With regards to the amounts of the substrates of the glutamate-glutamine cycle, the addition of 0.5mM [U-^{13}C]-glutamate did not seem to alter the metabolic profile of the glutamate – glutamine cycle in the epileptic tissue (as described in section 5.3.5). There was still no significant difference ($p \geq 0.05$; n= 8) between the control and the epileptic tissue in the amount of glutamate. The amount of glutamine was still significantly reduced ($p \leq 0.001$; n=8) in the epileptic tissue (0.00 ± 0.00 nmol/mg protein - non detectable) as compared against the control tissue (18.05 ± 3.08 nmol/mg protein). Tissue amount of GABA was still significantly elevated ($p \leq 0.001$; n=8) in the epileptic tissue (38.42 ± 1.85 nmol/mg protein) when compared against the control tissue (21.15 ± 1.82 nmol/mg protein).

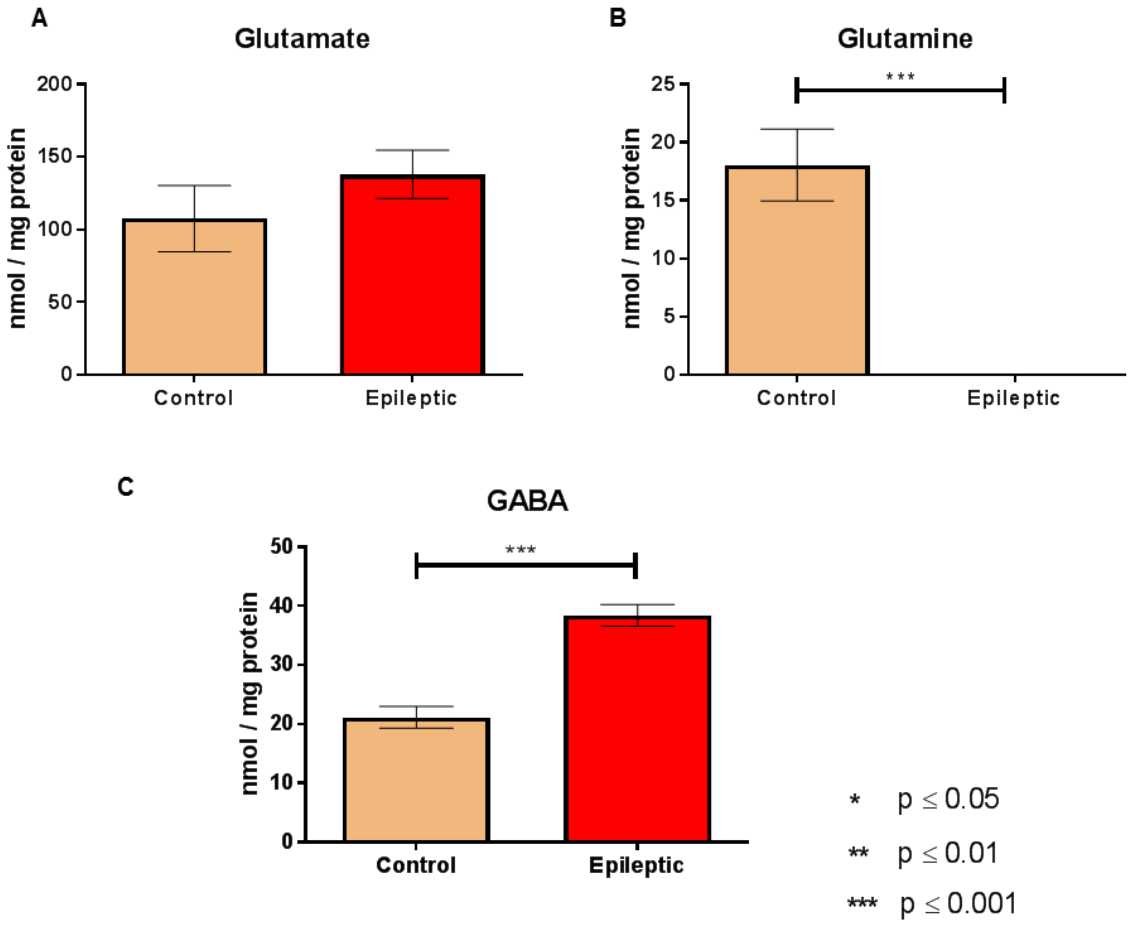

Figure 5-7 The addition of glutamate did not alter the metabolic profile of the epileptic tissue. Shown in A to C are amounts of glutamate, glutamine, and GABA respectively in the control and epileptic tissue following addition of 0.5mM [U-^{13}C]-glutamate. Results are from condition 5 and 6. Condition 5 indicates control and 6 indicates epileptic.

5.3.7 Glutamate can still enter the Krebs cycle despite inhibition of subsequent turns of the Krebs cycle

Glutamate enters the Krebs cycle via its intermediate, α-ketoglutarate (Hertz, 2013). Considering the severe impairment of the Krebs cycle brought about by the model (as described in section 5.3.2), it is important to investigate if the entry of glutamate into the Krebs cycle is affected as well. Therefore, I measured the incorporation of the ^{13}C labelling into the Krebs cycle's intermediates following incubation with 0.5mM [U-^{13}C]-glutamate (see Figure 5-8).

A

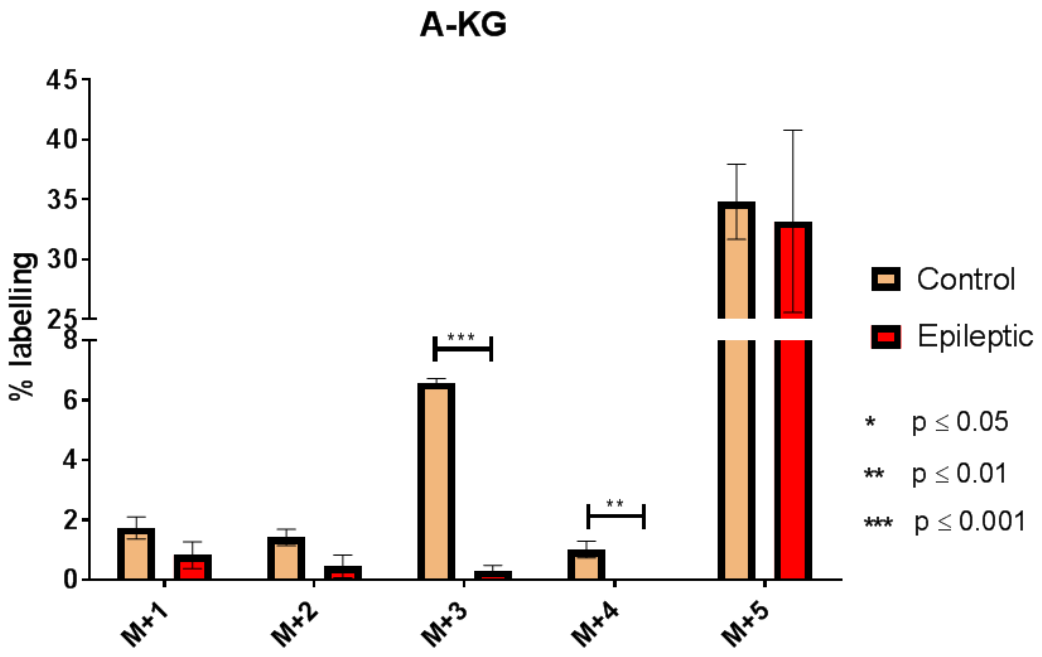
A-KG
% labelling
45
40
35
30
25
8
6
4
2
0
***
**
M+1
M+2
M+3
M+4
M+5
Control
Epileptic
* p ≤ 0.05
** p ≤ 0.01
*** p ≤ 0.001

B

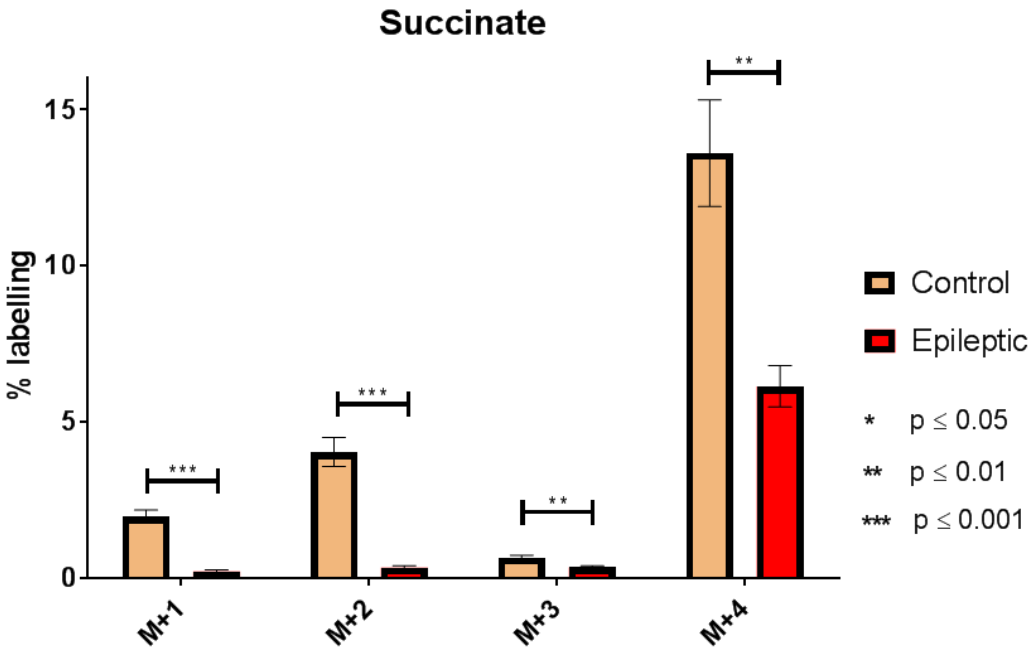
Succinate
% labelling
15
10
5
0
***
***
**
**
M+1
M+2
M+3
M+4
Control
Epileptic
* p ≤ 0.05
** p ≤ 0.01
*** p ≤ 0.001

C

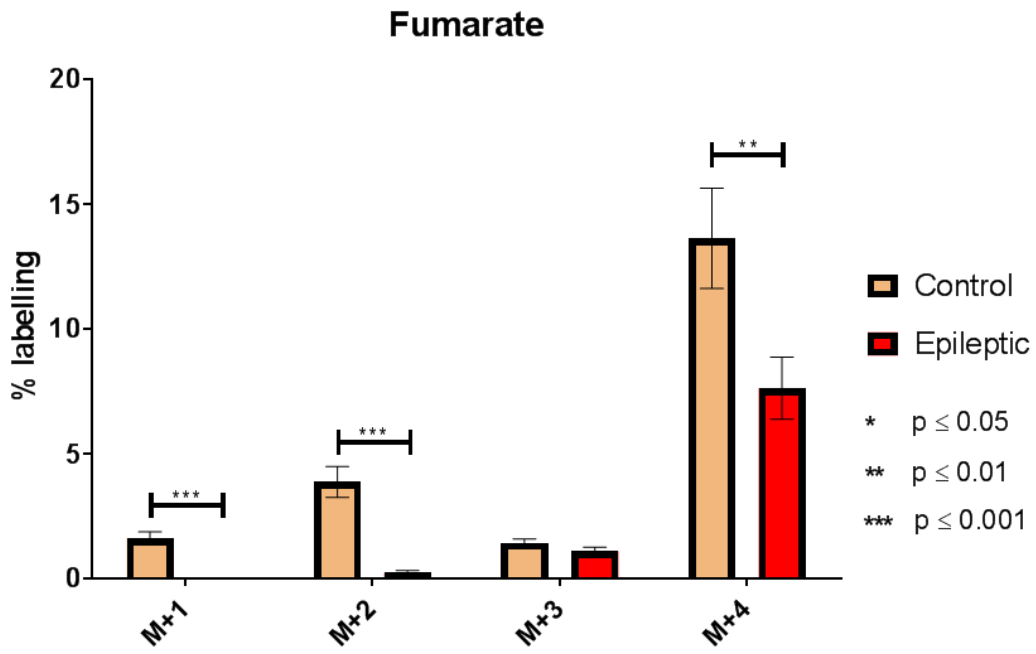
Fumarate
20
15
10
5
0
% labelling
***
***
**
M+1
M+2
M+3
M+4
Control
Epileptic
* p ≤ 0.05
** p ≤ 0.01
*** p ≤ 0.001

D

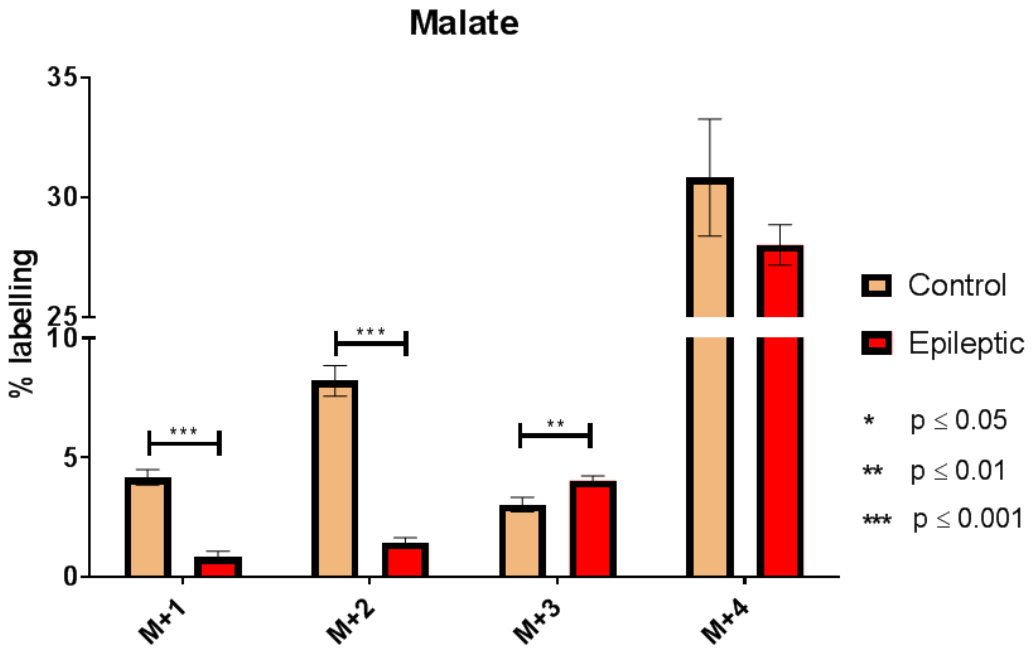
Malate
35
30
25
10
5
0
% labelling
***
***
**
M+1
M+2
M+3
M+4
Control
Epileptic
* p ≤ 0.05
** p ≤ 0.01
*** p ≤ 0.001

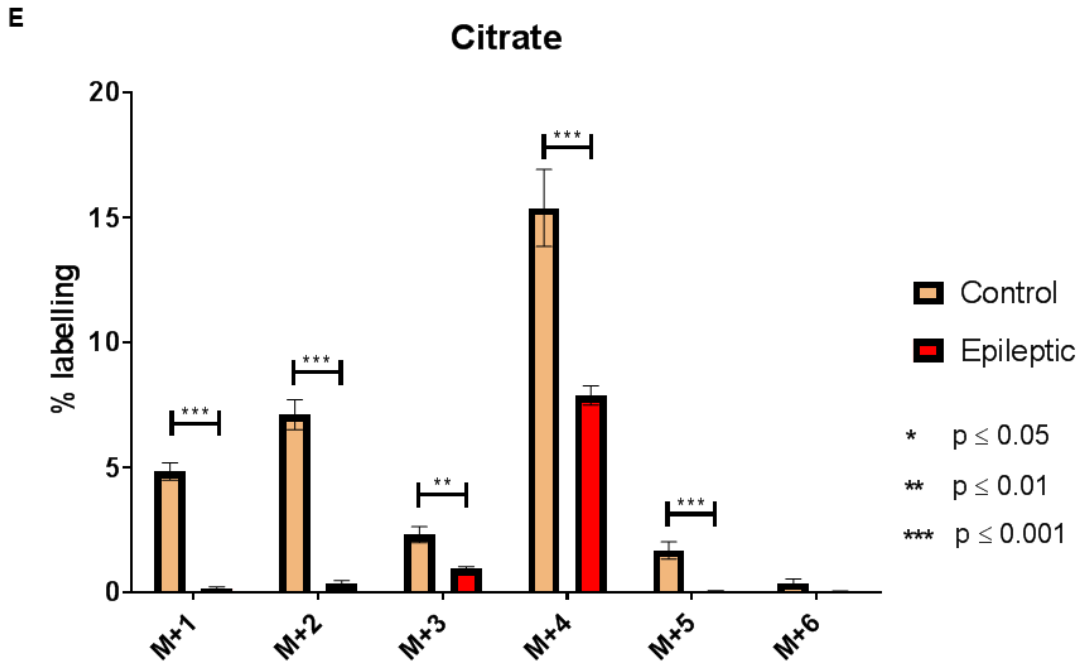

Figure 5-8 Glutamate's entry into the Krebs cycle is not affected but subsequent turns of Krebs cycle are inhibited by the mitochondrial epilepsy protocol. A-E shows the ^{13}C labelling for alpha-ketoglutarate, succinate, fumarate, malate, and citrate respectively. Results are from condition 5 and 6. Condition 5 indicates control and 6 indicates epileptic.

There was no significant difference ($p \geq 0.05$; n= 8) between the control and the epileptic group with regards to the alpha-ketoglutarate M+1, M+2, and M+5 labelling. There was a significant reduction ($p \leq 0.001$; n=8) in the epileptic group compared against the control group, with regards to the M+3 labelling (0.30 ± 0.19 % epileptic vs 6.58 ± 0.14 % control). There was also a significant reduction ($p \leq 0.01$; n=8) in the alpha-ketoglutarate M+4 labelling in the epileptic group (0.00 ± 0.00 % - non detectable) as compared against the control group (1.01 ± 0.28 %).

There was a significant reduction ($p \leq 0.001$; n=8) in the epileptic group compared against the control group, with regards to the succinate M+1 labelling (0.21 ± 0.05 % epileptic vs 1.98 ± 0.21% control) and the succinate M+2 labelling (0.34 ± 0.07 % epileptic vs 4.04 ± 0.47 % control). In addition, there was a significant reduction ($p \leq 0.01$; n=8) in the succinate M+3 labelling (0.35 ± 0.05 % epileptic vs 0.66 ± 0.08 % control) and M+4 labelling (6.14 ± 0.66 % epileptic vs 13.60 ± 1.71 % control).

With regards to fumarate, there was a significant reduction ($p \leq 0.001$; n=8) in the epileptic group compared against the control group, with regards to the M+1 labelling (0.00 ± 0.00 % - non detectable, epileptic vs 1.63 ± 0.26% control) and the M+2 labelling (0.24 ± 0.09 % epileptic vs 3.88 ± 0.62 % control). This was also seen in the fumarate M+4 labelling where there was a significant reduction ($p \leq 0.01$; n=8) of labelling in the epileptic tissue (7.64 ± 1.24 % epileptic vs 13.64 ± 2.01 % control). In contrast, there was no significant difference ($p \geq 0.05$; n= 8) between the control and the epileptic group with regards to the fumarate M+3 labelling.

In the epileptic group, there was a significant reduction ($p \leq 0.001$; n=8) in malate M+1 labelling when compared against the control group (0.84 ± 0.26 % epileptic vs 4.18 ± 0.32% control) and the malate M+2 labelling (1.44 ± 0.21 % epileptic vs 8.21 ± 0.63 % control). Interestingly, there was a significant increase ($p \leq 0.01$; n=8) in the malate M+3 labelling in the epileptic group (4.04 ± 0.20 %) when compared against the control group (3.04 ± 0.31 %). There was, however, no significant difference ($p \geq 0.05$; n= 8) between the control and the epileptic group with regards to the malate M+4 labelling.

Finally, a significant reduction ($p \leq 0.001$; n=8) was observed in the epileptic group as compared against the control group, with regards to the citrate M+1 labelling (0.16 ± 0.07 % epileptic vs 4.84 ± 0.35 % control), M+2 labelling (0.36 ± 0.11 % epileptic vs 7.11 ± 0.60 % control), M+4 labelling (7.89 ± 0.38 % epileptic vs 15.39 ± 1.54 % control), and M+5 labelling (0.05 ± 0.03 % epileptic vs 1.69 ± 0.35 % control). This was also observed in the citrate M+3 labelling as a significant reduction ($p \leq 0.01$; n=8), of labelling in the epileptic tissue (0.95 ± 0.09 % epileptic vs 2.31 ± 0.32 % control). Finally, there was no significant difference ($p \geq 0.05$; n= 8) between the control and the epileptic group with regards to the citrate M+6 labelling.

5.3.8 Aspartate formation is still reduced despite the addition of glutamate

In astrocytes, the formation of glutamate in the glutamate – glutamine cycle from the Krebs cycle intermediate, α-ketoglutarate, is coupled to the formation of oxaloacetate from aspartate (Bak *et al.*, 2006; Hertz, 2013). Therefore, it is important to consider the aspartate compartment when evaluating the effect of glutamate labelling (see Figure 5-9).

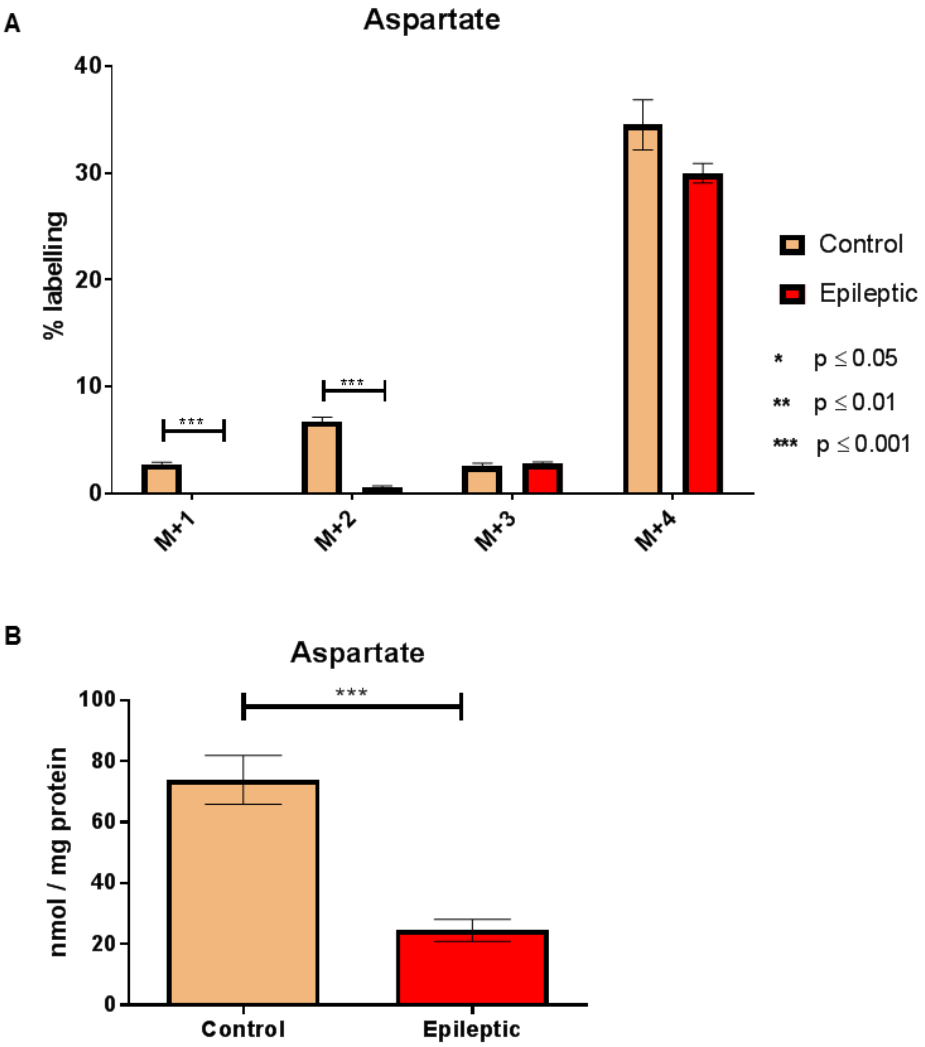

Figure 5-9 Aspartate labelling and amount is significantly reduced in the epileptic tissue, even with the addition of glutamate. Shown in A is the ^{13}C labelling for aspartate following incubation with 0.5mM [U-^{13}C]-glutamate and concurrently in B is the amount of aspartate in the same condition. Results are from condition 5 and 6. Condition 5 indicates control and 6 indicates epileptic.

There was a significant reduction ($p \leq 0.001$; n=8) in the epileptic group as compared against the control group, with regards to the aspartate M+1 labelling (0.00 ± 0.00 % - non detectable, epileptic vs 2.75 ± 0.15 % control) and the aspartate M+2 labelling (0.59 ± 0.12 % epileptic vs 6.76 ± 0.37 % control). Interestingly, there was no significant difference ($p \geq 0.05$; n= 8) between the control and the epileptic group with regards to either the aspartate M+3 or M+4 labelling.

This reduction in labelling was also accompanied by a significant reduction ($p \leq 0.001$; n=8) in the amount of aspartate in the epileptic group (24.52 ± 3.59 nmol/mg protein) when compared against the control group (73.89 ± 8.03 nmol/mg protein).

5.3.9 Unlike glutamate, the addition of glutamine was able to sustain GABA synthesis within the glutamate – glutamine cycle

Glutamine is a key player in the glutamate – glutamine cycle. It is the precursor amino acid to both glutamate and GABA. It also presents an alternate approach to the trafficking of neurotransmitters as it is a non-neuroactive compound, therefore allowing it to be released to the extracellular fluid safely without risk of neuronal depolarization (unlike glutamate) (Daikhin and Yudkoff, 2000). I have applied glutamine to the epileptic slices and found that the application of 2.5mM L-glutamine was able to suppress the epileptic activity significantly (as described in section 4.3.6.3). Given all this, I have applied the 'rescue' concentration of 2.5mM [U-^{13}C]-glutamine to trace the metabolic pathway that they underwent. By examining the incorporation of the ^{13}C atoms in the substrates of the cycle; glutamate, glutamine, and GABA; I would have an indication of the activity of the glutamate – glutamine cycle following the 'rescue' of the phenotype (see Figure 5-10).

There was a significant reduction ($p \leq 0.001$; n=10) in the epileptic group as compared against the control group, with regards to the glutamate M+1 labelling (0.33 ± 0.13 % epileptic vs 2.79 ± 0.25 % control), glutamate M+2 labelling (0.19 ± 0.08 % epileptic vs 2.24 ± 0.15 % control), and glutamate M+3 labelling (1.52 ± 0.30 % epileptic vs 8.97 ± 0.23 % control). Conversely, there was a statistically significant increase ($p \leq 0.001$; n=10) with regards to the glutamate M+4 labelling (3.65 ± 0.10 % epileptic vs 2.58 ± 0.13 % control) and the glutamate M+5 labelling (64.69 ± 1.58 % epileptic vs 49.24 ± 1.40 % control).

The labelling pattern in glutamine follows that of glutamate in these conditions. There was a significant reduction ($p \leq 0.001$; n=10) in the epileptic group compared against the control group, with regards to the M+1 labelling (0.11 ± 0.03 % epileptic vs 1.09 ± 0.06 % control), M+2 labelling (0.29 ± 0.08 % epileptic vs 1.01 ± 0.10 % control), and M+3 labelling (0.37 ± 0.01 % epileptic vs 4.33 ± 0.15 % control). In contrast, there was a significant increase ($p \leq 0.01$; n=10) in the M+4 labelling (4.16 ± 0.04 % epileptic vs 3.81 ± 0.12 % control) and also a significant increase ($p \leq 0.001$; n=10) in the M+5 labelling (93.09 ± 0.27 % epileptic vs 82.17 ± 1.11 % control).

A

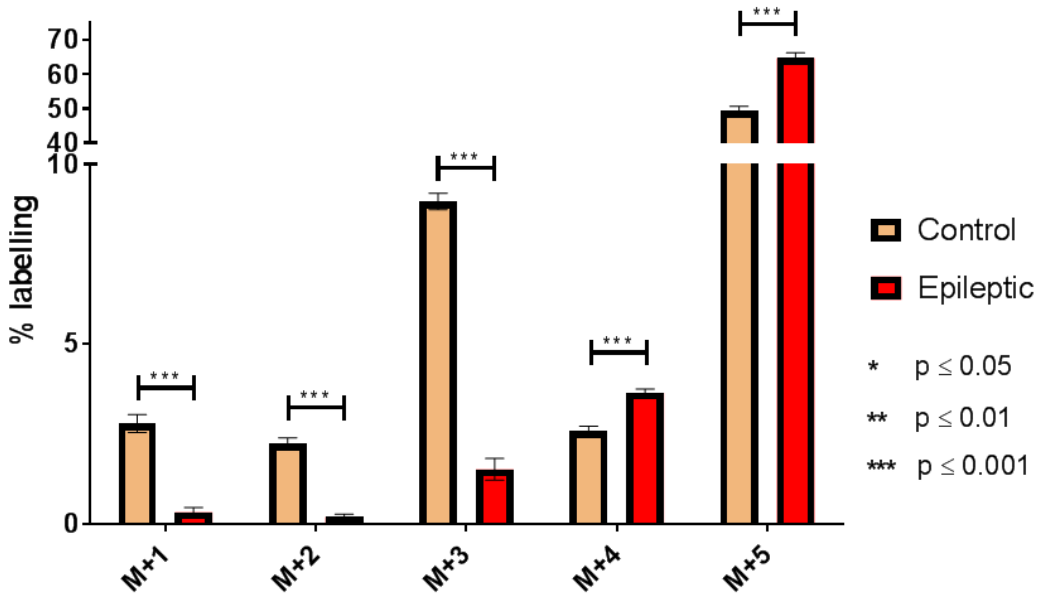
Glutamate
% labelling
70
60
50
40
10
5
0
***
M+1
M+2
M+3
M+4
M+5
Control
Epileptic
* p ≤ 0.05
** p ≤ 0.01
*** p ≤ 0.001

B

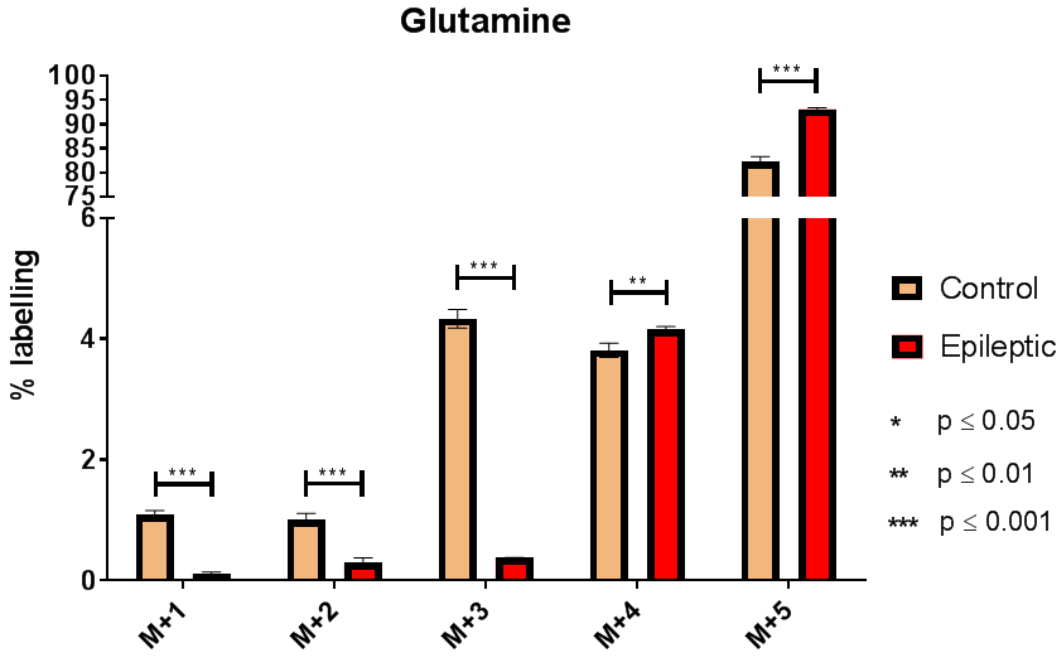
Glutamine
% labelling
100
95
90
85
80
75
6
4
2
0
***
**
M+1
M+2
M+3
M+4
M+5
Control
Epileptic
* p ≤ 0.05
** p ≤ 0.01
*** p ≤ 0.001

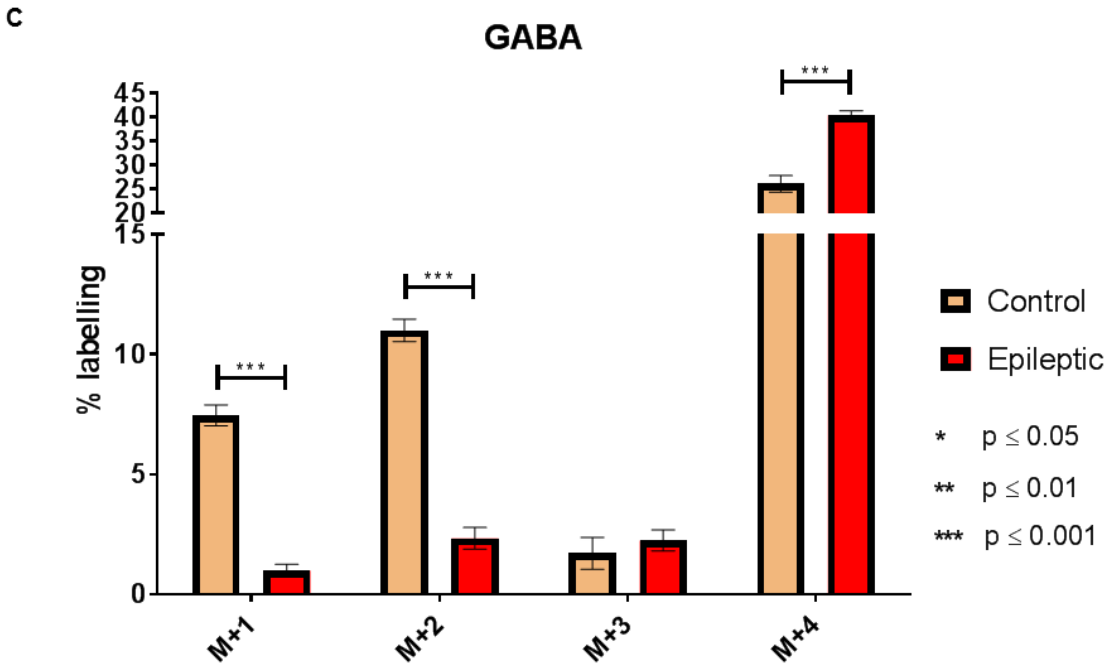

Figure 5-10 Glutamine addition did not rescue the recycling of the glutamate – glutamine cycle via the Krebs cycle but it did increase the synthesis of GABA. Shown in A to C are the ^{13}C labelling for glutamate, glutamine, and GABA respectively following addition of 2.5mM [U-13C]-glutamine. Results are from conditions 7 and 8. Condition 7 indicates control and 8 indicates epileptic.

In the epileptic group, there was a significant reduction ($p \leq 0.001$; n=10) in GABA M+1 labelling when compared against the control group (0.99 ± 0.26 % epileptic vs 7.45 ± 0.44 % control). This was similarly seen with regards to the M+2 labelling (2.33 ± 0.45 % epileptic vs 10.99 ± 0.47 % control). There was, however, no significant difference ($p \geq 0.05$; n= 10) in the GABA M+3 labelling between the control and the epileptic group. In contrast, there was a significant increase ($p \leq 0.001$; n=10) in the M+4 labelling of the epileptic group compared against the control group (40.33 ± 0.96 % epileptic vs 26.07 ± 1.74 % control).

The addition of 2.5mM [U-^{13}C]-glutamine as a 'rescue' treatment was able to significantly alter the metabolic profile of the epileptic tissue (unlike the addition of glutamate as described in section 5.3.6). There was a significant increase ($p \leq 0.01$; n=10) in the amount of glutamate in the epileptic tissue (420.10 ± 47.54 nmol/mg protein) as compared against the control tissue (259.80 ± 27.95 nmol/mg protein). The amount of glutamine was still significantly reduced ($p \leq 0.001$; n=8) in the epileptic tissue (153.10 ± 13.73 nmol/mg protein) as compared against the control tissue (279.80 ± 18.31 nmol/mg protein), albeit now being at a detectable amount in the epileptic tissue unlike any of the other conditions. Tissue amount of GABA was also still significantly increased ($p \leq 0.001$; n=8) in the epileptic tissue (35.33 ± 2.34 nmol/mg protein) when compared against the control tissue (17.54 ± 0.79 nmol/mg protein).

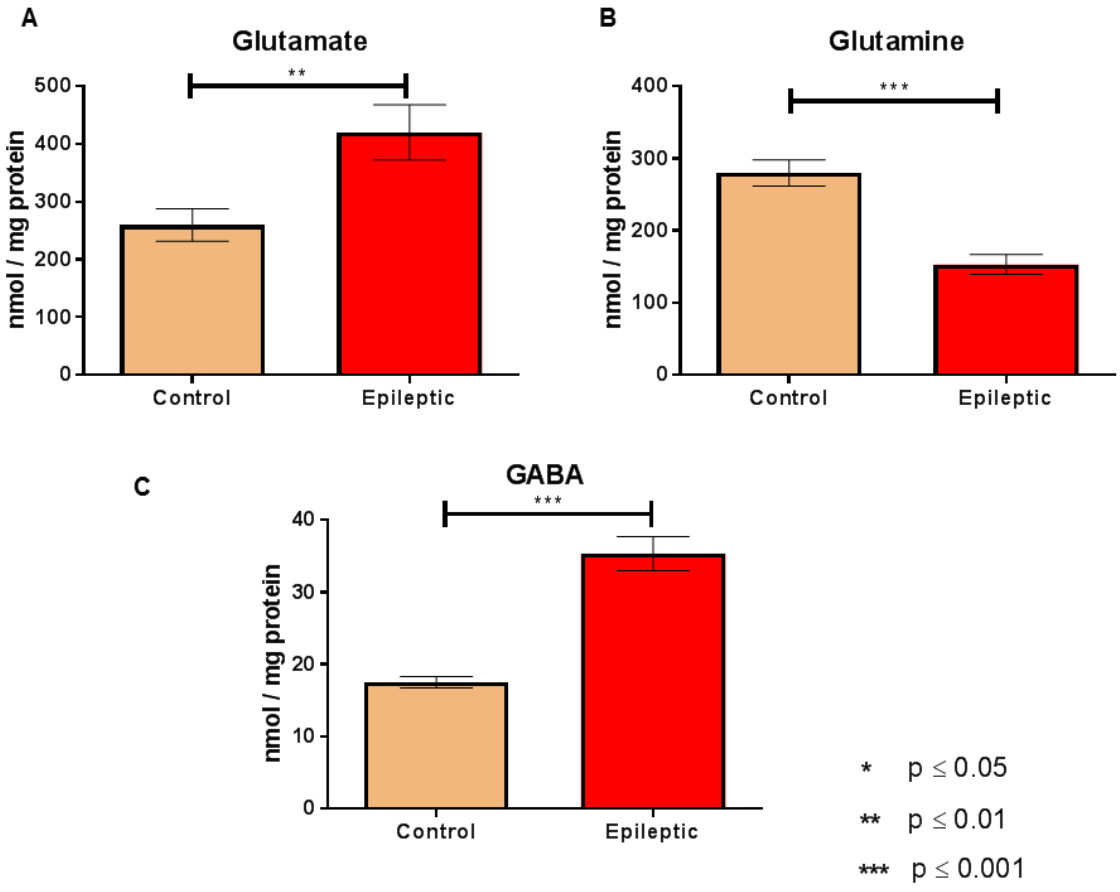

Figure 5-11 The addition of glutamine significantly alter the metabolic profile of the epileptic tissue. Shown in A to C are amounts of glutamate, glutamine, and GABA respectively in the control and the epileptic tissue following addition of 2.5mM [U-^{13}C]-glutamine. Results are from condition 7 and 8. Condition 7 indicates control and 8 indicates epileptic.

5.3.10 The entry of glutamine into the Krebs cycle is not impeded but subsequent turns of the Krebs cycle are inhibited

Glutamine does not directly enter the Krebs cycle, but, both glutamate and GABA are recycled (or degraded) mostly in astrocytes via the Krebs cycle. Glutamate enters the astrocytic and neuronal Krebs cycle via its intermediate, α-ketoglutarate whereas GABA enters the astrocytic Krebs cycle via succinyl-semialdehyde, which eventually is converted into succinate (Hertz, 2013). Therefore, it is also important in the context of incubation with ^{13}C-labelled glutamine to consider the incorporation of the ^{13}C in the Krebs cycle intermediates (see Figure 5-12).

There was no significant difference ($p \geq 0.05$; n= 10) in the labelling of all of the isotopologues of alpha-ketoglutarate (M+1, M+2, M+3, M+4, and M+5) between the control and the epileptic group.

In contrast, there was a significant reduction ($p \leq 0.001$; n=10) in the epileptic group when compared against the control group, with regards to the labelling of succinate M+1 (0.11 ± 0.04 % epileptic vs 0.98 ± 0.13 % control), M+2 (0.20 ± 0.05 % epileptic vs 2.64 ± 0.29 % control), M+3 (0.30 ± 0.05 % epileptic vs 0.66 ± 0.07 % control), and M+4 (3.84 ± 0.53 % epileptic vs 12.87 ± 1.88 % control).

Similarly, there was also a significant reduction ($p \leq 0.001$; n=10) in the labelling of fumarate in the epileptic group compared against the control group, with regards to the M+1 (0.33 ± 0.10 % epileptic vs 2.19 ± 0.24 % control), M+2 (0.69 ± 0.14 % epileptic vs 4.64 ± 0.39 % control), M+3 (1.17 ± 0.11 % epileptic vs 2.31 ± 0.31 % control), and M+4 (9.84 ± 0.90 % epileptic vs 20.13 ± 1.43 % control) isotopologues.

The labelling pattern of malate is unique to that of the other Krebs cycle intermediates in these incubation conditions. There was still a significant reduction ($p \leq 0.001$; n=10) in the epileptic group as compared against the control group, with regards to the M+1 (0.50 ± 0.19 % epileptic vs 4.53 ± 0.41 % control), M+2 (1.62 ± 0.25 % epileptic vs 8.60 ± 0.29 % control) and M+4 (30.28 ± 1.71 % epileptic vs 36.76 ± 1.49 % control) labelling. However, there was no significant difference ($p \geq 0.05$; n= 10) in the M+3 labelling of malate between the control and the epileptic group.

A

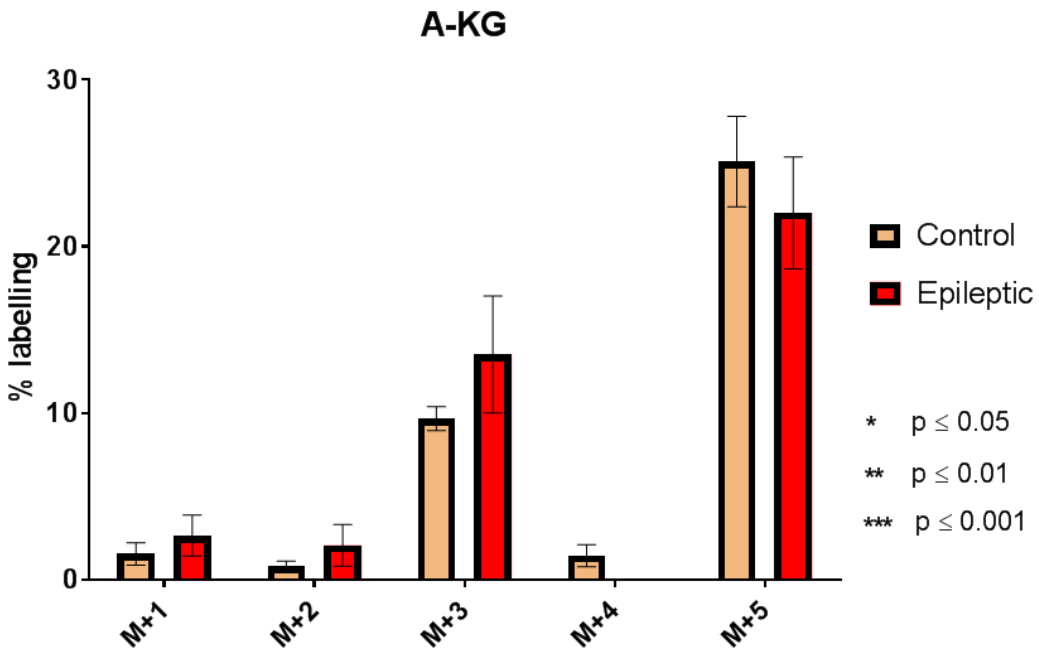
A-KG
30
20
10
0
% labelling
M+1
M+2
M+3
M+4
M+5
Control
Epileptic
* p ≤ 0.05
** p ≤ 0.01
*** p ≤ 0.001

B

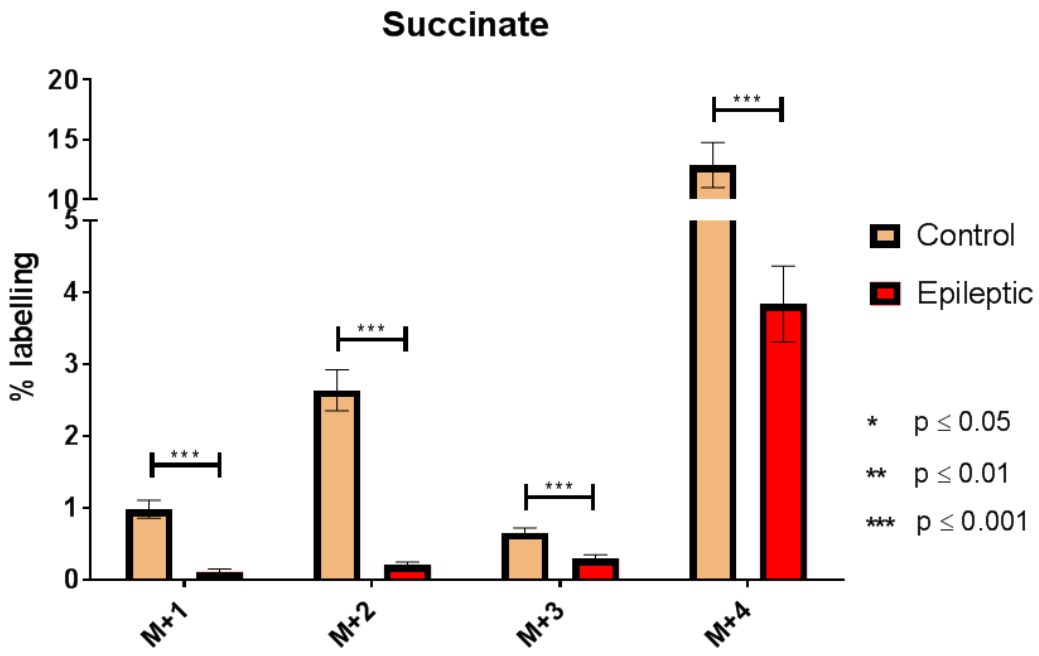
Succinate
20
15
10
5
4
3
2
1
0
% labelling
***
***
***
***
M+1
M+2
M+3
M+4
Control
Epileptic
* p ≤ 0.05
** p ≤ 0.01
*** p ≤ 0.001

C

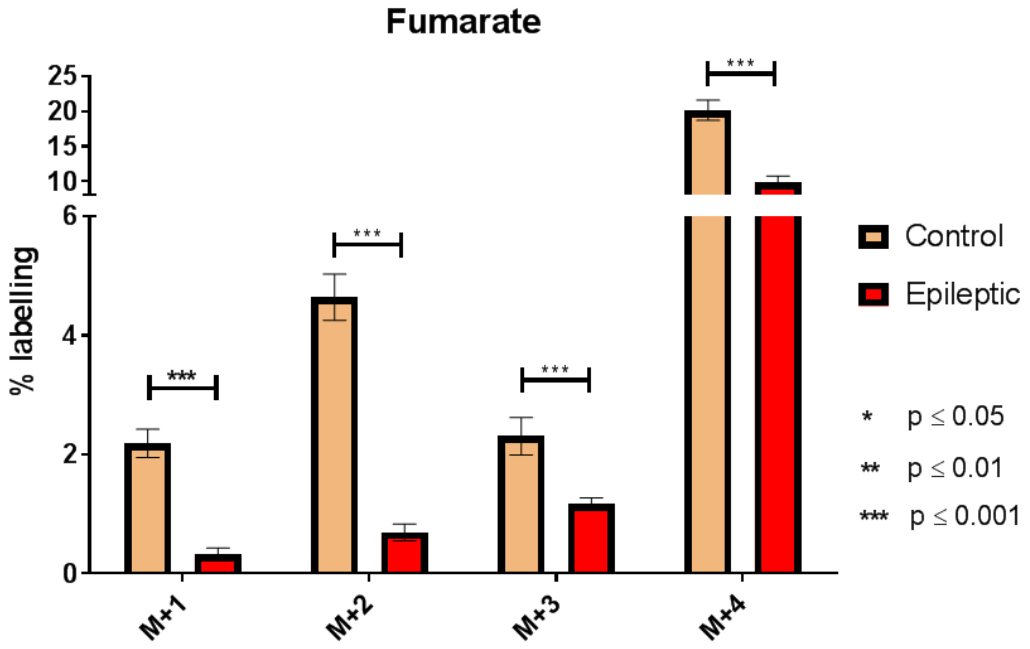
Fumarate
% labelling
25
20
15
10
6
4
2
0
***
***
***
***
M+1
M+2
M+3
M+4
Control
Epileptic
* p ≤ 0.05
** p ≤ 0.01
*** p ≤ 0.001

D

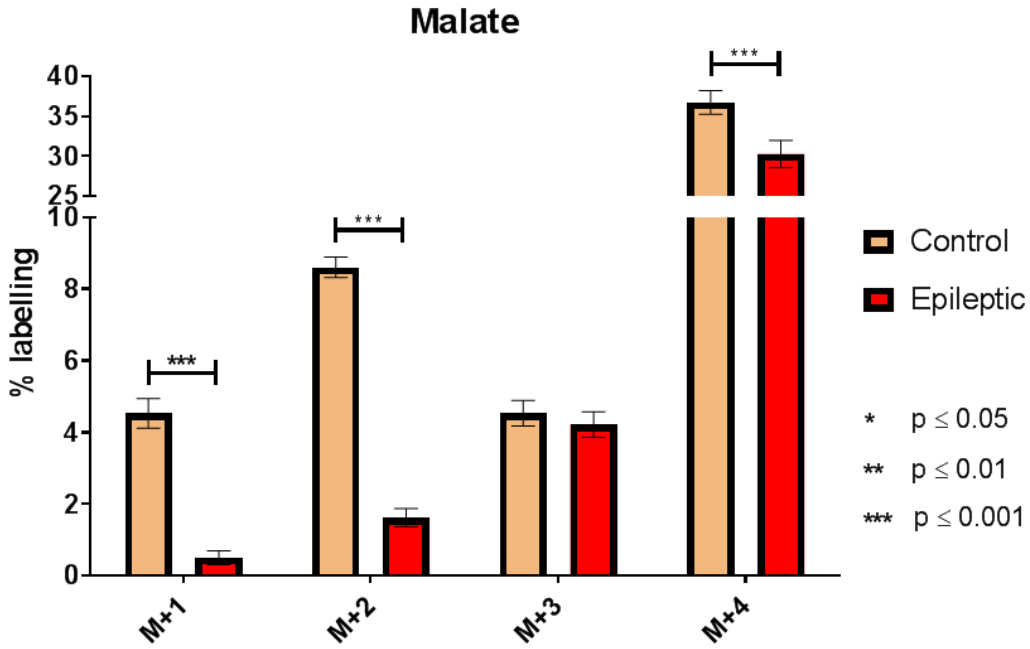
Malate
% labelling
40
35
30
25
10
8
6
4
2
0
***
***
***
M+1
M+2
M+3
M+4
Control
Epileptic
* p ≤ 0.05
** p ≤ 0.01
*** p ≤ 0.001

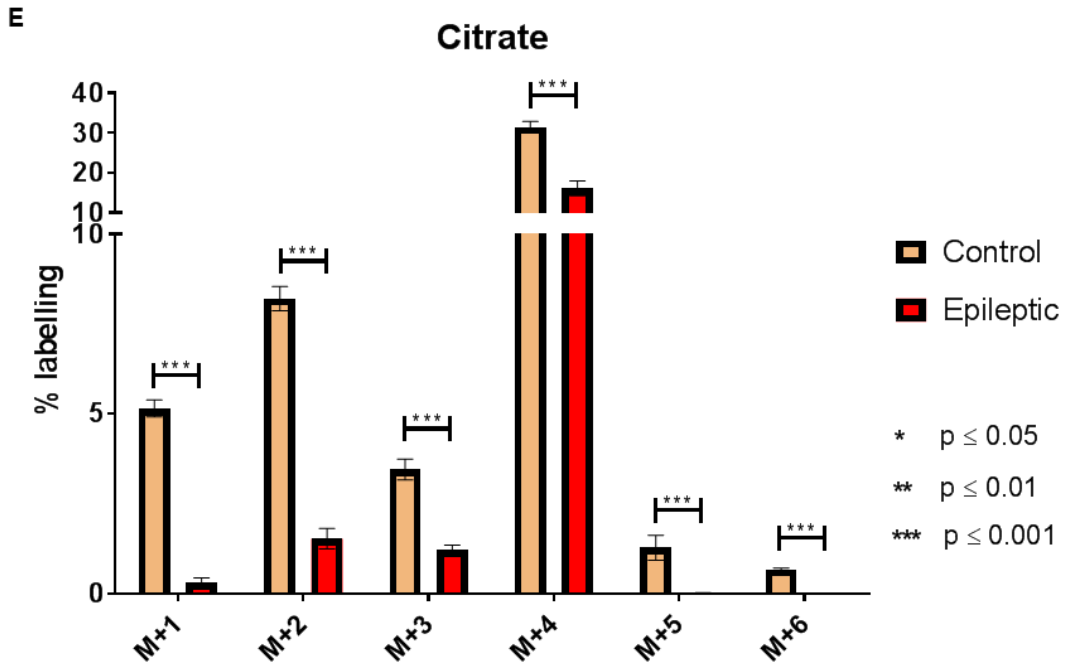

Figure 5-12 The entry of glutamine into the Krebs cycle is not affected but subsequent turns of Krebs cycle is inhibited by the mitochondrial epilepsy protocol. A-E shows the ^{13}C labelling for alpha-ketoglutarate, succinate, fumarate, malate, and citrate respectively. Results are from condition 7 and 8. Condition 7 indicates control and 8 indicates epileptic.

Again, there was a statistically significant reduction ($p \leq 0.001$; n=10) in the citrate labelling across all isotopologues in the epileptic group as compared against the control group. This includes the M+1 (0.30 ± 0.14 % epileptic vs 5.15 ± 0.24 % control), M+2 (1.53 ± 0.29 % epileptic vs 8.20 ± 0.34 % control), M+3 (1.23 ± 0.12 % epileptic vs 3.45 ± 0.30 % control), M+4 (16.15 ± 1.84 % epileptic vs 31.44 ± 1.36 % control), M+5 (0.01 ± 0.01 % epileptic vs 1.28 ± 0.35 % control), and M+6 (0.00 ± 0.00 % epileptic – non detectable vs 0.67 ± 0.05 % control) isotopologues.

5.3.11 Addition of glutamine favours the breakdown of aspartate

As described in section 5.3.8, the formation (or breakdown) of aspartate is coupled to the oxidative deamination of glutamate into alpha-ketoglutarate, catalysed by the enzyme glutamate dehydrogenase (Hertz, 2013). As such, it is important to examine the degree of aspartate labelling and the tissue levels of aspartate following this addition of the 'rescue' concentration of glutamine.

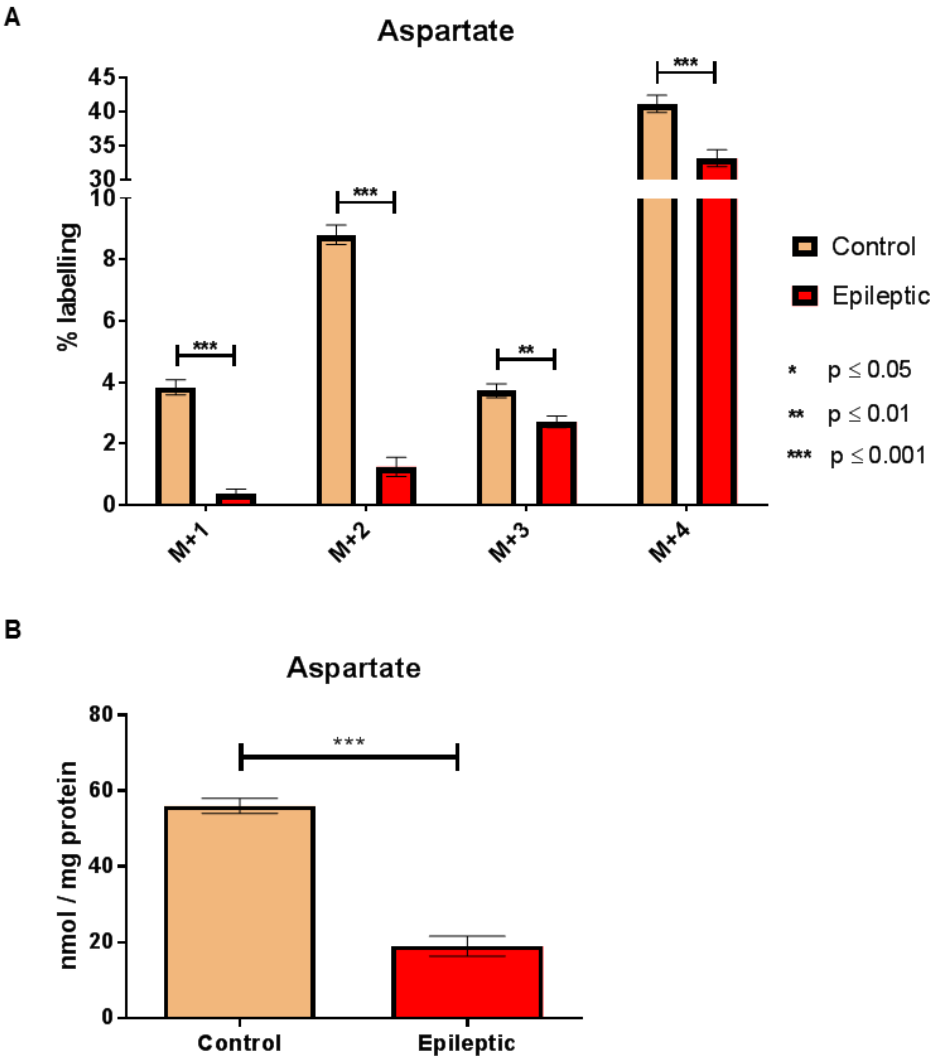

Figure 5-13 Glutamine addition favours the breakdown of aspartate. Shown in A is the ^{13}C labelling for aspartate following incubation with 2.5mM [U-^{13}C]-glutamine and in B is the amount of aspartate in the same condition. Results are from conditions 7 and 8. Condition 7 indicates control and 8 indicates epileptic.

There was a significant reduction ($p \leq 0.001$; n=10) in the epileptic group compared against the control group, with regards to the aspartate M+1 (0.37 ± 0.14 % epileptic vs 3.83 ± 0.25 % control), M+2 (1.24 ± 0.31 % epileptic vs 8.80 ± 0.32 % control), and M+4 (33.20 ± 1.24 % epileptic vs 41.18 ± 1.27 % control) labelling. This trend was also observed in the aspartate M+3 labelling where there is significant reduction ($p \leq 0.01$; n=10) in the epileptic group (2.70 ± 0.19 %) as compared against control (3.72 ± 0.23 %).

Similar to the labelling pattern, there was a significant reduction ($p \leq 0.001$; n=10) in the tissue level of aspartate in the epileptic group (19.00 ± 2.65 nmol/mg protein) when compared against the control group (56.00 ± 1.94 nmol/mg protein).

5.3.12 Neither glutamine nor glutamate addition decreased glycolysis in the epileptic tissue.

Finally, to examine the impact of the addition of 0.5mM L-glutamate or the 'rescue' concentration of 2.5mM L-glutamine, the amount of lactate released to the media was quantified following treatment with either [U-^{13}C]-glutamate or [U-^{13}C]-glutamine (see Figure 5-14).

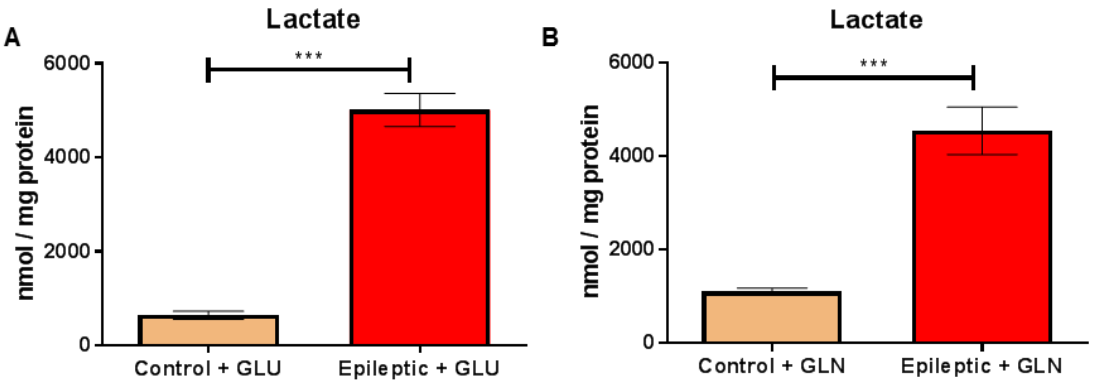

Figure 5-14. Lactate release from the media was not affected by treatment with either glutamate or glutamine. Shown in A and B are amount of lactate release into the media in the control and epileptic tissue following treatment with either [U-^{13}C]-glutamate (A) or [U-^{13}C]-glutamine (B). Results are from condition 5,6,7, and 8. Condition 5 indicates control + GLU, 6 indicates epileptic + GLU, 7 indicates control + GLN, and 8 indicates epileptic + GLN.

There was a significant increase ($p \leq 0.001$; n=8) in the amount of lactate release into the media in the epileptic tissue (5014.00 ± 350.10 nmol/mg protein) as compared against the control tissue (646.70 ± 83.74 nmol/mg protein) when incubated with 0.5mM L-glutamate. Similarly seen in tissues incubated with glutamine, there was also a significant increase ($p \leq 0.001$; n=10) in the level of lactate release in the epileptic tissue (4550.00 ± 509.00 nmol/mg protein) as compared against the control tissue (1107.0 ± 73.5 nmol/mg protein).

5.4 Discussion

The results presented in this Chapter are comprehensive assessment of the metabolic state of the tissue revealed using the metabolic mapping experiments. For transparency, all the data has been included in the results section and presented accordingly but from this point onwards, only relevant labelling data will be discussed.

5.4.1 Glycolysis

The results presented in section 5.3.1 detail the changes in glycolysis induced by the various components of the mitochondrial epilepsy protocol. There was a significant increase in the labelling of lactate M+3 and consequently, the tissue level of lactate by incubation of either fluorocitrate alone, rotenone and cyanide alone, or the combination when incubating with [U-^{13}C] glucose (see Figure 5-1). This indicates an upregulation in anaerobic glycolysis due to a change in the tissue redox state (Voet and Voet, 2011b). With any of the experimental conditions above, one would expect a severe inhibition of oxidative metabolism, hence causing a decrease in the NAD^+/NADH ratio. In order to replenish the supply of NAD^+, the excess NADH could be oxidized via the formation of the glycolytic by-product, lactate. In addition, under conditions of severe energy crisis, the formation of lactate is energetically favourable as it provides the NAD^+ necessary to drive the process of glycolysis, the net results of which would produce 2 ATP for each molecule of glucose. This increased level of lactate release is consistent with the clinical observation of lactic acidosis characteristic of the various phenotypes of mitochondrial epilepsy (Pavlakis *et al.*, 1984; Nishigaki *et al.*, 2003; Robinson, 2006).

Lactate, however, can be considered as a ‘dead end’ in metabolic terms and has to be converted back into pyruvate before it can be metabolized further (Berg *et al.*, 2012f). There has been some suggestion that lactate could provide the primary source of energy for neurons during high neural activity (Pellerin and Magistretti, 1994; Bélanger *et al.*, 2011) but our experiments, as described in section 4.3.5.3, have indicated that in this model, the induced seizure does not respond to lactate; indicating that lactate is not used as a metabolic substrate during the state of seizure. Furthermore, when comparing the value of lactate release in the control tissue (see Figure 5-1) against control tissue that was exposed to 0.5mM L-glutamate (see Figure 5-14), there was a slight decrease in lactate release following exposure to glutamate,

which directly challenges the astrocyte – neuron lactate shuttle hypothesis (ANLSH) (Pellerin and Magistretti, 1994). Taken together, our results agree with the critical review that evidence supporting the existence of this pathway is weak (Chih and Roberts, 2003), at least in the context of a pathological condition such as epilepsy.

Interestingly, there was also a trend towards an increase in the labelling of lactate M+2 in the group exposed to the combination (the 'epileptic' group) when compared against the control group (see Figure 5-1). This could be due to the upregulation of the pentose phosphate pathway. The pentose phosphate pathway (PPP) is an important alternate pathway to glycolysis as it is a critical source of NADPH and ATP in conditions of energy crisis. The NADPH generated is an important reducing agent against oxidative stress in the form of oxidized glutathione (GSSG) (Berg *et al.*, 2012b). This upregulation of PPP, therefore, suggests an ongoing process of oxidative stress in this model of mitochondrial epilepsy, which has been reported in other models and studies of mitochondrial epilepsy (Yamamoto and Tang, 1996; Liang and Patel, 2004; Rahman, 2012).

Interestingly, application of glutamate or glutamine to the epileptic tissue did not cause a reduction in lactate release (see section 5.3.12). In the case of glutamate, application of 0.5mM L-glutamate has been shown to not cause any change in the epileptic activity in the brain slices (see section 4.3.6.1), so, it is to unsurprising then that the addition of this concentration of glutamate did not modulate glycolytic activity. In the case of glutamine, application of 2.5mM L-glutamine has been shown to significantly suppress the epileptic activity *in vitro* (see section 4.3.6.3). However, glycolysis still seems to be significantly upregulated, even after suppression of epileptic activity. This suggests that even following suppression of epileptic activity, the underlying metabolic impairment could still be present and the tissue still heavily relies on glycolysis for metabolic sustainment.

Alanine is formed from pyruvate through a transamination reaction that is coupled with the deamination of glutamate into alpha-ketoglutarate (Berg *et al.*, 2012a). Alanine is, therefore, another useful indicator of glycolytic activity. The significant increase in alanine M+3 labelling across all the groups, again, confirmed that there is significant upregulation of glycolysis in the epileptic tissue. Interestingly, increase in tissue amounts of alanine is only observed in the tissue exposed to the fluorocitrate alone or to rotenone and cyanide alone, but not in the epileptic tissue which was exposed to the combination of all three compounds. This discrepancy may be

explained by the dependence of alanine biosynthesis on the donor of amino group from glutamate. Perhaps, in the epileptic tissue, glutamate is not as actively converted into alpha-ketoglutarate as it is required to sustain the hyperexcitable network state.

5.4.2 Krebs cycle

The Krebs cycle, also known as the citric acid cycle, is the final common pathways for the oxidation of carbohydrates, fatty acids, and amino acids (Berg *et al.*, 2012d). The intermediates of the cycle that can be detected via the GCMS measurements are citrate, alpha-ketoglutarate, succinate, fumarate, and malate.

The results presented in section 5.3.2 described the changes in the Krebs cycle as induced by the components of the mitochondrial epilepsy protocol. Citrate M+2 represents the entry point of pyruvate via conversion to acetyl-CoA into the first turn of the Krebs cycle. Subsequently, citrate is converted into isocitrate by the enzyme aconitase (Berg *et al.*, 2012b). Fluorocitrate, which is one of the critical components of the mitochondrial epilepsy protocol, is thought to be a selective astrocytic aconitase inhibitor (Paulsen *et al.*, 1987; Hassel *et al.*, 1992; Swanson and Graham, 1994). Accumulation of citrate M+2 in the tissue exposed to fluorocitrate only confirmed the inhibition of aconitase and this increase most likely reflects the contribution of the astrocytic Krebs cycle towards the overall labelling pattern. Interestingly, there was also an accumulation of citrate M+2 in the tissue exposed to rotenone and cyanide only. This could reflect the oxidative inactivation of mitochondrial aconitase that could occur during application of electron transport chain inhibitors (Cantu *et al.*, 2009). Another very interesting point is that there is no significant difference in the citrate M+2 labelling between the control group and the group exposed to the combination (the ‘epileptic’ group). This reflects the complexity of the metabolic alterations observed during the epileptic state as pyruvate may still enter the Krebs cycle even in the presence of all the metabolic inhibitors, including an inhibitor of aconitase. To a certain degree, the presence of an epileptiform activity at the tissue level must place a heavy metabolic demand on the tissue (Zsurka and Kunz, 2015), which may be met by utilizing the maximal capacity of the tissue for the Krebs cycle. There was, however, a subsequent decrease in all the other isotopologues of citrate in all conditions and this may reflect the downregulation of subsequent turns of the Krebs cycle in all the experimental conditions.

To trace the first turn of the Krebs cycle, the M+2 isotopologues is the ideal molecular substrate of the Krebs cycle to be examined. There was consistently a significant decrease in all the experimental conditions in the M+2 labelling of all subsequent substrates of the Krebs cycle (alpha-ketoglutarate, succinate, fumarate, and malate). This demonstrates the severe impairment of the Krebs cycle by the components of the mitochondrial epilepsy protocol. Interestingly, the decrease was always milder in the group exposed to fluorocitrate only as compared to the group exposed to rotenone and cyanide only or the group exposed to the combination. This again reaffirms the selective inhibition of the astrocytic Krebs cycle by fluorocitrate (Paulsen *et al.*, 1987; Hassel *et al.*, 1992; Swanson and Graham, 1994).

5.4.3 Aspartate

Aspartate is formed from oxaloacetate through a transamination reaction catalysed by aspartate aminotransferase with an amino group donor from glutamate, as alanine is (Berg *et al.*, 2012a). This makes aspartate a unique parameter for assessment of both the Krebs cycle and the glutamate – glutamine cycle.

Fluorocitrate exposure did not cause any significant change in both the aspartate isotopologues labelling and the tissue level of aspartate (see Figure 5-3). This supports the metabolic compartmentalization of aspartate as primarily a neuronal substrate (Baslow, 2003) and again reaffirms the selective inhibition of the astrocytic Krebs cycle by fluorocitrate (Paulsen *et al.*, 1987; Hassel *et al.*, 1992; Swanson and Graham, 1994). The addition of either rotenone and cyanide or the combination (with fluorocitrate) caused a significant decrease in both the aspartate isotopologues labelling and the tissue level of aspartate. This confirms the severe inhibition of Krebs cycle as described previously in section 5.4.2 and reflects the recruitment of the neuronal compartment in the metabolic inhibition caused by the electron transport chain inhibitors, rotenone and cyanide.

5.4.4 Glutamate – glutamine cycle

Since glucose is the primary source of the carbon atom required for synthesis of glutamate via alpha – ketoglutarate (Daikhin and Yudkoff, 2000), the results of the metabolic mapping with [U-^{13}C]-glucose as described in section 5.3.4 and 5.3.5 provides a crude assessment of the state of the glutamate – glutamine cycle although cycling is probably better assessed by incubation with one of the substrates of the cycle such as [U-^{13}C]-glutamate or [U-^{13}C]-glutamine.

Surprisingly, exposure to fluorocitrate did not cause any reduction in the M+2 labelling of either glutamate or glutamine, despite the significant reduction in the M+2 labelling of alpha-ketoglutarate (as described in section 5.4.2). Glutamine is primarily an astrocytic substrate due to the specific expression of glutamine synthetase in the glial family (Anlauf and Derouiche, 2013). This suggests that it is vital of the tissue to maintain the homeostatic balance of glutamate and glutamine by whatever Krebs cycle capacity is left in the astrocytes. This was confirmed by the maintained level of tissue glutamate and glutamine with fluorocitrate exposure (see Figure 5-5). Interestingly, there was a reduction in the M+2 labelling in GABA with exposure to fluorocitrate. This suggests that the tissue did not use the synthesized glutamate or glutamine (from glucose) for the synthesis of GABA in the presence of fluorocitrate. This is perhaps an important mechanism for the generation of mitochondrial epilepsy that is unique to fluorocitrate, which is to create a state of disinhibition, which has been described in previous study (Kaczor *et al.*, 2015). However, overall amounts of GABA seems to be unaffected by the fluorocitrate exposure.

Exposure to rotenone and cyanide caused a significant reduction in the M+2 labelling of glutamate, glutamine, and GABA which is concurrent with the severe impairment of the Krebs cycle in this group. Again, tissue amounts of glutamate and glutamine were sustained, which suggests the presence of a compensatory mechanism in the presence of these metabolic inhibitors. Interestingly, tissue amounts of GABA were increased with exposure to rotenone and cyanide; unlike fluorocitrate. This can be explained by the inhibition of GABA degradation via succinyl-coA, which is mediated by the enzyme succinic semialdehyde dehydrogenase. This enzyme is dependent on the NAD^+/NADH ratio (Olsen and Betz, 2006), which would be reduced by inhibition of the electron transport chain. Fluorocitrate did not inhibit the electron

transport chain and so would not modify the NAD^+/NADH ratio, hence the unaffected value of GABA.

Exposure to a combination of fluorocitrate, rotenone, and cyanide (which comprises the mitochondrial epilepsy protocol) caused a significant reduction in the M+2 labelling of glutamate, glutamine, and GABA, similar to the profile seen with exposure to rotenone and cyanide alone. However, there was also a significantly lower M+2 labelling in glutamine in this group as compared to the rotenone and cyanide group. This was accompanied by a concurrent significant reduction in tissue level of glutamine to an almost non-detectable level. This represents an interesting disparity to the rest of the experimental conditions. Two possibilities exist; either glutamine is utilized exclusively as metabolic fuel in the condition of seizure or a reflection of the complete shutdown of astrocyte function during a state of seizure; considering the exclusive localization of glutamine synthetase to the astrocytes (Anlauf and Derouiche, 2013). Whichever mechanism it may be; it is clear that glutamine (or the lack thereof) plays a pivotal role in the generation of seizure.

An important point to note here is that *in vivo*, two distinct pools of glutamate and GABA exists: the vesicular and the non-vesicular pools (Hassel and Dingledine, 2006; Olsen and Betz, 2006); both of which may be affected to a distinct manner by our treatments. Although HPLC is a very sensitive technique for detection of amino acids, it cannot differentiate between the two pools and so, one should be cautious in interpreting the glutamate and GABA readings from these measurements. Furthermore, this technique alone also cannot differentiate the astrocytic and neuronal origins of each of these substrates, although inferences can be made as demonstrated above.

Finally, the measured tissue GABA amount in the epileptic tissue does not correspond with the hypothesis presented earlier in section 4.5 that proposes a tissue deficiency of GABA based on the functional evidence. In addition to the technical limitations as discussed above, GABA-ergic inhibition is also shown to be very sensitive to the method of tissue preparation (Kuenzi *et al.*, 2000). Specifically, in slices prepared using the perfused method, GABA-ergic inhibition was shown to be preserved better as compared against the decapitation method (Kuenzi *et al.*, 2000). Therefore, the results in this Chapter, especially pertaining to GABA, should be taken with a degree of scepticism as the method of preparation used in the brain slice preparation (decapitation) may have significantly alter the GABA-ergic system in a manner unknown as of yet.

5.4.5 Addition of glutamate

Results presented in section 5.3.6, 5.3.7, and 5.3.8 described the results of metabolic mapping experiments following incubation with 0.5mM [U-^{13}C]-glutamate. As mentioned above in section 4.3.6.1, the application of this concentration of L-glutamate did not cause any change in the epileptic activity. This gives a unique opportunity for assessing the glutamate – glutamine cycle from the substrate's point of view without causing any interference in the seizure state.

There was an increase in glutamate M+5 and glutamine M+5 in the epileptic tissue as compared against control, which reflects lack of utilization of the [U-^{13}C]-glutamate as a metabolic substrate. Decreases in the other isotopologues of the glutamate and glutamine indicates the lack of recycling of glutamate via the Krebs cycle. As an example, if the [U-13C]-glutamate had recycled via the Krebs cycle, on the second turn of the glutamate cycle, M+3 labelling pattern would be expected from both glutamate and glutamine, which was reduced in the epileptic tissue. Level of tissue glutamate is unaffected by this addition of glutamate and interestingly, glutamine level is still depleted to a non-detectable level. As mentioned above, glutamine synthetase is almost exclusively expressed in astrocytes (Anlauf and Derouiche, 2013) and the lack of glutamine synthesis from this added glutamate supports the hypothesis of complete astrocyte shutdown during the epileptic state.

Interestingly, the labelling pattern for GABA M+4 is sustained unlike glutamate or glutamine. This means that the glutamate is still able to be taken up by the GABA-ergic neurons for sustainment of the GABA pool. However, since the flux of the glutamate and glutamine trafficking between neurons and astrocyte is very high, glutamate is more likely to be taken up by the astrocytes rather than neurons (Hassel and Dingledine, 2006), which makes glutamate a poor choice of substrates for sustaining GABA synthesis. This may explain why the addition of glutamate did not cause any change in the epileptiform activity, as it may have been taken up by the astrocytes rather than the neurons in need. GABA level is still significantly increased as was observed in the epileptic tissue (without addition of glutamate).

The Krebs cycle labelling results as described in section 5.3.7 also confirms the lack of recycling via the Krebs cycle. Interestingly, M+5 labelling of alpha-ketoglutarate is sustained in the epileptic tissue. This suggests that glutamate can still enter the

Krebs cycle via alpha-ketoglutarate but subsequent turns of the TCA cycle (into succinate, fumarate, malate, and citrate) are severely inhibited.

The aspartate labelling for M+1 and M+2 are significantly decreased, which again reflects the inhibition of the subsequent turns of the TCA cycle. This is also reflected by the significant reduction in tissue level of aspartate in the epileptic slices.

5.4.6 Addition of glutamine

Results presented in section 5.3.9, 5.3.10, and 5.3.11 described the results of metabolic mapping experiments following incubation with 2.5mM [U-^{13}C]-glutamine. As mentioned above in section 4.3.6.3, the application of this concentration of L-glutamine was able to suppress the epileptic activity, making this a 'rescue' concentration and the experiment an assessment of metabolic profile during a 'rescue' phenotype.

There is, again, an increase in glutamate and glutamine M+5 labelling, which may reflect the lack of utilization of [U-^{13}C]-glutamine as a metabolic substrate. This is supported by the decrease in other isotopologues (such as M+3), which reflects lack of recycling of glutamine via the Krebs cycle. Interestingly, there is now a significant increase in tissue glutamate amount and tissue glutamine amount is now detectable, albeit still lower than the control level, in the epileptic tissue. This casts doubt on the earlier hypothesis of the lack of utilization of [U-^{13}C]-glutamine as a metabolic substrate. Instead, the increase in the M+5 labelling may reflect an upregulation of the glutamate – glutamine cycle (more utilization of glutamine and more synthesis of glutamate). Krebs cycle cycling, however, is still significantly impeded.

Another interesting change to the metabolic profile is the significant enrichment in GABA M+4 in the epileptic tissue. Unlike glutamate, it seems that the addition of this 'rescue' concentration of glutamine was able to upregulate GABA synthesis. As explained above, this may be explained by the high flux of the cycle (Hassel and Dingledine, 2006) that makes glutamine an excellent source for sustainment of the GABA pool. Tissue level of GABA is still significantly increased, which may reflect either increased synthesis of GABA or the lack of GABA breakdown via the redox-dependent transamination reaction.

The Krebs cycle labelling results as described in section 5.3.10 shows a similar pattern of labelling as with the incubation of [U-^{13}C]-glutamate (detailed in section 5.3.7

and discussed in section 5.4.5). Glutamine can still enter the Krebs cycle via glutamate and alpha-ketoglutarate, as shown by the sustained M+5 alpha-ketoglutarate labelling. Interestingly, the addition of glutamine was able to sustain the M+3 labelling of alpha-ketoglutarate, unlike glutamate. M+3 alpha-ketoglutarate is obtained from the cycling of glutamine via the second turn of the Krebs cycle (see Figure 2-4) and although the level of labelling of the other substrates of Krebs cycle leading to that point (i.e succinate M+4, fumarate M+4, malate M+4, and citrate M+4) are all significantly reduced, their relative level is slightly higher than the level obtained from glutamate incubation (for example, citrate M+4 labelling is 16.15 ± 1.84% in epileptic with glutamine vs 7.89 ± 0.38% in epileptic with glutamate). This suggest that following glutamine addition, there may be a partial rescue of the capacity of Krebs cycle, at least up to the second turn of the cycle.

Finally, aspartate labelling pattern is very much similar to the results obtained from glutamate incubation (as shown in section 5.3.8 and discussed in section 5.4.5), except for a significant reduction in M+4 and M+3 aspartate. Both M+4 and M+3 aspartate are obtainable from recycling of glutamate or GABA via the Krebs cycle (see Figure 2-4). This again confirms the lack of recycling of glutamate or GABA via the Krebs cycle. Tissue amounts of aspartate are still significantly reduced which again supports this.

5.5 Summary, strength, and weakness

Overall, the metabolic mapping experiments provided a very comprehensive assessment of the metabolic state of the tissue following our mitochondrial epilepsy protocol. The tissue's metabolic profile is significantly modified during the epileptic state. There is a dependence on glycolysis for generation of energy during a state of seizure, which resulted in a significantly higher lactate release, consistent with what is observed in the patients. Krebs cycle is severely impaired, which may be reflective of severe inhibition of oxidative respiration. The glutamate – glutamine cycle is also significantly downregulated, particularly a significant loss of tissue glutamine during the seizure state. This, along with a series of other observations, indicates a complete shutdown of astrocyte's function in mitochondrial epilepsy. Glutamine, which may rescue the epileptic phenotype, is shown to be capable of sustaining GABA synthesis in the tissue, presumably restoring the cycle's homeostatic equilibrium. Compared to glutamate, glutamine is proven to be a better choice of metabolic substrate during mitochondrial epilepsy.

Findings from this chapter also provided us with the exquisite evidence of the selectivity of fluorocitrate inhibition of the Krebs cycle in the astrocytic compartment. Rotenone and cyanide, as an electron transport chain inhibitor, is shown to severely affect neuronal metabolism. This ties in with the 'dual neuronal – astrocytic hit hypothesis' in which both the astrocytic and neuronal compartment needs to be affected severely before epileptic activity is seen at the network level. In fact, astrocytes' metabolic function has to be completely silenced for epileptogenesis to occur.

Although these metabolic mapping experiments is very elegantly designed and conducted, there are some cautions in interpreting the results. The GCMS labelling pattern is presented as percentage of isotopologue labelling after being adjusted for the natural abundance but this does not represent the absolute value of the substrates discussed. In the case of some substrates (such as lactate, alanine, glutamate, glutamine, GABA, and aspartate), the absolute value may be obtained through HPLC measurements. In this case, it is imperative that the GCMS labelling is interpreted alongside consideration of the absolute value of the substrates discussed. In most cases (as with the Krebs cycle intermediates), the absolute value cannot be obtained through HPLC and as such, only inferences can be made on the relative activity of the Krebs cycle. Furthermore, measurements through GCMS or HPLC cannot distinguish

the origin of these substrates (vesicular vs non-vesicular pool or astrocytic vs neuronal pool), unless the substrate is metabolically compartmentalized (such as aspartate). These weaknesses however do not discredit the importance of these results in dissecting the mechanisms of seizure generation in mitochondrial epilepsy. It has provided a relative assessment of the metabolic state in the tissue during mitochondrial epilepsy and implicated several metabolic pathways that may be important targets for therapeutic interventions.

Chapter 6 Measuring metabolic fluxes in specific cellular population during mitochondrial epilepsy

6.1 Introduction

The experimental findings presented in Chapter 5 provided a comprehensive assessment of the state of tissue metabolism during mitochondrial epilepsy. However, the techniques used for this type of measurement do not directly measure mitochondrial respiration. One technique to address such gap is the use of Seahorse XF24 Flux Analyzer, which has been used extensively to measure mitochondrial respiration in tissues and isolated mitochondria (Beeson *et al.*, 2010; Rogers *et al.*, 2011; Sauerbeck *et al.*, 2011). This particular piece of equipment provides a live monitoring of oxygen consumption rates (OCR) and extracellular acidification rates (ECAR) as marker of mitochondrial respiration and glycolytic activity, respectively. However, most of the studies conducted with this technique has used cells that have been cultured on the Seahorse plate. It can be argued, however, that the use of *ex vivo* cell culture system would not accurately reflect the *in vivo* condition. As an example, the process of cell culture itself is known to impose oxidative stress (Halliwell and Whiteman, 2004), which would alter the metabolic profile of the cells. As such, this technique is not directly applicable for our purpose as the changes in the metabolic profile are due to pharmacological manipulations that may or may not induce a permanent change in the metabolism of the cells. Thus, a technique needs to be developed to be able to acutely isolate cells from fresh tissue preparation, which would resemble the *in vivo* condition as much as possible.

Another advent in cell isolation in recent years is the magnetic-activated cell sorting (MACS) technique, which uses magnetic beads that recognizes specific cell surface antigens (Miltenyi *et al.*, 1990). One advantage of such technique is the rapid cell isolation process, which does not affect cell viability (Miltenyi *et al.*, 1990). Furthermore, the use of the magnetic beads allows the sorting of isolated cells based on their expressed cell surface markers.

Our mitochondrial epilepsy model is heavily based on the ‘dual neuronal – astrocytic hit’ hypothesis (see section 3.5)**,** which postulates the necessary recruitment of both the neuronal and astrocytic compartment in the generation of mitochondrial epilepsy. The results described in Chapter 5 have supported the involvement of both the neuronal and astrocytic metabolism during the epileptic state, but again, no direct quantification of mitochondrial respiration in these two specific cellular compartments have been made.

To address this knowledge gap, I developed a novel technique by pairing the acute cell isolation using magnetic-activated cell sorting with the measurement of metabolic fluxes in these isolated cells using Seahorse XF24 Flux Analyzer. Since the two distinct cell compartments critical to my model are the neurons and astrocytes, I chose to isolate these from acutely prepared hippocampal slices. Subsequently, I designed and conducted various setup of metabolic experiments using the Seahorse XF24 Flux Analyzer, in order to first characterize these cell populations and then test specific hypothesis developed in relation to the mechanisms involved in the generation of mitochondrial epilepsy.

Finally, it is universally accepted that mitochondria are major source of endogenous reactive oxygen species and that oxidative stress is intimately linked with mitochondrial dysfunction (Tiwari *et al.*, 2002; Halliwell and Whiteman, 2004; Ott *et al.*, 2007). Furthermore, oxidative stress has been implicated in other models of mitochondrial epilepsy as a core pathophysiological process (Liang and Patel, 2004; Cantu *et al.*, 2009). To give an indication of the level of oxidative stress in our model of mitochondrial epilepsy, a measurement of carbonylated protein was performed to compare levels of protein peroxidation in control and epileptic tissue.

6.2 Methods

Animal preparation and cell isolation was as described in section 2.14. Following cell isolation, these cells were seeded onto the Seahorse XF24 microplate for measurement of metabolic fluxes as described in section 2.15. In order to test out the various hypothesis developed, I have used various composition of Seahorse experimental media as described in Table 6-1. The results of three experimental setups will be discussed in this chapter and the three experimental setups are as described in Table 6-2 and the cartridge setups are as described in Table 6-3.

Table 6-1 Composition of media used in the Seahorse experiments

No	Media	Composition
1	Control media	Seahorse XF media + 10mM D-glucose + 5mM pyruvate + 3% FBS
2	Control media + glutamine	As in no 1, but with 2.5mM L-glutamine
3	Epileptogenic media	As in no 1, but with 0.1mM fluorocitrate
4	Epileptogenic media + glutamine	As in no 2, but with 0.1mM fluorocitrate

Table 6-2 Groups in the experimental setups

Exp cond.	Group 1	Group 2	Group 3	Group 4
1	Astrocyte in control media	Astrocyte in control media + glutamine	Neurons in control media	Neurons in control media + glutamine
2	Astrocyte in control media		Neurons in control media	
3	Astrocyte in control media	Astrocyte in epileptogenic media	Neurons in control media	Neurons in epileptogenic media
4	Astrocyte in epileptogenic media	Astrocyte in epileptogenic media + glutamine	Neurons in epileptogenic media	Neurons in epileptogenic media + glutamine

Table 6-3 Cartridge setup in the experimental setups. FCCP refers to the ionophore carbonyl cyanide-p-trifluoromethoxyphenylhydrazone and 2D-G refers to 2-deoxy-D-glucose.

Exp cond.	Port A	Port B	Port C	Port D
1	Oligomycin (1mg/ml)	FCCP (3mM)	2D-G (10mM)	Rotenone (500nM) and antimycin-A (2.5µM)
2	Water (v/v)	DMSO (v/v)	Control media (v/v)	Ethanol (v/v)
3	Potassium cyanide (10µM)	Rotenone (500nM)	L-glutamine (2.5mM)	Antimycin-A (2.5µM)
4	Potassium cyanide (10µM)	Rotenone (50nM)	FCCP (3mM)	Antimycin-A (2.5µM)

Once each run in the Seahorse machine had concluded, the cells were fixed in 4% PFA and post-hoc immunofluorescence was conducted as described in section 2.16. The values of the Seahorse measurement were normalized against the viable cell count in each well. From these normalized values, various parameters were

quantified according to the bioenergetics profile measurement as described in other studies (Nicholls *et al.*, 2010; Tan *et al.*, 2015). Extracellular acidification rate was analysed using the mathematical model suggested in previous publication to account for the contributions of mitochondrial respiration and glycolysis to extracellular acid production (Mookerjee *et al.*, 2015).

Measurement of carbonylated protein was conducted as described in section 2.10. All the data was tabulated and analysed as described in section 2.9.

6.3 Results

6.3.1 Magnetic-activated cell sorting produced comparable yield and viability in astrocytes and neurons

Neurons and astrocytes were isolated using the magnetic-activated cell sorting techniques. The technique has produced comparable yield and viability within the two cellular compartments (see Figure 6-1). These cells were deemed viable to be used for the measurement of metabolic fluxes using the Seahorse XF24 Analyzer system.

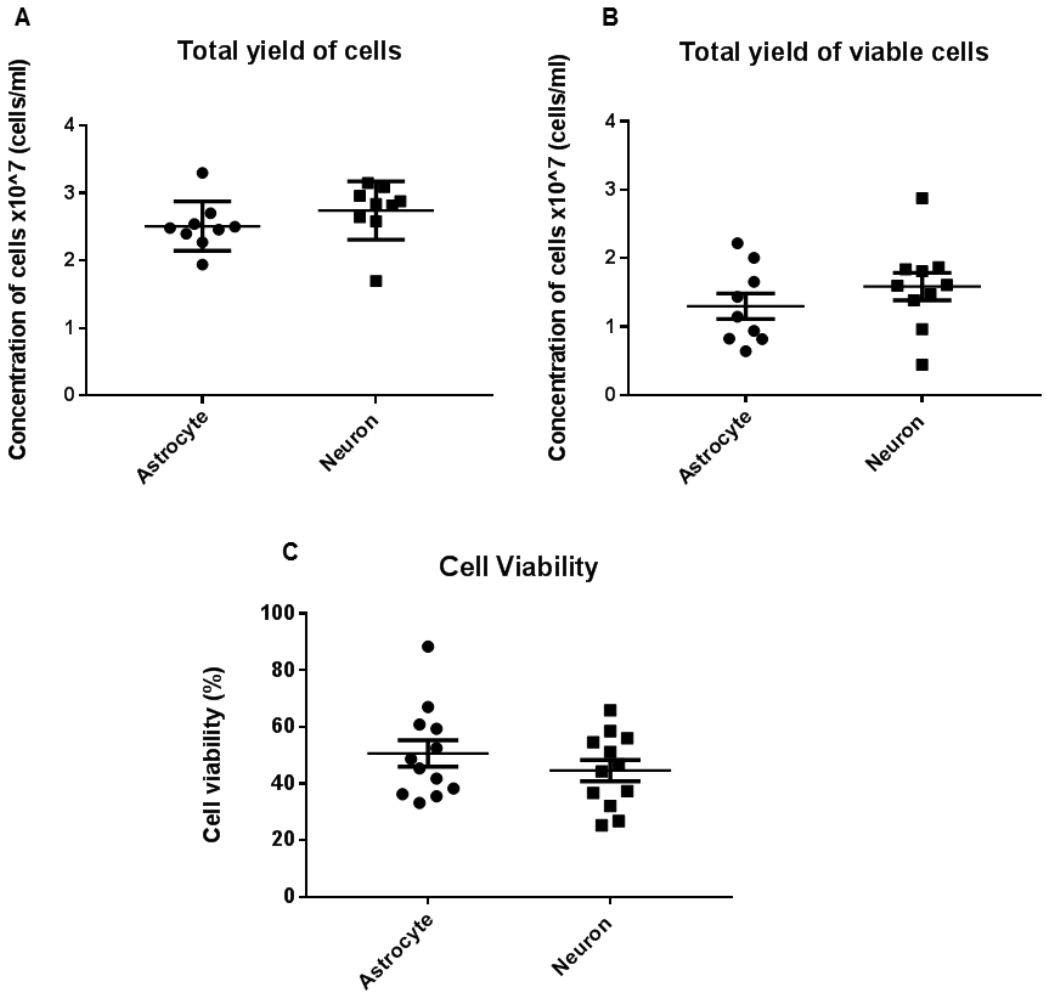

Figure 6-1 Cells isolated through MACS have comparable yield and viability. Shown in (A) is the total yield of cells isolated through the MACS protocol. The total yield of viable cells and percentage of cell viability was determined using tryptan blue cell viability assay and was calculated using automated cell counting, as shown in (B) and (C) respectively.

Overall, the total yield of the cells was significantly comparable ($p \geq 0.05$, $n = 9$), with average values of 2.51 ± 0.12 (x 10^7 cells/ml) for astrocytes and 2.74 ± 0.14 (x 10^7 cells/ml) with regards to neurons. The total yield of viable cells was also significantly comparable ($p \geq 0.05$, $n = 9$), with an overall mean value of 1.30 ± 0.19 (x 10^7 cells/ml) for astrocytes and 1.59 ± 0.20 (x 10^7 cells/ml) for neurons. Finally, the percentage of cell viability was not significantly different ($p \geq 0.05$, $n = 9$), with a calculated mean value of 50.62 ± 4.67 % viability for astrocytes and 44.63 ± 3.78 % viability for neurons.

6.3.2 Metabolic characterization of the isolated cellular compartments

The following sub-section described the results from experimental condition 1 (see Table 6-2 and Table 6-3). This experimental condition is designed to characterize the metabolic profile of the isolated cellular compartments using standard experimental protocol in measuring metabolic fluxes using the Seahorse XF24 Flux analyser. This standard protocol includes the sequential application of oligomycin, FCCP, 2-DG, and the co-application of rotenone and antimycin-A. Oligomycin is a well characterized inhibitor of ATP synthesis, by inhibiting the F0 portion of the catalytic subunit of mitochondrial respiratory chain complex V (ATP synthase) (Penefsky, 1985). FCCP is a mitochondrial uncoupler, which transports proton across the phospholipid bilayer membranes and uncouples mitochondrial respiration from ATP production (Benz and McLaughlin, 1983). This uncoupling causes the stimulation of oxygen consumption (mitochondrial respiration) without a concomitant increase in ATP synthesis, enabling the exploration of a cell's maximum respiratory capacity. 2-DG (2-deoxy-D-glucose) is a potent inhibitor of glycolysis, through the inhibition of the enzyme hexokinase (TeSlaa and Teitell, 2014). Finally, the co-application of rotenone, a mitochondrial complex I inhibitor, and antimycin-A, a mitochondrial complex III inhibitor, caused a complete inhibition of electron transport chain. The remaining rate of respiration can then be attributed to non-mitochondrial respiration. These experiments have demonstrated that the isolated astrocytes and neurons exhibited a distinct metabolic profile (see Figure 6-2).

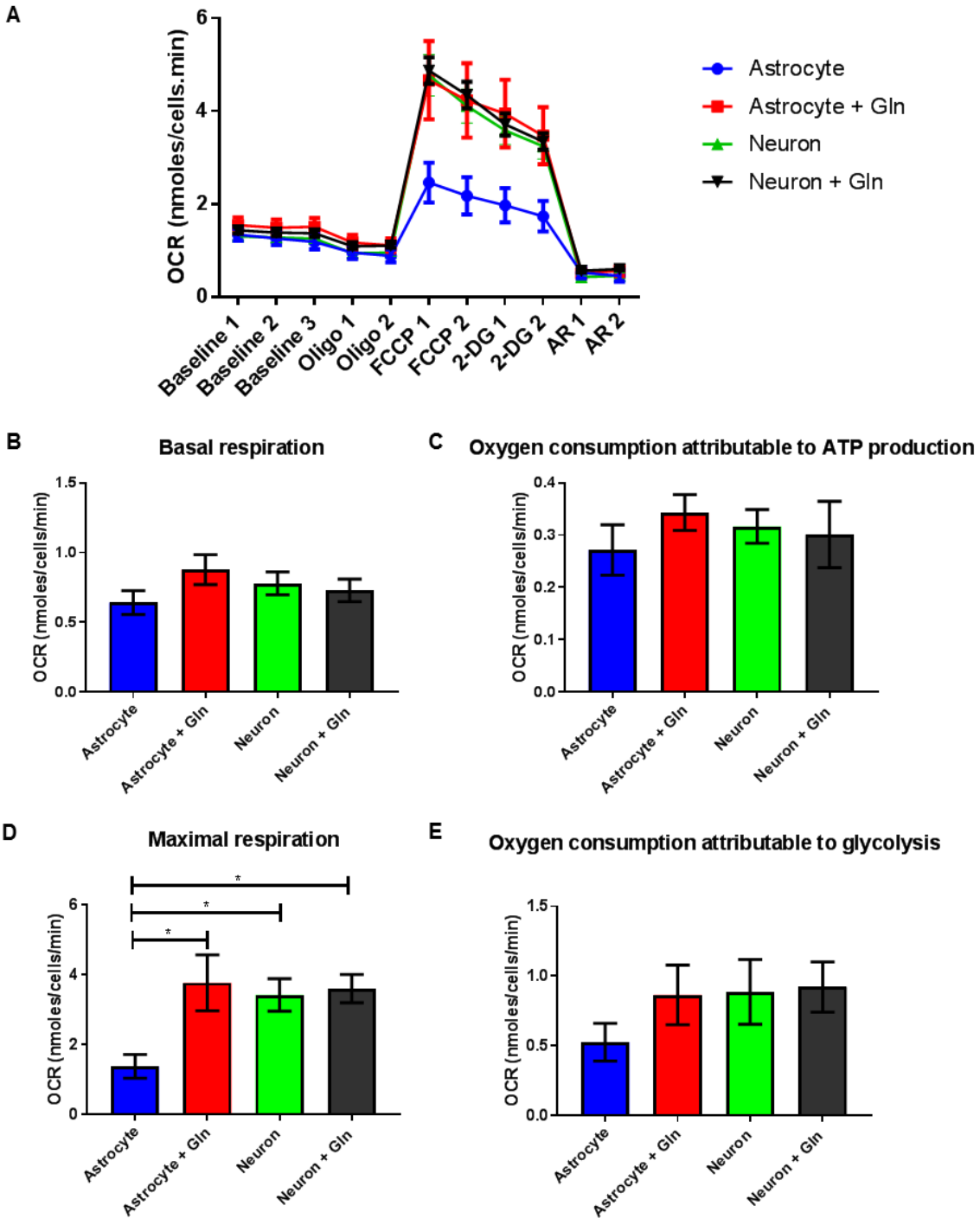

Figure 6-2 Oxygen consumption rate of astrocytes and neurons in the absence or presence of glutamine shows a distinct metabolic profile. Shown in (A) is the oxygen consumption rate following the experimental sequence as described in experimental condition 1 (see Table 6-2, N = 3 animals). Basal respiration, shown in (B), is obtained after subtracting the non-mitochondrial respiration rate from the baseline respiration rate. (C) and (E) shows the oxygen consumption rate that is attributable to ATP production and glycolysis, respectively. (D) shows the maximal respiration capacity attainable by each cell groups following the application of FCCP. * indicates statistical significance ($p \leq 0.05$).

Overall, the metabolic profile of the cells is relatively similar except for a distinct difference in the maximal respiratory capacity in the absence or presence of glutamine (n = 13 for astrocytes with or without glutamine, n =15 for neurons with or without glutamine). There was no significant difference ($p \geq 0.05$) in the basal respiration between all the groups (0.64 ± 0.08 nmoles/cells/min astrocytes vs 0.88 ± 0.11 nmoles/cells/min astrocytes + glutamine vs 0.78 ± 0.08 nmoles/cells/min neurons vs 0.73 ± 0.08 nmoles/cells/min neurons + glutamine). There was also no significant difference ($p \geq 0.05$) in the oxygen consumption attributable to either ATP production (0.27 ± 0.05 nmoles/cells/min astrocytes vs 0.34 ± 0.03 nmoles/cells/min astrocytes + glutamine vs 0.31 ± 0.03 nmoles/cells/min neurons vs 0.30 ± 0.06 nmoles/cells/min neuron + glutamine) or glycolysis (0.53 ± 0.14 nmoles/cells/min astrocytes vs 0.87 ± 0.21 nmoles/cells/min astrocytes + glutamine vs 0.89 ± 0.23 nmoles/cells/min neurons vs 0.92 ± 0.18 nmoles/cells/min neurons + glutamine) between all the groups. There was, however, a significant difference ($p \leq 0.05$) in the maximal respiration, where the maximal respiration of astrocyte (1.38 ± 0.34 nmoles/cells/min) was significantly lower ($p \leq 0.05$) than that of astrocyte in the presence of glutamine (3.78 ± 0.80 nmoles/cells/min) and of neurons in the absence (3.43 ± 0.47 nmoles/cells/min) or presence of glutamine (3.61 ± 0.40 nmoles/cells/min). This significant increase in maximal respiration by glutamine appears to be selective to astrocytes and is likely to enable astrocytes to achieve the maximal respiration capacity similar to that of neurons.

When analysing the ECAR data, I found that some of the cells have an ECAR profile that is directly correlated with the OCR measurements (see Figure 6-4.A). This means that 100% of the extracellular acid production is directly attributable to CO_2 generated as byproduct of mitochondrial respiration (from the TCA cycle). Specifically, following calculation according to the mathematical model (Mookerjee *et al.*, 2015), 6 out of 13 wells (46.15 %) of astrocytes had 100% of their ECAR attributable to CO_2 generated by oxidative respiration while 9 out of 14 wells (64.29 %) of neurons had 100 % of their ECAR attributable to CO_2 generated by oxidative respiration. This profile is slightly different when glutamine is present in the media. In the presence of glutamine, astrocytes become significantly more oxidative, $X^2(1,N=13) = 4.95$, $p = 0.03$, with 10 out of 13 wells (76.92 %) having 100 % of their ECAR attributable to CO_2 generated by oxidative respiration whereas neurons become significantly less oxidative, $X^2(1,N=15) = 3.85$, $p = 0.05$, with 6 out of 15 wells (40.00 %) having 100 % of their ECAR attributable to CO_2 generated by oxidative respiration.

The relative contribution of glycolysis towards ECAR in our isolated cellular system appears to be very low. Specifically, there was an average of 20.94 ± 9.29 % and 4.64 ± 2.40 % glycolytic contribution towards ECAR in astrocytes and neuron respectively. This appears to be quite different but is not statistically significant ($p \geq 0.05$), perhaps due to low sample size. In the presence of glutamine, this value has slightly changed with a calculated mean value of 4.64 ± 2.40 % and 12.40 ± 5.12 % glycolytic contribution towards ECAR in astrocytes and neuron respectively. This profile again seems to be different from the profile in absence of glutamine, but this difference is yet again not statistically significant ($p \geq 0.05$), possibly due to low sample size.

In general, our acutely isolated cells exhibited high oxidative respiration and in most cases, all of the ECAR is directly attributable to CO_2 generated from oxidative respiration. Therefore, ECAR cannot be used as a reliable indicator of glycolytic activity in our isolated cells system. However, these series of results (OCR and ECAR) truly demonstrated that the isolated cells are biologically viable and exhibited distinct metabolic profile, suggesting the relative selectivity of the isolation process. However, due to the inaccuracy of ECAR as a glycolytic indicator, for the remainder of this thesis, only OCR results will be presented and analysed.

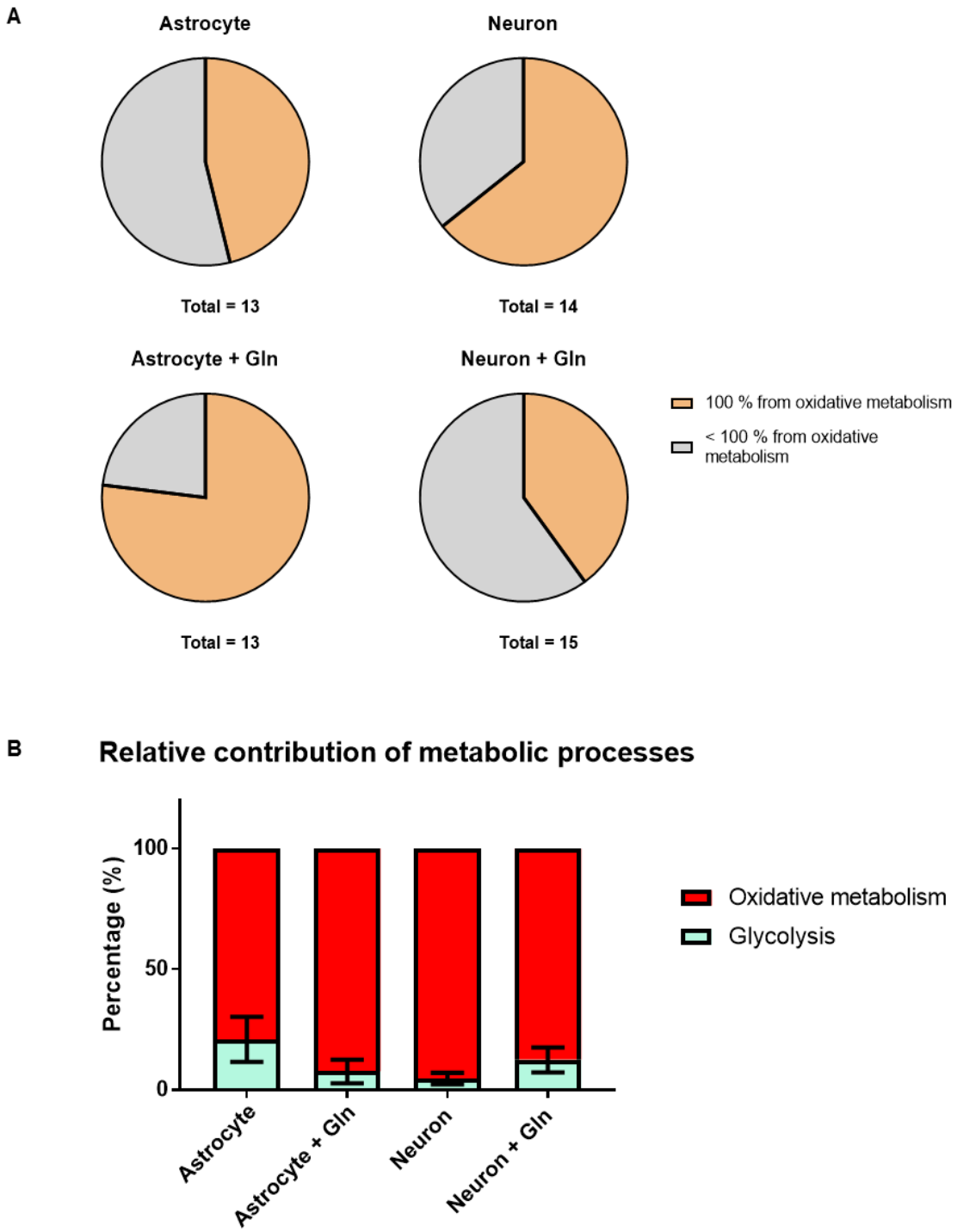

Figure 6-3 ECAR is mostly attributable to CO_2 generated from oxidative metabolism; yet still there exists a distinction between astrocytes and neurons. Shown in (A) is the proportion of wells in each group has their ECAR 100% attributable to CO_2 generated from oxidative metabolism following mathematical adjustment. Shown in (B) is the relative contribution of oxidative metabolism and glycolysis to the ECAR value following adjustment.

6.3.3 Cell's metabolic flux measurement is relatively stable over time

To examine the stability of the cell's metabolic flux measurement over time, I devised an experimental condition whereby the isolated cells were exposed to vehicle in accordance to the sequence of exposure in the experimental protocol (particularly pertaining to condition 3). The sequence of vehicle injection in the cartridge was as described in condition 2 in Table 6-3.

The oxygen consumption rate is very stable over time (see Figure 6-4) and is unaffected ($p \geq 0.05$) by exposure to the vehicle or time in both neurons (baseline 3: 1.33 ± 0.06 nmoles/cells/min vs ethanol 2: 1.40 ± 0.09 nmoles/cells/min, n=5) and astrocytes (baseline 3: 1.31 ± 0.21 nmoles/cells/min vs ethanol 2: 1.40 ± 0.09 nmoles/cells/min, n=5). These results further validate this technique for use to assess metabolic profile of acutely isolated neurons and astrocytes in various experimental conditions.

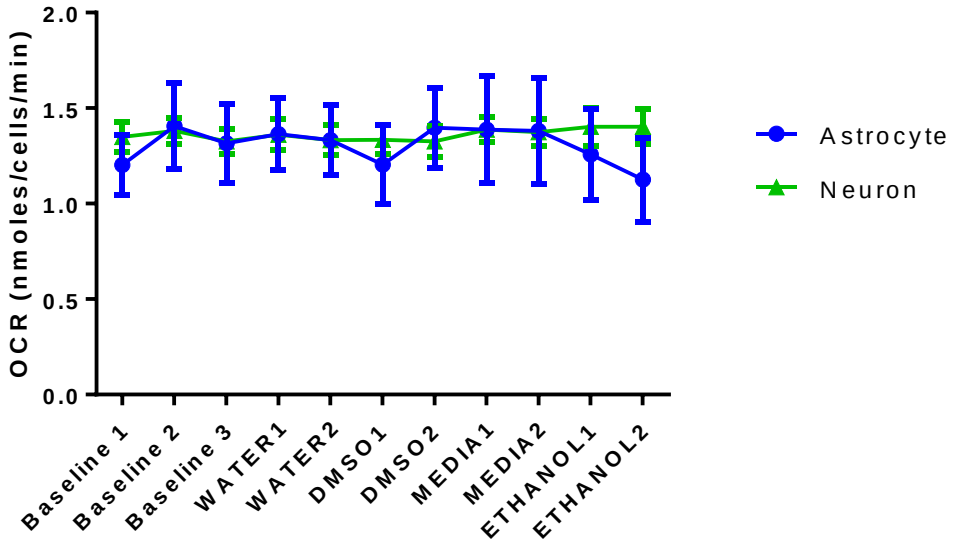

Figure 6-4 Oxygen consumption rate of astrocytes and neurons is relatively stable over time and unaffected by exposure to vehicle. These results are from condition 2 in Table 6-2 and Table 6-3 (N=1 animal).

6.3.4 Measurement of cellular mitochondrial respiration following the induction of mitochondrial epilepsy

After demonstrating the feasibility and stability of this technique, I designed an experimental setup to measure the degree of mitochondrial respiration as each component of the mitochondrial epilepsy protocol is applied onto the isolated cells (see condition 3 in Table 6-2 and Table 6-3). The isolated neurons and astrocytes were exposed to either the control media or the epileptogenic media. The epileptogenic media contains 0.1mM fluorocitrate in addition to the standard composition of the control media. The cells were then incubated in these media for 30 minutes prior to being measured in the Seahorse machine. This step is reminiscent of the pre-incubation with 0.1mM fluorocitrate in the standard mitochondrial epilepsy protocol (see section 2.5). Cyanide (10μM) was then injected through the cartridge first and rotenone (500nM) next, to see the acute impact of each of these mitochondrial inhibitors on oxygen consumption rate. Glutamine was then injected at the 'rescue' concentration of 2.5mM to examine if any acute rescue of the respiration is seen following the mitochondrial epilepsy protocol. Finally, antimycin-A was again applied to measure total mitochondrial respiration.

Basal respiration is not significantly different ($p \geq 0.05$) between the control and the epileptogenic media in both astrocytes (1.08 ± 0.12 nmol/cells/min control, n=12 vs 1.12 ± 0.12 nmol/cells/min with fluorocitrate, n=13) and neurons (1.33 ± 0.16 nmol/cells/min control, n=13 vs 1.15 ± 0.10 nmol/cells/min with fluorocitrate, n=15). Following the application of all of the components of the mitochondrial epilepsy protocol, mitochondrial respiration is almost completely inhibited (see Figure 6-5). There is no significant difference ($p \geq 0.05$) in the degree of mitochondrial respiration inhibition by cyanide (13.17 ± 3.94 % astrocyte vs 17.17 ± 5.61 % astrocyte with fluorocitrate vs 10.30 ± 2.08 % neuron vs 8.07 ± 1.45 % neuron with fluorocitrate) and rotenone (83.87 ± 2.79 % astrocyte vs 80.09 ± 4.18 % astrocyte with fluorocitrate vs 75.69 ± 3.37 % neuron vs 84.86 ± 3.76 % neuron with fluorocitrate) between all of the groups. Cyanide (10μM) inhibited an average of 12 % of mitochondrial respiration across all the groups while rotenone (500nM) inhibited an average of 81 % of mitochondrial respiration across all the groups. Glutamine did not cause any significant rescue in mitochondrial respiration and there was no significant difference ($p \geq 0.05$) between the responses of any of the groups towards the acute glutamine (2.5mM) application (3.43 ± 1.77 % astrocyte vs 4.74 ± 1.77 % astrocyte with fluorocitrate vs

0.90 ± 2.37 % neuron vs 4.17 ± 1.81 % neuron with fluorocitrate). On average, there was only about 3 % of mitochondrial respiration that was rescued by the acute glutamine application.

Overall, the pre-incubation with fluorocitrate did not inhibit mitochondrial respiration in both cellular compartments. The subsequent application of cyanide (10μM) and rotenone (500nM) inhibited most of the cells' mitochondrial respiration (circa 90%). The acute application of glutamine was not able to rescue mitochondrial respiration in this particular scenario, perhaps due to the almost complete inhibition of mitochondrial respiration by the inhibitors applied.

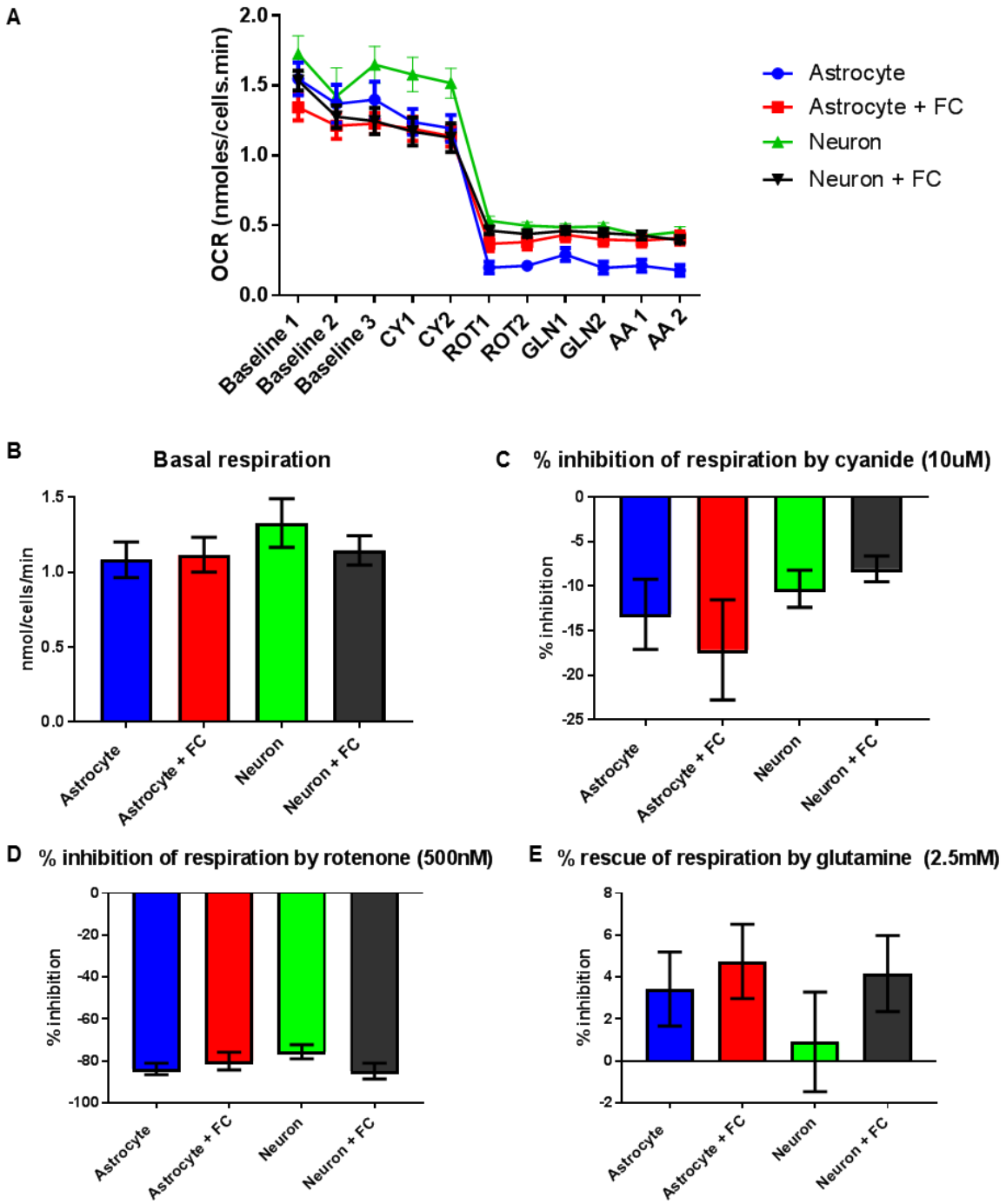

Figure 6-5 There is similar degree of inhibition of mitochondrial respiration by each components of mitochondrial respiration in astrocytes and neurons alike. Shown in (A) is the oxygen consumption rate following the experimental sequence as described in experimental condition 3 (see Table 6-2, N=3 animals). Basal respiration, shown in (B) is not different between the control and the epileptogenic media (for media composition, see Table 6-1). (C) and (D) shows the percentage of inhibition of mitochondrial respiration by the cyanide and rotenone component of the mitochondrial epilepsy induction protocol respectively. (E) shows the percentage of rescue of mitochondrial respiration by acute application of glutamine (2.5mM).

6.3.5 Glutamine may be able to rescue partial mitochondrial respiration inhibition, particularly in astrocytes

Despite the strength of this technique with regard to the metabolic assessment of discrete cellular populations, caution is advisable when attempting to translate the findings on a tissue level (brain slice) to a cellular level. In addition to housing the neurons and glial cells, a brain tissue (or slice) is also composed of extracellular matrix with unique properties and compositions such as proteoglycans and glycoproteins (Novak and Kaye, 2000). This extracellular matrix is particularly important when discussing the concept of drug delivery into brain tissue as it provides a physical form of barrier to diffusion of active compounds (Vargová and Syková, 2014). Therefore, the actual cellular concentration of a drug in a tissue setting would always be lower than the administered drug concentration. Hence, when designing a study at *ex vivo* isolated cell system, a submaximal concentration of the drug should be applied to more closely resemble the cellular concentration of the drug. However, the difficulty lies in measuring the actual cellular concentration of the drug at a tissue setting, which cannot easily and accurately be determined.

In my case, from results described in section 6.3.4, I find that exposure to both 10μM of cyanide and 500nM of rotenone resulted in an almost complete inhibition of mitochondrial respiration in both cellular compartments. One can safely infer that due to the generation of epileptic activity with this concentration of mitochondrial respiratory chain inhibitors at the tissue level that this concentration would not induce complete inhibition of mitochondrial respiration (otherwise, generalized energy failure would have occurred instead). To address this, I decided to re-examine the impact of glutamine on a partial mitochondrial respiratory chain inhibition using a lower concentration of the respiratory chain inhibitors. Since cyanide at its maximal concentration of 10μM only inhibited about 10% of mitochondrial respiration, I did not feel that it is necessary to titrate the concentration even lower. Instead, I decided to titrate the rotenone concentration, which was the major contributor to the complete respiratory chain inhibition in the previous experimental condition. Therefore, I chose a 10 times dilution of the rotenone concentration to 50nM to ensure a still potent respiratory chain inhibition without eliciting its maximal inhibitory effect. To examine the remaining mitochondrial respiration capacity in the cells following this partial respiratory chain inhibition, I decided to apply FCCP (3mM) following both the cyanide and rotenone application. Finally, antimycin-A was again applied to examine the non-

mitochondrial respiration. Furthermore, to properly examine the effect of glutamine on the metabolism, I decided to revert to pre-incubating the cells with glutamine in the media rather than acutely applying the glutamine through the cartridge injection. This allows accumulation of glutamine in the cells and the adaptation of the cellular metabolic machinery to the presence of glutamine prior to the respiratory chain inhibitions.

Overall, this combination of concentration of respiratory chain inhibitors was able to produce a partial inhibition of mitochondrial respiration (see Figure 6-6). Again, there was no significant difference ($p \geq 0.05$) in the degree of mitochondrial respiratory inhibition by cyanide (10μM) or the lower concentration of rotenone (50nM) across all of the groups. This lower concentration of rotenone (50nM) inhibited an average of 53 % mitochondrial respiration across all of the groups, instead of the average of 81 % inhibition with the maximal tissue concentration (500nM). There was, however, a trend where there was less inhibition of mitochondrial respiration by the 50nM rotenone in the astrocyte in the presence of glutamine in the media (62.85 ± 2.59 % astrocyte, n=5 vs 43.26 ± 4.70 % astrocyte with glutamine, n=5). There was a similar trend with regards to the neuron, but not as apparent as astrocytes (56.50 ± 8.28 % neuron, n=5 vs 47.88 ± 6.92 % neuron with glutamine, n=5). Due to a logistical limitation, I was unable to replicate this experiment, but with enough replicates, this trend would most probably be more apparent and reaches statistical significance. Again, there was no statistically significant difference ($p \geq 0.05$) in the maximal respiration capacity following the partial respiratory chain inhibition across all the groups. There was, however, a trend where there is slightly higher maximal respiration capacity in both neurons and astrocytes in the presence of glutamine (0.25 ± 0.05 nmol/cells/min astrocyte vs 0.30 ± 0.06 nmol/cells/min astrocyte with glutamine vs 0.27 ± 0.04 nmol/cells/min neuron vs 0.38 ± 0.04 nmol/cells/min neuron with glutamine). Again, with enough replicates of this experimental design, this trend would probably be more apparent and be a statistically significant difference.

Glutamine shows a promising potential as a potent mitochondrial respiration modulator and future works should focus on replicating this experimental design to truly validate this mitochondrial protective effect of glutamine.

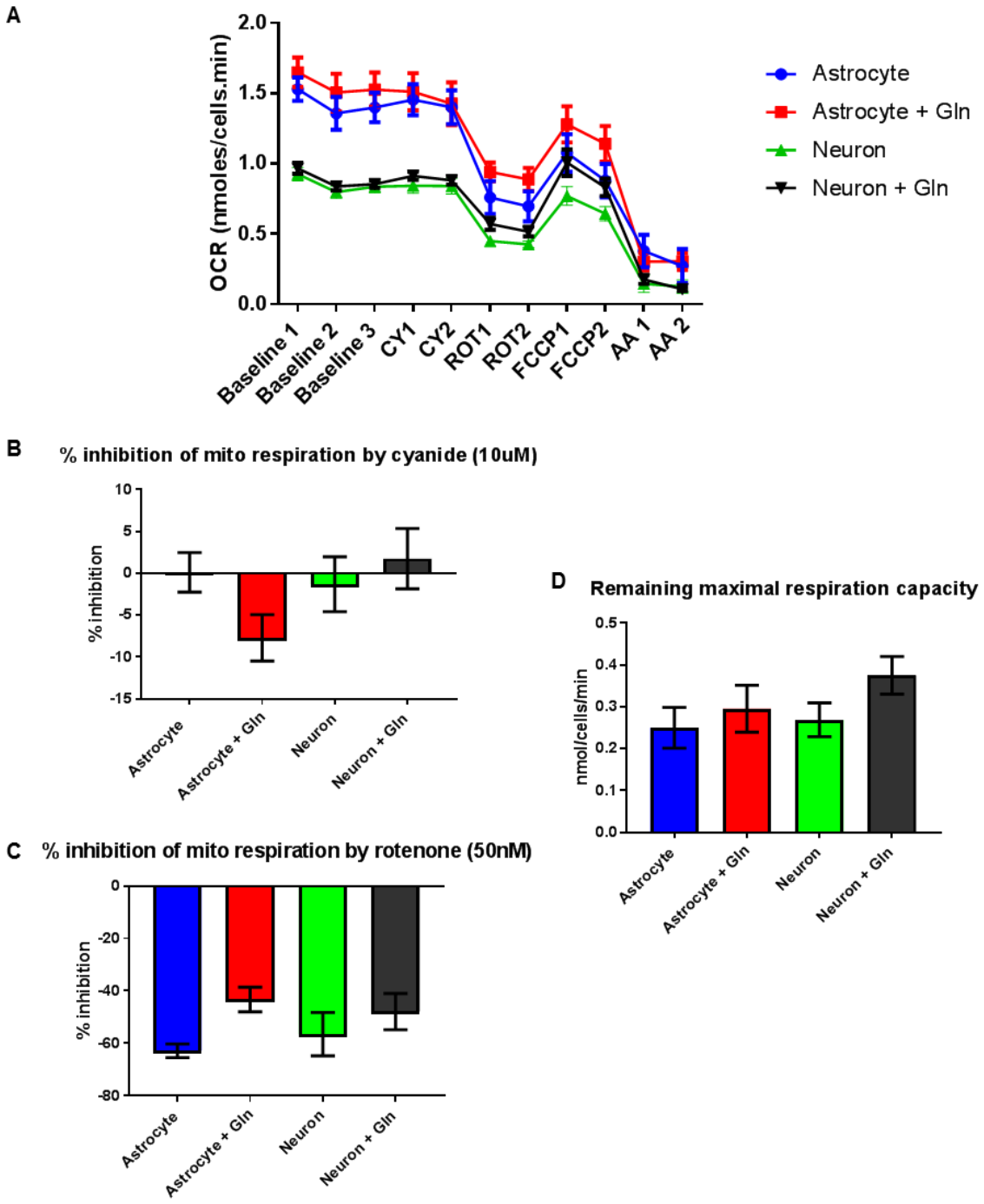

Figure 6-6 Glutamine may be able to rescue partial mitochondrial respiration inhibition, particularly in astrocytes. Shown in (A) is the oxygen consumption rate following the experimental sequence as described in experimental condition 4 (see Table 6-2, N = 1 animal). (B) and (C) shows the percentage of inhibition of mitochondrial respiration by cyanide (10μM) and a lower concentration of rotenone (50nM) in astrocytes and neurons in an epileptogenic media with or without glutamine (2.5mM). (D) shows the remaining maximal respiration capacity after the partial respiratory chain inhibition, as stimulated by the FCCP application.

6.3.6 There is significantly higher protein peroxidation in the epileptic tissue as compared against control tissue

Mitochondrial epilepsy has long been associated with a significant degree of oxidative stress in the tissue (Liang and Patel, 2004; Cantu *et al.*, 2009). As an indicator of oxidative stress, I measured carbonyl concentration in the tissue, which is a direct measure of protein peroxidation (Levine *et al.*, 1994; Suzuki *et al.*, 2010).

There is a significantly higher ($p \leq 0.05$) carbonyl concentration in the epileptic tissue (80.98 ± 16.30 nmol/mg protein, n = 8) as compared against the control tissue (29.03 ± 6.07 nmol/mg protein, n = 10).

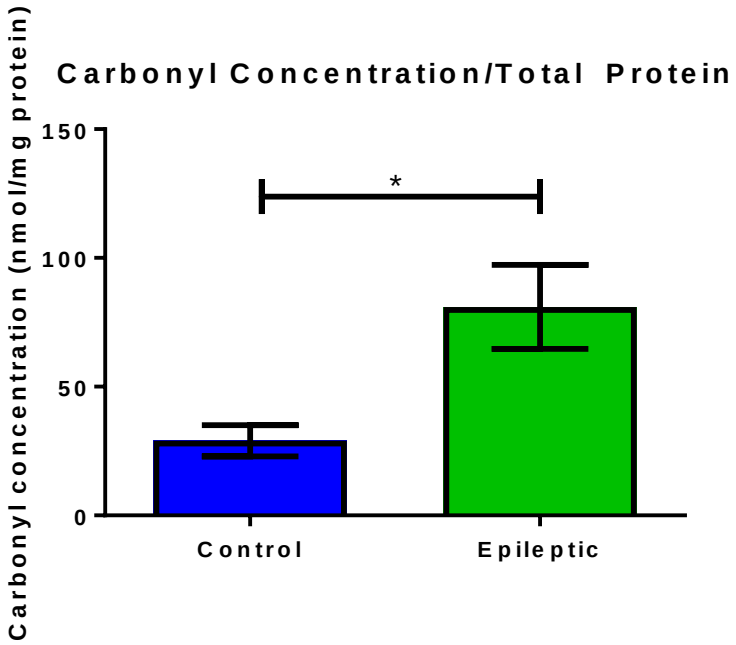

*Figure 6-7 There is a significantly higher carbonyl concentration in the epileptic tissue as compared against the control tissue. * indicates statistical significance ($p \leq 0.05$).*

6.4 Discussion

6.4.1 Cell isolation

As explained in section 6.1, there is a need to develop a method to acutely isolate specific cellular population from fresh tissue preparation to resemble the *in vivo* condition as much as possible. The method that I chose to work with was the magnetic-activated cell sorting (MACS) technique. In order to acutely isolate cells from fresh tissue, I required a cell isolation technique that was rapid and capable of producing a pure isolate. Previous studies have indeed shown that the MACS technique is fairly rapid and can produce a viable pure cell population, as it is separated through the specific conjugation between the magnetic beads and the cell's surface antigen (Miltenyi *et al.*, 1990; Marek *et al.*, 2008; Willasch *et al.*, 2009).

When I applied the MACS technique, I found that the cell isolation technique is relatively quick with the whole cell isolation process taking around 5 – 6 hours to complete for both the neuronal and astrocytic population. It also produced a relatively high total yield of cells with an average of around $2.6 \pm 1.0 \times 10^7$ cells/ml. Viability of the cells was slightly lower than the previously reported viability at around 50 %. This is probably due to the slightly older age of animals that I have used in my study. To conform with our other studies (electrophysiological and metabolic mapping), I decided to use the standard adult 10 weeks old Wistar rats for this study as well. It is well established, with other cell isolation techniques such as the density gradient separation, that cells from aged animals tend to be less viable (Brewer, 1997). The total yield of viable cells, however, was relatively comparable between both neurons and astrocytes.

Overall, the MACS technique has been able to isolate a relatively high yield of viable neurons and astrocytes for measurements of metabolic fluxes. The technique is unique to the other techniques (for example, the previously mentioned density gradient separation or immunopanning), in that it is relatively rapid and is quite specific in its separation of the cell population (to be discussed further in section 6.4.2.1).

6.4.2 Metabolic characterization of the cell isolates

Experimental condition 1 was designed to characterize the metabolic profile of cell's line by assessment of its capacity for ATP synthesis, glycolysis, and maximal respiration through the sequential application of various pharmacological inhibitors. Two parameters are continuously monitored throughout the experiment, namely the oxygen consumption rate (OCR) and the extracellular acidification rate (ECAR).

6.4.2.1 Oxygen consumption rate

Oxygen consumption rate is used as an indicator of cellular respiration (see Figure 6-2). After accounting for non-mitochondrial respiration obtained from the remaining respiration following complete mitochondrial inhibition with rotenone and antimycin-A, a basal respiration value is obtained as a parameter of mitochondrial respiration. The basal respiration rate was not significantly different between the neurons and astrocytes. This suggests that there is no difference in the oxygen consumption rate between astrocytes and neurons under physiological condition, which has been reported previously in a study on isolated mitochondria (Lopez-Fabuel *et al.*, 2016).

Inhibiting ATP synthase with oligomycin is a classic method to evaluate mitochondrial coupling as ATP production through phosphorylating respiration is stopped. Only a small amount of the oxygen consumption rate is attributable to this (an average of 0.3 nmoles/cells/min or about 30% of the basal respiration) and it is not significantly different between astrocytes and neurons. This value is comparable to previous studies on cultured neurons (Clerc and Polster, 2012). I also inhibited glycolysis with 2-deoxy-D-glucose to evaluate how much oxygen consumption is attributable to glycolysis and again, this was not significantly different between astrocytes and neurons. Overall, this finding suggests that oxygen consumption under physiological condition, that is attributable to both glycolysis and ATP production, is similar between astrocytes and neurons; confirming the inference made from the basal respiration rate.

Although all the other respiratory parameters are comparable between the neurons and the astrocytes, there is a distinct significant difference in maximal respiration capacity. The maximal respiration capacity is significantly higher in neurons

than in astrocytes. This distinction, as measured by FCCP, is comparable to previous observations on cultured cortical neurons and astrocytes (Divakaruni *et al.*, 2014). It is well established that astrocytes and neurons have different metabolic profile when responding to stress. The viability of neurons under a metabolic stress depend on provision of oxidative phosphorylation, whereas astrocytes depend more on glycolysis (Almeida *et al.*, 2001). Furthermore, there is a structural difference in the mitochondrial complex I assembly that has been shown to lead to a bioenergetics distinction between neurons and astrocytes. Specifically, it has been shown that in astrocytes, there is a higher proportion of free complex I as opposed to neurons, where most of the complex I is embedded into supercomplexes. This discrepancy leads to poor mitochondrial respiration but higher reactive oxygen species production in the astrocytes as compared to neurons (Lopez-Fabuel *et al.*, 2016). Although FCCP is not a metabolic stressor per se, the uncoupling mechanism artificially creates a system whereby the mitochondria are forced to operate at its maximal capacity, which would utilize the reserve capacity it had to respond to metabolic stress. Therefore, it would be unsurprising to see that neurons have much higher reserve capacity to upregulate their mitochondrial respiration under this artificial modulation.

This set of results can be viewed to add to the body of evidence that demonstrates that under basal physiological condition, there is no significant metabolic distinction between astrocytes and neurons. However, when exposed to metabolic stress or energetically demanding stimulus (such as electrical excitation), neurons had a much higher capacity for oxidative respiration than astrocytes. In addition to confirming the observations of other studies, this distinction also points to the selectivity of the cell isolation process using the MACS system to separate the cell population to the astrocytic and neuronal compartment.

6.4.2.2 Extracellular acidification rate

Extracellular acidification rate (ECAR) is a measure of the rate of proton (H^+) production, expressed as a change in the pH of the media over time. Two major factors contribute to the rate of extracellular acidification, namely glycolytic turnover and CO_2 production attributable to oxidative respiration (Divakaruni *et al.*, 2014; Mookerjee *et al.*, 2015).

In glycolysis, the conversion of glucose into lactate, irrespective of the pathways it undertake, necessitates the release of two protons molecule (Voet and Voet, 2011b; Berg *et al.*, 2012f), therefore acidifying the media. Another important component of glycolysis that can produce acidification is ATP hydrolysis. For every 2 moles of ATP that is hydrolysed in a system, one molecule of proton is released to the medium (Divakaruni *et al.*, 2014) and within the glycolytic breakdown of a molecule of glucose, two ATP molecules would be hydrolysed for each glucose molecule (Berg *et al.*, 2012f).

Initially, it was thought that ECAR is purely attributable to glycolysis but recent studies have demonstrated that CO_2 production from the Krebs cycle in oxidative metabolism may contribute towards the acidification process (Divakaruni *et al.*, 2014; Mookerjee *et al.*, 2015). The release of CO_2 into the aqueous media causes its reversible hydration and eventual dissociation into bicarbonate and a proton (Berg *et al.*, 2012c). In some systems, this may be particularly relevant as shown in a study using a pancreatic beta-cell line MIN6 that lacks lactate dehydrogenase expression, where the entire ECAR is shown to be attributable to the CO_2 release due to the oxidative metabolism of glucose (Sakamaki *et al.*, 2014).

Due to the varying nature of each cell line, it is recommended that the ECAR is initially evaluated by accounting for both the glycolytic turnover and the oxidative metabolism through a proposed mathematical model (Mookerjee *et al.*, 2015). In my system, a majority of the isolated cells were very oxidative (46% of astrocytes and 64% of neurons), meaning that 100% of the extracellular acid production is directly attributable to CO_2 generated from oxidative metabolism. This reflects previous observations where glycolytic turnover is generally not as robust in primary cells as in immortalized cells or proliferative cell cultures (Divakaruni *et al.*, 2014). This supports my view that the acutely isolated cells represent the *in vivo* condition better than a culture model, where metabolism may have significantly changed to adapt to the culture conditions. *In vivo,* it has been shown that both neurons and astrocytes are relatively oxidative (Hertz *et al.*, 2006; Ivanov *et al.*, 2013), which is what I have demonstrated in the isolated cells model. In addition, mitochondrial carbonic anhydrase, the enzyme responsible for the hydration and dissociation reaction as specified above, has been shown to be expressed exclusively in the neurons and astrocytes within the nervous system (Wong *et al.*, 1987; Ghandour *et al.*, 2000). Therefore, not surprisingly, both of our isolated neurons and astrocytes were able to generate substantial acidification through their oxidative metabolism.

When comparing the relative total contribution of glycolysis and oxidative metabolism towards extracellular acidification rate, a distinction exists between the astrocytes and neurons. Astrocytes are slightly less oxidative and more glycolytic than neurons. As mentioned above, the higher expression of free mitochondrial complex I in astrocytes suggests lower aerobic metabolism in astrocytes (Lopez-Fabuel *et al.*, 2016). Furthermore, astrocytes are shown to have higher capacity for glycolysis, due to the presence of the glycolysis-upregulating Pfkfb3 (6-phosphofructo-2-kinase/fructose-2, 6-bisphosphatase-3) protein; which is normally absent in the neurons (Herrero-Mendez *et al.*, 2009). Our observation, therefore, still supports this pattern and again reaffirms the selectivity of the isolation process.

Since the ECAR in our isolated cells is primarily reflective of the pattern of OCR, from this point forward, only relevant OCR data would be presented and discussed.

6.4.3 Stability of metabolic flux measurement

When working with primary cell isolates, the stability of the metabolic flux measurement over time needed to be established. Experimental condition 2 was designed to address this whilst also examining the presence or absence of vehicle effect.

Oxygen consumption rate is very stable in both neurons and astrocytes over time (see Figure 6-4), which indicate the viability of the cell isolates. Furthermore, the addition of all the vehicles used in the experimental designs during the metabolic flux measurements do not cause any significant change in the oxygen consumption rate. Out of all the vehicle, the most concerning vehicle would be the dimethyl sulfoxide (DMSO). Some studies have shown that DMSO may induce behavioural, cellular, or metabolic change at various concentrations (Cavas *et al.*, 2005; Nasrallah *et al.*, 2008; Galvao *et al.*, 2014). In my model, the addition of DMSO at the concentration used (0.1 %) did not affect the oxygen consumption rate in either neurons or astrocytes. This eliminates any concern for the ‘vehicle effect’ and validates further findings where drugs are applied using the vehicle as detailed below.

6.4.4 Mitochondrial respiration during mitochondrial epilepsy

Experimental condition 3 was designed to characterize the amount of mitochondrial respiration inhibited in neurons and astrocytes by the specific components of the mitochondrial epilepsy protocol.

Isolated cells were incubated in either a control or epileptogenic media (which contains 0.1 mM fluorocitrate). Pre-incubation with fluorocitrate did not alter the basal respiration of all the cells; neurons or astrocytes alike. As an inhibitor of astrocytic aconitase, fluorocitrate is expected to inhibit the Krebs cycle in astrocytes; which should bring about a subsequent reduction in oxidative metabolism. However, in this series of experiments, there was no change in the oxygen consumption rate in the astrocytes following fluorocitrate application. This supports previous finding where ATP level was found to be unaltered in the astrocytes following incubation with fluorocitrate; suggesting that fluorocitrate's inhibitory effect *in vivo* results from impairment of carbon flux rather than impairment of oxidative metabolism (Swanson and Graham, 1994). Furthermore, this discredits the idea that aconitase inhibition may produce high amount of reactive oxygen species which would impair mitochondrial respiration (Cantu *et al.*, 2009; Scandroglio *et al.*, 2014).

Potassium cyanide (10μM) caused a relatively low inhibition of mitochondrial respiration (about 15 % in astrocytes and 10 % in neurons). Cyanide is a well-established inhibitor of cytochrome-c-oxidase (complex IV) but the concentration I have used in this study (10μM) is relatively lower than the previously reported inhibitory values in other models (which is about 20μM) (Kalnenieks *et al.*, 2000; Leavesley *et al.*, 2008). Furthermore, it was suggested that mitochondrial respiration may consist of the cyanide-sensitive respiration and the cyanide-resistant respiration (CRR), which is shown to be associated with mitochondrial complex I (Esashi *et al.*, 1981; Veiga *et al.*, 2003). The effect of cyanide on mitochondrial respiration has not been well characterized within the central nervous system setting but it is well established that exposure to cyanide produces extensive reactive oxygen species, which may be beneficial at low concentrations (Correia *et al.*, 2012) or apoptotic-inducing at higher concentrations (Shou *et al.*, 2000). Either way, in our model, it would appear that there is a minimal inhibitory effect on respiration by the concentration of cyanide used (10μM). However, the absolute requirement of cyanide as a complex IV inhibitor in inducing mitochondrial epilepsy *in vitro* suggests that cyanide may have effects other than the

known metabolic actions. Cyanide has been shown in a multitude of studies to alter the electrophysiological properties of neurons, towards hyperexcitability and disinhibition (Brodie, 1959; Yamamoto and Tang, 1996; Whittaker *et al.*, 2011). In a study on inspiratory neuron, cyanide was found to shorten the duration of the burst and increase the frequency of the excitatory discharge (Brodie, 1959). In the intracellular recording of interneurons from the hippocampus, cyanide application reduced the firing rate significantly, whilst also inducing depolarization of the resting membrane potential (Whittaker *et al.*, 2011). Taken together, the effects that cyanide have on neurotransmission may represent an important mechanism by which cyanide, as part of the mitochondrial epilepsy induction protocol, modify the tissue to a state where it is prone to epileptogenesis. The exact mechanism, however, remains unknown.

Rotenone (500nM) caused a significant inhibition of mitochondrial respiration (about 80% in both astrocytes and neurons). Rotenone is well characterized as a selective inhibitor of mitochondrial complex I and the concentration I have used in this study (500nM) is again relatively lower than the previously reported IC_{50} (about 2μM) in isolated mitochondria (Gomez *et al.*, 2007; Frick *et al.*, 2013). However, in this study, the degree of inhibition by this concentration (500nM) is almost complete (circa 80%). This value is comparable to results in the HL-60 cell line (Li *et al.*, 2003) and is reflective of our cellular profile whereby our isolated cells rely heavily on oxidative metabolism (as explained above in section 6.4.2). As the largest mitochondrial complex (Janssen *et al.*, 2006), complex I is essential for the process of ATP production and is also a major source of mitochondrial reactive oxygen species. It is well known that inhibition of complex I causes extensive reactive oxygen species release and induces a significant degree of apoptosis (Testa *et al.*, 2005; Deng *et al.*, 2010; Siddiqui *et al.*, 2013). Combined, these may be responsible for the significant degree of inhibition of mitochondrial respiration by rotenone in our model.

Another interesting observation is that in the presence or absence of fluorocitrate, there seems to be no difference in the degree of mitochondrial respiration inhibition by either rotenone or cyanide. Therefore, it can be concluded that fluorocitrate did not increase the vulnerability of either astrocytes or neurons towards respiratory chain inhibition. Also, there is no significant difference in the degree of inhibition by both rotenone and cyanide in neurons as compared against astrocytes. This suggests there is no specific vulnerability of either neurons or astrocytes towards respiratory chain inhibition and that they are both equally inhibited by these inhibitors.

At this concentration, there was a much larger inhibition of mitochondrial respiration by the complex I inhibitor rather than the complex IV inhibitor. This reflects the original observation in the post-mortem neuropathological studies where there is a much larger complex I inhibition (~90%) and a much subtler complex IV inhibition (~40%) in the temporal cortex of the patients with mitochondrial epilepsy (Lax *et al.*, 2016).

Finally, as discussed above in section 6.3.5, when isolating neurons and astrocytes from their native tissue, the concentration of the drugs that these cells were exposed to is higher than the actual cellular concentration *in vivo*. This is primarily due to the dissociation of the extracellular matrix and other components of a tissue that would provide a physical barrier to the distribution of a drug onto the cells. Therefore, one should always be cautious in quantitatively analysing the pharmacological parameters (such as IC_{50}) of these drugs as it may not be directly comparable or relevant to the *in vivo* condition.

6.4.5 Effects of glutamine

The effects of glutamine have been addressed in a physiological (by experimental condition 1) as well as in a pathological context, during the state of metabolic inhibition during mitochondrial epilepsy (by experimental condition 3 and 4).

6.4.5.1 Physiological effects

The physiological effects of glutamine were examined in experimental condition 1, whereby the cells were either incubated in control media or media supplemented with 2.5mM L-glutamine. The effects of glutamine supplementation were evaluated by evaluating both parameters of a cell's metabolic state; the oxygen consumption rate (OCR) and the extracellular acidification rate (ECAR).

Glutamine did not alter the basal respiration of either astrocytes or neurons. The oxygen consumption attributable to both glycolysis and ATP production was also unaffected by glutamine incubation. However, glutamine significantly increased the maximal respiration of the astrocytes up to a level of maximal respiration value comparable to that observed in neurons (see Figure 6-2). This increase was only observed in astrocytes and was not seen in neurons exposed to the same

concentration of glutamine in the media. This finding suggests that glutamine can only be utilised by the astrocytes as metabolic fuel and not by neurons. Glutamine synthetase is exclusively expressed in the astrocytes (Anlauf and Derouiche, 2013); however, this enzyme is involved in the biosynthesis of glutamine and not in the utilisation (or degradation) of glutamine. The enzyme involved in the utilisation, glutaminase, is expressed in both neurons and astrocytes (Cardona *et al.*, 2015). Some studies have interestingly suggested that glutaminase activity is much higher in neurons than in astrocytes (Hogstad *et al.*, 1988). However, not much is known about the relative affinity of the glutaminase in neurons and astrocytes. In a study using tumour cell lines, it was found that during malignant transformation, there is an increase in oxidative respiration which is mediated by glutamine due to an increase in the affinity of glutaminase (Kovačević and Morris, 1972). There is, therefore, more to this effect than just the simple utilization of glutamine as a metabolic substrate. There may be a mechanism specific to the glial biology that is regulated by glutamine, of which with our current understanding remains unknown.

In terms of ECAR, glutamine altered the metabolic profile of the cells. Overall, the proportion of oxidative astrocytes significantly increase and the proportion of oxidative neurons significantly decrease. Therefore, it can be argued that glutamine somehow is able to upregulate oxidative respiration, as suggested by the OCR data as well. In recent studies, it is well characterized that glutamine is a key player in the growth of tumour cells. Glutamine has been shown to upregulate oxygen consumption, increase oxidative respiration, and to be an important carbon source for anaplerosis in these tumour cells (Reitzer *et al.*, 1979; DeBerardinis *et al.*, 2007; Weinberg *et al.*, 2010). The biology of glial cells is obviously very different to that of tumour cells but perhaps some of the insights obtained from the understanding of the role of glutamine in tumour cells may be applicable to the glial cells. In tumour cells, it is suggested that glutamine is essential for the generation of NADPH for its reductive power as well as for the anaplerosis of oxaloacetate for continued TCA cycle function (Kovačević and Morris, 1972). The study of complex I respiration in astrocytes has shown that due to the higher proportion of free complex I, oxidative respiration in astrocytes is characterized by high reactive oxygen species production and poorer mitochondrial respiration (Lopez-Fabuel *et al.*, 2016). Perhaps, the limiting factor in the spare respiratory capacity in astrocytes is the high reactive oxygen species that it would produce with its upregulation of aerobic respiration. Glutamine, as a source for NADPH

generation, could therefore compensate for this and essentially remove the limiting factor, allowing the astrocytes to reach its maximum spare respiratory capacity.

Regardless of the mechanism, the data produced in my studies has provided strong evidence that glutamine is a key player in astrocytic metabolism. It seems that glutamine has a positive effect towards modulating aerobic metabolism through mechanisms which remain unknown to this point.

6.4.5.2 Effects during mitochondrial epilepsy

Through experiments as discussed in section 4.3.6.3, glutamine was shown to have a suppressive effect on the induced mitochondrial epilepsy. Studies conducted in both Chapter 4 and Chapter 5 have suggested that one of the mechanism whereby glutamine has a 'rescue' effect is through the sustainment of GABA synthesis. To examine whether glutamine has a 'rescue' effect in terms of mitochondrial metabolism, I performed the metabolic flux measurement using the components of the mitochondrial epilepsy protocol and incorporate glutamine into the experimental design (see experimental condition 3 and 4).

In experimental condition 3 (see Figure 6-5), components of the mitochondrial epilepsy protocol were added and glutamine (2.5mM) was injected acutely through the cartridge following all the other components of the protocol. As explained in section 6.4.4, there was almost a complete inhibition of mitochondrial respiration following the injection of 10μM cyanide and 500nM rotenone in the presence or absence of 0.1mM fluorocitrate. Unsurprisingly, there was minimal effect of glutamine in terms of rescuing the mitochondrial respiration following this complete inhibition.

As argued in section 6.3.5, in the *in vitro* brain slice scenario, the cellular concentration of the inhibitors is unlikely to achieve the given bath concentration due to the physical barrier provided by the extracellular matrix. Therefore, the concentration I have applied during experimental condition 3 may be too high in terms of actual cellular concentration and I expect there to be only partial mitochondrial respiration block in the *in vitro* brain slice condition, rather than a complete inhibition. To simulate this, I titrated the concentration of the rotenone, which exhibited the biggest inhibitory effect, to a ten times diluted concentration (50nM). This produced approximately 50% inhibition in mitochondrial respiration and the effect of glutamine was evaluated by its

direct incorporation into the media rather than acute injection via the cartridge. In the presence of glutamine, there was a lower percentage of inhibition of mitochondrial respiration by rotenone (50nM) in neurons, but this reduction in complex I inhibition was more apparent in the astrocytes. This was not statistically significant due to the low power of the study (5 wells obtained from a single animal). However, this is promising evidence that glutamine may be able to attenuate mitochondrial respiration inhibition, in particular the complex I mediated respiration. Mechanisms by which it may induce this are currently unknown, but may be related to the reactive oxygen species, as discussed previously.

6.4.6 Oxidative stress during mitochondrial epilepsy

As outlined earlier, mitochondrial epilepsy has been intimately associated with a significant oxidative stress damage in the tissue (Liang and Patel, 2004; Cantu *et al.*, 2009). To assess oxidative stress in the epileptic tissue, I have chosen to measure the carbonyl concentration in the tissue. The carbonylation of the side chains of the amino acids occurs mostly due to protein peroxidation but can also occur due to the secondary reaction of aldehydes from lipid peroxidation (Dalle-Donne *et al.*, 2003). Regardless, it remains a good indicator of oxidative stress in the tissue and is the most commonly used biomarker due to its relative stability and ease of detection using the spectrophotometric assay following derivatization with DNPH (Suzuki *et al.*, 2010).

Unsurprisingly, there was a significantly higher concentration of carbonyl in the epileptic tissue as compared against the control tissue (see Figure 6-7). This confirms that there exists a significant degree of oxidative stress in the tissue following the induction of mitochondrial epilepsy. The source of this oxidative stress could be from any cells affected, but I postulate that this is correlated with the complete shutdown of the astrocyte population (as discussed in Chapter 3 to 5) during mitochondrial epilepsy. As discussed extensively in the previous subsections, the higher proportion of free complex I in the mitochondria of the astrocytes results in faster production and release of reactive oxygen species when compared with neurons (Lopez-Fabuel *et al.*, 2016). Therefore, it would be expected that when there is complete astrocytic shutdown that it would be accompanied by extensive reactive oxygen species in the tissue due to the loss of the extensive reducing power previously provided by the astrocyte.

6.5 Summary, strength, and weakness

In this chapter, I have presented a novel method of measuring metabolic fluxes in acutely isolated astrocytes and neurons by pairing the two powerful techniques of magnetic-activated cell sorting (MACS) and the Seahorse XF24 Metabolic Flux Analyzer. I have shown that the isolation process using MACS produced a relatively high yield of viable cells that is utilisable for the metabolic flux measurements. The astrocytes and neurons exhibited distinct metabolic profiles, supporting the specificity of the isolation process. In particular, the maximal respiratory capacity of neurons is much higher than that of astrocytes. In the presence of glutamine, however, the maximal respiratory capacity of astrocytes became similar to that of neurons. Both astrocytes and neurons are relatively oxidative in their respiration and most of their ATP production is attributable to oxidative phosphorylation. The presence of glutamine upregulated this oxidative metabolism in the astrocytes, but not in neurons.

Exposure to the components of the mitochondrial epilepsy at its *in vitro* concentration caused an almost complete inhibition of mitochondrial respiration. Interestingly, exposure to fluorocitrate did not cause any inhibition of mitochondrial respiration, supporting the previously reported effect of fluorocitrate on carbon flux rather than respiratory inhibition. The major respiratory inhibition originates from the rotenone component of the protocol. This reflects the original observation from the post-mortem neuropathological studies of patients with mitochondrial epilepsy. To examine the effect of glutamine in rescuing partial respiratory chain inhibition, I titrated the concentration of the rotenone and found that glutamine was able to attenuate the mitochondrial respiratory complex I inhibition specifically in the astrocytes.

Finally, to measure the degree of oxidative stress in the tissue, measurement of carbonylated protein was conducted. There was a significantly higher concentration of carbonylated protein in the epileptic tissue, suggesting an extensive oxidative damage in the epileptic tissue. I postulate that the major source of this oxidative damage is from the complete astrocytic shutdown during the state of epilepsy.

The technique shown and discussed in this chapter is novel in nature. Therefore, it requires a lot of optimization and validation to ensure its robustness. Some of these have been conducted, but ideally, a lot more validation can be performed (for instance with the media composition or modification to the isolation process to improve yield or purity). However, the process has shown to be promising and produce replicable

measurements. Some of these measurements conform very well to previously reported observations or values whilst some of them also provided novel interesting observation that needs to be followed up. Furthermore, confirmation that the isolation produces pure separate isolates have yet to be performed. This can be done through various means such as *post-hoc* immunofluorescence or the use of flow cytometry. Regardless, the use of this technique has provided the assessment of mitochondrial respiration in specific cellular population isolated from the acute brain slices; an issue that was not addressable by the techniques and experiments conducted in Chapter 5. Together, the studies in both Chapter 5 and Chapter 6 provided a very comprehensive assessment of the state of tissue and cellular metabolism during mitochondrial epilepsy.

Chapter 7 Final discussion and future work

7.1 Conceptualisation

The data presented in this thesis have focused on the development and understanding of a novel *in vitro* brain slice model of mitochondrial epilepsy. The rationale behind the development of this novel model has emanated from previously conducted neuropathological studies on patients with mitochondrial epilepsy. This work reported a profound loss of interneurons in the temporal neocortex of these patients and the remaining surviving interneurons presented with deficiency of mitochondrial complex I and complex IV subunit expression (Lax *et al.*, 2016). Using similar technique, the authors eventually also found that similar mitochondrial deficiency of complex I and complex IV was also observed in the astrocytes and there was also extensive reactive astrogliosis in the temporal neocortex of these patients (Lax *et al.*, unpublished data; see Figure 3-1). These findings provided the foundation to the functional modelling of mitochondrial epilepsy *in vitro*. Using a mitochondrial complex I inhibitor (rotenone), complex IV inhibitor (potassium cyanide), and a specific astrocytic aconitase inhibitor (fluorocitrate), I was able to robustly induce epileptiform discharges in the hippocampus CA3 in acutely prepared rodent brain slices. This induction is found to be specific to the concentrations and the incubation conditions used in this study (see section 3.3.1 for full details).

I further examined the face validity of this model by putting it through a battery of control experiments. First, I have described that the mitochondrial epilepsy induction is dependent on the presence of all three pharmacological components of the protocol. On its own, neither of these pharmacological agents at the concentrations used was able to induce epileptiform discharges in the hippocampus CA3. Additionally, the dual combination of either of these pharmacological agents was unable to induce the mitochondrial epileptic activity. Next, I have demonstrated that the induction is not specific to the mitochondrial complex inhibitor chosen (rotenone and potassium cyanide). The substitution with other established mitochondrial complex I and IV inhibitors (MPP^+-iodide and sodium azide respectively) was still able to induce epileptiform discharges in the hippocampus CA3 robustly. Finally, I have also shown that the mitochondrial epilepsy induction is not merely limited to acutely prepared brain slices from the Wistar rat. Using the same induction protocol, I was able to induce epileptiform discharges from the hippocampus CA3 of the C57BL/6 mice. Furthermore, using surgically resected human tissue from patients undergoing elective

neurosurgical procedure, I was also able to induce similar patterns of epileptiform discharges using the mitochondrial epilepsy induction protocol.

As a proof of concept, I have also examined the neuropathological changes in the hippocampus CA3 of the rodent brain slices following the epileptic induction. I have found severe neuronal loss across the whole brain slice, but especially in the hippocampus CA3. In particular, there was a selective loss of the inhibitory interneuron population, while the excitatory neuron population was relatively spared. I have also demonstrated significant astrogliosis across the whole area of the epileptic tissue. The degree of gliosis in the epileptic tissue is a severe reactive astrogliosis response with significant glial scar formation. All of these neuropathological findings have very closely recapitulated the neuropathological changes that were observed in the human post-mortem studies. This further added to the face validity of this *in vitro* model of mitochondrial epilepsy.

In addition, I have also examined the pharmacological profile of this model of mitochondrial epilepsy towards conventional antiepileptic drugs. I have found that most of the clinically used conventional antiepileptic drugs failed to control the epileptiform discharges induced in this model of mitochondrial epilepsy. This reflects very well the severe pharmacoresistance observed in the clinical setting during the care of patients with mitochondrial epilepsy using conventional means of antiepileptic drugs (Bindoff and Engelsen, 2012; Whittaker *et al.*, 2015). Therefore, the model not only recapitulates the neuropathological findings in the human study; but it also seems to produce epileptic phenotype that has a similar pharmacological profile to that seen in the clinical setting with patients suffering from mitochondrial epilepsy.

This study, therefore, has provided the scientific community with the first ever *in vitro* brain slice model of mitochondrial epilepsy. This model has been thoroughly validated and seems to reflect the phenotype of mitochondrial epilepsy very closely. It is very difficult to develop a model of this calibre *in vitro* but the approach that I have taken in the development of the model seems to have aided in the conceptualisation of this model. Therefore, it might be beneficial for future studies on modelling a human pathological condition *in vitro* to follow the framework that I have laid out in order to increase the validity of the model. This framework has been previously published and takes on the approach of utilizing the observations made from post-mortem studies on the end-stage of a disease before taking it to an *in vitro* system in an animal model to acutely recapitulate the changes seen in the human studies (Chan *et al.*, 2016).

7.2 Mechanisms

All the findings presented in the previous chapters in this thesis have clearly implicated the role of the two major cellular compartments in the brain, the neuronal and astrocytic compartment. This gives rise to the 'dual neuronal – astrocytic hit hypothesis'. The hypothesis focuses on the recruitment of both the neuronal and astrocytic compartment in the generation of epileptic activity in this *in vitro* model of mitochondrial epilepsy. Specific mechanisms have been postulated with regards to each cellular compartments that collectively may contribute towards the development of mitochondrial epilepsy.

It has been discussed above that there is a selective loss of inhibitory interneurons in this model of mitochondrial epilepsy. Mitochondrial respiratory chain inhibitors have been reported to selectively affect the inhibitory interneurons more than the excitatory neurons (Whittaker *et al.*, 2011). This selective loss of inhibitory interneurons would result in a generalized loss of inhibitory tone in the tissue. Furthermore, pharmacological studies have specifically implicated the role of $GABA_A$-R mediated inhibition in the generation of seizure. Any therapeutic strategy that upregulates or potentiate this $GABA_A$-R mediated inhibition has been able to silence the epileptic activity. This further indicates that there could be a loss of the tonic $GABA_A$-R mediated inhibitory tone due to the generalized loss of inhibitory interneurons in the epileptic tissue.

In terms of the astrocytic compartment, the glutamate-glutamine cycle has been implicated as the contributing mechanism in seizure generation. Metabolic tracing has showed that there was significantly less metabolic flux for the recycling of the neurotransmitters, glutamate and GABA. Glutamine seems to be a key player in the generation of seizure, as there was a significant reduction in tissue level of glutamine that is specific only to the epileptic tissue. As glutamine is the precursor to both glutamate and GABA, it would be unsurprising to then expect a deficiency of GABA due to the downstream deficiency of glutamine. This is indeed confirmed by the metabolic tracing experiments that have demonstrated less utilization of glutamine in the synthesis of GABA following the epileptic induction. Puzzlingly, the tissue level of GABA is sustained or increased in the epileptic tissue. This can be explained by the concept of metabolic compartmentalization. As both glutamate and GABA have a dual role in the brain tissue as both a neurotransmitter and a metabolic substrate; it is

possible that there is a distinct neurotransmitter pool and metabolic pool for these amino acids. It is unclear if the level of GABA measured by the technique used in Chapter 5 measures the neurotransmitter, metabolic, or both pool of GABA. Therefore, this finding should be taken with a grain of salt.

However, both the neuronal and the astrocytic mechanisms have converged on the mechanisms pertaining to reduced inhibition in the brain. This supports the recent school of thought on the 'inhibitory energy hypothesis' that suggests that the maintenance of inhibitory tone in the brain is more energetically demanding than the excitatory equivalent (Zsurka and Kunz, 2015; Kann, 2016; Lax *et al.*, 2016). Specifically, I have also demonstrated that astrocytes have a vital role in the maintenance of inhibitory tone through the glutamate – glutamine cycle. Therefore, future discussion on the inhibitory inputs in the brain should avoid the mere focus on the neuronal compartment and also critically examine the astrocytic compartment.

Metabolically, there is also a significant change in the tissue state of metabolism following the epileptic activity induction in this brain slice model. Particularly, glycolysis is significantly upregulated albeit not to the point of saturation. Lactic acid production is also significantly increased; which is reflective of the lactic acidosis commonly seen in patients with mitochondrial epilepsy (Pavlakis *et al.*, 1984; Ohno *et al.*, 1997; Bindoff and Engelsen, 2012; Steriade *et al.*, 2014). Oxidative metabolism is severely reduced in the epileptic tissue, as evidenced by the severe downregulation of the Krebs cycle. This was again confirmed in the metabolic flux analysis of the isolated tissue; showing that the oxygen consumption rates of both the neurons and the astrocytes are equally affected by exposure to the mitochondrial respiratory chain inhibitors.

Finally, there is also multiple evidence of the involvement of oxidative stress in this model of mitochondrial epilepsy. Carbonylated protein concentration is significantly higher in the epileptic tissue, suggesting increased reactive oxygen species damage of the protein (Levine *et al.*, 1994). The upregulation of the pentose-phosphate pathway during the epileptic state also suggested an ongoing process of oxidative stress as the pathway is an important source of NADPH, a potent endogenous cellular antioxidant (Berg *et al.*, 2012b). Although the use of coenzyme-Q, a potent cellular antioxidant, in this model of mitochondrial epilepsy showed no meaningful response; it does not necessarily exclude the presence of oxidative stress in the epileptic tissue. It may suggest, however, that oxidative stress is not the core pathogenic process in this *in vitro* model of mitochondrial epilepsy. Rather, it may be an end-stage consequence

of the epileptic tissue that could result in the upregulation of apoptotic cell death (Kannan and Jain, 2000), leading to the previously described neuronal loss in this model.

Much is still not understood about the specific mechanisms of seizure generation in mitochondrial epilepsy. However, this study has certainly provided some fresh insights into the potential pathogenic mechanisms implicated. Again, I would like to highlight the implication of the 'dual neuronal-astrocytic hit hypothesis' in mitochondrial epilepsy. Both the specific neuronal and astrocytic mechanisms discussed above seem to converge towards a generalized loss of inhibitory tone in the tissue. These findings have enabled me to reconstruct the old hypothesized model of seizure generation in mitochondrial epilepsy and propose a new model in understanding mitochondrial epilepsy (see Figure 7-1).

It is important to note at this point that this model has shown that an extraneous astrocytic dysfunction in the form of the failure of the glutamate – glutamine cycle is required for seizure generation. This is simulated in the model through the addition of fluorocitrate. However, it is currently unknown what specific mechanisms in the human patients with mitochondrial epilepsy led to the failure of this cycle. It is most likely not exclusively due to the respiratory chain deficiency through the mitochondrial DNA dysfunction. Therefore, it is advised that more studies are conducted on the post – mortem tissue of patients with mitochondrial epilepsy to better understand the nature of the astrocytic impairment.

Additionally, the model is dependent on the combination of a mitochondrial complex I and complex IV inhibitor. Whilst both inhibitors affected the neurons and astrocytes equally, the majority of the energy crisis is brought about by the complex I inhibition. It is unclear why the complex IV inhibition (simulated either by cyanide or sodium azide) is necessary but it may be related to the effect of complex IV inhibitors on inhibitory neurotransmission. Cyanide application has been demonstrated to significantly suppress inhibitory interneuron firing as well as depolarize the resting membrane potential of these fast spiking interneurons (Whittaker *et al.*, 2011). This mechanism may therefore contribute towards the generalized loss of inhibition.

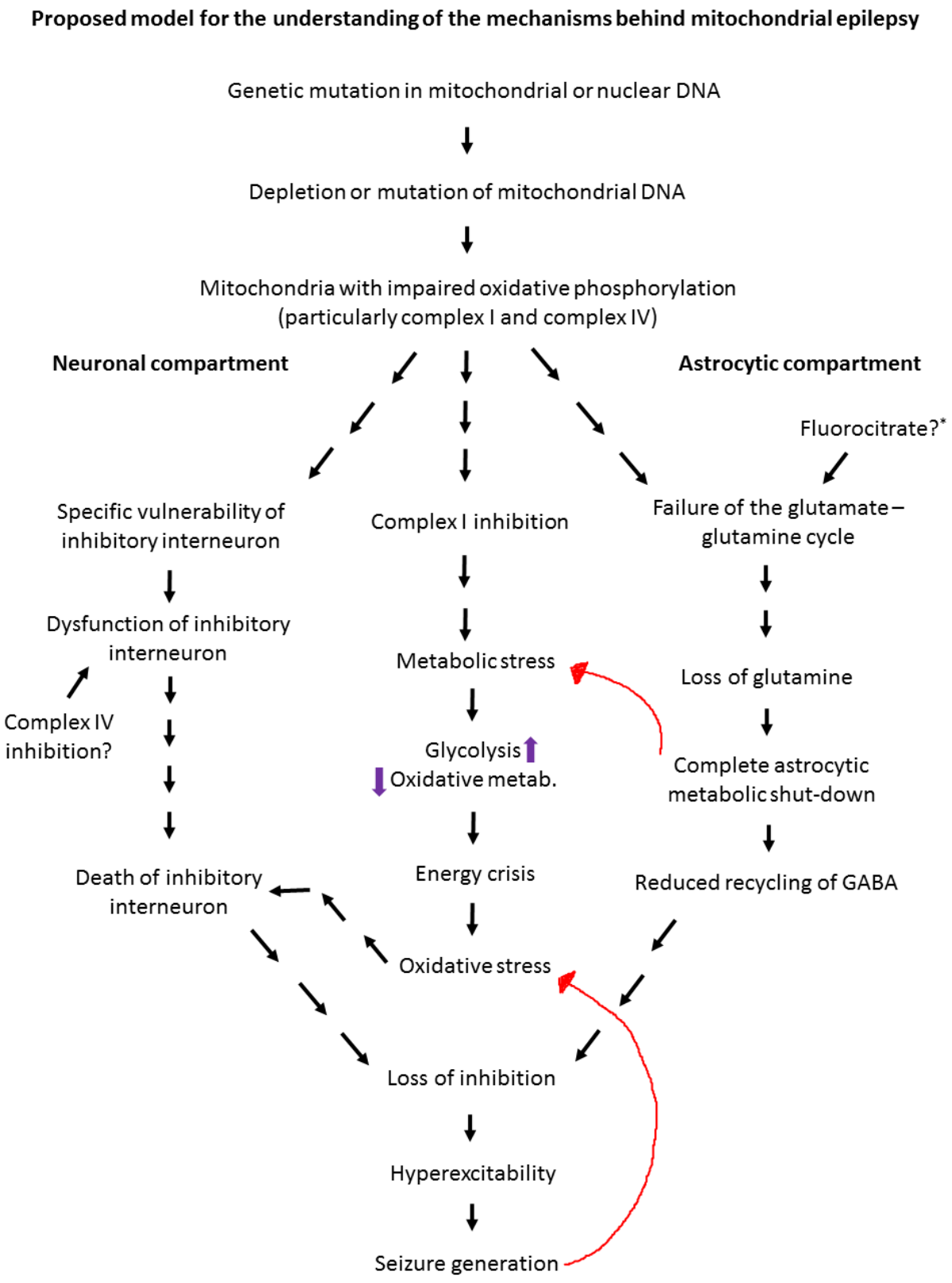

*Figure 7-1 Proposed model for the understanding of the mechanisms behind mitochondrial epilepsy. Shown are the specific mechanisms in the neuronal and the astrocytic compartment that contributes towards seizure generation. Red arrow indicates further upregulation of the target process. * Fluorocitrate is a vital component in this model which causes the failure of the glutamate – glutamine cycle when combined with the complex I and IV inhibition. However, in the human patients, it is unknown what mechanisms causes the astrocytic glutamate – glutamine cycle to fail in a manner that causes epileptic activity to be able to manifest.*

7.3 Therapeutic implications

The development of this novel *in vitro* brain slice model of epilepsy has also allowed me to evaluate several pharmacological approaches to the treatment of mitochondrial epilepsy. These findings have implicated three systems as a pharmacological target during the development of a pharmacological regime for patients with mitochondrial epilepsy. These three target systems are the AMPA-R system, the $GABA_A$-R system, and metabolic modulation (summarized in Figure 7-2).

7.3.1 AMPA-R

Antagonism of the AMPA-R seems to be a promising and viable approach in the treatment of mitochondrial epilepsy. The only currently available antiepileptic drug that modulates the AMPA-R are barbiturates and perampanel. Both these compounds were able to suppress the mitochondrial epilepsy in this model, although barbiturates are also modulator of $GABA_A$-R and so should be considered in its dual mechanisms of action. More selective to AMPA-R, perampanel is a well-characterized non-competitive antagonist (Hanada *et al.*, 2011; Ceolin *et al.*, 2012). I have demonstrated that perampanel can potently suppress the epileptic activity induced in this model. This supports the consideration of perampanel for use in the care of patients with mitochondrial epilepsy. Perhaps, a proper clinical trial to look into the efficacy of perampanel in patients with mitochondrial epilepsy can be considered.

Decanoic acid is a component of the ketogenic diet that has been proposed in the recent study as a potential antagonist of the AMPA-R (Chang *et al.*, 2015). I have indeed observed that decanoic acid application was able to suppress the induced epileptic activity. However, I have also shown that the same is true for octanoic acid; which was reported to not have any AMPA-R antagonism (Chang *et al.*, 2013; Chang *et al.*, 2015). Furthermore, the concentration whereby decanoic acid exhibits significant suppressive effect in this model is relatively higher than the usual concentration where it is indicated as an AMPA-R antagonist. Therefore, the effects by which decanoic acid and octanoic acid may suppress the epileptic activity are more likely attributable to other mechanism such as through metabolic modulation (discussed further below).

In addition, as described in detail in Chapter 4, many other compounds may also have an indirect effect in AMPA-R modulation which could contribute to their

pharmacological effect on this model of mitochondrial epilepsy. One such compound is β-hydroxybutyrate. At high concentration of β-hydroxybutyrate, it has been reported that it can upregulate the synthesis of kynurenic acid, an antagonist of AMPA-R (Weber *et al.*, 2001). Both octanoic acid and bezafibrate has also been reported to increase the production of β-hydroxybutyrate (Courchesne-Loyer *et al.*, 2015; Thevenet *et al.*, 2016); therefore, these compounds may also indirectly modulate the AMPA-R through the kynurenic acid production.

Regardless, it is inevitably clear that the antagonism of AMPA-R is a fruitful target in mitochondrial epilepsy. Should more compounds be developed in the future that modulate the AMPA-R, these compounds should be looked into for their effectiveness in mitochondrial epilepsy, both in pre-clinical studies and clinical trials.

7.3.2 $GABA_A$-R

The modulation of $GABA_A$-R is another recurring system in its implication in mitochondrial epilepsy. It has been discussed above that the converging mechanisms in the seizure generation in mitochondrial epilepsy seems to be through the loss of inhibition. Therefore, unsurprisingly the enhancement of inhibition through the modulation of the $GABA_A$-R system would be a viable approach for therapy in this condition.

The two antiepileptic drugs that modulate the $GABA_A$-R are benzodiazepines and barbiturates. Barbiturates have been shown to have a potent effect in suppressing the induced mitochondrial epilepsy. Benzodiazepines, however, do not suppress the epileptic activity, unless applied concomitantly with GABA. This discrepancy in pharmacological response is explained by the capacity of barbiturate to directly activate the $GABA_A$-R even in the absence of GABA (Rho *et al.*, 1996). Benzodiazepines, on the other hand, cannot modulate the $GABA_A$-R in the absence of GABA (Krisko *et al.*, 2017). Since the epileptic tissue is most likely devoid of GABA (as discussed above in section 7.2), the use of benzodiazepine clinically should be paired with other agents that can increase tissue concentration of GABA (such as gabapentin). Barbiturates, on the other hand, seems to be readily used as an antiepileptic of choice for the care of patients with mitochondrial epilepsy.

Another therapeutic strategy that can modulate the $GABA_A$-R is by increasing the level of the endogenous agonist of the receptor, GABA. I have demonstrated that the direct administration of GABA onto the epileptic tissue can suppress the induced mitochondrial epilepsy. Therefore, theoretically, the external supplementation of GABA should prove to be beneficial for these patients. GABA is indeed available as a nutritional supplement; however, its clinical efficacy and whether or not it crosses the blood-brain barrier is controversial and not well understood (Boonstra *et al.*, 2015). Analogues of GABA have been developed that crosses the blood-brain barrier, such as the infamous gamma-hydroxybutyrate (GHB) or baclofen (van Bree *et al.*, 1991; Bhattacharya and Boje, 2004). The use of these GABA analogues should be considered and examined in this model of mitochondrial epilepsy.

Taking a different approach to increase the tissue concentration of GABA is through the modulation of the glutamate – glutamine cycle. Glutamine has been discussed extensively as a promising therapeutic candidate due to its capacity to suppress the mitochondrial epileptic activity. This is thought to be due to a dual mechanisms of action; by increasing the production of GABA and by upregulating astrocytic oxidative respiration. Unlike GABA, glutamine readily crosses the blood – brain barrier (Ennis *et al.*, 1998; Xiang *et al.*, 2003). This makes glutamine a favourable candidate for therapeutic use as it can increase the bioavailability of GABA in the brain. Its use can therefore be potentially paired with other $GABA_A$ modulators such as benzodiazepine or barbiturate.

Nevertheless, again, the modulation of $GABA_A$-R is clearly a viable therapeutic approach in caring for patients with mitochondrial epilepsy. Recommendations can be made based on evidence presented in this study to support the use of barbiturates in this subset of epileptic patient. Benzodiazepine can be considered for use as a combination with other antiepileptic that can increase the bioavailability of GABA in the brain tissue. The direct supplementation of GABA through nutritional means or through the use of the GABA analogues should be examined further in this model or potentially in a clinical context. Finally, glutamine should seriously be considered as a novel therapeutic approach and strategy for its use in the clinical context should be developed.

7.3.3 Metabolic modulation

Inevitably, there is a severe change in the tissue metabolism following the mitochondrial epilepsy induction. I have found that metabolic modulation through alleviating the tissue's metabolic demand by the application of various substrates was also able to suppress the induced epileptiform discharges.

In this model, a significant upregulation of glycolysis, specifically anaerobic glycolysis resulting in lactate production, has been well – described. I have demonstrated that the extraneous addition of glucose and pyruvate was able to suppress the epileptiform discharges. This suggests that glycolysis is very much upregulated, but not to the point of saturation. Furthermore, it seems that there remains some degree of oxidative metabolism to accommodate the external pyruvate as an additional metabolic substrate. However, this suppressive effect was only achieved at very high concentrations (10-20mM). Although glucose and pyruvate are readily transported across the blood – brain barrier (Witt *et al.*, 2001), achieving such level of bioavailability in the brain tissue may be impractical or verging on impossible. Therefore, its use as a metabolic modulator should be considered in combination with other metabolic substrates to achieve a synergistic metabolic modulation.

As mentioned above, the modulation of glutamate – glutamine cycle is another approach in the treatment of mitochondrial epilepsy. Out of the three compounds tested, glutamine appears to be the most effective modulator of the glutamate – glutamine cycle. Application of glutamine has a dual effect in the modulation of metabolism; through the increased production of GABA as well as through the upregulation of astrocytic oxidative respiration. Therefore, as discussed above, glutamine should seriously be considered as a promising therapeutic intervention for patients with mitochondrial epilepsy. In rats, at least, it has been shown that oral glutamine administration was able to increase the level of GABA measured in the striatal tissue and the extracellular fluid (Wang *et al.*, 2007). Therefore, the concern of its distribution through the blood – brain barrier has somewhat been addressed and shows promises.

Interestingly, all three components of the ketogenic diet tested in this model (β-hydroxybutyrate, octanoic acid, and decanoic acid) exhibited an acute anticonvulsant effect. This strongly supports the consideration of ketogenic diet use in patients with mitochondrial epilepsy. Indeed, preliminary reports have shown that there is clinical

benefit to the use of ketogenic diet in these patients; although it is almost never used in isolation (Kang *et al.*, 2007; Martikainen *et al.*, 2012; Steriade *et al.*, 2014). It should be understood, however, that ketogenic diet is a systemic metabolic modulator and so further studies should look into the efficacy of ketogenic diet in mitochondrial epilepsy in an *in vivo* model.

An exciting observation that came about from the experiments on the components of ketogenic diet is that the modulation of lipid metabolism was also able to control the epileptiform discharges. Both octanoic and decanoic acid are fatty acids that are readily broken down as energy source through mitochondrial β-oxidation. Furthermore, bezafibrate, an agent shown to increase mitochondrial fatty acid β-oxidation (Krisko *et al.*, 2017), was also able to significantly suppress the epileptiform discharges. Therefore, the upregulation of fatty acid metabolism via mitochondrial β-oxidation may also be a viable therapeutic approach for intervention in patients with mitochondrial epilepsy.

To conclude, various forms of metabolic modulation is potentially beneficial for patients suffering from mitochondrial epilepsy. Out of all the metabolic substrates discussed, the most straightforward to be applied directly in clinical care of these patients is perhaps ketogenic diet. The role of fatty acid metabolism in this context should be evaluated further and may represent an entirely novel approach in metabolic modulation on these patients. Finally, the modulation of glycolysis as well as the glutamate – glutamine cycle should also be considered in the clinical setting.

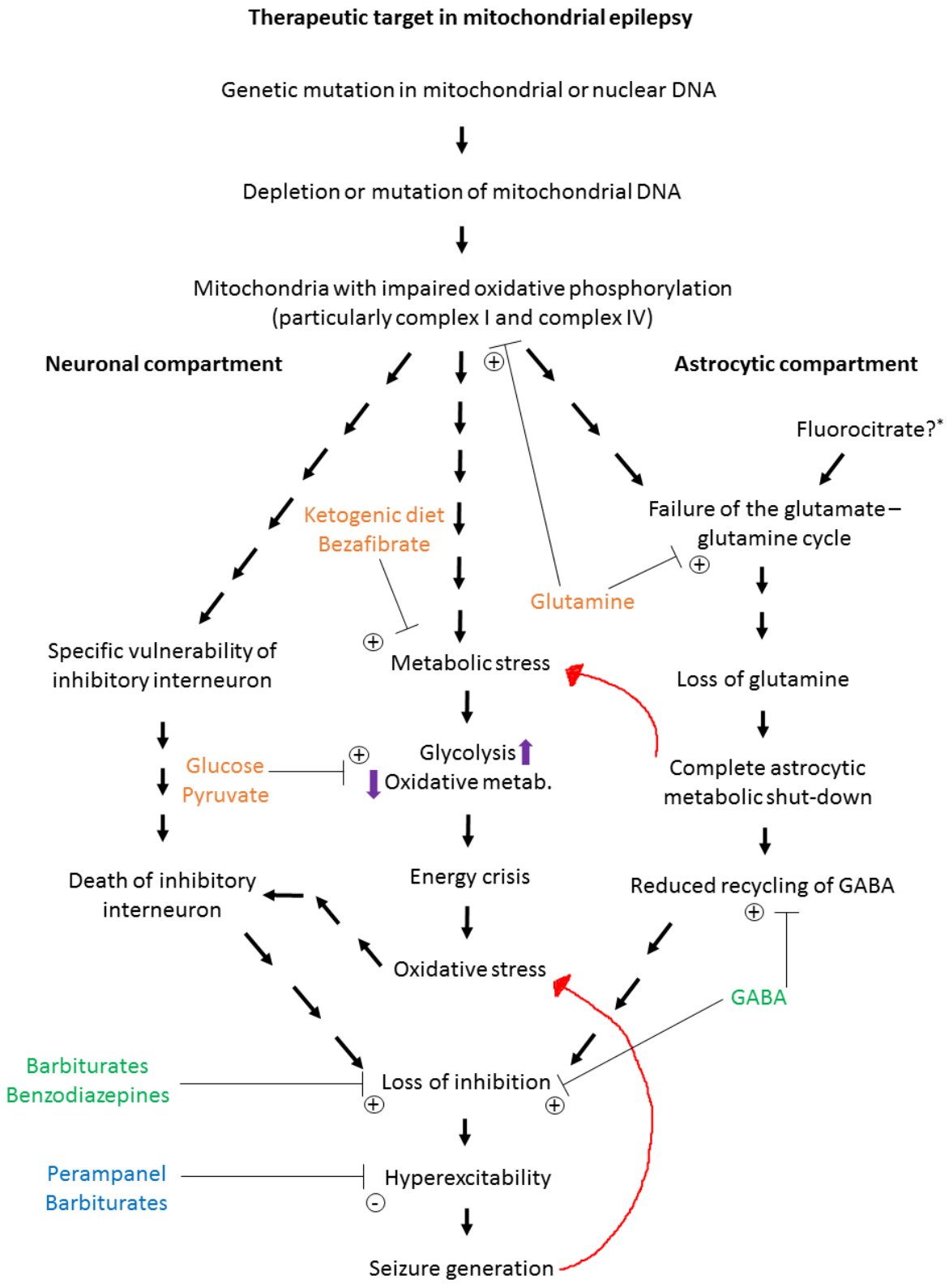

Figure 7-2 Therapeutic target in mitochondrial epilepsy. Shown is the proposed model of mechanisms underlying seizure generation in mitochondrial epilepsy along with the therapeutic interventions shown to have efficacy in this model and their respective therapeutic target. These therapeutic interventions fall into one of three categories: those working on the AMPA-R system (blue), $GABA_A$-R system (green), and metabolic modulators (orange). Each respective therapeutic intervention either inhibits (shown with the negative symbol) or upregulates / rescues (shown with the positive symbol) the respective system it targets.

7.4 Future work

This thesis has described the development of a novel *in vitro* brain slice model of mitochondrial epilepsy. Various mechanisms have been investigated in the context of understanding seizure generation in mitochondrial epilepsy. Extensive pharmacological studies have also been conducted to provide recommendations for creating a therapeutic regimen for patients with mitochondrial epilepsy.

Future studies should firstly try to further develop the model to another platform. As discussed above, despite the close resemblance of the *in vitro* rodent brain slice model to the human phenotype; some experimental design requires the use of an *in vivo* platform for scientifically accurate exploration (for instance, the examination of the effect of ketogenic diet). Therefore, efforts should be made, where possible, to try and extrapolate the findings from this model to developing an *in vivo* model of mitochondrial epilepsy. Furthermore, as discussed, this model is not a genetic model of mitochondrial disease *per se*, rather it is a model of the phenotypic manifestation of mitochondrial disease; the mitochondrial epilepsy. Hence, it is not by leaps and bounds to expect the development of a genetically modified animal model of mitochondrial epilepsy based on the findings from this study.

This model has also provided the opportunity of doing a pharmacological screen of various potential therapeutic interventions in mitochondrial epilepsy. Several of these interventions have shown very promising anticonvulsant effects that it should be further considered for use in a clinical setting. More pharmacological interventions can be screened for using this model and any leads from this initial screen can then be followed up through small clinical studies assessing efficacy of the treatment.

Finally, discussion on mechanisms that could potentially contribute towards seizure generation in mitochondrial epilepsy has been extensively argued for in the context of the model. These findings should be reassessed in the human patient study (such as using the post-mortem neuropathological study) to confirm that the mechanisms truly do contribute towards seizure generation in these patients. As discussed, mechanisms behind seizure generation may differ between an animal model and a human patient system. Therefore, as much as possible, a mechanistic investigation in an *in vitro* model, such as this, should be correlated with a human mechanistic study to ensure conservation of the pathogenic mechanisms across species.

Appendix 1. Matlab Script

Matlab script for analysis of epileptiform activity

```
function [coastline, numBursts, burstLengths, burstAmps] = getBurstParameters(data, threshold, gapSize)

coastline = sum(abs(diff(data)));

highpoints = find(data>threshold);
begs = highpoints(1);
ends = [];
burstLengths = [];
burstAmps = [];


for i = 1:length(highpoints)-1
    if ((highpoints(i+1)-highpoints(i))>gapSize)
        ends = [ends;highpoints(i)];
        begs = [begs;highpoints(i+1)];
    end
end
      ends = [ends;highpoints(length(highpoints))];

 for j = 1:length(begs)
     burstLengths = [burstLengths; (ends(j)-begs(j)+1)];
     burstAmps = [burstAmps; max(data(begs(j):ends(j)))];
 end
 numBursts = length(burstLengths);
end
```

Written by and used with permission of Dr. Katherine Newling

Published with MATLAB® 7.10

Matlab script for automated cell count analysis

```
folder = uigetdir
cd(folder)
currentFolder = dir(folder);

excelFilename = input(sprintf(['What would you like the Excel output \n' ...
    'file to be called? ']));

sensitivity = input(sprintf(['How sensitive do you want the counter \n' ...
    'to be between zero and one (default 0.85)? ']));

minCellRadius = input(sprintf(['What do you think is the minimum radius of your cells \n' ...
    ' in number of pixels (classically 10)? ']));

maxCellRadius = input(sprintf(['What do you think is the maximum radius of your cells \n' ...
    ' in number of pixels (classically 15)? ']));

counter = 1;
counts{counter,1} = 'Image';
counts{counter,2} = 'Number Of Cells';
for i = 1:length(currentFolder)
    if strfind(currentFolder(i).name,'.tif')
        if isempty(strfind(currentFolder(i).name,'.tif_'))
            counter = counter + 1;
            filename = currentFolder(i).name;
            [centers, radii, uniqueCount] = countCells(filename,sensitivity,minCellRadius,maxCellRadius);
            counts{counter,1} = filename;
            counts{counter,2} = uniqueCount;
        end
    end
end

xlswrite(excelFilename,counts);
```

Written by and used with permission of Stacey Aston

Published with MATLAB® 7.10

Appendix 2. Publications

Neuropharmacology 102 (2016) 48–58

Contents lists available at ScienceDirect

Neuropharmacology

journal homepage: www.elsevier.com/locate/neuropharm

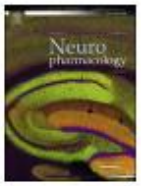

Invited review

Neuronal oscillations: A physiological correlate for targeting mitochondrial dysfunction in neurodegenerative diseases?

Felix Chan [a], Nichola Z. Lax [b], Ceri H. Davies [c, 1], Douglass M. Turnbull [b], Mark O. Cunningham [a, *]

[a] Institute of Neuroscience, The Medical School, Framlington Place, Newcastle University, Newcastle upon Tyne, UK
[b] Wellcome Trust Centre for Mitochondrial Research, Institute of Neuroscience, Newcastle University, Newcastle upon Tyne NE2 4HH, UK
[c] Neural Pathways DPU, GSK, 11 Biopolis Way, 138667, Singapore

ARTICLE INFO

Article history:
Received 18 August 2015
Received in revised form
19 October 2015
Accepted 24 October 2015
Available online 28 October 2015

Keywords:
Neuronal oscillation
Mitochondrial dysfunction
Neurodegenerative diseases
Physiological correlate
Biomarker

ABSTRACT

Increasingly in the realm of neurological disorders, particularly those involving neurodegeneration, mitochondrial dysfunction is emerging at the core of their pathogenic processes. Most of these diseases still lack effective treatment and are hampered by a shortfall in the development of novel medicines. Clearly new targets that translate well to the clinic are required. Physiological parameters in the form of neuronal network activity are increasingly being used as a therapeutic screening approach in drug development and disorders with mitochondrial dysfunction generally display neuronal network activity disturbance. However research directly linking the disturbances in neuronal network activity with mitochondrial dysfunction is only just starting to emerge. This review will summarize the breadth of knowledge linking neuronal network activity to mitochondrial dysfunction in neurodegenerative diseases and suggest potential avenues for exploration in respect to future drug development.

1. Mitochondria

Mitochondrion (plural-mitochondria) is a cell organelle primarily responsible for energy provision for cellular functioning. It has two layers, the inner and outer mitochondrial membrane, separated by the intermembrane space. It is within this inner mitochondrial membrane where most of the mitochondrial functions are performed. The inner mitochondrial membrane is further compartmentalized into foldings called cristae with spaces in between each cristae (matrix).

Mitochondria produce ATP (adenosine triphosphate) through a series of chain reactions, with most of the ATP generated by oxidative phosphorylation. Oxidative phosphorylation is carried out through consecutive oxidation of various substrates by respiratory complexes (complex I–IV) to generate a transmembrane potential which is used in complex V (ATP synthase) for ATP generation. Complex I and II oxidize NADH and $FADH_2$ respectively, and transfer electrons to ubiquinone. The resulting ubiquinone has its electron transferred to cytochrome c in complex III. This cytochrome c will then, via complex IV, transfer its electron to produce water (H_2O). In addition to ATP generation, mitochondria also serve various other important functions including calcium handling (Rizzuto et al., 2012), production of endogenous reactive oxygen species (ROS) (Sena and Chandel, 2012), and regulation of apoptosis (Wang and Youle, 2009).

Another unique property of the mitochondria is that they possess their own genome in the form of the circular mitochondrial DNA (mtDNA). In humans, this is approximately 16,569 base pairs in length with two strands, heavy and light strands, formed because of their different distribution of cytosine and guanine. This mtDNA contains just 37 genes in humans and is strictly derived through maternal inheritance (Tuppen et al., 2010).

Mitochondria continuously undergo turn-over through a fusion and fission cycle - processes that contribute to the ever-changing number and morphology of the organelle. Along with the process of mitophagy, this cycle essentially maintains the quality of mitochondria through continuous turn-over (Twig et al., 2008). Mitochondria are also mobile and undergo transport and trafficking to the areas of cells where they are needed the most (Chang and Reynolds, 2006). This is particularly important in neurones where mitochondria are distributed throughout somatic, axonal and

* Corresponding author. Institute of Neuroscience, The Medical School, Framlington Place, Newcastle University, Newcastle upon Tyne, NE2 4HH, UK.
E-mail address: mark.cunningham@ncl.ac.uk (M.O. Cunningham).
[1] Current address: CNS Drug Discovery Unit, Takeda Pharmaceutical Company Limited, 26-1, Muraoka-Higashi 2-chome, Fujisawa, Kanagawa, 251-8555, Japan

http://dx.doi.org/10.1016/j.neuropharm.2015.10.033
0028-3908/

dendritic compartments.

The brain derives most of its energy through aerobic metabolism using glucose as the main substrate. Hence, not surprisingly, neurons are highly dependent on mitochondria for their energy provision. The distribution of mitochondria within neurons also depends on the metabolic demand of different parts of the neurone with the dendritic area being the most metabolically active as measured by the cytochrome oxidase activity (Wong-Riley, 1989). Mitochondrial distribution is a dynamic process, however, with modulation of mitochondrial transport and trafficking depending on the level of synaptic activity (Chang et al., 2006). Without a doubt, neurons are one of the most metabolically active cell types in the human body. A human brain amounts to only 2% of total body weight yet it consumes 20% of the total oxygen consumption (Quastel and Wheatley, 1932). Advances in neuroimaging technique have also shown *in vivo* a very high physiological cerebral flow rate of about 45 ml per 100 g per minute concurrent with an extremely high global cerebral oxygen consumption of about 130 μmol per 100 g per minute (Jain et al., 2010). Therefore, the dependence of brain on optimal mitochondrial function should not be underestimated.

2. Mitochondrial disorders

Mitochondrial dysfunction can manifest as either (a) a primary mitochondrial disorder (often referred to simply as 'mitochondrial disease') arising from genetic mutations, either directly in the mitochondrial DNA or in nuclear DNA genes that regulate mitochondrial DNA maintenance or (b) a secondary mitochondrial disorder in which there is an established mitochondrial dysfunction component as a significant and integral component of a multifactorial pathogenic process. Secondary mitochondrial disorder may arise from genetic mutation in its familial form but these mutation does not compromise the mitochondrial DNA nor is it transmitted in the classic maternal inheritance pattern. It is beyond the scope of this review to cover every mitochondrial disorder and instead will primarily focus on neurodegenerative disorders which are established examples of secondary mitochondrial disorders. That said, it is important to note that exploration of primary mitochondrial disorders has driven much of our current understanding of mitochondria and how they contribute to this class of disease.

2.1. Primary mitochondrial disorders

Primary mitochondrial disorders (mitochondrial disease) arise from a genetic mutation, either in the mitochondrial or nuclear DNA, which causes a defect within the respiratory chain. Collectively, this clinical disorder currently represents a prevalence ratio of greater than 1 in 10,000 with pathogenic mutations occurring in at least 1 in 200 people within the general population (Chinnery et al., 2012; Gorman et al., 2015). Hitherto, the most common mutation is the m.3243A > G mutation which causes a spectrum of phenotypes that includes MELAS (Mitochondrial Encephalophaty, Lactic Acidosis, and Stroke like episode), MIDD (Maternally Inherited Deafness and Diabetes), and CPEO (Chronic Progressive External Ophthalmoplegia) (Nesbitt et al., 2013). However, these phenotypes are not exclusive to the mutation as other mutations can also lead to these phenotypic manifestations.

There are several unique features to primary mitochondrial disease. One of which exemplified above is that the same genetic mutation may cause a different phenotypic manifestation in different individuals. This arises in part because the mutant mtDNA coexists with normal mtDNA in a cell – a property known as heteroplasmy (Payne et al., 2013). Pathogenicity only occurs when the level of the mutant mtDNA exceeds a certain threshold level (Rossignol et al., 2003) and depending on which organ(s) has the excess mutant mtDNA, different clinical manifestations will occur. Since brain is one of the most metabolically demanding organs, it is unsurprising for primary mitochondrial disorders to in some way present with neurological impairment.

2.2. Secondary mitochondrial disorders

With increasing interest in mitochondrial medicine, more and more disorders have been identified to have mitochondrial dysfunction as a component of their pathogenesis. These secondary mitochondrial disorders comprise a wide range of multi-organ diseases with varying clinical manifestation. The most notable examples are Parkinson Disease (Abou-Sleiman et al., 2006), Alzheimer's Disease (Moreira et al., 2010), Huntington Disease (Oliveira, 2010), Amyotrophic Lateral Sclerosis (ALS) (Hervias et al., 2006), and psychiatric disorders such as schizophrenia and bipolar disorder (Clay et al., 2011).

2.3. Treatment of mitochondrial disorders

Drug development in primary mitochondrial disease is challenging as most studies on mitochondrial function have relied on cellular and molecular methods which often do not represent the actual tissue and organ environment in the patient. Mitochondrial parameters that are routinely measured are almost always structural or biochemical and there is often a lack of a physiological parameter in published reports which is disappointing because it is the physiological parameter that provides the most valuable information in translating pre-clinical research to clinical drug development. As such, currently, there is no specific treatment that has been developed for mitochondrial disease and treatment remains largely symptomatic and supportive (Parikh et al., 2009). That said several new treatments are being developed. Riboflavin and arginine have shown promising outcomes in patients with MELAS, whilst in patients with Leigh Syndrome and LHON, EPI-743 has proved positive. These drugs are now being tested in clinical trials in spite of a lack of a good clinical correlate or biomarkers for assessment of mitochondrial function (Pfeffer et al., 2013).

The same bleak image of the status of drug development for secondary mitochondrial disorder is also true. Thus, most of these diseases still do not have an effective curative pharmacological therapy at this time. Parkinson's disease patients, for instance, still exhibit many non-motor symptoms even when treated with the gold standard therapy levodopa that only addresses the loss of dopamine and possesses long-term maintenance issues (Obeso et al., 2010). Memantine and cholinesterase inhibitors are approved therapeutic agents for Alzheimer's disease. However both drugs have the issue of deteriorating efficacy with long-term use (Neugroschl and Sano, 2010) and do not address mitochondrial dysfunction. Mitochondrial focussed treatment for both Huntington disease (Ross and Tabrizi, 2011) and ALS (Kiernan et al., 2011) are also lacking.

3. Neuronal oscillations

Neuronal oscillations are a form of synchronized dynamic neuronal activity which is generated by specialized functional assemblies of neurons (Schnitzler and Gross, 2005). It can present at a range of different frequencies, including slow frequencies such as delta (0.5–3 Hz); theta (3.5–7 Hz); alpha (8–13 Hz); beta (14–30 Hz); and fast frequencies such as gamma (30–80 Hz) (Ward, 2003; Buzsáki and Draguhn, 2004). Due to their nature of high preservation across species (Buzsáki et al., 2013), neuronal oscillations have been shown to be a potentially important neurophysiological correlate for a variety of functional processes

including cognitive binding.

Neuronal oscillations have been recorded in many brain regions, both *in vivo* and *in vitro* including, but not limited to, the visual cortex (Edden et al., 2009), olfactory system (Ravel et al., 2003), hippocampus (Bragin et al., 1995), entorhinal cortex (Cunningham et al., 2003), prefrontal cortex (Benchenane et al., 2011), and sensorimotor cortex (Gray, 1994). Within each of these regions, oscillations can present at varying frequencies and each exhibit their own specific mechanism of generation and correlation to behavioural function. For example, in the motor cortex, gamma oscillations are associated with voluntary movement (Cheyne et al., 2008) whereas beta oscillations are associated with movement planning and maintenance (Rubino et al., 2006; Engel and Fries, 2010).

Although knowledge of the specific mechanisms that contribute to the generation and maintenance of neuronal oscillations in different brain regions has historically been sparse, significant advances have been made over recent years on understanding both the cellular and molecular mechanisms involved. Of all the cortical rhythms, the greatest insight has been gained with respect to the genesis of gamma frequency (30–80 Hz) oscillations in cortical microcircuits. Central to the generation of cortical gamma frequency oscillations is the functional output of inhibitory GABAergic interneurons, in particular the fast-spiking parvalbumin expressing basket cell (Bartos et al., 2007; Cardin et al., 2009; Sohal et al., 2009). More specifically, it is these perisomatic-targeting interneurons that provide rhythmic inhibitory input in the form of post-synaptic potentials onto pyramidal cells, synchronizing excitatory and inhibitory inputs, which in turn leads to the generation of gamma oscillations (Hájos and Paulsen, 2009). This balance between synaptic excitation and inhibition determines the frequency and the amplitude that the network oscillates at; two measures that are routinely used as quantitative assessments of the type and strength of oscillatory activity (Atallah and Scanziani, 2009). To induce oscillations *in vitro*, it is necessary to stimulate the aforementioned excitatory-inhibitory drive either with electrical stimulation or pharmacological manipulation by activation of cholinergic (Fisahn et al., 1998; Pálhalmi et al., 2004; Mann et al., 2005), glutamatergic receptors (Cunningham et al., 2003, 2004; Fisahn et al., 2004; Brown et al., 2006) or a combination of both (Buhl et al., 1998; Yamawaki et al., 2008) suggesting that synaptic inputs mediated by these receptor systems are likely to be involved in initiating/maintaining oscillatory activity *in vivo*.

In the remainder of this review, we will focus in on summarising our knowledge of the link between neuronal oscillations and mitochondrial function in the context of secondary mitochondrial disorders, and specifically those that affect CNS function because there are only a few studies that have looked at the interaction between mitochondrial dysfunction and neuronal network oscillations in primary mitochondrial disease.

Neuronal oscillations have started to gain credibility as a good parameter to provide neurophysiological correlates during the drug discovery process. It has been most widely used for pharmaceutical development of psychiatric medicines (Whittington et al., 2000; Millan et al., 2012) as it provides a physiological correlate to EEG signatures that have been recorded from this patient population (schizophrenia and major depressive disorder) and there are few other model systems that have proved useful in representing these diseases. However the evidence that mitochondrial dysfunction is a key component of these diseases is not as well developed as for neurodegenerative diseases which is described in detail below.

4. Mitochondrial function and neuronal oscillation in neurodegeneration: the missing link?

More and more neurodegenerative diseases are being identified as secondary mitochondrial disorders and more often than not, and perhaps somewhat surprisingly, most of these diseases also exhibit a dysfunction in neuronal network activity or neuronal oscillations. Therefore, it is not unrealistic to speculate that these two phenomena could be mechanistically interrelated to one another. Taking examples from two classical neurodegenerative disorders; Huntington Disease and Parkinson's Disease; we will examine the evidence for the occurrence of both phenomena (mitochondrial and neuronal oscillation dysfunction) in these disorders within the context of their clinical manifestation and establish what we know and where the gaps are in our understanding that could be addressed to strengthen or refute such a hypothesis (refer to Fig. 1).

4.1. Huntington Disease

4.1.1. Clinical manifestation

Huntington Disease (HD) is an autosomal dominant inherited neurodegenerative disorder and in Western populations, its prevalence is relatively stable at about 4 in 100,000 cases (Ross and Tabrizi, 2011). The disease occurs because of a mutation in the huntingtin gene (at chromosome 4p16.3) which causes an expanded CAG repeat (Duyao et al., 1993) which in turn leads to an abnormally lengthened polyglutamine stretch within the encoded huntingtin protein (htt). Notably the length of the trinucleotide repeat (or polyglutamine stretch) correlates with the severity and timing of manifestation of the symptoms of the disease.

Originally known as Huntington chorea due to the classic symptom of 'dancing' movement (chorea), it is now understood that HD also presents with various cognitive and psychiatric disturbances (most notably sleep disturbances) in addition to the motor impairment (Sturrock and Leavitt, 2010). Huntington Disease is progressive and it is during its prodromal stage that subtle cognitive and psychiatric symptoms occur commensurate with the start of neuronal impairment. It is only at the later stage of the disease that chorea and motor symptoms emerge concurrent with the neurons starting to undergo apoptosis and degeneration (Tabrizi et al., 2011). By this stage, permanent neurological damage has occurred and it is extremely difficult to reverse the degeneration process. This emphasizes yet again the importance of targeting the subtle cognitive and psychiatric changes (exemplified by impairment in neuronal network activity) instead of the motor symptoms to prevent neurodegeneration from progressing further. Neuropathological analysis of post-mortem HD brain has demonstrated that these degenerative changes occur most extensively in the striatum (caudate and putamen) as well as in the cortex. Within the striatum, cell loss seems to be preferential to the GABAergic medium spiny neurons (MSNs). More specifically, it is the enkephalin-expressing MSNs that are selectively affected in the early stage and the substance-P expressing MSNs in the later stages (Zuccato et al., 2010).

Many animal models have been generated for HD using various approaches that have yielded relatively satisfying reproducibility of symptoms (Ramaswamy et al., 2007). The most notable and commonly used animal models are the neurotoxin models (particularly the 3-NP model described later) and the transgenic rodent models (using insertion of mutant htt – with the most commonly used models being R6/1 and R6/2 mice which employ random insertion of the human htt sequence).

4.1.2. Mitochondrial dysfunction

Huntington Disease has an established mitochondrial dysfunction component. Postmortem biochemical analysis of HD patient's caudate has shown a severe respiratory chain defect, especially in complex II-III and to a lesser extent in complex IV (Gu et al., 1996; Browne et al., 1997; Tabrizi et al., 1999). These defects appear to be

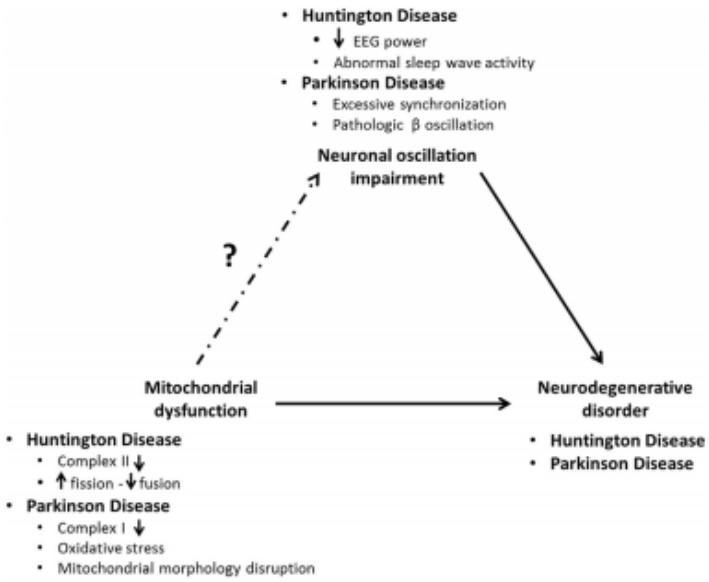

Fig. 1. The missing link between mitochondrial dysfunction and neuronal oscillation impairment in the context of neurodegenerative disorders. Summarized are the mitochondrial dysfunction and neuronal oscillation impairment observed in two neurodegenerative disorders (Huntington's Disease and Parkinson's Disease). Although much is known about both of these components, there is a gap in understanding whether or not the mitochondrial dysfunction observed can lead to the neuronal oscillation impairment seen in these neurodegenerative diseases.

regionally specific with the caudate and putamen being the most severely affected (Brennan et al., 1985). Furthermore, there also appears to be evidence of regionally-specific oxidative damage to the mitochondrial DNA, especially within the parietal cortex (Polidori et al., 1999) and mitochondrial DNA deletion is increased significantly in the frontal and temporal cortex of HD patients (Horton et al., 1995).

Having identified these mitochondrial dysfunction components, the mitochondrial complex II inhibitors were used in an attempt to generate a Huntington Disease neurotoxic animal model. The most successful inhibitor used in generating this animal model is 3-nitropropionic acid (3-NP), which is a suicide inhibitor of mitochondrial complex II (succinate dehydrogenase). The reason for why this inhibitor was chosen corresponds to an outbreak in China where children were ingesting moldy sugarcane contaminated with 3-NP and developed symptoms resembling Huntington Disease (Liu et al., 1992; Ming, 1995). Subsequently, it was found that intrastriatal injection of 3-NP induced age-dependent, striatal-specific degeneration with a histochemical profile and behavioural manifestation resembling that seen in HD patients (Beal et al., 1993a; Borlongan et al., 1995). Other methods of administration such as intraperitoneal injection were also able to induce these symptoms but it was chronic systemic administration of the 3-NP that most accurately replicated HD features observed in humans (Beal et al., 1993b). This protocol is now widely accepted as a reliable neurotoxin model for HD and has been used in various species ranging from rodent up to non-human primate to generate consistent and reproducible neurodegenerative features (Brouillet et al., 1995; Palfi et al., 1996).

In addition to the compelling evidence of respiratory chain deficiency in HD, there also appears to be another side of the coin to the mitochondrial dysfunction in HD, one found in recent years, that being impaired mitochondrial dynamics. Immunohistochemical analysis of mitochondria extracted from MSNs in HD brain show disrupted mitochondrial morphology that results from increased fission and reduced fusion, creating fragmented mitochondria (Kim et al., 2010). It was now known that mutant huntingtin binds to the mitochondrial fission protein, Drp1, and upregulates its enzymatic activity leading to increased mitochondrial fission (Song et al., 2011) which causes various downstream events ranging from reduced mitochondrial biogenesis, synaptic degeneration, and impaired mitochondrial trafficking (Johri et al., 2011; Shirendeb et al., 2012).

4.1.3. Neuronal network activity

Consistent with the observed neurodegeneration, Huntington Disease has also been associated with dysfunctional neuronal network activity that associates closely with the severity/profile of its symptoms. Specifically, EEG analysis in one cohort of HD patients revealed a pattern of reduced EEG power associated with increased theta and reduced alpha wave activity. (Scott et al., 1972; Streletz et al., 1990) whereas another study with resting EEG analysis revealed reductions in alpha and theta power concurrent with an increase in delta and beta power. These abnormal EEG patterns were shown to correlate with the neurological and neurocognitive impairment of the patients (Bylsma et al., 1994). More recently, a rigorous EEG study on a larger sample of HD patients showed a pattern of EEG wave slowing characterized by a decrease in alpha and beta power; and an increase in delta and theta power (Painold et al., 2010). The authors associated this abnormal electrophysiological pattern to an inhibited cortical network induced by the lack of excitatory oscillatory waves (fast wave activity – alpha and beta). This conclusion is somewhat misleading as we now understand that fast network activity corresponds to a gamma band (30–80 Hz) instead of the alpha or beta band. Certainly, when Hans Berger first described the neuronal oscillation band, he observed both the alpha (8–14 Hz) and the beta band (14–30 Hz) and classified this range as 'fast network activity' (Berger, 1929) but

this classification has since become outdated. This highlights the merit of revisiting all these old studies to truly establish and characterize the nature of the neuronal network impairment in these patients. An abnormal EEG slowing is also seen in preclinical HD patients with reduced alpha power in EEG during memory activation tasks (de Tommaso et al., 2003; van der Hiele et al., 2007). Sleep wave EEG and concurrent cranial CT scanning also reveal reduced slow wave sleep activity in HD patients which is associated with caudate atrophy (Wiegand et al., 1991) and analysis of recordings taken from microelectrode implants in patients undergoing Deep Brain Stimulation (DBS) surgery has confirmed a reduction in oscillatory activity over the frequency range of 2–35 Hz at rest (Starr et al., 2008). Taken together this collection of evidence despite the controversial conclusion clearly demonstrates impairment of neuronal oscillations pattern particularly a slowing of the EEG rhythms of patients with Huntington Disease.

This impairment is also observed in preclinical animal models of HD. *In vivo* electrophysiological recordings from the hippocampus and neocortex of R6/1 mice show a pattern of ectopic theta burst (increased theta-decreased delta) oscillatory patterning during slow wave state in freely behaving mice, which is not physiological. These bursts are interspersed with interictal spikes, suggesting hyperexcitability within the neuronal network (Pignatelli et al., 2012). Indeed, R6/2 mice are shown to be susceptible to developing seizures following glutamate challenge (Estrada-Sánchez et al., 2009). These changes however contrast with findings from single unit recording where it was shown that pyramidal neurons extracted from R6/2 mice display reduced AMPA and NMDA receptor-mediated currents and less sensitivity to glutamate agonists, suggesting hypoexcitability (André et al., 2006).

Recent studies have also described dysfunctional patterns of sleep EEG activity in these transgenic HD mice model. Chronic implanted electrode recording in R6/1 mice has shown ectopic β-wave activity (20–35 Hz) which evolves as the disease progresses and strengthens as the sleep cycle takes place (Jeantet et al., 2013). Similar implant recording in the frontal region of R6/2 mice revealed reduction in slow wave activity, in particular theta rhythm, along with an abnormal ectopic gamma wave (30–40 Hz) activity that appears independent of sleep cycle stage (Kantor et al., 2013). Conflicting results were obtained by another group which found an increase in beta and gamma activity in all sleep/wake states, an increase in theta in non-REM and REM sleep state, and a decreased delta in non-REM sleep state in R6/2 mice (Fisher et al., 2013). These conflicting results demonstrate the challenges faced when working with transgenic models of HD as no one particular model has been shown to accurately reflect the changes observed in human HD patients.

With regards to the neurotoxin models of HD, some pattern of neuronal network dysfunction has also been observed. In the quinolonic acid model, a marked reduction in EEG power is observed in the frontal cortex of the rat across a wide range of frequencies (Popoli et al., 1994) although the most pronounced changes are a specific reduction in the alpha and beta wave range (Reggio et al., 1999). The 3-NP model of HD also shows a marked pattern of electrophysiological impairment. For example, in striatal cell cultures, significant depolarization of the resting membrane potential and Na^+ channel inactivation are found in current clamp recordings from HD neurons (Greene et al., 1998). In vitro recording from brain slices exposed to 3-NP show reduced striatal field potential strength in the absence of Mg^{2+} where NMDA receptor activation is induced (Centonze et al., 2006) and abnormal enhancement of the long-term potentiation (LTP) of NMDA-facilitated synaptic EPSP specific to striatal MSNs and not in the striatal cholinergic neurons (Calabresi et al., 2001). This ectopic LTP induction is shown to be dependent on dopamine D2 receptor and metabotropic glutamate receptor 1 (mGlu1) activation (Calabresi et al., 2001; Gubellini et al., 2004). Collectively, these evidence implicated cell-specific synaptic dysfunction at a molecular level yet despite these clear effects on synaptic activity, the effect of 3-NP on neuronal activity at a population level and how it affects neuronal network oscillatory power and frequency is not known. The expectation is that it would have an impact but the precise manner in which this would manifest clearly requires experimental exploration.

It is interesting to note that compounds that have produced improvement of symptoms in rodent HD models have not yet shown significant effects in clinical trials and their effects on neuronal network activity have not been documented. Although this could suggest low translatability of the currently available models (Crook and Housman, 2011) there are also a number of other reasons (e.g., lack of target engagement because of restricted dose or CNS penetration) why these clinical studies have not been as successful as might have been expected.

4.2. Parkinson Disease

4.2.1. Clinical manifestation

Similar to Huntington Disease, Parkinson's Disease (PD) is a progressive neurodegenerative disorder and although it too is characterized as a movement disorder its profile is different with the most common symptoms being tremor, rigidity, and bradykinesia – the so-called 'triad of cardinal motor symptoms' (Xia and Mao, 2012). In addition to the classical motor symptoms, several cognitive impairment (in memory, visuospatial, and executive function) as well as psychiatric symptoms (such as delusion or hallucination) have been reported in patients with PD (Aarsland et al., 2010; Forsaa et al., 2010). Dementia is highly associated with PD with a staggeringly high cumulative prevalence rate of 75% in the lifetime of PD patients (Aarsland and Kurz, 2010). As with HD, Parkinson's Disease has also been shown to have a long preclinical stage with various non-specific subtle symptoms such as anxiety or sleep disturbance presenting during this stage (Savica et al., 2010).

Classically, Parkinson's Disease results from the loss of dopaminergic neurons of the substantia nigra pars compacta in the basal ganglia (Damier et al., 1999). A further neuropathological hallmark of Parkinson's Disease is the intranuclear inclusion of aggregates of the misfolded presynaptic protein, α-synuclein. These aggregates present as a spherical Lewy Body in the cell body (soma) of the neurons or as elongated and branching Lewy-neurite in the neuronal processes (Braak et al., 2002).

As with HD, many animal models have also been generated for Parkinson's Disease although in contrast to HD most research has focused on neurotoxin rather than transgenic driven models. Two groups of neurotoxins are most commonly used: those that interfere with the catecholaminergic neurotransmission (such as reserpine, methamphetamine, 6-OHDA) or those that interfere with mitochondrial function (explained in more detail below but include agents such as MPTP, rotenone, and Paraquat-Maneb) (Blesa et al., 2012). Transgenic models for PD have also been developed; most notably by overexpression of mutant human α-synuclein or by interfering with genes found to be associated with familial Parkinson Disease (such as Parkin, PINK-1, DJ-1) (Dawson et al., 2010).

4.2.2. Mitochondrial dysfunction

The body of literature linking Parkinson's Disease to mitochondrial dysfunction is even greater than that for HD (for a comprehensive review, see (Exner et al., 2012)). Mitochondrial respiratory chain assessment in post-mortem PD brain has shown significant reduction in complex I activity (Schapira et al., 1990); a finding consistent with cases of patients developing Parkinsonism

after exposure to MPTP, a contaminant in an opioid preparation used by drug addicts, whose metabolite, MPP^+, is a potent inhibitor of mitochondrial complex I (Ballard et al., 1985). Furthermore, chronic exposure to the pesticide, rotenone which inhibits complex I, also produces Parkinsonism (Betarbet et al., 2000), further validating the presence of complex I impairment as an underlying feature of PD. Given their PD-like effects in man, complex I inhibitors, such as MPTP or rotenone, have been used extensively to recreate Parkinsonism in rodents and non-human primates. Complex I dysfunction in PD is not only limited to a reduction in enzyme activity as (Mizuno et al., 1989) have shown a reduction in complex I subunit composition among mitochondria isolated from the striatum of post-mortem PD brain. More in depth analysis revealed a decrease in its 8kDA subunit and a significant increase in protein carbonyls attached to its catalytic subunit, suggesting a protein peroxidative damage in the subunits composing complex I. This oxidative process is suggested to arise from an internal autooxidative process, correlated with complex I misassembly (Keeney et al., 2006). Recently, it was also discovered that there was high level of deletion in mitochondrial DNA (mtDNA) in the substantia nigra and striatum of Parkinson's Disease patients (Ikebe et al., 1990; Bender et al., 2006), further corroborating the role of mitochondrial genetics in Parkinson's Disease. This wealth of evidence attests to the importance of complex I dysfunction in the pathogenesis of Parkinson's Disease.

Further evidence for a role of mitochondrial dysfunction in PD comes from recent studies describing many genes implicated in familial Parkinson's Disease; most of which are associated with mitochondrial function. It is beyond the scope of this review to individually summarize the genes and its associated mitochondrial dysfunction but the most important is the triad of Parkin-PINK1-DJ1 genes. Parkin is a gene which encodes a protein with a E3 ubiquitin ligase function that is selectively recruited into damaged mitochondria and promotes autophagy (Narendra et al., 2008). A loss-of-function mutation of Parkin, associated with human familial PD, causes complex I and IV dysfunction as well as oxidative stress (Palacino et al., 2004). Other than promoting autophagy, Parkin is also at the core of many other mitochondrial functions, including prevention of mitochondrial swelling and protection against mitochondrial cell death (Darios et al., 2003). Another important gene identified in familial PD is PINK-1 which encodes a mitochondrial-targeting serine/threonine kinase. PINK-1 mutations cause severe multi-system mitochondrial impairment (e.g., disruption of mitochondrial morphology causing a fragmented mitochondria appearance (Clark et al., 2006; Exner et al., 2007)) which is rescued by Parkin overexpression, suggesting PINK-1 acts upstream of Parkin (Clark et al., 2006). The final protein in the triad, DJ-1 is another gene which is reported to have a mitochondrial function in scavenging reactive oxygen species (ROS) (Canet-Avilés et al., 2004; Taira et al., 2004). DJ-1 mutations cause increased vulnerability to oxidative stress and hypersensitivity to complex I inhibition (Kim et al., 2005). Furthermore, Parkin associates with DJ-1 and controls the stability of this protein (Moore et al., 2005). All in all these three genes play major roles in mitochondrial function and are tightly associated with the mitochondrial dysfunction implicated in Parkinson Disease.

4.2.3. Neuronal network activity

EEG abnormalities have long been described in Parkinson's Disease. A generalized slowing of EEG oscillatory activities is commonly observed with a reduction in the alpha and beta rhythm activity concurrent with an increase in the slower delta and theta wave activity (Soikkeli et al., 1991). These EEG abnormalities are correlated with the severity of the patient's clinical manifestation. For instance, PD patients with dementia have a much slower frequency activity dominating the EEG compared to those without dementia (Soikkeli et al., 1991; Neufeld et al., 1994; Sinanović et al., 2005). Bradykinesia has also been shown to be associated with a reduction of alpha and beta wave activity in the motor cortex; effects that are attenuated by levodopa administration (Brown and Marsden, 1999; Alonso-Frech et al., 2006). It is now well accepted that, motor symptoms in Parkinson's are associated with task-related EEG activity and show improvement after levodopa administration (Brown and Marsden, 1999; Wang et al., 1999), supporting strong association of motor impairment with EEG oscillatory activity impairment.

In addition to the evidence provided by EEG studies, the recent increase in the number of surgical procedures conducted on PD patients has provided a unique opportunity to record from deep areas of the brain to analyse activity beyond the reach of standard EEG recording approaches. In patients with tremor, single neuron analysis from subthalamic nucleus and basal ganglia revealed excessive high frequency synchronization consistent with the dynamic pattern of an oscillatory activity (Levy et al., 2000, 2002). This ectopic oscillatory activity is recorded yet again on local field potential recordings from the subthalamic nucleus, specifically in the gamma frequency range, among PD patients who present with tremor (Weinberger et al., 2009). Data obtained from depth recordings on patients undergoing Deep Brain Stimulation also showed the presence of excessive synchronization in the form of 'pathological' beta oscillations in the subthalamic nucleus; a phenomenon that was correlated with the degree to which patient's respond to dopaminergic medication (Weinberger et al., 2006; Ray et al., 2008; Kühn et al., 2009).

Animal models of Parkinson's Disease have also provided robust evidence of impaired neuronal network synchronization. In the neurotoxic rodent model using 6-hydroxydopamine (6-OHDA), excessive synchronization in the beta range (similar to the 'pathological beta' phenomenon in human) is found in recordings from the subthalamic nucleus (Mallet et al., 2008). Furthermore, in the substantia nigra of this 6-OHDA-rat model, increased alpha band oscillatory activity was observed that correlated with single neuron firing at the same frequency range and was associated with abnormal involuntary movement (Meissner et al., 2006). Acute application of 6-OHDA also resulted in increased power and coherence of the beta oscillation recorded *in vivo* in both the frontal cortex and subthalamic nucleus in the awake rat (Sharott et al., 2005). In a non-human primate MPTP model, recordings made from the primary motor cortex revealed hypersynchronous firing which was generated independently of basal ganglia input and could not generate detectable movement – hence making it an abnormal/pathological hypersynchronous activity (Goldberg et al., 2002). Similarly, in the globus pallidus and substantia nigra, neurons become oscillatory and fire with increased correlation in the beta frequency range (Nini et al., 1995; Wichmann et al., 1999; Raz et al., 2000). Taken together these observations suggest that excessive neuronal synchronization in the slow oscillatory range, most consistently at beta frequency, is a common phenomenon observed in neurotoxin induced PD animal models; an effect that translates through to observations made in human patients. Mechanistically, these changes are believed to be due to the reorganization of the inherent basal ganglia – thalamocortical neuronal network (Moran et al., 2011) but the exact mechanism as to how this reorganization occurs is yet to be elucidated.

5. Filling in the gap between mitochondrial dysfunction and neuronal oscillation

As described above, a lot is known about the presence, and importance, of mitochondrial dysfunction or neuronal oscillation

impairment in neurodegenerative disorders. However, little is known about the correlation between these two components. In particular, does mitochondrial dysfunction lead to the specific pattern of neuronal oscillation impairment causing the clinical manifestation observed in these neurodegenerative diseases? In order to answer this question, it is imperative to understand first whether mitochondrial function plays a role in generating physiological neuronal oscillatory activity. Few studies have tried to address this issue but the evidence generated to date points to mitochondrial function being vital for the generation of network activity.

In vitro brain slice studies have provided most of the evidence on the role of mitochondrial function in the generation of neuronal network activity. In the CA3 region of the hippocampus, it has been shown that gamma frequency oscillations require a higher level of pO_2, much higher than the 'critical' threshold value at which generalized energy failure in the form of spreading depression starts to occur (Huchzermeyer et al., 2008). This suggests that gamma frequency oscillations as a neuronal network activity has a higher energy demand than simple neuronal activity. This higher energy demand is met by the near-limit utilization of the mitochondrial oxidative phosphorylation capacity (Kann et al., 2011). In particular, in areas where gamma frequency oscillations are much higher in amplitude and frequency (such as CA3 compared to CA1 or dentate gyrus), a higher expression of mitochondrial complex I subunits and a concurrent higher oxygen consumption is observed (Kann et al., 2011). Additional support for the argument that gamma oscillations are tightly coupled with mitochondrial function comes from the observation that the reduction in gamma oscillation amplitude and frequency associated with aging in rodent brain slice is attributable to an increase in mitochondrial depolarization which limits the functional performance of the aged mitochondria (Lu et al., 2012).

The high dependence of oscillatory activity on mitochondrial function also renders the hippocampal network particularly sensitive to mitochondrial dysfunction. In this respect, it has been shown that both mitochondrial complex I (Kann et al., 2011) and complex IV inhibition (Whittaker et al., 2011) can abolish hippocampal gamma oscillations. Notably mitochondrial complex inhibition has cellular-specific effects with the interneurons being particularly vulnerable to damage compared to pyramidal cells (Whittaker et al., 2011). This cellular susceptibility is an important concept since different cellular ensembles are involved in the generation of neuronal oscillations in distinct brain regions and the specific cellular susceptibility in one brain region could explain why the same form of mitochondrial dysfunction could manifest differently in different brain regions the—so-called phenotypic variability. Thus, considering that we do observe that mitochondrial complex inhibition affects local field network activity, the next obvious question to ask is whether the effect is due to the selective vulnerability of a subset of cells (for instace interneurons) or whether it is due to a global knockout of mitochondrial function in all cellular components involved in the rhythmogenesis (see Fig. 2)? — an area of investigation that is starting to develop. The current school of thought seems to favour the 'interneuron energy hypothesis' that proposes an underlying susceptibility of fast-spiking interneurons to oxidative damage and mitochondrial dysfunction (Whittaker et al., 2011; Kann, 2015; Lax et al., 2015) but this hypothesis still lacks concrete evidence and the opposing idea of a global mitochondrial knockout has yet to be entertained. Nevertheless, the few studies that have addressed this gap between mitochondrial function and physiological neuronal network activity seems to agree on the idea that mitochondrial function is vital for the generation of synchronized neuronal oscillatory activity.

It is important to note at this instance that all the literature we have reviewed in the field of neurodegenerative diseases have quoted an impairment in various neuronal oscillation band, such as alpha, beta, and delta. Yet, most of the neuroenergetics study have focused on the gamma oscillation band. Whilst one can argue that these findings could be generalized to other form of neuronal oscillation, it can be an oversimplification and clearly represents a gap in our knowledge of the cellular energetics of neuronal oscillation. This warrants more studies on the mitochondrial bioenergetics of neuronal oscillations in discrete bands within the context of the neurodegenerative diseases. We now propose a framework to address this issue (see Section 6).

6. Suggested approach for neuropharmacological study in mitochondrial disorder

Drug discovery for mitochondrial disorders is challenging not least because we currently lack a parameter that can translate well to a clinical setting. The best parameter to use for this purpose is a physiological parameter and in terms of neurological disorders, one parameter that has been shown to be promising is assessment of neuronal oscillation power and patterning — an activity indicative of neuronal network function that generates behavioural response. Whilst extensive evidence exists to suggest that both mitochondrial dysfunction and neuronal network impairment are present in neurodegenerative disorders, no correlation has yet been made between the two in respect to the clinical disorder. Some studies have shown that, under physiological condition, neuronal oscillatory activity does require a supra-threshold utilization of mitochondrial oxidative capacity. Hence, logically, in the context of neurodegeneration where mitochondrial dysfunction exists, it would make sense that the neuronal network activity would be impaired (which is indeed what is seen in these disorders). Therefore, an interesting novel approach that could be undertaken now is to assess in these neurodegenerative disorders whether the mitochondrial dysfunction observed leads to the neuronal oscillatory impairment found in these disorders.

The simplest method to do so is to use the *in vitro* brain slice approach, which has various advantages such as the use of a tissue setting with the preservation of a viable neuronal network (unlike cultured cell electrophysiology studies) and the ability to perform controlled pharmacological manipulation. We propose a framework for neuropharmacological study which incorporates this method as a platform for a pilot study to try and develop a model system that replicates neuronal disturbances seen in a mitochondrial disorder and then to attempt to "treat" this to provide insight as to how a drug discovery programme could be configured to treat real patients (refer to Fig. 3). Our approach was to take the mitochondrial dysfunction observed in human pathological analyses and use various established mitochondrial inhibitors, to replicate the dysfunction observed in humans. Specifically our approach is to study the impact of mitochondrial inhibition on neuronal network activity and address the question: Does this pharmacological challenge echo the pattern of impairment seen in the human electrophysiology studies in patients ? If it does, we would have achieved the first evidence to suggest that in that particular neurodegenerative disorder, the mitochondrial dysfunction gives rise to the neuronal network impairment. In effect the resultant model would be an *in vitro* brain slice model of the 'mitochondrial dysfunction — neuronal network impairment coupling' of that particular disorder. The model could then be validated further by the use of *post-hoc* immunohistochemical or biochemical analyses to verify if indeed the use of the mitochondrial inhibitors has replicated the same pattern of mitochondrial dysfunction and/or neurodegeneration seen in human pathology. After this validation, the model system can then be used faithfully for drug discovery

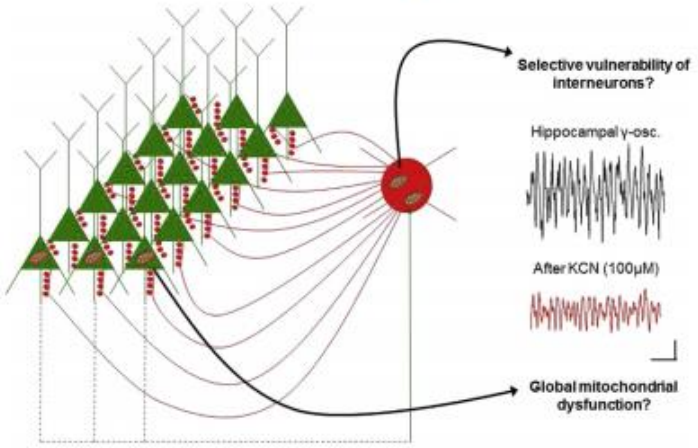

Fig. 2. Neuronal oscillation and mitochondrial function coupling. The figure shows the cellular component understood to generate neuronal oscillation from studies done in hippocampus—the interaction between pyramidal cells (shown in green) and inhibitory interneuron (shown in red). Inhibitory interneurons have been shown to have more mitochondria than pyramidal cells, implying a higher metabolic demand. Also shown is a demonstration of the vulnerability of neuronal oscillatory activity to mitochondrial complex inhibition where significant reduction is seen after the addition of potassium cyanide – (KCN) – a complex IV inhibitor. The issue to consider is then whether this disruption in neuronal oscillatory activity is attributable to the selective vulnerability of the interneurons or a global mitochondrial dysfunction of the entire neuronal network. (For interpretation of the references to colour in this figure legend, the reader is referred to the web version of this article.)

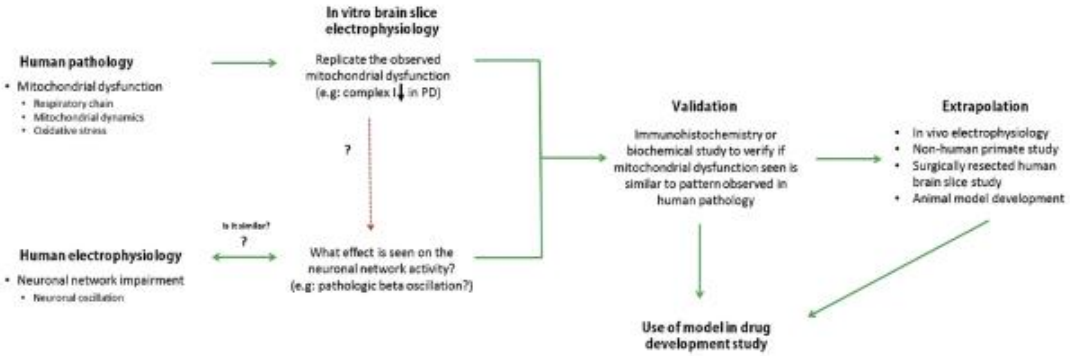

Fig. 3. Suggested framework for neuropharmacological study in mitochondrial disorder. Four main stages are identified: extrapolation from human neuropathological and/or electrophysiological study, *in vitro* brain slice electrophysiology study (as the pilot stage), validation, and further extrapolation. *In vitro* work can employ pure or nested oscillation model and should ideally be conducted in relevant brain region according to the neuropathological findings.

studies involving the evaluation of novel compounds. If successful it can also be engineered to a higher complexity setting such as the use of *in vivo* electrophysiology, non-human primate electrophysiology, or surgically resected human brain slice electrophysiology (where applicable in cases in which relevant area to the disorder could be obtained via routine surgical procedures). Following through this framework would provide scientists the opportunity to pursue detailed neuropharmacological analysis of mitochondrial disorders via a neurophysiological approach that could fill in the gap for translation to the clinical setting and thereby hopefully, improve the probability of successfully developing medicines that could treat mitochondrial disorders that severely impact the quality life of these patients.

Thus, we would like to propose neuronal oscillation as a possible physiological parameter to be used in drug development studies for mitochondrial disorder. It could potentially be able to fill the gap for physiological biomarkers that are desperately required for assessment of mitochondrial function.

Acknowledgements

FC is funded by a GSK/EPSRC CASE (EP/K50499X/1) studentship. NZL and DMT are supported by The Wellcome Trust (074454/Z/04/Z). We would like to thank Nicholas Lynch for assistance in the graphical design of a figure in this paper.

References

Aarsland, D., Bronnick, K., Williams-Gray, C., Weintraub, D., Marder, K., Kulisevsky, J., Burn, D., Barone, P., Pagonabarraga, J., Allcock, L., Santangelo, G., Foltynie, T., Janvin, C., Larsen, J.P., Barker, R.A., Emre, M., 2010. Mild cognitive impairment in Parkinson disease: a multicenter pooled analysis. Neurology 75 (12), 1062–1069.

Aarsland, D., Kurz, M.W., 2010. The epidemiology of dementia associated with Parkinson disease. J. Neurol. Sci. 289 (1–2), 18–22.

Abou-Sleiman, P.M., Muqit, M.M.K., Wood, N.W., 2006. Expanding insights of

mitochondrial dysfunction in Parkinson's disease. Nat. Rev. Neurosci. 7 (3), 207–219.
Alonso-Frech, F., Zamarbide, I., Alegre, M., Rodríguez-Oroz, M.C., Guridi, J., Manrique, M., Valencia, M., Artieda, J., Obeso, J.A., 2006. Slow oscillatory activity and levodopa-induced dyskinesias in Parkinson's disease. Brain 129 (7), 1748–1757.
André, V.M., Cepeda, C., Venegas, A., Gomez, Y., Levine, M.S., 2006. Altered cortical glutamate receptor function in the R6/2 model of Huntington's disease. J. Neurophysiol. 95 (4), 2108–2119.
Atallah, B.V., Scanziani, M., 2009. Instantaneous modulation of gamma oscillation frequency by balancing excitation with inhibition. Neuron 62 (4), 566–577.
Ballard, P.A., Tetrud, J.W., Langston, J.W., 1985. Permanent human parkinsonism due to 1-methy1–4-phenyl-1,2,3,6-tetrahydropyridine (MPTP): seven cases. Neurology 35 (7), 949.
Bartos, M., Vida, I., Jonas, P., 2007. Synaptic mechanisms of synchronized gamma oscillations in inhibitory interneuron networks. Nat. Rev. Neurosci. 8 (1), 45–56.
Beal, M.F., Brouillet, E., Jenkins, B., Henshaw, R., Rosen, B., Hyman, B.T., 1993a. Age-dependent striatal excitotoxic lesions produced by the endogenous mitochondrial inhibitor malonate. J. Neurochem. 61 (3), 1147–1150.
Beal, M.F., Brouillet, E., Jenkins, B.G., Ferrante, R.J., Kowall, N.W., Miller, J.M., Storey, E., Srivastava, R., Rosen, B.R., Hyman, B.T., 1993b. Neurochemical and histologic characterization of striatal excitotoxic lesions produced by the mitochondrial toxin 3-nitropropionic acid. J. Neurosci. 13 (10), 4181–4192.
Benchenane, K., Tiesinga, P.H., Battaglia, F.P., 2011. Oscillations in the prefrontal cortex: a gateway to memory and attention. Curr. Opin. Neurobiol. 21 (3), 475–485.
Bender, A., Krishnan, K.J., Morris, C.M., Taylor, G.A., Reeve, A.K., Perry, R.H., Jaros, E., Hersheson, J.S., Betts, J., Klopstock, T., Taylor, R.W., Turnbull, D.M., 2006. High levels of mitochondrial DNA deletions in substantia nigra neurons in aging and Parkinson disease. Nat. Genet. 38 (5), 515–517.
Berger, H., 1929. Über das Elektrenkephalogramm des Menschen. Arch. für Psychiatr. Nervenkrankh. 87 (1), 527–570.
Betarbet, R., Sherer, T.B., MacKenzie, G., Garcia-Osuna, M., Panov, A.V., Greenamyre, J.T., 2000. Chronic systemic pesticide exposure reproduces features of Parkinson's disease. Nat. Neurosci. 3, 1301–1306.
Blesa, J., Phani, S., Jackson-Lewis, V., Przedborski, S., 2012. Classic and new animal models of Parkinson's disease. J. Biomed. Biotechnol. 2012, 10.
Borlongan, C.V., Koutouzis, T.K., Freeman, T.B., Cahill, D.W., Sanberg, P.R., 1995. Behavioral pathology induced by repeated systemic injections of 3-nitropropionic acid mimics the motoric symptoms of Huntington's disease. Brain Res. 697 (1–2), 254–257.
Braak, H., Del Tredici, K., Bratzke, H., Hamm-Clement, J., Sandmann-Keil, D., Rüb, U., 2002. Staging of the intracerebral inclusion body pathology associated with idiopathic Parkinson's disease (preclinical and clinical stages). J. Neurol. 249 (3), iii1–iii5.
Bragin, A., Jando, G., Nadasdy, Z., Hetke, J., Wise, K., Buzsaki, G., 1995. Gamma (40-100 Hz) oscillation in the hippocampus of the behaving rat. J. Neurosci. 15 (1), 47–60.
Brennan, W.A., Bird, E.D., Aprille, J.R., 1985. Regional mitochondrial respiratory activity in Huntington's disease brain. J. Neurochem. 44 (6), 1948–1950.
Brouillet, E., Hantraye, P., Ferrante, R.J., Dolan, R., Leroy-Willig, A., Kowall, N.W., Beal, M.F., 1995. Chronic mitochondrial energy impairment produces selective striatal degeneration and abnormal choreiform movements in primates. Proc. Natl. Acad. Sci. 92 (15), 7105–7109.
Brown, J.T., Teriakidis, A., Randall, A.D., 2006. A pharmacological investigation of the role of GLUK5-containing receptors in kainate-driven hippocampal gamma band oscillations. Neuropharmacology 50 (1), 47–56.
Brown, P., Marsden, C.D., 1999. Bradykinesia and impairment of EEG desynchronization in Parkinson's disease. Mov. Disord. 14 (3), 423–429.
Browne, S.E., Bowling, A.C., Macgarvey, U., Baik, M.J., Berger, S.C., Muquit, M.M.K., Bird, E.D., Beal, M.F., 1997. Oxidative damage and metabolic dysfunction in Huntington's disease: selective vulnerability of the basal ganglia. Ann. Neurol. 41 (5), 646–653.
Buhl, E.H., Tamás, G., Fisahn, A., 1998. Cholinergic activation and tonic excitation induce persistent gamma oscillations in mouse somatosensory cortex in vitro. J. Physiol. 513 (1), 117–126.
Buzsáki, G., Draguhn, A., 2004. Neuronal oscillations in cortical networks. Science 304 (5679), 1926–1929.
Buzsáki, G., Logothetis, N., Singer, W., 2013. Scaling brain size, keeping timing: evolutionary preservation of brain rhythms. Neuron 80 (3), 751–764.
Bylsma, F.W., Peyser, C.E., Folstein, S.E., Ross, C., Brandt, J., 1994. EEG power spectra in huntington's disease: clinical and neuropsychological correlates. Neuropsychologia 32 (2), 137–150.
Calabresi, P., Gubellini, P., Picconi, B., Centonze, D., Pisani, A., Bonsi, P., Greengard, P., Hipskind, R.A., Borrelli, E., Bernardi, G., 2001. Inhibition of mitochondrial complex II induces a long-term potentiation of NMDA-mediated synaptic excitation in the striatum requiring endogenous dopamine. J. Neurosci. 21 (14), 5110–5120.
Canet-Avilés, R.M., Wilson, M.A., Miller, D.W., Ahmad, R., McLendon, C., Bandyopadhyay, S., Baptista, M.J., Ringe, D., Petsko, G.A., Cookson, M.R., 2004. The Parkinson's disease protein DJ-1 is neuroprotective due to cysteine-sulfinic acid-driven mitochondrial localization. Proc. Natl. Acad. Sci. U. S. A. 101 (24), 9103–9108.
Cardin, J.A., Carlen, M., Meletis, K., Knoblich, U., Zhang, F., Deisseroth, K., Tsai, L.-H., Moore, C.I., 2009. Driving fast-spiking cells induces gamma rhythm and controls sensory responses. Nature 459 (7247), 663–667.
Centonze, D., Prosperetti, C., Barone, I., Rossi, S., Picconi, B., Tscherter, A., De Chiara, V., Bernardi, G., Calabresi, P., 2006. NR2B-containing NMDA receptors promote the neurotoxic effects of 3-nitropropionic acid but not of rotenone in the striatum. Exp. Neurol. 202 (2), 470–479.
Chang, D.T.W., Honick, A.S., Reynolds, I.J., 2006. Mitochondrial trafficking to synapses in cultured primary cortical neurons. J. Neurosci. 26 (26), 7035–7045.
Chang, D.T.W., Reynolds, I.J., 2006. Mitochondrial trafficking and morphology in healthy and injured neurons. Prog. Neurobiol. 80 (5), 241–268.
Cheyne, D., Bells, S., Ferrari, P., Gaetz, W., Bostan, A.C., 2008. Self-paced movements induce high-frequency gamma oscillations in primary motor cortex. Neuroimage 42 (1), 332–342.
Chinnery, P.F., Elliott, H.R., Hudson, G., Samuels, D.C., Relton, C.L., 2012. Epigenetics, epidemiology and mitochondrial DNA diseases. Int. J. Epidemiol. 41 (1), 177–187.
Clark, I.E., Dodson, M.W., Jiang, C., Cao, J.H., Huh, J.R., Seol, J.H., Yoo, S.J., Hay, B.A., Guo, M., 2006. Drosophila pink1 is required for mitochondrial function and interacts genetically with parkin. Nature 441 (7097), 1162–1166.
Clay, H.B., Sillivan, S., Konradi, C., 2011. Mitochondrial dysfunction and pathology in bipolar disorder and schizophrenia. Int. J. Dev. Neurosci. 29 (3), 311–324.
Crook, Z.R., Housman, D., 2011. Huntington's disease: can mice lead the way to treatment? Neuron 69 (3), 423–435.
Cunningham, M.O., Davies, C.H., Buhl, E.H., Kopell, N., Whittington, M.A., 2003. Gamma oscillations induced by kainate receptor activation in the entorhinal cortex in vitro. J. Neurosci. 23 (30), 9761–9769.
Cunningham, M.O., Whittington, M.A., Bibbig, A., Roopun, A., LeBeau, F.E.N., Vogt, A., Monyer, H., Buhl, E.H., Traub, R.D., 2004. A role for fast rhythmic bursting neurons in cortical gamma oscillations in vitro. Proc. Natl. Acad. Sci. U. S. A. 101 (18), 7152–7157.
Damier, P., Hirsch, E.C., Agid, Y., Graybiel, A.M., 1999. The substantia nigra of the human brain: II. Patterns of loss of dopamine-containing neurons in Parkinson's disease. Brain 122 (8), 1437–1448.
Darios, F., Corti, O., Lücking, C.B., Hampe, C., Muriel, M.-P., Abbas, N., Gu, W.-J., Hirsch, E.C., Rooney, T., Ruberg, M., Brice, A., 2003. Parkin prevents mitochondrial swelling and cytochrome c release in mitochondria-dependent cell death. Hum. Mol. Genet. 12 (5), 517–526.
Dawson, T.M., Ko, H.S., Dawson, V.L., 2010. Genetic animal models of Parkinson's disease. Neuron 66 (5), 646–661.
de Tommaso, M., De Carlo, F., Difruscolo, O., Massafra, R., Sciruicchio, V., Bellotti, R., 2003. Detection of subclinical brain electrical activity changes in Huntington's disease using artificial neural networks. Clin. Neurophysiol. 114 (7), 1237–1245.
Duyao, M., Ambrose, C., Myers, R., Novelletto, A., Persichetti, F., Frontali, M., Folstein, S., Ross, C., Franz, M., Abbott, M., Gray, J., Conneally, P., Young, A., Penney, J., Hollingsworth, Z., Shoulson, I., Lazzarini, A., Falek, A., Koroshetz, W., Sax, D., Bird, E., Vonsattel, J., Bonilla, E., Alvir, J., Bickham Conde, J., Cha, J.H., Dure, L., Gomez, F., Ramos, M., Sanchez-Ramos, J., Snodgrass, S., de Young, M., Wexler, N., Moscowitz, C., Penchaszadeh, G., MacFarlane, H., Anderson, M., Jenkins, B., Srinidhi, J., Barnes, G., Gusella, J., MacDonald, M., 1993. Trinucleotide repeat length instability and age of onset in Huntington's disease. Nat. Genet. 4 (4), 387–392.
Edden, R.A.E., Muthukumaraswamy, S.D., Freeman, T.C.A., Singh, K.D., 2009. Orientation discrimination performance is predicted by GABA concentration and gamma oscillation frequency in human primary visual cortex. J. Neurosci. 29 (50), 15721–15726.
Engel, A.K., Fries, P., 2010. Beta-band oscillations—signalling the status quo? Curr. Opin. Neurobiol. 20 (2), 156–165.
Estrada-Sánchez, A.M., Montiel, T., Segovia, J., Massieu, L., 2009. Glutamate toxicity in the striatum of the R6/2 Huntington's disease transgenic mice is age-dependent and correlates with decreased levels of glutamate transporters. Neurobiol. Dis. 34 (1), 78–86.
Exner, N., Lutz, A.K., Haass, C., Winklhofer, K.F., 2012. Mitochondrial dysfunction in Parkinson|'s disease: molecular mechanisms and pathophysiological consequences. EMBO J. 31 (14), 3038–3062.
Exner, N., Treske, B., Paquet, D., Holmström, K., Schiesling, C., Gispert, S., Carballo-Carbajal, I., Berg, D., Hoepken, H.-H., Gasser, T., Krüger, R., Winklhofer, K.F., Vogel, F., Reichert, A.S., Auburger, G., Kahle, P.J., Schmid, B., Haass, C., 2007. Loss-of-Function of human PINK1 results in mitochondrial pathology and can be rescued by Parkin. J. Neurosci. 27 (45), 12413–12418.
Fisahn, A., Contractor, A., Traub, R.D., Buhl, E.H., Heinemann, S.F., McBain, C.J., 2004. Distinct roles for the kainate receptor subunits GluR5 and GluR6 in kainate-induced hippocampal gamma oscillations. J. Neurosci. 24 (43), 9658–9668.
Fisahn, A., Pike, F.G., Buhl, E.H., Paulsen, O., 1998. Cholinergic induction of network oscillations at 40 Hz in the hippocampus in vitro. Nature 394 (6689), 186–189.
Fisher, S.P., Black, S.W., Schwartz, M.D., Wilk, A.J., Chen, T.-M., Lincoln, W.U., Liu, H.W., Kilduff, T.S., Morairty, S.R., 2013. Longitudinal analysis of the electroencephalogram and sleep phenotype in the R6/2 mouse model of Huntington's disease. Brain 136 (7), 2159–2172.
Forsaa, E.B., Larsen, J., Wentzel-Larsen, T., et al., 2010. A 12-year population-based study of psychosis in parkinson disease. Arch. Neurol. 67 (8), 996–1001.
Goldberg, J.A., Boraud, T., Maraton, S., Haber, S.N., Vaadia, E., Bergman, H., 2002. Enhanced synchrony among primary motor cortex neurons in the 1-methyl-4-phenyl-1,2,3,6-tetrahydropyridine primate model of Parkinson's disease. J. Neurosci. 22 (11), 4639–4653.
Gorman, G.S., Schaefer, A.M., Ng, Y., Gomez, N., Blakely, E.L., Alston, C.L., Feeney, C.,

Horvath, R., Yu-Wai-Man, P., Chinnery, P.F., Taylor, R.W., Turnbull, D.M., McFarland, R., 2015. Prevalence of nuclear and mitochondrial DNA mutations related to adult mitochondrial disease. Ann. Neurol. 77 (5), 753–759.
Gray, C., 1994. Synchronous oscillations in neuronal systems: mechanisms and functions. J. Comput. Neurosci. 1 (1–2), 11–38.
Greene, J.G., Sheu, S.S., Gross, R.A., Greenamyre, J.T., 1998. 3-Nitropropionic acid exacerbates N-methyl-d-aspartate toxicity in striatal culture by multiple mechanisms. Neuroscience 84 (2), 503–510.
Gu, M., Gash, M.T., Mann, V.M., Javoy-Agid, F., Cooper, J.M., Schapira, A.H.V., 1996. Mitochondrial defect in Huntington's disease caudate nucleus. Ann. Neurol. 39 (3), 385–389.
Gubellini, P., Centonze, D., Tropepi, D., Bernardi, G., Calabresi, P., 2004. Induction of corticostriatal LTP by 3-nitropropionic acid requires the activation of mGluR1/PKC pathway. Neuropharmacology 46 (6), 761–769.
Hájos, N., Paulsen, O., 2009. Network mechanisms of gamma oscillations in the CA3 region of the hippocampus. Neural Netw. 22 (8), 1113–1119.
Hervias, I., Beal, M.F., Manfredi, G., 2006. Mitochondrial dysfunction and amyotrophic lateral sclerosis. Muscle & Nerve 33 (5), 598–608.
Horton, T., Graham, B., Corral-Debrinski, M., Shoffner, J., Kaufman, A., Beal, M., Wallace, D., 1995. Marked increase in mitochondrial DNA deletion levels in the cerebral cortex of Huntington's disease patients. Neurology 45 (10), 1879–1893.
Huchzermeyer, C., Albus, K., Gabriel, H.-J., Otáhal, J., Taubenberger, N., Heinemann, U., Kovács, R., Kann, O., 2008. Gamma oscillations and spontaneous network activity in the Hippocampus are highly sensitive to decreases in pO2 and concomitant changes in mitochondrial redox state. J. Neurosci. 28 (5), 1153–1162.
Ikebe, S.-i., Tanaka, M., Ohno, K., Sato, W., Hattori, K., Kondo, T., Mizuno, Y., Ozawa, T., 1990. Increase of deleted mitochondrial DNA in the striatum in Parkinson's disease and senescence. Biochem. Biophys. Res. Commun. 170 (3), 1044–1048.
Jain, V., Langham, M.C., Wehrli, F.W., 2010. MRI estimation of global brain oxygen consumption rate. J. Cereb. Blood Flow Metab. Off. J. Int. Soc. Cereb. Blood Flow Metab. 30 (9), 1598–1607.
Jeantet, Y., Cayzac, S., Cho, Y.H., 2013. β oscillation during slow wave sleep and rapid eye movement sleep in the electroencephalogram of a transgenic mouse model of Huntington's disease. PLoS One 8 (11), e79509.
Johri, A., Chaturvedi, R.K., Beal, M.F., 2011. Hugging tight in Huntington's. Nat. Med. 17 (3), 245–246.
Kann, O., 2015. The interneuron energy hypothesis: implications for brain disease. Neurobiol. Dis. S0969-9961(15)30025-5.
Kann, O., Huchzermeyer, C., Kovács, R., Wirtz, S., Schuelke, M., 2011. Gamma oscillations in the hippocampus require high complex I gene expression and strong functional performance of mitochondria. Brain 134 (2), 345–358.
Kantor, S., Szabo, L., Varga, J., Cuesta, M., Morton, A.J., 2013. Progressive sleep and electroencephalogram changes in mice carrying the Huntington's disease mutation. Brain 136 (7), 2147–2158.
Keeney, P.M., Xie, J., Capaldi, R.A., Bennett, J.P., 2006. Parkinson's disease brain mitochondrial complex I has oxidatively damaged subunits and is functionally impaired and misassembled. J. Neurosci. 26 (19), 5256–5264.
Kiernan, M.C., Vucic, S., Cheah, B.C., Turner, M.R., Eisen, A., Hardiman, O., Burrell, J.R., Zoing, M.C., 2011. Amyotrophic lateral sclerosis. Lancet 377 (9769), 942–955.
Kim, J., Moody, J.P., Edgerly, C.K., Bordiuk, O.L., Cormier, K., smith, K., Beal, M.F., Ferrante, R.J., 2010. Mitochondrial loss, dysfunction, and altered dynamics in Huntington's disease. Hum. Mol. Genet. 19 (20), 3919–3935.
Kim, R.H., Smith, P.D., Aleyasin, H., Hayley, S., Mount, M.P., Pownall, S., Wakeham, A., You-Ten, A.J., Kalia, S.K., Horne, P., Westaway, D., Lozano, A.M., Anisman, H., Park, D.S., Mak, T.W., 2005. Hypersensitivity of DJ-1-deficient mice to 1-methyl-4-phenyl-1,2,3,6-tetrahydropyrindine (MPTP) and oxidative stress. Proc. Natl. Acad. Sci. U. S. A. 102 (14), 5215–5220.
Kühn, A.A., Tsui, A., Aziz, T., Ray, N., Brücke, C., Kupsch, A., Schneider, G.-H., Brown, P., 2009. Pathological synchronisation in the subthalamic nucleus of patients with Parkinson's disease relates to both bradykinesia and rigidity. Exp. Neurol. 215 (2), 380–387.
Lax, N.Z., Grady, J., Laude, A., Chan, F., Hepplewhite, P.D., Gorman, G., Whittaker, R.G., Ng, Y., Cunningham, M.O., Turnbull, D.M., 2015. Extensive respiratory chain defects in inhibitory interneurones in patients with mitochondrial disease. Neuropathol. Appl. Neurobiol. http://dx.doi.org/10.1111/nan.12238.
Levy, R., Hutchison, W.D., Lozano, A.M., Dostrovsky, J.O., 2000. High-frequency synchronization of neuronal activity in the subthalamic nucleus of Parkinsonian patients with limb tremor. J. Neurosci. 20 (20), 7766–7775.
Levy, R., Hutchison, W.D., Lozano, A.M., Dostrovsky, J.O., 2002. Synchronized neuronal discharge in the basal ganglia of Parkinsonian patients is limited to oscillatory activity. J. Neurosci. 22 (7), 2855–2861.
Liu, X., Luo, X., Hu, W., 1992. Studies on the epidemiology and etiology of moldy sugarcane poisoning in China. Biomed. Environ. Sci. BES 5 (2), 161–177.
Lu, C.B., Vreugdenhil, M., Toescu, E.C., 2012. The effect of aging-associated impaired mitochondrial status on kainate-evoked hippocampal gamma oscillations. Neurobiol. Aging 33 (11), 2692–2703.
Mallet, N., Pogosyan, A., Sharott, A., Csicsvari, J., Bolam, J.P., Brown, P., Magill, P.J., 2008. Disrupted dopamine transmission and the emergence of exaggerated beta oscillations in subthalamic nucleus and cerebral cortex. J. Neurosci. 28 (18), 4795–4806.
Mann, E.O., Suckling, J.M., Hajos, N., Greenfield, S.A., Paulsen, O., 2005. Perisomatic feedback inhibition underlies cholinergically induced fast network oscillations in the rat Hippocampus in vitro. Neuron 45 (1), 105–117.
Meissner, W., Ravenscroft, P., Reese, R., Harnack, D., Morgenstern, R., Kupsch, A., Klitgaard, H., Bioulac, B., Gross, C.E., Bezard, E., Boraud, T., 2006. Increased slow oscillatory activity in substantia nigra pars reticulata triggers abnormal involuntary movements in the 6-OHDA-lesioned rat in the presence of excessive extracellular striatal dopamine. Neurobiol. Dis. 22 (3), 586–598.
Millan, M.J., Agid, Y., Brüne, M., Bullmore, E.T., Carter, C.S., Clayton, N.S., Connor, R., Davis, S., Deakin, B., DeRubeis, R.J., Dubois, B., Geyer, M.A., Goodwin, G.M., Gorwood, P., Jay, T.M., Joëls, M., Mansuy, I.M., Meyer-Lindenberg, A., Murphy, D., Rolls, E., Saletu, B., Spedding, M., Sweeney, J., Whittington, M., Young, L.J., 2012. Cognitive dysfunction in psychiatric disorders: characteristics, causes and the quest for improved therapy. Nat. Rev. Drug Discov. 11 (2), 141–168.
Ming, L., 1995. Moldy sugarcane poisoning— a case report with a brief review. Clin. Toxicol. 33 (4), 363–367.
Mizuno, Y., Ohta, S., Tanaka, M., Takamiya, S., Suzuki, K., Sato, T., Oya, H., Ozawa, T., Kagawa, Y., 1989. Deficiencies in complex I subunits of the respiratory chain in Parkinson's disease. Biochem. Biophys. Res. Commun. 163 (3), 1450–1455.
Moore, D.J., Zhang, L., Troncoso, J., Lee, M.K., Hattori, N., Mizuno, Y., Dawson, T.M., Dawson, V.L., 2005. Association of DJ-1 and parkin mediated by pathogenic DJ-1 mutations and oxidative stress. Hum. Mol. Genet. 14 (1), 71–84.
Moran, R.J., Mallet, N., Litvak, V., Dolan, R.J., Magill, P.J., Friston, K.J., Brown, P., 2011. Alterations in brain connectivity underlying beta oscillations in Parkinsonism. PLoS Comput. Biol. 7 (8), e1002124.
Moreira, P.I., Carvalho, C., Zhu, X., Smith, M.A., Perry, G., 2010. Mitochondrial dysfunction is a trigger of Alzheimer's disease pathophysiology. Biochim. Biophys. Acta (BBA) Mol. Basis Dis. 1802 (1), 2–10.
Narendra, D., Tanaka, A., Suen, D.-F., Youle, R.J., 2008. Parkin is recruited selectively to impaired mitochondria and promotes their autophagy. J. Cell Biol. 183 (5), 795–803.
Nesbitt, V., Pitceathly, R.D.S., Turnbull, D.M., Taylor, R.W., Sweeney, M.G., Mudanohwo, E.E., Rahman, S., Hanna, M.G., McFarland, R., 2013. The UK MRC mitochondrial disease patient cohort study: clinical phenotypes associated with the m.3243A>G mutation—implications for diagnosis and management. J. Neurol. Neurosurg. Psychiatry 84 (8), 936–938.
Neufeld, M.Y., Blumen, S., Aitkin, I., Parmet, Y., Korczyn, A.D., 1994. EEG frequency analysis in demented and nondemented Parkinsonian patients. Dement. Geriatr. Cogn. Disord. 5 (1), 23–28.
Neugroschl, J., Sano, M., 2010. Current treatment and recent clinical research in Alzheimer's disease. Mt. Sinai J. Med. A J. Transl. Personalized Med. 77 (1), 3–16.
Nini, A., Feingold, A., Slovin, H., Bergman, H., 1995. Neurons in the globus pallidus do not show correlated activity in the normal monkey, but phase-locked oscillations appear in the MPTP model of parkinsonism. J. Neurophysiol. 74 (4), 1800–1805.
Obeso, J.A., Rodriguez-Oroz, M.C., Goetz, C.G., Marin, C., Kordower, J.H., Rodriguez, M., Hirsch, E.C., Farrer, M., Schapira, A.H.V., Halliday, G., 2010. Missing pieces in the Parkinson's disease puzzle. Nat. Med. 16 (6), 653–661.
Oliveira, J.M.A., 2010. Nature and cause of mitochondrial dysfunction in Huntington's disease: focusing on huntingtin and the striatum. J. Neurochem. 114 (1), 1–12.
Painold, A., Anderer, P., Holl, A., Letmaier, M., Saletu-Zyhlarz, G., Saletu, B., Bonelli, R., 2010. Comparative EEG mapping studies in Huntington's disease patients and controls. J. Neural Transm. 117 (11), 1307–1318.
Palacino, J.J., Sagi, D., Goldberg, M.S., Krauss, S., Motz, C., Wacker, M., Klose, J., Shen, J., 2004. Mitochondrial dysfunction and oxidative damage in parkin-deficient mice. J. Biol. Chem. 279 (18), 18614–18622.
Palfi, S., Ferrante, R.J., Brouillet, E., Beal, M.F., Dolan, R., Guyot, M.C., Peschanski, M., Hantraye, P., 1996. Chronic 3-Nitropropionic acid treatment in baboons replicates the cognitive and motor deficits of Huntington's disease. J. Neurosci. 16 (9), 3019–3025.
Pálhalmi, J., Paulsen, O., Freund, T.F., Hájos, N., 2004. Distinct properties of carbachol- and DHPG-induced network oscillations in hippocampal slices. Neuropharmacology 47 (3), 381–389.
Parikh, S., Saneto, R., Falk, M., Anselm, I., Cohen, B., Haas, R., 2009. A modern approach to the treatment of mitochondrial disease. Curr. Treat. Options Neurol. 11 (6), 414–430.
Payne, B.A.I., Wilson, I.J., Yu-Wai-Man, P., Coxhead, J., Deehan, D., Horvath, R., Taylor, R.W., Samuels, D.C., Santibanez-Koref, M., Chinnery, P.F., 2013. Universal heteroplasmy of human mitochondrial DNA. Hum. Mol. Genet. 22 (2), 384–390.
Pfeffer, G., Horvath, R., Klopstock, T., Mootha, V.K., Suomalainen, A., Koene, S., Hirano, M., Zeviani, M., Bindoff, L.A., Yu-Wai-Man, P., Hanna, M., Carelli, V., McFarland, R., Majamaa, K., Turnbull, D.M., Smeitink, J., Chinnery, P.F., 2013. New treatments for mitochondrial disease—no time to drop our standards. Nat. Rev. Neurol. 9 (8), 474–481.
Pignatelli, M., Lebreton, F., Cho, Y.H., Leinekugel, X., 2012. "Ectopic" theta oscillations and interictal activity during slow-wave state in the R6/1 mouse model of Huntington's disease. Neurobiol. Dis. 48 (3), 409–417.
Polidori, M.C., Mecocci, P., Browne, S.E., Senin, U., Beal, M.F., 1999. Oxidative damage to mitochondrial DNA in Huntington's disease parietal cortex. Neurosci. Lett. 272 (1), 53–56.
Popoli, P., Pèzzola, A., Domenici, M.R., Sagratella, S., Diana, G., Caporali, M.G., Bronzetti, E., Vega, J., de Carolis, A.S., 1994. Behavioral and electrophysiological correlates of the quinolinic acid rat model of Huntington's disease in rats. Brain Res. Bull. 35 (4), 329–335.
Quastel, J.H., Wheatley, A.H.M., 1932. Oxidations by the brain. Biochem. J. 26 (3), 725–744.

Ramaswamy, S., McBride, J.L., Kordower, J.H., 2007. Animal models of Huntington's disease. ILAR J. 48 (4), 356–373.
Ravel, N., Chabaud, P., Martin, C., Gaveau, V., Hugues, E., Tallon-Baudry, C., Bertrand, O., Gervais, R., 2003. Olfactory learning modifies the expression of odour-induced oscillatory responses in the gamma (60–90 Hz) and beta (15–40 Hz) bands in the rat olfactory bulb. Eur. J. Neurosci. 17 (2), 350–358.
Ray, N.J., Jenkinson, N., Wang, S., Holland, P., Brittain, J.S., Joint, C., Stein, J.F., Aziz, T., 2008. Local field potential beta activity in the subthalamic nucleus of patients with Parkinson's disease is associated with improvements in bradykinesia after dopamine and deep brain stimulation. Exp. Neurol. 213 (1), 108–113.
Raz, A., Vaadia, E., Bergman, H., 2000. Firing patterns and correlations of spontaneous discharge of pallidal neurons in the Normal and the tremulous 1-methyl-4-phenyl-1,2,3,6-tetrahydropyridine vervet model of Parkinsonism. J. Neurosci. 20 (22), 8559–8571.
Reggio, R., Pèzzola, A., Popoli, P., 1999. The intrastratial injection of an adenosine A2 receptor antagonist prevents frontal cortex EEG abnormalities in a rat model of Huntington's disease. Brain Res. 831 (1–2), 315–318.
Rizzuto, R., De Stefani, D., Raffaello, A., Mammucari, C., 2012. Mitochondria as sensors and regulators of calcium signalling. Nat. Rev. Mol. Cell Biol. 13 (9), 566–578.
Ross, C.A., Tabrizi, S.J., 2011. Huntington's disease: from molecular pathogenesis to clinical treatment. Lancet Neurol. 10 (1), 83–98.
Rossignol, R., Faustin, B., Rocher, C., Malgat, M., Mazat, J.-P., Letellier, T., 2003. Mitochondrial threshold effects. Biochem. J. 370 (3), 751–762.
Rubino, D., Robbins, K.A., Hatsopoulos, N.G., 2006. Propagating waves mediate information transfer in the motor cortex. Nat. Neurosci. 9 (12), 1549–1557.
Savica, R., Rocca, W.A., Ahlskog, J., 2010. When does parkinson disease start? Arch. Neurol. 67 (7), 798–801.
Schapira, A.H.V., Cooper, J.M., Dexter, D., Clark, J.B., Jenner, P., Marsden, C.D., 1990. Mitochondrial complex I deficiency in Parkinson's disease. J. Neurochem. 54 (3), 823–827.
Schnitzler, A., Gross, J., 2005. Normal and pathological oscillatory communication in the brain. Nat. Rev. Neurosci. 6 (4), 285–296.
Scott, D.F., Heathfield, K.W.G., Toone, B., Margerison, J.H., 1972. The EEG in Huntington's chorea: a clinical and neuropathological study. J. Neurol. Neurosurg. Psychiatry 35 (1), 97–102.
Sena, Laura A., Chandel, Navdeep S., 2012. Physiological roles of mitochondrial reactive oxygen species. Mol. Cell 48 (2), 158–167.
Sharott, A., Magill, P.J., Harnack, D., Kupsch, A., Meissner, W., Brown, P., 2005. Dopamine depletion increases the power and coherence of β-oscillations in the cerebral cortex and subthalamic nucleus of the awake rat. Eur. J. Neurosci. 21 (5), 1413–1422.
Shirendeb, U.P., Calkins, M.J., Manczak, M., Anekonda, V., Dufour, B., McBride, J.L., Mao, P., Reddy, P.H., 2012. Mutant huntingtin's interaction with mitochondrial protein Drp1 impairs mitochondrial biogenesis and causes defective axonal transport and synaptic degeneration in Huntington's disease. Hum. Mol. Genet. 21 (2), 406–420.
Sinanović, O., Kapidzić, A., Kovacević, L., Hudić, J., Smajlović, D., 2005. EEG frequency and cognitive dysfunction in patients with Parkinson's disease. Med. Arh. 59 (5), 286–287.
Sohal, V.S., Zhang, F., Yizhar, O., Deisseroth, K., 2009. Parvalbumin neurons and gamma rhythms enhance cortical circuit performance. Nature 459 (7247), 698–702.
Soikkeli, R., Partanen, J., Soininen, H., Pääkkönen, A., Riekkinen Sr, P., 1991. Slowing of EEG in Parkinson's disease. Electroencephalogr. Clin. Neurophysiol. 79 (3), 159–165.
Song, W., Chen, J., Petrilli, A., Liot, G., Klinglmayr, E., Zhou, Y., Poquiz, P., Tjong, J., Pouladi, M.A., Hayden, M.R., Masliah, E., Ellisman, M., Rouiller, I., Schwarzenbacher, R., Bossy, B., Perkins, G., Bossy-Wetzel, E., 2011. Mutant huntingtin binds the mitochondrial fission GTPase dynamin-related protein-1 and increases its enzymatic activity. Nat. Med. 17 (3), 377–382.
Starr, P.A., Kang, G.A., Heath, S., Shimamoto, S., Turner, R.S., 2008. Pallidal neuronal discharge in Huntington's disease: support for selective loss of striatal cells originating the indirect pathway. Exp. Neurol. 211 (1), 227–233.
Streletz, L.J., Reyes, P.F., Zalewska, M., Katz, L., Fariello, R.G., 1990. Computer analysis of EEG activity in dementia of the Alzheimer's type and Huntington's disease. Neurobiol. Aging 11 (1), 15–20.
Sturrock, A., Leavitt, B.R., 2010. The clinical and genetic features of Huntington disease. J. Geriatr. Psychiatry Neurol. 23 (4), 243–259.
Tabrizi, S.J., Cleeter, M.W.J., Xuereb, J., Taanman, J.W., Cooper, J.M., Schapira, A.H.V., 1999. Biochemical abnormalities and excitotoxicity in Huntington's disease brain. Ann. Neurol. 45 (1), 25–32.
Tabrizi, S.J., Scahill, R.I., Durr, A., Roos, R.A.C., Leavitt, B.R., Jones, R., Landwehrmeyer, G.B., Fox, N.C., Johnson, H., Hicks, S.L., Kennard, C., Craufurd, D., Frost, C., Langbehn, D.R., Reilmann, R., Stout, J.C., 2011. Biological and clinical changes in premanifest and early stage Huntington's disease in the TRACK-HD study: the 12-month longitudinal analysis. Lancet Neurol. 10 (1), 31–42.
Taira, T., Saito, Y., Niki, T., Iguchi-Ariga, S.M.M., Takahashi, K., Ariga, H., 2004. DJ-1 has a role in antioxidative stress to prevent cell death. EMBO Rep. 5 (2), 213–218.
Tuppen, H.A.L., Blakely, E.L., Turnbull, D.M., Taylor, R.W., 2010. Mitochondrial DNA mutations and human disease. Biochim. Biophys. Acta (BBA) Bioenerg. 1797 (2), 113–128.
Twig, G., Hyde, B., Shirihai, O.S., 2008. Mitochondrial fusion, fission and autophagy as a quality control axis: the bioenergetic view. Biochim. Biophys. Acta (BBA) Bioenerg. 1777 (9), 1092–1097.
van der Hiele, K., Jurgens, C.K., Vein, A.A., Reijntjes, R.H.A.M., Witjes-Ané, M.-N.W., Roos, R.A.C., van Dijk, G., Middelkoop, H.A.M., 2007. Memory activation reveals abnormal EEG in preclinical Huntington's disease. Mov. Disord. 22 (5), 690–695.
Wang, C., Youle, R.J., 2009. The role of mitochondria in apoptosis*. Annu. Rev. Genet. 43 (1), 95–118.
Wang, H.-C., Lees, A.J., Brown, P., 1999. Impairment of EEG desynchronisation before and during movement and its relation to bradykinesia in Parkinson's disease. J. Neurol. Neurosurg. Psychiatry 66 (4), 442–446.
Ward, L.M., 2003. Synchronous neural oscillations and cognitive processes. Trends Cogn. Sci. 7 (12), 553–559.
Weinberger, M., Hutchison, W.D., Lozano, A.M., Hodaie, M., Dostrovsky, J.O., 2009. Increased gamma oscillatory activity in the subthalamic nucleus during tremor in Parkinson's disease patients. J. Neurophysiol. 101 (2), 789–802.
Weinberger, M., Mahant, N., Hutchison, W.D., Lozano, A.M., Moro, E., Hodaie, M., Lang, A.E., Dostrovsky, J.O., 2006. Beta oscillatory activity in the subthalamic nucleus and its relation to dopaminergic response in Parkinson's disease. J. Neurophysiol. 96 (6), 3248–3256.
Whittaker, R.G., Turnbull, D.M., Whittington, M.A., Cunningham, M.O., 2011. Impaired mitochondrial function abolishes gamma oscillations in the hippocampus through an effect on fast-spiking interneurons. Brain 134 (7), e180.
Whittington, M.A., Faulkner, H.J., Doheny, H.C., Traub, R.D., 2000. Neuronal fast oscillations as a target site for psychoactive drugs. Pharmacol. Ther. 86 (2), 171–190.
Wichmann, T., Bergman, H., Starr, P.A., Subramanian, T., Watts, R.L., DeLong, M.R., 1999. Comparison of MPTP-induced changes in spontaneous neuronal discharge in the internal pallidal segment and in the substantia nigra pars reticulata in primates. Exp. Brain Res. 125 (4), 397–409.
Wiegand, M., Möller, A.A., Lauer, C.J., Stolz, S., Schreiber, W., Dose, M., Krieg, J.C., 1991. Nocturnal sleep in huntington's disease. J. Neurol. 238 (4), 203–208.
Wong-Riley, M.T.T., 1989. Cytochrome oxidase: an endogenous metabolic marker for neuronal activity. Trends Neurosci. 12 (3), 94–101.
Xia, R., Mao, Z.-H., 2012. Progression of motor symptoms in Parkinson's disease. Neurosci. Bull. 28 (1), 39–48.
Yamawaki, N., Stanford, I.M., Hall, S.D., Woodhall, G.L., 2008. Pharmacologically induced and stimulus evoked rhythmic neuronal oscillatory activity in the primary motor cortex in vitro. Neuroscience 151 (2), 386–395.
Zuccato, C., Valenza, M., Cattaneo, E., 2010. Molecular mechanisms and potential therapeutical targets in Huntington's disease. Physiol. Rev. 90 (3), 905–981.

Bibliography

Abbott, N.J., Ronnback, L. and Hansson, E. (2006) 'Astrocyte-endothelial interactions at the blood-brain barrier', *Nat Rev Neurosci*, 7(1), pp. 41-53.

Abou-Khalil, B.W., Siegel, G.J., Chris Sackellares, J., Gilman, S., Hichwa, R. and Marshall, R. (1987) 'Positron emission tomography studies of cerebral glucose metabolism in chronic partial epilepsy', *Annals of Neurology*, 22(4), pp. 480-486.

Adam-Vizi, V. (2005) 'Production of reactive oxygen species in brain mitochondria: contribution by electron transport chain and non-electron transport chain sources', *Antioxid Redox Signal*, 7(9-10), pp. 1140-9.

Almeida, A., Almeida, J., Bolaños, J.P. and Moncada, S. (2001) 'Different responses of astrocytes and neurons to nitric oxide: The role of glycolytically generated ATP in astrocyte protection', *Proceedings of the National Academy of Sciences*, 98(26), pp. 15294-15299.

Amico-Ruvio, Stacy A., Murthy, Swetha E., Smith, Thomas P. and Popescu, Gabriela K. (2011) 'Zinc Effects on NMDA Receptor Gating Kinetics', *Biophysical Journal*, 100(8), pp. 1910-1918.

Andrews, R.M., Kubacka, I., Chinnery, P.F., Lightowlers, R.N., Turnbull, D.M. and Howell, N. (1999) 'Reanalysis and revision of the Cambridge reference sequence for human mitochondrial DNA', *Nat Genet*, 23(2), pp. 147-147.

Anlauf, E. and Derouiche, A. (2013) 'Glutamine Synthetase as an Astrocytic Marker: Its Cell Type and Vesicle Localization', *Frontiers in Endocrinology*, 4, p. 144.

Antoniadis, A., Müller, W.E. and Wollert, U. (1980) 'Inhibition of GABA and benzodiazepine receptor binding by penicillins', *Neuroscience Letters*, 18(3), pp. 309-312.

Aronica, E., Van Vliet, E.A., Mayboroda, O.A., Troost, D., Da Silva, F.H.L. and Gorter, J.A. (2000) 'Upregulation of metabotropic glutamate receptor subtype mGluR3 and mGluR5 in reactive astrocytes in a rat model of mesial temporal lobe epilepsy', *European Journal of Neuroscience*, 12(7), pp. 2333-2344.

Arvanian, V.L. and Mendell, L.M. (2001) 'Removal of NMDA Receptor Mg²⁺ Block Extends the Action of NT-3 on Synaptic Transmission in Neonatal Rat Motoneurons', *Journal of Neurophysiology*, 86(1), pp. 123-129.

Auestad, N., Korsak, R.A., Morrow, J.W. and Edmond, J. (1991) 'Fatty Acid Oxidation and Ketogenesis by Astrocytes in Primary Culture', *Journal of Neurochemistry*, 56(4), pp. 1376-1386.

Avoli, M. (2007) 'The Epileptic Hippocampus Revisited: Back to the Future', *Epilepsy Currents*, 7(4), pp. 116-118.

Avula, S., Parikh, S., Demarest, S., Kurz, J. and Gropman, A. (2014) 'Treatment of Mitochondrial Disorders', *Current Treatment Options in Neurology*, 16(6), p. 292.

Bak, L.K., Schousboe, A. and Waagepetersen, H.S. (2006) 'The glutamate/GABA-glutamine cycle: aspects of transport, neurotransmitter homeostasis and ammonia transfer', *Journal of Neurochemistry*, 98(3), pp. 641-653.

Balla, A., Koneru, R., Smiley, J., Sershen, H. and Javitt, D.C. (2001) 'Continuous Phencyclidine Treatment Induces Schizophrenia-Like Hyperreactivity of Striatal Dopamine Release', *Neuropsychopharmacology*, 25(2), pp. 157-164.

Bartos, M. and Elgueta, C. (2012) 'Functional characteristics of parvalbumin- and cholecystokinin-expressing basket cells', *The Journal of Physiology*, 590(Pt 4), pp. 669-681.

Baslow, M.H. (2003) 'N-Acetylaspartate in the Vertebrate Brain: Metabolism and Function', *Neurochemical Research*, 28(6), pp. 941-953.

Bastin, J., Aubey, F., Rötig, A.s., Munnich, A. and Djouadi, F. (2008) 'Activation of Peroxisome Proliferator-Activated Receptor Pathway Stimulates the Mitochondrial Respiratory Chain and Can Correct Deficiencies in Patients' Cells Lacking Its Components', *The Journal of Clinical Endocrinology & Metabolism*, 93(4), pp. 1433-1441.

Bates, K.A., Martins, R.N. and Harvey, A.R. (2007) 'Oxidative stress in a rat model of chronic gliosis', *Neurobiology of Aging*, 28(7), pp. 995-1008.

Baxendale, S. (2008) 'The impact of epilepsy surgery on cognition and behavior', *Epilepsy & Behavior*, 12(4), pp. 592-599.

Baxter, P.S. and Hardingham, G.E. (2016) 'Adaptive regulation of the brain's antioxidant defences by neurons and astrocytes', *Free Radical Biology & Medicine*, 100, pp. 147-152.

Bear, M.F., Connors, B.W. and Paradiso, M.A. (2016a) 'Molecular Mechanisms of Learning and Memory', in *Neuroscience : Explring the Brain*. 4 edn. China: Wolters Kluwer, pp. 865-899.

Bear, M.F., Connors, B.W. and Paradiso, M.A. (2016b) 'Neurotransmitter Systems', in *Neuroscience : Explring the Brain*. 4 edn. China: Wolters Kluwer, pp. 143-178.

Beeson, C.C., Beeson, G.C. and Schnellmann, R.G. (2010) 'A high-throughput respirometric assay for mitochondrial biogenesis and toxicity', *Analytical Biochemistry*, 404(1), pp. 75-81.

Bekkers, J.M. (2011) 'Pyramidal neurons', *Current Biology*, 21(24), p. R975.

Bélanger, M., Allaman, I. and Magistretti, Pierre J. (2011) 'Brain Energy Metabolism: Focus on Astrocyte-Neuron Metabolic Cooperation', *Cell Metabolism*, 14(6), pp. 724-738.

Benson, D.L., Isackson, P.J., Gall, C.M. and Jones, E.G. (1992) 'Contrasting patterns in the localization of glutamic acid decarboxylase and Ca2+ /calmodulin protein kinase gene expression in the rat centrat nervous system', *Neuroscience*, 46(4), pp. 825-849.

Benz, R. and McLaughlin, S. (1983) 'The molecular mechanism of action of the proton ionophore FCCP (carbonylcyanide p-trifluoromethoxyphenylhydrazone)', *Biophysical Journal*, 41(3), pp. 381-398.

Berg, J.M., Tymoczko, J.L., Stryer, L. and Gregory J. Gatto, J. (2012a) 'The Biosynthesis of Amino Acids', in *Biochemistry*. 7 edn. United States of America: W. H. Freeman and Company, pp. 729-759.

Berg, J.M., Tymoczko, J.L., Stryer, L. and Gregory J. Gatto, J. (2012b) 'The Calvin Cycle and the Pentose Phosphate Pathway', in *Biochemistry*. 7 edn. United States of America: W. H. Freeman and Company, pp. 609-635.

Berg, J.M., Tymoczko, J.L., Stryer, L. and Gregory J. Gatto, J. (2012c) 'Catalytic Strategies', in *Biochemistry*. 7 edn. United States of America: W. H. Freeman and Company, pp. 261-297.

Berg, J.M., Tymoczko, J.L., Stryer, L. and Gregory J. Gatto, J. (2012d) 'The Citric Acid Cycle', in *Biochemistry*. 7 edn. United States of America: W. H. Freeman and Company, pp. 515-542.

Berg, J.M., Tymoczko, J.L., Stryer, L. and Gregory J. Gatto, J. (2012e) 'Fatty Acid Metabolism', in *Biochemistry*. 7 edn. United States of America: W. H. Freeman and Company, pp. 663-696.

Berg, J.M., Tymoczko, J.L., Stryer, L. and Gregory J. Gatto, J. (2012f) 'Glycolysis and Gluconeogenesis', in *Biochemistry*. 7 edn. United States of America: W. H. Freeman and Company, pp. 469-513.

Berg, J.M., Tymoczko, J.L., Stryer, L. and Gregory J. Gatto, J. (2012g) 'Oxidative Phosphorylation', in *Biochemistry*. 7 edn. United States of America: W. H. Freeman and Company, pp. 543-584.

Bergmann, R., Kongsbak, K., Sørensen, P.L., Sander, T. and Balle, T. (2013) 'A Unified Model of the GABAA Receptor Comprising Agonist and Benzodiazepine Binding Sites', *PLOS ONE*, 8(1), p. e52323.

Betteridge, D.J. (2000) 'What is oxidative stress?', *Metabolism*, 49(2), pp. 3-8.

Beydoun, A.A., Farrell, K. and Nasreddine, W.M. (2008) 'Valproate', in Jerome Engel, J. and Pedley, T.A. (eds.) *Epilepsy : A Comprehensive Textbook*. United States of America: Lippincott Williams & Wilkins, pp. 1673-1681.

Bhattacharya, I. and Boje, K.M.K. (2004) 'GHB (γ-Hydroxybutyrate) Carrier-Mediated Transport across the Blood-Brain Barrier', *Journal of Pharmacology and Experimental Therapeutics*, 311(1), pp. 92-98.

Bindoff, L.A. and Engelsen, B.A. (2012) 'Mitochondrial diseases and epilepsy', *Epilepsia*, 53, pp. 92-97.

Birbeck, Gretchen L., Hays, Ron D., Cui, X. and Vickrey, Barbara G. (2002) 'Seizure Reduction and Quality of Life Improvements in People with Epilepsy', *Epilepsia*, 43(5), pp. 535-538.

Bittner, B. and Mountfield, R.J. (2002) 'Intravenous administration of poorly soluble new drug entities in early drug discovery: the potential impact of formulation on pharmacokinetic parameters', *Current opinion in drug discovery & development*, 5(1), pp. 59-71.

Bonnefont, J.-P., Bastin, J., Behin, A. and Djouadi, F. (2009) 'Bezafibrate for an Inborn Mitochondrial Beta-Oxidation Defect', *New England Journal of Medicine*, 360(8), pp. 838-840.

Boonstra, E., de Kleijn, R., Colzato, L.S., Alkemade, A., Forstmann, B.U. and Nieuwenhuis, S. (2015) 'Neurotransmitters as food supplements: the effects of GABA on brain and behavior', *Frontiers in Psychology*, 6, p. 1520.

Borges, C.G., Canani, C.R., Fernandes, C.G., Zanatta, Â., Seminotti, B., Ribeiro, C.A.J., Leipnitz, G., Vargas, C.R. and Wajner, M. (2015) 'Reactive nitrogen species mediate oxidative stress and astrogliosis provoked by in vivo administration of phytanic acid in cerebellum of adolescent rats: A potential

contributing pathomechanism of cerebellar injury in peroxisomal disorders', *Neuroscience*, 304, pp. 122-132.

Bozzo, L., Puyal, J. and Chatton, J.-Y. (2013) 'Lactate Modulates the Activity of Primary Cortical Neurons through a Receptor-Mediated Pathway', *PLOS ONE*, 8(8), p. e71721.

Bradl, M. and Lassmann, H. (2010) 'Oligodendrocytes: biology and pathology', *Acta Neuropathologica*, 119(1), pp. 37-53.

Branco, A.F., Ferreira, A., Simões, R.F., Magalhães-Novais, S., Zehowski, C., Cope, E., Silva, A.M., Pereira, D., Sardão, V.A. and Cunha-Oliveira, T. (2016) 'Ketogenic diets: from cancer to mitochondrial diseases and beyond', *European Journal of Clinical Investigation*, 46(3), pp. 285-298.

Brewer, G.J. (1997) 'Isolation and culture of adult rat hippocampal neurons', *Journal of Neuroscience Methods*, 71(2), pp. 143-155.

Brodie, D.A. (1959) 'THE EFFECT OF THIOPENTAL AND CYANIDE ON THE ACTIVITY OF INSPIRATORY NEURONS', *Journal of Pharmacology and Experimental Therapeutics*, 126(3), pp. 264-269.

Brown, A.M. and Ransom, B.R. (2007) 'Astrocyte glycogen and brain energy metabolism', *Glia*, 55(12), pp. 1263-1271.

Brown, W.M., George, M. and Wilson, A.C. (1979) 'Rapid evolution of animal mitochondrial DNA', *Proceedings of the National Academy of Sciences*, 76(4), pp. 1967-1971.

Bureau, M.H. and Olsen, R.W. (1993) 'GABAA Receptor Subtypes: Ligand Binding Heterogeneity Demonstrated by Photoaffinity Labeling and Autoradiography', *Journal of Neurochemistry*, 61(4), pp. 1479-1491.

Bush, T.G., Puvanachandra, N., Horner, C.H., Polito, A., Ostenfeld, T., Svendsen, C.N., Mucke, L., Johnson, M.H. and Sofroniew, M.V. (1999) 'Leukocyte Infiltration, Neuronal Degeneration, and Neurite Outgrowth after Ablation of Scar-Forming, Reactive Astrocytes in Adult Transgenic Mice', *Neuron*, 23(2), pp. 297-308.

Buskila, Y., Breen, P.P., Tapson, J., van Schaik, A., Barton, M. and Morley, J.W. (2014) 'Extending the viability of acute brain slices', *Scientific Reports*, 4, p. 5309.

Cannady, R., Fisher, K.R., Durant, B., Besheer, J. and Hodge, C.W. (2013) 'Enhanced AMPA receptor activity increases operant alcohol self-administration and cue-induced reinstatement', *Addiction Biology*, 18(1), pp. 54-65.

Cantu, D., Schaack, J. and Patel, M. (2009) 'Oxidative Inactivation of Mitochondrial Aconitase Results in Iron and H2O2-Mediated Neurotoxicity in Rat Primary Mesencephalic Cultures', *PLOS ONE*, 4(9), p. e7095.

Cardona, C., Sánchez-Mejías, E., Dávila, J.C., Martín-Rufián, M., Campos-Sandoval, J.A., Vitorica, J., Alonso, F.J., Matés, J.M., Segura, J.A., Norenberg, M.D., Rama Rao, K.V., Jayakumar, A.R., Gutiérrez, A. and Márquez, J. (2015) 'Expression of Gls and Gls2 glutaminase isoforms in astrocytes', *Glia*, 63(3), pp. 365-382.

Cavas, M., Beltrán, D. and Navarro, J.F. (2005) 'Behavioural effects of dimethyl sulfoxide (DMSO): Changes in sleep architecture in rats', *Toxicology Letters*, 157(3), pp. 221-232.

Ceolin, L., Bortolotto, Z.A., Bannister, N., Collingridge, G.L., Lodge, D. and Volianskis, A. (2012) 'A novel anti-epileptic agent, perampanel, selectively inhibits AMPA receptor-mediated synaptic transmission in the hippocampus', *Neurochemistry International*, 61(4), pp. 517-522.

Chan, F., Lax, N.Z., Davies, C.H., Turnbull, D.M. and Cunningham, M.O. (2016) 'Neuronal oscillations: A physiological correlate for targeting mitochondrial dysfunction in neurodegenerative diseases?', *Neuropharmacology*, 102, pp. 48-58.

Chandra, A., Sharma, A., Calingasan, N.Y., White, J.M., Shurubor, Y., Yang, X.W., Beal, M.F. and Johri, A. (2016) 'Enhanced mitochondrial biogenesis ameliorates disease phenotype in a full-length mouse model of Huntington's disease', *Human Molecular Genetics*, 25(11), pp. 2269-2282.

Chang, P., Augustin, K., Boddum, K., Williams, S., Sun, M., Terschak, J.A., Hardege, J.D., Chen, P.E., Walker, M.C. and Williams, R.S.B. (2015) 'Seizure control by decanoic acid through direct AMPA receptor inhibition', *Brain*.

Chang, P., Terbach, N., Plant, N., Chen, P.E., Walker, M.C. and Williams, R.S.B. (2013) 'Seizure control by ketogenic diet-associated medium chain fatty acids', *Neuropharmacology*, 69, pp. 105-114.

Chen, C.-Y., Matt, L., Hell, J.W. and Rogawski, M.A. (2014) 'Perampanel Inhibition of AMPA Receptor Currents in Cultured Hippocampal Neurons', *PLOS ONE*, 9(9), p. e108021.

Chesler, M. (2003) 'Regulation and Modulation of pH in the Brain', *Physiological Reviews*, 83(4), pp. 1183-1221.

Chevallier, J.A., Von Allmen, G.K. and Koenig, M.K. (2014) 'Seizure semiology and EEG findings in mitochondrial diseases', *Epilepsia*, 55(5), pp. 707-712.

Chih, C.-P. and Roberts, E.L. (2003) 'Energy Substrates for Neurons during Neural Activity: A Critical Review of the Astrocyte-Neuron Lactate Shuttle Hypothesis', *Journal of Cerebral Blood Flow & Metabolism*, 23(11), pp. 1263-1281.

Chinnery, P.F. and Turnbull, D.M. (2001) 'Epidemiology and treatment of mitochondrial disorders', *American Journal of Medical Genetics*, 106(1), pp. 94-101.

Chiron, C., Marchand, M.C., Tran, A., Rey, E., d'Athis, P., Vincent, J., Dulac, O. and Pons, G. (2000) 'Stiripentol in severe myoclonic epilepsy in infancy: a randomised placebo-controlled syndrome-dedicated trial', *The Lancet*, 356(9242), pp. 1638-1642.

Chmiel-Perzyńska, I., Kloc, R., Perzyński, A., Rudzki, S. and Urbańska, E.M. (2011) 'Novel Aspect of Ketone Action: β-Hydroxybutyrate Increases Brain Synthesis of Kynurenic Acid In Vitro', *Neurotoxicity Research*, 20(1), pp. 40-50.

Chuang, Y.-C., Chang, A.Y.W., Lin, J.-W., Hsu, S.-P. and Chan, S.H.H. (2004) 'Mitochondrial Dysfunction and Ultrastructural Damage in the Hippocampus during Kainic Acid–induced Status Epilepticus in the Rat', *Epilepsia*, 45(10), pp. 1202-1209.

Cirillo, G. and Papa, M. (2016) 'Beyond peripheral nerve injury: spinal gliopathy and maladaptive synaptic plasticity', *Neural Regeneration Research*, 11(9), pp. 1422-1423.

Clerc, P. and Polster, B.M. (2012) 'Investigation of Mitochondrial Dysfunction by Sequential Microplate-Based Respiration Measurements from Intact and Permeabilized Neurons', *PLOS ONE*, 7(4), p. e34465.

Cock, H.R., Tong, X., Hargreaves, I.P., Heales, S.J.R., Clark, J.B., Patsalos, P.N., Thom, M., Groves, M., Schapira, A.H.V., Shorvon, S.D. and Walker, M.C. (2002) 'Mitochondrial dysfunction associated with neuronal death following status epilepticus in rat', *Epilepsy Research*, 48(3), pp. 157-168.

Collingridge, G.L. (1995) 'The brain slice preparation: a tribute to the pioneer Henry McIlwain', *Journal of Neuroscience Methods*, 59(1), pp. 5-9.

Consortium, R.G.S.P. (2004) 'Genome sequence of the Brown Norway rat yields insights into mammalian evolution', *Nature*, 428(6982), pp. 493-521.

Cooper, J.R., Bloom, F.E. and Roth, R.H. (2003) 'Amino Acid Transmitters', in *The Biochemical Basis of Neuropharmacology*. 8th edn. United States of America: Oxford University Press, pp. 105-150.

Correia, S.C., Santos, R.X., Cardoso, S.M., Santos, M.S., Oliveira, C.R. and Moreira, P.I. (2012) 'Cyanide preconditioning protects brain endothelial and NT2 neuron-like cells against glucotoxicity: Role of mitochondrial reactive oxygen species and HIF-1α', *Neurobiology of Disease*, 45(1), pp. 206-218.

Courchesne-Loyer, A., St-Pierre, V., Hennebelle, M., Castellano, C.-A., Fortier, M., Tessier, D. and Cunnane, S.C. (2015) 'Ketogenic response to cotreatment with bezafibrate and medium chain triacylglycerols in healthy humans', *Nutrition*, 31(10), pp. 1255-1259.

Cowen, M.S., Schroff, K.C., Gass, P., Sprengel, R. and Spanagel, R. (2003) 'Neurobehavioral effects of alcohol in AMPA receptor subunit (GluR1) deficient mice', *Neuropharmacology*, 45(3), pp. 325-333.

Cummings, K.A. and Popescu, G.K. (2015) 'Glycine-dependent activation of NMDA receptors', *The Journal of General Physiology*, 145(6), pp. 513-527.

Cunningham, M.O., Roopun, A., Schofield, I.S., Whittaker, R.G., Duncan, R., Russell, A., Jenkins, A., Nicholson, C., Whittington, M.A. and Traub, R.D. (2012) 'Glissandi: transient fast electrocorticographic oscillations of steadily increasing frequency, explained by temporally increasing gap junction conductance', *Epilepsia*, 53(7), pp. 1205-1214.

Daikhin, Y. and Yudkoff, M. (2000) 'Compartmentation of Brain Glutamate Metabolism in Neurons and Glia', *The Journal of Nutrition*, 130(4), p. 1026.

Dailey, M.E., Marrs, G.S. and Kurpius, D. (2011) 'Maintaining Live Cells and Tissue Slices in the Imaging Setup', *Cold Spring Harbor protocols*, 2011(4), pp. pdb.top105-pdb.top105.

Dalle-Donne, I., Rossi, R., Giustarini, D., Milzani, A. and Colombo, R. (2003) 'Protein carbonyl groups as biomarkers of oxidative stress', *Clinica Chimica Acta*, 329(1–2), pp. 23-38.

Dam, A.M. (1980) 'Epilepsy and Neuron Loss in the Hippocampus', *Epilepsia*, 21(6), pp. 617-629.

de Lima, P.A., de Brito Sampaio, L.P. and Damasceno, N.R.T. (2014) 'Neurobiochemical mechanisms of a ketogenic diet in refractory epilepsy', *Clinics*, 69(10), pp. 699-705.

DeBerardinis, R.J., Mancuso, A., Daikhin, E., Nissim, I., Yudkoff, M., Wehrli, S. and Thompson, C.B. (2007) 'Beyond aerobic glycolysis: Transformed cells can engage in glutamine metabolism that exceeds the requirement for protein and nucleotide synthesis', *Proceedings of the National Academy of Sciences*, 104(49), pp. 19345-19350.

Demeulemeester, H., Arckens, L., Vandesande, F., Orban, G.A., Heizmann, C.W. and Pochet, R. (1991) 'Calcium binding proteins and neuropeptides as molecular markers of GABAergic interneurons in the cat visual cortex', *Experimental Brain Research*, 84(3), pp. 538-544.

Deng, Y.-T., Huang, H.-C. and Lin, J.-K. (2010) 'Rotenone induces apoptosis in MCF-7 human breast cancer cell-mediated ROS through JNK and p38 signaling', *Molecular Carcinogenesis*, 49(2), pp. 141-151.

Deshpande, L.S., Lou, J.K., Mian, A., Blair, R.E., Sombati, S., Attkisson, E. and DeLorenzo, R.J. (2008) 'Time course and mechanism of hippocampal neuronal death in an in vitro model of status epilepticus: Role of NMDA receptor activation and NMDA dependent calcium entry', *European journal of pharmacology*, 583(1), pp. 73-83.

Deshpande, L.S., Lou, J.K., Mian, A., Blair, R.E., Sombati, S. and DeLorenzo, R.J. (2007) 'In vitro status epilepticus but not spontaneous recurrent seizures cause cell death in cultured hippocampal neurons', *Epilepsy research*, 75(2-3), pp. 171-179.

Detmer, S.A. and Chan, D.C. (2007) 'Functions and dysfunctions of mitochondrial dynamics', *Nat Rev Mol Cell Biol*, 8(11), pp. 870-879.

Devi, P.U., Manocha, A. and Vohora, D. (2008) 'Seizures, antiepileptics, antioxidants and oxidative stress: an insight for researchers', *Expert Opinion on Pharmacotherapy*, 9(18), pp. 3169-3177.

Dienel, G.A. (2014) 'Energy Metabolism in the Brain', in *From Molecules to Networks : An Introduction to Cellular and Molecular Neuroscience*. 3 edn. United Kingdom: Academic Press, pp. 53-117.

Dingledine, R., Varvel, N.H. and Dudek, F.E. (2014) 'When and How Do Seizures Kill Neurons, and Is Cell Death Relevant to Epileptogenesis?', *Advances in experimental medicine and biology*, 813, pp. 109-122.

Divakaruni, A.S., Paradyse, A., Ferrick, D.A., Murphy, A.N. and Jastroch, M. (2014) 'Analysis and Interpretation of Microplate-Based Oxygen Consumption and pH Data', *Methods in Enzymology*, 547, pp. 309-354.

Domino, E.F. and Luby, E.D. (2012) 'Phencyclidine/Schizophrenia: One View Toward the Past, The Other to the Future', *Schizophrenia Bulletin*, 38(5), pp. 914-919.

Dubé, C., Boyet, S., Marescaux, C. and Nehlig, A. (2001) 'Relationship between Neuronal Loss and Interictal Glucose Metabolism during the Chronic Phase of the Lithium-Pilocarpine Model of Epilepsy in the Immature and Adult Rat', *Experimental Neurology*, 167(2), pp. 227-241.

Duberley, K.E., Heales, S.J.R., Abramov, A.Y., Chalasani, A., Land, J.M., Rahman, S. and Hargreaves, I.P. (2014) 'Effect of Coenzyme Q10 supplementation on mitochondrial electron transport chain activity

and mitochondrial oxidative stress in Coenzyme Q10 deficient human neuronal cells', *The International Journal of Biochemistry & Cell Biology*, 50, pp. 60-63.

Dudkina, N.V., Eubel, H., Keegstra, W., Boekema, E.J. and Braun, H.-P. (2005) 'Structure of a mitochondrial supercomplex formed by respiratory-chain complexes I and III', *Proceedings of the National Academy of Sciences of the United States of America*, 102(9), pp. 3225-3229.

Dunn, D.A., Cannon, M.V., Irwin, M.H. and Pinkert, C.A. (2012) 'Animal models of human mitochondrial DNA mutations', *Biochimica et Biophysica Acta*, 1820(5), pp. 601-607.

Eadie, M.J. and Kwan, P. (2008) 'Phenobarbital and Other Barbiturates', in Jerome Engel, J. and Pedley, T.A. (eds.) *Epilepsy : A Comprehensive Textbook*. United States of America: Lippincott Williams & Wilkins, pp. 1599-1607.

Elston, T., Wang, H. and Oster, G. (1998) 'Energy transduction in ATP synthase', *Nature*, 391(6666), pp. 510-513.

Engel, J. (2003) 'A Greater Role for Surgical Treatment of Epilepsy: Why and When?', *Epilepsy Currents*, 3(2), pp. 37-40.

Engel, J., McDermott, M.P., Wiebe, S. and et al. (2012) 'Early surgical therapy for drug-resistant temporal lobe epilepsy: A randomized trial', *JAMA*, 307(9), pp. 922-930.

Engel Jr, J. (1996) 'Introduction to temporal lobe epilepsy', *Epilepsy Research*, 26(1), pp. 141-150.

Ennis, S.R., Kawai, N., Ren, X.-d., Abdelkarim, G.E. and Keep, R.F. (1998) 'Glutamine Uptake at the Blood-Brain Barrier Is Mediated by N-System Transport', *Journal of Neurochemistry*, 71(6), pp. 2565-2573.

Esashi, Y., Sakai, Y. and Ushizawa, R. (1981) 'Cyanide-sensitive and Cyanide-resistant Respiration in the Germination of Cocklebur Seeds', *Plant Physiology*, 67(3), pp. 503-508.

Ettema, T.J.G. (2016) 'Evolution: Mitochondria in the second act', *Nature*, 531(7592), pp. 39-40.

Fabricius, M., Fuhr, S., Bhatia, R., Boutelle, M., Hashemi, P., Strong, A.J. and Lauritzen, M. (2006) 'Cortical spreading depression and peri-infarct depolarization in acutely injured human cerebral cortex', *Brain*, 129(3), pp. 778-790.

Fabricius, M., Fuhr, S., Willumsen, L., Dreier, J.P., Bhatia, R., Boutelle, M.G., Hartings, J.A., Bullock, R., Strong, A.J. and Lauritzen, M. (2008) 'Association of seizures with cortical spreading depression and peri-infarct depolarisations in the acutely injured human brain', *Clinical Neurophysiology*, 119(9), pp. 1973-1984.

Fan, D., Grooms, S.Y., Araneda, R.C., Johnson, A.B., Dobrenis, K., Kessler, J.A. and Zukin, R.S. (1999) 'AMPA receptor protein expression and function in astrocytes cultured from hippocampus', *Journal of Neuroscience Research*, 57(4), pp. 557-571.

Farrar, G.J., Chadderton, N., Kenna, P.F. and Millington-Ward, S. (2013) 'Mitochondrial disorders: aetiologies, models systems, and candidate therapies', *Trends in Genetics*, 29(8), pp. 488-497.

Faulkner, J.R., Herrmann, J.E., Woo, M.J., Tansey, K.E., Doan, N.B. and Sofroniew, M.V. (2004) 'Reactive Astrocytes Protect Tissue and Preserve Function after Spinal Cord Injury', *The Journal of Neuroscience*, 24(9), pp. 2143-2155.

Feindel, W., Leblanc, R. and De Almeida, A.N. (2009) 'Epilepsy Surgery: Historical Highlights 1909–2009', *Epilepsia*, 50, pp. 131-151.

Fernandez-Fernandez, S., Almeida, A. and Bolaños, Juan P. (2012) 'Antioxidant and bioenergetic coupling between neurons and astrocytes', *Biochemical Journal*, 443(1), pp. 3-11.

Ferrea, E., Maccione, A., Medrihan, L., Nieus, T., Ghezzi, D., Baldelli, P., Benfenati, F. and Berdondini, L. (2012) 'Large-scale, high-resolution electrophysiological imaging of field potentials in brain slices with microelectronic multielectrode arrays', *Frontiers in Neural Circuits*, 6, p. 80.

Fertig, E.J. and Mattson, R.H. (2008) 'Carbamazepine', in Jerome Engel, J. and Pedley, T.A. (eds.) *Epilepsy : A Comprehensive Textbook*. United States of America: Lippincott Williams & Wilkins, pp. 1543 - 1555.

Finsterer, J. and Mahjoub, S.Z. (2013) 'Presentation of adult mitochondrial epilepsy', *Seizure*, 22(2), pp. 119-123.

Fisher, J.L. (2011) 'The effects of stiripentol on GABAA receptors', *Epilepsia*, 52, pp. 76-78.

Fisher, R.S., Acevedo, C., Arzimanoglou, A., Bogacz, A., Cross, J.H., Elger, C.E., Engel, J., Forsgren, L., French, J.A., Glynn, M., Hesdorffer, D.C., Lee, B.I., Mathern, G.W., Moshé, S.L., Perucca, E., Scheffer, I.E., Tomson, T., Watanabe, M. and Wiebe, S. (2014) 'ILAE Official Report: A practical clinical definition of epilepsy', *Epilepsia*, 55(4), pp. 475-482.

Fleming, J.J. and England, P.M. (2010) 'AMPA receptors and synaptic plasticity: a chemist's perspective', *Nat Chem Biol*, 6(2), pp. 89-97.

Fonnum, F., Johnsen, A. and Hassel, B. (1997) 'Use of Fluorocitrate and Fluoroacetate in the Study of Brain Metabolism', *Glia*, 21, pp. 106-113.

Forman, S.A., Feng, H.-J., Chou, J., Mao, J. and Lo, E.H. (2017) 'Pharmacology of GABAergic and Glutamatergic Neurotransmission', in Golan, D.E., Armstrong, E.J. and Armstrong, A.W. (eds.) *Principles of Pharmacology : The Pathophysiologic Basis of Drug Therapy*. China: Wolters Kluwer, pp. 184-205.

Frantz, M.-C. and Wipf, P. (2010) 'Mitochondria as a target in treatment', *Environmental and molecular mutagenesis*, 51(5), pp. 462-475.

Fraser, D.D., Mudrick-Donnon, L.A. and Macvicar, B.A. (1994) 'Astrocytic GABA receptors', *Glia*, 11(2), pp. 83-93.

French, J.A., Krauss, G.L., Steinhoff, B.J., Squillacote, D., Yang, H., Kumar, D. and Laurenza, A. (2013) 'Evaluation of adjunctive perampanel in patients with refractory partial-onset seizures: Results of randomized global phase III study 305', *Epilepsia*, 54(1), pp. 117-125.

Freund, T.F. and Buzsaki, G. (1996) 'Interneurons of the Hippocampus', *Hippocampus*, 6, pp. 347-470.

Frey, T.G. and Mannella, C.A. (2000) 'The internal structure of mitochondria', *Trends in Biochemical Sciences*, 25(7), pp. 319-324.

Frick, A., Suzuki, O., Butz, N., Chan, E. and Wiltshire, T. (2013) 'In Vitro and In Vivo Mouse Models for Pharmacogenetic Studies', in Innocenti, F. and van Schaik, R.H.N. (eds.) *Pharmacogenomics: Methods and Protocols*. Totowa, NJ: Humana Press, pp. 263-278.

Fritsch, B., Reis, J., Gasior, M., Kaminski, R.M. and Rogawski, M.A. (2014) 'Role of GluK1 Kainate Receptors in Seizures, Epileptic Discharges, and Epileptogenesis', *The Journal of Neuroscience*, 34(17), pp. 5765-5775.

Frotscher, M., Schlander, M. and Léránth, C. (1986) 'Cholinergic neurons in the hippocampus', *Cell and Tissue Research*, 246(2), pp. 293-301.

Gadea, A., Schinelli, S. and Gallo, V. (2008) 'Endothelin-1 Regulates Astrocyte Proliferation and Reactive Gliosis via a JNK/c-Jun Signaling Pathway', *The Journal of Neuroscience*, 28(10), pp. 2394-2408.

Galanopoulou, A.S. (2008) 'GABA(A) Receptors in Normal Development and Seizures: Friends or Foes?', *Current Neuropharmacology*, 6(1), pp. 1-20.

Gáll, Z., Orbán-Kis, K. and Szilágyi, T. (2017) 'Differential effects of sodium channel blockers on in vitro induced epileptiform activities', *Archives of Pharmacal Research*, 40(1), pp. 112-121.

Galvao, J., Davis, B., Tilley, M., Normando, E., Duchen, M.R. and Cordeiro, M.F. (2014) 'Unexpected low-dose toxicity of the universal solvent DMSO', *The FASEB Journal*, 28(3), pp. 1317-1330.

Gao, J., Chi, Z.-F., Liu, X.-W., Shan, P.-Y. and Wang, R. (2007) 'Mitochondrial dysfunction and ultrastructural damage in the hippocampus of pilocarpine-induced epileptic rat', *Neuroscience Letters*, 411(2), pp. 152-157.

García-Marín, V., García-López, P. and Freire, M. (2007) 'Cajal's contributions to glia research', *Trends in Neurosciences*, 30(9), pp. 479-487.

Garzillo, Cibele L. and Mello, Luiz E.A.M. (2002) 'Characterization of Reactive Astrocytes in the Chronic Phase of the Pilocarpine Model of Epilepsy', *Epilepsia*, 43, pp. 107-109.

Genc, S., Kurnaz, I.A. and Ozilgen, M. (2011) 'Astrocyte - neuron lactate shuttle may boost more ATP supply to the neuron under hypoxic conditions - in silico study supported by in vitro expression data', *BMC Systems Biology*, 5(1), p. 162.

Ghandour, M.S., Parkkila, A.-K., Parkkila, S., Waheed, A. and Sly, W.S. (2000) 'Mitochondrial Carbonic Anhydrase in the Nervous System', *Journal of Neurochemistry*, 75(5), pp. 2212-2220.

Giles, R.E., Blanc, H., Cann, H.M. and Wallace, D.C. (1980) 'Maternal inheritance of human mitochondrial DNA', *Proceedings of the National Academy of Sciences*, 77(11), pp. 6715-6719.

Giménez-Cassina, A., Martínez-François, J.R., Fisher, J.K., Szlyk, B., Polak, K., Wiwczar, J., Tanner, G.R., Lutas, A., Yellen, G. and Danial, N.N. (2012) 'BAD-Dependent Regulation of Fuel Metabolism and K(ATP) Channel Activity Confers Resistance to Epileptic Seizures', *Neuron*, 74(4), pp. 719-730.

Glauser, T.A. (2011) 'Biomarkers for antiepileptic drug response', *Biomarkers in Medicine*, 5(5), pp. 635-641.

Gomez, C., Bandez, M.J. and Navarro, A. (2007) 'Pesticides and impairment of mitochondrial function in relation with the parkinsonian syndrome', *Frontiers in bioscience : a journal and virtual library*, 12, pp. 1079-1093 [Online]. Available at: http://europepmc.org/abstract/MED/17127363

http://dx.doi.org/10.2741/2128 DOI: 10.2741/2128 (Accessed: 2007).

Gorman, G.S., Schaefer, A.M., Ng, Y., Gomez, N., Blakely, E.L., Alston, C.L., Feeney, C., Horvath, R., Yu‐Wai‐Man, P., Chinnery, P.F., Taylor, R.W., Turnbull, D.M. and McFarland, R. (2015) 'Prevalence of nuclear and mitochondrial DNA mutations related to adult mitochondrial disease', *Annals of Neurology*, 77(5), pp. 753-759.

Gouaux, E. (2004) 'Structure and function of AMPA receptors', *The Journal of Physiology*, 554(Pt 2), pp. 249-253.

Green, D. and Reed, J. (1998) 'Mitochondria and Apoptosis', *Science*, 281(5381), pp. 1309-1312.

Greenfield Jr, L.J. (2013) 'Molecular mechanisms of antiseizure drug activity at GABAA receptors', *Seizure*, 22(8), pp. 589-600.

Grosenbaugh, D.K. and Mott, D.D. (2013) 'Stiripentol in refractory status epilepticus', *Epilepsia*, 54, pp. 103-105.

Gulyás, A.I., Buzsáki, G., Freund, T.F. and Hirase, H. (2006) 'Populations of hippocampal inhibitory neurons express different levels of cytochrome c', *European Journal of Neuroscience*, 23(10), pp. 2581-2594.

Gunter, T.E. and Pfeiffer, D.R. (1990) 'Mechanisms by which mitochondria transport calcium', *American Journal of Physiology - Cell Physiology*, 258(5), p. C755.

Gupta, A., Perez, M., Lee, K., Taylor, J. and Farrow, K. (2015) 'SOD2 Activity Is not Impacted by Hyperoxia in Murine Neonatal Pulmonary Artery Smooth Muscle Cells and Mice', *International Journal of Molecular Sciences*, 16(3), p. 6373.

Gusel'nikova, V.V. and Korzhevskiy, D.E. (2015) 'NeuN As a Neuronal Nuclear Antigen and Neuron Differentiation Marker', *Acta Naturae*, 7(2), pp. 42-47.

Gyung, W.K. and Pak, H.C. (2002) 'Involvement of Superoxide in Excitotoxicity and DNA Fragmentation in Striatal Vulnerability in Mice after Treatment with the Mitochondrial Toxin, 3-Nitropropionic Acid', *Journal of Cerebral Blood Flow & Metabolism*, 22(7), pp. 798-809.

Haberek, G., Tomczyk, T., Zuchora, B., Wielosz, M., Turski, W.A. and Urbanska, E.M. (2000) 'Proconvulsive effects of the mitochondrial respiratory chain inhibitor — 3-nitropropionic acid', *European Journal of Pharmacology*, 403(3), pp. 229-233.

Haidukewych, D., Forsythe, W.I. and Sills, M. (1982) 'Monitoring octanoic and decanoic acids in plasma from children with intractable epilepsy treated with medium-chain triglyceride diet', *Clinical Chemistry*, 28(4), pp. 642-645.

Hall, R.A. and Soderling, T.R. (1997) 'Quantitation of AMPA receptor surface expression in cultured hippocampal neurons', *Neuroscience*, 78(2), pp. 361-371.

Halliwell, B. and Whiteman, M. (2004) 'Measuring reactive species and oxidative damage in vivo and in cell culture: how should you do it and what do the results mean?', *British Journal of Pharmacology*, 142(2), pp. 231-255.

Hanada, T., Hashizume, Y., Tokuhara, N., Takenaka, O., Kohmura, N., Ogasawara, A., Hatakeyama, S., Ohgoh, M., Ueno, M. and Nishizawa, Y. (2011) 'Perampanel: A novel, orally active, noncompetitive AMPA-receptor antagonist that reduces seizure activity in rodent models of epilepsy', *Epilepsia*, 52(7), pp. 1331-1340.

Hansen, D.B., Garrido-Comas, N., Salter, M. and Fern, R. (2015) 'HCO3−-independent pH Regulation in Astrocytes in Situ Is Dominated by V-ATPase', *Journal of Biological Chemistry*, 290(13), pp. 8039-8047.

Hargreaves, I.P. (2014) 'Coenzyme Q10 as a therapy for mitochondrial disease', *The International Journal of Biochemistry & Cell Biology*, 49, pp. 105-111.

Hassel, B. and Dingledine, R. (2006) 'Glutamate', in Siegel, G.J., Albers, R.W., Brady, S.T. and Price, D.L. (eds.) *Basic Neurochemistry: Molecular, Cellular, and Medical Aspects*. 7 edn. China: Elsevier, pp. 267-290.

Hassel, B., Paulsen, R.E., Johnsen, A. and Fonnum, F. (1992) 'Selective inhibition of glial cell metabolism in vivo by fluorocitrate', *Brain Research*, 576(1), pp. 120-124.

Hatefi, Y. (1985) 'The Mitochondrial Electron Transport and Oxidative Phosphorylation System', *Annual Review of Biochemistry*, 54(1), pp. 1015-1069.

Hazelton, J.L., Petrasheuskaya, M., Fiskum, G. and Kristián, T. (2009) 'Cyclophilin D is predominantly expressed in mitochondria of GABAergic interneurons', *Journal of neuroscience research*, 87(5), pp. 1250-1259.

Henderson, J.W. and Brooks, A. (2010) 'Improved Amino Acid Methods using Agilent ZORBAX Eclipse Plus C18 Columns for a Variety of Agilent LC Instrumentation and Separation Goals', [Online]. Available at: http://www.agilent.com/cs/library/applications/5990-4547EN.pdf (Accessed: 19 January 2017).

Henry, T.R., Frey, K.A., Sackellares, J.C., Gilman, S., Koeppe, R.A., Brunberg, J.A., Ross, D.A., Berent, S., Young, A.B. and Kuhl, D.E. (1993) 'In vivo cerebral metabolism and central benzodiazepine ‐ receptor binding in temporal lobe epilepsy', *Neurology*, 43(10), p. 1998.

Herrero-Mendez, A., Almeida, A., Fernandez, E., Maestre, C., Moncada, S. and Bolanos, J.P. (2009) 'The bioenergetic and antioxidant status of neurons is controlled by continuous degradation of a key glycolytic enzyme by APC/C-Cdh1', *Nat Cell Biol*, 11(6), pp. 747-752.

Hertz, L. (2004) 'The Astrocyte-Neuron Lactate Shuttle: A Challenge of a Challenge', *Journal of Cerebral Blood Flow & Metabolism*, 24(11), pp. 1241-1248.

Hertz, L. (2013) 'The Glutamate–Glutamine (GABA) Cycle: Importance of Late Postnatal Development and Potential Reciprocal Interactions between Biosynthesis and Degradation', *Frontiers in Endocrinology*, 4, p. 59.

Hertz, L., Peng, L. and Dienel, G.A. (2006) 'Energy Metabolism in Astrocytes: High Rate of Oxidative Metabolism and Spatiotemporal Dependence on Glycolysis/Glycogenolysis', *Journal of Cerebral Blood Flow & Metabolism*, 27(2), pp. 219-249.

Hertz, L. and Rothman, D.L. (2016) 'Glucose, Lactate, β-Hydroxybutyrate, Acetate, GABA, and Succinate as Substrates for Synthesis of Glutamate and GABA in the Glutamine–Glutamate/GABA Cycle', in Schousboe, A. and Sonnewald, U. (eds.) *The Glutamate/GABA-Glutamine Cycle: Amino Acid Neurotransmitter Homeostasis*. Cham: Springer International Publishing, pp. 9-42.

Hertz, L. and Zielke, H.R. (2004) 'Astrocytic control of glutamatergic activity: astrocytes as stars of the show', *Trends in Neurosciences*, 27(12), pp. 735-743.

Herx, L.M. and Yong, V.W. (2001) 'Interleukin-1β is Required for the Early Evolution of Reactive Astrogliosis Following CNS Lesion', *Journal of Neuropathology & Experimental Neurology*, 60(10), pp. 961-971.

Hitiris, N., Mohanraj, R., Norrie, J., Sills, G.J. and Brodie, M.J. (2007) 'Predictors of pharmacoresistant epilepsy', *Epilepsy Research*, 75(2–3), pp. 192-196.

Hof, P.R., Kidd, G., DeFelipe, J., Vellis, J.d., sosa, M.A.G., Elder, G.A. and Trapp, B.D. (2014) 'Cellular Components of Nervous Tissue', in *From Molecules to Networks : An Introduction to Cellular and Molecular Neuroscience*. 3 edn. United Kingdom: Academic Press, pp. 1-22.

Hogstad, S., Svenneby, G., Torgner, I.A., Kvamme, E., Hertz, L. and Schousboe, A. (1988) 'Glutaminase in neurons and astrocytes cultured from mouse brain: Kinetic properties and effects of phosphate, glutamate, and ammonia', *Neurochemical Research*, 13(4), pp. 383-388.

Hol, E.M. and Pekny, M. (2015) 'Glial fibrillary acidic protein (GFAP) and the astrocyte intermediate filament system in diseases of the central nervous system', *Current Opinion in Cell Biology*, 32, pp. 121-130.

Hornfeldt, C.S. and Larson, A.A. (1990) 'Seizures induced by fluoroacetic acid and fluorocitric acid may involve chelation of divalent cations in the spinal cord', *European Journal of Pharmacology*, 179(3), pp. 307-313.

Hubbard, J.A., Hsu, M.S., Seldin, M.M. and Binder, D.K. (2015) 'Expression of the Astrocyte Water Channel Aquaporin-4 in the Mouse Brain', *ASN Neuro*, 7(5), p. 1759091415605486.

Huchzermeyer, C., Albus, K., Gabriel, H.-J., Otáhal, J., Taubenberger, N., Heinemann, U., Kovács, R. and Kann, O. (2008) 'Gamma Oscillations and Spontaneous Network Activity in the Hippocampus Are Highly

Sensitive to Decreases in pO₂ and Concomitant Changes in Mitochondrial Redox State', *The Journal of Neuroscience*, 28(5), pp. 1153-1162.

Hughes, S.D., Kanabus, M., Anderson, G., Hargreaves, I.P., Rutherford, T., Donnell, M.O., Cross, J.H., Rahman, S., Eaton, S. and Heales, S.J.R. (2014) 'The ketogenic diet component decanoic acid increases mitochondrial citrate synthase and complex I activity in neuronal cells', *Journal of Neurochemistry*, 129(3), pp. 426-433.

Humpel, C. (2015) 'Organotypic brain slice cultures: A review', *Neuroscience*, 305, pp. 86-98.

Huttenlocher, P.R., Wilbourn, A.J. and Signore, J.M. (1971) 'Medium‐chain triglycerides as a therapy for intractable childhood epilepsy', *Neurology*, 21(11), p. 1097.

Inoue, Y., Ohtsuka, Y., Oguni, H., Tohyama, J., Baba, H., Fukushima, K., Ohtani, H., Takahashi, Y. and Ikeda, S. (2009) 'Stiripentol open study in Japanese patients with Dravet syndrome', *Epilepsia*, 50(11), pp. 2362-2368.

Isaac, J.T.R., Ashby, M.C. and McBain, C.J. (2007) 'The Role of the GluR2 Subunit in AMPA Receptor Function and Synaptic Plasticity', *Neuron*, 54(6), pp. 859-871.

Isaeva, E., Isaev, D., Savrasova, A., Khazipov, R. and Holmes, G.L. (2010) 'Recurrent neonatal seizures result in long-term increases in neuronal network excitability in the rat neocortex', *European Journal of Neuroscience*, 31(8), pp. 1446-1455.

Ivanov, A.I., Malkov, A.E., Waseem, T., Mukhtarov, M., Buldakova, S., Gubkina, O., Zilberter, M. and Zilberter, Y. (2013) 'Glycolysis and Oxidative Phosphorylation in Neurons and Astrocytes during Network Activity in Hippocampal Slices', *Journal of Cerebral Blood Flow & Metabolism*, 34(3), pp. 397-407.

Jain, V., Langham, M.C. and Wehrli, F.W. (2010) 'MRI Estimation of Global Brain Oxygen Consumption Rate', *Journal of Cerebral Blood Flow & Metabolism*, 30(9), pp. 1598-1607.

Janssen, R.J.R.J., Nijtmans, L.G., Heuvel, L.P.v.d. and Smeitink, J.A.M. (2006) 'Mitochondrial complex I: Structure, function and pathology', *Journal of Inherited Metabolic Disease*, 29(4), pp. 499-515.

Janzer, R.C. and Raff, M.C. (1987) 'Astrocytes induce blood-brain barrier properties in endothelial cells', *Nature*, 325(6101), pp. 253-257.

Jessen, S.B., Mathiesen, C., Lind, B.L. and Lauritzen, M. (2017) 'Interneuron Deficit Associates Attenuated Network Synchronization to Mismatch of Energy Supply and Demand in Aging Mouse Brains', *Cerebral Cortex*, 27(1), pp. 646-659.

Jia, Z., Agopyan, N., Miu, P., Xiong, Z., Henderson, J., Gerlai, R., Taverna, F.A., Velumian, A., MacDonald, J., Carlen, P., Abramow-Newerly, W. and Roder, J. (2014) 'Enhanced LTP in Mice Deficient in the AMPA Receptor GluR2', *Neuron*, 17(5), pp. 945-956.

Jiang, F., Liu, T., Cheng, M., Pang, X.-Y., Bai, Z.-T., Zhou, J.-J. and Ji, Y.-H. (2009) 'Spinal astrocyte and microglial activation contributes to rat pain-related behaviors induced by the venom of scorpion Buthus martensi Karch', *European Journal of Pharmacology*, 623(1–3), pp. 52-64.

Jobst, B. (2010) 'Brain stimulation for surgical epilepsy', *Epilepsy Research*, 89(1), pp. 154-161.

Johri, A., Calingasan, N.Y., Hennessey, T.M., Sharma, A., Yang, L., Wille, E., Chandra, A. and Beal, M.F. (2012) 'Pharmacologic activation of mitochondrial biogenesis exerts widespread beneficial effects in a transgenic mouse model of Huntington's disease', *Human Molecular Genetics*, 21(5), pp. 1124-1137.

Jones, E.G. (2009) 'The Origins of Cortical Interneurons: Mouse versus Monkey and Human', *Cerebral Cortex*, 19(9), pp. 1953-1956.

Jones, E.V., Cook, D. and Murai, K.K. (2012) 'A Neuron-Astrocyte Co-Culture System to Investigate Astrocyte-Secreted Factors in Mouse Neuronal Development', in Milner, R. (ed.) *Astrocytes: Methods and Protocols*. Totowa, NJ: Humana Press, pp. 341-352.

Jones, R.S.G., da Silva, A.B., Whittaker, R.G., Woodhall, G.L. and Cunningham, M.O. (2016) 'Human brain slices for epilepsy research: Pitfalls, solutions and future challenges', *Journal of Neuroscience Methods*, 260, pp. 221-232.

Joo, M.D.Daisy T., Xiong, P.D.Z., MacDonald, P.D.John F., Jia, P.D.Z., Roder, P.D.J., Sonner, M.D.J. and Orser, M.D.P.D.F.R.C.P.C.Beverley A. (1999) 'Blockade of Glutamate Receptors and Barbiturate Anesthesia Increased Sensitivity to Pentobarbital-induced Anesthesia Despite Reduced Inhibition of AMPA Receptors in GluR2 Null Mutant Mice', *Anesthesiology*, 91(5), pp. 1329-1329.

Kaczor, P., Rakus, D. and Mozrzymas, J.W. (2015) 'Neuron-astrocyte interaction enhance GABAergic synaptic transmission in a manner dependent on key metabolic enzymes', *Frontiers in Cellular Neuroscience*, 9, p. 120.

Kalnenieks, U., Galinina, N., Toma, M.M. and Poole, R.K. (2000) 'Cyanide inhibits respiration yet stimulates aerobic growth of Zymomonas mobilis', *Microbiology*, 146(6), pp. 1259-1266.

Kane, D.A. (2014) 'Lactate oxidation at the mitochondria: a lactate-malate-aspartate shuttle at work', *Frontiers in Neuroscience*, 8, p. 366.

Kang, H.-C., Lee, Y.-M., Kim, H.D., Lee, J.S. and Slama, A. (2007) 'Safe and Effective Use of the Ketogenic Diet in Children with Epilepsy and Mitochondrial Respiratory Chain Complex Defects', *Epilepsia*, 48(1), pp. 82-88.

Kann, O. (2016) 'The interneuron energy hypothesis: Implications for brain disease', *Neurobiology of Disease*, 90, pp. 75-85.

Kann, O., Huchzermeyer, C., Kovács, R., Wirtz, S. and Schuelke, M. (2011) 'Gamma oscillations in the hippocampus require high complex I gene expression and strong functional performance of mitochondria', *Brain*, 134(2), pp. 345-358.

Kann, O., Papageorgiou, I.E. and Draguhn, A. (2014) 'Highly energized inhibitory interneurons are a central element for information processing in cortical networks', *Journal of Cerebral Blood Flow & Metabolism*, 34(8), pp. 1270-1282.

Kannan, K. and Jain, S.K. (2000) 'Oxidative stress and apoptosis', *Pathophysiology*, 7(3), pp. 153-163.

Kelsom, C. and Lu, W. (2013) 'Development and specification of GABAergic cortical interneurons', *Cell & Bioscience*, 3(1), p. 19.

Kepecs, A. and Fishell, G. (2014) 'Interneuron cell types are fit to function', *Nature*, 505(7483), pp. 318-326.

Kew, J.N.C. and Kemp, J.A. (2005) 'Ionotropic and metabotropic glutamate receptor structure and pharmacology', *Psychopharmacology*, 179(1), pp. 4-29.

Khurana, D.S., Salganicoff, L., Melvin, J.J., Hobdell, E.F., Valencia, I., Hardison, H.H., Marks, H.G., Grover, W.D. and Legido, A. (2008) 'Epilepsy and Respiratory Chain Defects in Children with Mitochondrial Encephalopathies', *Neuropediatrics*, 39(01), pp. 8-13.

Kimelberg, H.K. and Nedergaard, M. (2010) 'Functions of Astrocytes and their Potential As Therapeutic Targets', *Neurotherapeutics*, 7(4), pp. 338-353.

Kofuji, P. and Newman, E.A. (2004) 'POTASSIUM BUFFERING IN THE CENTRAL NERVOUS SYSTEM', *Neuroscience*, 129(4), pp. 1045-1056.

Kolbaev, S.N., Sharonova, I.N., Vorobjev, V.S. and Skrebitsky, V.G. (2002) 'Mechanisms of GABAA receptor blockade by millimolar concentrations of furosemide in isolated rat Purkinje cells', *Neuropharmacology*, 42(7), pp. 913-921.

Korpi, E.R. and Lüddens, H. (1997) 'Furosemide interactions with brain GABA(A) receptors', *British Journal of Pharmacology*, 120(5), pp. 741-748.

Kossoff, E.H., McGrogan, J.R., Bluml, R.M., Pillas, D.J., Rubenstein, J.E. and Vining, E.P. (2006) 'A Modified Atkins Diet Is Effective for the Treatment of Intractable Pediatric Epilepsy', *Epilepsia*, 47(2), pp. 421-424.

Kovac, S., Domijan, A.M., Walker, M.C. and Abramov, A.Y. (2014) 'Seizure activity results in calcium- and mitochondria-independent ROS production via NADPH and xanthine oxidase activation', *Cell Death & Disease*, 5(10), p. e1442.

Kovačević, Z. and Morris, H.P. (1972) 'The Role of Glutamine in the Oxidative Metabolism of Malignant Cells', *Cancer Research*, 32(2), pp. 326-333.

Krisko, T.I., Armstrong, E.J. and Cohen, D.E. (2017) 'Pharmacology of Cholesterol and Lipoprotein Metabolism', in Golan, D.E., Armstrong, E.J. and Armstrong, A.W. (eds.) *Principles of Pharmacology: The Pathophysiologic Basis of Drug Therapy*. 4th edn. China: Wolters Kluwer, pp. 336-357.

Kucken, A.M., Wagner, D.A., Ward, P.R., Teissére, J.A., Boileau, A.J. and Czajkowski, C. (2000) 'Identification of Benzodiazepine Binding Site Residues in the γ2 Subunit of the γ-Aminobutyric Acid_A Receptor', *Molecular Pharmacology*, 57(5), pp. 932-939.

Kudin, A.P., Debska-Vielhaber, G., Vielhaber, S., Elger, C.E. and Kunz, W.S. (2004) 'The Mechanism of Neuroprotection by Topiramate in an Animal Model of Epilepsy', *Epilepsia*, 45(12), pp. 1478-1487.

Kudin, A.P., Kudina, T.A., Seyfried, J., Vielhaber, S., Beck, H., Elger, C.E. and Kunz, W.S. (2002) 'Seizure-dependent modulation of mitochondrial oxidative phosphorylation in rat hippocampus', *European Journal of Neuroscience*, 15(7), pp. 1105-1114.

Kudin, A.P., Malinska, D. and Kunz, W.S. (2008) 'Sites of generation of reactive oxygen species in homogenates of brain tissue determined with the use of respiratory substrates and inhibitors', *Biochimica et Biophysica Acta (BBA) - Bioenergetics*, 1777(7–8), pp. 689-695.

Kuenzi, F.M., Fitzjohn, S.M., Morton, R.A., Collingridge, G.L. and Seabrook, G.R. (2000) 'Reduced long-term potentiation in hippocampal slices prepared using sucrose-based artificial cerebrospinal fluid', *Journal of Neuroscience Methods*, 100(1–2), pp. 117-122.

Kwan, P., Arzimanoglou, A., Berg, A.T., Brodie, M.J., Allen Hauser, W., Mathern, G., Moshé, S.L., Perucca, E., Wiebe, S. and French, J. (2010) 'Definition of drug resistant epilepsy: Consensus proposal by the ad hoc Task Force of the ILAE Commission on Therapeutic Strategies', *Epilepsia*, 51(6), pp. 1069-1077.

Kwan, P. and Brodie, M.J. (2000) 'Early Identification of Refractory Epilepsy', *New England Journal of Medicine*, 342(5), pp. 314-319.

Laffel, L. (1999) 'Ketone bodies: a review of physiology, pathophysiology, and application of monitoring to diabetes', *Diabetes Metabolism, Research, and Reviews*, 15(6), pp. 412-426.

Lambert, J.J., Belelli, D., Peden, D.R., Vardy, A.W. and Peters, J.A. (2003) 'Neurosteroid modulation of GABAA receptors', *Progress in Neurobiology*, 71(1), pp. 67-80.

Lambrechts, D.A.J.E., de Kinderen, R.J.A., Vles, J.S.H., de Louw, A.J.A., Aldenkamp, A.P. and Majoie, H.J.M. (2017) 'A randomized controlled trial of the ketogenic diet in refractory childhood epilepsy', *Acta Neurologica Scandinavica*, 135(2), pp. 231-239.

Lapuente-Brun, E., Moreno-Loshuertos, R., Acín-Pérez, R., Latorre-Pellicer, A., Colás, C., Balsa, E., Perales-Clemente, E., Quirós, P.M., Calvo, E., Rodríguez-Hernández, M.A., Navas, P., Cruz, R., Carracedo, Á., López-Otín, C., Pérez-Martos, A., Fernández-Silva, P., Fernández-Vizarra, E. and Enríquez, J.A. (2013) 'Supercomplex Assembly Determines Electron Flux in the Mitochondrial Electron Transport Chain', *Science*, 340(6140), pp. 1567-1570.

Largo, C., Ibarz, J.M. and Herreras, O. (1997) 'Effects of the Gliotoxin Fluorocitrate on Spreading Depression and Glial Membrane Potential in Rat Brain In Situ', *Journal of Neurophysiology*, 78(1), pp. 295-307.

Lauble, H., Kennedy, M.C., Emptage, M.H., Beinert, H. and Stout, C.D. (1996) 'The reaction of fluorocitrate with aconitase and the crystal structure of the enzyme-inhibitor complex', *Proceedings of the National Academy of Sciences*, 93(24), pp. 13699-13703.

Lauritzen, M. (1987) 'Cortical spreading depression as a putative migraine mechanism', *Trends in Neurosciences*, 10(1), pp. 8-13.

Lax, N.Z., Gorman, G.S. and Turnbull, D.M. (2017) 'Review: Central nervous system involvement in mitochondrial disease', *Neuropathology and Applied Neurobiology*, 43(2), pp. 102-118.

Lax, N.Z., Grady, J., Laude, A., Chan, F., Hepplewhite, P.D., Gorman, G., Whittaker, R.G., Ng, Y., Cunningham, M.O. and Turnbull, D.M. (2016) 'Extensive respiratory chain defects in inhibitory interneurones in patients with mitochondrial disease', *Neuropathology and Applied Neurobiology*, 42(2), pp. 180-193.

Leavesley, H.B., Li, L., Prabhakaran, K., Borowitz, J.L. and Isom, G.E. (2008) 'Interaction of Cyanide and Nitric Oxide with Cytochrome c Oxidase: Implications for Acute Cyanide Toxicity', *Toxicological Sciences*, 101(1), pp. 101-111.

Lee, E., Williams, Z., Goodman, C.B., Oriaku, E.T., Harris, C., Thomas, M. and Soliman, K.F.A. (2006) 'Effects of NMDA receptor inhibition by phencyclidine on the neuronal differentiation of PC12 cells', *NeuroToxicology*, 27(4), pp. 558-566.

Leibovitz, B., Hu, M.L. and Tappel, A.L. (1990) 'Dietary supplements of vitamin E, beta-carotene, coenzyme Q10 and selenium protect tissues against lipid peroxidation in rat tissue slices', *The Journal of nutrition*, 120(1), pp. 97-104.

Leppik, I.E. (2003) 'Classification of the Myoclonic Epilepsies', *Epilepsia*, 44, pp. 2-6.

Levine, R.L., Williams, J.A., Stadtman, E.R. and Shacter, E. (1994) 'Carbonyl assays for determination of oxidatively modified proteins', *Methods Enzymol*, 233, pp. 346-57.

Li, H., Fukuda, S., Hasegawa, Y., Kobayashi, H., Purevsuren, J., Mushimoto, Y. and Yamaguchi, S. (2010) 'Effect of heat stress and bezafibrate on mitochondrial β-oxidation: Comparison between cultured cells from normal and mitochondrial fatty acid oxidation disorder children using in vitro probe acylcarnitine profiling assay', *Brain and Development*, 32(5), pp. 362-370.

Li, N., Ragheb, K., Lawler, G., Sturgis, J., Rajwa, B., Melendez, J.A. and Robinson, J.P. (2003) 'Mitochondrial Complex I Inhibitor Rotenone Induces Apoptosis through Enhancing Mitochondrial Reactive Oxygen Species Production', *Journal of Biological Chemistry*, 278(10), pp. 8516-8525.

Li, S., Guo, J., Ying, Z., Chen, S., Yang, L., Chen, K., Long, Q., Qin, D., Pei, D. and Liu, X. (2015) 'Valproic acid-induced hepatotoxicity in alpers syndrome is associated with mitochondrial permeability transition pore opening-dependent apoptotic sensitivity in an induced pluripotent stem cell model', *Hepatology*, 61(5), pp. 1730-1739.

Li, W.C., Soffe, S.R. and Roberts, A. (2004) 'A Direct Comparison of Whole Cell Patch and Sharp Electrodes by Simultaneous Recording From Single Spinal Neurons in Frog Tadpoles', *Journal of Neurophysiology*, 92(1), pp. 380-386.

Lian, X.-Y. and Stringer, J.L. (2004) 'Inhibition of aconitase in astrocytes increases the sensitivity to chemical convulsants', *Epilepsy Research*, 60(1), pp. 41-52.

Liang, H. and Ward, W.F. (2006) 'PGC-1α: a key regulator of energy metabolism', *Advances in Physiology Education*, 30(4), pp. 145-151.

Liang, L.-P. and Patel, M. (2004) 'Mitochondrial oxidative stress and increased seizure susceptibility in Sod2−/+ mice', *Free Radical Biology and Medicine*, 36(5), pp. 542-554.

Liang, L.P., Ho, Y.S. and Patel, M. (2000) 'Mitochondrial superoxide production in kainate-induced hippocampal damage', *Neuroscience*, 101(3), pp. 563-570.

Lightowlers, R.N., Chinnery, P.F., Turnbull, D.M. and Howell, N. (1997) 'Mammalian mitochondrial genetics: heredity, heteroplasmy and disease', *Trends in Genetics*, 13(11), pp. 450-455.

Likhodii, S.S., Musa, K., Mendonca, A., Dell, C., Burnham, W.M. and Cunnane, S.C. (2000) 'Dietary Fat, Ketosis, and Seizure Resistance in Rats on the Ketogenic Diet', *Epilepsia*, 41(11), pp. 1400-1410.

Lin-Hendel, Erika G., McManus, Meagan J., Wallace, Douglas C., Anderson, Stewart A. and Golden, Jeffrey A. (2016) 'Differential Mitochondrial Requirements for Radially and Non-radially Migrating Cortical Neurons: Implications for Mitochondrial Disorders', *Cell Reports*, 15(2), pp. 229-237.

Lin, C.-J., Lee, C.-C., Shih, Y.-L., Lin, C.-H., Wang, S.-H., Chen, T.-H. and Shih, C.-M. (2012) 'Inhibition of Mitochondria- and Endoplasmic Reticulum Stress-Mediated Autophagy Augments Temozolomide-Induced Apoptosis in Glioma Cells', *PLOS ONE*, 7(6), p. e38706.

Lin, C.-M. and Thajeb, P. (2007) 'Valproic Acid Aggravates Epilepsy due to MELAS in a Patient with an A3243G Mutation of Mitochondrial DNA', *Metabolic Brain Disease*, 22(1), p. 105.

Lindquist, C.E.L., Laver, D.R. and Birnir, B. (2005) 'The mechanism of SR95531 inhibition at GABAA receptors examined in human α1β1 and α1β1γ2S receptors', *Journal of Neurochemistry*, 94(2), pp. 491-501.

Ling, C., Hendrickson, M.L. and Kalil, R.E. (2012) 'Resolving the Detailed Structure of Cortical and Thalamic Neurons in the Adult Rat Brain with Refined Biotinylated Dextran Amine Labeling', *PLOS ONE*, 7(11), p. e45886.

Liu, X.-B. and Murray, K.D. (2012) 'Neuronal excitability and calcium/calmodulin-dependent protein kinase type II: Location, location, location', *Epilepsia*, 53, pp. 45-52.

Liuzzi, F.J. and Lasek, R.J. (1987) 'Astrocytes block axonal regeneration in mammals by activating the physiological stop pathway', *Science*, 237(4815), pp. 642-645.

Livne-Bar, I., Lam, S., Chan, D., Guo, X., Askar, I., Nahirnyj, A., Flanagan, J.G. and Sivak, J.M. (2016) 'Pharmacologic inhibition of reactive gliosis blocks TNF-[alpha]-mediated neuronal apoptosis', *Cell Death Dis*, 7, p. e2386.

Lopez-Fabuel, I., Le Douce, J., Logan, A., James, A.M., Bonvento, G., Murphy, M.P., Almeida, A. and Bolaños, J.P. (2016) 'Complex I assembly into supercomplexes determines differential mitochondrial ROS production in neurons and astrocytes', *Proceedings of the National Academy of Sciences*, 113(46), pp. 13063-13068.

Löscher, W. (2002) 'Basic Pharmacology of Valproate', *CNS Drugs*, 16(10), pp. 669-694.

Löscher, W. (2011) 'Critical review of current animal models of seizures and epilepsy used in the discovery and development of new antiepileptic drugs', *Seizure*, 20(5), pp. 359-368.

Lynch, B.A., Lambeng, N., Nocka, K., Kensel-Hammes, P., Bajjalieh, S.M., Matagne, A. and Fuks, B. (2004) 'The synaptic vesicle protein SV2A is the binding site for the antiepileptic drug levetiracetam',

Proceedings of the National Academy of Sciences of the United States of America, 101(26), pp. 9861-9866.

Maccaferri, G. and Lacaille, J.-C. (2003) 'Interneuron Diversity series: Hippocampal interneuron classifications – making things as simple as possible, not simpler', *Trends in Neurosciences*, 26(10), pp. 564-571.

Macdonald, R.L. and Rogawski, M.A. (2008) 'Cellular Effects of Antiepileptic Drugs', in Jerome Engel, J. and Pedley, T.A. (eds.) *Epilepsy : A Comprehensive Textbook*. United States of America: Lippincott Williams & Wilkins, pp. 1433 - 1445.

Mancuso, M., Orsucci, D., Angelini, C., Bertini, E., Carelli, V., Comi, G.P., Donati, A., Minetti, C., Moggio, M., Mongini, T., Servidei, S., Tonin, P., Toscano, A., Uziel, G., Bruno, C., Ienco, E.C., Filosto, M., Lamperti, C., Catteruccia, M., Moroni, I., Musumeci, O., Pegoraro, E., Ronchi, D., Santorelli, F.M., Sauchelli, D., Scarpelli, M., Sciacco, M., Valentino, M.L., Vercelli, L., Zeviani, M. and Siciliano, G. (2014) 'The m.3243A>G mitochondrial DNA mutation and related phenotypes. A matter of gender?', *Journal of Neurology*, 261(3), pp. 504-510.

Mangia, S., Simpson, I.A., Vannucci, S.J. and Carruthers, A. (2009) 'The in vivo neuron-to-astrocyte lactate shuttle in human brain', *J Neurochem*, 109.

Maranzana, E., Barbero, G., Falasca, A.I., Lenaz, G. and Genova, M.L. (2013) 'Mitochondrial Respiratory Supercomplex Association Limits Production of Reactive Oxygen Species from Complex I', *Antioxidants & Redox Signaling*, 19(13), pp. 1469-1480.

Marek, R., Caruso, M., Rostami, A., Grinspan, J.B. and Sarma, J.D. (2008) 'Magnetic cell sorting: A fast and effective method of concurrent isolation of high purity viable astrocytes and microglia from neonatal mouse brain tissue', *Journal of Neuroscience Methods*, 175(1), pp. 108-118.

Markram, H., Toledo-Rodriguez, M., Wang, Y., Gupta, A., Silberberg, G. and Wu, C. (2004) 'Interneurons of the neocortical inhibitory system', *Nat Rev Neurosci*, 5(10), pp. 793-807.

Martikainen, M.H., Paivarinta, M., Jaaskelainen, S. and Majamaa, K. (2012) 'Successful treatment of POLG-related mitochondrial epilepsy with antiepileptic drugs and low glycaemic index diet', *Epileptic Disorders*, 14(4), pp. 438-441.

Martin, K., Jackson, C.F., Levy, R.G. and Cooper, P.N. (2016) 'Ketogenic diet and other dietary treatments for epilepsy', *Cochrane Database of Systematic Reviews*, (2).

Martin, L.J., Blackstone, C.D., Levey, A.I., Huganir, R.L. and Price, D.L. (1993) 'AMPA glutamate receptor subunits are differentially distributed in rat brain', *Neuroscience*, 53(2), pp. 327-358.

Matthews, P.M., Ford, B., Dandurand, R.J., Eidelman, D.H., O'Connor, D., Sherwin, A., Karpati, G., Andermann, F. and Arnold, D.L. (1993) 'Coenzyme Q10 with multiple vitamins is generally ineffective in treatment of mitochondrial disease', *Neurology*, 43(5), p. 884.

Mattman, A., Sirrs, S., Mezei, M.M., Salvarinova-Zivkovic, R., Alfadhel, M. and Lillquist, Y. (2011) 'Mitochondrial disease clinical manifestations: An overview', *BC Medical Journal*, 53(4), pp. 183-187.

Matyash, V. and Kettenmann, H. (2010) 'Heterogeneity in astrocyte morphology and physiology', *Brain Research Reviews*, 63(1–2), pp. 2-10.

Mayevsky, A., Doron, A., Manor, T., Meilin, S., Zarchin, N. and Ouaknine, G.E. (1996) 'Cortical spreading depression recorded from the human brain using a multiparametric monitoring system', *Brain Research*, 740(1–2), pp. 268-274.

McFarland, R., Taylor, R.W. and Turnbull, D.M. (2012) 'A neurological perspective on mitochondrial disease', *The Lancet Neurology*, 9(8), pp. 829-840.

McKenna, M.C., Gruetter, R., Sonnewald, U., Waagepetersen, H.S. and Schousboe, A. (2006) 'Energy Metabolism of the Brain', in Siegel, G.J., Albers, R.W., Brady, S.T. and Price, D.L. (eds.) *Basic Neurochemistry : Molecular, Cellular, and Medical Aspects*. 7th edn. China: Elsevier, pp. 531-557.

McKenzie, M., Lazarou, M., Thorburn, D.R. and Ryan, M.T. (2006) 'Mitochondrial Respiratory Chain Supercomplexes Are Destabilized in Barth Syndrome Patients', *Journal of Molecular Biology*, 361(3), pp. 462-469.

McNair, L.F., Kornfelt, R., Walls, A.B., Andersen, J.V., Aldana, B.I., Nissen, J.D., Schousboe, A. and Waagepetersen, H.S. (2016) 'Metabolic Characterization of Acutely Isolated Hippocampal and Cerebral Cortical Slices Using [U-13C]Glucose and [1,2-13C]Acetate as Substrates', *Neurochemical Research*, pp. 1-17.

McNamara, J.O. (2011) 'Pharmacotherapy of the Epilepsies', in Brunton, L., Chabner, B. and Knollman, B. (eds.) *Goodman and Gilman's The Pharmacological Basis of Therapeutics*. 12 edn. China: McGraw Hills, pp. 583-607.

Mehlman, M.A. (1968) 'Inhibition of Pyruvate Carboxylation by Fluorocitrate in Rat Kidney Mitochondria', *Journal of Biological Chemistry*, 243(8), pp. 1919-1925.

Meldrum, B.S. (1993) 'Excitotoxicity and Selective Neuronal Loss in Epilepsy', *Brain Pathology*, 3(4), pp. 405-412.

Mendenhall, B. and Murphey, R.K. (1974) 'The morphology of cricket giant interneurons', *Journal of Neurobiology*, 5(6), pp. 565-580.

Mendez-Armenta, M., Nava-Ruiz, C., Juarez-Rebollar, D., Rodriquez-Marinez, E. and Gomez, P.Y. (2014) 'Oxidative Stress Associated with Neuronal Apoptosis in Experimental Models of Epilepsy', *Oxidative Medicine and Cellular Longevity*, 2014, p. 12.

Miller, P.S. and Aricescu, A.R. (2014) 'Crystal structure of a human GABA(A) receptor', *Nature*, 512(7514), pp. 270-275.

Miltenyi, S., Müller, W., Weichel, W. and Radbruch, A. (1990) 'High gradient magnetic cell separation with MACS', *Cytometry*, 11(2), pp. 231-238.

Minlebaev, M. and Khazipov, R. (2011) 'Antiepileptic effects of endogenous beta-hydroxybutyrate in suckling infant rats', *Epilepsy Research*, 95(1–2), pp. 100-109.

Miranda, M.J., Turner, Z. and Magrath, G. (2012) 'Alternative diets to the classical ketogenic diet—Can we be more liberal?', *Epilepsy Research*, 100(3), pp. 278-285.

Mirsattari, S.M., Shen, B., Leung, L.S. and Rajakumar, N. (2008) 'A gliotoxin model of occipital seizures in rats', *Seizure*, 17(6), pp. 483-489.

Mohanan, P.V. and Yamamoto, H.-a. (2002) 'Preventive effect of melatonin against brain mitochondria DNA damage, lipid peroxidation and seizures induced by kainic acid', *Toxicology Letters*, 129(1–2), pp. 99-105.

Mookerjee, S.A., Goncalves, R.L.S., Gerencser, A.A., Nicholls, D.G. and Brand, M.D. (2015) 'The contributions of respiration and glycolysis to extracellular acid production', *Biochimica et Biophysica Acta (BBA) - Bioenergetics*, 1847(2), pp. 171-181.

Moriyoshi, K., Masu, M., Ishii, T., Shigemoto, R., Mizuno, N. and Nakanishi, S. (1991) 'Molecular cloning and characterization of the rat NMDA receptor', *Nature*, 354(6348), pp. 31-37.

Mosienko, V., Teschemacher, A.G. and Kasparov, S. (2015) 'Is L-lactate a novel signaling molecule in the brain?', *Journal of Cerebral Blood Flow & Metabolism*, 35(7), pp. 1069-1075.

Möykkynen, T. and Korpi, E.R. (2012) 'Acute Effects of Ethanol on Glutamate Receptors', *Basic & Clinical Pharmacology & Toxicology*, 111(1), pp. 4-13.

Murphy, E.J. (2014) 'Carbon recycling goes full circle: fatty acids to excitatory amino acids and now excitatory amino acids to fatty acids', *Journal of Neurochemistry*, 129(3), pp. 363-365.

Muzykewicz, D.A., Lyczkowski, D.A., Memon, N., Conant, K.D., Pfeifer, H.H. and Thiele, E.A. (2009) 'Efficacy, safety, and tolerability of the low glycemic index treatment in pediatric epilepsy', *Epilepsia*, 50(5), pp. 1118-1126.

Myer, D.J., Gurkoff, G.G., Lee, S.M., Hovda, D.A. and Sofroniew, M.V. (2006) 'Essential protective roles of reactive astrocytes in traumatic brain injury', *Brain*, 129(10), pp. 2761-2772.

Nardou, R., Yamamoto, S., Bhar, A., Burnashev, N., Ben-Ari, Y. and Khalilov, I. (2011) 'Phenobarbital but Not Diazepam Reduces AMPA/kainate Receptor Mediated Currents and Exerts Opposite Actions on Initial Seizures in the Neonatal Rat Hippocampus', *Frontiers in Cellular Neuroscience*, 5, p. 16.

Nasrallah, F.A., Garner, B., Ball, G.E. and Rae, C. (2008) 'Modulation of brain metabolism by very low concentrations of the commonly used drug delivery vehicle dimethyl sulfoxide (DMSO)', *Journal of Neuroscience Research*, 86(1), pp. 208-214.

Navarro-Sastre, A., Tort, F., Stehling, O., Uzarska, Marta A., Arranz, José A., del Toro, M., Labayru, M T., Landa, J., Font, A., Garcia-Villoria, J., Merinero, B., Ugarte, M., Gutierrez-Solana, Luis G., Campistol, J., Garcia-Cazorla, A., Vaquerizo, J., Riudor, E., Briones, P., Elpeleg, O., Ribes, A. and Lill, R. (2011) 'A Fatal Mitochondrial Disease Is Associated with Defective NFU1 Function in the Maturation of a Subset of Mitochondrial Fe-S Proteins', *American Journal of Human Genetics*, 89(5), pp. 656-667.

Neal, E.G., Chaffe, H., Schwartz, R.H., Lawson, M.S., Edwards, N., Fitzsimmons, G., Whitney, A. and Cross, J.H. (2008) 'The ketogenic diet for the treatment of childhood epilepsy: a randomised controlled trial', *The Lancet Neurology*, 7(6), pp. 500-506.

Nesbitt, V. and McFarland, R. (2011) 'Phenotypic spectrum of m.3243A>G mitochondrial DNA mutation in children', *Archives of Disease in Childhood*, 96(Suppl 1), pp. A28-A28.

Ng, Y.S., Gorman, G., Nesbitt, V., Pitceathly, R., Grady, J., Schaefer, A., Bright, A., Feeney, C., Rahman, S., Poulton, J., Taylor, R., Hanna, M., Turnbull, D. and McFarland, R. (2015) 'Phenotypes and Genotypes of Mitochondrial Disease- Findings from A National Mitochondrial Disease Cohort (P2.061)', *Neurology*, 84(14 Supplement).

Ng, Y.S. and Turnbull, D.M. (2016) 'Mitochondrial disease: genetics and management', *Journal of Neurology*, 263, pp. 179-191.

Nicholls, D.G., Darley-Usmar, V.M., Wu, M., Jensen, P.B., Rogers, G.W. and Ferrick, D.A. (2010) 'Bioenergetic Profile Experiment using C2C12 Myoblast Cells', *Journal of Visualized Experiments : JoVE*, (46), p. 2511.

Nikolaev, M.V., Magazanik, L.G. and Tikhonov, D.B. (2012) 'Influence of external magnesium ions on the NMDA receptor channel block by different types of organic cations', *Neuropharmacology*, 62(5–6), pp. 2078-2085.

Nishigaki, Y., Tadesse, S., Bonilla, E., Shungu, D., Hersh, S., Keats, B.J.B., Berlin, C.I., Goldberg, M.F., Vockley, J., DiMauro, S. and Hirano, M. (2003) 'A novel mitochondrial tRNALeu(UUR) mutation in a patient with features of MERRF and Kearns–Sayre syndrome', *Neuromuscular Disorders*, 13(4), pp. 334-340.

Nordli, D.R. and De Vivo, D.C. (1997) 'The Ketogenic Diet Revisited: Back to the Future', *Epilepsia*, 38(7), pp. 743-749.

Noseda, R. and Burstein, R. (2013) 'Migraine pathophysiology: Anatomy of the trigeminovascular pathway and associated neurological symptoms, cortical spreading depression, sensitization, and modulation of pain', *PAIN®*, 154, Supplement 1, pp. S44-S53.

Novak, U. and Kaye, A.H. (2000) 'Extracellular matrix and the brain: components and function', *Journal of Clinical Neuroscience*, 7(4), pp. 280-290.

Nutt, D. (2006) 'GABAA receptors: subtypes, regional distribution, and function', *Journal of clinical sleep medicine : JCSM : official publication of the American Academy of Sleep Medicine*, 2(2), pp. S7-11.

Nylen, K., Likhodii, S. and Burnham, W.M. (2009) 'The ketogenic diet: Proposed mechanisms of action', *Neurotherapeutics*, 6(2), pp. 402-405.

O'Dowd, B.S., Gibbs, M.E., Sedman, G.L. and Ng, K.T. (1994) 'Astrocytes implicated in the energizing of intermediate memory processes in neonate chicks', *Cognitive Brain Research*, 2(2), pp. 93-102.

Obel, L.F., Müller, M.S., Walls, A.B., Sickmann, H.M., Bak, L.K., Waagepetersen, H.S. and Schousboe, A. (2012) 'Brain glycogen—new perspectives on its metabolic function and regulation at the subcellular level', *Frontiers in Neuroenergetics*, 4, p. 3.

Oberheim, N.A., Takano, T., Han, X., He, W., Lin, J.H.C., Wang, F., Xu, Q., Wyatt, J.D., Pilcher, W., Ojemann, J.G., Ransom, B.R., Goldman, S.A. and Nedergaard, M. (2009) 'Uniquely Hominid Features of Adult Human Astrocytes', *The Journal of Neuroscience*, 29(10), pp. 3276-3287.

Ohno, K., Isotani, E. and Hirakawa, K. (1997) 'MELAS presenting as migraine complicated by stroke: case report', *Neuroradiology*, 39(11), pp. 781-784.

Olav, B.S., Mussie, G.H., Tanya, S.M., Ursula, S. and Karin, B. (2013) 'Brain Mitochondrial Metabolic Dysfunction and Glutamate Level Reduction in the Pilocarpine Model of Temporal Lobe Epilepsy in Mice', *Journal of Cerebral Blood Flow & Metabolism*, 33(7), pp. 1090-1097.

Olsen, R.W. (2002) 'Phenobarbital and Other Barbiturates: Mechanisms of Action', in Levy, R.H., Mattson, R.H., Meldrum, B.S. and Perucca, E. (eds.) *Antiepileptic Drugs*. 5th edn. United States of America: Lippincott Williams & Wilkins, pp. 489-495.

Olsen, R.W. (2006) 'Picrotoxin-like channel blockers of GABAA receptors', *Proceedings of the National Academy of Sciences*, 103(16), pp. 6081-6082.

Olsen, R.W. and Betz, H. (2006) 'GABA and Glycine', in Siegel, G.J., Albers, R.W., Brady, S.T. and Price, D.L. (eds.) *Basic Neurochemistry: Molecular, Cellular, and Medical Aspects*. 7 edn. China: Elsevier, pp. 291-301.

Olude, M.A., Mustapha, O.A., Aderounmu, O.A., Olopade, J.O. and Ihunwo, A.O. (2015) 'Astrocyte morphology, heterogeneity, and density in the developing African giant rat (Cricetomys gambianus)', *Frontiers in Neuroanatomy*, 9, p. 67.

Ortinski, P.I., Dong, J., Mungenast, A., Yue, C., Takano, H., Watson, D.J., Haydon, P.G. and Coulter, D.A. (2010) 'Selective induction of astrocytic gliosis generates deficits in neuronal inhibition', *Nat Neurosci*, 13(5), pp. 584-591.

Ott, M., Gogvadze, V., Orrenius, S. and Zhivotovsky, B. (2007) 'Mitochondria, oxidative stress and cell death', *Apoptosis*, 12(5), pp. 913-922.

Owen, O.E. (2005) 'Ketone bodies as a fuel for the brain during starvation', *Biochemistry and Molecular Biology Education*, 33(4), pp. 246-251.

Panov, A., Orynbayeva, Z., Vavilin, V. and Lyakhovich, V. (2014) 'Fatty Acids in Energy Metabolism of the Central Nervous System', *BioMed Research International*, 2014, p. 22.

Parikh, S., Saneto, R., Falk, M.J., Anselm, I., Cohen, B.H., Haas, R. and The Mitochondrial Medicine, S. (2009) 'A Modern Approach to the Treatment of Mitochondrial Disease', *Current treatment options in neurology*, 11(6), pp. 414-430.

Park, J.-J. and Cunningham, M.G. (2007) 'Thin Sectioning of Slice Preparations for Immunohistochemistry', *Journal of Visualized Experiments : JoVE*, (3), p. 194.

Paulsen, R.E., Contestabile, A., Villani, L. and Fonnum, F. (1987) 'An In Vivo Model for Studying Function of Brain Tissue Temporarily Devoid of Glial Cell Metabolism: The Use of Fluorocitrate', *Journal of Neurochemistry*, 48(5), pp. 1377-1385.

Paulson, O.B. (2002) 'Blood–brain barrier, brain metabolism and cerebral blood flow', *European Neuropsychopharmacology*, 12(6), pp. 495-501.

Pavlakis, S.G., Phillips, P.C., DiMauro, S., De Vivo, D.C. and Rowland, L.P. (1984) 'Mitochondrial myopathy, encephalopathy, lactic acidosis, and strokelike episodes: A distinctive clinical syndrome', *Annals of Neurology*, 16(4), pp. 481-488.

Pekny, M. and Pekna, M. (2014) 'Astrocyte Reactivity and Reactive Astrogliosis: Costs and Benefits', *Physiological Reviews*, 94(4), pp. 1077-1098.

Pekny, M., Wilhelmsson, U. and Pekna, M. (2014) 'The dual role of astrocyte activation and reactive gliosis', *Neuroscience Letters*, 565, pp. 30-38.

Pellerin, L. and Magistretti, P.J. (1994) 'Glutamate uptake into astrocytes stimulates aerobic glycolysis: a mechanism coupling neuronal activity to glucose utilization', *Proceedings of the National Academy of Sciences*, 91(22), pp. 10625-10629.

Penefsky, H.S. (1985) 'Mechanism of inhibition of mitochondrial adenosine triphosphatase by dicyclohexylcarbodiimide and oligomycin: relationship to ATP synthesis', *Proceedings of the National Academy of Sciences of the United States of America*, 82(6), pp. 1589-1593.

Perea, G., Navarrete, M. and Araque, A. (2009) 'Tripartite synapses: astrocytes process and control synaptic information', *Trends in Neurosciences*, 32(8), pp. 421-431.

Pfeffer, G., Majamaa, K., Turnbull, D.M., Thorburn, D. and Chinnery, P.F. (2012) 'Treatment for mitochondrial disorders', *Cochrane Database of Systematic Reviews*, (4).

Picard, M. and McEwen, B.S. (2014) 'Mitochondria impact brain function and cognition', *Proceedings of the National Academy of Sciences*, 111(1), pp. 7-8.

Picot, M.-C., Baldy-Moulinier, M., Daurès, J.-P., Dujols, P. and Crespel, A. (2008) 'The prevalence of epilepsy and pharmacoresistant epilepsy in adults: A population-based study in a Western European country', *Epilepsia*, 49(7), pp. 1230-1238.

Popa-Wagner, A., Mitran, S., Sivanesan, S., Chang, E. and Buga, A.-M. (2013) 'ROS and Brain Diseases: The Good, the Bad, and the Ugly', *Oxidative Medicine and Cellular Longevity*, 2013, p. 14.

Potokar, M., Jorgačevski, J. and Zorec, R. (2016) 'Astrocyte Aquaporin Dynamics in Health and Disease', *International Journal of Molecular Sciences*, 17(7), p. 1121.

Prinz, M. and Priller, J. (2014) 'Microglia and brain macrophages in the molecular age: from origin to neuropsychiatric disease', *Nat Rev Neurosci*, 15(5), pp. 300-312.

Puttachary, S., Sharma, S., Stark, S. and Thippeswamy, T. (2015) 'Seizure-Induced Oxidative Stress in Temporal Lobe Epilepsy', *BioMed Research International*, 2015, p. 20.

Quastel, J.H. and Wheatley, A.H.M. (1932) 'Oxidations by the brain', *Biochemical Journal*, 26(3), pp. 725-744.

Quilichini, P.P., Chiron, C., Ben-Ari, Y. and Gozlan, H. (2006) 'Stiripentol, a Putative Antiepileptic Drug, Enhances the Duration of Opening of GABAA-Receptor Channels', *Epilepsia*, 47(4), pp. 704-716.

Rahman, S. (2012) 'Mitochondrial disease and epilepsy', *Developmental Medicine & Child Neurology*, 54(5), pp. 397-406.

Rahman, S. (2015) 'Pathophysiology of mitochondrial disease causing epilepsy and status epilepticus', *Epilepsy & Behavior*, 49, pp. 71-75.

Randle, J.C.R., Guet, T., Cordi, A. and Lepagnol, J.M. (1992) 'Competitive inhibition by NBQX of kainate/AMPA receptor currents and excitatory synaptic potentials: importance of 6-nitro substitution', *European Journal of Pharmacology*, 215(2), pp. 237-244.

Raybaud, C., Shroff, M., Rutka, J.T. and Chuang, S.H. (2006) 'Imaging surgical epilepsy in children', *Child's Nervous System*, 22(8), pp. 786-809.

Reddy, D.S. and Kuruba, R. (2013) 'Experimental Models of Status Epilepticus and Neuronal Injury for Evaluation of Therapeutic Interventions', *International Journal of Molecular Sciences*, 14(9), pp. 18284-18318.

Reitzer, L.J., Wice, B.M. and Kennell, D. (1979) 'Evidence that glutamine, not sugar, is the major energy source for cultured HeLa cells', *Journal of Biological Chemistry*, 254(8), pp. 2669-2676.

Represa, A., Niquet, J., Pollard, H. and Ben-Ari, Y. (1995) 'Cell death, gliosis, and synaptic remodeling in the hippocampus of epileptic rats', *Journal of Neurobiology*, 26(3), pp. 413-425.

Rho, Jong M., Anderson, Gail D., Donevan, Sean D. and White, H.S. (2002) 'Acetoacetate, Acetone, and Dibenzylamine (a Contaminant in l-(+)-β-Hydroxybutyrate) Exhibit Direct Anticonvulsant Actions in Vivo', *Epilepsia*, 43(4), pp. 358-361.

Rho, J.M., Donevan, S.D. and Rogawski, M.A. (1996) 'Direct activation of GABAA receptors by barbiturates in cultured rat hippocampal neurons', *The Journal of Physiology*, 497(2), pp. 509-522.

Robel, S., Buckingham, S.C., Boni, J.L., Campbell, S.L., Danbolt, N.C., Riedemann, T., Sutor, B. and Sontheimer, H. (2015) 'Reactive Astrogliosis Causes the Development of Spontaneous Seizures', *The Journal of Neuroscience*, 35(8), pp. 3330-3345.

Robinson, B.H. (2006) 'Lactic acidemia and mitochondrial disease', *Molecular Genetics and Metabolism*, 89(1–2), pp. 3-13.

Rodrigues, J.V. and Gomes, C.M. (2012) 'Mechanism of superoxide and hydrogen peroxide generation by human electron-transfer flavoprotein and pathological variants', *Free Radical Biology and Medicine*, 53(1), pp. 12-19.

Rogawski, M.A. (2013) 'AMPA Receptors as a Molecular Target in Epilepsy Therapy', *Acta neurologica Scandinavica. Supplementum*, (197), pp. 9-18.

Rogawski, M.A. and Hanada, T. (2013) 'Preclinical pharmacology of perampanel, a selective non-competitive AMPA receptor antagonist', *Acta neurologica Scandinavica. Supplementum*, (197), pp. 19-24.

Rogers, G.W., Brand, M.D., Petrosyan, S., Ashok, D., Elorza, A.A., Ferrick, D.A. and Murphy, A.N. (2011) 'High Throughput Microplate Respiratory Measurements Using Minimal Quantities Of Isolated Mitochondria', *PLOS ONE*, 6(7), p. e21746.

Romano, A., Koczwara, J.B., Gallelli, C.A., Vergara, D., Micioni Di Bonaventura, M.V., Gaetani, S. and Giudetti, A.M. (2017) 'Fats for thoughts: An update on brain fatty acid metabolism', *The International Journal of Biochemistry & Cell Biology*, 84, pp. 40-45.

Ronald Zielke, H., Zielke, C.L., Baab, P.J. and Tyson Tildon, J. (2007) 'Effect of fluorocitrate on cerebral oxidation of lactate and glucose in freely moving rats', *Journal of Neurochemistry*, 101(1), pp. 9-16.

Roopun, A.K., Simonotto, J.D., Pierce, M.L., Jenkins, A., Nicholson, C., Schofield, I.S., Whittaker, R.G., Kaiser, M., Whittington, M.A., Traub, R.D. and Cunningham, M.O. (2010) 'A nonsynaptic mechanism underlying interictal discharges in human epileptic neocortex', *Proceedings of the National Academy of Sciences*, 107(1), pp. 338-343.

Rossignol, R., Faustin, B., Rocher, C., Malgat, M., Mazat, J.-P. and Letellier, T. (2003) 'Mitochondrial threshold effects', *Biochemical Journal*, 370(Pt 3), pp. 751-762.

Rossokhin, A.V., Sharonova, I.N., Bukanova, J.V., Kolbaev, S.N. and Skrebitsky, V.G. (2014) 'Block of GABAA receptor ion channel by penicillin: Electrophysiological and modeling insights toward the mechanism', *Molecular and Cellular Neuroscience*, 63, pp. 72-82.

Rowe, W.B., Blalock, E.M., Chen, K.-C., Kadish, I., Wang, D., Barrett, J.E., Thibault, O., Porter, N.M., Rose, G.M. and Landfield, P.W. (2007) 'Hippocampal Expression Analyses Reveal Selective Association of Immediate-Early, Neuroenergetic, and Myelinogenic Pathways with Cognitive Impairment in Aged Rats', *The Journal of Neuroscience*, 27(12), pp. 3098-3110.

Roy, A., Jana, M., Corbett, Grant T., Ramaswamy, S., Kordower, Jeffrey H., Gonzalez, Frank J. and Pahan, K. (2013) 'Regulation of Cyclic AMP Response Element Binding and Hippocampal Plasticity-Related Genes by Peroxisome Proliferator-Activated Receptor α', *Cell Reports*, 4(4), pp. 724-737.

Sada, N., Lee, S., Katsu, T., Otsuki, T. and Inoue, T. (2015) 'Targeting LDH enzymes with a stiripentol analog to treat epilepsy', *Science*, 347(6228), pp. 1362-1367.

Sakamaki, J.-I., Fu, A., Reeks, C., Baird, S., Depatie, C., Al Azzabi, M., Bardeesy, N., Gingras, A.-C., Yee, S.-P. and Screaton, R.A. (2014) 'Role of the SIK2–p35–PJA2 complex in pancreatic β-cell functional compensation', *Nat Cell Biol*, 16(3), pp. 234-244.

Sanchez, H., Zoll, J., Bigard, X., Veksler, V., Mettauer, B., Lampert, E., Lonsdorfer, J. and Ventura-Clapier, R. (2001) 'Effect of cyclosporin A and its vehicle on cardiac and skeletal muscle mitochondria: relationship to efficacy of the respiratory chain', *British Journal of Pharmacology*, 133(6), pp. 781-788.

Sandbank, U. and Lerman, P. (1972) 'Progressive cerebral poliodystrophy – Alpers' disease', *Disorganized giant neuronal mitochondria on electron microscopy*, 35(6), pp. 749-755.

Sato, M. and Sato, K. (2013) 'Maternal inheritance of mitochondrial DNA by diverse mechanisms to eliminate paternal mitochondrial DNA', *Biochimica et Biophysica Acta (BBA) - Molecular Cell Research*, 1833(8), pp. 1979-1984.

Satoh, J.-i., Tabunoki, H., Yamamura, T., Arima, K. and Konno, H. (2007) 'Human astrocytes express aquaporin-1 and aquaporin-4 in vitro and in vivo', *Neuropathology*, 27(3), pp. 245-256.

Sauerbeck, A., Pandya, J., Singh, I., Bittman, K., Readnower, R., Bing, G. and Sullivan, P. (2011) 'Analysis of regional brain mitochondrial bioenergetics and susceptibility to mitochondrial inhibition utilizing a microplate based system', *Journal of Neuroscience Methods*, 198(1), pp. 36-43.

Saxton, W.M. and Hollenbeck, P.J. (2012) 'The axonal transport of mitochondria', *Journal of Cell Science*, 125(9), pp. 2095-2104.

Scaglia, F. (2012) 'Nuclear Gene Defects in Mitochondrial Disorders', in Wong, P.D.L.-J.C. (ed.) *Mitochondrial Disorders: Biochemical and Molecular Analysis*. Totowa, NJ: Humana Press, pp. 17-34.

Scandroglio, F., Tórtora, V., Radi, R. and Castro, L. (2014) 'Metabolic control analysis of mitochondrial aconitase: influence over respiration and mitochondrial superoxide and hydrogen peroxide production', *Free Radical Research*, 48(6), pp. 684-693.

Scarpulla, R.C. (1997) 'Nuclear Control of Respiratory Chain Expression in Mammalian Cells', *Journal of Bioenergetics and Biomembranes*, 29(2), pp. 109-119.

Scatena, R., Bottoni, P., Vincenzoni, F., Messana, I., Martorana, G.E., Nocca, G., De Sole, P., Maggiano, N., Castagnola, M. and Giardina, B. (2003) 'Bezafibrate Induces a Mitochondrial Derangement in Human Cell Lines: A PPAR-Independent Mechanism for a Peroxisome Proliferator', *Chemical Research in Toxicology*, 16(11), pp. 1440-1447.

Schaefer, A.M., McFarland, R., Hart, Y. and Turnbull, D.M. (2010) 'Newcastle Mitochondrial Disease Guidelines - Epilepsy in Adult Mitochondrial Disease : Investigation and Management', [Online]. Available at: http://www.mitochondrialncg.nhs.uk/documents/Epilepsy_Guidelines_2011.pdf (Accessed: 22 December 2016).

Schägger, H. and Pfeiffer, K. (2000) 'Supercomplexes in the respiratory chains of yeast and mammalian mitochondria', *The EMBO Journal*, 19(8), pp. 1777-1783.

Schapira, A.H.V. (2010) 'Complex I: Inhibitors, inhibition and neurodegeneration', *Experimental Neurology*, 224(2), pp. 331-335.

Schildge, S., Bohrer, C., Beck, K. and Schachtrup, C. (2013) 'Isolation and Culture of Mouse Cortical Astrocytes', *Journal of Visualized Experiments : JoVE*, (71), p. 50079.

Schmidt, D. and Wilensky, A.J. (2008) 'Benzodiazepines', in Jerome Engel, J. and Pedley, T.A. (eds.) *Epilepsy : A Comprehensive Textbook*. United States of America: Lippincott Williams & Wilkins, pp. 1531-1541.

Schon, E.A., DiMauro, S., Hirano, M. and Gilkerson, R.W. (2010) 'Therapeutic prospects for mitochondrial disease', *Trends in Molecular Medicine*, 16(6), pp. 268-276.

Schönfeld, P. and Reiser, G. (2013) 'Why does brain metabolism not favor burning of fatty acids to provide energy? - Reflections on disadvantages of the use of free fatty acids as fuel for brain', *Journal of Cerebral Blood Flow & Metabolism*, 33(10), pp. 1493-1499.

Schönfeld, P. and Wojtczak, L. (2012) 'Brown adipose tissue mitochondria oxidizing fatty acids generate high levels of reactive oxygen species irrespective of the uncoupling protein-1 activity state', *Biochimica et Biophysica Acta (BBA) - Bioenergetics*, 1817(3), pp. 410-418.

Scorza, F.A., Arida, R.M., Priel, M.R., Calderazzo, L. and Cavalheiro, E.A. (2002) 'Glucose utilisation during status epilepticus in an epilepsy model induced by pilocarpine: a qualitative study', *Arquivos de Neuro-Psiquiatria*, 60, pp. 198-203.

Seifert, G. and Steinhäuser, C. (1995) 'Glial Cells in the Mouse Hippocampus Express AMPA Receptors with an Intermediate Ca2+ Permeability', *European Journal of Neuroscience*, 7(9), pp. 1872-1881.

Seress, L. (2007) 'Comparative anatomy of the hippocampal dentate gyrus in adult and developing rodents, non-human primates and humans', in Helen, E.S. (ed.) *Progress in Brain Research*. Elsevier, pp. 23-798.

Shank, R.P., Bennett, G.S., Freytag, S.O. and Campbell, G.L. (1985) 'Pyruvate carboxylase: an astrocyte-specific enzyme implicated in the replenishment of amino acid neurotransmitter pools', *Brain Research*, 329(1–2), pp. 364-367.

Sharott, A. (2013) 'Local Field Potential, Methods of Recording', in Jaeger, D. and Jung, R. (eds.) *Encyclopedia of Computational Neuroscience*. New York, NY: Springer New York, pp. 1-3.

Shin, E.-J., Jeong, J.H., Chung, Y.H., Kim, W.-K., Ko, K.-H., Bach, J.-H., Hong, J.-S., Yoneda, Y. and Kim, H.-C. (2011) 'Role of oxidative stress in epileptic seizures', *Neurochemistry international*, 59(2), pp. 122-137.

Shou, Y., Gunasekar, P.G., Borowitz, J.L. and Isom, G.E. (2000) 'Cyanide-Induced Apoptosis Involves Oxidative-Stress-Activated NF-κB in Cortical Neurons', *Toxicology and Applied Pharmacology*, 164(2), pp. 196-205.

Siddiqui, M.A., Ahmad, J., Farshori, N.N., Saquib, Q., Jahan, S., Kashyap, M.P., Ahamed, M., Musarrat, J. and Al-Khedhairy, A.A. (2013) 'Rotenone-induced oxidative stress and apoptosis in human liver HepG2 cells', *Molecular and Cellular Biochemistry*, 384(1), pp. 59-69.

Sigel, E. and Steinmann, M.E. (2012) 'Structure, Function, and Modulation of GABAA Receptors', *Journal of Biological Chemistry*, 287(48), pp. 40224-40231.

Sills, G. (2014) 'Anti-epileptic drug treatment', 04 [Online]. Available at: https://www.epilepsyresearch.org.uk/wp-content/uploads/2014/04/AEDs.pdf (Accessed: 21 December 2016).

Sills, M.A., Forsythe, W.I. and Haidukewych, D. (1986) 'Role of octanoic and decanoic acids in the control of seizures', *Archives of Disease in Childhood*, 61(12), pp. 1173-1177.

Silver, I.A. and Erecinska, M. (1994) 'Extracellular glucose concentration in mammalian brain: continuous monitoring of changes during increased neuronal activity and upon limitation in oxygen supply in normo-, hypo-, and hyperglycemic animals', *The Journal of Neuroscience*, 14(8), pp. 5068-5076.

Silver, J. (2016) 'The glial scar is more than just astrocytes', *Experimental Neurology*, 286, pp. 147-149.

Simon, A., Traub, R.D., Vladimirov, N., Jenkins, A., Nicholson, C., Whittaker, R.G., Schofield, I., Clowry, G.J., Cunningham, M.O. and Whittington, M.A. (2014) 'Gap junction networks can generate both ripple-like and fast ripple-like oscillations', *European Journal of Neuroscience*, 39(1), pp. 46-60.

Sinha, K., Das, J., Pal, P.B. and Sil, P.C. (2013) 'Oxidative stress: the mitochondria-dependent and mitochondria-independent pathways of apoptosis', *Archives of Toxicology*, 87(7), pp. 1157-1180.

Sirven, J., Whedon, B., Caplan, D., Liporace, J., Glosser, D., O'Dwyer, J. and Sperling, M.R. (1999) 'The Ketogenic Diet for Intractable Epilepsy in Adults: Preliminary Results', *Epilepsia*, 40(12), pp. 1721-1726.

Sleven, H., Gibbs, J.E., Heales, S., Thom, M. and Cock, H.R. (2006) 'Depletion of reduced glutathione precedes inactivation of mitochondrial enzymes following limbic status epilepticus in the rat hippocampus', *Neurochemistry International*, 48(2), pp. 75-82.

Smith, T.A.D. (2001) 'Type A (gamma)-aminobutyric acid (GABA(A)) receptor subunits and benzodiazepine binding: Significance to clinical syndromes and their treatment', *British Journal of Biomedical Science*, 58(2), p. 111.

Snow, D.M., Lemmon, V., Carrino, D.A., Caplan, A.I. and Silver, J. (1990) 'Sulfated proteoglycans in astroglial barriers inhibit neurite outgrowth in vitro', *Experimental Neurology*, 109(1), pp. 111-130.

Sofroniew, M.V. (2009) 'Molecular dissection of reactive astrogliosis and glial scar formation', *Trends in Neurosciences*, 32(12), pp. 638-647.

Sofroniew, M.V. and Vinters, H.V. (2010) 'Astrocytes: biology and pathology', *Acta Neuropathologica*, 119(1), pp. 7-35.

Sowa-Kućma, M., Szewczyk, B., Sadlik, K., Piekoszewski, W., Trela, F., Opoka, W., Poleszak, E., Pilc, A. and Nowak, G. (2013) 'Zinc, magnesium and NMDA receptor alterations in the hippocampus of suicide victims', *Journal of Affective Disorders*, 151(3), pp. 924-931.

Spruston, N. (2008) 'Pyramidal neurons: dendritic structure and synaptic integration', *Nat Rev Neurosci*, 9(3), pp. 206-221.

Srinivasan, R., Lu, T.-Y., Chai, H., Xu, J., Huang, B.S., Golshani, P., Coppola, G. and Khakh, B.S. (2016) 'New Transgenic Mouse Lines for Selectively Targeting Astrocytes and Studying Calcium Signals in Astrocyte Processes In Situ and In Vivo', *Neuron*, 92(6), pp. 1181-1195.

Steele, H.E. and Chinnery, P.F. (2015) 'Mitochondrial Causes of Epilepsy: Evaluation, Diagnosis, and Treatment', *Semin Neurol*, 35(03), pp. 300-309.

Steriade, C., Andrade, D.M., Faghfoury, H., Tarnopolsky, M.A. and Tai, P. (2014) 'Mitochondrial Encephalopathy With Lactic Acidosis and Stroke-like Episodes (MELAS) May Respond to Adjunctive Ketogenic Diet', *Pediatric Neurology*, 50(5), pp. 498-502.

Stern, J.M., Perucca, E. and Brown, T.R. (2008) 'Phenytoin, Fosphenytoin, and Other Hydantoins', in Jerome Engel, J. and Pedley, T.A. (eds.) *Epilepsy : A Comprehensive Textbook*. United States of America: Lippincott Williams & Wilkins, pp. 1609-1627.

Stewart, J.B. and Chinnery, P.F. (2015) 'The dynamics of mitochondrial DNA heteroplasmy: implications for human health and disease', *Nat Rev Genet*, 16(9), pp. 530-542.

Sugimoto, M., Fukami, S., Kayakiri, H., Yamazaki, S., Matsuoka, N., Uchida, I. and Mashimo, T. (2002) 'The β-lactam antibiotics, penicillin-G and cefoselis have different mechanisms and sites of action at GABA(A) receptors', *British Journal of Pharmacology*, 135(2), pp. 427-432.

Sung, C.-S., Cherng, C.-H., Wen, Z.-H., Chang, W.-K., Huang, S.-Y., Lin, S.-L., Chan, K.-H. and Wong, C.-S. (2012) 'Minocycline and fluorocitrate suppress spinal nociceptive signaling in intrathecal IL-1B-induced thermal hyperalgesic rats', *Glia*, 60(12), pp. 2004-2017.

Suzuki, Y.J., Carini, M. and Butterfield, D.A. (2010) 'Protein Carbonylation', *Antioxidants & Redox Signaling*, 12(3), pp. 323-325.

Swanson, R.A. and Graham, S.H. (1994) 'Fluorocitrate and fluoroacetate effects on astrocyte metabolism in vitro', *Brain Research*, 664(1–2), pp. 94-100.

Takahashi, S., Iizumi, T., Mashima, K., Abe, T. and Suzuki, N. (2014) 'Roles and Regulation of Ketogenesis in Cultured Astroglia and Neurons Under Hypoxia and Hypoglycemia', *ASN NEURO*, 6(5), p. 1759091414550997.

Takano, T., Tian, G.-F., Peng, W., Lou, N., Lovatt, D., Hansen, A.J., Kasischke, K.A. and Nedergaard, M. (2007) 'Cortical spreading depression causes and coincides with tissue hypoxia', *Nat Neurosci*, 10(6), pp. 754-762.

Tan, B., Xiao, H., Li, F., Zeng, L. and Yin, Y. (2015) 'The profiles of mitochondrial respiration and glycolysis using extracellular flux analysis in porcine enterocyte IPEC-J2', *Animal Nutrition*, 1(3), pp. 239-243.

Téllez-Zenteno, J.F. and Hernández-Ronquillo, L. (2012) 'A Review of the Epidemiology of Temporal Lobe Epilepsy', *Epilepsy Research and Treatment*, 2012, p. 5.

Terada, H. (1990) 'Uncouplers of oxidative phosphorylation', *Environmental Health Perspectives*, 87, pp. 213-218.

TeSlaa, T. and Teitell, M.A. (2014) 'Techniques to Monitor Glycolysis', *Methods in enzymology*, 542, pp. 91-114.

Testa, C.M., Sherer, T.B. and Greenamyre, J.T. (2005) 'Rotenone induces oxidative stress and dopaminergic neuron damage in organotypic substantia nigra cultures', *Molecular Brain Research*, 134(1), pp. 109-118.

Thevenet, J., De Marchi, U., Domingo, J.S., Christinat, N., Bultot, L., Lefebvre, G., Sakamoto, K., Descombes, P., Masoodi, M. and Wiederkehr, A. (2016) 'Medium-chain fatty acids inhibit mitochondrial metabolism in astrocytes promoting astrocyte–neuron lactate and ketone body shuttle systems', *The FASEB Journal*, 30(5), pp. 1913-1926.

Thom, M. (2014) 'Review: Hippocampal sclerosis in epilepsy: a neuropathology review', *Neuropathology and Applied Neurobiology*, 40(5), pp. 520-543.

Tidman, L., Saravanan, K. and Gibbs, J. (2003) 'Epilepsy in mainstream and special educational primary school settings', *Seizure*, 12(1), pp. 47-51.

Ting, J.T., Daigle, T.L., Chen, Q. and Feng, G. (2014) 'Acute brain slice methods for adult and aging animals: application of targeted patch clampanalysis and optogenetics', *Methods in molecular biology (Clifton, N.J.)*, 1183, pp. 221-242.

Tiwari, B.S., Belenghi, B. and Levine, A. (2002) 'Oxidative Stress Increased Respiration and Generation of Reactive Oxygen Species, Resulting in ATP Depletion, Opening of Mitochondrial Permeability Transition, and Programmed Cell Death', *Plant Physiology*, 128(4), pp. 1271-1281.

Tokudome, K., Okumura, T., Shimizu, S., Mashimo, T., Takizawa, A., Serikawa, T., Terada, R., Ishihara, S., Kunisawa, N., Sasa, M. and Ohno, Y. (2016) 'Synaptic vesicle glycoprotein 2A (SV2A) regulates kindling epileptogenesis via GABAergic neurotransmission', *Scientific Reports*, 6, p. 27420.

Tomson, T., Stephen, L.J. and Brodie, M.J. (2008) 'Lamotrigine', in Jerome Engel, J. and Pedley, T.A. (eds.) *Epilepsy : A Comprehensive Textbook*. United States of America: Lippincott Williams & Wilkins, pp. 1575-1582.

Torbergsen, T., Mathiesen, E. and Aasly, J. (1991) 'Epilepsy in a mitochondrial disorder', *Journal of Neurology, Neurosurgery & Psychiatry*, 54(12), pp. 1073-1076.

Tremblay-Mercier, J., Tessier, D., Plourde, M., Fortier, M., Lorrain, D. and Cunnane, S.C. (2010) 'Bezafibrate Mildly Stimulates Ketogenesis and Fatty Acid Metabolism in Hypertriglyceridemic Subjects', *Journal of Pharmacology and Experimental Therapeutics*, 334(1), pp. 341-346.

Tsuda, A., Ito, M., Kishi, K., Shiraishi, H., Tsuda, H. and Mori, C. (1994) 'Effect of penicillin on GABA-gated chloride ion influx', *Neurochemical Research*, 19(1), pp. 1-4.

Tuppen, H.A.L., Blakely, E.L., Turnbull, D.M. and Taylor, R.W. (2010) 'Mitochondrial DNA mutations and human disease', *Biochimica et Biophysica Acta (BBA) - Bioenergetics*, 1797(2), pp. 113-128.

Tyynismaa, H. and Suomalainen, A. (2009) 'Mouse models of mitochondrial DNA defects and their relevance for human disease', *EMBO Reports*, 10(2), pp. 137-143.

Ünal-Çevik, I., Kılınç, M., Gürsoy-Özdemir, Y., Gurer, G. and Dalkara, T. (2004) 'Loss of NeuN immunoreactivity after cerebral ischemia does not indicate neuronal cell loss: a cautionary note', *Brain Research*, 1015(1–2), pp. 169-174.

Van Brederode, J.F.M., Mulligan, K.A. and Hendrickson, A.E. (1990) 'Calcium-binding proteins as markers for subpopulations of GABAergic neurons in monkey striate cortex', *The Journal of Comparative Neurology*, 298(1), pp. 1-22.

van Bree, J.B.M.M., Heijligers-Feijen, C.D., de Boer, A.G., Danhof, M. and Breimer, D.D. (1991) 'Stereoselective Transport of Baclofen Across the Blood–Brain Barrier in Rats as Determined by the Unit Impulse Response Methodology', *Pharmaceutical Research*, 8(2), pp. 259-262.

van Delft, R., Lambrechts, D., Verschuure, P., Hulsman, J. and Majoie, M. (2010) 'Blood beta-hydroxybutyrate correlates better with seizure reduction due to ketogenic diet than do ketones in the urine', *Seizure*, 19(1), pp. 36-39.

van der Bliek, A.M., Shen, Q. and Kawajiri, S. (2013) 'Mechanisms of Mitochondrial Fission and Fusion', *Cold Spring Harbor Perspectives in Biology*, 5(6).

Van Remmen, H., Salvador, C., Yang, H., Huang, T.T., Epstein, C.J. and Richardson, A. (1999) 'Characterization of the Antioxidant Status of the Heterozygous Manganese Superoxide Dismutase Knockout Mouse', *Archives of Biochemistry and Biophysics*, 363(1), pp. 91-97.

Vandenberghe, W., Robberecht, W. and Brorson, J.R. (2000) 'AMPA Receptor Calcium Permeability, GluR2 Expression, and Selective Motoneuron Vulnerability', *The Journal of Neuroscience*, 20(1), pp. 123-132.

Vargová, L. and Syková, E. (2014) 'Astrocytes and extracellular matrix in extrasynaptic volume transmission', *Philosophical Transactions of the Royal Society B: Biological Sciences*, 369(1654).

Veiga, A., Arrabaça, J.D. and Loureiro-Dias, M.C. (2003) 'Cyanide-resistant respiration, a very frequent metabolic pathway in yeasts', *FEMS Yeast Research*, 3(3), pp. 239-245.

Vezzani, A., French, J., Bartfai, T. and Baram, T.Z. (2011) 'The role of inflammation in epilepsy', *Nature Reviews. Neurology*, 7(1), pp. 31-40.

Vincent, P. and Mulle, C. (2009) 'Kainate receptors in epilepsy and excitotoxicity', *Neuroscience*, 158(1), pp. 309-323.

Voet, D. and Voet, J.G. (2011a) 'Electron Transport and Oxidative Phosphorylation', in *Biochemistry*. United States of America: Wiley, pp. 823-870.

Voet, D. and Voet, J.G. (2011b) 'Glycolysis', in *Biochemistry*. United States of America: Wiley, pp. 593-637.

Volmering, E., Niehusmann, P., Peeva, V., Grote, A., Zsurka, G., Altmüller, J., Nürnberg, P., Becker, A.J., Schoch, S., Elger, C.E. and Kunz, W.S. (2016) 'Neuropathological signs of inflammation correlate with mitochondrial DNA deletions in mesial temporal lobe epilepsy', *Acta Neuropathologica*, 132(2), pp. 277-288.

Voskuhl, R.R., Peterson, R.S., Song, B., Ao, Y., Morales, L.B.J., Tiwari-Woodruff, S. and Sofroniew, M.V. (2009) 'Reactive Astrocytes Form Scar-Like Perivascular Barriers to Leukocytes during Adaptive Immune Inflammation of the CNS', *The Journal of Neuroscience*, 29(37), pp. 11511-11522.

Waldbaum, S. and Patel, M. (2010) 'Mitochondria, oxidative stress, and temporal lobe epilepsy', *Epilepsy Research*, 88(1), pp. 23-45.

Walker, L.E., Mirza, N., Yip, V.L.M., Marson, A.G. and Pirmohamed, M. (2015) 'Personalized medicine approaches in epilepsy', *Journal of Internal Medicine*, 277(2), pp. 218-234.

Wallace, D.C. and Chalkia, D. (2013) 'Mitochondrial DNA Genetics and the Heteroplasmy Conundrum in Evolution and Disease', *Cold Spring Harbor Perspectives in Biology*, 5(11), p. a021220.

Walls, A.B., Bak, L.K., Sonnewald, U., Schousboe, A. and Waagepetersen, H.S. (2014) 'Metabolic mapping of astrocytes and neurons in culture using stable isotopes and gas chromatography-mass spectrometry (GC-MS)', in Hirrlinger, J. and Waagepetersen, H.S. (eds.) *Brain Energy Metabolism*. 5th edn. New York: Humana Press, pp. 73-106.

Wanders, R.J.A., Van Roermund, C.W.T., Visser, W.F., Ferdinandusse, S., Jansen, G.A., Van den Brink, D.M., Gloerich, J. and Waterham, H.R. (2003) 'Peroxisomal Fatty Acid Alpha-and Beta-Oxidation in Health and Disease: New insights', in Roels, F., Baes, M. and De Bie, S. (eds.) *Peroxisomal Disorders and Regulation of Genes*. Boston, MA: Springer US, pp. 293-302.

Wang, L., Maher, T.J. and Wurtman, R.J. (2007) 'Oral l-glutamine increases GABA levels in striatal tissue and extracellular fluid', *The FASEB Journal*, 21(4), pp. 1227-1232.

Wang, M. (2011) 'Neurosteroids and GABA-A Receptor Function', *Frontiers in Endocrinology*, 2(44).

Wang, X., Zhang, C., Szábo, G. and Sun, Q.-Q. (2013) 'Distribution of CaMKIIα expression in the brain in vivo, studied by CaMKIIα-GFP mice', *Brain research*, 1518, pp. 9-25.

Wanner, I.B., Anderson, M.A., Song, B., Levine, J., Fernandez, A., Gray-Thompson, Z., Ao, Y. and Sofroniew, M.V. (2013) 'Glial Scar Borders Are Formed by Newly Proliferated, Elongated Astrocytes That Interact to Corral Inflammatory and Fibrotic Cells via STAT3-Dependent Mechanisms after Spinal Cord Injury', *The Journal of Neuroscience*, 33(31), pp. 12870-12886.

Warden, A., Truitt, J., Merriman, M., Ponomareva, O., Jameson, K., Ferguson, L.B., Mayfield, R.D. and Harris, R.A. (2016) 'Localization of PPAR isotypes in the adult mouse and human brain', *Scientific Reports*, 6, p. 27618.

Waxham, M.N. (2014) 'Neurotransmitter Receptors', in *From Molecules to Networks : An Introduction to Cellular and Molecular Neuroscience*. 3 edn. United Kingdom: Academic Press, pp. 285-321.

Weber, M., Dietrich, D., Gräsel, I., Reuter, G., Seifert, G. and Steinhäuser, C. (2001) '6-Hydroxykynurenic acid and kynurenic acid differently antagonise AMPA and NMDA receptors in hippocampal neurones', *Journal of Neurochemistry*, 77(4), pp. 1108-1115.

Weinberg, F., Hamanaka, R., Wheaton, W.W., Weinberg, S., Joseph, J., Lopez, M., Kalyanaraman, B., Mutlu, G.M., Budinger, G.R.S. and Chandel, N.S. (2010) 'Mitochondrial metabolism and ROS generation are essential for Kras-mediated tumorigenicity', *Proceedings of the National Academy of Sciences*, 107(19), pp. 8788-8793.

Weiss, M., Tikhonov, D. and Buldakova, S. (2002) 'Effect of Flumazenil on GABAA Receptors in Isolated Rat Hippocampal Neurons', *Neurochemical Research*, 27(12), pp. 1605-1612.

Westergaard, N., Sonnewald, U. and Schousboe, A. (1995) 'Metabolic Trafficking between Neurons and Astrocytes: The Glutamate/Glutamine Cycle Revisited', *Developmental Neuroscience*, 17(4), pp. 203-211.

Whittaker, R.G., Devine, H.E., Gorman, G.S., Schaefer, A.M., Horvath, R., Ng, Y., Nesbitt, V., Lax, N.Z., McFarland, R., Cunningham, M.O., Taylor, R.W. and Turnbull, D.M. (2015) 'Epilepsy in adults with mitochondrial disease: A cohort study', *Annals of neurology*, 78(6), pp. 949-957.

Whittaker, R.G., Turnbull, D.M., Whittington, M.A. and Cunningham, M.O. (2011) 'Impaired mitochondrial function abolishes gamma oscillations in the hippocampus through an effect on fast-spiking interneurons', *Brain*, 134(7), pp. e180-e180.

Whittington, M.A., Traub, R.D. and Jefferys, J.G. (1995) 'Erosion of inhibition contributes to the progression of low magnesium bursts in rat hippocampal slices', *The Journal of Physiology*, 486(3), pp. 723-734.

Wild, J.M., Williams, M.N., Howie, G.J. and Mooney, R. (2005) 'Calcium-binding proteins define interneurons in HVC of the zebra finch (Taeniopygia guttata)', *The Journal of Comparative Neurology*, 483(1), pp. 76-90.

Willasch, A., Eing, S., Weber, G., Kuci, S., Schneider, G., Soerensen, J., Jarisch, A., Rettinger, E., Koehl, U., Klingebiel, T., Kreyenberg, H. and Bader, P. (2009) 'Enrichment of cell subpopulations applying automated MACS technique: purity, recovery and applicability for PCR-based chimerism analysis', *Bone Marrow Transplant*, 45(1), pp. 181-189.

Williams, M.D., Van Remmen, H., Conrad, C.C., Huang, T.T., Epstein, C.J. and Richardson, A. (1998) 'Increased Oxidative Damage Is Correlated to Altered Mitochondrial Function in Heterozygous Manganese Superoxide Dismutase Knockout Mice', *Journal of Biological Chemistry*, 273(43), pp. 28510-28515.

Williamson, R. and Wheal, H.V. (1992) 'The contribution of AMPA and NMDA receptors to graded bursting activity in the hippocampal CA1 region in an acute in vitro model of epilepsy', *Epilepsy Research*, 12(2), pp. 179-188.

Willoughby, J.O., Mackenzie, L., Broberg, M., Thoren, A.E., Medvedev, A., Sims, N.R. and Nilsson, M. (2003) 'Fluorocitrate-mediated astroglial dysfunction causes seizures', *Journal of Neuroscience Research*, 74(1), pp. 160-166.

Witt, K.A., Gillespie, T.J., Huber, J.D., Egleton, R.D. and Davis, T.P. (2001) 'Peptide drug modifications to enhance bioavailability and blood-brain barrier permeability', *Peptides*, 22(12), pp. 2329-2343.

Witthoft, A., Filosa, Jessica A. and Karniadakis, George E. (2013) 'Potassium Buffering in the Neurovascular Unit: Models and Sensitivity Analysis', *Biophysical Journal*, 105(9), pp. 2046-2054.

Wlaź, P., Socała, K., Nieoczym, D., Łuszczki, J.J., Żarnowska, I., Żarnowski, T., Czuczwar, S.J. and Gasior, M. (2012) 'Anticonvulsant profile of caprylic acid, a main constituent of the medium-chain triglyceride (MCT) ketogenic diet, in mice', *Neuropharmacology*, 62(4), pp. 1882-1889.

Wlaź, P., Socała, K., Nieoczym, D., Żarnowski, T., Żarnowska, I., Czuczwar, S.J. and Gasior, M. (2015) 'Acute anticonvulsant effects of capric acid in seizure tests in mice', *Progress in Neuro-Psychopharmacology and Biological Psychiatry*, 57, pp. 110-116.

Wong, V., Barrett, C.P., Donati, E.J. and Guth, L. (1987) 'Distribution of Carbonic Anhydrase Activity in Neurons of the Rat', *The Journal of Comparative Neurology*, 257, pp. 122-129.

Wright, A. and Vissel, B. (2012) 'The essential role of AMPA receptor GluR2 subunit RNA editing in the normal and diseased brain', *Frontiers in Molecular Neuroscience*, 5(34).

Wu, Y.-N., Shen, K.-Z. and Johnson, S.W. (1999) 'Presynaptic inhibition preferentially reduces the NMDA receptor-mediated component of transmission in rat midbrain dopamine neurons', *British Journal of Pharmacology*, 127(6), pp. 1422-1430.

Xiang, J., Ennis, S.R., Abdelkarim, G.E., Fujisawa, M., Kawai, N. and Keep, R.F. (2003) 'Glutamine transport at the blood–brain and blood–cerebrospinal fluid barriers', *Neurochemistry International*, 43(4–5), pp. 279-288.

Xu, Y., Cheng, G., Zhu, Y., Zhang, X., Pu, S., Wu, J., Lv, Y. and Du, D. (2016) 'Anti-nociceptive roles of the glia-specific metabolic inhibitor fluorocitrate in paclitaxel-evoked neuropathic pain', *Acta Biochimica et Biophysica Sinica*, 48(10), pp. 902-908.

Yamamoto, H.-a. and Mohanan, P.V. (2003) 'Ganglioside GT1B and melatonin inhibit brain mitochondrial DNA damage and seizures induced by kainic acid in mice', *Brain Research*, 964(1), pp. 100-106.

Yamamoto, H.-a. and Tang, H.-w. (1996) 'Preventive effect of melatonin against cyanide-induced seizures and lipid peroxidation in mice', *Neuroscience Letters*, 207(2), pp. 89-92.

Yatsuga, S. and Suomalainen, A. (2012) 'Effect of bezafibrate treatment on late-onset mitochondrial myopathy in mice', *Human Molecular Genetics*, 21(3), pp. 526-535.

Yonemura, K., Hasegawa, Y., Kimura, K., Minematsu, K. and Yamaguchi, T. (2001) 'Diffusion-weighted MR Imaging in a Case of Mitochondrial Myopathy, Encephalopathy, Lactic Acidosis, and Strokelike Episodes', *American Journal of Neuroradiology*, 22(2), pp. 269-272.

Young, B., Heath, J.W., Stevens, A. and Lowe, J.S. (2000) 'Nervous tissues', in Young, B. and heath, J.W. (eds.) *Wheater's Functional Histology : a text and colour atlas*. 4 edn. United Kingdom: Churchill Livingstone, pp. 116-142.

Yu, P., Wang, H., Katagiri, Y. and Geller, H.M. (2012) 'An In Vitro Model of Reactive Astrogliosis and Its Effect on Neuronal Growth', *Methods in molecular biology (Clifton, N.J.)*, 814, pp. 327-340.

Yu, Z., Yu, P., Chen, H. and Geller, H.M. (2014) 'Targeted inhibition of KCa3.1 attenuates TGF-β-induced reactive astrogliosis through the Smad2/3 signaling pathway', *Journal of Neurochemistry*, 130(1), pp. 41-49.

Yuen, A.W.C. and Sander, J.W. (2011) 'Impaired mitochondrial energy production: The basis of pharmacoresistance in epilepsy', *Medical Hypotheses*, 77(4), pp. 536-540.

Yum, M.-S., Ko, T.-S. and Kim, D.W. (2012a) 'Anticonvulsant Effects of β-Hydroxybutyrate in Mice', *Journal of Epilepsy Research*, 2(2), pp. 29-32.

Yum, M.-S., Ko, T.-S. and Kim, D.W. (2012b) 'β-Hydroxybutyrate increases the pilocarpine-induced seizure threshold in young mice', *Brain and Development*, 34(3), pp. 181-184.

Zaitsev, A.V., Gonzalez-Burgos, G., Povysheva, N.V., Kröner, S., Lewis, D.A. and Krimer, L.S. (2005) 'Localization of Calcium-binding Proteins in Physiologically and Morphologically Characterized Interneurons of Monkey Dorsolateral Prefrontal Cortex', *Cerebral Cortex*, 15(8), pp. 1178-1186.

Zamanian, J.L., Xu, L., Foo, L.C., Nouri, N., Zhou, L., Giffard, R.G. and Barres, B.A. (2012) 'Genomic Analysis of Reactive Astrogliosis', *The Journal of neuroscience : the official journal of the Society for Neuroscience*, 32(18), pp. 6391-6410.

Zijlmans, M., Huiskamp, G., Hersevoort, M., Seppenwoolde, J.-H., van Huffelen, A.C. and Leijten, F.S.S. (2007) 'EEG-fMRI in the preoperative work-up for epilepsy surgery', *Brain*, 130(9), pp. 2343-2353.

Zorov, D.B., Juhaszova, M. and Sollott, S.J. (2006) 'Mitochondrial ROS-induced ROS release: An update and review', *Biochimica et Biophysica Acta (BBA) - Bioenergetics*, 1757(5–6), pp. 509-517.

Zorov, D.B., Juhaszova, M. and Sollott, S.J. (2014) 'Mitochondrial Reactive Oxygen Species (ROS) and ROS-Induced ROS Release', *Physiological Reviews*, 94(3), pp. 909-950.

Zsurka, G. and Kunz, W.S. (2015) 'Mitochondrial dysfunction and seizures: the neuronal energy crisis', *The Lancet Neurology*, 14(9), pp. 956-966.

Zuchora, B., Turski, W.A., Wielosz, M. and Urbańska, E.M. (2001) 'Protective effect of adenosine receptor agonists in a new model of epilepsy – seizures evoked by mitochondrial toxin, 3-nitropropionic acid, in mice', *Neuroscience Letters*, 305(2), pp. 91-94.